

## National Transportation Library

### Section 508 and Accessibility Compliance

The National Transportation Library (NTL) both links to and collects electronic documents in a variety of formats from a variety of sources. The NTL makes every effort to ensure that the documents it collects are accessible to all persons in accordance with Section 508 of the Rehabilitation Act Amendments of 1998 (29 USC 794d), however, the NTL, as a library and digital repository, collects documents it does not create, and is not responsible for the content or form of documents created by third parties. Since June 21, 2001, all electronic documents developed, procured, maintained or used by the federal government are required to comply with the requirements of Section 508.

If you encounter problems when accessing our collection, please let us know by writing to [librarian@bts.gov](mailto:librarian@bts.gov) or by contacting us at (800) 853-1351. Telephone assistance is available 9AM to 6:30PM Eastern Time, 5 days a week (except Federal holidays). We will attempt to provide the information you need or, if possible, to help you obtain the information in an alternate format. Additionally, the NTL staff can provide assistance by reading documents, facilitate access to specialists with further technical information, and when requested, submit the documents or parts of documents for further conversion.

### Document Transcriptions

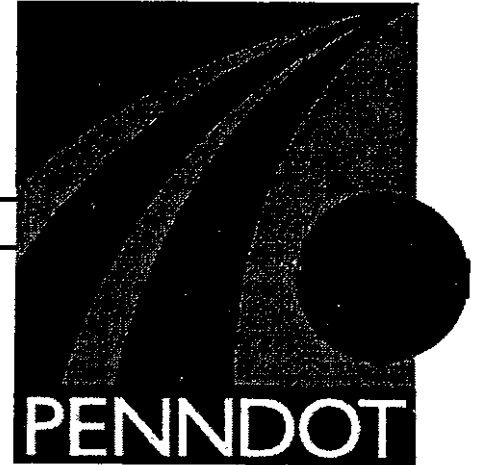
In an effort to preserve and provide access to older documents, the NTL has chosen to selectively transcribe printed documents into electronic format. This has been achieved by making an OCR (optical character recognition) scan of a printed copy. Transcriptions have been proofed and compared to the originals, but these are NOT exact copies of the official, final documents. Variations in fonts, line spacing, and other typographical elements will differ from the original. All transcribed documents are noted as "Not a True Copy."

The NTL Web site provides access to a graphical representation of certain documents. Thus, if you have any questions or comments regarding our transcription of a document's text, please contact the NTL at [librarian@bts.gov](mailto:librarian@bts.gov). If you have any comment regarding the content of a document, please contact the author and/or the original publisher.

---

**COMMONWEALTH OF PENNSYLVANIA  
DEPARTMENT OF TRANSPORTATION**

**PENNDOT RESEARCH**



---

---

**EVALUATION OF ERECTION PROCEDURES  
OF THE HORIZONTALLY CURVED STEEL  
I-GIRDER FORD CITY VETERANS BRIDGE**

**University-Based Research, Education,  
and Technology Transfer Program  
AGREEMENT NO. 359704, WORK ORDER 74**

**FINAL REPORT**

**March 2002**

**By B. W. Chavel and C. J. Earls**

**PENNS**STATE

---

---

**Pennsylvania Transportation Institute**

**The Pennsylvania State University  
Transportation Research Building  
University Park, PA 16802-4710  
(814) 865-1891 [www.pti.psu.edu](http://www.pti.psu.edu)**

<b>1. Report No.</b> FHWA-PA-2002-003-97-04 (74)	<b>2. Government Accession No.</b>	<b>3. Recipient's Catalog No.</b>	
<b>4. Title and Subtitle</b> Evaluation of Erection Procedures of the Horizontally Curved Steel I-Girder Ford City Veteran's Bridge		<b>5. Report Date</b> March 6, 2002	
<b>7. Author(s)</b> Brandon W. Chavel and Christopher J. Earls		<b>6. Performing Organization Code</b>  <b>8. Performing Organization Report No.</b> 2002-23	
<b>9. Performing Organization Name and Address</b>  The Pennsylvania Transportation Institute Transportation Research Building The Pennsylvania State University University Park, PA 16802-4710		<b>10. Work Unit No. (TRAIS)</b>	
<b>12. Sponsoring Organization Name and Address</b>  The Pennsylvania Department of Transportation Bureau of Planning and Research Commonwealth Keystone Building 400 North Street, 6 <sup>th</sup> Floor Harrisburg, PA 17120-0064		<b>11. Contract or Grant No. 359704</b> Work Order 74	
<b>15. Supplementary Notes</b> COTR: Tom Macioce (717) 787-7504		<b>13. Type of Report and Period Covered</b>  Final Report, 7/10/2000 - 3/9/2002	
<b>16. Abstract</b> <p>In the case of horizontally steel curved I-girder bridges, it is important to carefully analyze the erection sequence of the superstructure so as to ensure that difficulties do not arise in the field during construction of the bridge. Generally, problems with curved girder bridges result from unwanted displacements, stresses, and instabilities that occur during erection. For this reason, the bridge engineer should explore a variety of erection sequences to ensure each phase of construction proceeds as anticipated to make certain that the steel superstructure satisfies the intended design parameters (i.e. deck elevations, girder web plumbness, etc).</p> <p>Additional construction difficulties can result from inconsistent detailing of cross-frame members, which are primary load carrying members in steel curved I-girder bridges. Given that horizontally curved I-girders deflect vertically and horizontally upon loading, the web of the girders cannot remain plumb both before and after load is applied. An inconsistency occurs when the design engineer, the bridge erector, or the owner desires to have the web or the girders plumb before and after erection. For example, if the girders are fabricated to fit cross-frames in a web-plumb, no load condition, but the cross-frames are detailed to connect girders in a web-plumb after load application, an inconsistency develops. In some cases, the inconsistent detailing cross-frame members can lead to extreme problems during construction of curved I-girder bridge.</p> <p>The steel erection sequence of the Ford City Bridge is recreated through a computer simulation using the commercial finite element program ABAQUS. Displacements, stresses, and support reactions are monitored for each stage of the construction. The finite element modeling techniques used in this study displayed favorable agreement with available experimental data resulting from the erection studies carried out as part of the Curved Steel Bridge research project (CSBRP). Using these verified techniques, a nonlinear finite element model of the Ford City Bridge is constructed and the notion of inconsistent detailing is examined. A substantial difference in cross-frame member lengths is observed to result from the inconsistent detailing of the cross-frames. Such length differences imply the need for extremely large forces to be applied in the field during erection.</p>		<b>14. Sponsoring Agency Code</b>	
<b>17. Key Words</b> Gravity-On/Off, inconsistent Detailing of Cross-Frames, No-Load State of Construction, Nonlinear Finite Element Analysis, Steel Curved I-Girder Bridge, Steel Curved I-Girder Bridge Erection, Temporary Support Reactions Web-Out-of-Plumb Condition, Web-Plumb Condition		<b>18. Distribution Statement</b> No restrictions. This document is available from the National Technical Information Service, Springfield, VA 22161	
<b>19. Security Classif. (of this report)</b>  Unclassified	<b>20. Security Classif. (of this page)</b>  Unclassified	<b>21. No. of Pages</b>	<b>22. Price</b>

EVALUATION OF ERECTION PROCEDURES OF THE HORIZONTALLY  
CURVED STEEL I-GIRDER FORD CITY VETERANS BRIDGE  
University-Based Research, Education, and Technology Transfer  
Agreement No. 359704  
Work Order 74

FINAL REPORT

Prepared for

Commonwealth of Pennsylvania  
Department of Transportation

By

Brandon W. Chavel, Research Assistant  
And  
Christopher J. Earls, Assistant Professor and William Kepler Whiteford Faculty  
Scholar

Department of Civil and Environmental Engineering  
University of Pittsburgh

The Pennsylvania Transportation Institute  
The Pennsylvania State University  
Transportation Research Building  
University Park, PA 16802-4710

March 2002

This work was sponsored by the Pennsylvania Department of Transportation and the U.S. Department of Transportation, Federal Highway Administration. The contents of this report reflect the views of the authors, who are responsible for the facts and the accuracy of the data presented herein. The contents do not necessarily reflect the official views or policies of either the Federal Highway Administration, U.S. Department of Transportation, or the Commonwealth of Pennsylvania at the time of publication. This report does not constitute a standard, specification, or regulation.

PTI 2002-23

## **ABSTRACT**

### **EVALUATION OF ERECTION PROCEDURES OF THE HORIZONTALLY CURVED STEEL I-GIRDER FORD CITY VETERANS BRIDGE**

Brandon W. Chavel, Research Assistant

and

Christopher J. Earls, Assistant Professor and William Kepler Whiteford Faculty Fellow

Department of Civil and Environmental Engineering

University of Pittsburgh

In the case of horizontally steel curved I-girder bridges, it is important to carefully analyze the erection sequence of the superstructure so as to ensure that difficulties do not arise in the field during construction of the bridge. Generally, problems with curved girder bridges result from unwanted displacements, stresses, and instabilities that occur during erection. For this reason, the bridge engineer should explore a variety of erection sequences to ensure each phase of construction proceeds as anticipated to make certain that the steel superstructure satisfies the intended design parameters (i.e. deck elevations, girder web plumbness, etc.).

Additional construction difficulties can result from inconsistent detailing of cross-frame members, which are primary load carrying members in steel curved I-girder bridges. Given that horizontally curved I-girders deflect vertically and horizontally upon loading, the web of the girders cannot remain plumb both before and after load is applied. An inconsistency occurs when the design engineer, the bridge erector, or the owner desires to have the web of the girders plumb before and after erection. For example, if the girders are fabricated to fit cross-frames in a web-plumb, no load condition, but the cross-frames are detailed to connect girders in a web-plumb position after load application, an inconsistency develops. In some cases, the inconsistent detailing of cross-frame members can lead to extreme problems during construction of curved I-girder bridges.

The steel erection sequence of the Ford City Bridge is recreated through a computer simulation using the commercial finite element program ABAQUS. Displacements, stresses, and support reactions are monitored for each stage of the construction. The finite element modeling techniques used in this study displayed favorable agreement with available experimental data resulting from the erection studies carried out as part of the Curved Steel Bridge Research Project (CSBRP). Using these verified techniques, a nonlinear finite element model of the Ford City Bridge is constructed and the notion of inconsistent detailing is examined. A substantial difference in cross-frame member lengths is observed to result from the inconsistent detailing of the cross-frames. Such length differences imply the need for extremely large forces to be applied in the field during erection.

## DESCRIPTORS

Gravity-On/Off	Inconsistent Detailing of Cross-Frames
No-Load State of Construction	Nonlinear Finite Element Analysis
Steel Curved I-Girder Bridge	Steel Curved I-Girder Bridge Erection
Temporary Support Reactions	Web-Out-of-Plumb Condition
Web-Plumb Condition	

## TABLE OF CONTENTS

	Page
ACKNOWLEDGEMENTS .....	ii
ABSTRACT .....	iii
LIST OF FIGURES .....	xi
LIST OF TABLES .....	xxxii
NOMENCLATURE (Symbols, Acronyms, Curved I-Girder Bridge Terminology) .....	xxxiv
1.0 INTRODUCTION .....	1
1.1 Objectives .....	4
2.0 LITERATURE REVIEW .....	7
2.1 Introduction .....	7
2.2 Horizontally Curved Steel I-Girder Bridge Construction .....	9
2.2.1 Construction Study of FHWA CSBRP Experimental Bridge .....	9
2.2.2 Minnesota DOT Project .....	18
2.3 Horizontally Curved I-Girder Bridge Construction Concerns .....	25
2.3.1 Construction Issues .....	26
2.3.2 NCHRP Report 424 .....	28
2.4 Horizontally Curved I-Girder Bridge Construction Related Research .....	30
2.4.1 Lifting of Horizontally Curved I-Girders During Construction .....	30
2.4.2 Lateral Bracing and Construction Effects .....	32
2.4.3 Field Measurements of Camber Loss and Temperature Effects .....	33

	Page
2.5 Single Curved I-Girder and I-Girder Bridge Behavior .....	35
2.5.1 FHWA Horizontally Curved Steel Bridge Research Project (CSBRP) .....	35
2.6 Other Significant References Relevant to the Current Research .....	37
3.0 DESCRIPTION OF THE FORD CITY BRIDGE .....	41
3.1 Introduction .....	41
3.2 I-Girder Details .....	45
3.3 Cross-Frame Details .....	51
3.3.1 Incorrect Detailing of Cross-Frame Members .....	51
3.4 Falsework Details (Temporary Supports) .....	56
3.5 Miscellaneous Details .....	57
4.0 FORD CITY BRIDGE ERECTION SEQUENCE DETAILS .....	60
4.1 Curved Section Steel Erection Overview .....	61
4.2 “As-Built” Erection Procedure of Bridge Curved Section .....	66
5.0 VERIFICATION STUDY .....	112
5.1 CSBRP “ES1-4” Erection Study Test Frame Description .....	113
5.2 CSBRP “ES1-4” Erection Study Experimental Results .....	115
5.3 “ES1-4” Erection Study Finite Element Model .....	118
5.3.1 Finite Element Model Element Characteristics .....	118
5.3.2 Boundary Conditions .....	123
5.3.3 Loading Conditions .....	124
5.3.4 Loading Conditions .....	124

	Page
5.4 Discussion of Verification Results .....	125
6.0 FORD CITY BRIDGE FINITE ELEMENT MODEL .....	131
6.1 Element Types .....	131
6.2 Boundary Conditions .....	136
6.3 Loading Conditions .....	137
6.4 Additional Finite Element Model Details .....	138
7.0 ANALYTICAL STUDY OF FORD CITY BRIDGE ERECTION SEQUENCE .....	139
7.1 “As-Built” Erection Sequence Analytical Studies .....	140
7.1.1 Construction Stage 1 .....	141
7.1.2 Construction Stage 4 .....	144
7.1.3 Construction Stage 5 .....	147
7.1.4 Construction Stage 8 .....	152
7.1.5 Construction Stage 9 .....	156
7.1.6 Construction Stage 10 .....	162
7.1.7 Construction Stage 11 .....	166
7.1.8 Construction Stage 12 .....	172
7.1.9 Construction Stages 13 and 14 .....	178
7.1.10 Construction Stage 15 .....	183
7.1.11 Construction Stage 16 .....	188
7.1.12 Removal of Falsework 1 and Falsework 2A .....	193
7.2 “Planned” Erection Sequence Analytical Studies .....	195

	Page
7.2.1 Construction Stage 13 .....	197
7.2.2 Construction Stage 14 .....	203
7.2.3 Construction Stage 15 .....	211
7.2.4 Construction Stage 16 .....	216
7.3 Comparison of Construction Reactions for the Ford City Bridge With Incorrectly Detailed Cross-Frames and Cross-Frames Detailed for the No- Load Case .....	217
7.3.1 Construction Stage 4 Support Reaction Comparisons .....	219
7.3.2 Construction Stage 8 Support Reaction Comparisons .....	220
7.3.3 Construction Stage 12 Support Reaction Comparisons .....	220
7.3.4 Construction Stage 14 Support Reaction Comparisons .....	221
7.3.5 Construction Stage 16 Support Reaction Comparisons .....	222
7.4 Summary of Ford City Bridge Erection Sequence Analytical Studies .....	223
8.0 INCONSISTENT DETAILING OF CROSS-FRAME MEMBERS .....	225
8.1 Typical Inconsistent Detailing of Cross-Frames in Curved Steel I-Girder Bridges .....	227
8.1.1 Detailing of Cross-Frames to Girder Web-Plumb Condition at the Beginning of Construction .....	234
8.1.2 Detailing of Cross-Frames to Girder Web Out-Of-Plumb Condition at the Beginning of Construction .....	240
8.1.3 Difference in Cross-Frame Member Lengths Due to Inconsistent Detailing Procedures .....	247
8.1.3.1 Analysis and Results .....	248
8.1.3.2 Consequences of Results .....	257

8.2 Ford City Bridge – Cross-Frames Incorrectly Detailed for Girder Web-Plumb Condition After Application of Concrete Deck Load Only .....	258
8.2.1 Difference in Cross-Frame Member Lengths Due to Incorrect Detailing Procedures .....	259
8.2.2 Comparison of Field-Surveyed Elevations of Steel Superstructure Prior to Concrete Deck Placement with Finite Element Model Predictions .....	268
9.0 CONCLUSIONS .....	271
9.1 Recommended Future Research .....	274
APPENDIX A INTERVIEW TRANSCRIPTS .....	276
APPENDIX B ABAQUS FINITE ELEMENT MODELING TERMINOLOGY .....	282
APPENDIX C RESULTS FROM ANALYTICAL STUDIES OF BRIDGE ERECTION SEQUENCES .....	287
APPENDIX D INCONSISTENT DETAILING RESULTS .....	395
APPENDIX E HAND CALCULATION OF CROSS-FRAME MEMBER LENGTH FOR THE WEB-OUT-OF PLUMB CONDITION AT THE NO-LOAD POSITION .....	450
APPENDIX F SUMMARY OF CONSEQUENCES RELATED TO INCONSISTENT DETAILING OF CROSS-FRAMES .....	460
BIBLIOGRAPHY .....	463

## LIST OF FIGURES

Figure No.		Page
1	Ford City Veterans Bridge steel superstructure .....	2
2	CSBRP experimental bridge .....	11
3	Typical cross-frame .....	12
4	Construction study framing plans .....	14
5	MNDOT Bridge framing plan and typical cross-frame elevation view .....	19
6	MNDOT vibrating wire strain gauge placement .....	21
7	Lifting schemes .....	31
8	Plan view of Ford City Bridge (Sheet 1) .....	42
9	Plan view of Ford City Bridge (Sheet 2) .....	43
10	Ford city bridge naming convention .....	44
11	Comparison view depicting girder size .....	45
12	Elevation view of girder G1 .....	47
13	Elevation view of girder G2 .....	48
14	Elevation view of girder G3 .....	49
15	Elevation view of girder G4 .....	50
16	Cross-frame CF-1 detail. ....	52
17	Cross-frame CF-2 detail. ....	53
18	Cross-frame CF-3 detail. ....	54
19	Cross-frame CF-4 detail. ....	55

Figure No.		Page
20	Falsework structure .....	56
21	Field-splice 1, girder G4 .....	57
22	Typical concrete deck profile .....	59
23	Lifting crane .....	61
24	Falsework 1, 2A, and 2; prior to “bearing” assembly .....	62
25	Falsework 1, 2A, and 2; after “bearing” assembly .....	63
26	Side view of falsework 2A .....	64
27	Railway transport of girders .....	65
28	Barge transport of girders .....	65
29	Lifting of G3-1 .....	67
30	Clamping device used to lift G3-2 .....	68
31	Placement of cross-frame 1B at abutment 1 to stabilize G3-2 .....	69
32	Erection of girder G2-1 .....	70
33	Erection of girder G4-1 .....	71
34	Connection cross-frames 1C and 7C between G3-1 and G4-1 .....	72
35	Erection of G1-1 .....	73
36	Placing cross-frame 4A, G1-1 is on the right .....	74
37	Placing cross-frame 7A .....	74
38	Lifting of G3-2 .....	75
39	Lifting truss and lifting lug, G2-2 .....	76
40	Erected cross-frames on both sides of F3-2 at falsework 2A and 2 .....	77

Figure No.		Page
41	Erection of girder G1-2 .....	78
42	Typically used cantilevered “com-along” assembly .....	79
43	Girder G2 field-splice 1 .....	80
44	Placement of cross-frame 16B .....	81
45	Lifting of G4-1 .....	82
46	Lifting of G1-2 .....	84
47	Placement of cross-frame 11A, connecting G1-2 with G2-2 .....	84
48	Completed steel erection of bridge section 1 and 2 .....	85
49	Girder G3 pier 1 bracket construction .....	86
50	Completed pier 1 brackets for girders G2 and G3 .....	87
51	Lifting of G3-4 .....	88
52	G3-4 after cross-frames 27B and C were erected .....	89
53	Erection of cross-frame 26B .....	89
54	Lifting of G2-4 .....	90
55	Erection of cross-frame 25B .....	91
56	Erection of cross-frame 24B .....	91
57	Erection of cross-frame 23B .....	92
58	Lifting of G3-3 .....	94
59	Erection of G3-3 .....	94
60	G3-3; field-splice 2 .....	95
61	G3-3; field-splice 3 .....	95

Figure No.		Page
62	G3-3; field-splice 3 .....	96
63	G3-3; field-splice 3 .....	96
64	G3-3 is held in place with second and third cranes (third crane is on right, barely visible) .....	97
65	Lifting of G2-3 .....	99
66	Placing G2-3 in between sections 2 and 4 .....	99
67	G2-3, field-splice 3 .....	100
68	G2-3, field-splice 2 .....	100
69	Section 3; all four cranes holding girders and placing cross-frames .....	101
70	10/25/99, lifting crane still attached to G2-3 .....	102
71	Erection of G4-4 .....	103
72	Lifting of G1-4 .....	104
73	Erection of cross-frames 28A, G1-4 held in place .....	105
74	Erection of G4-4 .....	106
75	Lifting of G1-3 .....	108
76	G1-3 and section 3 cross-frames .....	108
77	Beginning the removal of falsework 2A .....	109
78	Falsework 2A has been completely removed .....	110
79	Completed curved section of the Ford City Bridge .....	111
80	CSBRP experimental bridge .....	114
81	ES1-4 experimental results; G1 midspan displacement vs. reactions .....	117
82	Verification study finite element model .....	121

Figure No.	Page
83	Verification study finite element mesh (close-up) ..... 122
84	ES1-4 Experimental and analytical results; G1 midspan displacement vs. reactions ..... 126
85	ES1-4 study; G1 top and bottom flange longitudinal strains at cross-frame 7 at maximum G1 midspan displacement ..... 127
86	ES1-4 study; G1 top and bottom flange longitudinal strains at cross-frame 5R at maximum G1 midspan displacement. .... 128
87	Deformed finite element model (Magnification factor of 25) ..... 129
88	Undeformed (darker) and deformed (lighter) models (Magnification factor of 25) ..... 130
89	Finite element mesh, girder G3 section 1 ..... 134
90	Finite element model of entire Ford City Bridge (meshes not shown for clarity) ..... 135
91	Finite element model of the curved section (meshes not shown for clarity) ..... 136
92	Construction stage 1 – Plan view of finite element model ..... 142
93	Construction stage 1 – Out-of-plane displacement, centerline of bottom flange ..... 143
94	Construction stage 1 – Out-of-plane displacement, centerline of top flange ..... 143
95	Construction stage 4 – Plan view of finite element model ..... 145
96	Construction stage 5 – Plan view of finite element model ..... 149
97	Construction Stage 5 – View above abutment 1 of finite element model ..... 150
98	Construction stage 5 – Out-of-plane displacement, centerline of bottom flange ..... 151

Figure No.	Page
99	Construction stage 5 – Out-of-plane displacement, centerline of top flange ..... 151
100	Construction stage 8 – Plan view of finite element model ..... 153
101	Construction stage 8 – Vertical displacement, centerline of bottom flange ..... 154
102	Construction stage 9 – Plan view of finite element model ..... 158
103	Construction stage 9 – Out-of-plane (radial) displacement, centerline of bottom flange ..... 159
104	Construction state 9 – Out-of-plane (radial) displacement, centerline of top flange ..... 160
105	Construction stage 9 – Vertical displacement, centerline of bottom flange ..... 161
106	Construction stage 10 – Plan view of finite element model ..... 164
107	Construction stage 10 – Vertical displacement, centerline of bottom flange ..... 165
108	Construction stage 11 – Plan view of finite element model ..... 168
109	Construction stage 11 – Out-of-plane (radial) displacement, centerline of top flange ..... 169
110	Construction stage 11 – Vertical displacement, centerline of bottom flange ..... 170
111	Construction stage 12 – Plan view of finite element model ..... 174
112	Construction stage 12 – Out-of-plane (radial) displacement, centerline of top flange ..... 175
113	Construction stage 12 – Vertical displacement, centerline of bottom flange ..... 176
114	Construction stage 14 – Plan view of finite element model ..... 180

Figure No.	Page
115 Construction stage 14 – Out-of-plane (radial) displacement, centerline of top flange .....	181
116 Construction stage 14 – Vertical displacement, centerline of bottom flange .....	182
117 Construction stage 15 – Plan view of finite element model .....	185
118 Construction stage 15 – Out-of-plane (radial) displacement, centerline of top flange .....	186
119 Construction stage 15 – Vertical displacement, centerline of bottom flange .....	187
120 Construction stage 16 – Plan view of finite element model .....	190
121 Construction stage 16 – Out-of-plane (radial) displacement, centerline of top flange .....	191
122 Construction stage 16 – Vertical displacement, centerline of bottom flange .....	192
123 After removal of falsework 1 and 2A – Vertical displacement, centerline of bottom flange .....	194
124 “In Field” construction stage 13 – Out-of-plane (radial) displacement, centerline of top flange .....	198
125 “Planned” construction stage 13 – Out-of-plane (radial) displacement, centerline of top flange .....	199
126 “In Field” construction stage 13 – Vertical displacement, centerline of bottom flange .....	200
127 “Planned” construction stage 13 – Vertical displacement, centerline of bottom flange .....	201
128 “In Field” construction stage 14 – Plan view of finite element model .....	205
129 “Planned” construction stage 14 – Plan view of finite element model .....	206

Figure No.		Page
130	“In Field” construction stage 14 – Out-of-plane (radial) displacement, centerline of top flange .....	207
131	“Planned” construction stage 14 – Out-of-plane (radial) displacement, centerline of top flange .....	208
132	“In Field” construction stage 14 – Vertical displacement, centerline of bottom flange .....	209
133	“Planned” construction stage 14 – Vertical displacement, centerline of bottom flange .....	210
134	“In Field” construction stage 15 – Vertical displacement, centerline of bottom flange .....	213
135	“Planned” construction stage 15 – Vertical displacement, centerline of bottom flange .....	214
136	Curved I-girder center of gravity .....	227
137	Displacement of finite element model – Displacement magnified by a factor of 10 (displaced structure is colored white, original structure is darker shade) .....	229
138	Vertical displacement of Ford City Bridge finite element model .....	230
139	Out-of-plane (radial) displacement at the bottom flange of the Ford City Bridge finite element model .....	231
140	Out-of-plane (radial) displacement at the top flange of the Ford City Bridge finite element model .....	232
141	Girder web rotation of the Ford City Bridge finite element model .....	233
142	Cross-sectional view of bridge at cross-frame 14 – Undeformed structure with cross-frames detailed for the no-load, web-plumb condition .....	236
143	Cross-sectional view of bridge at cross-frame 14 – Deformed structure due to steel self-weight with cross-frames detailed for the no-load, web-plumb condition .....	236

Figure No.		Page
144	Displacement of finite element model with cross-frames detailed for the no-load, web-plumb condition (displaced structure is colored white, original structure is darker shade) .....	238
145	Displacement of finite element model with cross-frames detailed for the no-load, web-plumb condition – Displacement magnified by a factor of 5 (displaced structure is colored white, original structure is darker shade) .....	239
146	Cross-sectional view of bridge at cross-frame 14 – Deformed structure due to steel self-weight with cross-frames detailed for the no-load web-plumb condition (Displacement magnified by a factor of 5) .....	242
147	Cross-sectional view of bridge at cross-frame 14 – Girder webs rotated back to web-plumb position (Displacement magnified by a factor of 5) .....	243
148	Cross-sectional view of bridge at cross-frame 14 – Girder webs rotated back to a web-plumb position and new cross-frame members are inserted (Displacement magnified by a factor of 5) .....	244
149	Cross-sectional view of bridge at cross-frame 14 – Web-plumb versus non-web-plumb at beginning of construction (Displacement magnified by a factor of 5) .....	246
150	Inconsistent detailing – naming convention for cross-frame members .....	249
151	Cross-sectional view of bridge at cross-frame 14 – Difference in cross-frame member lengths between web-plumb and non-web-plumb girders at no-load (Displacement magnified by a factor of 5) (No-load condition not shown for clarity) .....	250
152	Cross-frame member ‘F’ – Non-web-plumb detail vs. web-plumb detail length difference .....	253
153	Cross-frame member ‘M’ – Non-web-plumb detail vs. web-plumb detail length difference .....	254
154	Cross-frame top chord – Non-web-plumb detail vs. web-plumb detail length difference .....	255

Figure No.	Page
155	Cross-frame bottom chord – Non-web-plumb detail vs. web-plumb detail length difference ..... 256
156	Representative cross-frame member length difference due to incorrect detailing (application of concrete deck load) ..... 262
157	Cross-frame member ‘F’ – Web-plumb at concrete deck load detail vs. web-plumb at no-load detail length difference ..... 263
158	Cross-frame member ‘M’ – Web-plumb at concrete deck load detail vs. we-plumb at no-load detail length difference ..... 264
159	Cross-frame top chord – Web-plumb at concrete deck load detail vs. we-plumb at no-load detail length difference ..... 265
160	Cross-frame bottom chord – Web-plumb at concrete deck load detail vs. we-plumb at no-load detail length difference ..... 266
161	G4 – Elevation profile, STA 1+540 to 1+555; Analytical model versus field-surveyed data ..... 270
B-1	MPC LINEAR constraint ..... 285
C-1	Construction stage 1 – Plan view of finite element model ..... 289
C-2	Construction stage 1 – Field-splice location deflections and support reactions summary ..... 290
C-3	Construction stage 1 – Out-of-plane (radial) displacement, centerline of bottom flange ..... 291
C-4	Construction stage 1 – Out-of-plane (radial) displacement, centerline of top flange ..... 292
C-5	Construction stage 1 – Vertical displacement, centerline of bottom flange ..... 293
C-6	Construction stage 2 – Plan view of finite element model ..... 294
C-7	Construction stage 2 – Field-splice location deflections and support reactions summary ..... 295

Figure No.	Page
C-8 Construction stage 2 – Out-of-plane (radial) displacement, centerline of bottom flange .....	296
C-9 Construction stage 2 – Out-of-plane (radial) displacement, centerline of top flange .....	297
C-10 Construction stage 2 – Vertical displacement, centerline of bottom flange .....	298
C-11 Construction stage 3 – Plan view of finite element model .....	299
C-12 Construction stage 3 – Field-splice location deflections and support reactions summary .....	300
C-13 Construction stage 3 – Out-of-plane (radial) displacement, centerline of bottom flange .....	301
C-14 Construction stage 3 – Out-of-plane (radial) displacement, centerline of top flange .....	302
C-15 Construction stage 3 – Vertical displacement, centerline of bottom flange .....	303
C-16 Construction stage 4 – Plan view of finite element model .....	304
C-17 Construction stage 4 – Field-splice location deflections and support reactions summary .....	305
C-18 Construction stage 4 – Out-of-plane (radial) displacement, centerline of bottom flange .....	306
C-19 Construction stage 4 – Out-of-plane (radial) displacement, centerline of top flange .....	307
C-20 Construction stage 4 – Vertical displacement, centerline of bottom flange .....	308
C-21 Construction stage 5 – Plan view of finite element model .....	309
C-22 Construction stage 5 – Field-splice location deflections and support reactions summary .....	310

Figure No.	Page
C-23 Construction stage 5 – Out-of-plane (radial) displacement, centerline of bottom flange .....	311
C-24 Construction stage 5 – Out-of-plane (radial) displacement, centerline of top flange .....	312
C-25 Construction stage 5 – Vertical displacement, centerline of bottom flange .....	313
C-26 Construction stage 6 – Plan view of finite element model .....	314
C-27 Construction stage 6 – Field-splice location deflections and support reactions summary .....	315
C-28 Construction stage 6 – Out-of-plane (radial) displacement, centerline of bottom flange .....	316
C-29 Construction stage 6 – Out-of-plane (radial) displacement, centerline of top flange .....	317
C-30 Construction stage 6 – Vertical displacement, centerline of bottom flange .....	318
C-31 Construction stage 7 – Plan view of finite element model .....	319
C-32 Construction stage 7 – Field-splice location deflections and support reactions summary .....	320
C-33 Construction stage 7 – Out-of-plane (radial) displacement, centerline of bottom flange .....	321
C-34 Construction stage 7 – Out-of-plane (radial) displacement, centerline of top flange .....	322
C-35 Construction stage 7 – Vertical displacement, centerline of bottom flange .....	323
C-36 Construction stage 8 – Plan view of finite element model .....	324
C-37 Construction stage 8 – Field-splice location deflections and support reactions summary .....	325

Figure No.	Page
C-38 Construction stage 8 – Out-of-plane (radial) displacement, centerline of bottom flange .....	326
C-39 Construction stage 8 – Out-of-plane (radial) displacement, centerline of top flange .....	327
C-40 Construction stage 8 – Vertical displacement, centerline of bottom flange .....	328
C-41 Construction stage 9 – Plan view of finite element model .....	329
C-42 Construction stage 9 – Field-splice location deflections and support reactions summary .....	330
C-43 Construction stage 9 – Out-of-plane (radial) displacement, centerline of bottom flange .....	331
C-44 Construction stage 9 – Out-of-plane (radial) displacement, centerline of top flange .....	332
C-45 Construction stage 9 – Vertical displacement, centerline of bottom flange .....	333
C-46 Construction stage 10 – Plan view of finite element model .....	334
C-47 Construction stage 10 – Field-splice location deflections and support reactions summary .....	335
C-48 Construction stage 10 – Out-of-plane (radial) displacement, centerline of bottom flange .....	336
C-49 Construction stage 10 – Out-of-plane (radial) displacement, centerline of top flange .....	337
C-50 Construction stage 10 – Vertical displacement, centerline of bottom flange .....	338
C-51 Construction stage 11 – Plan view of finite element model .....	339
C-52 Construction stage 11 – Field-splice location deflections and support reactions summary .....	340

Figure No.	Page
C-53 Construction stage 11 – Out-of-plane (radial) displacement, centerline of bottom flange .....	341
C-54 Construction stage 11 – Out-of-plane (radial) displacement, centerline of top flange .....	342
C-55 Construction stage 12 – Vertical displacement, centerline of bottom flange .....	343
C-56 Construction stage 12 – Plan view of finite element model .....	344
C-57 Construction stage 12 – Field-splice location deflections and support reactions summary .....	345
C-58 Construction stage 12 – Out-of-plane (radial) displacement, centerline of bottom flange .....	346
C-59 Construction stage 12 – Out-of-plane (radial) displacement, centerline of top flange .....	347
C-60 Construction stage 12 – Vertical displacement, centerline of bottom flange .....	348
C-61 Construction stage 13 – Plan view of finite element model .....	349
C-62 Construction stage 13 – Field-splice location deflections and support reactions summary .....	350
C-63 Construction stage 13 – Out-of-plane (radial) displacement, centerline of bottom flange .....	351
C-64 Construction stage 13 – Out-of-plane (radial) displacement, centerline of top flange .....	352
C-65 Construction stage 13 – Vertical displacement, centerline of bottom flange .....	353
C-66 Construction stage 14 – Plan view of finite element model .....	354
C-67 Construction stage 14 – Field-splice location deflections and support reactions summary .....	355

Figure No.	Page
C-68 Construction stage 14 – Out-of-plane (radial) displacement, centerline of bottom flange .....	356
C-69 Construction stage 14 – Out-of-plane (radial) displacement, centerline of top flange .....	357
C-70 Construction stage 14 – Vertical displacement, centerline of bottom flange .....	358
C-71 Construction stage 15 – Plan view of finite element model .....	359
C-72 Construction stage 15 – Field-splice location deflections and support reactions summary .....	360
C-73 Construction stage 15 – Out-of-plane (radial) displacement, centerline of bottom flange .....	361
C-74 Construction stage 15 – Out-of-plane (radial) displacement, centerline of top flange .....	362
C-75 Construction stage 15 – Vertical displacement, centerline of bottom flange .....	363
C-76 Construction stage 16 – Plan view of finite element model .....	364
C-77 Construction stage 16 – Field-splice location deflections and support reactions summary .....	365
C-78 Construction stage 16 – Out-of-plane (radial) displacement, centerline of bottom flange .....	366
C-79 Construction stage 16 – Out-of-plane (radial) displacement, centerline of top flange .....	367
C-80 Construction stage 16 – Vertical displacement, centerline of bottom flange .....	368
C-81 Removal of Falsework 1 and Falsework 2A – Plan view of finite element model .....	369
C-82 Removal of Falsework 1 and Falsework 2A – Field-splice location deflections and support reactions summary .....	370

Figure No.	Page
C-83	Removal of Falsework 1 and Falsework 2A – Out-of-plane (radial) displacement, centerline of bottom flange ..... 371
C-84	Removal of Falsework 1 and Falsework 2A – Out-of-plane (radial) displacement, centerline of top flange ..... 372
C-85	Removal of Falsework 1 and Falsework 2A – Vertical displacement, centerline of bottom flange ..... 373
C-86	“Planned” construction stage 13 – Plan view of finite element model ..... 375
C-87	“Planned” construction stage 13 – Field-splice location deflections and support reactions summary ..... 376
C-88	“Planned” construction stage 13 – Out-of-plane (radial) displacement, centerline of bottom flange ..... 377
C-89	“Planned” construction stage 13 – Out-of-plane (radial) displacement, centerline of top flange ..... 378
C-90	“Planned” construction stage 13 – Vertical displacement, centerline of bottom flange ..... 379
C-91	“Planned” construction stage 14 – Plan view of finite element model ..... 380
C-92	“Planned” construction stage 14 – Field-splice location deflections and support reactions summary ..... 381
C-93	“Planned” construction stage 14 – Out-of-plane (radial) displacement, centerline of bottom flange ..... 382
C-94	“Planned” construction stage 14 – Out-of-plane (radial) displacement, centerline of top flange ..... 383
C-95	“Planned” construction stage 14 – Vertical displacement, centerline of bottom flange ..... 384
C-96	“Planned” construction stage 15 – Plan view of finite element model ..... 385
C-97	“Planned” construction 15 – Field-splice location deflections and support reactions summary ..... 386

Figure No.	Page
C-98 “Planned” construction stage 15 – Out-of-plane (radial) displacement, centerline of bottom flange .....	387
C-99 “Planned” construction stage 15 – Out-of-plane (radial) displacement, centerline of top flange .....	388
C-100 “Planned” construction stage 15 – Vertical displacement, centerline of bottom flange .....	389
C-101 “Planned” construction stage 16 – Plan view of finite element model .....	390
C-102 “Planned” construction 16 – Field-splice location deflections and support reactions summary .....	391
C-103 “Planned” construction stage 16 – Out-of-plane (radial) displacement, centerline of bottom flange .....	392
C-104 “Planned “ construction stage 16 – Out-of-plane (radial) displacement, centerline of top flange .....	393
C-105 “Planned” construction stage 16 – Vertical displacement, centerline of bottom flange .....	394
D-1 Inconsistent detailing – naming convention for cross-frame members .....	397
D-2 Cross-frame member ‘F’ – Non-web plumb detail vs. web-plumb detail length difference .....	405
D-3 Cross-frame member ‘M’ – Non-web-plumb detail vs. web-plumb detail length difference .....	406
D-4 Cross-frame top chord – Non-web-plumb detail vs. web-plumb detail length difference .....	407
D-5 Cross-frame bottom chord – Non-web-plumb detail vs. web-plumb detail length difference .....	408
D-6 Cross-frame member ‘F’ – Web-plumb at concrete deck load detail vs. web-plumb at no-load detail length difference .....	417
D-7 Cross-frame member ‘M’ – Web-plumb at concrete deck load detail vs. web-plumb at no-load detail length difference .....	418

Figure No.	Page
D-8	419
D-9	420
D-10	422
D-11	423
D-12	424
D-13	425
D-14	426
D-15	427
D-16	428
D-17	429
D-18	430
D-19	431
D-20	432
D-21	433

Figure No.	Page
D-22 G2 – Elevation profile, STA 1+585 to 1+600; Analytical model versus field-surveyed data .....	434
D-23 G2 – Elevation profile, STA 1+600 to 1+615; Analytical model versus field-surveyed data .....	435
D-24 G3 – Elevation profile, STA 1+510 to 1+525; Analytical model versus field-surveyed data .....	436
D-25 G3 – Elevation profile, STA 1+525 to 1+540; Analytical model versus field-surveyed data .....	437
D-26 G3 – Elevation profile, STA 1+540 to 1+555; Analytical model versus field-surveyed data .....	438
D-27 G3 – Elevation profile, STA 1+555 to 1+570; Analytical model versus field-surveyed data .....	439
D-28 G3 – Elevation profile, STA 1+570 to 1+585; Analytical model versus field-surveyed data .....	440
D-29 G3 – Elevation profile, STA 1+585 to 1+600; Analytical model versus field-surveyed data .....	441
D-30 G3 – Elevation profile, STA 1+600 to 1+615; Analytical model versus field-surveyed data .....	442
D-31 G4 – Elevation profile, STA 1+510 to 1+525; Analytical model versus field-surveyed data .....	443
D-32 G4 – Elevation profile, STA 1+525 to 1+540; Analytical model versus field-surveyed data .....	444
D-33 G4 – Elevation profile, STA 1+540 to 1+555; Analytical model versus field-surveyed data .....	445
D-34 G4 – Elevation profile, STA 1+555 to 1+570; Analytical model versus field-surveyed data .....	446
D-35 G4 – Elevation profile, STA 1+570 to 1+585; Analytical model versus field-surveyed data .....	447

Figure No.	Page
D-36 G4 – Elevation profile, STA 1+585 to 1+600; Analytical model versus field-surveyed data .....	448
D-37 G4 – Elevation profile, STA 1 +600 to 1+615; Analytical model versus field-surveyed data .....	449
E-1 Girder Displacements for Hand Calculation .....	452
E-2 Web-Out-of-plumb Cross-Frames Inserted for Hand Calculation .....	453
E-3 Girder position for girder webs out-of-plumb at the beginning of construction .....	445

## LIST OF TABLES

Table No.		Page
1	CSBRP Bridge data. ....	11
2	ES2-1 reaction distribution (approximate values from graphs by Linzell 1999) .....	16
3	Ford City Bridge girder geometric data .....	46
4	CSBRP Bridge data. ....	114
5	Construction stage 4 – Support reactions .....	146
6	Construction stages 1 through 4 – Support reactions .....	146
7	Construction stages 1 through 8 – Support reactions .....	155
8	Construction stages 9 and 10 – Pier 1 support reactions .....	166
9	Construction stage 11 – Support reactions .....	171
10	Construction stage 11 and 12 – Support reactions .....	177
11	Construction stages 12 through 14 – Pier 1 reactions .....	179
12	Construction stage 15 – Falsework 2 and pier 1 reactions .....	184
13	Construction stage 16 – Support reactions .....	189
14	After removal falsework 1 and 2A – Support reactions .....	193
15	Difference in erection sequences .....	196
16	“In Field” vs. “Planned” construction stage 13 vertical displacements .....	202
17	“In Field” vs. “Planned” construction stage 13 support reactions – section 1 and 2 .....	203
18	“In Field” vs. “Planned” construction stage 14 support reactions .....	211

Table No.	Page
19	“In Field” vs. “Planned” construction stage 15 support reactions ..... 215
20	Erections sequence support reactions for bridge with incorrectly detailed cross-frames (Case 1) and cross-frames detailed for the web-plumb, no-load case (Case 2) ..... 218
21	Cross-frames 10A – 20A – Dimensions for web-plumb at no-load condition versus web-non-plumb at no-load condition ..... 251
22	Cross-frames 10A – 20A – Dimensions for web-plumb at no-load and web-plumb for concrete deck load ..... 260
D-1	Cross-frames 1 through 8 – Detailing dimensions for web-plumb positions at no-load condition versus web-non-plumb position at no-load condition ..... 398
D-2	Cross-frames 9 through 12 – Detailing dimensions for web-plumb position at no-load condition versus web-non-plumb position at no-load condition ..... 399
D-3	Cross-frames 13 through 16 – Detailing dimensions for web-plumb position at no-load condition versus web-non-plumb position at no-load condition ..... 400
D-4	Cross-frames 17 through 20 – Detailing dimensions for web-plumb position at no-load condition versus web-non-plumb position at no-load condition ..... 401
D-5	Cross-frames 21 through 24 – Detailing dimensions for web-plumb position at no-load condition versus web-non-plumb position at no-load condition ..... 402
D-6	Cross-frames 25 through 28 – Detailing dimensions for web-plumb position at no-load condition versus web-non-plumb position at no-load condition ..... 403
D-7	Cross-frames 29 – Detailing dimensions for web-plumb position at no-load condition versus web-non-plumb position at no-load condition. .... 404
D-8	Cross-frames 1 through 8 – Detailing dimensions for web-plumb position at no-load condition versus web-plumb position after application of concrete deck load ..... 410

Table No.		Page
D-9	Cross-frames 9 through 12 – Detailing dimensions for web-plumb position at no-load condition versus web-plumb position after application of concrete deck load .....	411
D-10	Cross-frames 13 through 16 – Detailing dimensions for web-plumb position at no-load condition versus web-plumb position after application of concrete deck load .....	412
D-11	Cross-frames 17 through 20 – Detailing dimensions for web-plumb position at no-load condition versus web-plumb position after application of concrete deck load .....	413
D-12	Cross-frames 21 through 24 – Detailing dimensions for web-plumb position at no-load condition versus web-plumb position after application of concrete deck load .....	414
D-13	Cross-frames 25 through 28 – Detailing dimensions for web-plumb position at no-load condition versus web-plumb position after application of concrete deck load .....	415
D-14	Cross-frames 29 – Detailing dimensions for web-plumb position at no-load condition versus web-plumb position after application of concrete deck load .....	416
E-1	Analytical girder G1 displacements of the entire Ford City Bridge due to steel self-weight only .....	456
E-2	Analytical girder G2 displacements of the entire Ford City Bridge due to steel self-weight only .....	457
E-3	Analytical girder G3 displacements of the entire Ford City Bridge due to steel self-weight only .....	458
E-4	Analytical girder G4 displacements of the entire Ford City Bridge due to steel self-weight only .....	459

## NOMENCLATURE

1A, 1B, 4C, etc.	Cross-frame designations for the Ford City Bridge; cross-frame line A is the outermost of the curved span cross-frames
A	Area of a cross-section
CF-1, CF-2, CF-3, CF-4	Cross-frame types for the Ford City Bridge
COG	Center of Gravity
D, d	Girder web depth
ES1-4	CSBRP Bridge erection study
G1, G2, G3, G4	<ol style="list-style-type: none"><li>1. Ford City Bridge girders, G1 is the outside girder (largest radius)</li><li>2. CSBRP ES1-4 bridge girders, G1 is the inside girder (smallest radius)</li></ol>
G1-1, G1-2, G2-1, etc.	Ford City Bridge - Girder 1 Section 1, Girder 1 Section 2, Girder 2 Section 1, etc.
$I_{xx}$ , $I_{yy}$ , I	Moments of inertia of a cross-section
L	Curved length, or span length
R	Radius of Curvature
XF	Cross-frame

## Symbols

$\alpha$	Temperature constant
$\Delta$	Deflection due to temperature change
$\Delta T$	Internal temperature gradient
$\Theta$	Girder arc length angle

## Acronyms

AASHTO	American Association of State Highway and Transportation Officials
CSBRP	Curved Steel Bridge Research Project
FHWA	Federal Highway Administration
PennDot	Pennsylvania Department of Transportation
NCHRP	National Cooperative Highway Research Program

## Curved I-Girder Bridge Terminology

Gravity on/off	Analytical condition of applying load to the bridge structure, usually including steel self-weight. Gravity-on means self-weight is analytically considered; gravity-off means self-weight is not analytically considered.
No-load	Theoretical condition in which the bridge is subject to no stresses or displacements. Accomplished in the field during construction by using temporary supports.
Web out-of-plumb (Non-web-plumb)	The bridge girder webs are not vertical, not perpendicular to the horizon.
Web-plumb	The bridge girder webs are vertical, perpendicular to the horizon.

## 1.0 INTRODUCTION

In the case of horizontally curved steel I-girder bridges, it is important to carefully analyze the steel erection sequence of the bridge system to ensure that difficulties do not occur in the field during construction of the bridge. Generally, problems with curved girder bridges result from unwanted displacements, stresses, and instabilities during erection, which are typically unaccounted for by the designer. For this reason, the bridge engineer should explore a variety of erection sequences to ensure each phase of construction proceeds as anticipated to make certain that the steel superstructure satisfies the intended design parameters (i.e. deck elevations, girder web plumbness, etc.).

Additional construction difficulties can result from inconsistent detailing of cross-frame members, which are primary load carrying members in curved steel I-girder bridges. The fabrication of a curved I-girder to one load condition and the cross-frames to another load condition will induce additional stresses and deflections unaccounted for in the original design. The purpose of this research is to analyze these construction issues by means of monitoring critical curved girder response parameters through an analytical model of a recently constructed curved I-girder bridge.

The Pennsylvania Department of Transportation (PENNDOT) recently completed (July 2000) the new, 232 meters (1060 foot), three-span continuous Ford City Veterans Bridge, which carries Pennsylvania State Route 128 over the Allegheny River, approximately 50 miles northeast of Pittsburgh. The bridge consists of 44 individual girder sections, utilizing 4.275m (14ft) deep I-girders spaced at 4.1m (13.5ft) on center.

The northernmost span of the Ford City Bridge is curved, with a mean radius of 156m (511ft), and a curved length of approximately 89m (292ft), ending 8.8m (28.8ft) short of the northernmost pier. Figure 1 shows a photograph of the steel superstructure of the Ford City Bridge immediately prior to deck pan placement. The bridge is a longitudinal hybrid structure that employs HPS70W steel for the webs and flanges in the negative moment regions over the piers and grade 50 weathering steel throughout the remainder of the structure.

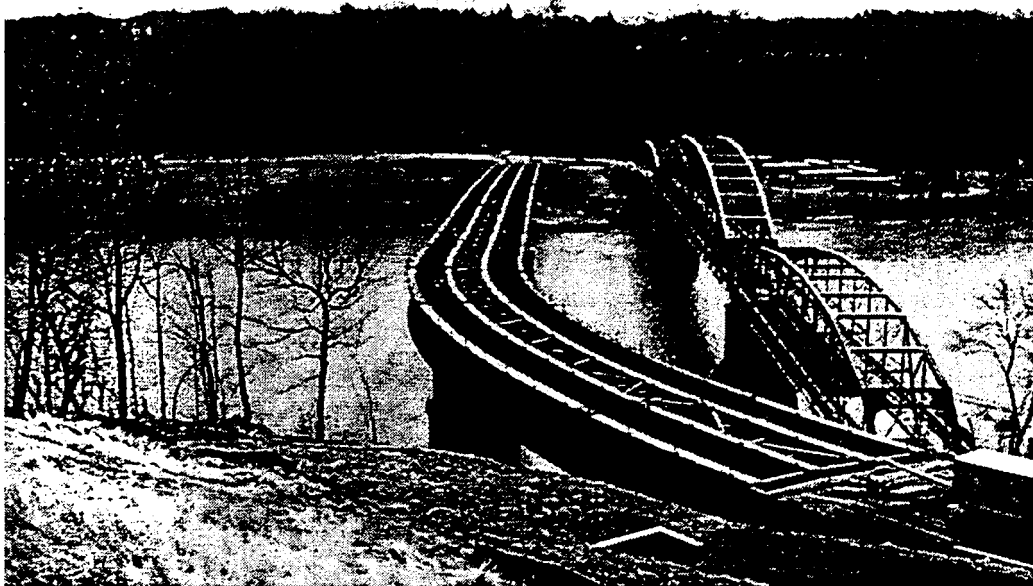


**Figure 1** Ford City Veterans Bridge steel superstructure

The geometrical complexities of the Ford City Bridge curved span make it an ideal candidate for studying issues relating to curved I-girder bridge erection methodologies. As part of the current research, the steel erection sequence is recreated through a computer simulation using the commercial finite element program ABAQUS.

The finite element modeling techniques used in this study display a favorable agreement with experimental data found in the literature. A nonlinear finite element model of the subject bridge, incorporating the verified modeling techniques, is used to analyze the erection sequence employed in the actual construction of the bridge. The construction of the model follows the construction sequence of the actual bridge; each individual phase of construction is analyzed so that temporary support reactions, displacements, and stresses induced during steel erection can be monitored.

Furthermore, given that horizontally curved girders deflect vertically and horizontally upon loading, the web of the girders cannot remain plumb both before and after a load is applied. An inconsistency occurs when the girders of a bridge are detailed to one geometric condition and the cross-frames to another. For example, if the girders are fabricated to fit cross-frames in a web-plumb (no-load) condition, but the cross-frames are detailed to connect the girders in a non-web-plumb (loaded) position, an inconsistency develops (Yadlosky 2001). In some cases, this inconsistency can lead to extreme problems during construction of curved I-girder bridges. The analytical model of the Ford City Bridge is used to illustrate that a substantial difference in cross-frame member lengths results from application of the different detailing methods (web-plumb and non-web-plumb).

## 1.1 Objectives

This current research consists of four major tasks:

1. Interviews are conducted that include PENNDOT site engineers involved in the erection of the curved girder span, and engineers from Michael Baker Engineering, Inc. who developed the design of the bridge and portions of the erection scheme. (See Appendix A.)
2. An extensive literature survey is performed to identify previous experimental and analytical research related to curved I-girder bridge construction.
3. A detailed nonlinear finite element model is created in order that behavior associated with the “in-field” construction of the curved span of the Ford City Bridge may be observed. The commercial finite element program ABAQUS is used to accomplish this task. The girders are modeled using meshes of shell elements for the webs and flanges, and beam elements for the “X” type cross-frames. The modeling techniques used to build the Ford City Bridge model show favorable agreement with experimental data found in the literature. The “as-built” construction sequence of the bridge is analyzed by replicating the placement of the girders and cross-frames directly in the finite element model.
4. An investigation is carried out to evaluate the difference in cross-frame dimensions using the analytical model of the Ford City Bridge under application of the different detailing methods (web-plumb and non-web-plumb under a given loading condition).

Currently, no design specification guidelines exist as pertains to the erection of curved I-girder bridges. It is hoped that this study will contribute to the available data related to erection of curved I-girder bridges, and identify possible improvements in erection schemes for future curved girder bridges of this type. Of course, there is no unique erection scheme suitable for all curved I-girder bridges, but certain bridge responses (temporary support reactions, displacements, and stresses) during erection may be generalized to this class of bridges. The current research endeavors to point out these generalities is organized as follows:

Section 2 contains an extensive literature review that identifies previous experimental and analytical research related to curved I-girder bridges. Section 3 provides a detailed description of the Ford City Bridge, detailing framing plans, girder dimensions, cross-frame members, and etc. Section 4 details each construction stage of the curved span of the Ford City Bridge. Photographs presented in section 4 depict the events associated with each construction stage. A verification study of the finite element modeling techniques employed in this research is discussed in section 5. The verification study utilizes results presented in the literature as part of the CSBRP ES1-4 erection study. In section 6, the construction of a detailed nonlinear finite element model of the Ford City Bridge, using the verified techniques of section 5, is presented. A detailed description of each element as well as ABAQUS nomenclature used in the finite element models can be found in Appendix B

Section 7 of the current study presents the analytical results for most of the construction stages used to erect the Ford City Bridge. Section 7 also provides analytical

comparisons related to differences between the “as-built” erection sequence and the “planned” erection sequence of the curved span. Comparisons in regard to support reactions are also made between the “planned” erection sequence of the bridge employing cross-frames detailed for the web-plumb position at the no-load condition, and the “planned” erection sequence of the bridge employing cross-frames detailed for the web-plumb position at application of the concrete deck load (which occurs in the actual structure). Appendix C provides all of the data related to this section.

Section 8 provides an in depth investigation in regard to inconsistent detailing of cross-frame members in curved steel I-girder bridges. This section specifies the discrepancies between detailing cross-frames for the web-plumb position at the no-load condition, and detailing cross-frames for the non-web-plumb position at the no-load condition, while in both cases girders are detailed for the web-plumb position at the no-load condition. Cross-frame member length differences are presented and discussed for both detailing methods. Additionally, cross-frame member length differences are presented for the detailing conditions of web-plumb at the no-load condition, and web-plumb at the application of concrete deck load. Appendix D displays all of the data in regard to the inconsistent detailing of cross-frame members.

Conclusions and future research recommendations are presented in Section 9. Additionally, transcripts of interviews conducted as part of the current research are shown in Appendix A.

## 2.0 LITERATURE REVIEW

### 2.1 Introduction

An enormous amount of research has been accomplished in regard to the behavior of horizontally curved steel I-girders however, little of this research has focused on the construction aspects of horizontally curved steel I-girder bridges. Over the last half of the 20<sup>th</sup> century, horizontally curved I-girder bridge construction has steadily increased. It now comprises almost one-third of the total steel bridge market in the United States (Burrell et al. 1997)<sup>1</sup>. Zureick et al. (1994) published a report as part of the Federal Highway Administration's (FHWA) Curved Steel Bridge Research Project (CSBRP) which summarized the large amount of research that has been accomplished analytically, experimentally, and theoretically. Approximately 750 references were collected, and 540 of these were considered significant and briefly discussed in the FHWA report. Of these, only one discussed construction aspects related to cross-frame requirements during construction.

Prior to the initiation of the CSBRP in 1992, the development of the curved steel bridge design specifications in the United States stemmed from research work accomplished by the Consortium of University Research Teams (CURT) in the 1960's and 1970's. The CURT project included researchers from Carnegie Mellon University, the University of Pennsylvania, the University of Rhode Island, and Syracuse University.

---

<sup>1</sup>Parentetical references placed in the line of text refer to the bibliography.

Research was conducted experimentally and analytically in regard to nominal bending strength, lateral stability, local buckling, and so forth. An allowable stress design format was developed based mostly on the work carried out as part of the CURT project. During the late 1970's, a load factor design criteria for curved girder bridges was developed based on work done by Galambos (1978) and Stegmann (1975) at Washington University. The developed allowable stress design criteria and the load factor design criteria ultimately became the AASHTO Guide Specifications for Horizontally Curved Highway Bridges in 1980 (revised 1993 (AASHTO 1993)), which contained design criteria for curved I-girder and box girder bridges, hybrid I-girder bridges, and curved box girder bridges. However, little if any attention was given to the behavior of horizontally curved I-girder bridges during construction.

More recently, two major contributions to the behavior of horizontally curved I-girder bridges during construction have appeared in the literature. One such contribution emanated from a portion of the FHWA-CSBRP project wherein a full-scale horizontally curved I-girder bridge structure was experimentally tested at the Turner-Fairbank Highway Research Center. A construction study was conducted as the structure was being erected wherein a series of elastic tests were performed that studied the behavior of portions of the experimental bridge as shoring was removed and replaced from underneath the girders. The experimental results, as well as comparison analytical results using the finite element program ABAQUS, were presented by Linzell (1999).

Galambos et al. (1996) completed a substantial "in-field" experimental investigation of the erection behavior of a horizontally curved steel I-girder bridge.

Results of this study were also presented by Pulver (1996), and finite element verification studies and analyses were conducted by Huang (1996). The objective of this research was to investigate the strains in the steel superstructure during the erection of a curved I-girder bridge built near Minneapolis, Minnesota. These field measurements were then compared with results obtained using a finite element program developed at the University of Minnesota.

Since the primary goal of the present research is related to the behavior of horizontally curved I-girder bridges during construction, this literature review will mainly focus on the CSBRP construction study and the Minnesota project. In addition, other related research that applies to the behavior of horizontally curved I-girders during construction will be presented and briefly summarized as part of the current survey of the literature.

## **2.2 Horizontally Curved Steel I-Girder Bridge Construction**

### **2.2.1 Construction Study of FHWA CSBRP Experimental Bridge (Linzell 1999, 2000)**

In 1992, the FHWA initiated the Curved Steel Bridge Research Project (CSBRP) in order to study and better characterize the behavior of horizontally curved I-girder bridges. The experimental program involved testing of a series of full-scale curved steel I-girder components in bending and shear, as well as a full size bridge, under realistic

loads and boundary conditions (Duwadi 2000). The bending and shear experimental program is not germane to the present research, and will only be briefly discussed later as part of the current literature survey. Tests were conducted on the CSBRP bridge, as reported by Linzell (1999), which studied the behavior of curved I-girder bridges during construction. These tests consisted of a series of elastic experimental loadings that were carried out as the bridge was being constructed. During this testing, bridge response was monitored as shoring was removed and replaced. Linzell focused on the deformations and load redistribution that took place as the structure was erected.

The CSBRP bridge was designed so that linear elastic behavior was guaranteed for the portion of the structure that was not part of the flexure and shear specimen tests. The CSBRP bridge, illustrated in figure 2, consists of three concentric I-girders, spaced at approximately 8.75 feet, and each having a depth of 48 inches. The bending component specimens were placed in the G3 girder line and were 25.4ft (7.7m) in length and centered about the midspan of G3. The remainder of the structure served as the testing frame. Flanges of the testing frame girders were flame cut, and not heat curved. Table 1 shows the applicable data for each girder, noting that G2 was fabricated from AASHTO M270 Grade 70W in order to guarantee it remained elastic throughout the testing.

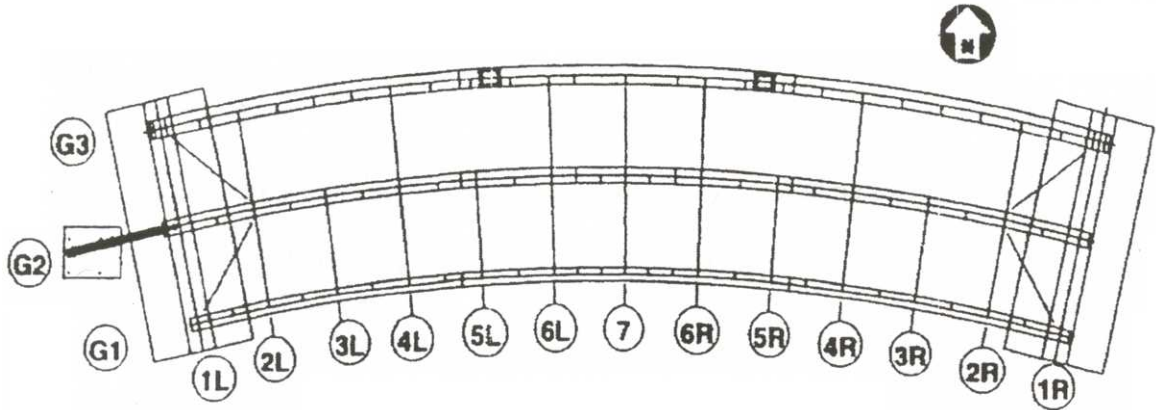


**Figure 2** CSBRP experimental bridge (Linzell 1999)

**Table 1** CSBRP Bridge data

<b>Girder</b>	<b>Radius</b>	<b>Spans</b>	<b>Yield Stress</b>	<b>Flange Width</b>
<b>G1</b>	191.25 ft (58.3 m)	86 ft (26.2 m)	50 ksi	16 in
<b>G2</b>	200 ft (61.0 m)	90 ft. (27.4 m)	70 ksi	20 in
<b>G3</b>	208.75 ft (63.6 m)	94 ft. (28.6 m)	50 ksi	24 in

As shown in figure 2, for each girder, transverse stiffeners were placed as single stiffeners at, and in between, the cross-frames. Back-to-back stiffeners were placed at the end supports, and at the load points used for the bending component tests. The radially orientated abutments supported the experimental bridge so that the structure was elevated approximately 2m above the floor. Spherical bearings and Teflon pads were used to

minimize the frictional forces and provide the desired degrees of freedom at the abutments. Guided bearings at both ends prevented radial translation, and a tangential support frame at the one end (used in order to stabilize the system) restricted G2's movement. The tangential support frame was pinned at the neutral axis of girder G2.

The lower lateral bracing in the end bays consisted of WT sections. Cross-frames consisted of "K" type frames, as shown in figure 3. All members of the cross-frames were fabricated from 60 ksi yield steel, and were of tubular cross-section, with a diameter of 5in and a wall thickness of 0.25in. Results from additional tests on tubular members completed by Linzell showed that the tubular members provided increased torsional stiffness when compared to similarly sized angle or tee sections, which are typically used in curved I-girder bridges.

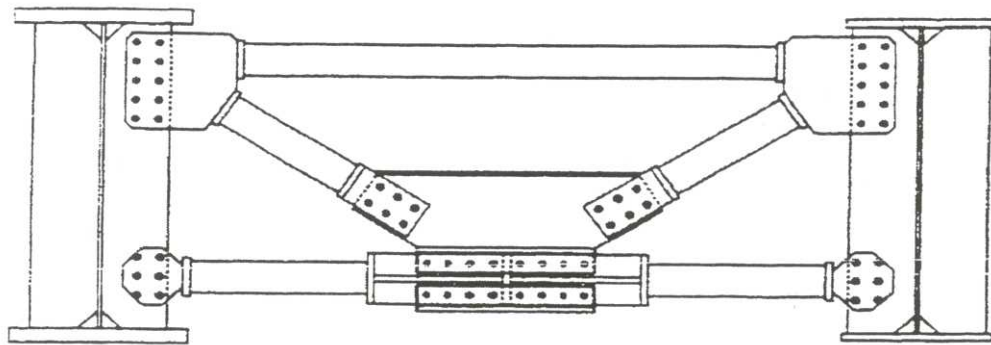


**Figure 3** Typical cross-frame (not to scale) (Linzell 1999)

Linzell discussed the instrumentation of the bridge in detail since it was of great importance due to the constraints associated with the project. To summarize, data was recorded as shoring was removed and replaced for each erection study. Load cells were

used at the abutment supports, and at intermediate shoring locations. Vibrating wire strain gauges were used to measure the strain at given locations on the girders. Resistance strain gauges were used at approximately mid length of all cross-frame members. Standard displacement and rotation transducers were used to measure girder deformations while at set increments along the top and bottom flanges laser and total station systems were also employed.

A series of nine different construction study tests were accomplished, using 6 different framing plans. Six ES1 tests were completed with G1 and G2 erected, where shoring beneath G1 was removed and then replaced while G2 was always fully shored; two ES2 tests where shoring was removed and replaced from beneath G1 and G2; and one ES3 test in which all three girders were in place and shoring was removed and replaced from beneath all three girders. All of the construction study tests began with the system completely shored so it was in the “no-load” position, which was determined from measurements at the fabrication plant, and from analytical models. The only load on the girders was their self-weight, no additional loads were placed on the experimental structure for any of the construction study tests. Figure 4 shows framing plans for the construction studies that were conducted by Linzell.

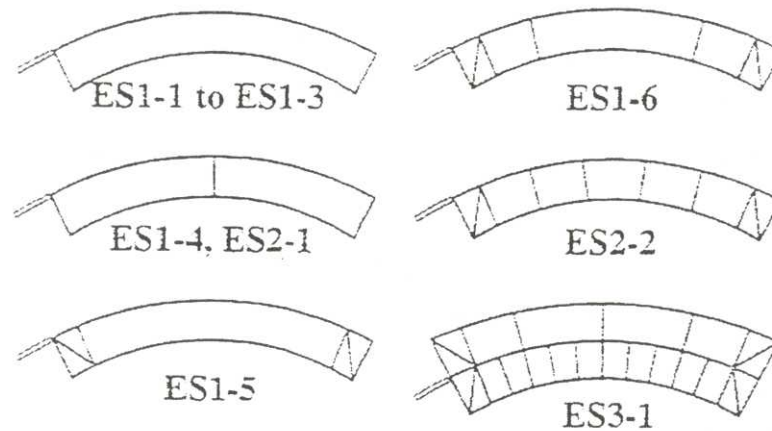


**Figure 4** Construction study framing plans (Linzell 2000)

In general, results from all of the construction study tests were consistent with engineering judgment. For the ES1-3 test, G2 was completely shored, as shoring beneath G1 at midspan was lowered incrementally, with all other G1 shoring removed once the “no-load” condition was reached. A G1 midspan vertical deflection of approximately 10 inches was achieved before the test was stopped, to ensure that the girder would return elastically back to its initial position. As shown in figure 4, the ES1-4 test was conducted with the cross-frame seven inserted at midspan. Again, G1 was lowered, as in the ES1-3 test, and a maximum G1 midspan vertical deflection of approximately 0.35 inch was obtained. It is obvious that the cross-frame at midspan played a significant role in controlling the deflection of G1 as shoring was removed. As the ES1-4 test progressed, the forces in cross-frame 7 continuously increased, with an internal maximum force of 8 kips reached in the diagonal members at the end of the test. In noting the final strains of the top and bottom flange at midspan of G1, it was shown that the top flange experienced compression on the outside (of curve) edge, and tension on the inside (of curve) edge;

while the bottom flange experienced tension on the outside edge, and compression on the inside edge. This result may be due to the presence of the cross-frame at midspan. While the observed stresses were significantly less than the yield stress, they did point to the type of girder behavior that occurred during the subject test.

A maximum G1 midspan vertical deflection of approximately 0.45 inch was obtained from the ES1-6 test, in which there was no center cross-frame, but cross-frames were in place near the ends, as shown in figure 4. The ES1-6 test followed the same shoring removal sequence as the ES1-3 and ES1-4 tests. In regard to the subject shoring removal sequence, the ES1-6 test again showed the importance of the midspan cross-frame as it related to the deflection of G1. Additionally, small values of strain were measured at G1 midspan, where the top flange experienced tension on the outside (of curve) edge, and compression on the inside (of curve) edge; while the bottom flange experienced compression on the outside edge, and tension on the inside edge. This is opposite to what occurred as a result of the ES1-4 test, which may be due to the fact that cross-frame seven was removed for the ES1-6 test.

The ES2 tests focused on the twin-girder system, in which shoring at midspan was lowered incrementally from beneath G1, and removed, then lowered from beneath G2, and removed. Upon full removal of shoring beneath G1 only, the G1 midspan vertical deflection was 0.4in. After G2 midspan shoring was completely removed, G1 midspan vertical deflection was approximately 0.7in, and G2 midspan vertical deflection was approximately 2.5in. Additionally, load redistribution occurred, in which the G2 girder abutments assumed most of the reaction in the structure's final state, as shown in Table 2.

**Table 2** ES2-1 reaction distribution (approximate values from graphs by Linzell)

<b>Girder Location</b>	<b>Re-action Force (kips)</b>		
	<b>Prior to any Shoring Removal</b>	<b>After G1 Midspan shoring removed</b>	<b>After G2 Midspan shoring removed</b>
G1 – Left Abutment	2.3	7.0	1.5
G1 – Right Abutment	3.0	8.0	2.0
G2 – Left Abutment	2.0	5.0	25.0
G2 – Right Abutment	3.7	6.0	22.0
G2 – Midspan	7.3	22.0	0.0

In comparison with the ES1-4 study, the internal forces in cross-frame seven increased significantly; to where most of the cross-frame members have a force of approximately 20 kips at the end of the test.

The ES2-2 test followed the same shoring removal sequence as the ES2-1 test, but with a different cross-frame configuration, as shown in figure 3. The final midspan vertical deflections were 0.4 inch and 1.4 inches, for G1 and G2, respectively. The inclusion of more cross-frames limited the overall deflection of the structure, in comparison with the ES2-1 study. Furthermore, a similar load redistribution occurred, as in the ES2-1 study, where the G2 girder abutments assumed most of the reaction after all shoring was removed. It was also shown in the ES3-1 study that as the shoring was removed, the load shifted to the exterior girder, G3.

In addition to presenting all the data for the experimental constructions studies, Linzell also developed detailed analytical models of the bridge systems using the finite

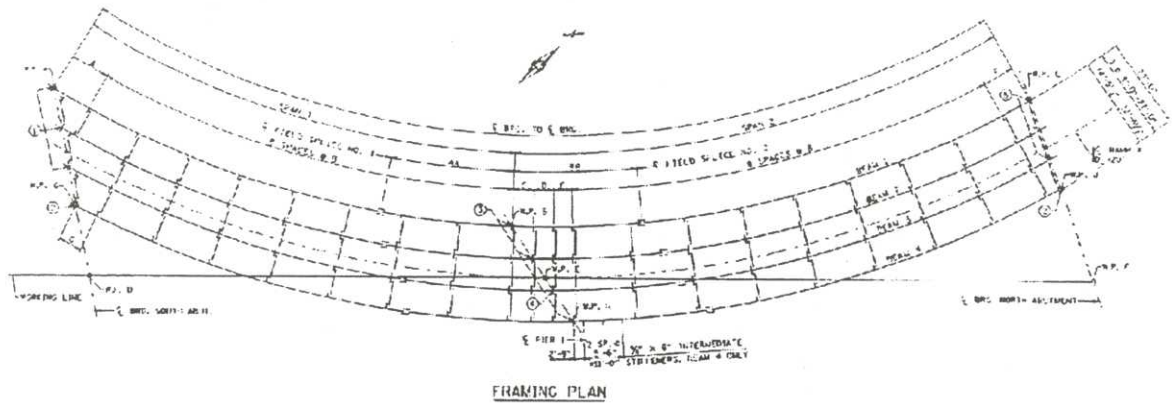
element program ABAQUS for comparison. The ABAQUS models were elastic, but did consider nonlinear geometry. The finite element analyses followed the same shoring removal and replacement sequences as were carried out experimentally. Self-weight was applied to all the girders, and additional point loads were used at cross-frame locations to account for the dead load of cross-frame connection plates and such, which were not explicitly modeled. Analytical and experimental results for support reactions, vertical displacements, girder strains, and cross-frame internal forces were compared and shown to have very good agreement. However, there were some differences in the comparisons, which was a direct result of discrepancies that occurred during the experimental testing. One of these discrepancies was that G2 was incorrectly cambered, and was heated and forced back to its intended camber, therefore causing locked-in stresses that were unaccounted for in the analytical models. Also, forces induced when fitting the cross-frames in between the girders were not measured, and could not be duplicated in the analytical models.

Linzell's work showed that finite element models, using a program such as ABAQUS, could predict the experimental behavior that occurred throughout the construction studies, with very limited error. The construction studies also provided insight related to the load redistribution that occurs during curved I-girder bridge construction, and subsequent deformations. Additional elastic analyses carried out as part of the CSBRP project indicated that for the completed structure, the final deflected shape and load distribution would be different if a different erection sequence was followed (Duwadi et al. 2000).

### **2.2.2 Minnesota DOT Project (Galambos et al. 1996, 2000; Pulver 1996; Huang 1996)**

Researchers at the University of Minnesota, in conjunction with the Minnesota Department of Transportation, performed significant research related to horizontally curved I-girder bridge construction. A field investigation was carried out on a two span continuous horizontally curved I-girder bridge as it was being erected, near Minneapolis. The objective of the MNDOT project was to study the behavior of the steel superstructure during all phases of construction via strain measurements, and determine whether actual stresses were well represented by linear elastic software typically used (Galambos et al. 2000). Field measurements were compared with results obtained from a linear elastic analysis program developed specifically for the MNDOT research (Huang 1996).

As shown in figure 5, the MNDOT Bridge (Bridge No. 27998) had four continuous concentric I-girders spaced at approximately 9ft, in which each girder was actually three sections field-spliced together at points along the longitudinal axis. The girder depths ranged from 50in for the inside girder, to 72in for the outside girder, and all girder steel had a yield stress of 50 ksi. The length of the spans ranged from 130-155ft, and the radius of curvature ranged from 270-300ft. Cross-frames, fabricated from a tee section (bottom chord), and double angles (top chord and “X” brace), were used to connect the girders. At the abutments, instead of cross-frames, stiff I-shaped diaphragms were used.



DIAPHRAGM SPACING							
	A	B	C	D	E	F	G
BEAM 1	21'-0"	16'-0"	6'-5 1/2"	5'-11 1/2"	5'-6 1/2"	3'-5 1/2"	---
BEAM 2	---	15'-6 3/4"	6'-8 3/4"	6'-2"	5'-8 3/4"	8'-0"	---
BEAM 3	---	17'-0 1/2"	6'-10 1/2"	6'-4 1/2"	5'-10 1/2"	6'-6 1/2"	13'-7 1/2"
BEAM 4	---	17'-0"	7'-5 1/2"	6'-6 1/2"	5'-0 1/2"	5'-4 1/2"	6'-8 1/2"

FIELD SPLICE LOCATIONS		
	AA	BB
BEAM 1	21'-0"	30'-0"
BEAM 2	43'-0"	34'-0"
BEAM 3	42'-0"	37'-0"
BEAM 4	47'-0"	39'-0"

SPAN LENGTHS			
	RADIUS	SPAN 1	SPAN 2
BEAM 1	272'-0 1/2"	139'-10 1/2"	155'-4 1/2"
BEAM 2	261'-0 1/2"	143'-0 1/2"	152'-3 1/2"
BEAM 3	290'-0 1/2"	146'-3 1/2"	148'-3 1/2"
BEAM 4	275'-0 1/2"	149'-6 1/2"	152'-10 1/2"

- ① MILLERIZED EXPANSION CURVED PLATE BEARING ASSEMBLY, TYPE 1
- ② MILLERIZED EXPANSION CURVED PLATE BEARING ASSEMBLY, TYPE 2
- ③ FIXED CURVED PLATE BEARING ASSEMBLY, TYPE 1
- ④ FIXED CURVED PLATE BEARING ASSEMBLY, TYPE 2
- ⑤ MILLERIZED EXPANSION CURVED PLATE BEARING ASSEMBLY, TYPE 1

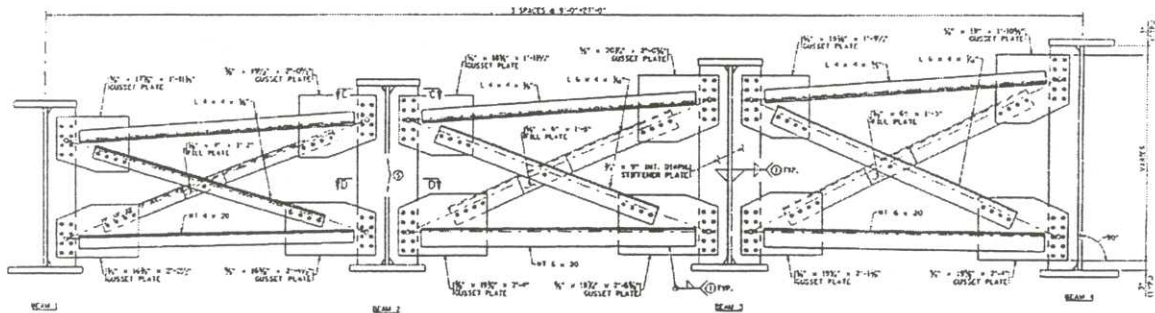
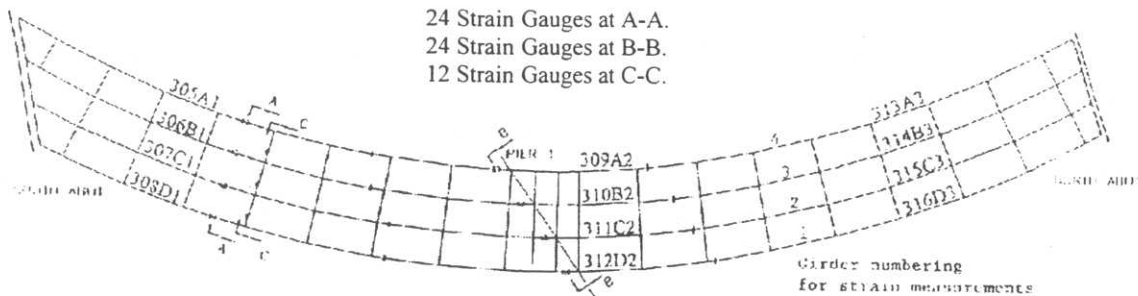
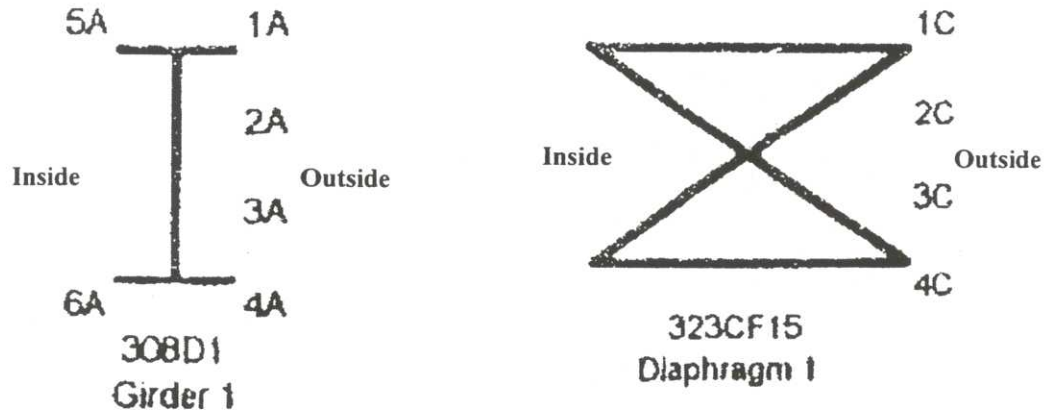


Figure 5 MNDOT Bridge framing plan and typical cross-frame elevation view (Galambos et al.1996)

In order to determine the stresses resulting from the erection of the bridge girders, 60 vibrating wire strain gauges were installed on the bridge in the fabrication shop and in the field. Twenty-four gauges were placed on the girders near the midspan of section 1, and twenty-four additional gauges were placed on the girders over the pier, as shown in figure 6. In each case, six strain gauges were used on each girder so as to measure the flange and web strains. Twelve strain gauges, were placed on the diagonal members of the cross-frames located near the midspan of section 1, with 4 gauges used per a cross-frame.



Strain Gauge Layout



Typical Girder - Section A-A or B-B

Most Outside Cross-Frame - Section C-C

**Figure 6** MNDOT vibrating wire strain gauge placement (Galambos et al. 1996)

Field measurements were taken for different critical loading stages during the construction sequence. Strains were measured for stages during the erection of the steel superstructure, during the placement of the concrete deck, and during the application of truck live loading. Only the strains measured during the erection of the steel superstructure are relevant to the current research, and will be further discussed. Field measurements were taken for four different stages during the erection of the steel superstructure (Galambos et al. 1996):

1. After Span 1 was erected including the section over the pier; with cross-frame bolts in place but loose; with shoring towers in place under all Span 1 girders.
2. After the outside (of curve) half of Span 2 was erected; with cross-frame bolts loose; with shoring towers in place under all Span 1 girders.
3. After all girders and cross-frames were erected; with cross-frame bolts loose.
4. After all girders and cross-frames were erected; with the structure “rattled up,” all bolts were tightened.

The analytical study of the curved I-girder system steel superstructure employed the grillage method. The horizontally curved I-girders were modeled by a three-dimensional, two node beam element having 5 degrees of freedom (DOF) at each node. The five DOF included two translational components (one vertical and one axial to account for the thermal expansion that could occur), two rotational components, and a component to account for the warping effect (Huang 1996). The cross-frames were modeled as individual trusses, comprised of 4 pinned-ends, and only axial force was assumed. The boundary conditions consisted of pins at the center support, rollers at the abutments, and twist was restrained at the abutments and the center pier (Galambos et al. 2000). Residual stresses and stresses due to fit-up were not modeled.

In general, the construction of the steel superstructure proceeded smoothly. Steel erection took place toward the end of July, and was completed during the early morning hours. Two 100-ton cranes, and one 50-ton crane were utilized during the steel erection. Girders were assembled one at a time, not in pairs, as one of the cranes was utilized to stabilize one girder while cross-frames or a second girder was placed.

Field measurements obtained for erection stages 1 and 2 provided for little direct correlation with the given erection stage. However, the outside girder (Girder 312D32) over the pier did show a somewhat significant increase in flange stress after the completion of erection stage 2. An increase of approximately 6 ksi, in tension, occurred in the outside of the top flange. Otherwise, all other girder stresses remained less than 3 ksi, as well as the cross-frames except for the most outside cross-frame, in which a stress of 5.9 ksi was obtained. This cross-frame stress may have been due to a fit-up constraint that occurred during the construction.

A better correlation of the measured data with appropriate erection stage was found for stages 3 and 4. Again, measured stresses were relatively small however, stresses in the top flanges indicated that warping had occurred in girders 1, 2 and 3 due to the curvature of the girders. The “rattling-up” of the structure between stages 3 and 4, did not result in a significant change in stress in any of the girders or cross-frames. The change in stress from before and after all bolts were tightened, ranged from  $-0.87$  ksi to 1.15 ksi.

The range of stresses in the completed steel superstructure, as well as throughout the erection process, remained well below the yield stress of the steel. The final range of stress after all steel was erected and tightened was as follows; at midspan of Span 1, the stress ranged from  $-3.78$  ksi to 2.87 ksi; at the pier, the stress ranged from  $-4.75$  ksi to 6.74 ksi; at the cross-frames, the stress ranged from  $-3.04$  ksi to 4.41 ksi. The largest girder stress occurred over the pier, in the outside top flange of the most outside girder and was 6.74 ksi. The largest cross-frame stress occurred in the most outside cross-

frame, and was 4.41 ksi. Moderate load redistribution to the outside girders was observed, as the erection of the steel superstructure progressed.

Computational results were compared with the obtained field measurements, and showed better correlation as erection of the steel superstructure proceeded. For the first two erection stages, little correlation was achieved, which could have been the result of two discrepancies (Huang 1996). The shoring towers were modeled as rigid supports in the analytical study, which did not simulate the actual elastic supports. Differences may also have resulted from the fact that the connection bolts between the cross-frames and the girders were not fully tightened, and the minor fit-up stresses dominated the results.

The research completed as part of the MNDOT/University of Minnesota project showed that the structure was controlled by stiffness, not strength, while it was temporarily shored during the steel erection. Stresses during construction remained well below yield stress for all steel superstructure erection stages. Stresses due to fit-up constraints were evident from the field measurements, especially in the cross-frames. Generally, computational results matched well with the recorded field measurements. Minor differences developed due to the modeling of the temporary supports, the erratic effects of warping restraint and minor axis bending on the field measurements, and the unpredictability associated with loose girder-to-cross-frame connections.

## **2.3 Horizontally Curved I-Girder Bridge Construction Concerns**

### **2.3.1 Construction Issues (Grubb, Yadlosky, and Duwadi 1996)**

Grubb et al. (1996) detailed important construction issues that pertained to the fabrication and erection of horizontally curved I-girder bridges. In the paper, Grubb et al. pointed out that most problems during construction have been related to unanticipated and unaccounted for deformations that occurred. Issues regarding camber, lifting of girders, erection sequencing, cross-frame installation, and temporary shoring were discussed as well as how, if it at all, they were related to current guidelines.

Horizontally curved I-girders are cambered to offset vertical displacement due to self-weight, just as in straight girder bridges. Even though curved I-girders twist and rotate immediately upon receiving load, including self-weight, they usually are not cambered to offset this rotation. If the structure is not shored and/or braced properly, unanticipated deflection and twist can occur which can lead to abnormalities in the geometric profile. Limits on lateral rotation or girder plumbness are not currently specified in construction practice, and cambers to offset the twist are generally not specified (Grubb et al. 1996). Furthermore, in general, cambering does not reflect the deflections that will occur as part of the erection sequence used to construct the given bridge.

Lifting of a single horizontally curved I-girder during construction has also been an area of concern, since lifting points must be chosen so that the girder remains stable.

The center of gravity of a curved girder in plan view, does not coincide with the cross sectional centroid, and therefore if the girder is not lifted in the proper location, it will rotate immediately due to self-weight. As an alternative, if possible, pairs of girders previously connected by cross-frames could be erected as a unit to provide additional torsional stiffness.

Guidelines for determining the need for temporary shoring of horizontally curved I-girders during the erection sequence are currently lacking in practice (Grubb et al. 1996). Providing for stability during erection, and limiting excess deflections and rotations of curved I-girders, are issues of primary concern during the erection sequence. As erection of a horizontally curved I-girder bridge proceeds, load paths and associated deflections and rotations change based on the erection sequence.

Girder fit-up is usually accomplished at the fabrication shop with each girder in the “no-load” state, meaning that each girder is sufficiently supported so there is “zero” stress in the girder. If curved I-girders are not fully shored during erection to match the conditions used in the fabrication shop to verify fit-up, girders will begin to deflect and rotate immediately upon erection due to their self-weight unless they are restrained by cross-frames attached to adjacent girders or shoring (Grubb et al. 1996). Unpredicted deflections and rotations result in cross-frame connection and field splice connection difficulties. Slopes and elevations at field splices may vary significantly from what was expected, and incorrect final steel elevations may be produced. Two cranes are often used to prevent unwanted deflections and rotations. Within such a scenario, one crane erects the girder, while another crane stabilizes the girder as cross-frames are attached.

Horizontally curved I-girders depend on their connections to adjacent girders, via cross-frames, for stability. Based on this fact, Grubb et al. recommended, that cross-frame connections not be left loose and instead be firmly tightened. Loosely connected cross-frames and oversized or slotted holes should not be specified in horizontally curved I-girder bridges, as they would compromise the girder alignment and plumbness, and make cross-frame fit-up difficult (Grubb et al. 1996).

The use of temporary shoring can provide additional aid in controlling instability that can occur during erection of horizontally curved I-girder bridges. The use of temporary shoring has been shown to improve girder fit-up because the condition simulates the “no-load” condition assumed when connections were detailed. There are currently no guidelines upon which to base rational decisions as to whether temporary shoring should be provided during construction (Grubb et al. 1996).

### **2.3.2 NCHRP Report 424 (Hall et al. 1999)**

The National Cooperative Highway Research Program (NCHRP) produced a revised guide specification for horizontally curved I-girder bridges based on practice and technology that was available. Significant deficiencies in the AASHTO Guidelines (1993) led to the pursuit of this revision. Part of the NCHRP research problem statement dictated that, “other critical deficiencies include lack of fabrication and erection procedures, insufficient guidance on analytical procedures for both preliminary and final design” (Hall et al. 1999). Various designers, builders, and owners have pointed out that the AASHTO Guidelines (1993) lack provisions directly related to construction and erection issues. The NCHRP Report 424 has provided some guidance with regard to some of the construction issues at the heart of many curved I-girder bridge erection problems.

The majority of problems in curved I-girder bridges have typically occurred during construction of the bridge, and are related to unaccounted for deflections and rotations. Hall et al. have pointed out that in the case of cantilever construction of horizontally curved I-girder bridges, insertion of a suspended span becomes problematic because the vertical camber and rotation are always coupled. Additionally, as erection proceeds, an interior girder may actually become an exterior girder at some point during construction, which could result in a larger moment or load in the girder than what was expected in the final structure. Also, when a girder is only partially braced, it may rotate enough to make it very difficult to attach cross-frames. Another problem encountered by

erectors is related to the use of oversized bolt holes. Oversized bolt holes have been shown to permit unpredictable deflections and associated stresses that are different from those determined by analyses. Problems are very difficult to rectify in the field, because curved girders interact through the cross-frames as a complete system, and therefore it is difficult to adjust one girder to obtain the needed elevations.

The NCHRP report also provided direction that future research might follow (Hall et al. 1999):

- There is a need for better fundamental understanding of the structural behavior of curved I-girders during construction. A greater confidence in girder behavior during construction should lead to bolder designs.
- Research is required to determine when lateral deflection and twist limitations are needed in curved I-girder bridge construction to ensure that stresses and deflections do not exceed reasonable limits.
- The validity of small deflection theory when analyzing curved I-girders needs to be investigated, since curved I-girders deflect a great deal laterally at times during construction and lifting when unbraced lengths are very large.
- Unsymmetrical curved I-girder sections need to be studied since they are most commonly used in practice.

## **2.4 Horizontally Curved I-Girder Bridge Construction Related Research**

### **2.4.1 Lifting of Horizontally Curved I-Girders During Construction (Davidson 1996)**

Davidson (1996) analytically investigated the behavior of a single horizontally curved I-girder subjected to various lifting schemes. Three different lifting schemes were analyzed using finite element models, as shown in figure 7. Lifting scheme 1 was used to model a girder being lifted at the center of the span only. Lifting scheme 2 simulated the condition where a girder has been lifted vertically by cables at two locations separated by a spreader beam. The two locations are at the intersection of a line through the center of gravity of the curved I-girder. Lifting scheme 3 replicated the condition where a girder would be lifted at two locations, but only by cables attached to a single lifting point above the center of gravity of the curved I-girder. Three different size cross sections were used, where sections 2 and 3 only differed in bottom flange size. The section 3 bottom flange was 2 inches wider, and a  $\frac{1}{2}$  inch thicker. Section 1 had a depth of 60in while sections 2 and 3 had a depth of 84in. Lengths of the girders were chosen in order to have consistent L/d for each lifting scheme test; L/d of 20 for lifting scheme 1, and L/d of 30 for lifting scheme 2 and 3. Loading of the girder was due to self-weight only, and for nonlinear geometric analyses, the load was incrementally applied up to 3 times the self-weight to compensate for inertial effects.

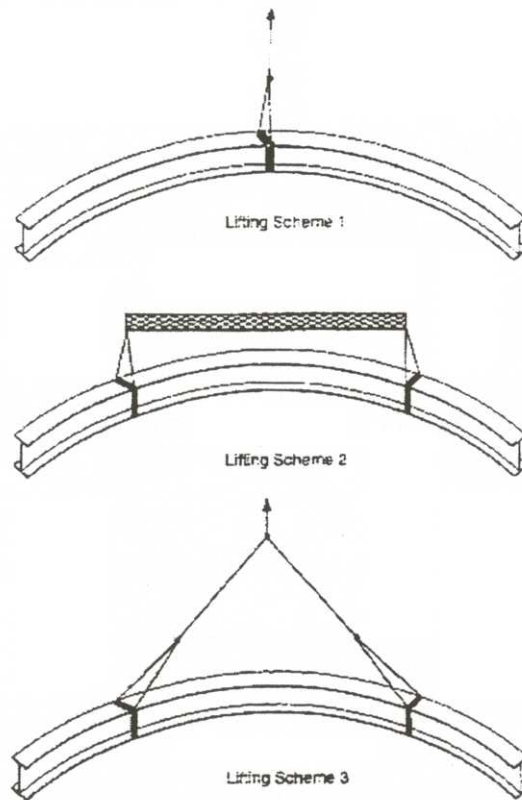


**Figure 7** Lifting schemes (Davidson 1996)

The results showed that lifting scheme 1 and lifting scheme 3 should not be used in practice. Lifting scheme 1 allowed the girder to “roll” an extreme amount. Lifting scheme 3 showed that forces due to the inclined cables caused significant minor-axis bending at the center of the span. Also, when cables are attached to the top flange only, the top flange could experience much more internal force and moment than the bottom flange. Lifting scheme 2 was shown to be the better lifting scheme analyzed. As additional load was applied, beyond self-weight, the deflections at the center of the span and at the ends remained far less than those for the other lifting schemes. Also, in comparing the symmetrical and unsymmetrical cross sections, sections 2 and 3

respectively, for lifting scheme 2; section 3 had a greater transverse displacement at the end and center of the span, approximately 1 inch; section 2 had a greater vertical deflection at the end and center of the span, approximately 1 inch; and section 2 had a greater rotation at the end and center of the span.

#### **2.4.2 Lateral Bracing and Construction Effects (Schelling et al. 1989)**

Schelling et al. (1989) proposed guidelines via a parametric study that quantified the effect that top and bottom lateral bracing had upon the stress levels within the main curved I-girder elements of a curved I-girder bridge. These guidelines were intended to prevent overstress during construction. The study examined the response of a curved single span, two-girder system due to self-weight. The researchers developed equations that defined the dead load distribution throughout the superstructure system.

A 3-dimensional space frame was used to model the curved I-girders, cross-frames, and lateral bracing system. This model permitted the consideration of three moments and three normal forces at the end of each member, thus allowing bending about two major axes, torsion, and the influence of warping to be incorporated into the analysis. The model properties were determined by comparing the model results to girder stresses and deformations based on statics, and adjusted until agreement between statics and the space frame model was achieved.

It was shown that the top and bottom lateral bracing act together in the construction stage to effectively reduce the dead load stresses by creating a pseudobox

girder with a higher torsional rigidity. Distribution factors based on diaphragm spacing, girder spacing, span length, and radius were developed. The concept of distribution factors requires a relation between the response of the forces in a system to those forces developed in a single isolated girder subjected to a set of wheel loads (or in the present case, self-weight), i.e.:

D.F. = (Curved System Function) / (Curved Single Girder Function) (AASHTO 1993).

Distribution Factor equations were developed for the following relationships:

- Curved to straight girder response with cross-frames and without lateral bracing.
- Curved to straight girder response with cross-frames and with full lateral bracing.
- Braced to un-braced curved girder response.
- Bracing stress – related lateral bracing stress to cross-frame stress.

#### **2.4.3 Field Measurements of Camber Loss and Temperature Effects (Hilton 1984)**

Hilton (1984) addressed the issue of additional camber that had to be provided for in steel I-girders that were heat curved. Field measurements were obtained from a horizontally curved I-girder bridge, which consisted of four girders spaced at 10ft – 8in, with a 140ft span, and a radius of curvature that varied from 802.5ft to 834.51ft. Hilton showed that the camber loss from construction loads was approximately  $\frac{1}{4}$  of that predicted from the AASHTO equation, and that the average camber loss for the completed in-service structure was approximately 13% of the AASHTO value. Therefore the subject AASHTO equation was modified to its present form.

The results that Hilton provided in regard to temperature effects during the construction of the subject bridge are related to the current research. Hilton showed that considerable deflections occurred due to thermal effects. Thermocouples were placed on the top and bottom flanges at midspan and the one-fourth point of the girders. Measurements were taken before the deck was in place, but with the framework for the deck in place, therefore allowing a portion of the girders to be shielded from direct sunlight. As a result of this configuration, top flanges were exposed to direct solar radiation, where as the lower portion was exposed to only the ambient air temperature. The subject bridge was orientated in a north to south direction, thus, in the morning the sunlight was directly on the eastern girder, and in the afternoon the sunlight was directly on the western girder. The bridge was located in Virginia, and readings were taken on a typical sunny day in August, with the initial reading at 7:30 AM.

It was found that there was a net thermal differential between the upper and lower flanges that resulted in an internal moment over the cross section, which in turn caused the girder to deflect upward an amount related to the solar radiation intensity, time of day, and so on. At 3:00 PM a maximum differential of 36-degrees between the top and bottom flange was noted, where the top flange was warmer. At 3:00 PM, the vertical deflections were maximum, and the defection at midspan was found to be 1.25 inches upward from the 7:25 AM “zero” reading. This indicates that if steel erection was to be accomplished (installation of cross-frames for instance), members could fit-up extremely tightly, inducing further unaccounted for stresses. It should be noted that all girders

deflected vertically 1.25 in, due to the rigid I-shaped diaphragm connections, and one would expect the thermal response of an individual curved element to be more severe.

Hilton pointed out that the thermal effects on girder deflection must be taken into account if deflections due to self-weight are measured. Calculations to determine thermal deflections must consider the upper portion of the web above the neutral axis, since that portion participates in the development of forces and moments due to the internal temperature gradient from the top to the bottom of the web. Hilton provided a simple equation to determine the deflection ( $\Delta$ ) at a given location based on  $F=A E \alpha \Delta T$ :

$$\Delta = \alpha A \Delta T d L^2 / 8I \quad (2-1)$$

This equation was shown to be within 1% of the vertical deflection measured at 3:00 PM.

## **2.5 Single Curved I-Girder and I-Girder Bridge Behavior**

### **2.5.1 FHWA Horizontally Curved Steel Bridge Research Project (CSBRP)**

The CSBRP studied the behavior of horizontally curved girders through theoretical, analytical, and experimental research. As stated previously, most of the research accomplished as part of the CSBRP is not directly related to the current research that is focusing on curved I-girder bridge construction. However, due to the importance of the research conducted by the CSBRP, it is presented as part of this literature review.

Duwadi et al. (2000) provided a summary of the investigation conducted as part of the CSBRP in regard to the development and refinement of predictor equations and the

testing of full-scale bending and shear curved I-girder components. Davidson, Ballance and Yoo have conducted a large amount of analytical research leading to the development of equations for nominal bending and shear strength of curved I-sections. Davidson et al. have published papers which:

- i. Presented an analytical model that was used to predict the transverse displacement and induced plate bending stress of curved I-shaped girder webs subjected to bending. Presented the effects of curvature on elastic buckling behavior of curved web panels. Also, provided a “lateral pressure” analogy that could be conservatively applied to approximate the “bulging” transverse displacement of the web (1999a).
- ii. Developed equations that represent the reduction in nominal strength of curved webs due to the effects of curvature based on results from geometric nonlinear finite element analyses. Provided formulations for the reduction in allowable web slenderness ( $D/t_w$ ) due to curvature, based on a limit of allowable “bulging” transverse displacement and maximum allowable stress (1999b).
- iii. Analytically investigated the buckling and finite-displacement behavior of curved web panels under combined bending and shear. Also, showed that predictor equations previously published by the writers derived for pure bending were somewhat conservative (2000a).
- iv. Examined the optimum location and strength effects of one and two longitudinal stiffeners attached to curved I-shaped plate girders (2000b).
- v. Employed the use of detailed finite element models, representing the CSBRP three girder test frame, which was the same structure studied by Linzell (1999), and

evaluated the effects of curvature on the bending strength of curved I-girders. Previously developed predictor equations by the writers were shown to have good correlations that would be conservative for design use (2000c).

Duwadi et al. (2000) summarized much of the research accomplished by Davidson, Ballance, and Yoo, as well as other relevant references. In addition to the discussion provided, concerning the bending and shear component tests, a brief summary of the erection study and the girder displacements for various configurations were presented. The same results are part of Linzell's (1999) study.

Simpson (2000) also performed analytical studies that employed ANSYS finite element models, in order to study the FHWA-CSBRP bridge behavior. These studies were conducted as "predictive" studies since they were accomplished prior to the experimental studies. Simpson analytically examined the erection sequence of the test frame and the inserted bending components. It was found that the erection sequence of the test frame significantly affected the dead load distribution of reactions and internal girder moments.

## **2.6 Other Significant References Relevant to the Current Research**

Davidson et al. (1996) investigated the effects of a number of parameters on the behavior of a curved I-girder system. ABAQUS was used to investigate a three girder system, where shell elements were used for the web, and beam elements for the flanges. The model was assumed to remain linear elastic, and deformations were assumed to

remain within the limits of small deflection theory. The researchers determined that the dead-load condition, where the uncured concrete deck was applied to the non-composite bridge model, resulted in the greatest curvature effects on the warping stresses with respect to the vertical bending stresses. It was concluded that parameters such as the span length, radius of curvature, flange width, and cross-frame spacing had the greatest effect on the warping-to-bending stress ratio.

Brennan et al. (1970) utilized a methodology that was developed previously by Brennan et al., in which a bridge structure was scaled down using similitude relations, and developed a small-scale experimental model of Ramp CBW over Huyck Stream of the Mall Arterial Highway, Interstate Route 540, in Albany, New York. The small-scale structure was used to evaluate a three-dimensional analytical model program developed at Syracuse University. Comparisons between experimental and analytical bending moment results showed good agreement. Brennan and Mandel (1979) expanded the previous research and performed experimental tests on a variety of small-scale structural configurations, with and without a concrete deck. As before, comparisons between experimental and analytical bending moments showed good agreement however, the analytical results significantly underestimated the vertical deflections of the bridge. The analytical models used chords instead of curves to analyze the girders, therefore neglecting the torsional moments induced by a curved beam. The torsional moments in a horizontally curved member cause additional vertical deflection. The three-dimensional analytical models were changed and curved members added, and agreement was achieved in predicting the vertical deflections and bending moments.

Mozer and Culver (1970) and Mozer et al. (1971 and 1973) produced a series of three reports that summarized their efforts to investigate the experimental behavior of curved I-girders. The experimental structures were not full-scale tests, but nonetheless, provided valuable data. The first set of experimental tests (Mozer and Culver 1970) evaluated local flange buckling behavior of a single curved I-girders, and provided preliminary investigation of curved web panel shear behavior and post buckling strength. The second report (Mozer et al. 1971) summarized the investigation of flexural failure, shear failure, and combined flexural and shear failure of a singly curved I-girder. In this study, the researchers found that full depth transverse stiffeners seemed to assist in preventing cross section deformation, but the effect on ultimate strength was minimal. In the final set of experimental investigations (Mozer et al. 1973) eight static tests were conducted on a small-scale simple span, two girder curved bridge without a concrete deck. The I-girders were connected by end diaphragms and intermediate cross-frames. Some of the tests were carried out with and without certain cross-frames in place, in order to study the response of the steel structure for different framing configurations. Mozer et al. concluded that cross-frames play a major role in curved I-girder bridge behavior; particularly when the structure acts as an open grid system, which is the case during construction when there is no concrete deck in place. A drastic loss of torsional rigidity occurred in one of the tests, in which the diagonals from two sets of installed cross-frames were removed.

Zureick and Naqib (1999) presented a detailed report that provides highlights of analytical research conducted on horizontally curved I-girder bridges; both approximate

and refined methods are discussed. Approximate methods were considered to require minimal modeling effort and can be used as preliminary calculations: such methods include the plane-grid, space-frame, and V-load methods. Refined methods were considered to be more elaborate and computationally intensive and should be used for a detailed analysis: such methods include the finite element method, the finite-strip method, the finite-difference method, and the slope deflection method. Zureick and Naqib presented summaries of work conducted by other researchers using the finite element method for curved I-girder bridges.

### **3.0 DESCRIPTION OF THE FORD CITY BRIDGE**

#### **3.1 Introduction**

The Ford City Bridge is a three span continuous steel I-girder bridge with 98m (322ft) end spans and a 127m (417ft) center span. The bridge consists of 44 individual girder sections, spaced at 4.1m (13.5ft) on center, aligned in four girder lines. The deck of the bridge has a width of 14.7m (48.2ft) and is comprised of two vehicular lanes and a pedestrian walkway.

The northern most span of the Ford City Bridge consists of a horizontally curved span, approximately 89m (292ft) in length. The curved section has a mean radius of 155.9m (511ft), and ends just short of the northern most pier by 8.7m (28.8ft). Figures 8 and 9 show plan views of the Ford City Bridge. Figure 10 shows the naming convention for the cross-frames and girders to be used throughout the remainder of this research.

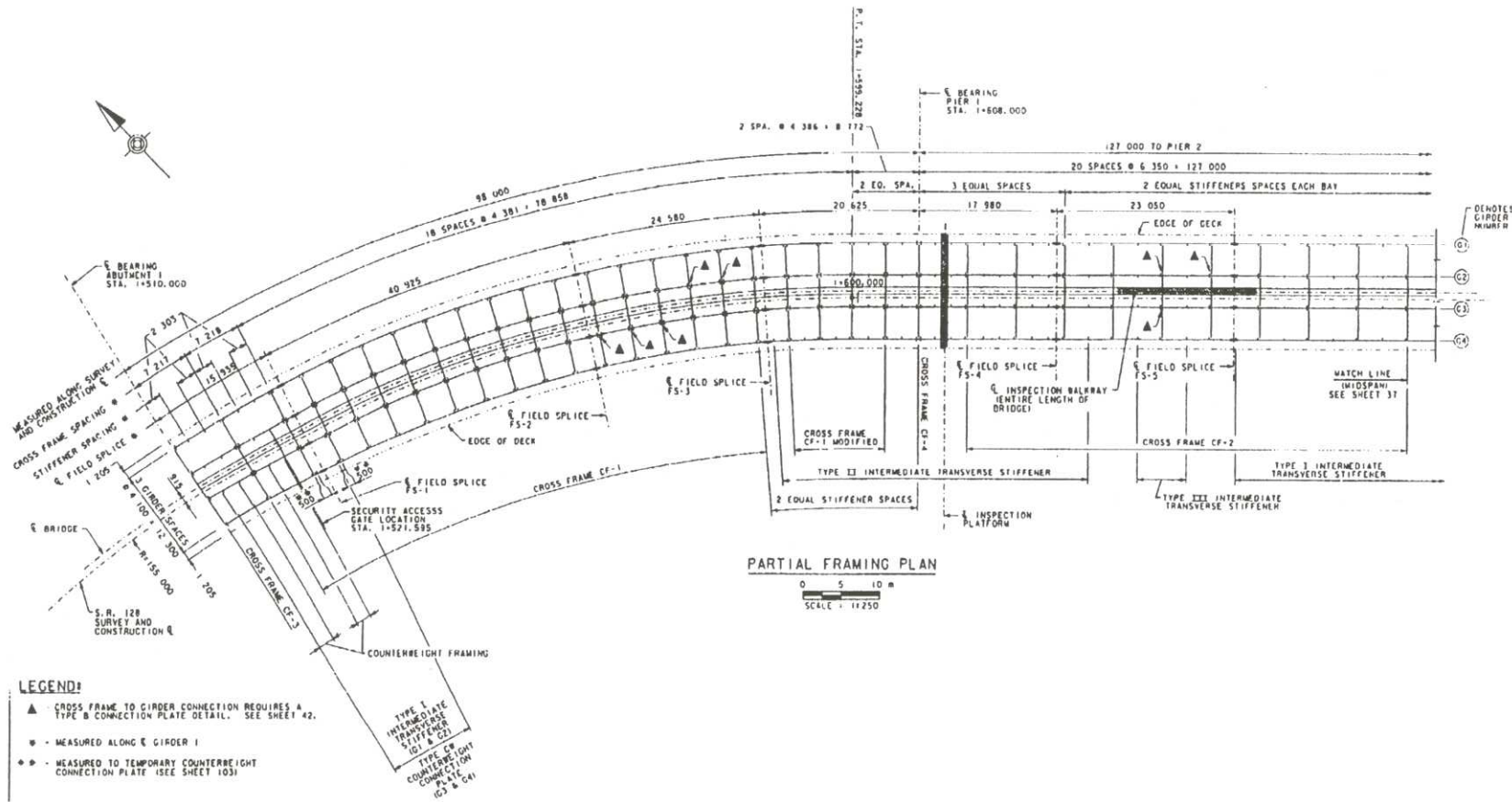


Figure 8 Plan view of Ford City Bridge (Sheet 1) (PENNDOT1998)

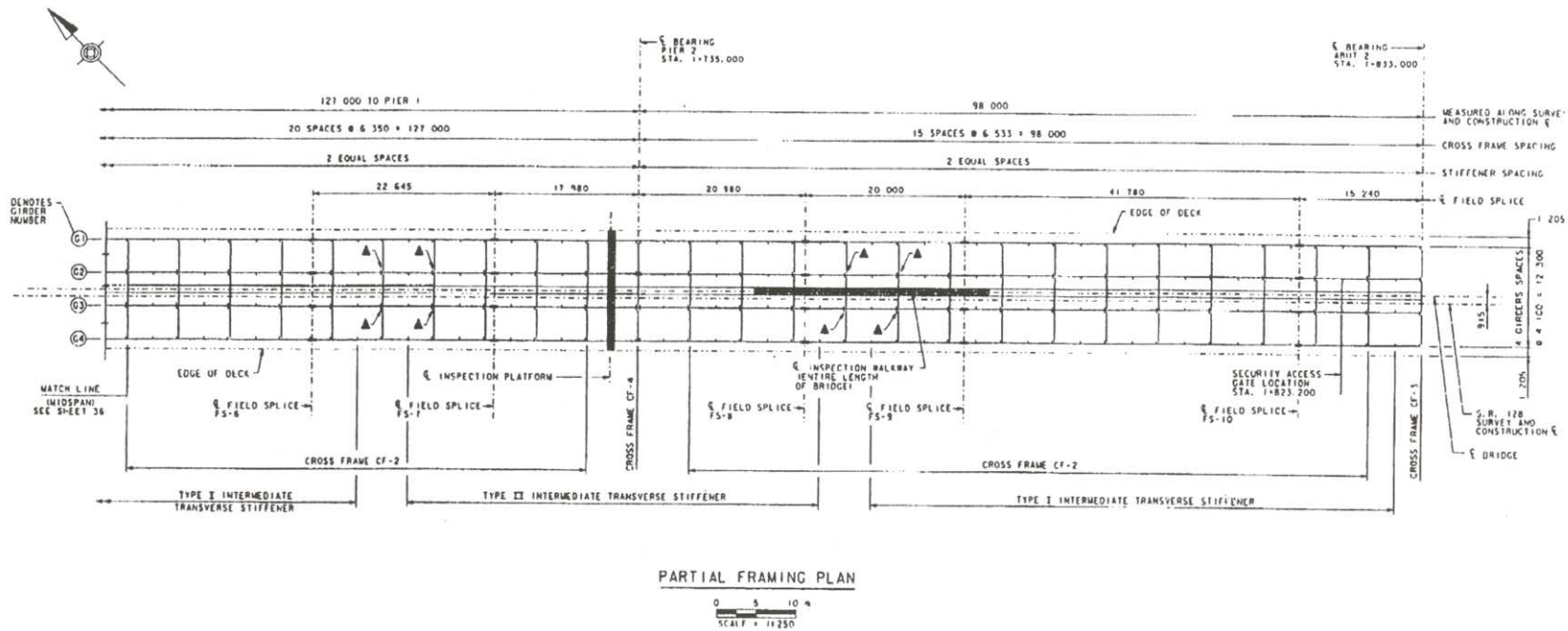
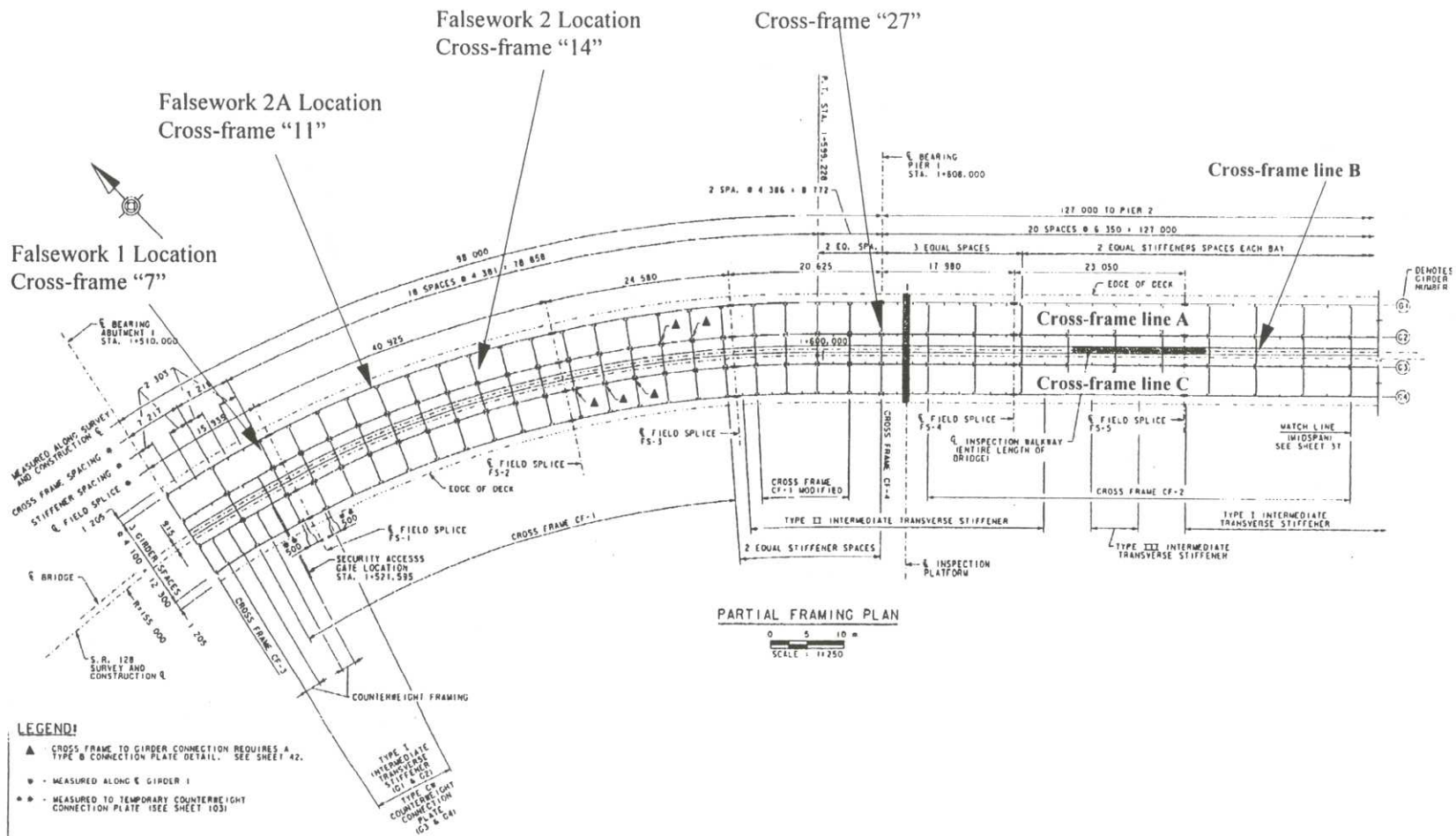
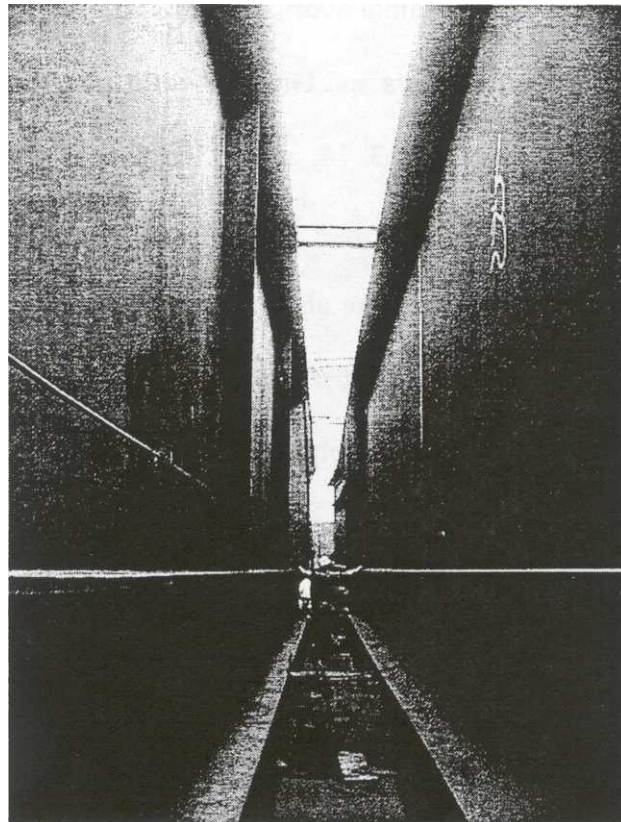


Figure 9 Plan view of Ford City Bridge (Sheet 2) (PENNDOT1998)



### 3.2 I-Girder Details

In general, the geometric properties of each individual girder section vary, especially in the curved span. In many cases, flange thickness and widths differ from one section to another, and unsymmetrical cross-sections are often used; however the web height remains a constant 4.275m (14ft) throughout the structure. Figure 11 depicts the enormous size of the girders used in the Ford City Bridge. Table 3 summarizes the geometric data of the curved span.



**Figure 11** Comparison view depicting girder size

**Table 3** Ford City Bridge girder geometric data

<b>Girder</b>	<b>Radius m (ft)</b>	<b>Curved Length m (ft)</b>
G1	162.1 (531.7)	93.3 (306.1)
G2	158.0 (518.3)	90.9 (298.3)
G3	153.9 (504.8)	88.6 (290.6)
G4	149.8 (491.4)	86.2 (282.9)

Also, the bridge is a longitudinal hybrid structure that employs HPS70W steel at negative moment regions over the piers and Grade 50 weathering steel throughout the remainder of the structure. Figures 12, 13, 14, and 15 illustrate elevation views of girders G1, G2, G3, and G4 respectively.

Longitudinal stiffeners are also used throughout the bridge girders, as shown on the elevation view figures. Cross-frame connection plates are full-depth transverse stiffeners, in most cases these are placed on both sides of the web connection (i.e. side by side, at a given cross-frame connection) at each cross-frame location. Additional full-depth transverse stiffeners are used in the section 1 girders of the bridge, and larger bearing stiffeners are utilized at the abutments and piers.

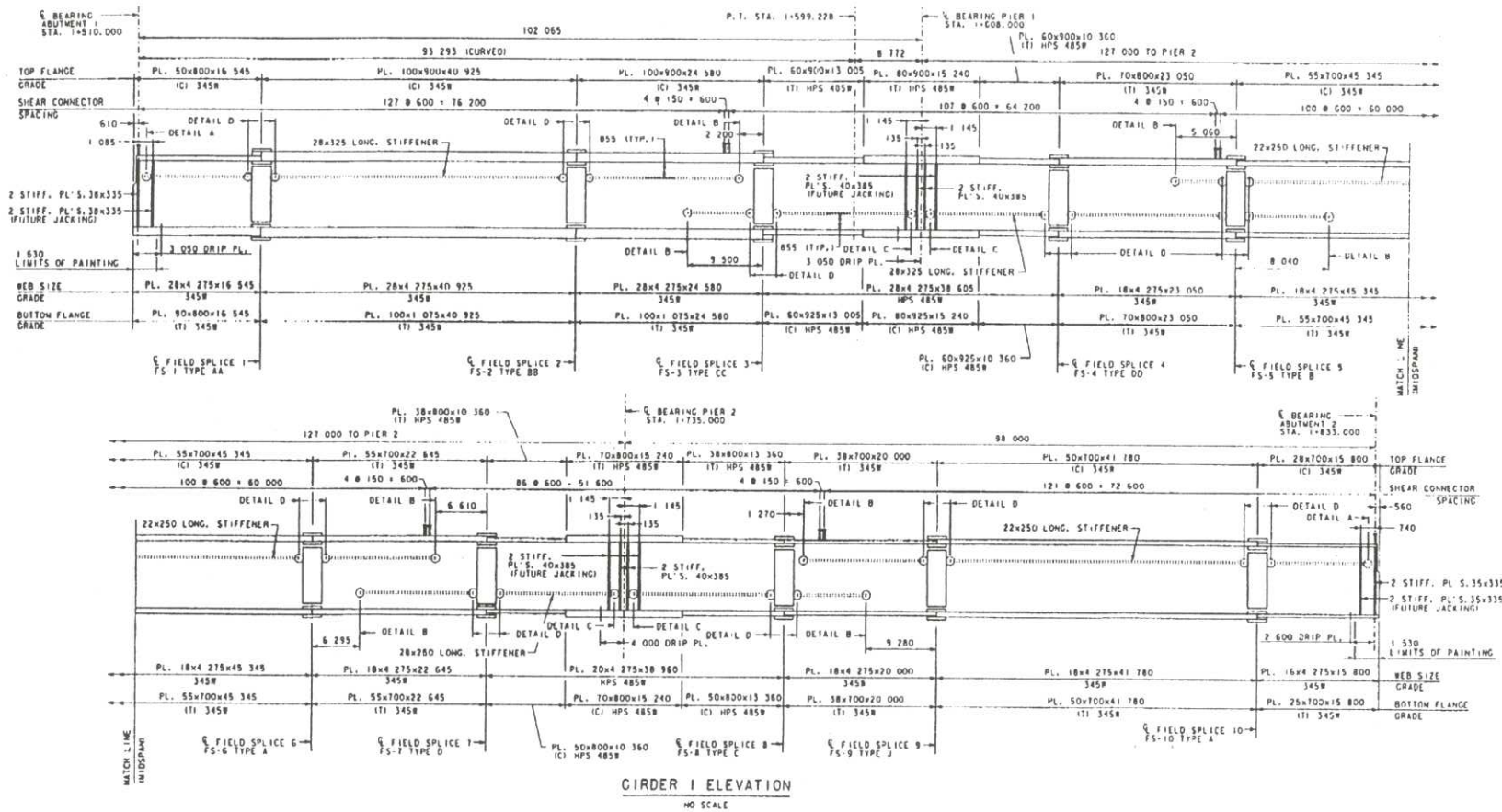


Figure 12 Elevation view of girder G1 (PENNDOT 1998)

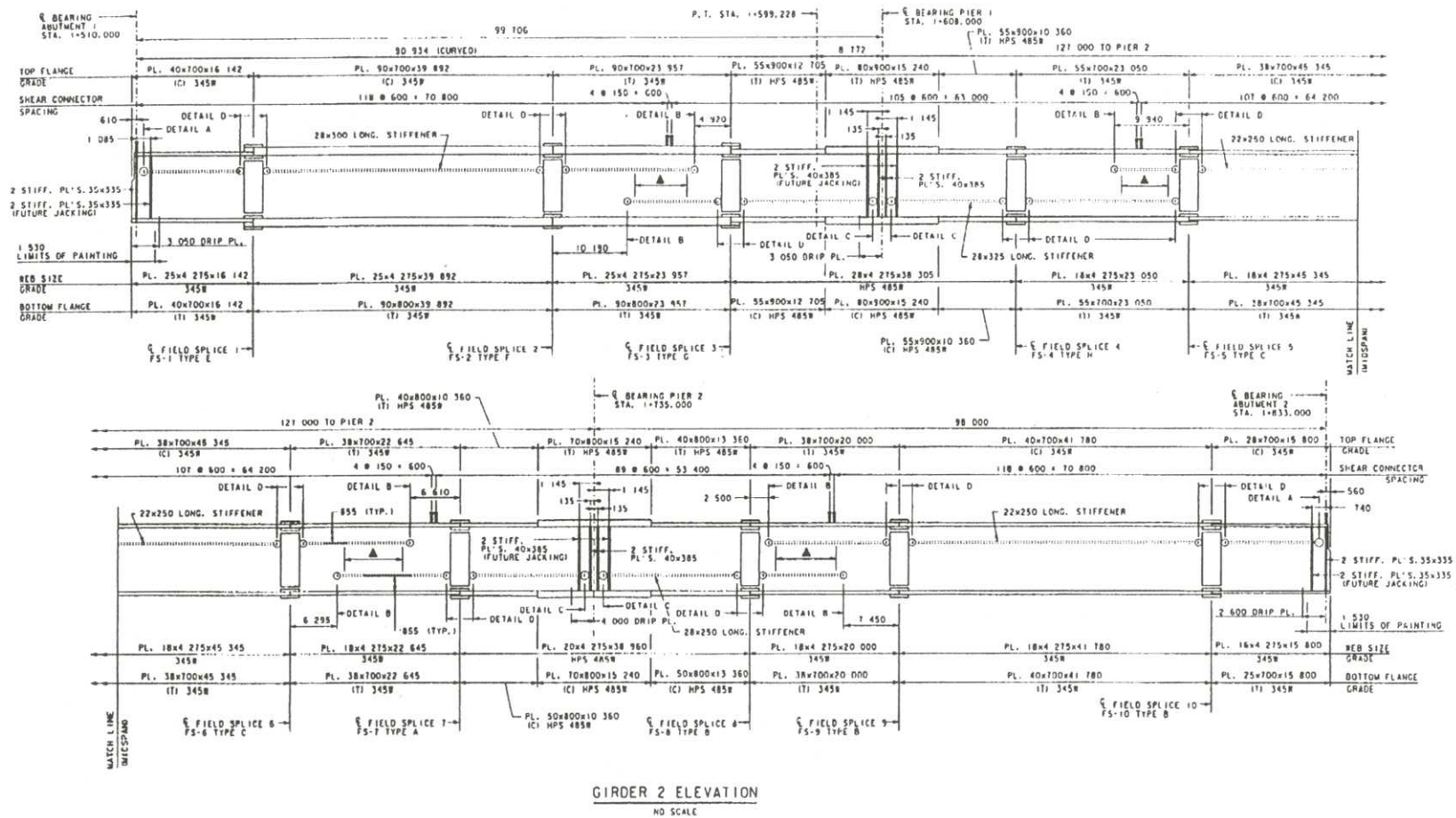


Figure 13 Elevation view of girder G2 (PENNDOT 1998)

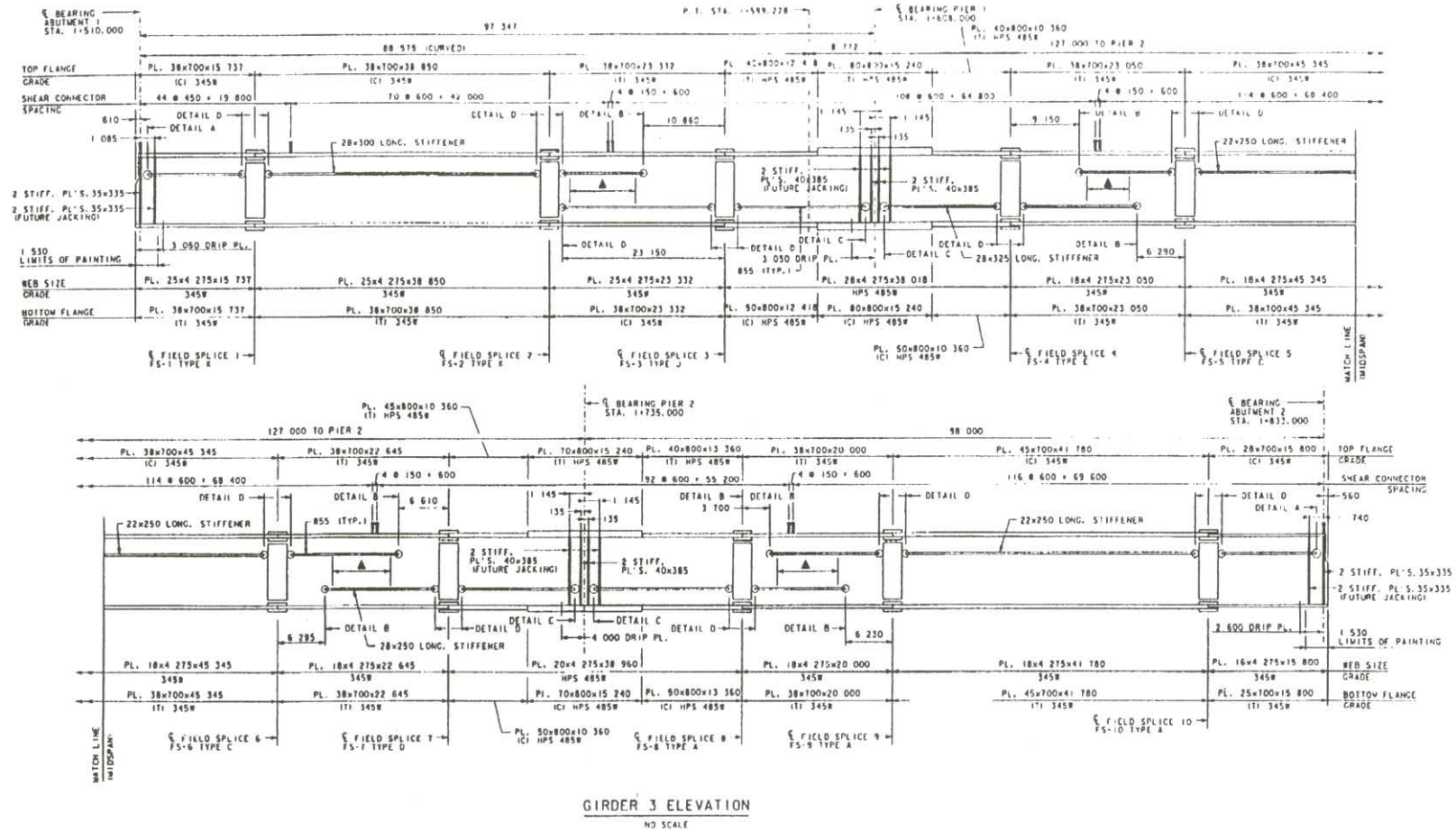


Figure 14 Elevation view of girder G3 (PENNDOT 1998)

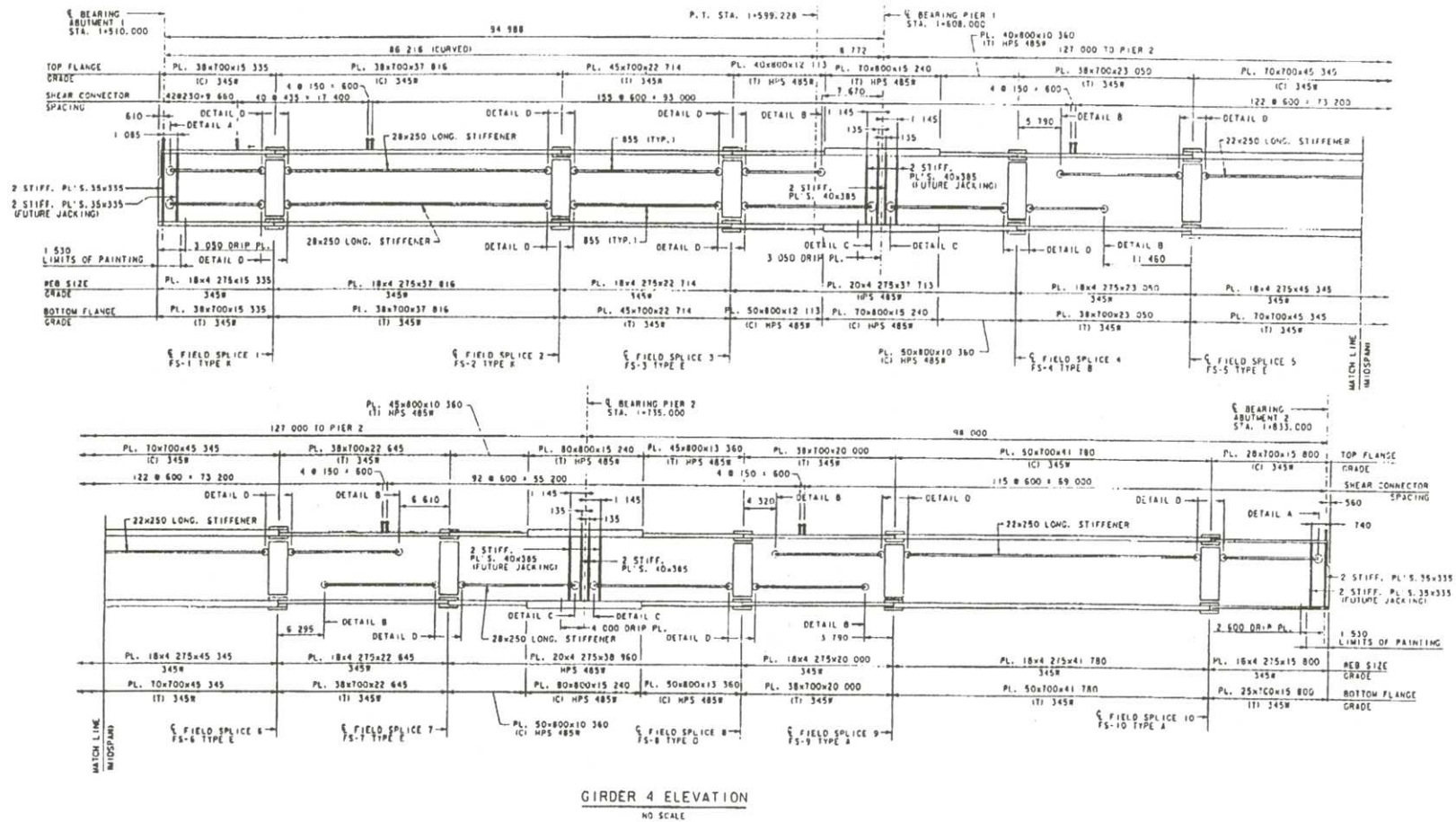


Figure 15 Elevation view of girder G4 (PENNDOT 1998)

### 3.3 Cross-Frame Details

In regard to span 1 of the Ford City Bridge, cross-frames are placed at equal radial intervals along the span. The cross-frame spacing differs near abutment 1 and in the region of pier 1. Four different cross-frame sizes are used in the four northern most sections of the bridge, including the curved section, as shown in figure 8 (CF-1, CF-2, CF-3, and CF-4). Figures 16, 17, 18, and 19 illustrate the cross-frames that are used, including the member sizes. All of the cross-frames were assembled and “pre-drilled” at the fabrication shop and transported to the bridge site. As shown in the figures, the cross-frame connections on the girders employ one full-depth stiffener and a connection plate, which enclose the cross-frame where it connects to the girder.

#### 3.3.1 Incorrect Detailing of Cross-Frame Members

It should be noted that an error occurred during the fabrication of the cross-frames. The cross-frames were incorrectly detailed, such that the concrete deck load case was used to detail the girders, instead of the no-load case, or the steel self-weight only load case. (An in depth analysis of the difference between detailing to the web-plumb no-load condition versus detailing to the web-plumb at steel self-weight condition is given in section 8.0 of the current study.) These incorrectly detailed cross-frames were still used in the bridge structure.

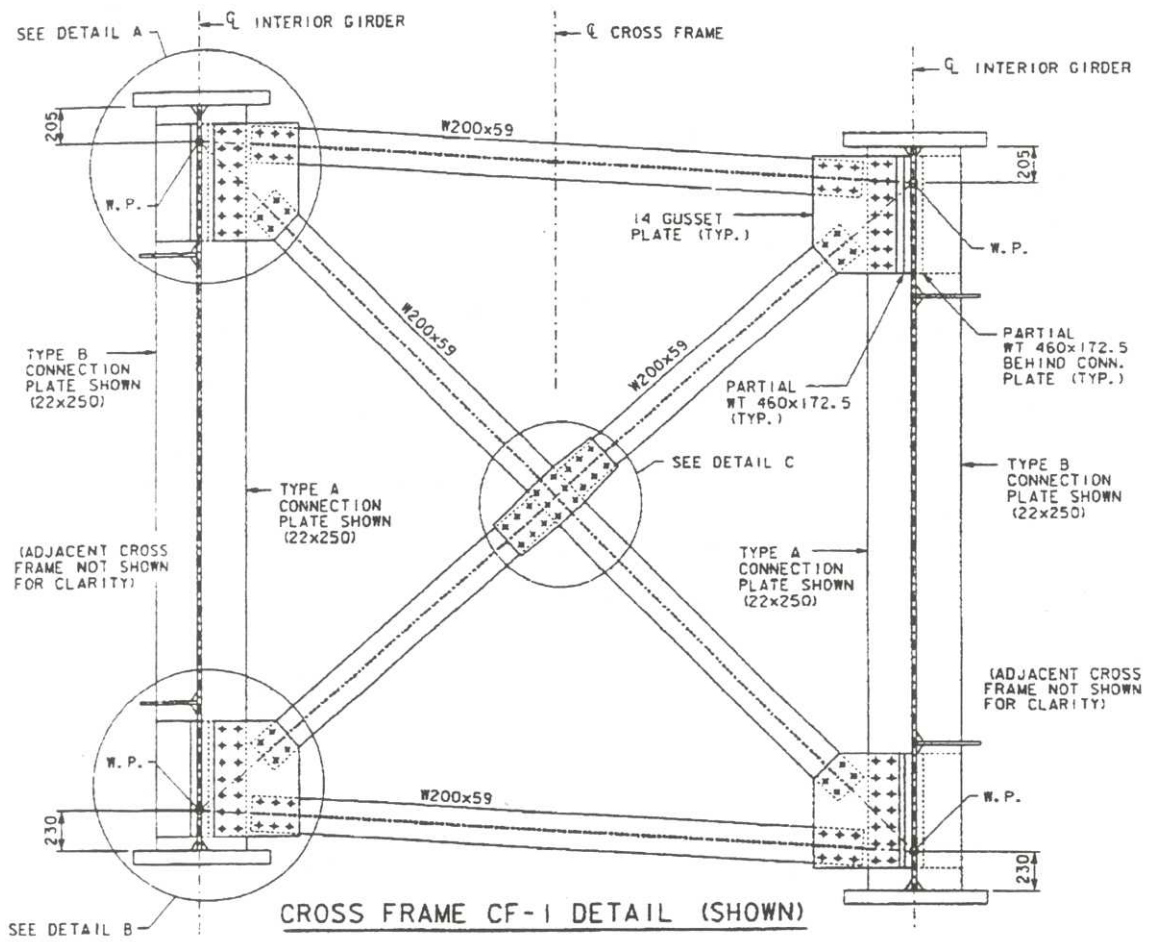


Figure 16 Cross-frame CF-1 detail (PENNDOT 1998)

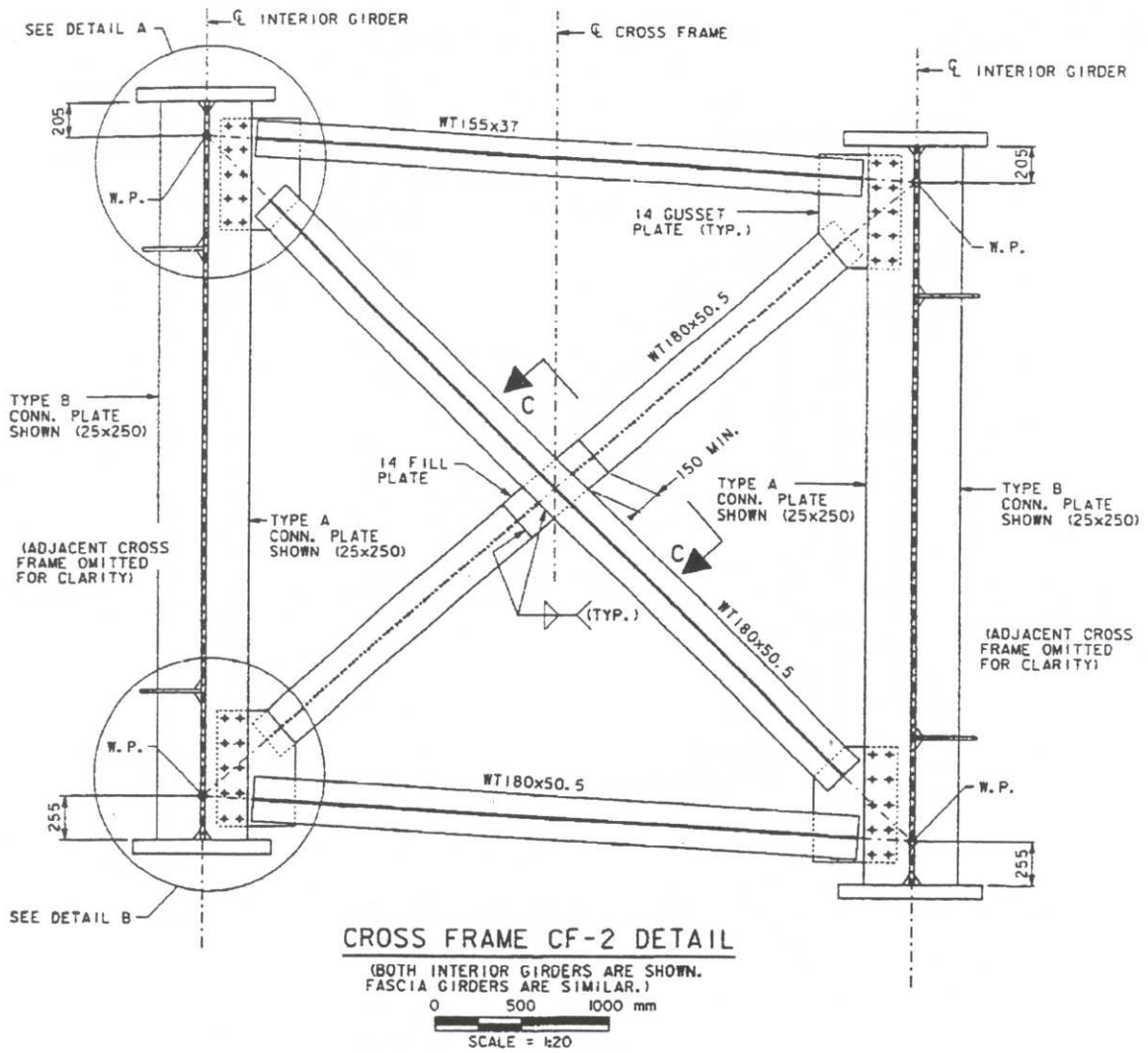


Figure 17 Cross-frame CF-2 detail (PENNDOT 1998)

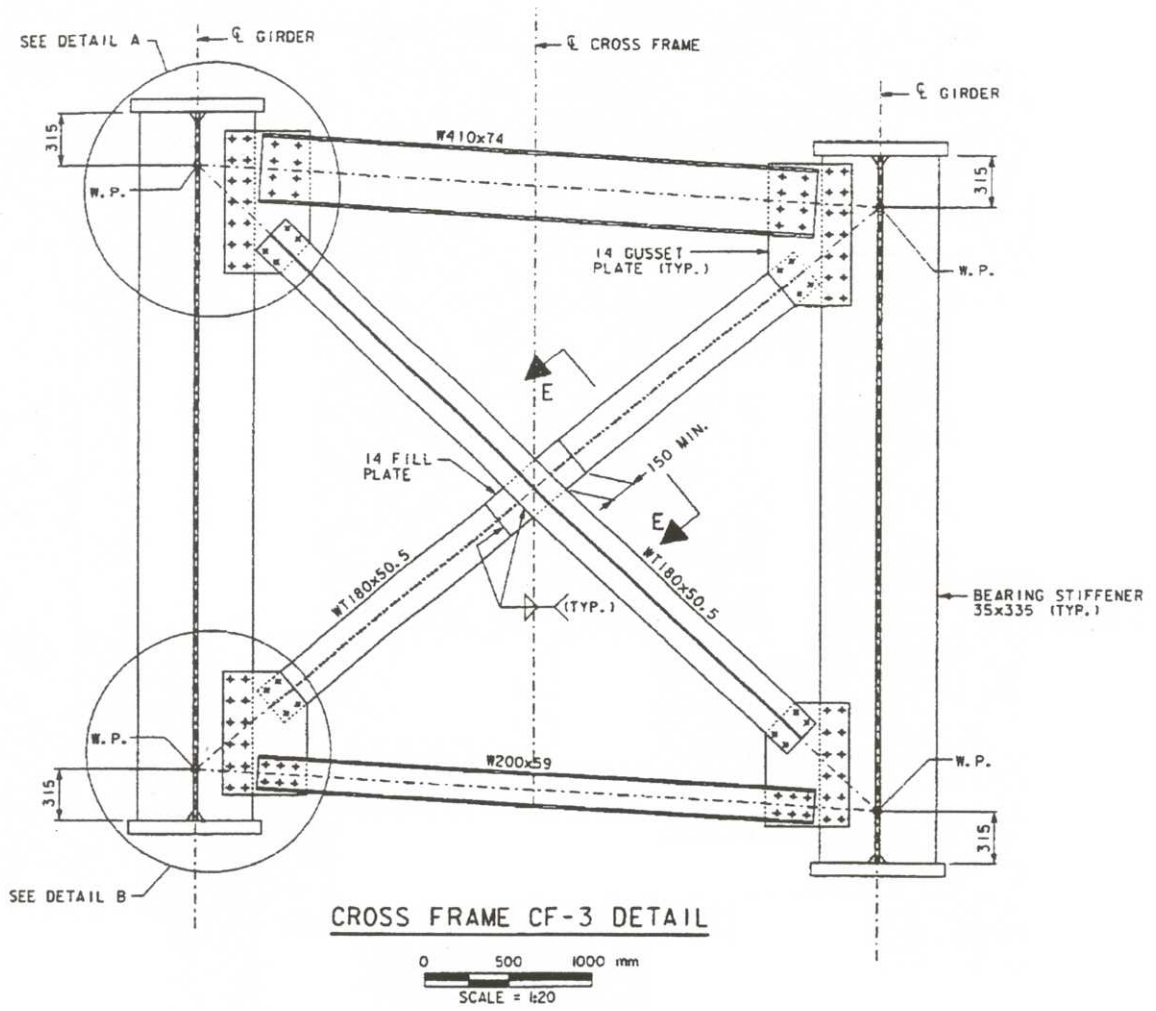


Figure 18 Cross-frame CF-3 detail (PENNDOT 1998)

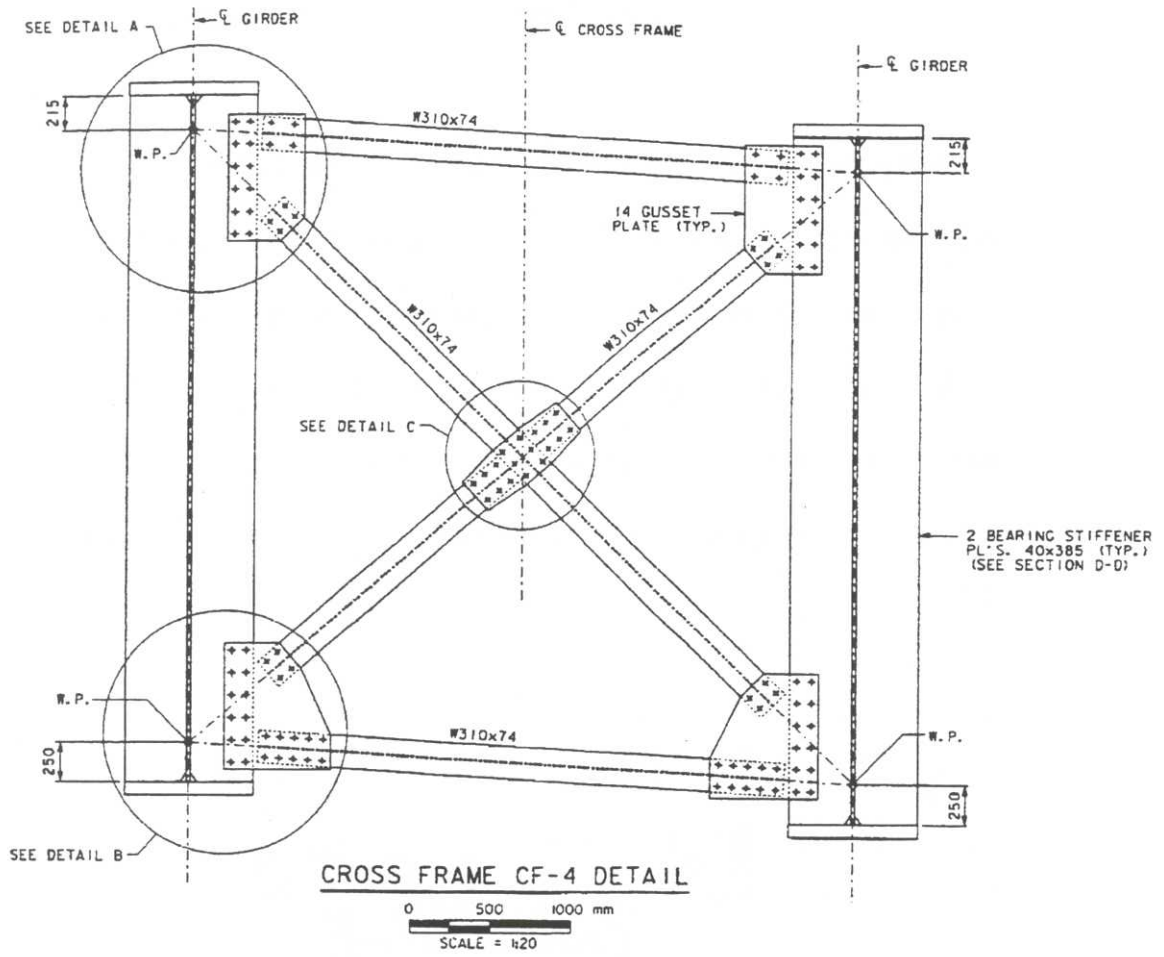
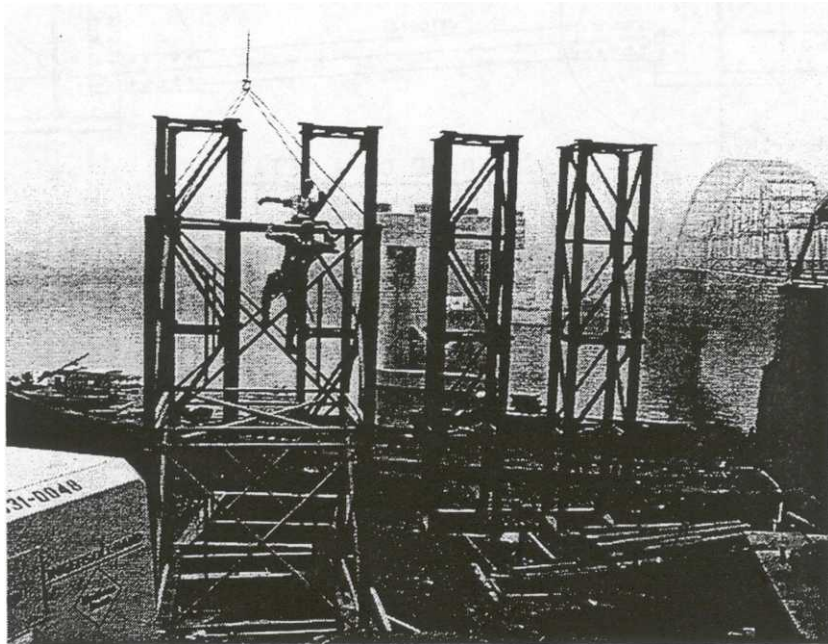


Figure 19 Cross-frame CF-4 detail (PENNDOT 1998)

### 3.4 Falsework Details (Temporary Supports)

During the erection of the curved span of the Ford City Bridge, three separate temporary supports are used in order to limit deflections and stabilize the girders. The temporary supports are truss-type structures, as shown in figure 20, with support below all four girders at each location. Falsework 1 is placed below the cross-frame 7 location; falsework 2A is placed below the cross-frame 11 location; and falsework 2 is placed below the cross-frame 14 location. The locations of the falseworks are shown in figure 10.



**Figure 20** Falsework structure

### 3.5 Miscellaneous Details

Forty field-splices are used throughout the entire superstructure, with the first three sets of field splices occurring in the curved span. In general, sizes of the top flange, bottom flange, and web splice plates vary from one girder to another, and from one field-splice to another. In cases where flanges thickness varies between two girders at a field-splice, filler plates are used. Therefore, at these locations on the top and bottom flanges, it is necessary to place bolts through four members of the connection; the top piece of the flange splice, the filler plate, the flange itself, and the bottom piece of the flange splice. Figure 21 illustrates girder G4, field-splice 1.

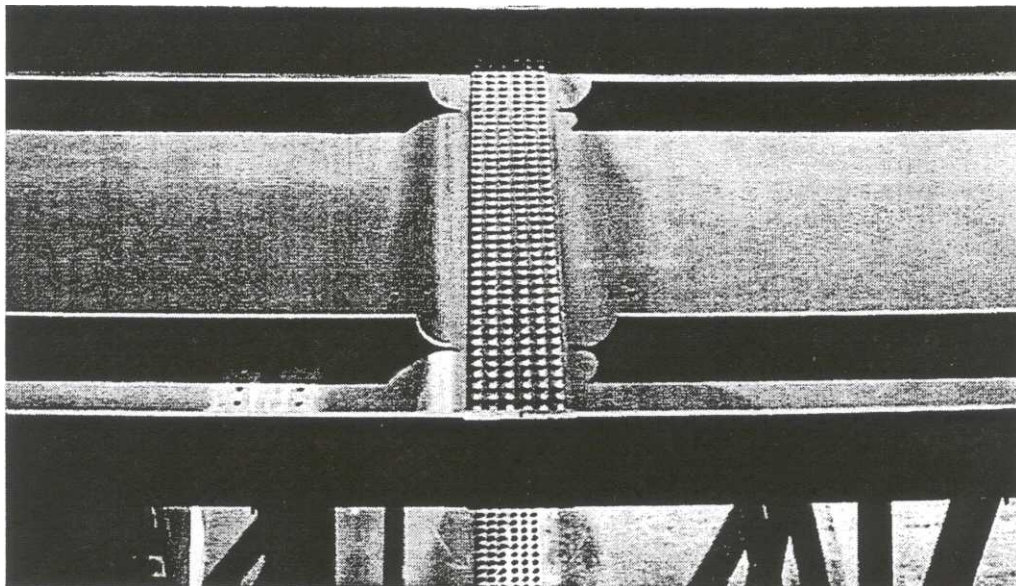


**Figure 21** Field-splice 1, girder G4

In addition to the cross-frame connection plates, also serving as transverse stiffeners, intermediate full-depth transverse stiffeners are also used in the curved section, specifically sections 1 and 4 of the bridge. In section 1, 22x250 plates are used, and in section 4, 30x350 plates are employed as transverse stiffeners.

Lateral bracing at the top of the girders is also used in order to limit out of plane deflections to due wind loads, especially in the straight section of the bridge. The lateral bracing was added after the design was completed. Lateral bracing members were positioned in between girders G2 and G3, and “field-drilled” connections were utilized to install the lateral bracing.

As shown in figure 22, the concrete deck is 240mm (9.45in) thick, and overhangs the fascia girders on each side by 1205mm. (47.4in). The haunch over girders G1 and G2 is designed to be 140mm (5.5in), and 130mm (5.1in) over girders G3 and G4. Additionally, welded stud shear connectors are employed on the top flange of the girders throughout the structure.

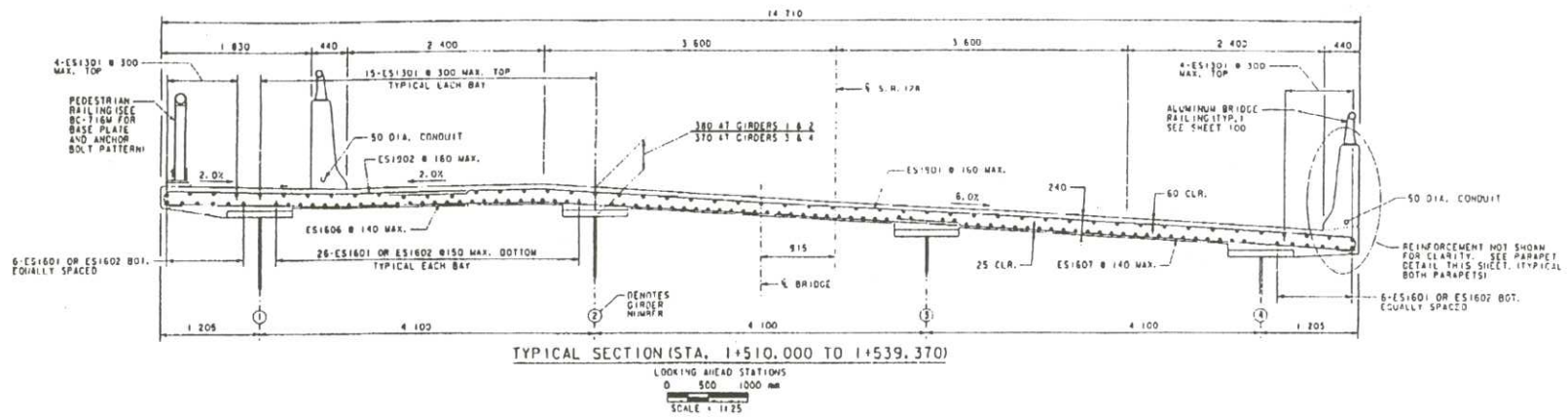


Figure 22 Typical concrete deck profile (PENNDOT 1998)

## **4.0 FORD CITY BRIDGE ERECTION SEQUENCE DETAILS**

This section describes the “as-built” erection sequence of the curved steel superstructure section of the Ford City Bridge. For each workday, descriptions are given for: the method of girder lifting; the connection of cross-frames and field splices; the equipment used in each erection step; and problems that developed as a result of the erection procedure. It should be noted that the steel superstructure erection was completed prior to the start of the present study. Therefore, for this chapter, the “in-field” construction of the bridge is recreated using field paperwork, a video chronicling portions of the construction, and photographs supplied by the Pennsylvania Department of Transportation (PennDOT) site engineers for the bridge project. Interviews conducted with the PennDOT personnel also provided information important to this section.

### **4.1 Curved Section Steel Erection Overview**

The erection of the curved section of the steel superstructure took place during daytime hours only. The erection of the curved section of the superstructure began on September 13, 1999, and finished on November 6, 1999. Abutments 1 and 2, piers 1 and 2, and falsework 1, 2, and 2A, had been constructed prior to the erection of the curved steel section.

A total of four separate cranes were used in the erection of the curved section, however, only in a few instances were all four cranes used at once. The 200-ton capacity

lifting crane, shown in figure 23, was equipped with a 200-foot boom and an 88,200 pound counter weight. The three other cranes were 4-wheel-type cranes; one primarily used to lift and place cross-frames; the second was used to stabilize the girders when needed; and the third was used to lift workers and equipment onto the bridge, as well as place cross-frames in some cases.

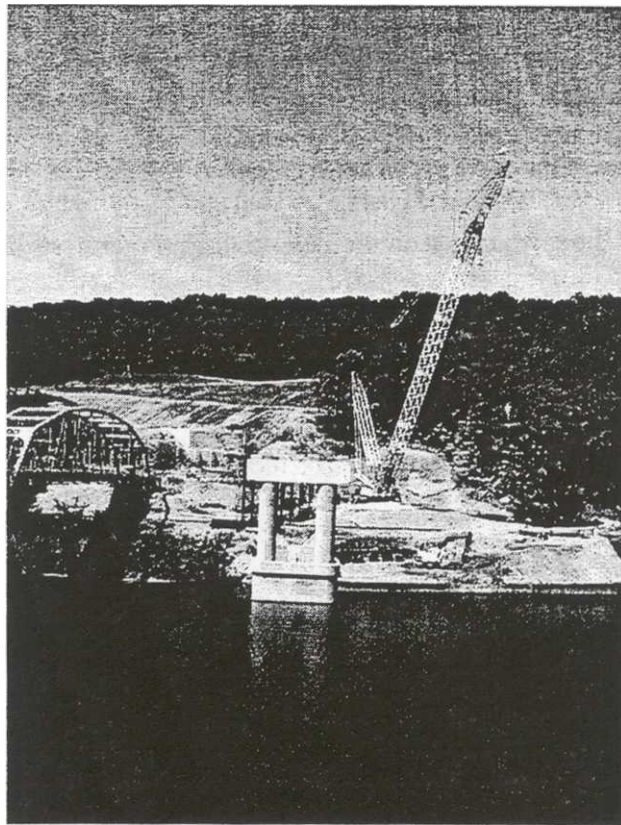


**Figure 23** Lifting crane

Three falsework towers were erected underneath the curved section of the bridge and supported all four girders at each location. Falsework 1 was placed underneath the cross-frame 7 location; falsework 2A was erected underneath the cross-frame 11 position; and falsework 2 was erected beneath the cross-frame 14 location. The girder supports on

the falsework consisted of steel blocking and steel shims, enclosing a jacking device, with a steel plate, a beveled plate, an elastomeric pad, and polytetrafluoroethylene (TFE) pads in between the jack and the girder. Figure 24 shows all of the falsework towers prior to the placement of the jacking devices, shim packs, and such. Figure 25 shows the falsework towers after the placement of the jacking devices, shim packs, and such. Figure 26 provides a side view of the falsework 2A structure. Sections of the falsework were prefabricated, and the sections were assembled and erected at the work-site.

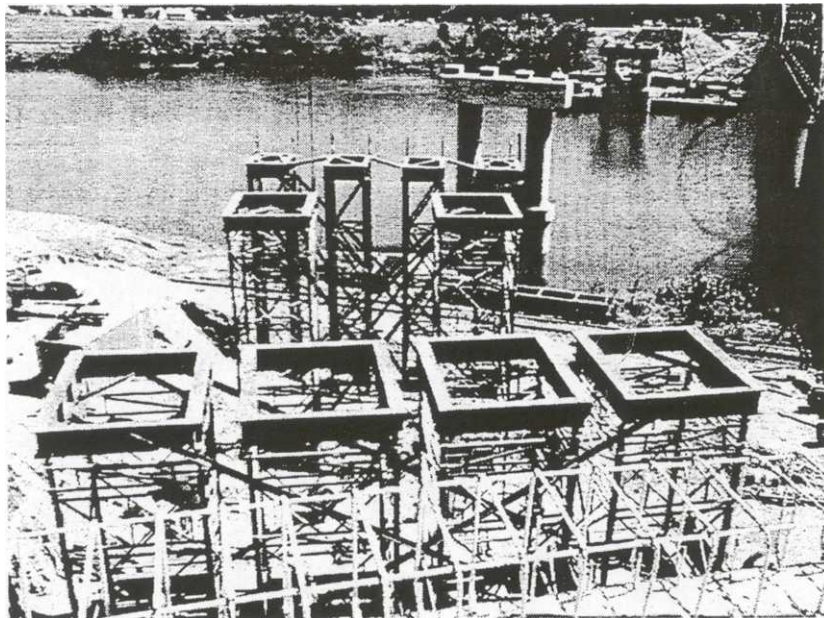


**Figure 24** Falsework 1, 2A, and 2; prior to “bearing” assembly

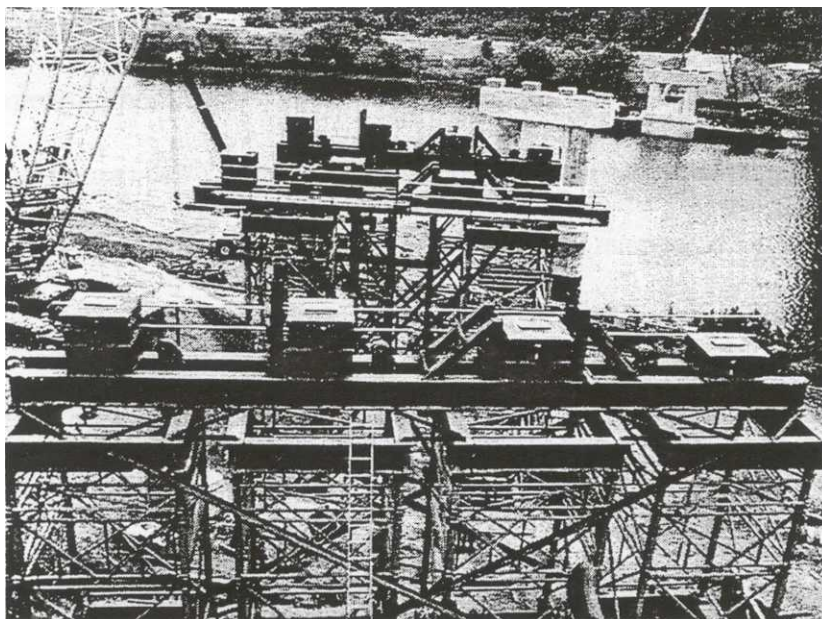


**Figure 25** Falsework 1, 2A, and 2; after “bearing” assembly

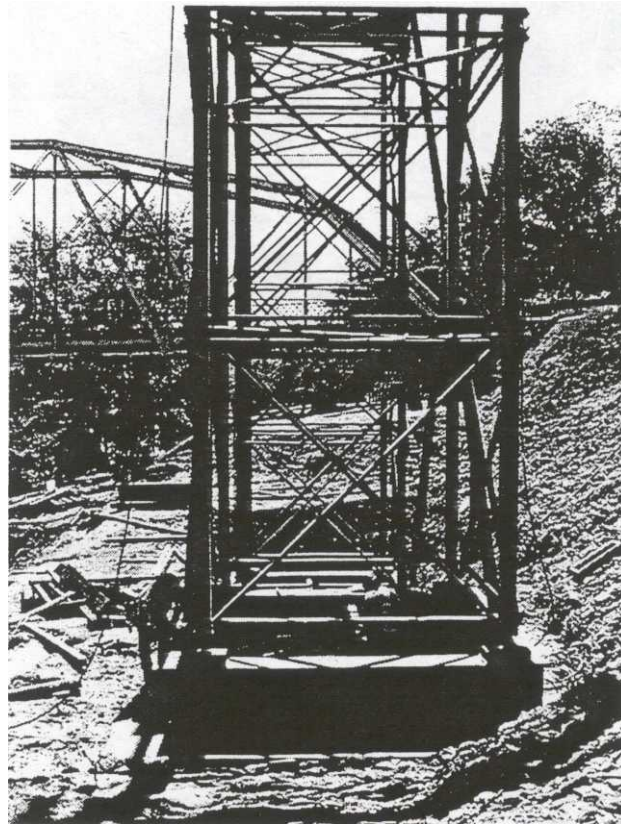


**Figure 26** Side view of falsework 2A

Girders were transported to the work-site by the railway that passed under the future bridge, and by barge, using the navigable waters of the Allegheny River, as shown in figures 27 and 28, respectively.

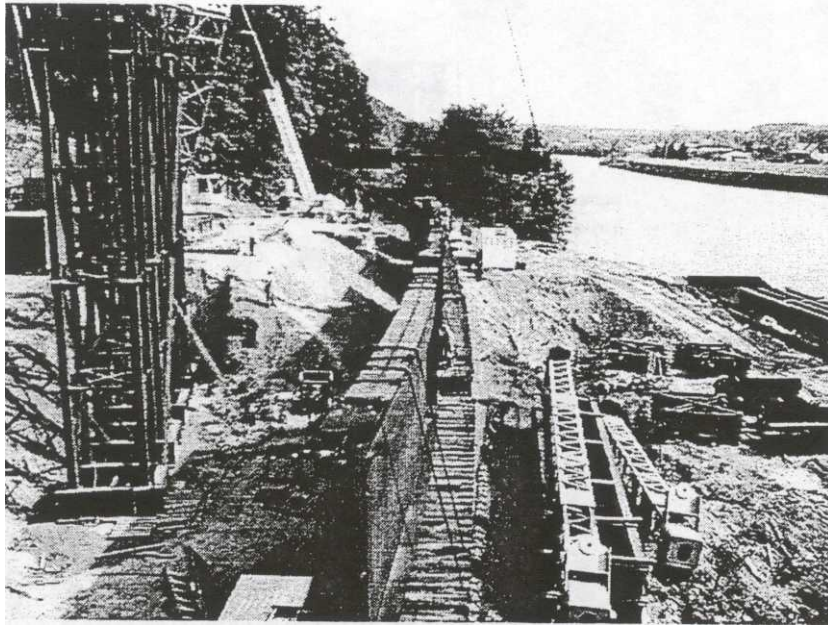


**Figure 27** Railway transport of girders

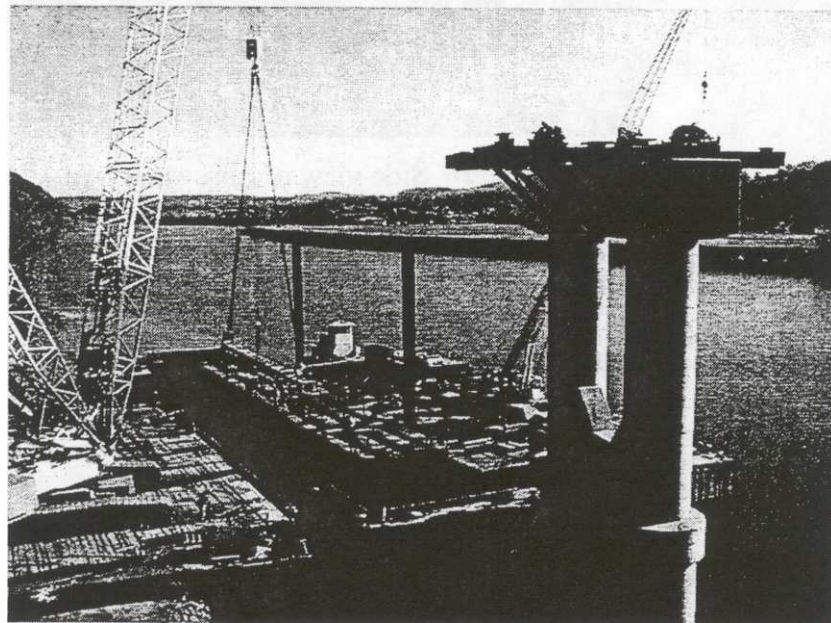


**Figure 28** Barge transport of girders

## 4.2 “As-Built” Erection Procedure of Curved Section

### 9/13/99 (Stage 1 of Bridge Erection Plans)

Girder G3 section 1 (G3-1) was erected: clamping devices separated by a spreader beam were used on the top flange to lift the girder, as shown in figure 29 and 30. Cross-frames at abutment 1 (B and C) and at falsework 1 (B and C) were attached after G3-1 was placed on the bearings at abutment 1 and falsework 1. A second crane was used to place the subject cross frames, as the lifting crane was used to stabilize G3-1 as the cross frames were attached, as shown in figure 31. Cross-frames were attached to G3-1 and blocked and tied down at abutment1 and falsework 1. G3-1 was blocked laterally at the bottom flange at abutment 1 and falsework 1. Once the cross-frame tie-downs were secure, and the bottom flange was blocked, the lifting crane released G3-1.

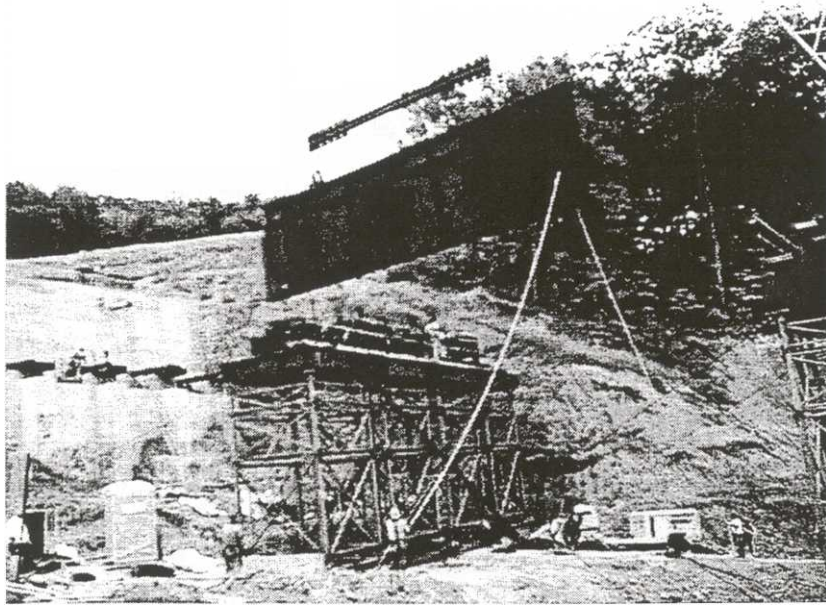


**Figure 29** Lifting of G3-1

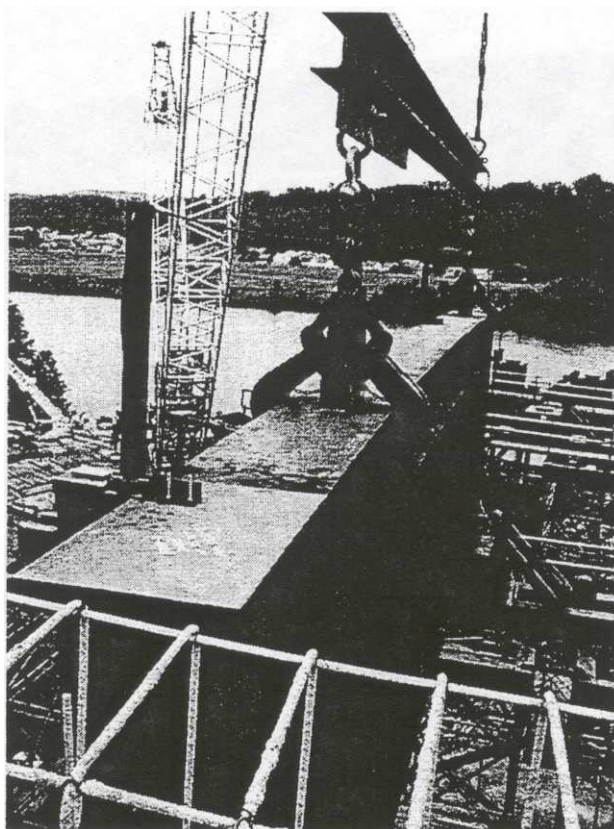


**Figure 30** Clamping device used to lift G3-1

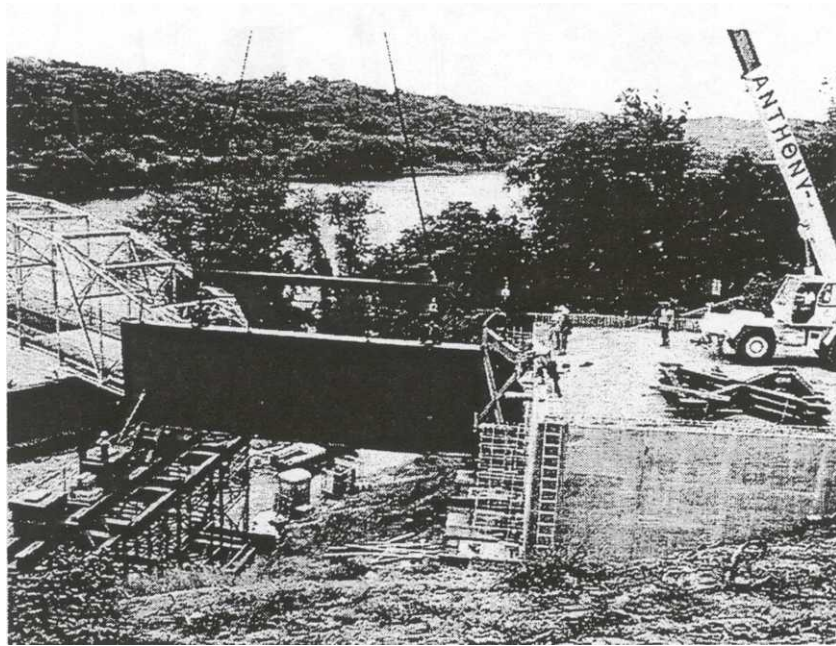


**Figure 31** Placement of cross-frame 1B at abutment 1 to stabilize G3-1

9/14/99 (Stage 1 of Bridge Erection Plans)

Girder G2 section 1 (G2-1) was lifted and placed via the clamping device. Once G2-1 was placed on abutment 1 and falsework 1, it was held in place by the lifting crane as it was connected to G3-1 by the previously installed cross-frames 1B and 7B. Figure 32 shows G2-1 being lifted into place, as well as cross-frame 7B attached to G3-1 over falsework 1. Once cross-frames 1B and 7B were connected, cross-frame 4B was placed, then the lifting crane released G2-1.

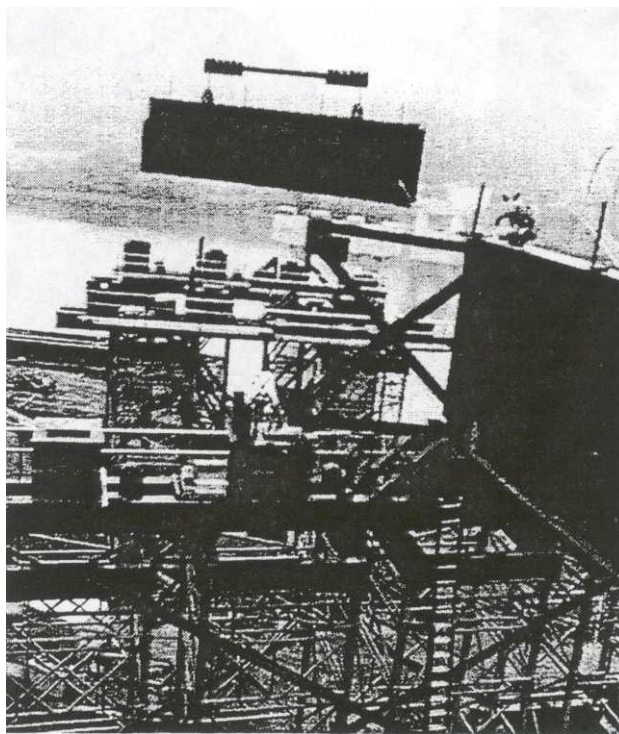


**Figure 32** Erection of girder G2-1

Girder G4 section 1 (G4-1) was lifted and placed via the clamping device. G4-1 was connected to G3-1 by cross-frames 1C and 7C, which were previously connected to G3-1, as shown in figures 33 and 34. G4-1 was held in place with the erecting crane, as another crane placed cross-frame 4C. After cross-frame 4C connections were made with girders G3-1 and G4-1, the lifting crane released G4-1.

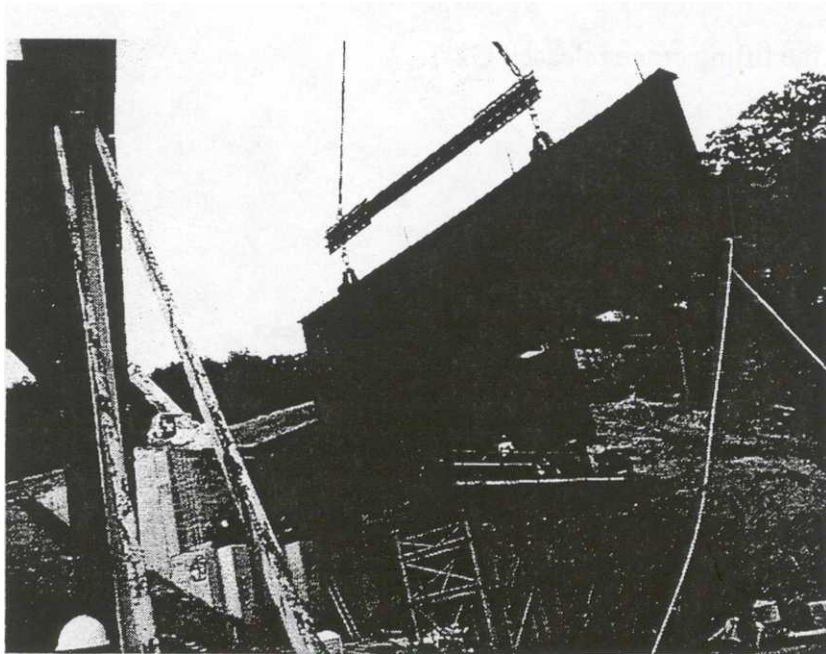


**Figure 33** Erection of girder G4-1

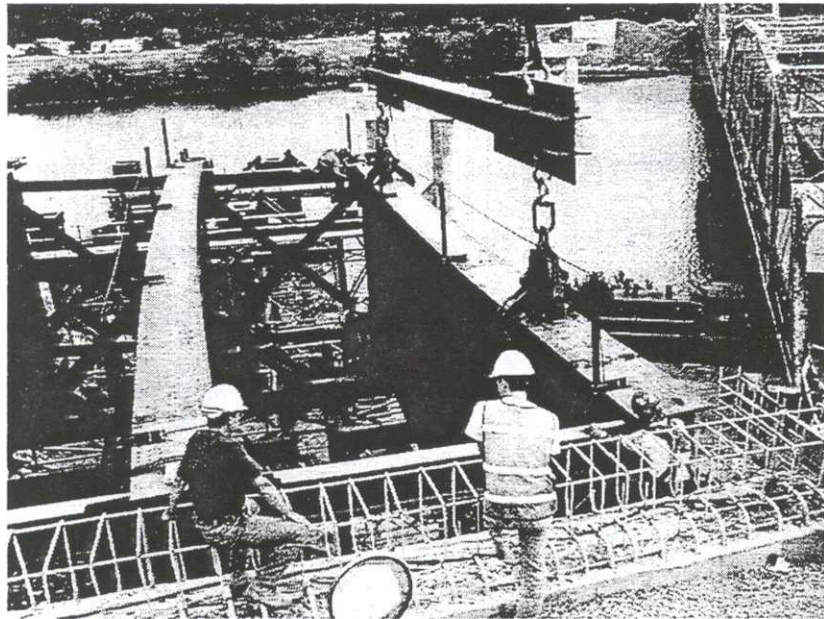


**Figure 34** Connecting cross-frames 1C and 7C between G3-1 and G4-1

9/15/99 (Stage 1 of Bridge Erection Plans)

Girder G1 section 1 (G1-1) was erected, using the same clamp and spreader beam device, as is shown in figure 35. Once G1-1 was set on abutment 1 and falsework 1, it was held in place by the lifting crane as the connection to cross-frame 1A was made. Cross-frame 1A was previously attached to G2-1, prior to the erection of G1-1. G1-1 continued to be held in place by the lifting crane, as the second crane placed cross-frame 4A and then cross-frame 7A, as shown in figures 36 and 37 respectively. After cross-frame 4A and 7A connections were made with girders G1-1 and G2-1, the lifting crane released G2-1.

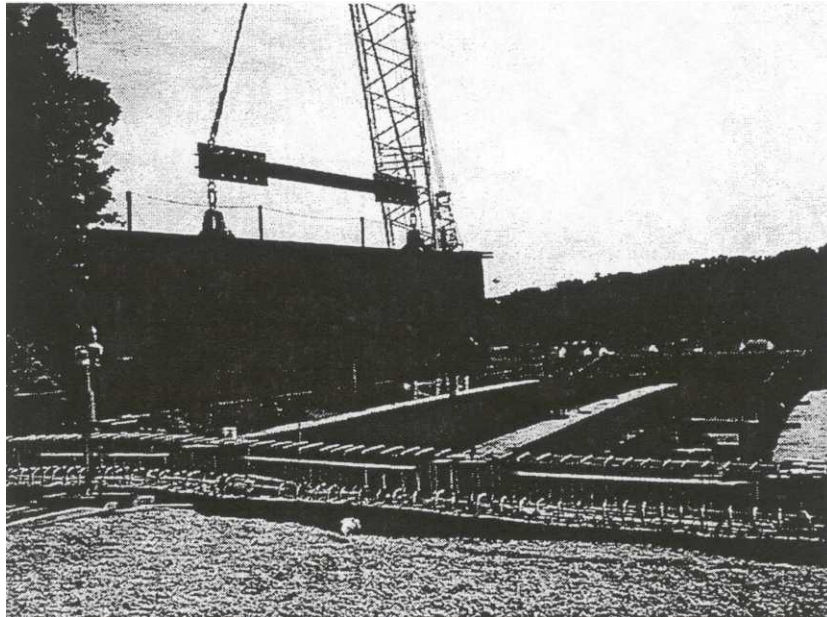


**Figure 35** Erection of G1-1

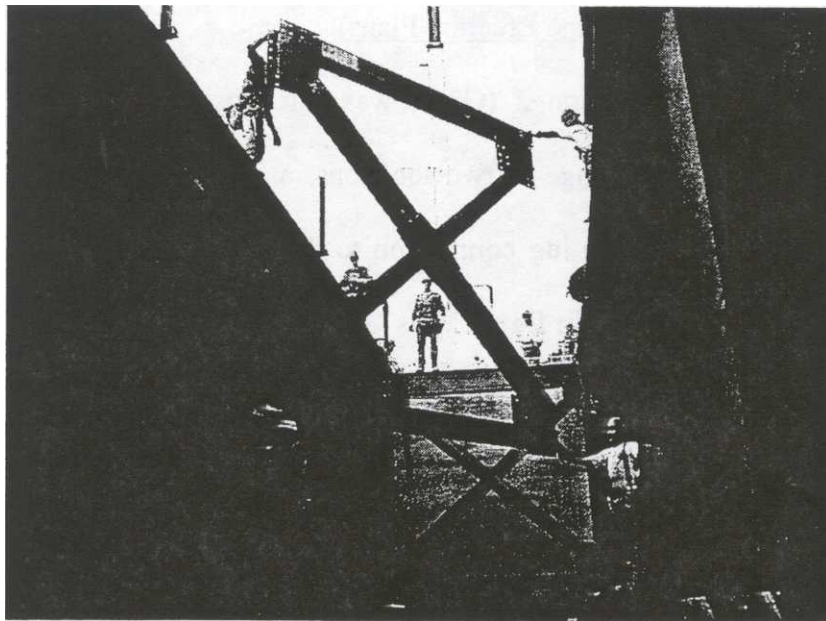


**Figure 36** Placing cross-frame 4A, G1 -1 is on the right

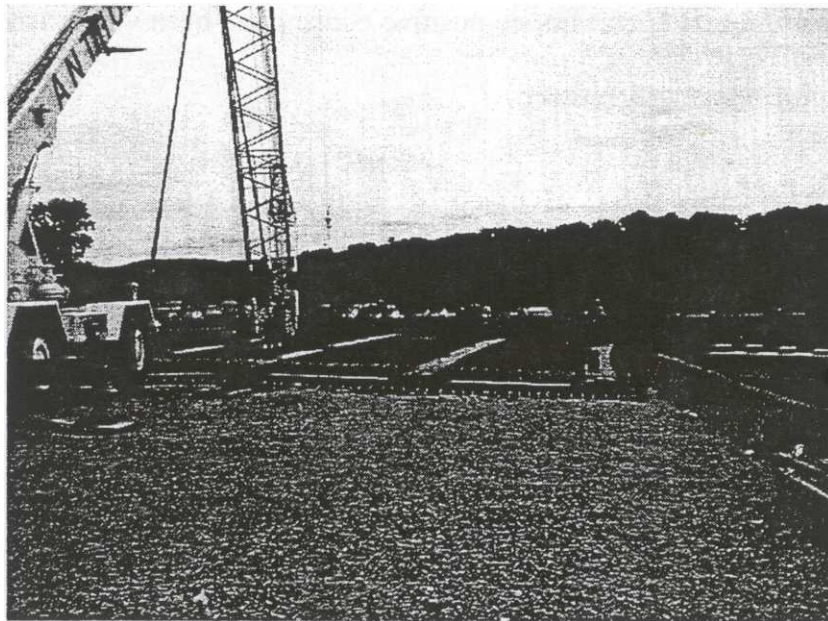


**Figure 37** Placing cross-frame 7A

9/17/99 (Stage 2 of Bridge Erection Plans)

Girder G3 section 2 (G3-2) was lifted using a lifting truss, with lifting lugs attached to the top flange at two locations, as shown in figure 38. A close-up of the lifting truss, and lifting lug connection to the top flange is shown in figure 39. (Note: while the girder shown in figure 17 is G2 section 2, the same lifting device is used on all girders employing the lifting truss and lifting lugs.) As G3-2 was held in place on falsework 2A and falsework 2 by the lifting crane, field-splice 1 was completed. A second crane individually lifted cross-frames 11B, 11C, 14B and 14C, which were then attached to G3-2 and falsework 2A and 2, respectively, as shown in figure 40. The cross-frames were blocked and tied-down, G3-2 was blocked laterally at the bottom flange at falsework 2A and 2, and once positive contact had been verified at falsework 2A and 2, the lifting crane was released.

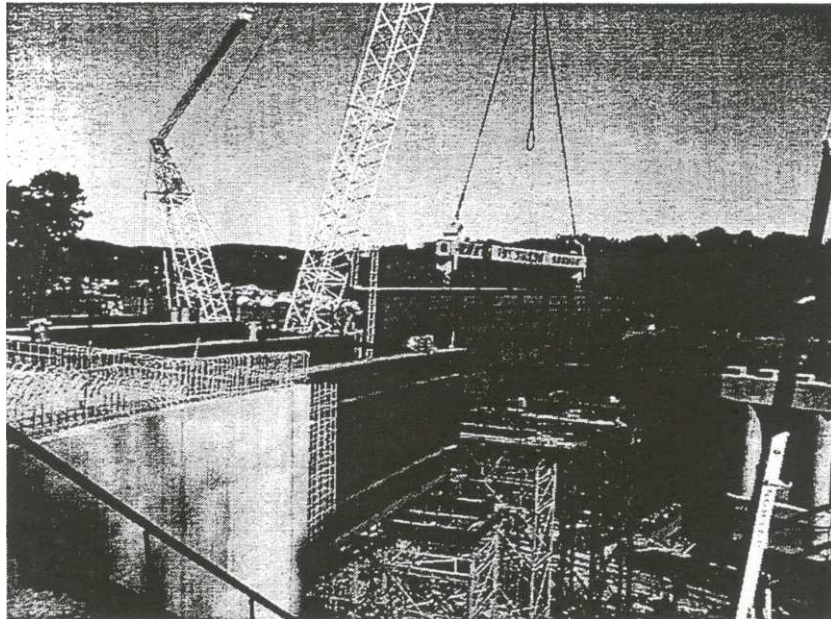


**Figure 38** Lifting of G3-2

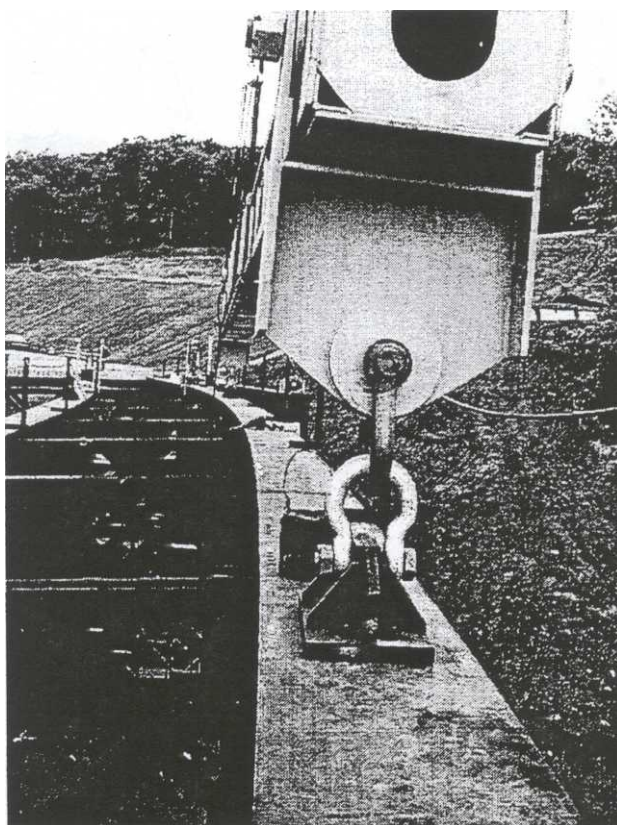


**Figure 39** Lifting truss and lifting lug, G2-2

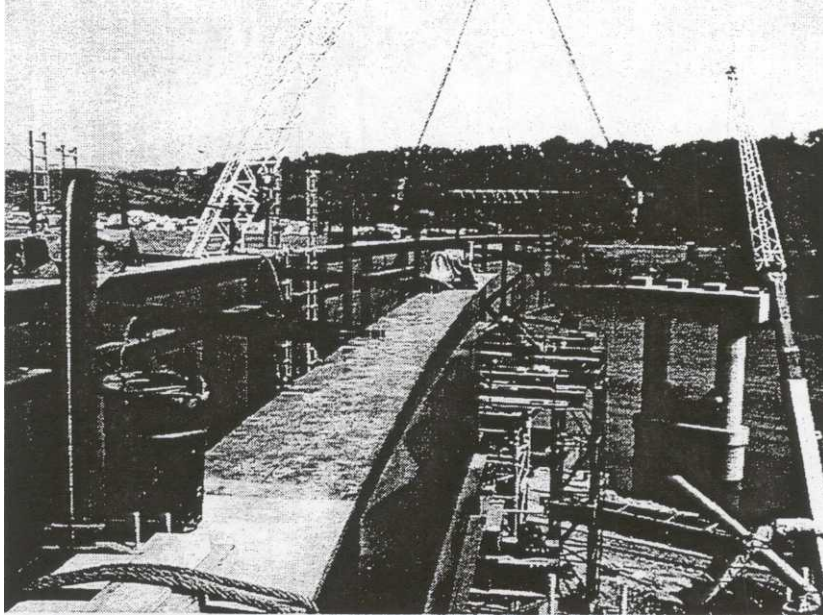


**Figure 40** Erected cross-frames on both sides of G3-2 at falsework 2A and 2

9/20/99 (Stage 2 of Bridge Erection Plans)

Girder G2 section 2 (G2-2) was lifted by the lifting truss with lifting lugs connected to the top flange, and placed on falsework 2A and 2, as shown in figure 41. A cantilevered “come-along” assembly, as shown in figure 42 (different girder section shown), was also used when G2-2 was lifted, which prevented the girder from rotating. G2-2 was held in place by the lifting crane as cross-frames 11B and 14B, previously attached to G3-2, were connected to G2-2, and field-splice 1 was made. Figure 43 shows field-splice 1 nearly completed. G2-2 was still held in place by the lifting crane, as the second crane lifted and placed, in order, cross-frames 8B, 9B, 10B, 12B, 13B, 15B and 16B. Figure 44 shows cross-frame 16B being placed.

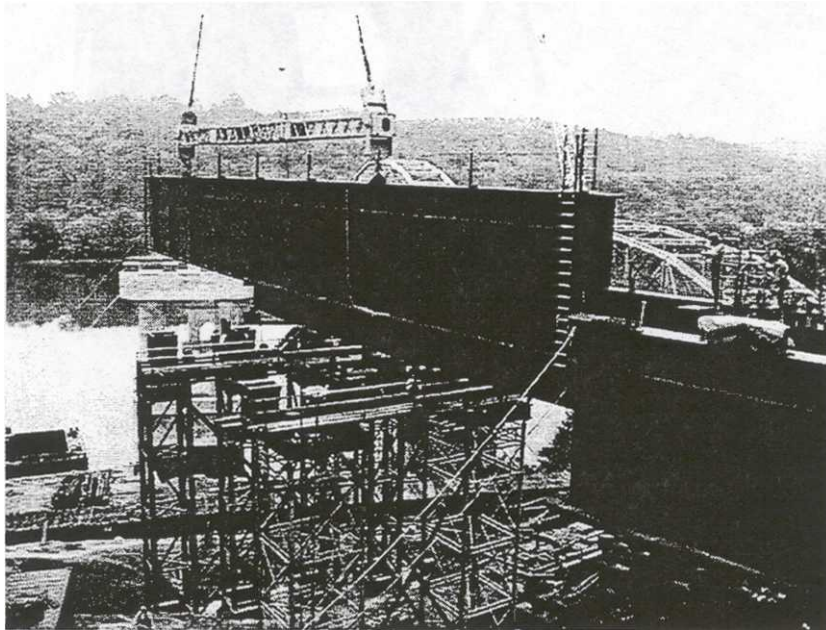


**Figure 41** Erection of girder G1-2

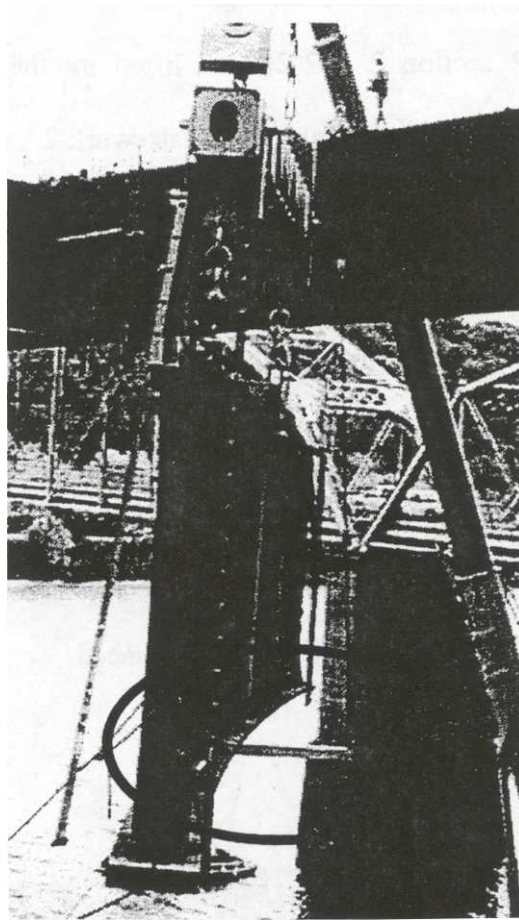


**Figure 42** Typically used cantilevered “come-along” assembly (circled)

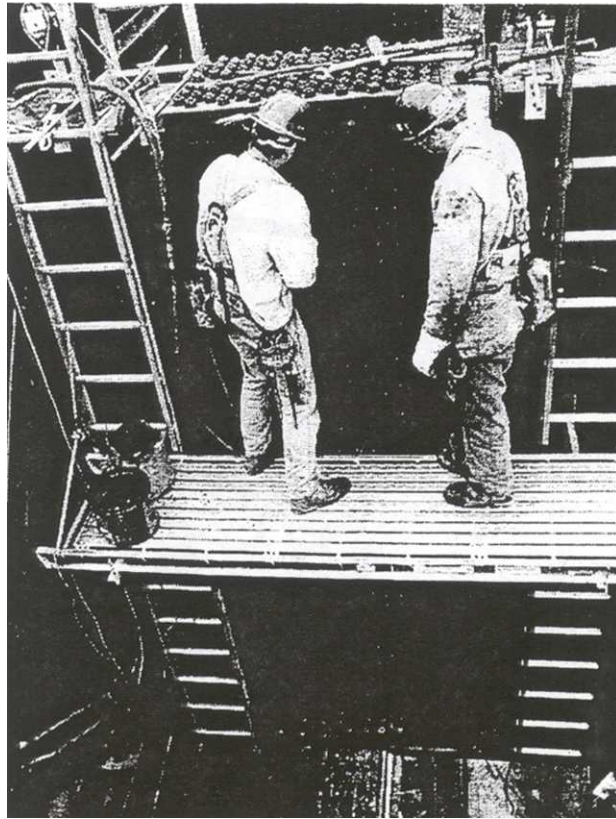


**Figure 43** Girder G2 field-splice 1

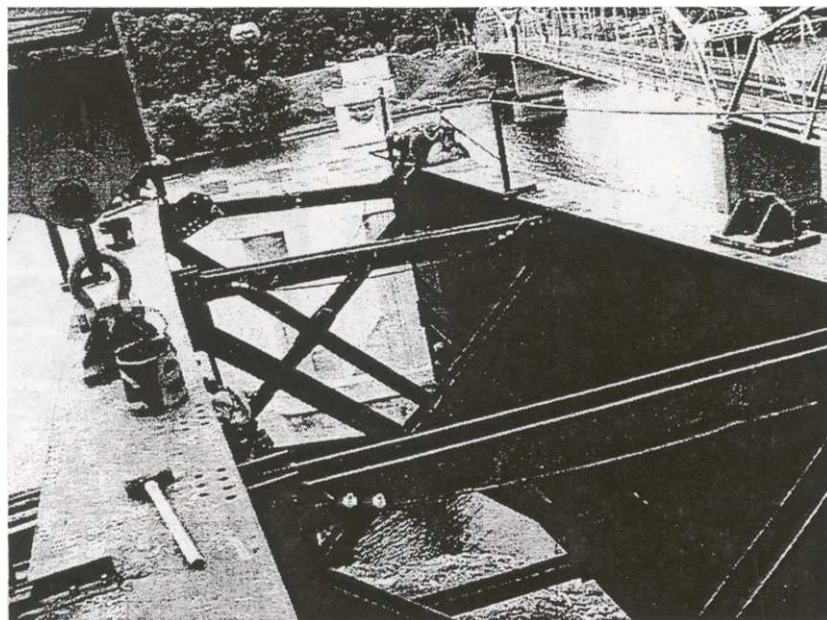


**Figure 44** Placement of cross-frame 16B

9/21/99 (Stage 2 of Bridge Erection Plans)

Girder G4 section 2 (G4-2) was lifted via the lifting truss, with lifting lugs connected to the top flange of the girder, and placed on falsework 2A and 2. A “come-along” device was also used when G4-2 was lifted, as shown in figure 45. As G4-2 was held in place by the lifting crane, connections to cross-frames 11C and 14C at falsework 2A and 2, respectively, were made, and field-splice 1 was completed.

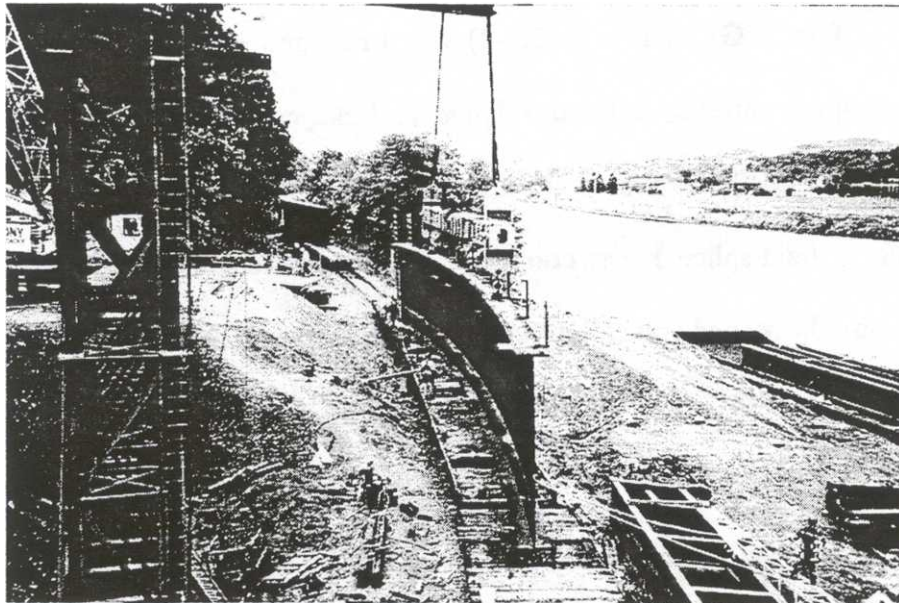


**Figure 45** Lifting of G4-1

9/22/99 (Stage 2 of Bridge Erection Plans)

Cross-frames 8C, 9C, 10C, 12C, 13C, 15C, and 16C were placed and connected between girders G4-2 and G3-2. Based on the field record, it is unknown if the lifting crane released G4-2 prior to the night of 9/21/99, before the installation of the subject cross-frames was executed on 9/22/99. (No pictures were available for this day.)

9/23/99 (Stage 2 of Bridge Erection Plans)

Girder G1 section 2 (G1-2) was lifted and placed using the lifting truss, with lifting lugs connected to the top flange, and the “come-along” device, as shown in figure 46. Once G1-2 was placed on falsework 2A and 2, it was held in place by the lifting crane as field-splice 1 was completed, and cross-frames 11A and 14A were lifted into place by the second crane, individually, as shown in figure 47.

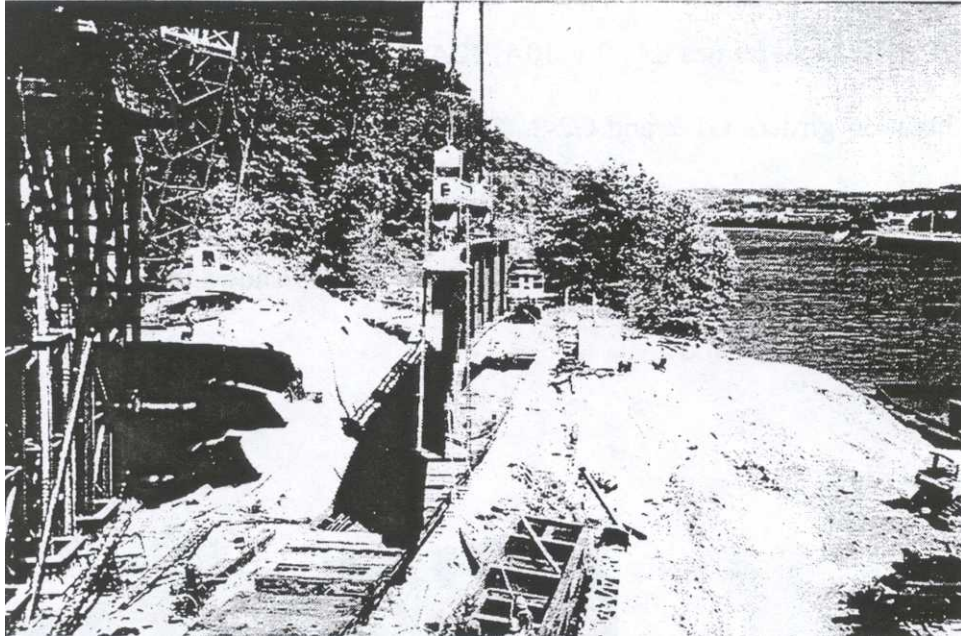


**Figure 46** Lifting of G1 -2

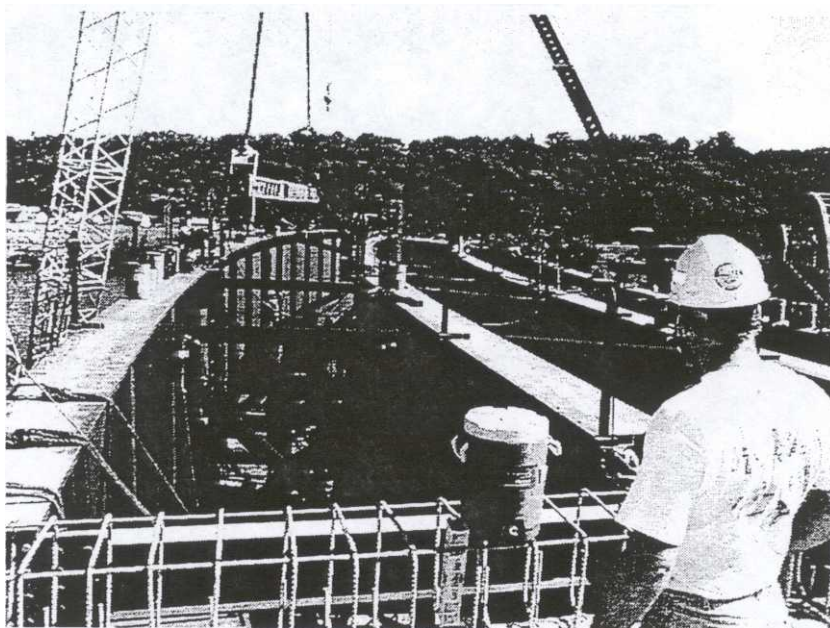


**Figure 47** Placement of cross-frame 11A, connecting G1-2 with G2-2

9/24/99 (Stage 2 of Bridge Erection Plans)

Cross-frames 8A, 9A, 10A, 12A, 13A, 15A, and 16A were placed and connected between girders G1-2 and G2-2. Based on the best available data, it is unknown if the lifting crane released G1 -2 prior to the night of 9/23/99, and hence prior to the installation of the subject cross-frames on 9/24/99. Figure 48 shows the completed steel erection of bridge sections 1 and 2.

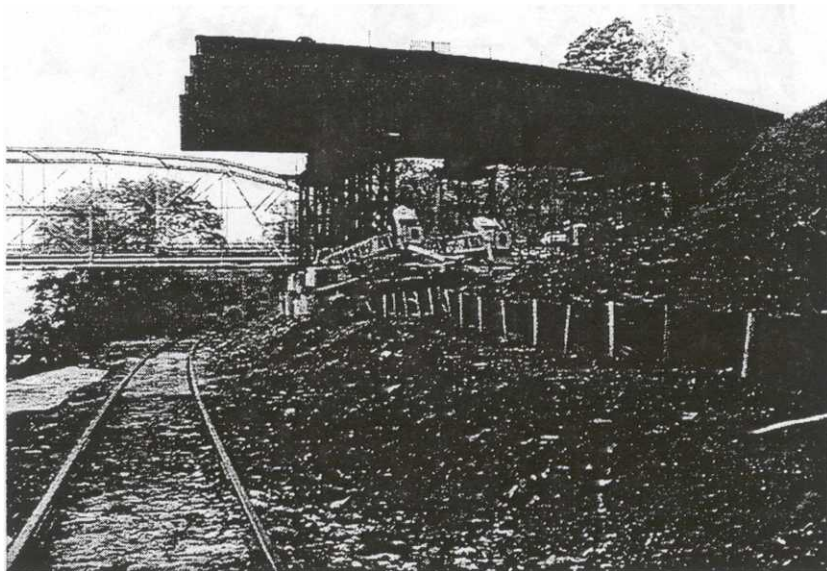


**Figure 48** Completed steel erection of bridge section 1 and 2

10/8/99 thru 10/14/99 (Stage 3 of Bridge Erection Plans)

Pier brackets for girders G2 and G3 at pier 1 were set and adjusted, as shown in figures 49 and 50, and pier 1 bearings were adjusted.

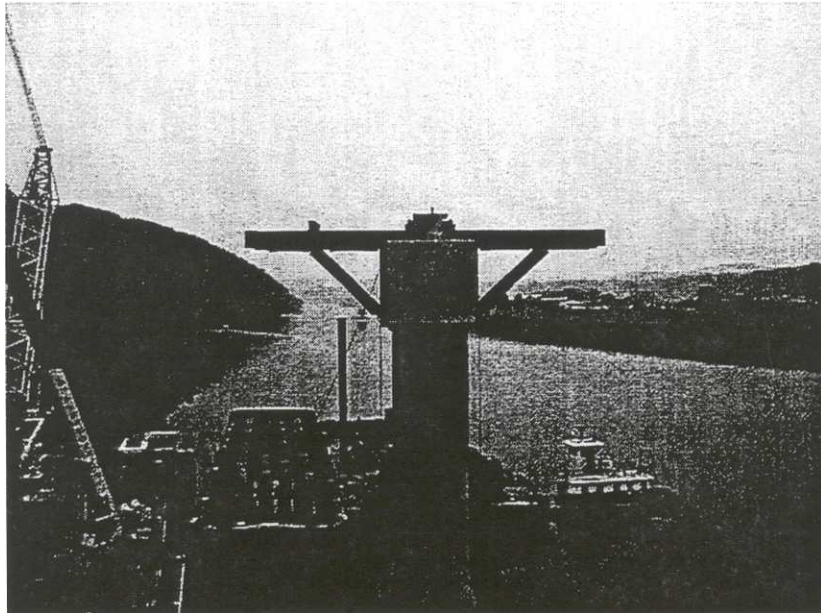


**Figure 49** Girder G3 pier 1 bracket construction

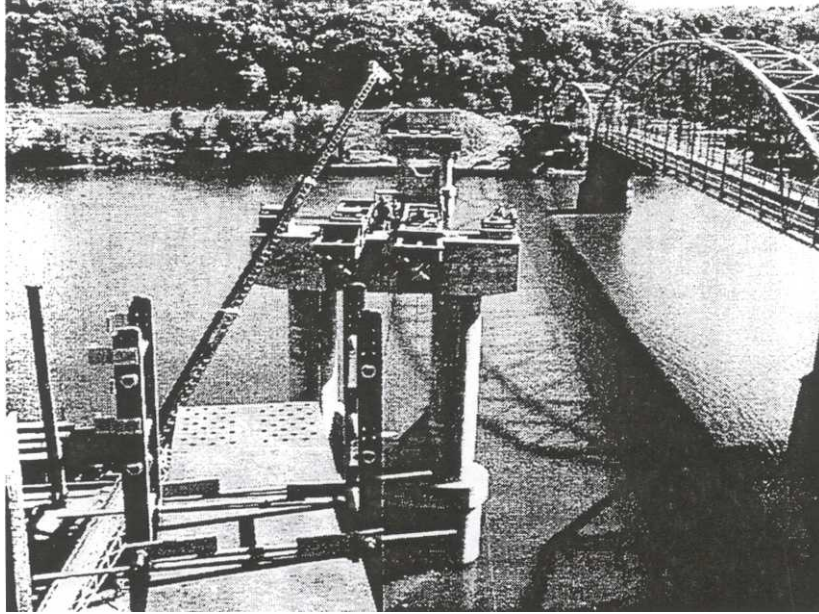


**Figure 50** Completed pier 1 brackets for girders G2 and G3

10/15/99 (Stage 3 of Bridge Erection Plans)

Girder G3 section 4 (G3-4) was lifted and placed onto pier 1 and the pier 1 brackets. The girder was lifted via the lifting truss with the lifting lugs attached to the top flange of the girder as shown in figure 51. Once G3-4 was placed on pier 1, it was held in place with the lifting crane as a second crane placed cross-frames 27B and C over pier 1, as shown in figure 52. G3 4 was still held in place by the lifting crane, as the second crane erected the cross-frames at both ends of the pier 1 brackets, cross-frames 26B, and then 28B. The erection of cross frame 26B is shown in figure 53. Once the cross-frames were blocked and tied-down to the pier and pier brackets, the lifting crane was released.

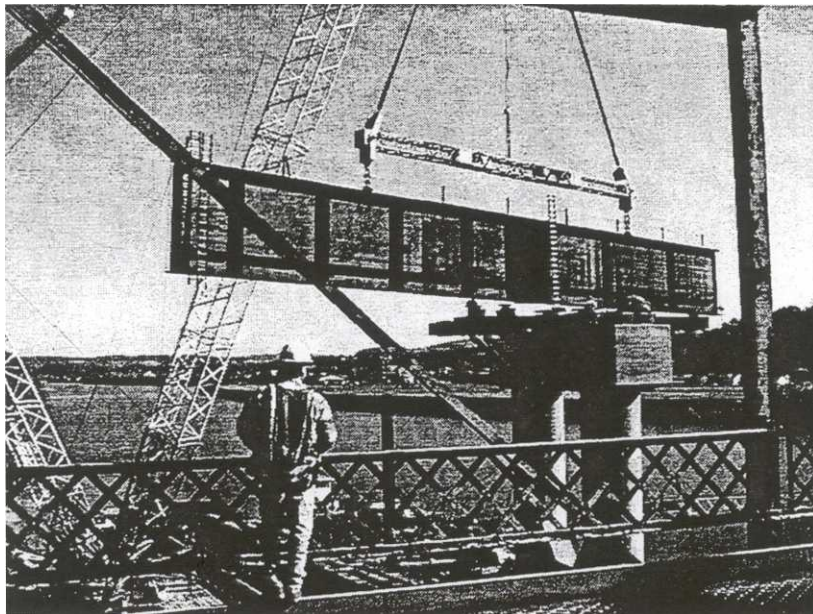


**Figure 51** Lifting of G3-4

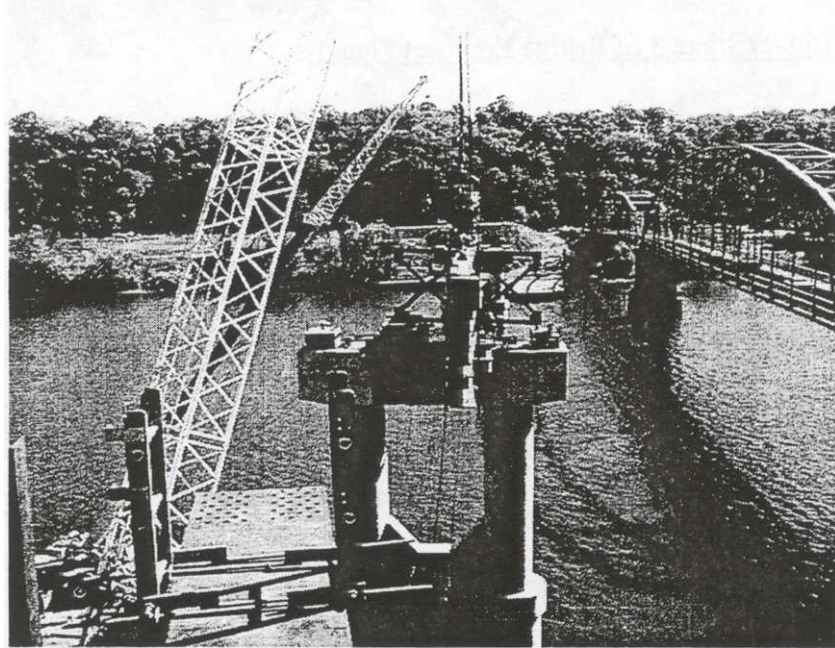


**Figure 52** G3-4 after cross-frames 27B and C were erected

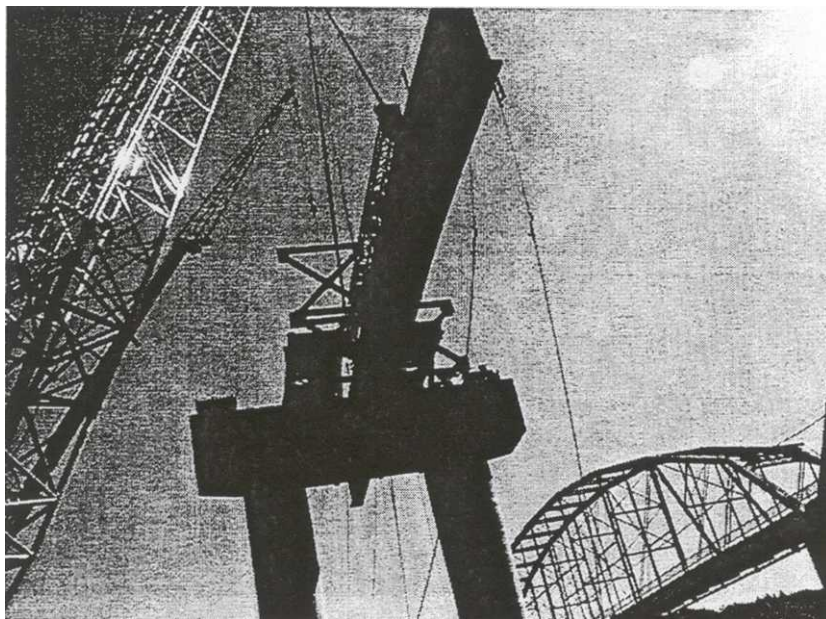


**Figure 53** Erection of cross-frame 26B

10/16/99 (Stage 4 of Bridge Erection Plans)

Girder G2 section 4 (G2-4) was erected, with the lifting truss and lifting lugs being used to lift the girder, as shown in figure 54. The lifting crane held G2-4 in place as the connections to cross-frames 26B, 27B, and 28B were made, which were previously attached to G3-4. A second crane then placed cross-frames in the following order, 25B, 24B, 23B and 29B, as G2-4 was held in place. The erection of cross-frames 25B, 24B, and 23B are shown in figures 55, 56 and 57, respectively. Once cross-frame 25B was placed, the lifting crane released G2-4 (Note: lifting crane is not holding G2-4 in figure 56).



**Figure 54** Lifting of G2-4

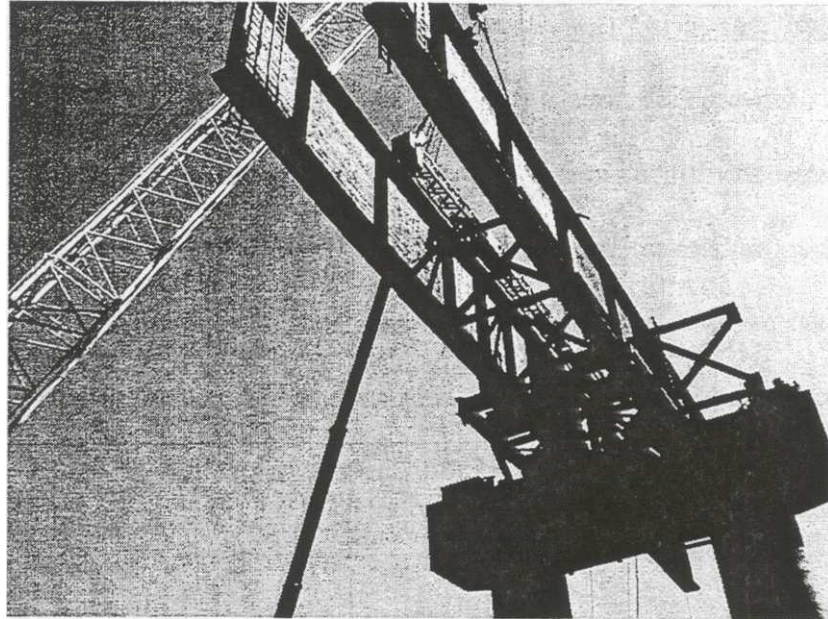


**Figure 55** Erection of cross-frame 25B

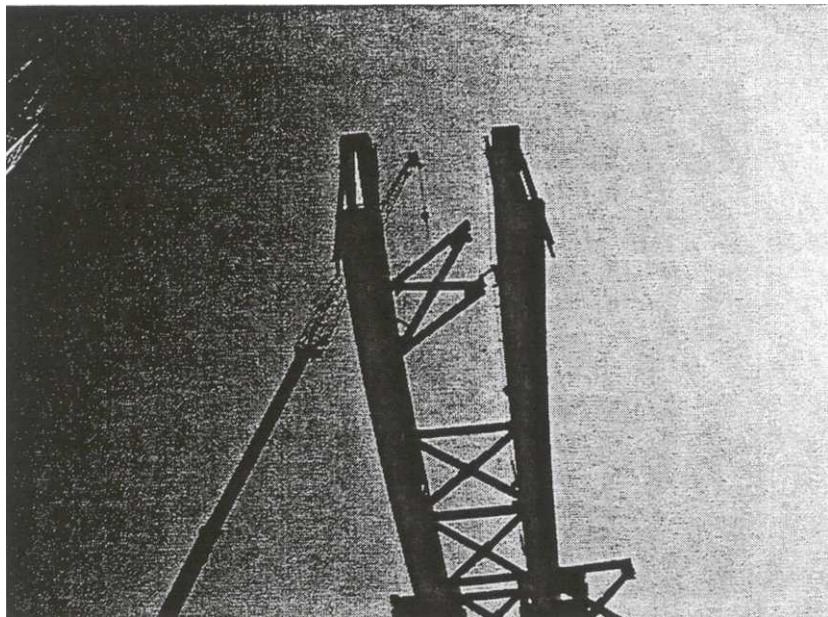


**Figure 56** Erection of cross-frame 24B

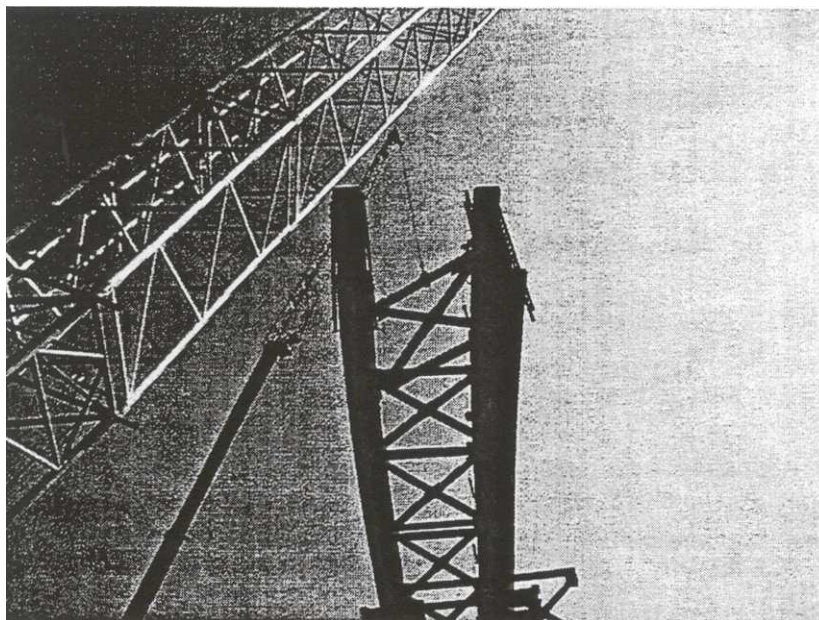


**Figure 57** Erection of cross-frame 23B

10/19/99 (Stage 4A of Bridge Erection Plans)

The lifting crane hoisted girder G3 section 3 (G3-3) using the lifting truss, with clamps attached to the top flange of the girder, as shown in figure 58. A cantilevered “come-along” assembly was also used, in order to prevent the girder from rotating as it was lifted. As can be seen in figure 59, it was necessary to place G3-3 in between previously erected section 2 and 4. This “drop-in” section created some difficulties in placing pins that were part of field-splices 2 and 3. A few alignment problems for both field-splices were noted, however the field-splices were atleast partially made at this point in the construction. Figure 60 shows field-splice 2, and figures 61, 62, and 63 show field-splice 3 for G3-3. Second and third cranes were attached to G3-3, as shown in figure 64, and the lifting crane was released. Based on the best information available to the researchers, it is unknown if the lifting crane held G3-3 in place overnight, or if the second and third cranes were left to hold G3-3 overnight, in order to stabilize the girder until the next workday.

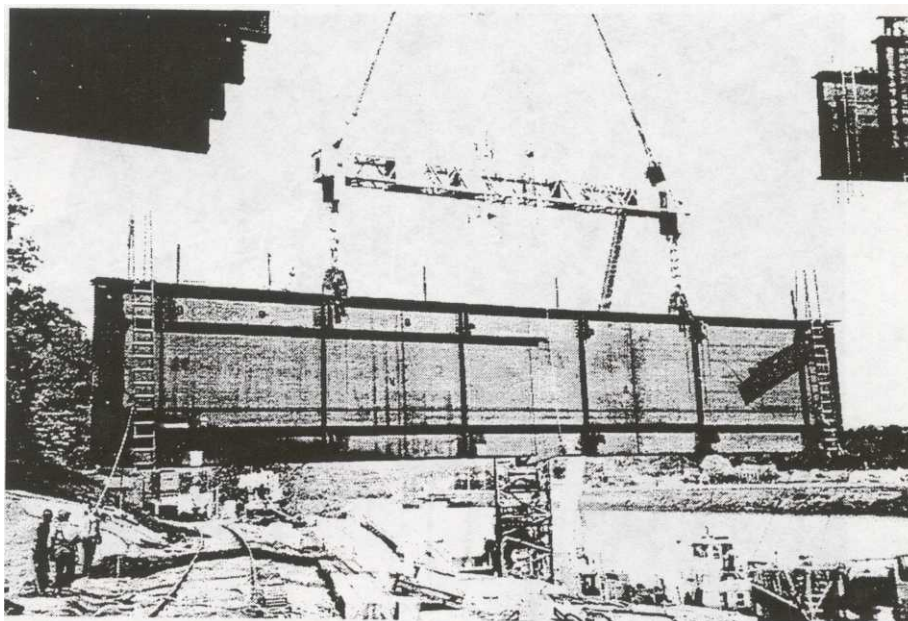


**Figure 58** Lifting of G3-3

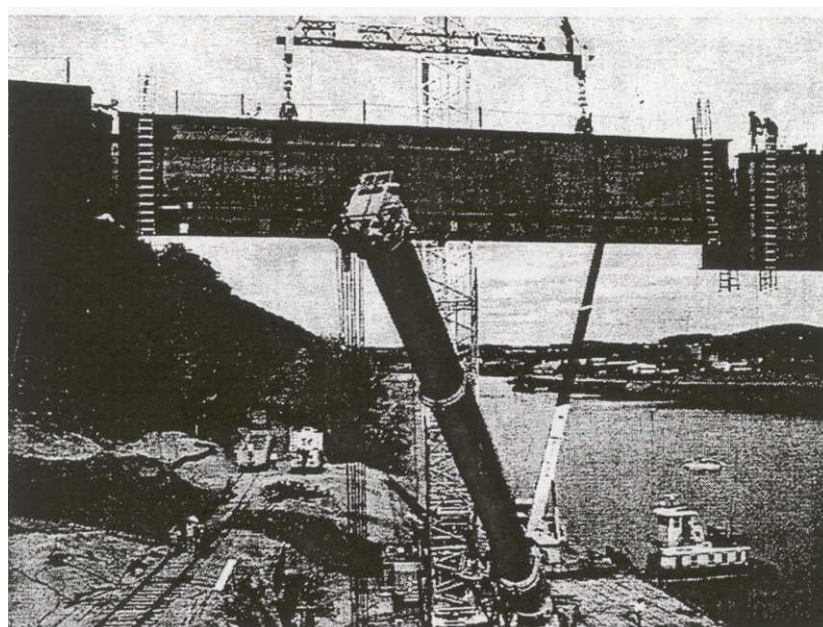


**Figure 59** Erection of G3-3

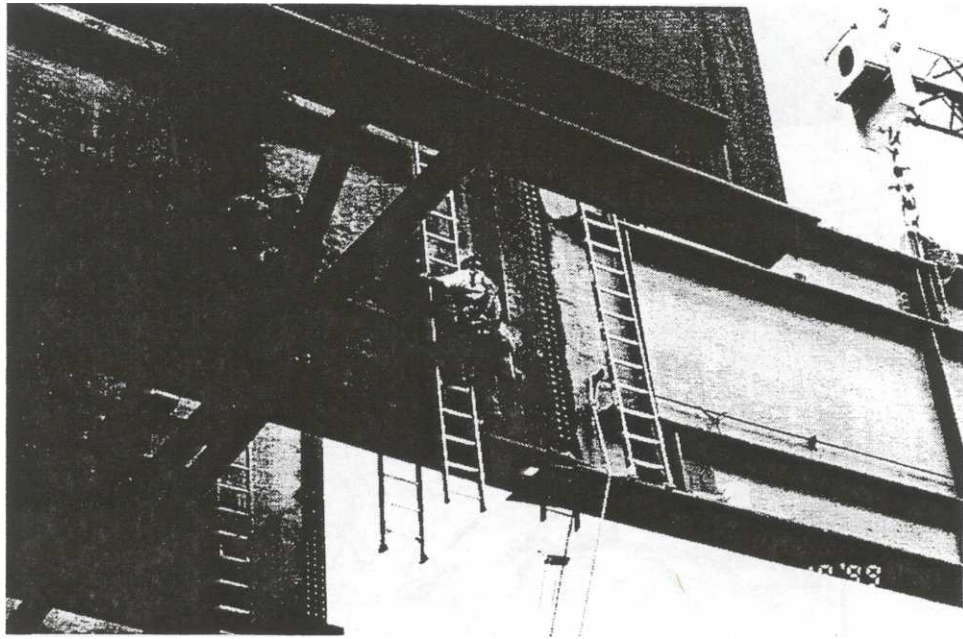


**Figure 60** G3-3; field-splice 2

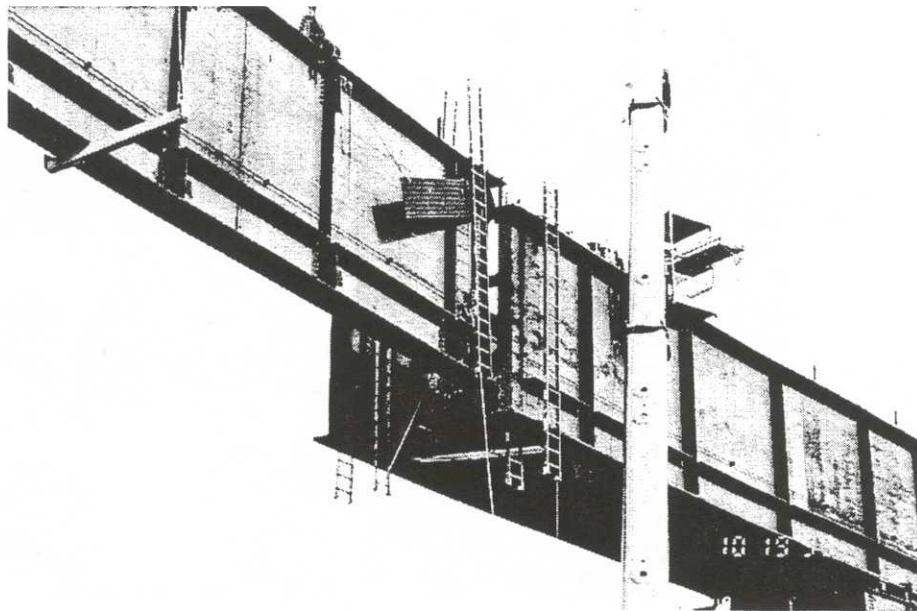


**Figure 61** G3-3; field-splice 3

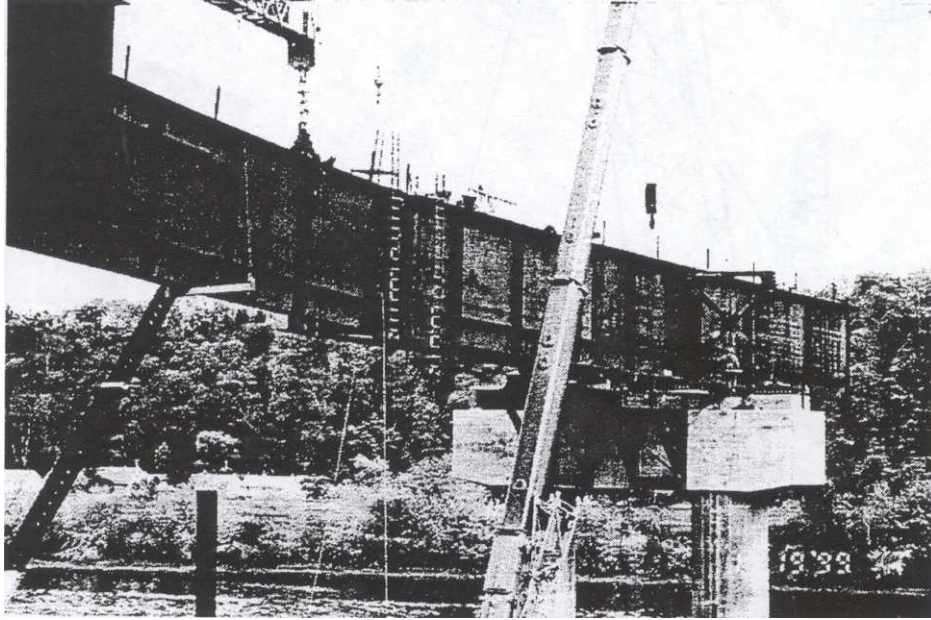


**Figure 62** G3-3; field-splice 3

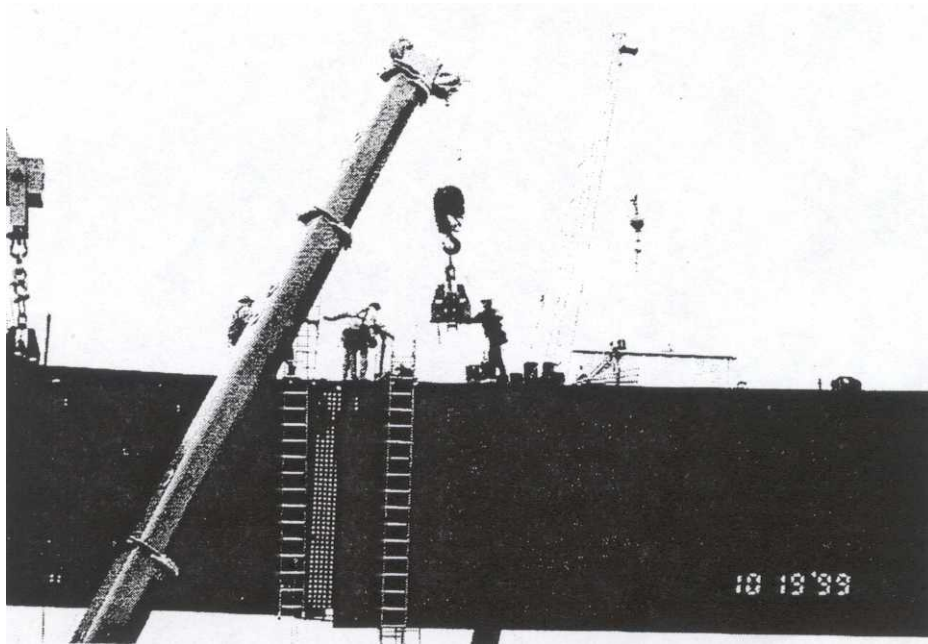


**Figure 63** G3-3; field-splice 3

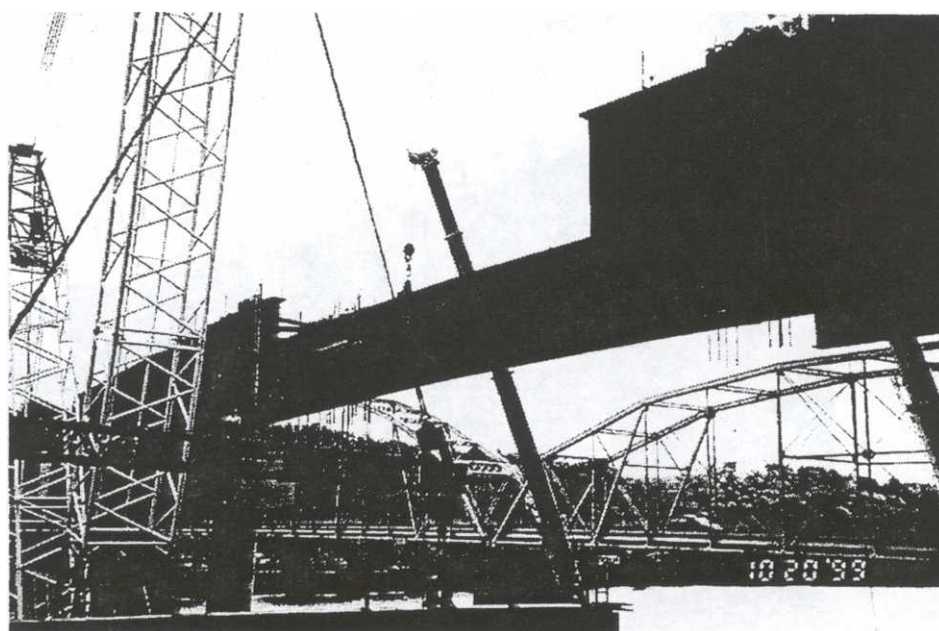


**Figure 64** G3-3 is held in place with second and third cranes (third crane is on right, barely visible)

10/20/99 (Stage 4A of Bridge Erection Plans)

The lifting crane lifted girder G2 section 3 (G2-3) using the lifting truss, with clamps attached to the top flange of the girder, as shown in figure 65. A cantilevered “come-along” assembly was also used, in order to prevent the girder from rotating as it was lifted. Figure 66 shows G2-3 being maneuvered in between sections 2 and 4, field-splice 2 is on the right. Field-splice 3 for G2-3 was then made, however extreme difficulties were encountered in trying to connect field-splice 2. Longitudinal jacking devices at abutment 1 were used to close the gap for field-splice 2. Figures 67 and 68 show construction personnel working on field-splices 3 and 2, respectively. Even though field-splice 2 was not fully made, a fourth crane placed cross-frames 17B, 18B, 19B, and 22B; the order of placement is unknown. Figure 69 shows GM being held in place by two cranes, G2-3 being held in place with the lifting crane, and the fourth crane that was used to erect the aforementioned cross-frames.

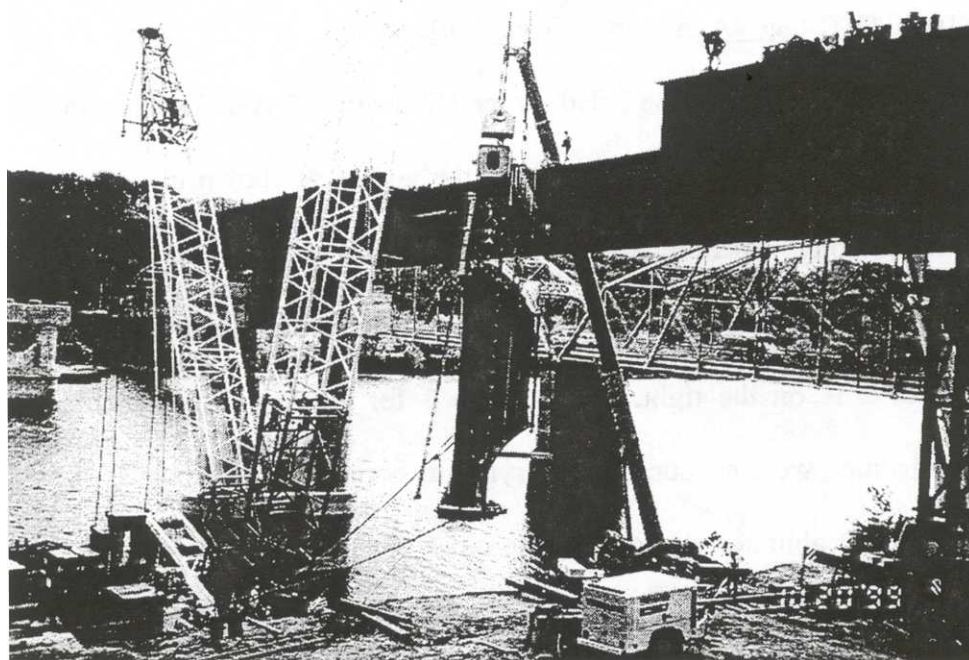


**Figure 65** Lifting of G2-3

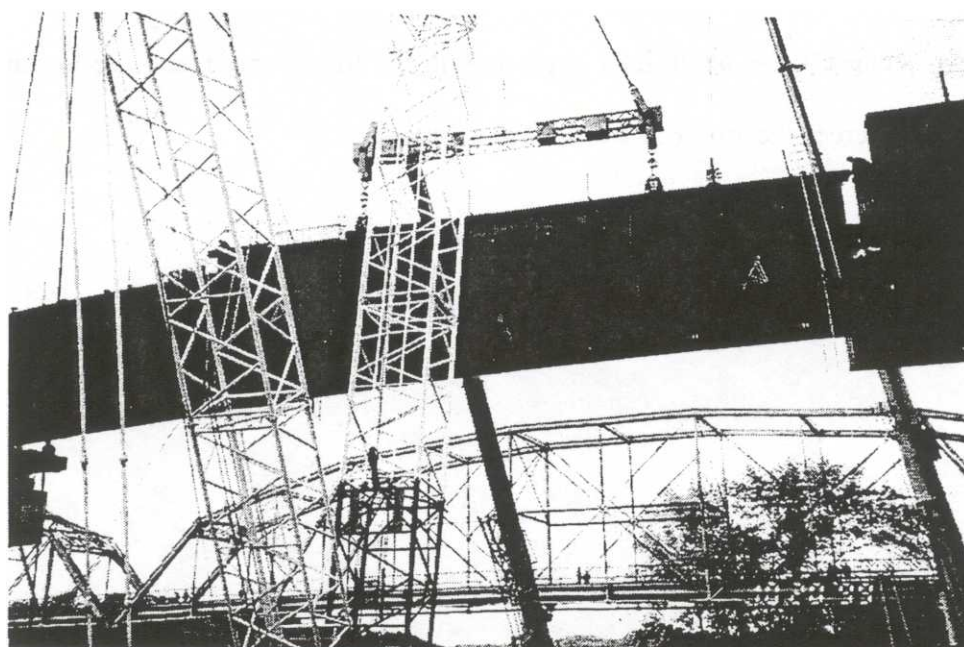


**Figure 66** Placing G2-3 in between sections 2 and 4

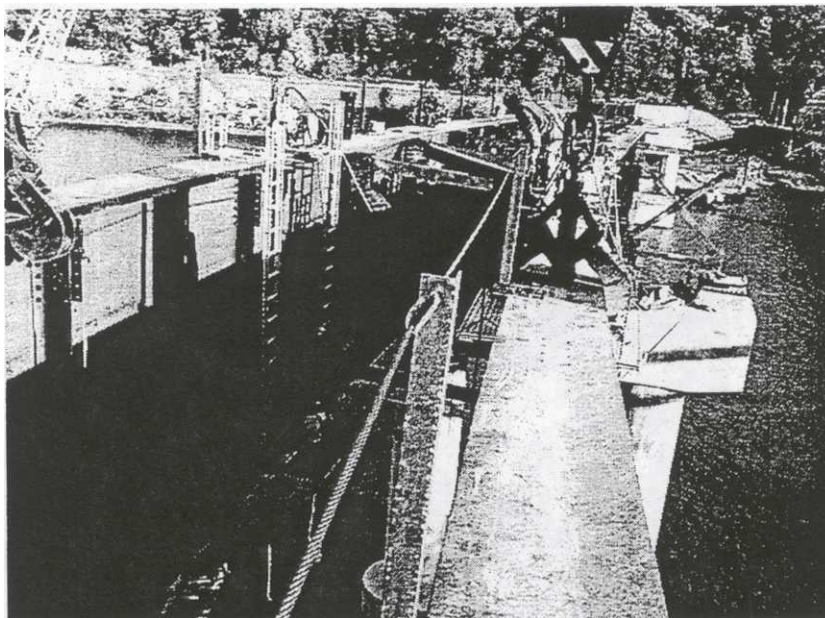


**Figure 67** G2-3, field-splice 3

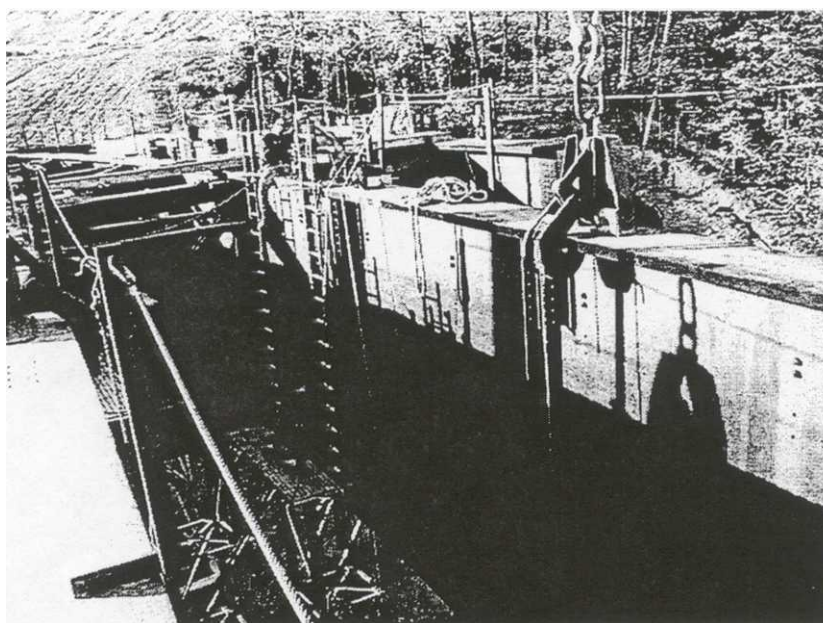


**Figure 68** G2-3, field-splice 2

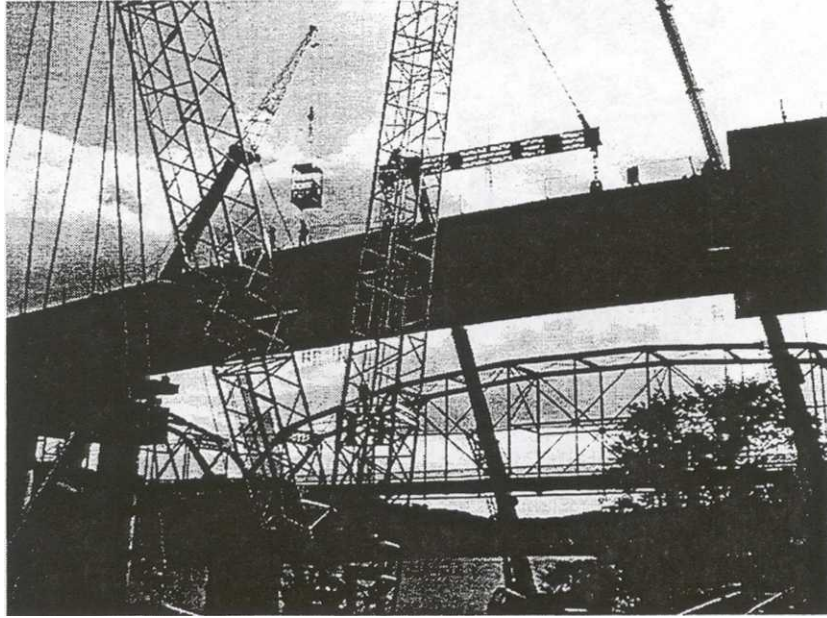


**Figure 69** Section 3; all four cranes holding girders and placing cross-frames

10/21/99 (Stage 4A of Bridge Erection Plans)

Cross-frames 20B and 21B were erected by the fourth crane. G2-3 was held in place by the lifting crane as the cross-frames were erected. Work continued on making field-splice 2 for girder G2. Field-splice 2 was not fully completed until 10/27/99.

10/25/99 (Stage 4A of Bridge Erection Plans)

The lifting crane was still attached to G2-3, as shown in figure 70 (this picture was taken on 10/25/99). Based on the available records, it is unknown if this lifting crane was released at anytime prior to this workday. Work continued on making field-splice 2 on girder G2, and cross-frame connections between G2-3 and G3-3 were tightened. Also, removal of pier 1 brackets began.

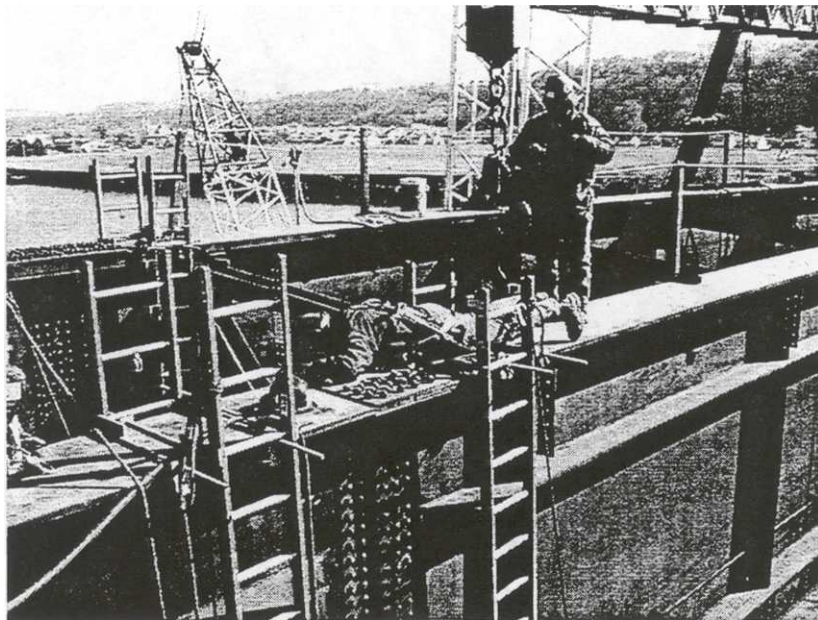


**Figure 70** 10/25/99, lifting crane still attached to G2-3

10/26/99 (Stage 4A of Bridge Erection Plans)

Pier 1 brackets were fully removed. Work on field-splice 2, girder G2, continued.

10/27/99 (Stage 4B of Bridge Erection Plans)

Field-splice 2, girder G2 was completed. Girder G4 section 4 (G4-4) was lifted and placed over pier 1, as shown in figure 71. The girder was lifted with the lifting truss and lifting lug combination. Previously erected cross-frame 27C was then attached to G4-4, over pier 1. As G4-4 was held in place by the lifting crane, a second crane erected cross-frames 23C, 24C, 25C, 26C, 28C, and 29C (the order of cross-frame erection is unknown).

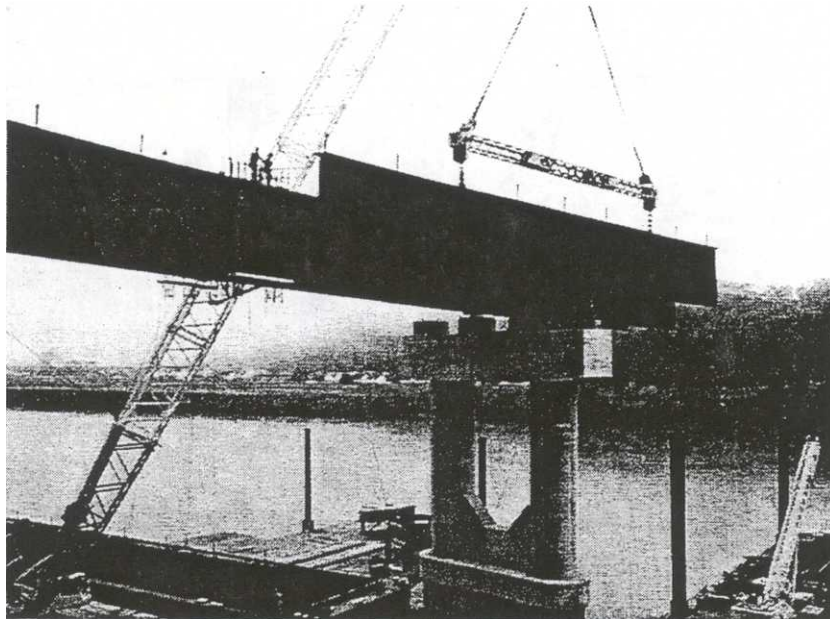


**Figure 71** Erection of G4-4

10/28/99 (Stage 4C of Bridge Erection Plans)

Girder G1 section 4 (G1-4) was lifted and placed over pier 1, using the lifting truss and lifting lugs attached to the top flange of the girder. Figure 72 shows G1-4 being lifted into place. As G1-4 was held in place by the lifting crane, the second crane, as shown in figure 73, erected cross-frame 27A then 28A. Cross-frames 29A and 26A were then placed by the second crane.

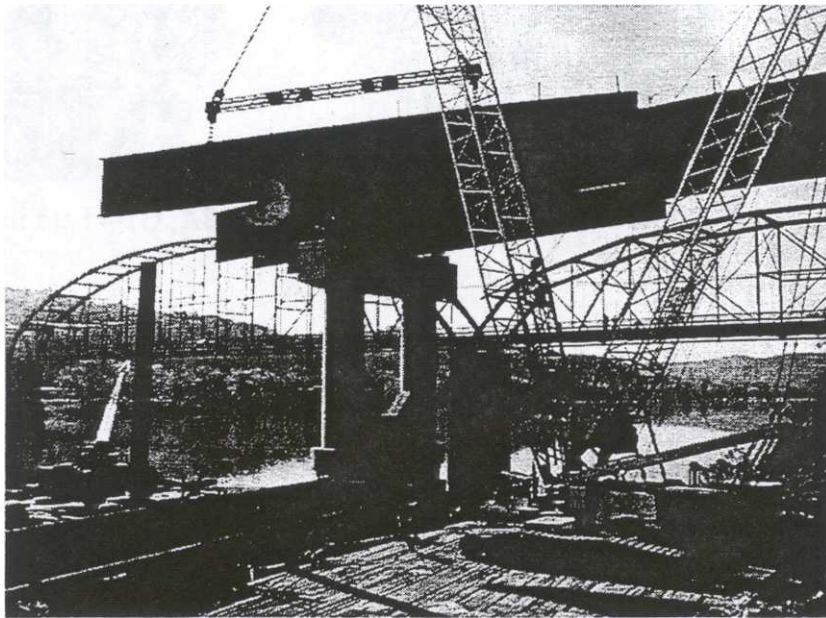


**Figure 72** Lifting of G1-4

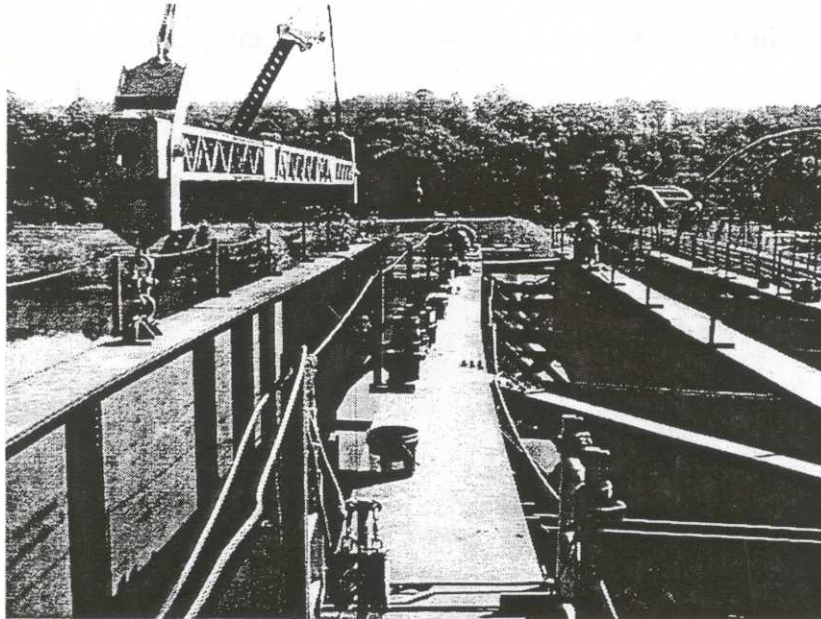


**Figure 73** Erection of cross-frame 28A, G1-4 held in place

10/29/99 (Stage 4C of Bridge Erection Plans)

Cross-frames 23A, 24A, and 25A were erected (it is unknown if the lifting crane held G1-4 in place as these cross-frames were erected).

10/30/99 (Stage 4B of Bridge Erection Plans)

Girder G4 section 3 (G4-3) was lifted using the lifting truss and clamps attached to the top flange of the girder. The “come-along” device was also used in the lifting of G4-3. G4-3 was “dropped-in,” between sections 2 and 4, as shown in figure 74. Field-splice 3 was made, and then field-splice 2 was closed using the jacking device at abutment 1. Field-splice 2 was made with little or no alignment problems. The lifting crane held G4-3 in place, as the second crane placed cross-frames in between G4-3 and G3-3. Cross-frames 17C, 18C, 19C, 20C, 21C, and 22C were erected by the second crane (it is unknown in which order these cross-frames were erected).

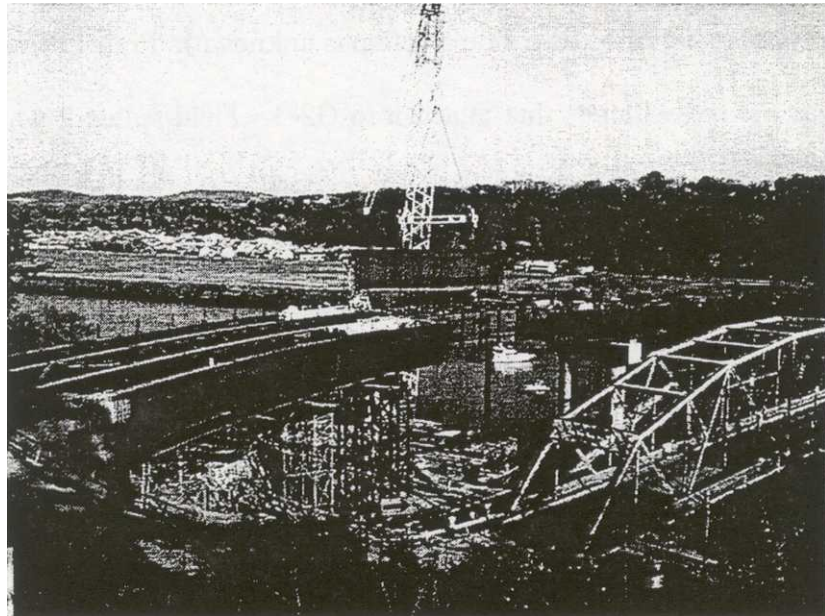


**Figure 74** Erection of G4-4

10/31/99 (Stage 4C of Bridge Erection Plans)

Girder G1 section 3 (G1-3) was lifted with the lifting truss, attached to the top flange of the girder via the lifting lugs, and a “come-along” device, as shown in figure 75. Alignment problems occurred as the field-splices were being connected. Field-splice 3 was made, and then problems developed as the girders did not align properly for field-splice 2. Again, a jacking device at abutment 1 was used to try to close the gap for field-splice 2. The lifting crane held G1-3 in place, as a second crane erected the cross-frames, which attach to G1-3 and G2-3, even though field-splice 2 had only been partially completed. Cross-frames 17A, 18A, 19A, 20A, 21A, and 22A were erected. It was noted, that some alignment problems also occurred in placing the cross-frames for this section (the order of cross-frame erection is unknown). Figure 76 shows G1-3 erected, as well as the cross-frames that attach it to G2-3. Field-splice 2 was not fully completed until 11/6/99.

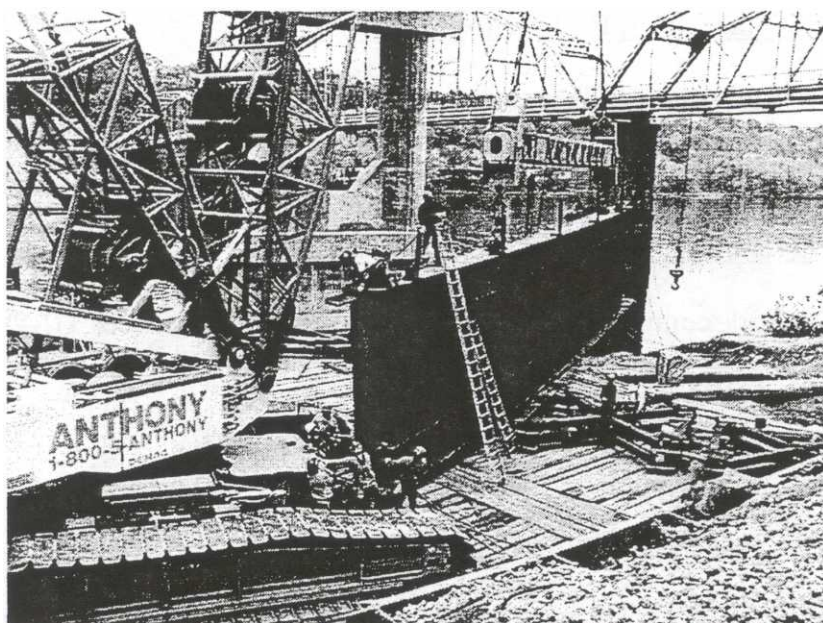


**Figure 75** Lifting of G1-3

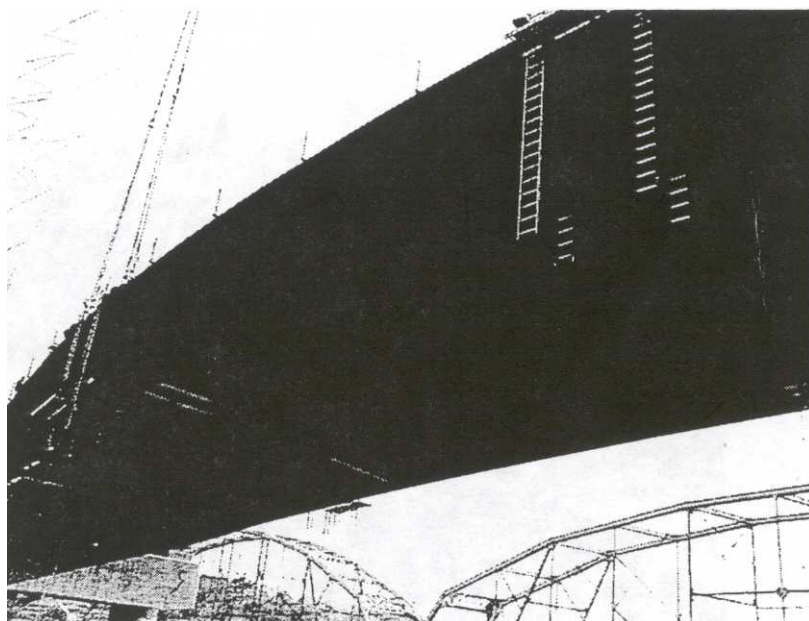


**Figure 76** G1-3 and section 3 cross-frames

11/4/99 (Stage 4C of Bridge Erection Plans)

Work continued on making field-splice 2, in between G1-2 and G1-3.

11/5/99 (Stage 4C of Bridge Erection Plans)

Work continued on making field-splice 2, in between G1-2 and G1-3. Removal of falsework 2A began.

11/6/99 (Stage 4C of Bridge Erection Plans)

Field-splice 2 was completed, in between G1-2 and G1-3. As shown in figures 77 and 78, falsework 2A was completely removed from underneath the structure.

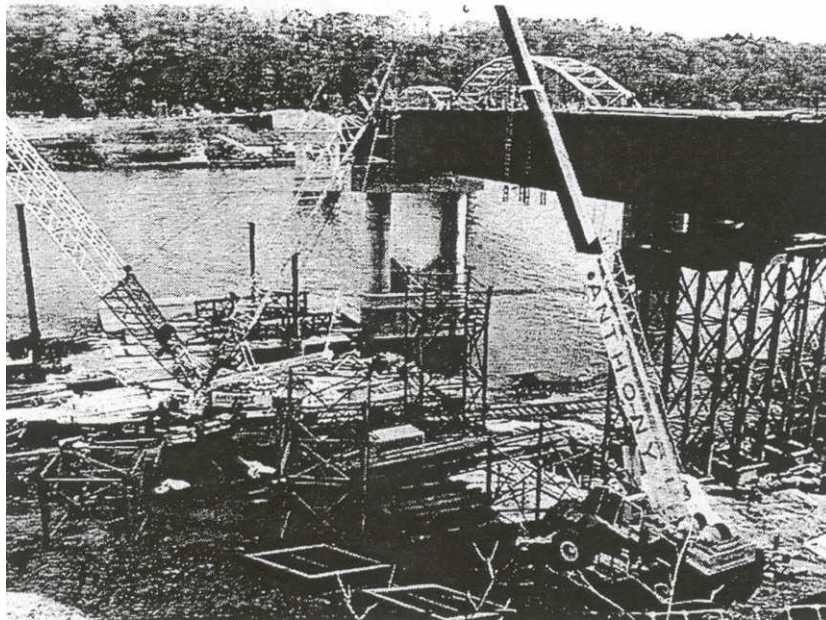


**Figure 77** Beginning the removal of falsework 2A

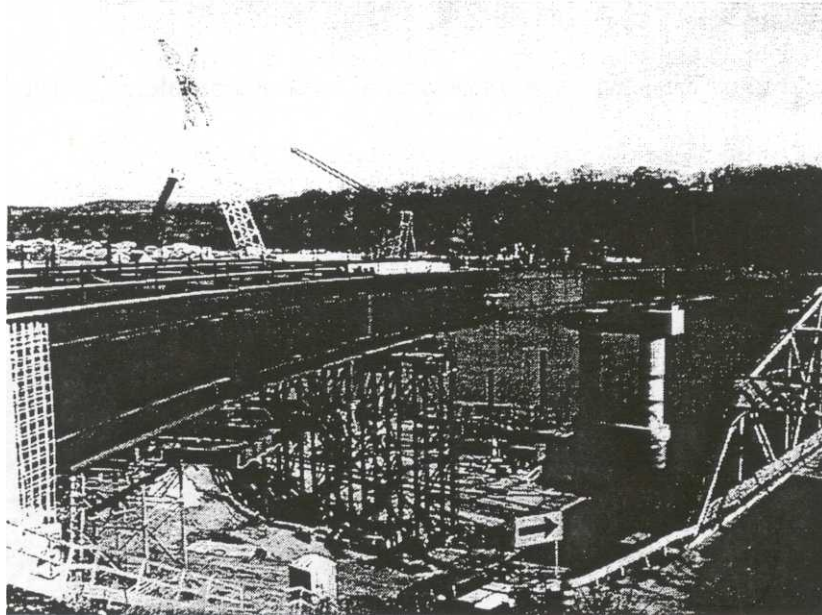


**Figure 78** Falsework 2A has been completely removed

12/8/99 – 12/9/99 (Stage 4A of Bridge Erection Plans)

Falsework 1 was removed from underneath section 1. (No pictures were available for this day.)

### Completed Curved Section of Bridge

Figure 79 shows a photograph of the completed curved steel superstructure section of the Ford City Bridge.

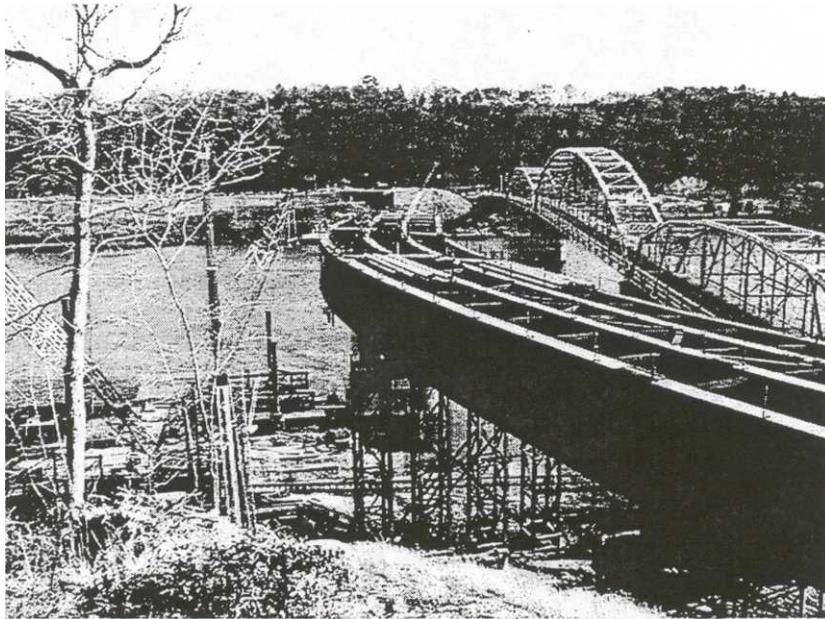


**Figure 79** Completed curved section of the Ford City Bridge

## 5.0 VERIFICATION STUDY

A validated finite element model is one of the best tools available to study the behavior of a complex structural system. Once modeling techniques are verified with an actual structural system, the same modeling techniques can be used to predict structural responses for which no experimental data exists. It is extremely important to verify results from a finite element analysis with experimental results in order to ensure the reliability and accuracy of the finite element model. Therefore, prior to developing the finite element model for the curved span of the Ford City Bridge, it is necessary to develop modeling techniques that display favorable agreement with experimental data found in the literature. Since a minute amount of field data was obtained during the erection of the curved span of the Ford City Bridge, it is required that previous experimental results from a curved steel I-girder erection study be used as a basis for this verification study. The experimental data from the Curved Steel Bridge Research Project (CSBRP) erection study, as presented by Linzell, is suitable for the verification of the modeling techniques used in the present research (Linzell 1999). A detailed synopsis of the CSBRP erection study is presented as a component of the literature review in the current report.

As part of the current section, a brief summary of the CSBRP erection study test frame is presented, and the experimental results of the ES1-4 erection study are defined (Linzell 1999). The finite element model of the CSBRP ES1-4 study, created as part of the present research follows (including detailed explanations of modeling techniques

employed). Lastly, the experimental results of the CSBRP ES1-4 study and the analytical results of the finite element verification model are compared.

### 5.1 CSBRP ES1-4 Erection Study Test Frame Description

The entire CSBRP bridge, illustrated in figure 80, consists of three concentric I-girders, spaced at approximately 8.75 feet (2.67 meters), and each having a depth of 48 inches (1.22 meters). The ES1-4 erection study includes girders G1 and G2, and cross-frames 1L, 7, and 1R only. Girders G1 and G2 were designed in order to guarantee they remained elastic for all of the CSBRP erection and bending component tests. Table 4 provides the applicable girder data for ES1-4 erection study.

As shown in figure 80, for each girder, transverse stiffeners were placed as single stiffeners at, and in between, the cross-frames. Back-to-back stiffeners were placed at the end supports, and at load points used for the bending component tests. The radially orientated abutment supported the experimental bridge so that the structure was elevated approximately 6.5 ft (2 m) above the floor. Spherical bearings and Teflon pads were used to minimize frictional forces and provide the desired degrees of freedom at the abutments. Guided bearings at both ends were used to prevent radial translation, and a tangential support frame at the one end restricted G2's movement. The tangential support frame was pinned at the neutral axis of girder G2. The cross-frames consisted of "K" type cross-frames, as shown previously in the literature review section. All members of

the cross-frames were fabricated from 60 ksi yield steel, and were of tubular cross-section, with a diameter of 5 in and a wall thickness of 0.25 in.

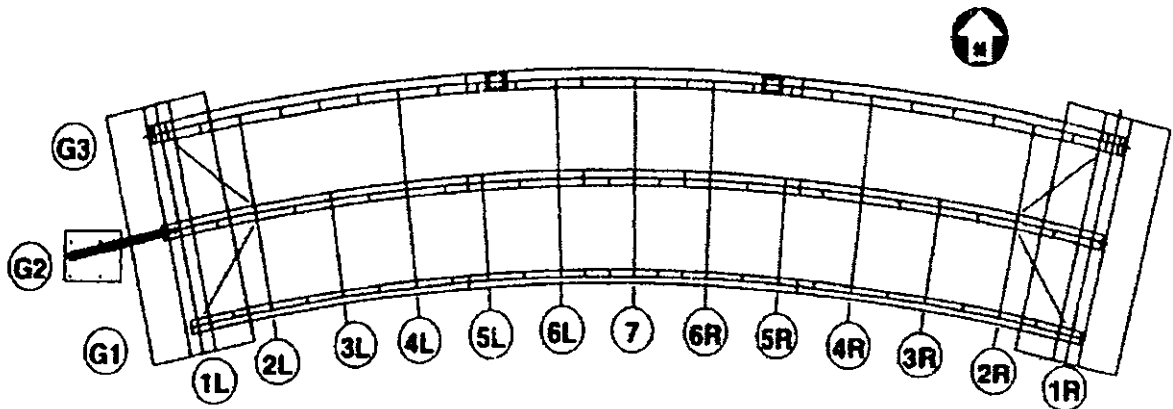


**Figure 80** CSBRP experimental bridge (Linzell 1999)

**Table 4** CSBRP Bridge data

<b>Girder</b>	<b>Radius</b>	<b>Spans</b>	<b>Yield Stress</b>	<b>Flange Width</b>
<b>G1</b>	191.25 ft (58.3 m)	86ft (26.2 m)	50 ksi	16 in
<b>G2</b>	200 ft (61.0 m)	90 ft (27.4 m)	70 ksi	20 in

It is important to note that girder G2 was incorrectly cambered during the fabrication process. Therefore, girder G2 was re-cambered using “V” heats on particular sections of the web, in order to obtain the correct camber.

Reactions are measured using load cells at the abutment supports and at intermediate shoring locations. Vibrating wire gauges are used to measure the strain at given locations on the girders. Girder deformations are monitored at set increments along

the top and bottom of the girder cross-section using standard displacement and rotation transducers, and also employing the use of laser and total station systems.

## **5.2 CSBRP ES1-4 Erection Study Experimental Results**

The ES1-4 experimental erection study began with the structure, girders G1, G2 and cross-frames 1L, 1R, and 7, in the “no-load” position, as predicted by preliminary finite element analyses. Shoring was placed below both girders at cross-frame locations 3L, 5L, 7, 5R, and 3R in order to achieve the “no-load” state. The “no-load” state was achieved once the load cells at the shoring locations measured the same reactions as predicted by the finite element results (Linzell 1999). Once the “no-load” condition was reached, shoring under G1 at cross-frame locations 3L, 5L, 5R, and 3R was removed, and the ES1-4 erection test began.

The shoring under G1 at cross-frame 7 was then lowered incrementally, until it was fully removed. The load cell at the shoring measured a reaction of approximately 12 kips at the beginning of the test and was reduced in a series of steps to 2 kips by increments of 2 kips for each step; then reduced by 1 kip to a load reading of 1 kip; then reduced by 0.5 kips twice, at which time the shoring was completely removed. The shoring was then replaced, and incrementally raised, following the same series of steps in which it was lowered. Reactions at the abutments and at cross-frame seven were measured at each shoring removal step. The replacing sequence of the shoring is not germane to the present verification study.

From data presented by Linzell, figure 81 shows the reactions at the abutments and cross-frame 7 shoring location of G1, as the G1 mid-span shoring was removed (Linzell 1999). The measured vertical displacement at mid-span of G1 was approximately 0.35 inches, after the G1 mid-span shoring was completely removed. It was noted by Linzell that minimal mid-span girder rotation existed when G1 was in the fully deflected position (Linzell 1999).

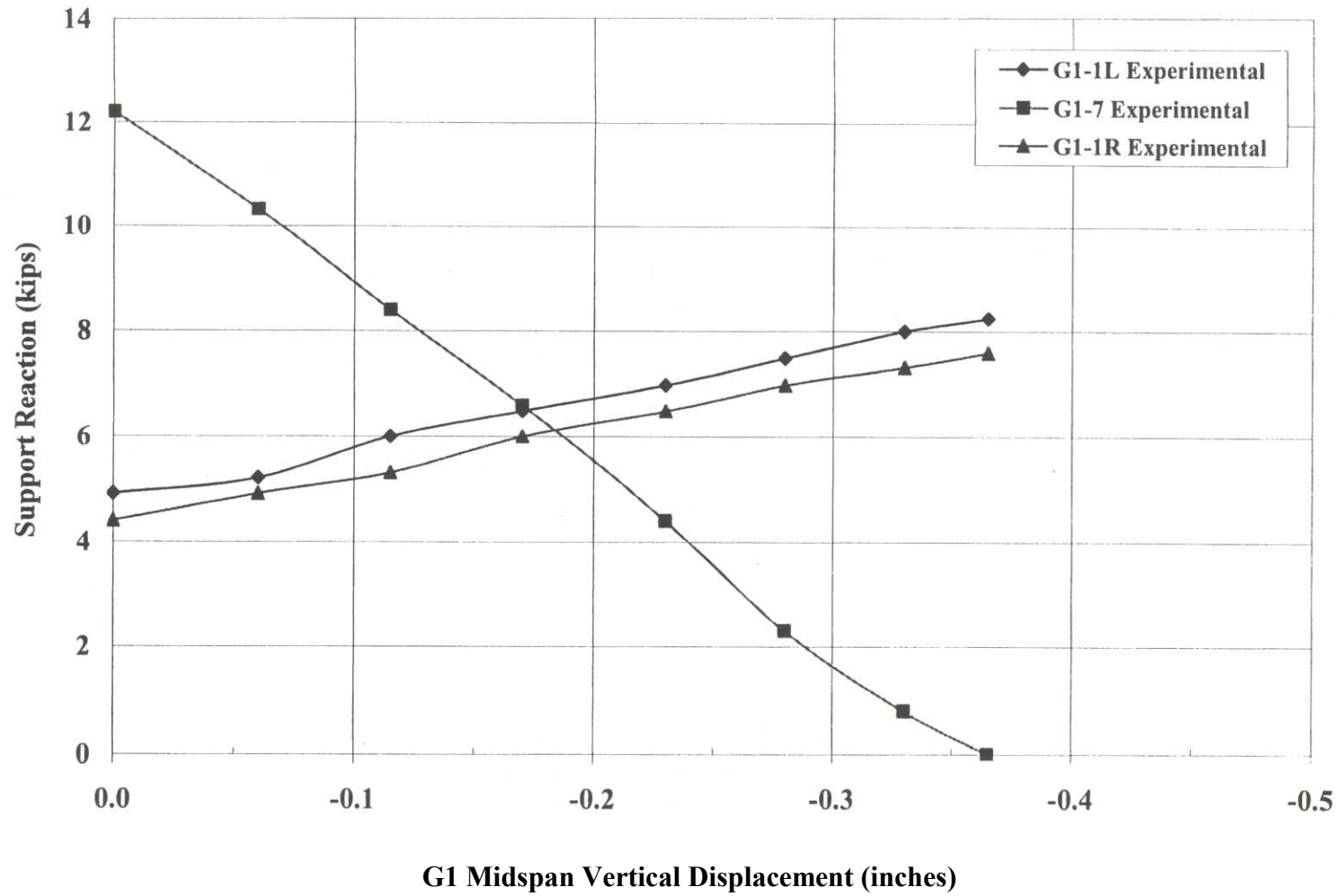


**Figure 81** ES1-4 experimental results; G1 midspan displacement vs. reactions (Linzell 1999)

### 5.3 ES1-4 Erection Study Finite Element Model

An extremely detailed finite element model of the ES1-4 erection study for the CSBRP experimental structure is created with the commercial finite element program ABAQUS. The finite element model, shown in figure 82, considers nonlinear geometric effects, but does not consider material nonlinearity. Due to the geometric complexities of a curved I-girder, nonlinear geometric effects are thought to be important and are thus considered in the analysis. Additionally, given that the structure is designed to remain elastic throughout the erection study, effects of nonlinear material properties are not considered in the analysis; the consideration of the nonlinear material effects would greatly increase the amount of computational resources needed. The analysis procedure of the finite element model replicates the actual shoring removal sequence.

#### 5.3.1 Finite Element Model Element Characteristics

After much consideration and mesh refinement, a very dense mesh of shell elements is utilized to model girders G1 and G2. The flanges, webs, and transverse stiffeners of girders G1 and G2 are modeled using ABAQUS S4R shell elements. A very dense mesh, as shown in figure 83, is used since the ES1-4 tests bridge is serving as a verification study, to ensure a similarly dense model can be effectively employed for the Ford City Bridge erection study. It is desired to keep a consistent number of rows of

elements across the top and bottom flange, for both the verification study and Ford City Bridge analysis.

A length to width aspect ratio of slightly less than 2 to 1 is maintained for the shell elements used for the flanges, and near 1.5 to 1 for the webs and transverse stiffeners in both girders. (Length for the flanges is regarded as along the tangential length of the flange; and length for the webs and stiffeners is considered to be the vertical length.) A lesser amount of available computational resources is required when using an aspect ratio of near 2 to 1, or 1.5 to 1, in lieu of 1 to 1. The amount of available computational resources is of vital importance in light of the anticipated model size of the Ford City Bridge; therefore it is necessary to verify that an aspect ratio other than 1 to 1, but less than 2 to 1, is satisfactory via this verification study.

Taking into consideration various trial shell element meshes, an element mesh was chosen that fit the geometric constraints. Girder G1 is modeled with 16 elements across the flanges, and 18 elements vertically along the web and transverse stiffeners. Girder G2 is modeled with 20 elements across the flanges, and 18 elements vertically along the web and transverse stiffeners.

The cross-frames at the abutments and mid-span, 1L, 1R and 7, respectively, are modeled using ABAQUS B31 beam elements. Each member of the cross-frame is explicitly modeled, and connected by the adjoining end nodes to form the “K” type cross-frame. The cross sectional data for these elements is consistent with what was used in the experimental structure, such as moment of inertia and cross-sectional area. The cross-frames are attached to the girders at their respective locations, using the ABAQUS MPC

TIE command. For simplicity sake, cross-frame connection plates (gusset plates) were not explicitly modeled.

ABAQUS unidirectional GAP elements are used at the abutments and shoring supports for both girders, in conjunction with the prescribed boundary conditions. The unidirectional GAP elements permit the girders to “lift-off” the supports during the analysis, therefore simulating actual field type conditions associated with the tendency of curved I-girder “roll.”

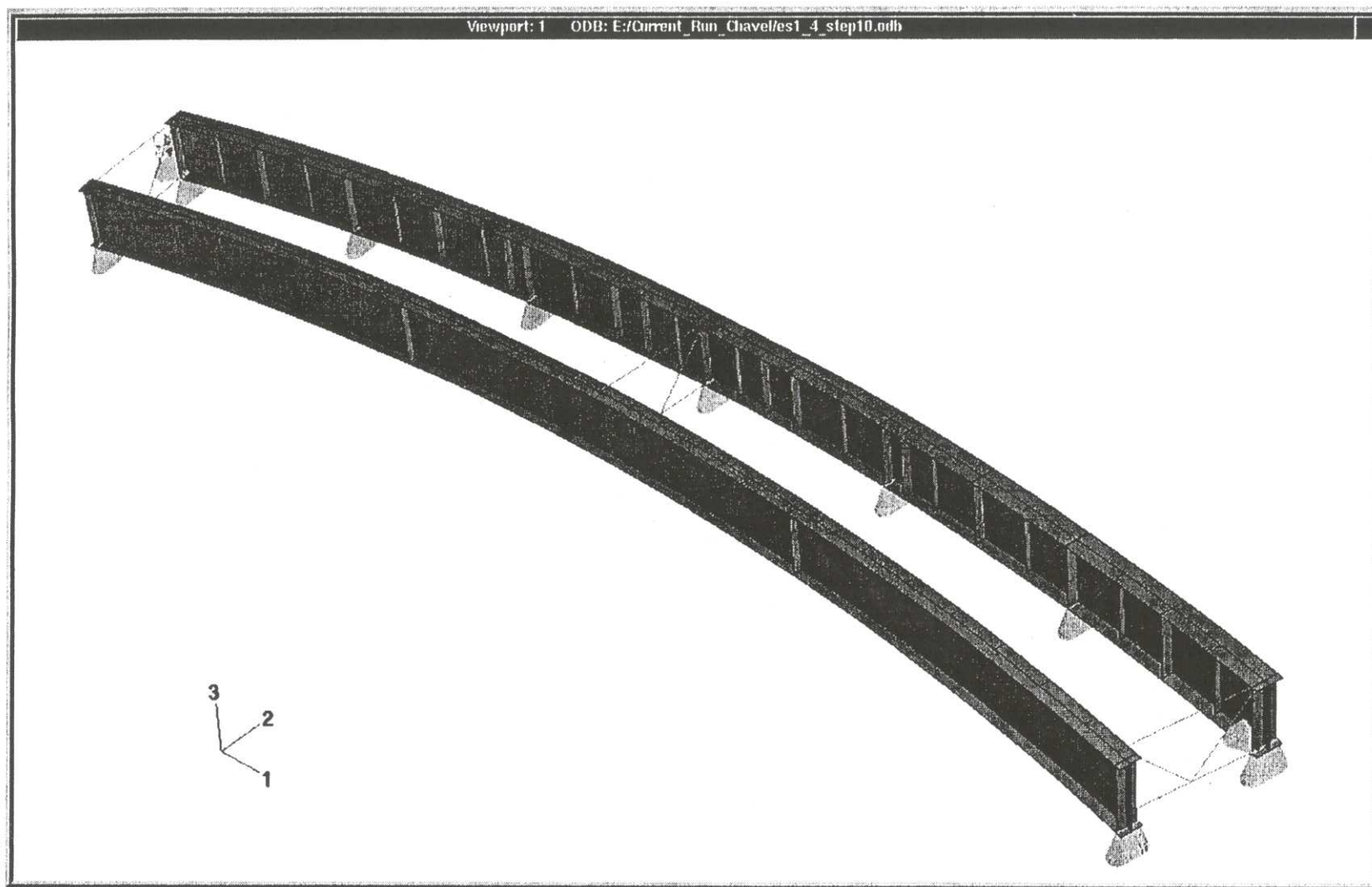


**Figure 82** Verification study finite element model

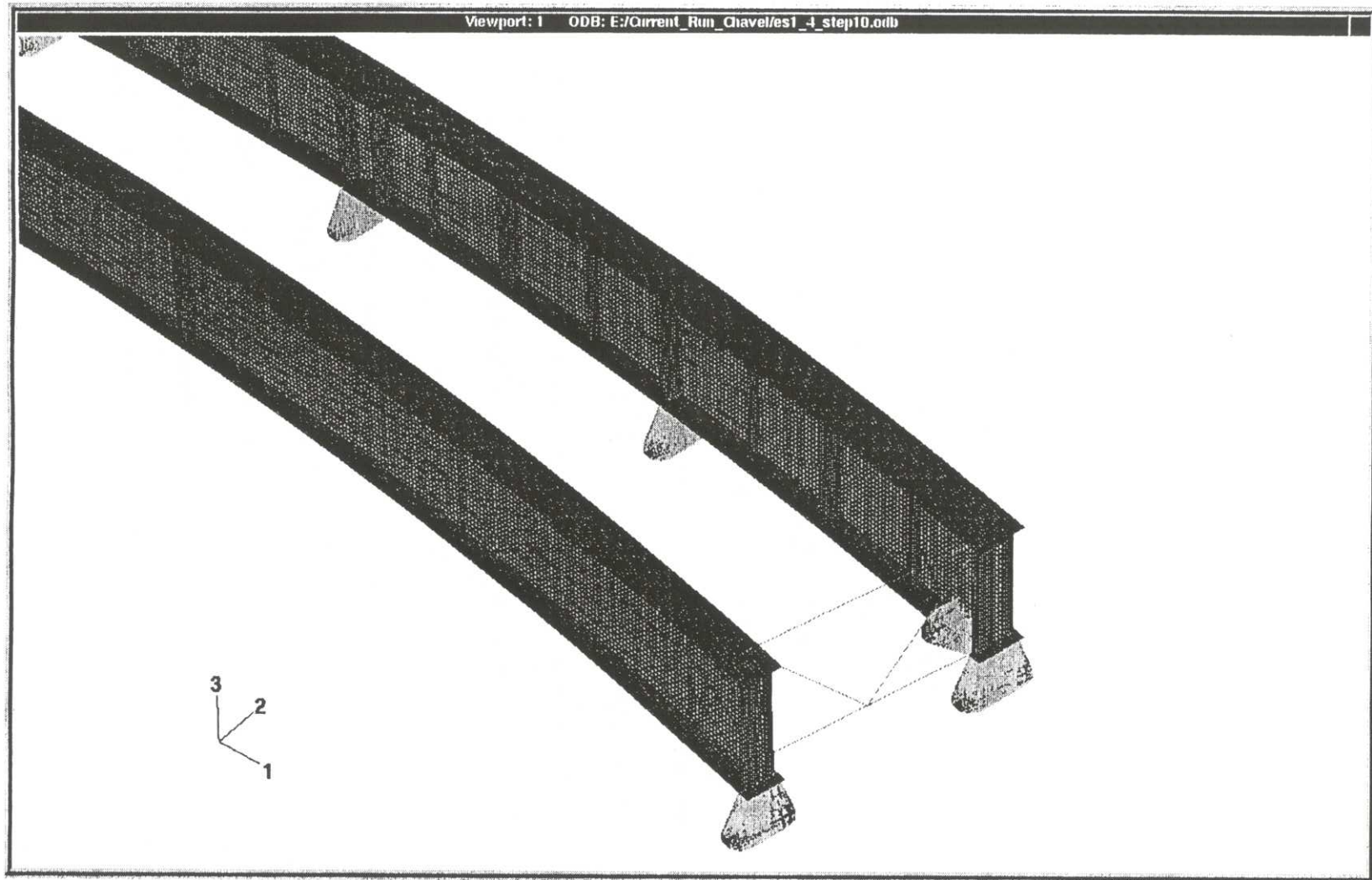


**Figure 83** Verification study finite element mesh (close-up)

### 5.3.2 Boundary Conditions

As stated previously, spherical bearings are used at both abutment supports of girder G1. Theoretically spherical bearings will provide for rotation and translation in any direction except vertically, and consequentially the abutment support locations of girder G1 need only be restrained in the vertical (u3) direction. Additionally, unidirectional GAP elements, with a minute length, are used in the vertical direction at the G1 abutment supports in order to permit “lift-off”. Therefore to simulate the abutment support, the nodes that correspond with the GAP elements along the bottom flange, at the abutment bearing stiffeners, are restrained in the vertical direction.

Guided bearings were employed at the abutment supports of girder G2, therefore not permitting vertical and radial (out-of-plane) translation. Again, ABAQUS unidirectional GAP elements are used in the vertical direction at these locations. Not only are the abutment location nodes restrained as in the case of girder G1, but they are also restrained in the radial direction. Also, the support frame connected to G2 at the girder neutral axis via a single hole, at the abutment, did not allow any translation in the tangential direction. To simulate the support frame condition, the node at girder G2's neutral axis is restricted from translation in the tangential direction.

The intermediate shoring locations under girders G1 and G2 are also replicated in the finite element model. At the shoring locations, nodes along the bottom flanges are restrained in the vertical direction, and ABAQUS unidirectional GAP elements are used.

Therefore, vertical translation downward is prevented, and the girders are capable of “lift-off.”

### **5.3.3 Loading Conditions**

Self-weight of the girders and cross-frames are the only loads considered for the ES1-4 verification study. A standard structural steel density of  $7,850 \text{ kg/m}^3$  ( $490 \text{ lbs/ft}^3$ ) is applied to the girder shell elements, to account for the girder weights. Cross-frame weights are divided into four equal point loads, with each load applied to the respective top and bottom cross-frame connection points on the girders. Only the cross-frame lengths and sizes are known, therefore, the total load for a single cross-frame was increased by 10% to account for the large gusset plate connections. Otherwise, no other external loads are applied to the finite element model.

### **5.3.4 Other Modeling Considerations**

It should be noted that the finite element modeling undertaken as part of this verification study did not consider the effect of residual stresses and the connection details associated with the cross-frames. Furthermore, the geometric imperfection due to the incorrect cambering and re-cambering of girder G2 is not recreated.

## 5.4 Discussion of Verification Results

Favorable agreement is shown between the results of the experimental ES1-4 study and the finite element results completed as part of this verification study. G1 mid-span deflection / abutment reaction response, for both experimental and analytical studies, is shown in figure 84. The curves agree favorably, but not exactly. Some of the disagreement may be due to the discrepancy with the camber of girder G2, or due to the exclusion of cross-frame connection plates. Illustrations of the resulting longitudinal strains in the top and bottom flanges of girder G1, at maximum G1 mid-span displacement, are shown in figures 85 and 86. It is evident that the finite element model predicts the flange strain of the subject structure adequately. Figures 87 and 88 illustrate the undeformed and entirely deformed finite element model. Inspection of the subject figures shows that the cross-frame seven connection between G1 and G2 prevents extreme rotation of girder G1 at mid-span.

Given that this verification study is employed to identify the most efficient and accurate modeling techniques to be used for the finite element modeling of the Ford City Bridge, agreement between the experimental and analytical data is sufficient to show that the modeling techniques developed are useful for the present study.

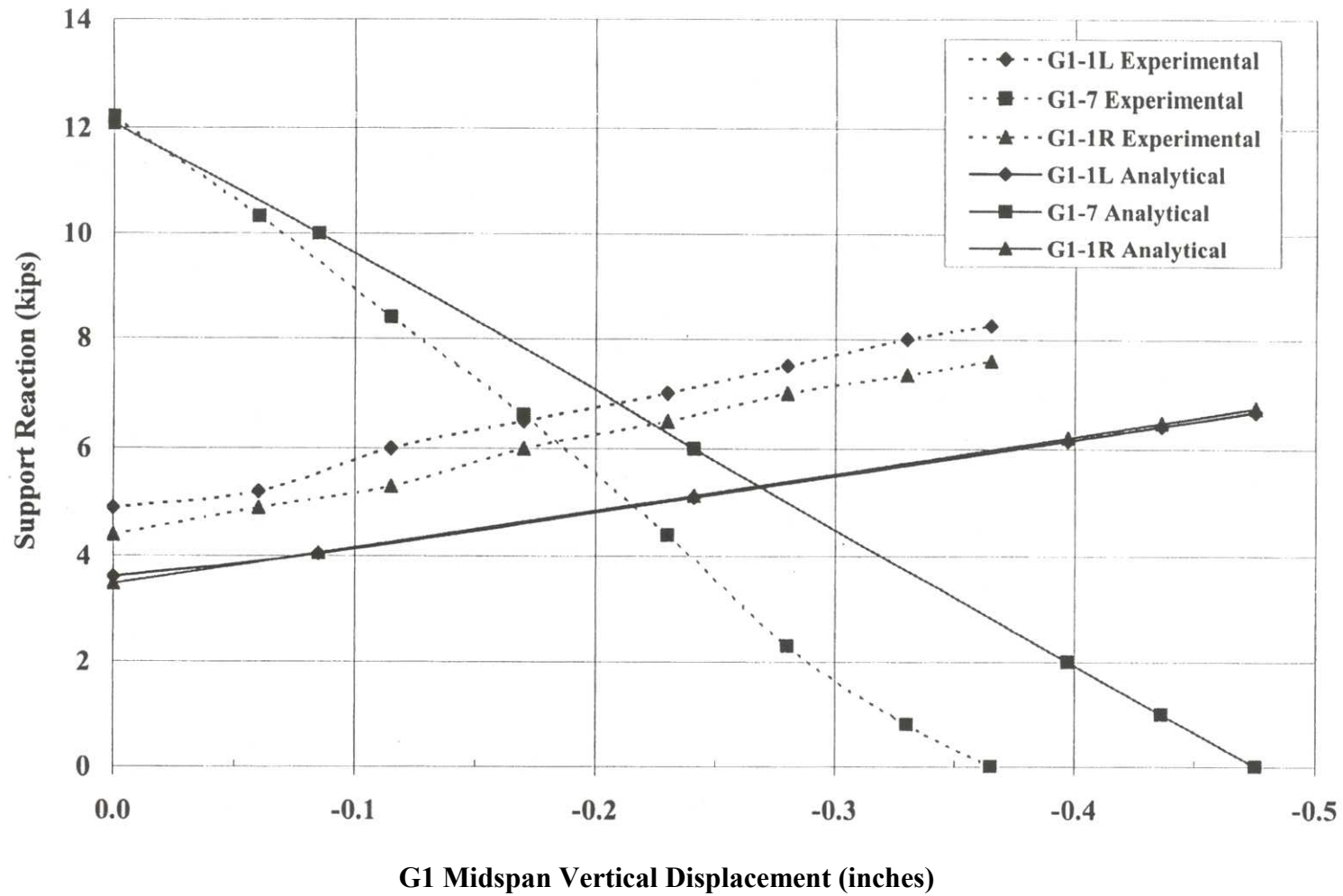


**Figure 84** ES1-4 Experimental and analytical results; G1 midspan displacement vs. reactions

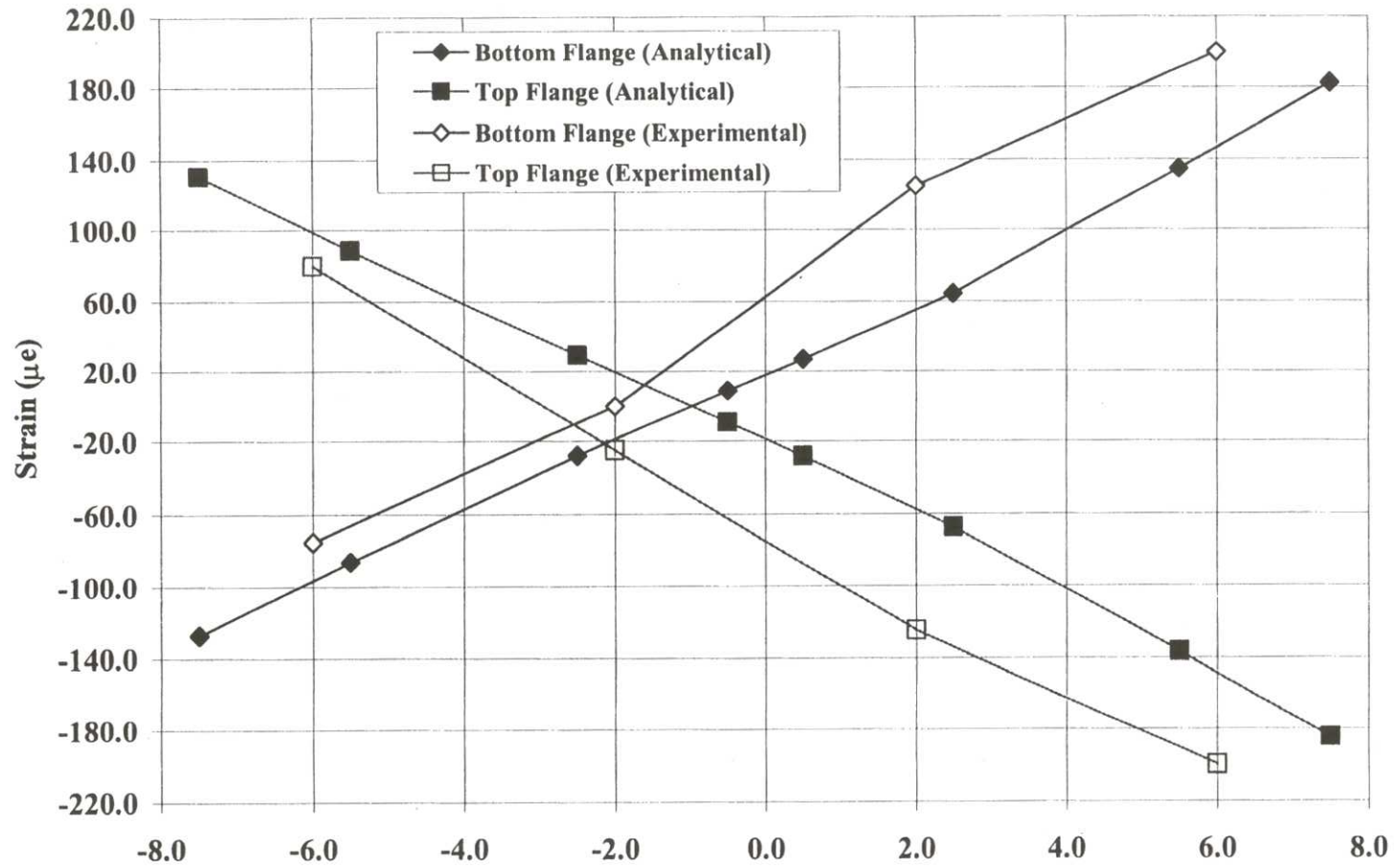


**Figure 85** ES1-4 study; G1 top and bottom flange longitudinal strains at cross-frame 7 at maximum G1 midspan displacement

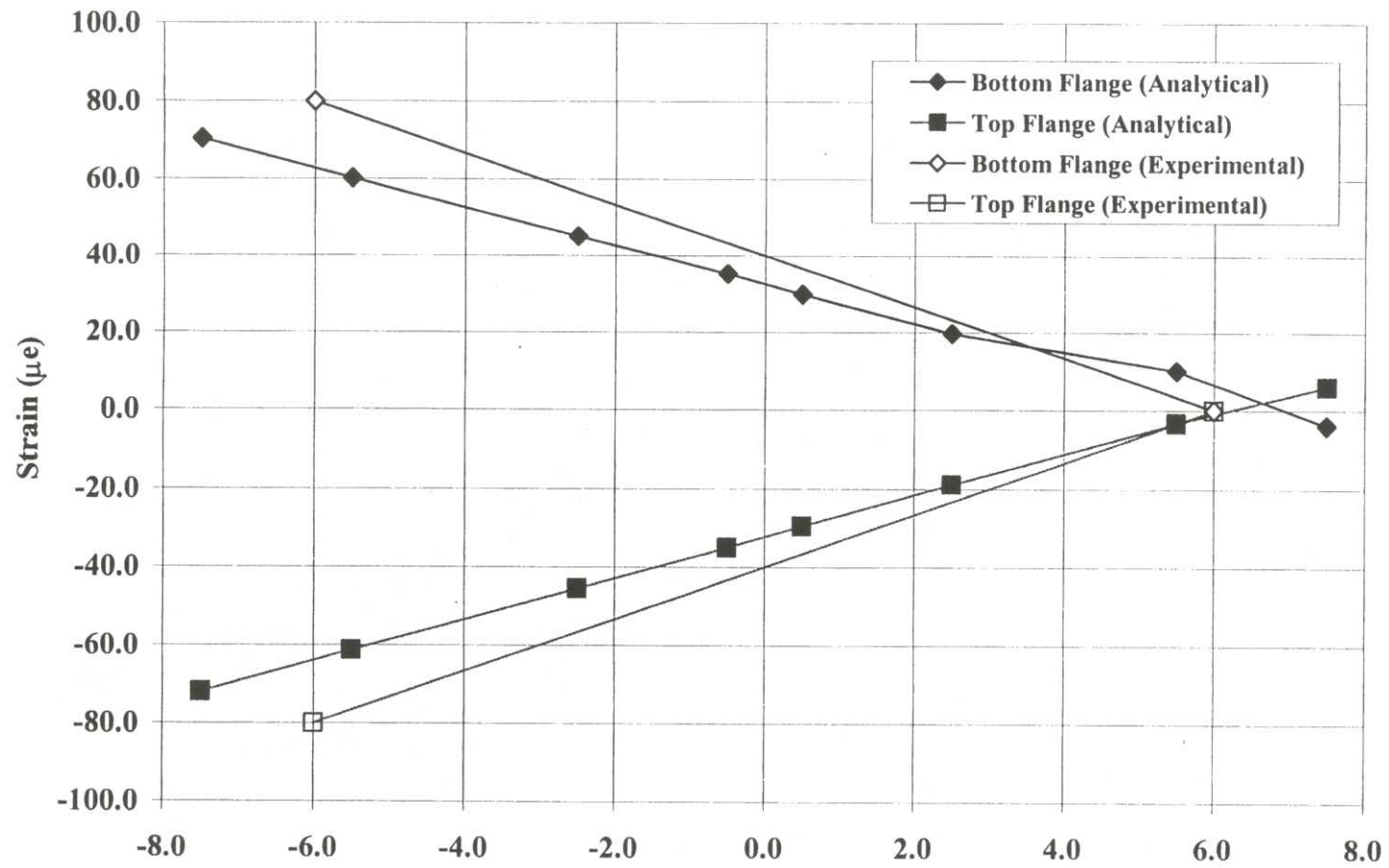


**Figure 86** ES1-4 study; G1 top and bottom flange longitudinal strains at cross-frame 5R at maximum G1 midspan displacement

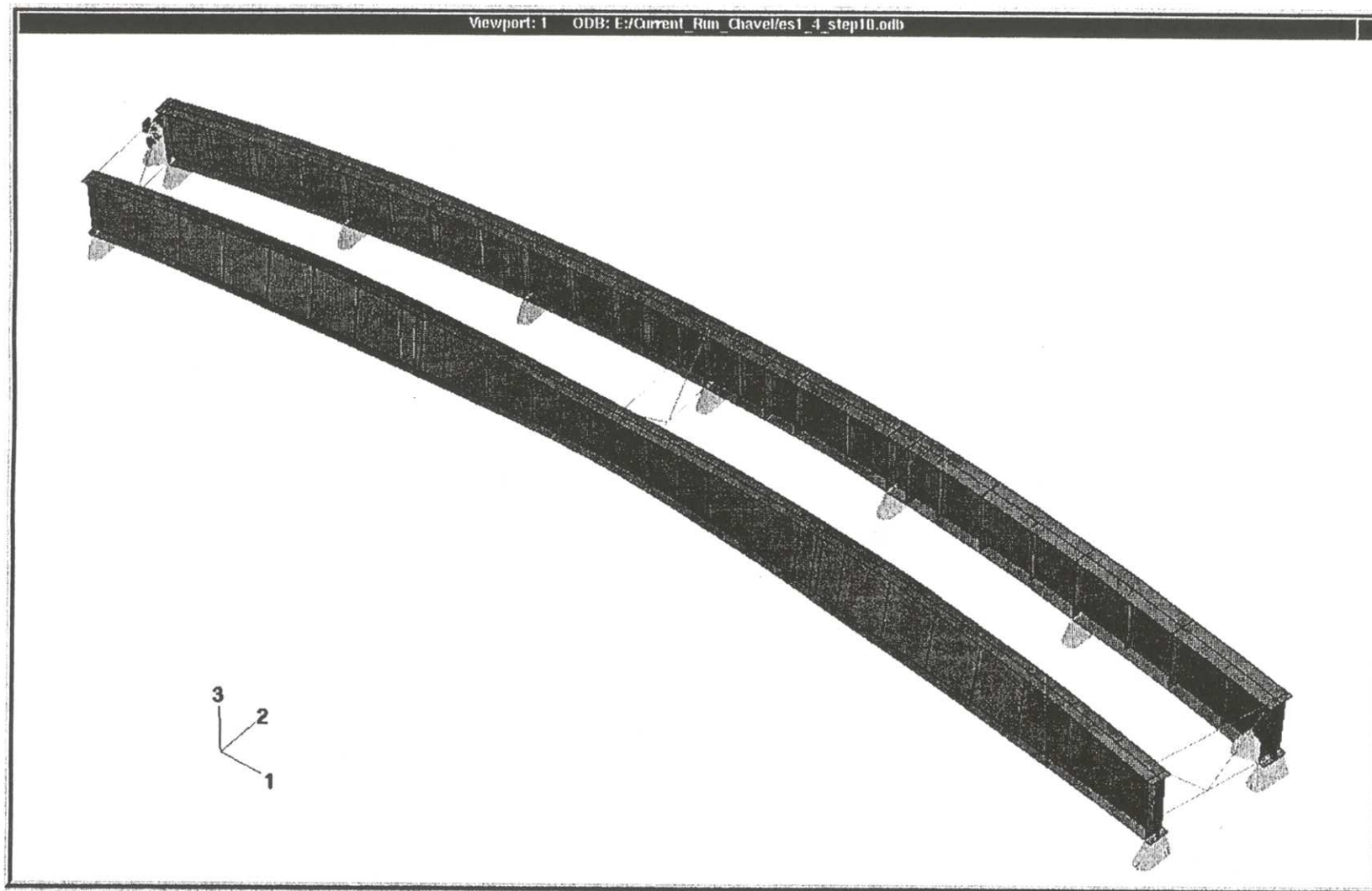


**Figure 87** Deformed finite element model (Magnification factor of 25)

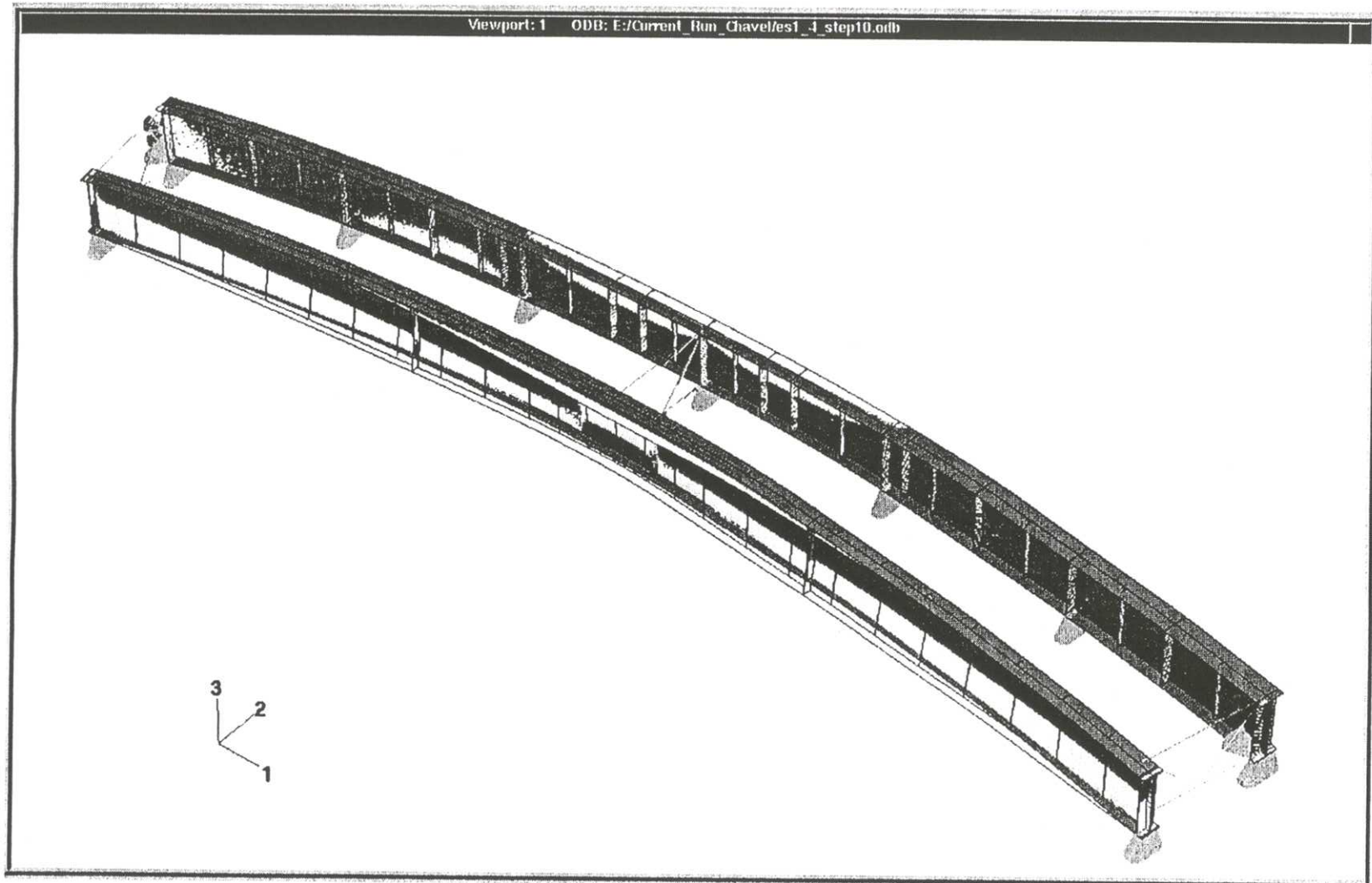


**Figure 88** Undeformed (darker) and deformed (lighter) models (Magnification factor of 25)

## **6.0 FORD CITY BRIDGE FINITE ELEMENT MODEL**

An extremely detailed finite element model is created to analyze the behavior of the Ford City Bridge steel superstructure during its construction as well as to illustrate the difference in cross-frame sizes resulting from application of different detailing methods. The commercial finite element software package ABAQUS is used for all of the analyses conducted as part of the current research. Most of the model preprocessing, such as node and element data, is carried out using Microsoft Excel spreadsheets, and then imported into the ABAQUS input files. The model of the entire bridge uses more than 210,000 elements with over 1,260,000 degrees of freedom. The modeling techniques used to develop the Ford City Bridge model are based on the same techniques utilized for the verification study as described in section 5.0 of the current study.

### **6.1 Element Types**

Each of the sixteen total girder sections of the curved span is individually discretized into meshes of shell elements placed along the middle surfaces of the plate components making up the girders. Such a modeling strategy is adopted due to the fact that most of the girders have different width flanges, and because of the different spacing intervals for cross-frames from one girder to another. The ABAQUS S4R element (4 noded, reduced integration, shear deformable, shell element) is used for the flanges, webs, longitudinal stiffeners, and transverse stiffeners of each curved I-girder. (A

detailed description of each element as well as ABAQUS nomenclature used in this section, can be found in Appendix B of the current study.)

Throughout the model it is desired to keep a consistent number of rows of elements across the top and bottom flange. Therefore, for any single girder, the width of the elements used on the flanges varies slightly. This is caused by the desire to have flange nodes align properly with the transverse stiffeners nodes, and maintain the same number of rows of elements from one girder to another. The length to width aspect ratio for elements on any flange never exceeds 1.5 to 1. (Length of the flange is regarded as the tangential length of the flange.) The same principles that apply to the modeling of the flanges, also apply to the modeling of the longitudinal stiffeners. Each girder in the curved span is modeled with 8 elements across the width of each flange.

The webs of each curved span girder also employ the ABAQUS S4R shell element, and the number of elements that are used along the web height vary from one girder to another. The length to width aspect ratio for web elements never exceeds 2 to 1. (Length for the web is considered to be the vertical length.) It was shown via the verification study conducted as part of the current research, that the use of web elements that have a 2 to 1 aspect ratio perform very well for an elastic analysis such as this. These same modeling principles are followed for the development of the transverse stiffeners. Depending on the element size used for the flanges and the webs (and transverse stiffeners) of the girders, either 17, 21, or 24 elements occur through the depth of the web.

Given that only the consideration of the curved span is germane to the current research, the straight spans of the Ford City Bridge employ a more simplified modeling strategy. ABAQUS B32 beam elements (3-node, quadratic beam) are used to model the straight spans of the bridge, 28 sections total. Appropriate cross-sectional properties are input for each girder section; such as moment of inertia and cross-sectional area. These beam elements are attached to the neutral axis of the girders modeled with shell elements at the end of the curved span (Section 4). Mesh conformity at the inter element boundary between the shell sections and beam element is accomplished via the plane section hypothesis being enforced at the transition interface using rigid beam elements (ABAQUS RB3D2 elements, 2-node rigid beam with a unit area).

Field splices are not explicitly modeled with shell elements, however their influence is modeled using the ABAQUS multi-point constraints (MPQ types “TIE” and “LINEAR.” These two constraint types are used to join the girders at the field splice locations. The “TIE” constraint is used to enforce on the slave node all translations and rotations of the master node, and the “LINEAR” constraint is used when a slave node must lie along a line defined by two master nodes

The “X” type cross-frames are modeled with ABAQUS B31 beam elements (2-node, linear beam). Each member of the cross-frame is modeled, 6 in all, with 2 each being used for the diagonal members due to the welded connection at the middle of the “X” Again, appropriate cross-sectional properties are input for each cross-frame section, such as moment of inertia and cross-sectional area. For simplicity sake, the cross-frame connection plates (gusset plates) are not explicitly modeled. The cross-frames are

attached to the girders using the appropriate ABAQUS MPC commands. The cross-frames used in every model for the current research are detailed to the “no load” state of stress.

Figure 89 illustrates a typical girder finite element mesh, in this case for girder G3 section 1. Figure 90 shows the entire finite element model of the Ford City Bridge, and figure 91 illustrates the curved section only.

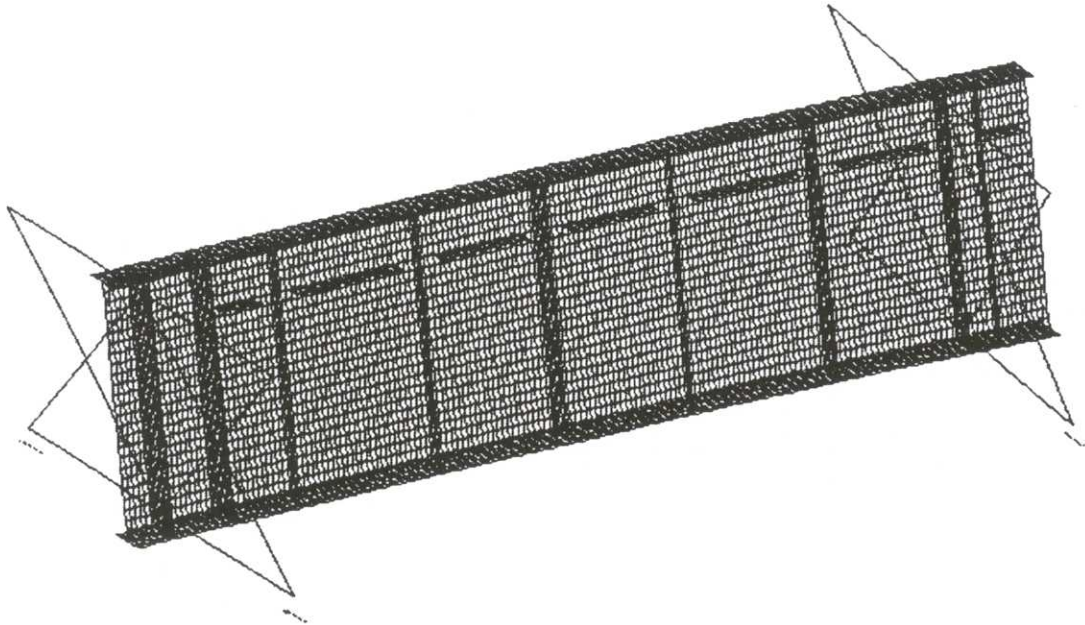


**Figure 89** Finite element mesh, girder G3 section 1

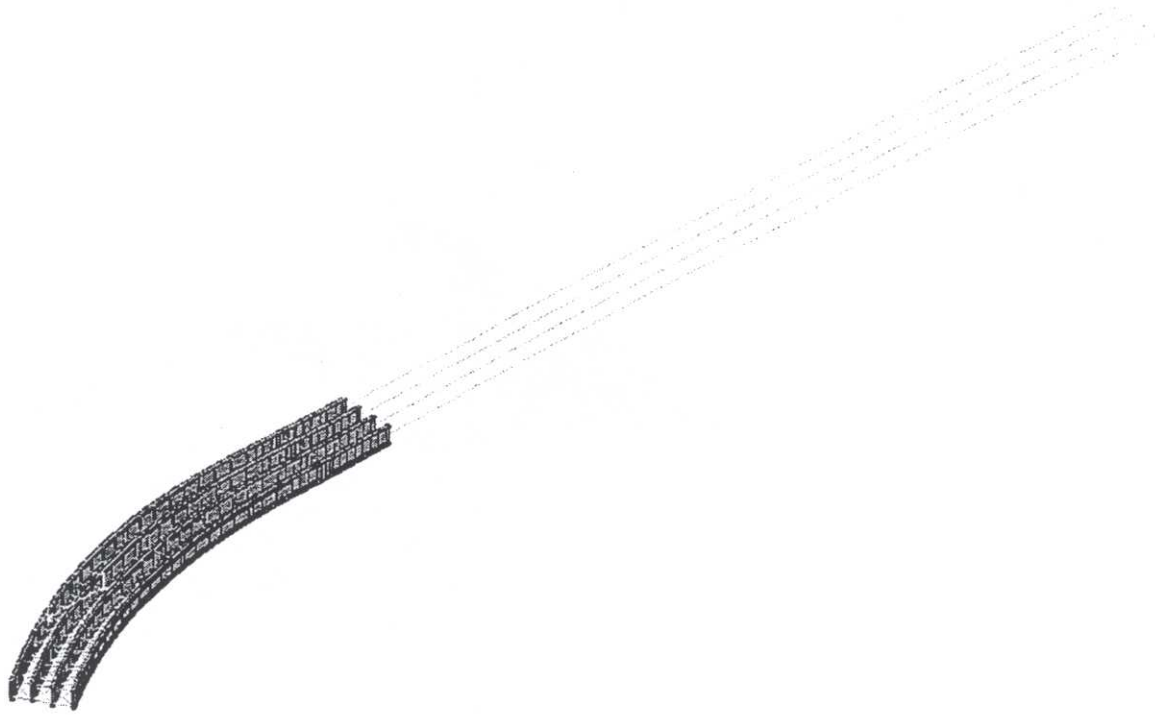


**Figure 90** Finite element model of entire Ford City Bridge (meshes not shown for clarity)

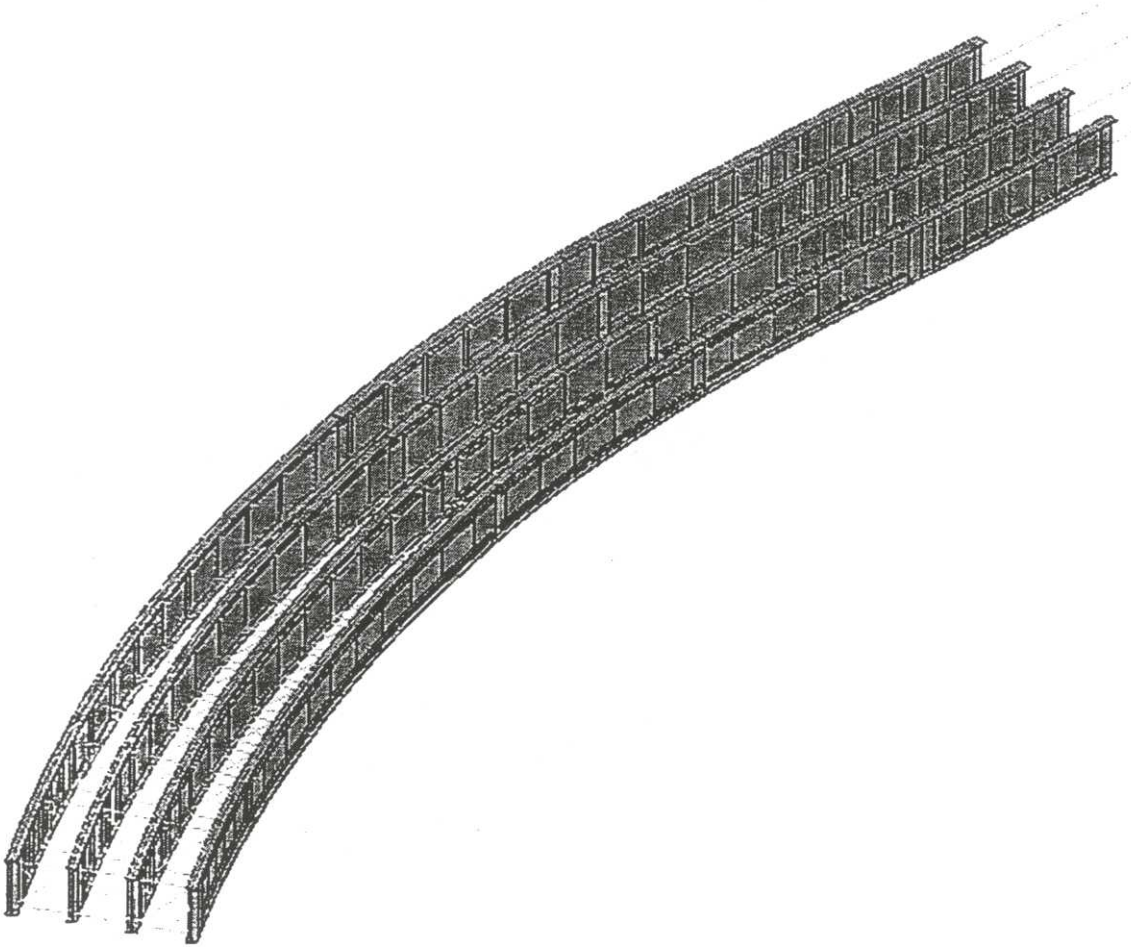


**Figure 91** Finite element model of the curved section (meshes not shown for clarity)

## 6.2 Boundary Conditions

The bearing supports of the Ford City Bridge are not explicitly modeled (i.e. connection plates, pistons, elastomer, and etc.). Fixed bearings and expansion bearing are used at the abutments and piers, and also at falsework locations during the construction of the bridge.

In the case of fixed bearings, the girders are restrained at the support locations in the radial (out-of-plane) direction in the finite element model. For all of the support locations ABAQUS unidirectional GAP elements are used, with the bottom end restrained in the vertical direction. The unidirectional GAP elements permit the bridge girders to “lift-off” the support during the analysis, as they would be able to during the construction of the bridge. The use of GAP elements is especially important when using temporary supports, as will be shown later as part of the current thesis. The use of GAP elements constitutes a rudimentary consideration of the contact problem at the supports using hard frictionless contact.

### **6.3 Loading Conditions**

The loads implemented in this study consist of the self-weight of the steel superstructure components only. There are no other external loads applied to the model during the analyses. A standard steel density of  $7.85 \times 10^3 \text{ kg/m}^3$  ( $490 \text{ lb/ft}^3$ ) is used for all of the girder components throughout the modeling. The steel density is increased by 10% for the cross-frame members in order to account for gusset plate connections that are not explicitly modeled.

#### 6.4 Additional Finite Element Model Details

The finite element model of the Ford City Bridge considers nonlinear geometric effects, but does not consider material nonlinearity. Due to the geometric complexities of a curved I-girder, nonlinear geometric effects are thought to be important and are thus considered in the analysis. However, given that the steel superstructure is designed to remain elastic throughout the erection, effects of nonlinear material properties are not considered in the analysis.

The “in-field” and “planned” erection sequences of the Ford City Bridge are replicated through a series of finite element models. Individual girder sections, and attaching cross-frames, are inserted into the model in the same order as they were erected in the field employing the use of the ABAQUS MODEL CHANGE feature.

Residual stresses and temperature effects are not included in any of the finite element models employed for the current research. Additionally, nominal dimensions from the bridge plans and geometric properties are used for all of the finite elements models.

## 7.0 ANALYTICAL STUDY OF FORD CITY BRIDGE ERECTION SEQUENCE

The nonlinear finite element model of the Ford City Bridge is used to recreate the “as-built,” and intended steel erection sequence of the curved span. The “as-built” erection of the bridge is discussed in Section 4.0 of the current study. During the final stages of steel construction of the curved span, the “as-built” and intended erection sequences differ slightly, and therefore both are analyzed. Since the steel superstructure erection was completed prior to the start of the present study, the only data obtained from the field construction was the final steel elevations after completion of the steel superstructure. Therefore, quantitatively, no basis of comparison for the “as-built” and analytical erection sequences exists for each erection stage of the curved section. Instead, for the later stages of construction, comparisons will be made in regard to the “as-built” erection and proposed erection sequence analytical models. For each erection stage, the temporary support reactions, displacements, and stresses induced during steel erection are monitored.

In addition, the analytical models used for the current study employ cross-frames detailed for the “no-load” case. However, as stated previously, a discrepancy results from the incorrect fabrication of the cross-frames, in which they are detailed for the concrete deck load case. The erection plans for the Ford City Bridge (HDR 1999), are developed for the bridge with the incorrect cross-frames (concrete deck load case). A table of temporary reactions is given for the entire erection sequence, and is used as a basis of comparison for the current research in regard to the current erection study.

## 7.1 “As-built” Erection Sequence Analytical Studies

Each stage of the erection sequence is recreated using the developed finite element model of the Ford City Bridge. Sixteen different stages are analyzed, one for the placement of each girder in the curved section. Each individual phase of the construction is analyzed, and the temporary support reactions, girder displacements, and girder stresses are observed. This section will highlight particular construction stages, while the data for each erection stage can be found in Appendix C of the current research. Again, it should be noted that all of the models employed in this study utilize cross-frames detailed for the web-plumb position at the no-load condition.

### 7.1.1 Construction Stage 1

The construction of the Ford City Bridge begins with girder G3 section 1 (G3-1), and cross-frames 1B, 1C, 7B, and 7C. The girder is supported by abutment 1 and falsework 1, located directly below cross-frame 7. The south end of the girder section overhangs falsework 1 by approximately 1.4m (4.6ft). Figure 92 depicts the plan view of the finite element model for construction stage 1 (in relation to remainder of the curved section).

Deflections at midspan of girder G3-1 in both the vertical and out-of-plane (radial) directions are minimal, and less than 1mm. This is consistent with engineering judgment, when considering the theoretical vertical deflection is estimated as

$5wL^4/384EI$ . The moment of inertia,  $I$ , for the subject girder is quite large ( $4.102 \times 10^{11} \text{ mm}^4$ ), while the span of the section is moderately short (13.34m). Owing to the rotation of the girder, at midspan, the bottom flange deflects 0.7mm to the inside of the curve, while the top flange deflects 0.7mm to the outside of the curve. As shown in figures 93 and 94, these out-of-plane (radial) deflections are small, but are consistent with engineering judgment.

The maximum von Mises stress occurs on the inside-of-curve-edge of the top and bottom flanges, and is approximately 5 MPa (0.73 ksi), well below the yield stress.

The vertical reaction at abutment 1 is 25.2 kips, and 26.9 kips at falsework 1. Also, a vertical reaction at the cross-frame tie-down points is observed; approximately 0.73 kip and 0.85 kip for cross-frames 1B and 7B, respectively; and approximately 0.34 kip and 0.49 kip for cross-frames 1C and 7C, respectively.

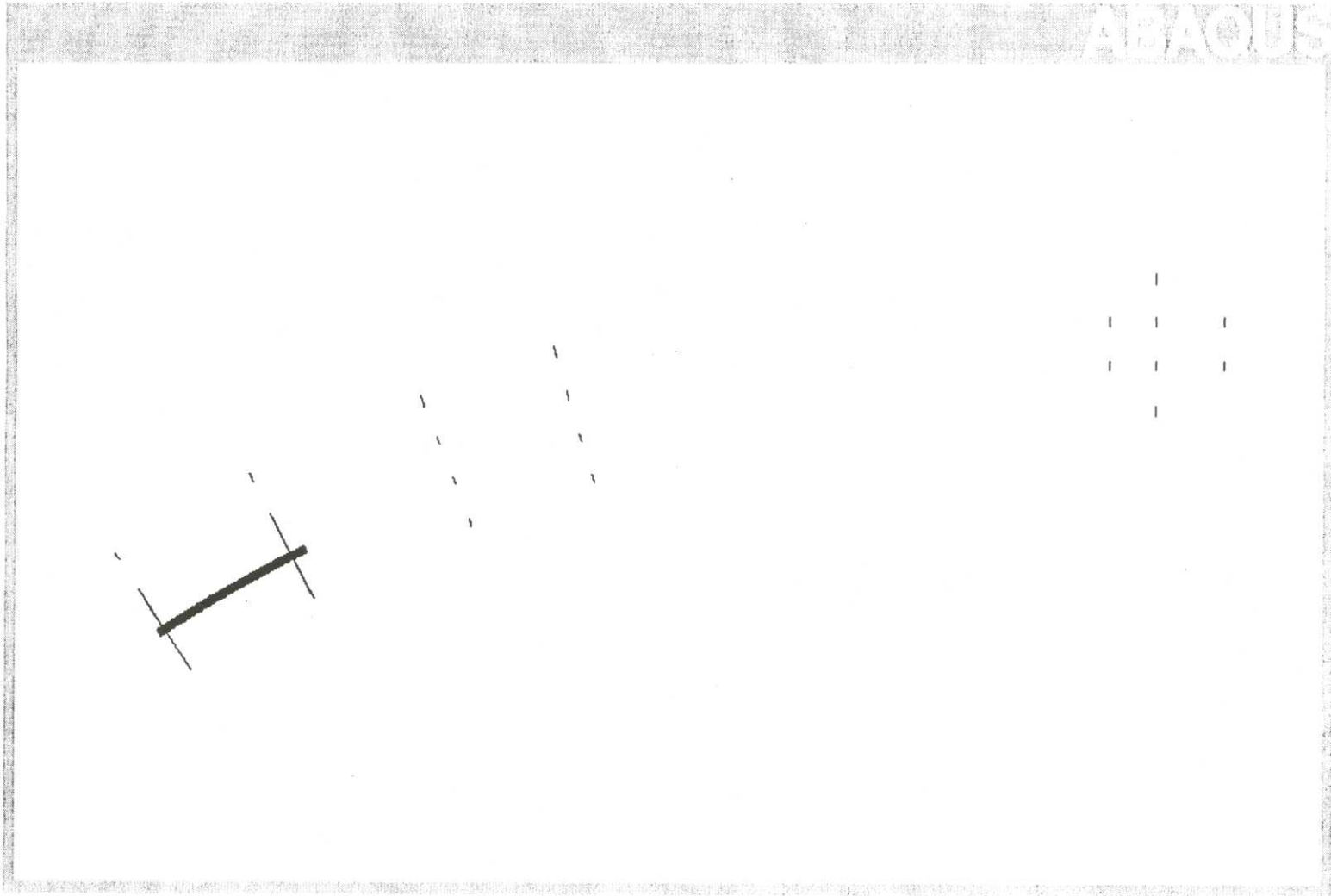
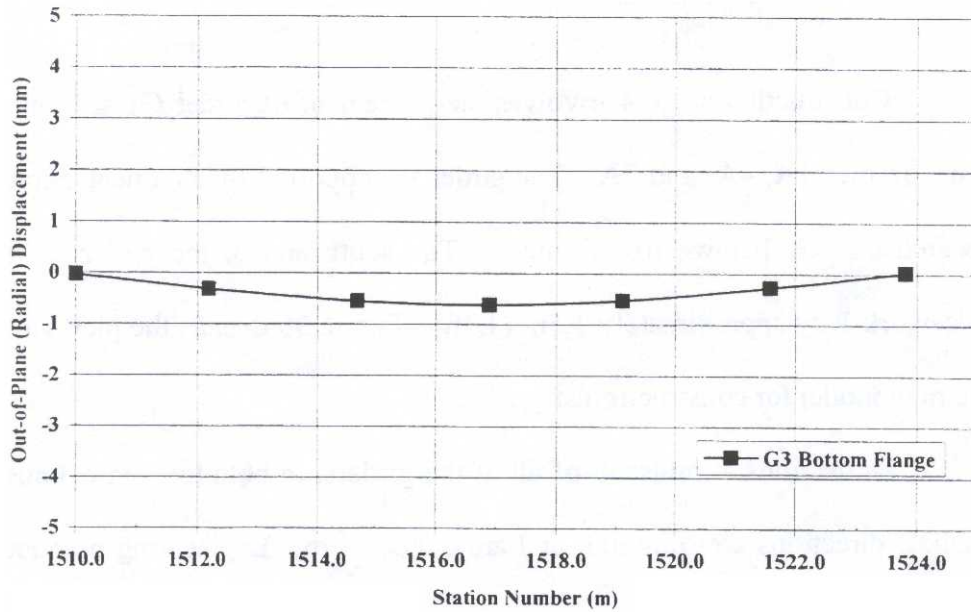
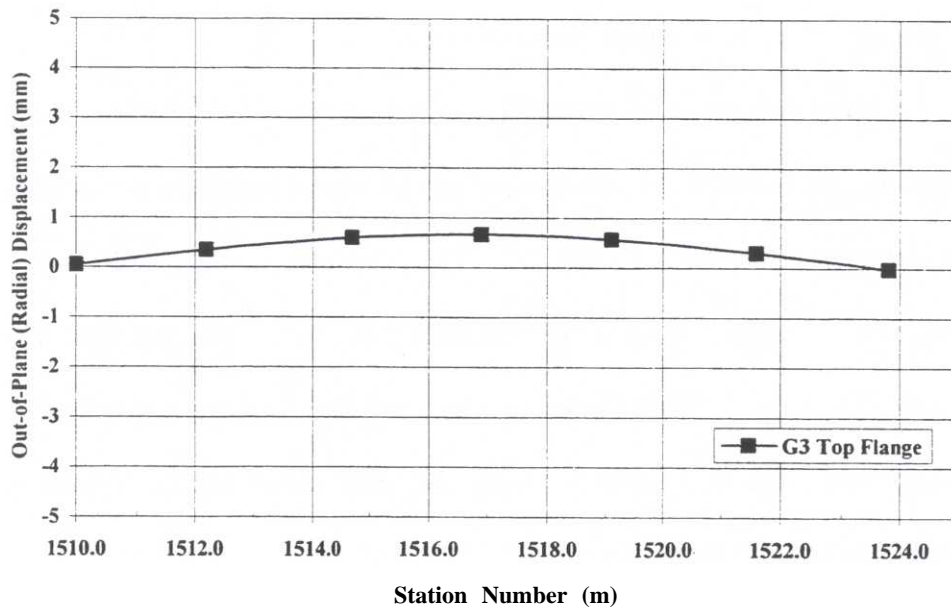


**Figure 92** Construction stage 1 - Plan view of finite element model



(“-“ is displacement inward of curve; “+” is displacement outward of curve)

**Figure 93** Construction stage 1 - Out-of-plane displacement, centerline of bottom flange



(“-“ is displacement inward of curve; “+” is displacement outward of curve)

**Figure 94** Construction stage 1 - Out-of-plane displacement, centerline of top flange

### 7.1.2 Construction Stage 4

Construction stage 4 involves the placement of girder G1 section 1 (G1-1), and cross-frames 1A, 4A, and 7A. The girder is supported by abutment 1 and falsework 1, located directly below cross-frame 7. The south end of the girder section overhangs falsework 1 by approximately 1.5m (4.9ft). Figure 95 depicts the plan view of the finite element model for construction stage 4.

Deflections at midspan of all of the girders, in both the vertical and out-of-plane (radial) directions are minimal, and are almost zero. Engineering practice dictates that during the construction of a horizontally curved steel bridge, it is desired to maintain the “no-load” condition, and this is shown to be the case with the current model. The von Mises stresses are minimal, with a maximum stress of approximately 4 MPa (0.58 ksi) occurring in the top flange of girder G1-1.

The reactions at abutment 1 and falsework 1 are consistent with engineering judgment, given that the finite element model results indicate that the total load is being transferred to the outside girder, G1. The maximum reactions occur at the supports of girder G1; abutment 1 and falsework 1 each experience a reaction force of approximately 40 kips (178 kN). Table 5 shows the reactions for all of the girders that are members of construction stage 4. Table 6 shows the progression of the support reactions from construction stage 1 through stage 4.

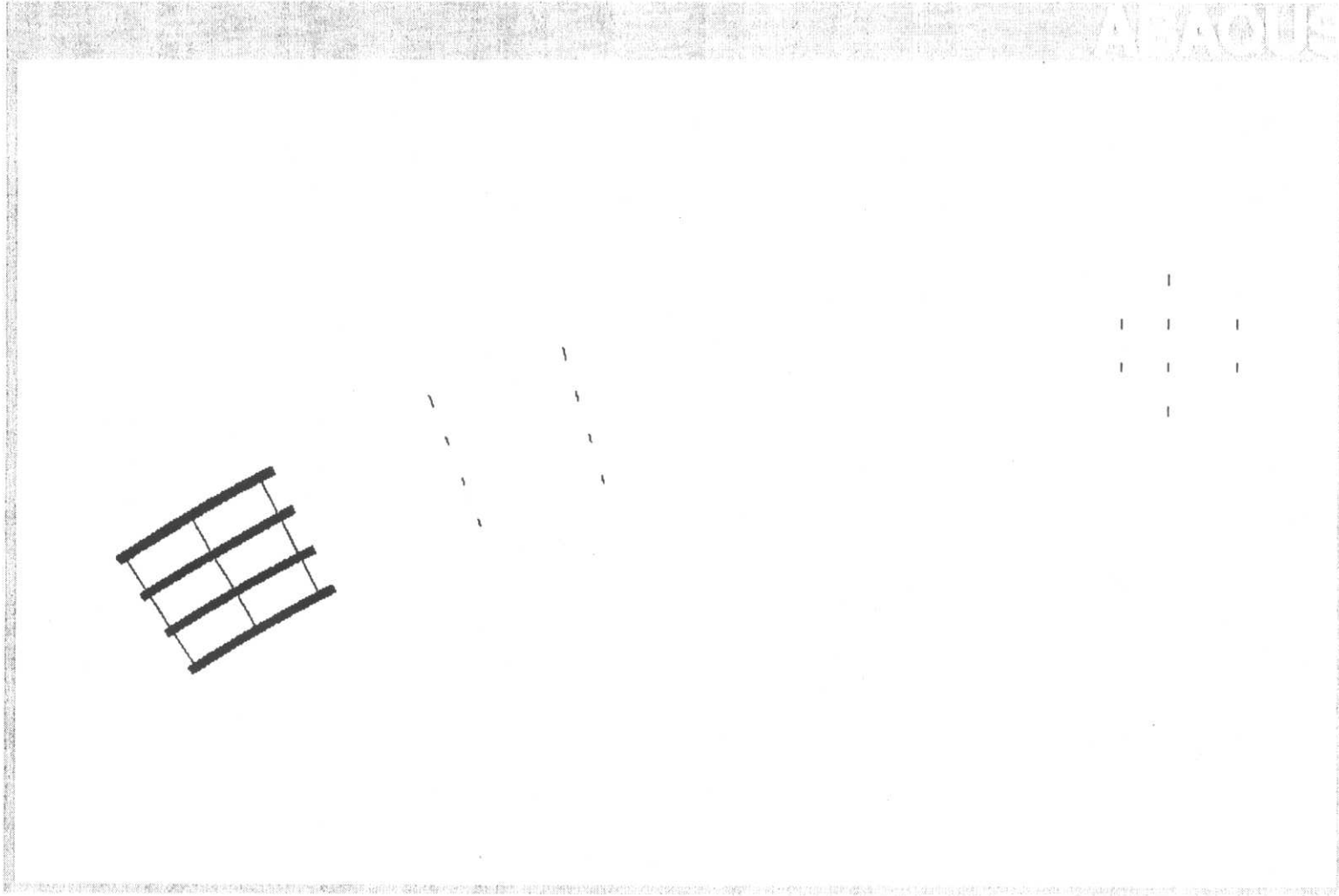


**Figure 95** Construction stage 4 - Plan view of finite element model

**Table 5** Construction stage 4 – Support reactions

<b>Girder</b>	<b>Abutment 1</b>	<b>Falsework 1</b>
<b>G1</b>	39.6 kips (176.3 kN)	40.3 kips (179.1 kN)
<b>G2</b>	27.1 kips (120.5 kN)	27.8 kips (123.7 kN)
<b>G3</b>	26.1 kips (116.2 kN)	28.1 kips 125.1 (kN)
<b>G4</b>	21.8 kips (97.1 kN)	22.5 kips (100.1 kN)

**Table 6** Construction stages 1 through 4 – Support reactions

<b>Construction Stage</b>	<b>Erected Girder</b>	<b>Abutment 1 (kips)</b>				<b>Falsework 1 (kips)</b>			
		G1	G2	G3	G4	G1	G2	G3	G4
<b>1</b>	<b>G3-1</b>			25			27		
<b>2</b>	<b>G2-1</b>		28	25			30	27	
<b>3</b>	<b>G4-1</b>		28	26	21		29	29	22
<b>4</b>	<b>G1-1</b>	40	27	26	22	40	28	28	23

### 7.1.3 Construction Stage 5

Girder G3 section 2 (G3-2) and cross-frames 11B, 11C, 14B, and 14C, are placed as part of construction stage 5. Using the ABAQUS MPC “TIE” and “LINEAR” constraints, field-splice 1 is analytically achieved. This same technique is used for all of the construction stages. G3-2 is supported by falsework 2A, below cross-frame 11, and by falsework 2, below cross-frame 14. The erected cross-frames also aid in stabilizing G3-2. The south end of the girder section overhangs falsework 2 by approximately 11.16m (36.6ft). Figure 96 portrays the plan view of the finite element model for construction stage 5, and figure 97 illustrates a second view of the finite element model.

Vertical and out-of-plane (radial) displacements are minimal throughout the structure at this construction stage. However, a downward vertical deflection of 1.12 occurs at the overhang end of girder G3-2. At this same location, an out-of-plane (radial) deflection is observed in which the bottom flange centerline deflects outward (of curve) 1.7mm, and the top flange centerline deflects inward (of curve) 1.9mm. Figures 98 and 99 illustrate the out-of-plane (radial) displacements for the current construction stage.

The maximum von Mises stress occurs on the outside-of-curve edge, on the top flange of G3-2 above falsework 2, and is approximately 8 MPa (1.16 ksi). The monitored stress in the longitudinal direction at the same location is approximately 7 MPa (1.02 ksi).

Due to the addition of G3-2, the vertical reaction of girder G3 at falsework 1 increases from 28.1 kips (125.1 kN) in construction stage 4, to 58.8 kips (261.7 kN). The reactions at falsework 2A and 2 are 32.7 kips (145.5 kN) and 66.0 kips (293.5 kN),

respectively. Reactions at other girder support locations (abutment 1 and falsework 1) basically remain the same as what is observed in construction stage 4. Vertical reactions also exist at the cross-frame tie-down locations at falsework 2A and 2, cross-frames 11B and C, and cross-frames 14B and C, respectively. A maximum vertical reaction of approximately 3 kips (13.3 kN) occurs at cross-frame 14C tie-down point at falsework 2; while a vertical reaction of 0.2 kips is shown to be acting at the tie-down point of cross-frame 14B. This appears to show that girder G3-2 is rotating inward, as is also shown by the out-of-plane and vertical displacements at the overhang end. This inward rotation, while it is minor, is possibly due to the placement of the temporary supports, falsework 2A and 2.

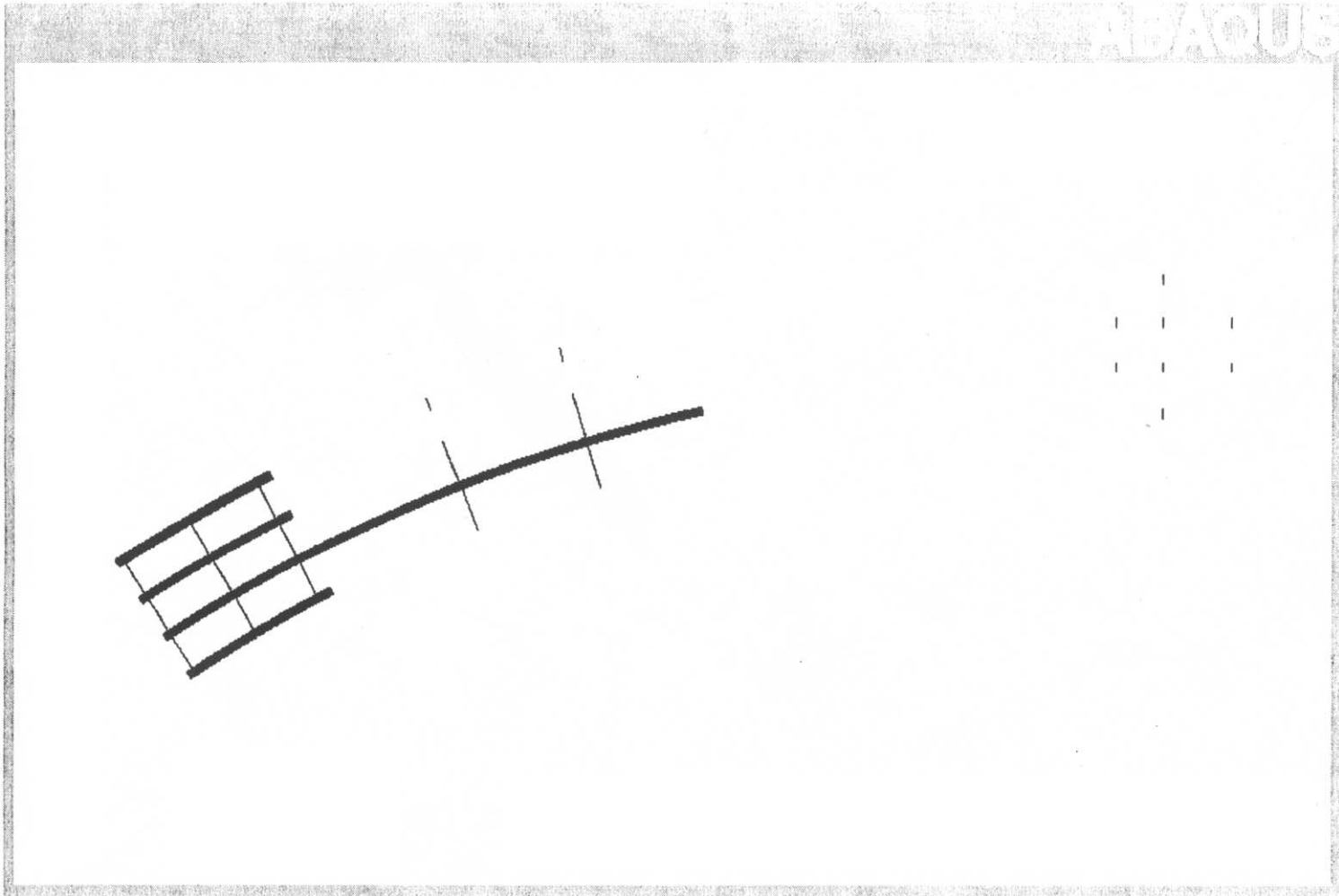


**Figure 96** Construction stage 5 - Plan view of finite element model

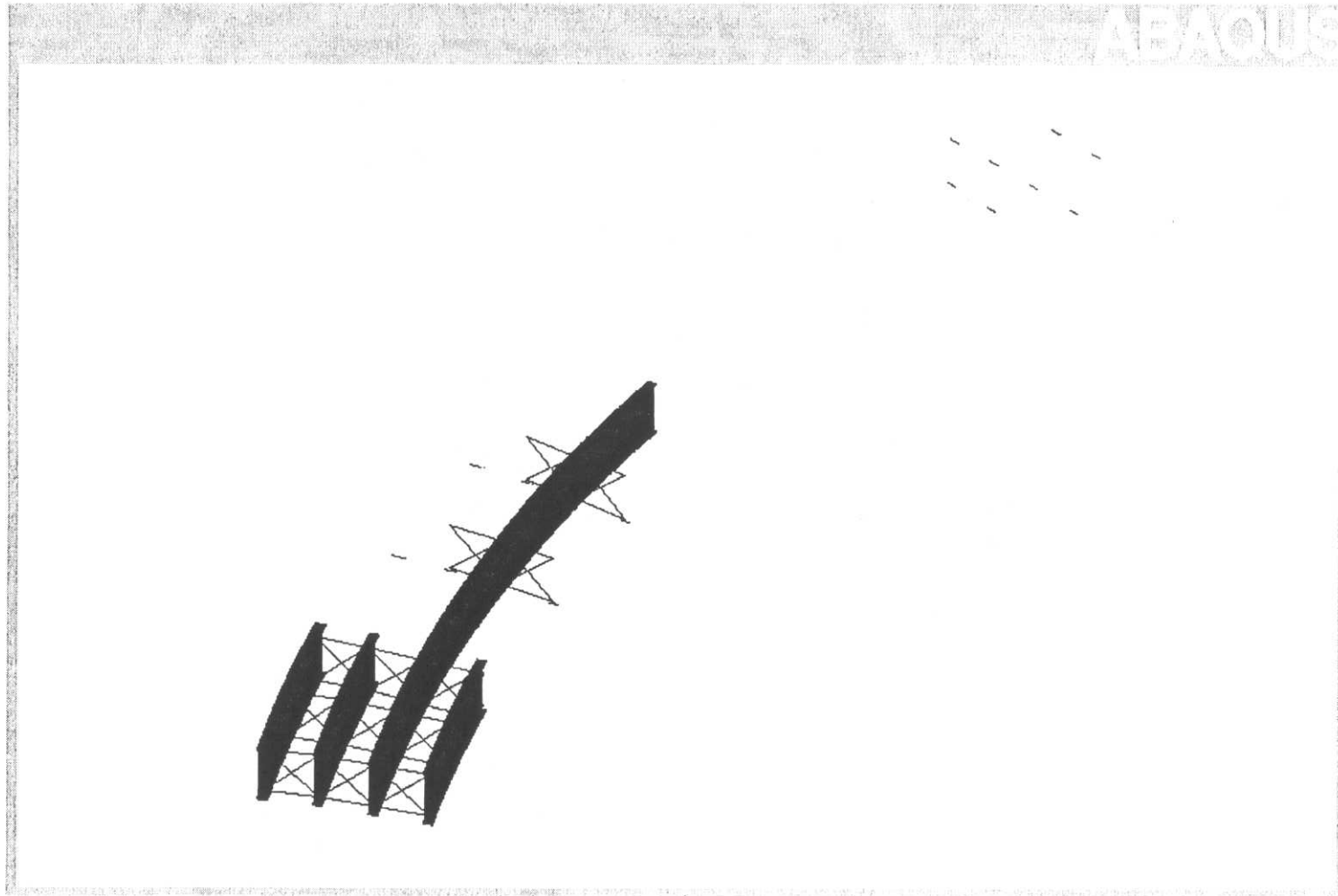
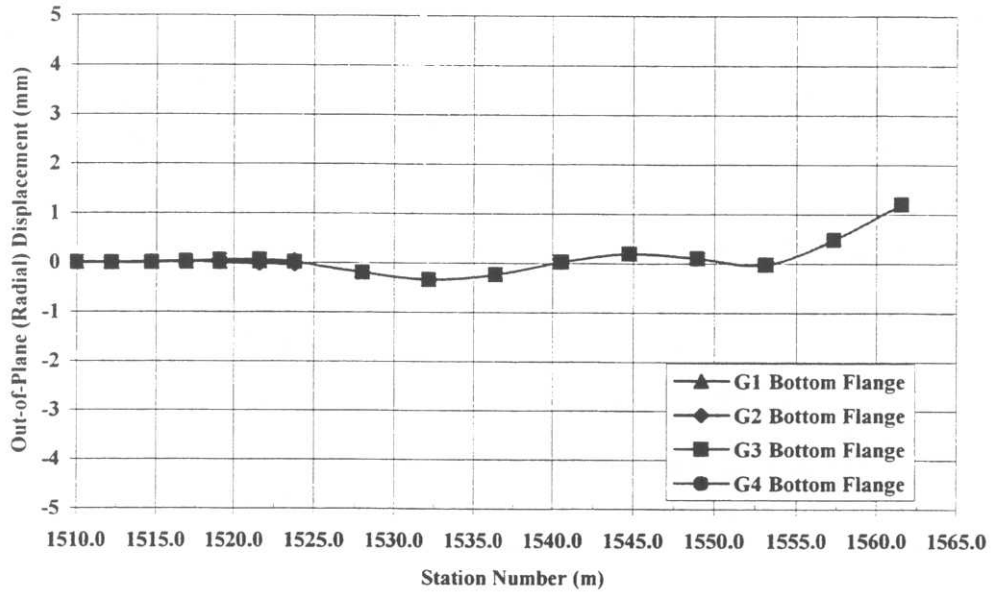
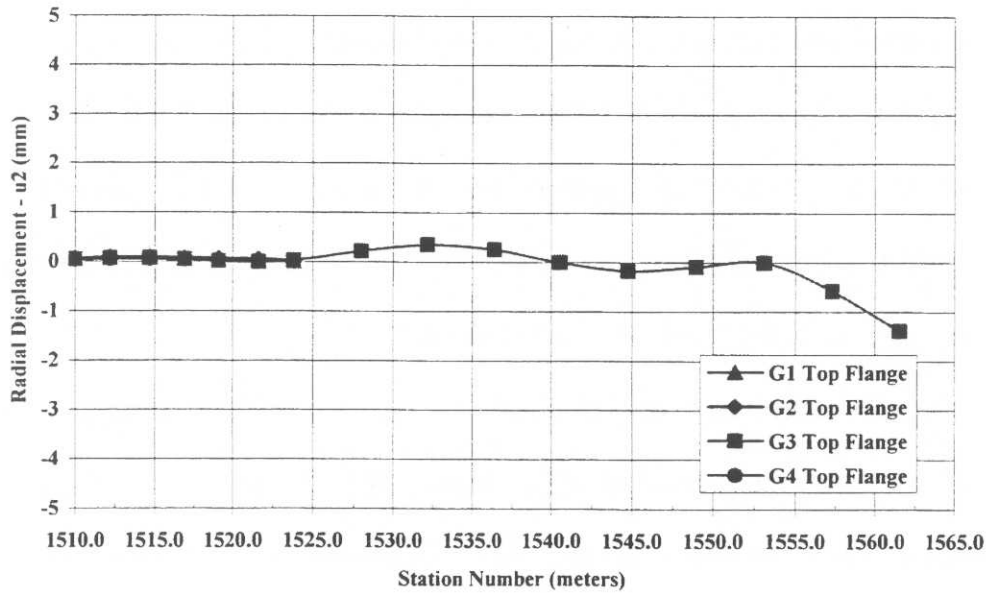


**Figure 97** Construction Stage 5 - View above abutment 1 of finite element model



(“-“ is displacement inward of curve; “+” is displacement outward of curve)

**Figure 98** Construction stage 5 - Out-of-plane displacement, centerline of bottom flange



(“-“ is displacement inward of curve; “+” is displacement outward of curve)

**Figure 99** Construction stage 5 - Out-of-plane displacement, centerline of top flange

#### 7.1.4 Construction Stage 8

Girder G1 section 2 (G1-1) and cross-frames 8A through 16A are placed as part of construction stage 8, completing section 2 of the steel superstructure. G1-2 is supported by falsework 2A below cross-frame 11, and by falsework 2 below cross-frame 14. The south end of G1-2 extends beyond falsework 2 by approximately 11.76m (38.6ft). Figure 100 illustrates the finite element model at construction stage 8.

The vertical and out-of-plane (radial) deflections are extremely small throughout the structure, and bordering close to zero. As shown in figure 101, for all four girders, a downward vertical deflection of approximately 1mm exists at the end of the cantilevered portion of the structure.

The maximum von Mises stress for the current structure is approximately 8 MPa (1.16ksi), and occurs in the top flange of girders G2, G3, and G4 above falsework 2. Coupled with the observed deflections, it can be concluded that the structure continues to remain in its theoretical “no-load” state of stress, up to this point of the construction sequence. The temporary supports (falseworks 1, 2A, and 2) play a key role in keeping the structure in the “no-load” state of stress.

The maximum vertical reactions at each support location develop under girder G1, with the largest reaction of 121 kips (538.1 kN) occurring at falsework 2. Table 7 shows the progression of the reactions throughout the structure beginning with construction stage 1. In comparing construction stages 7 and 8, the support reactions of girders G2, G3, and G4 do not significantly change with the addition of girder G1-2.

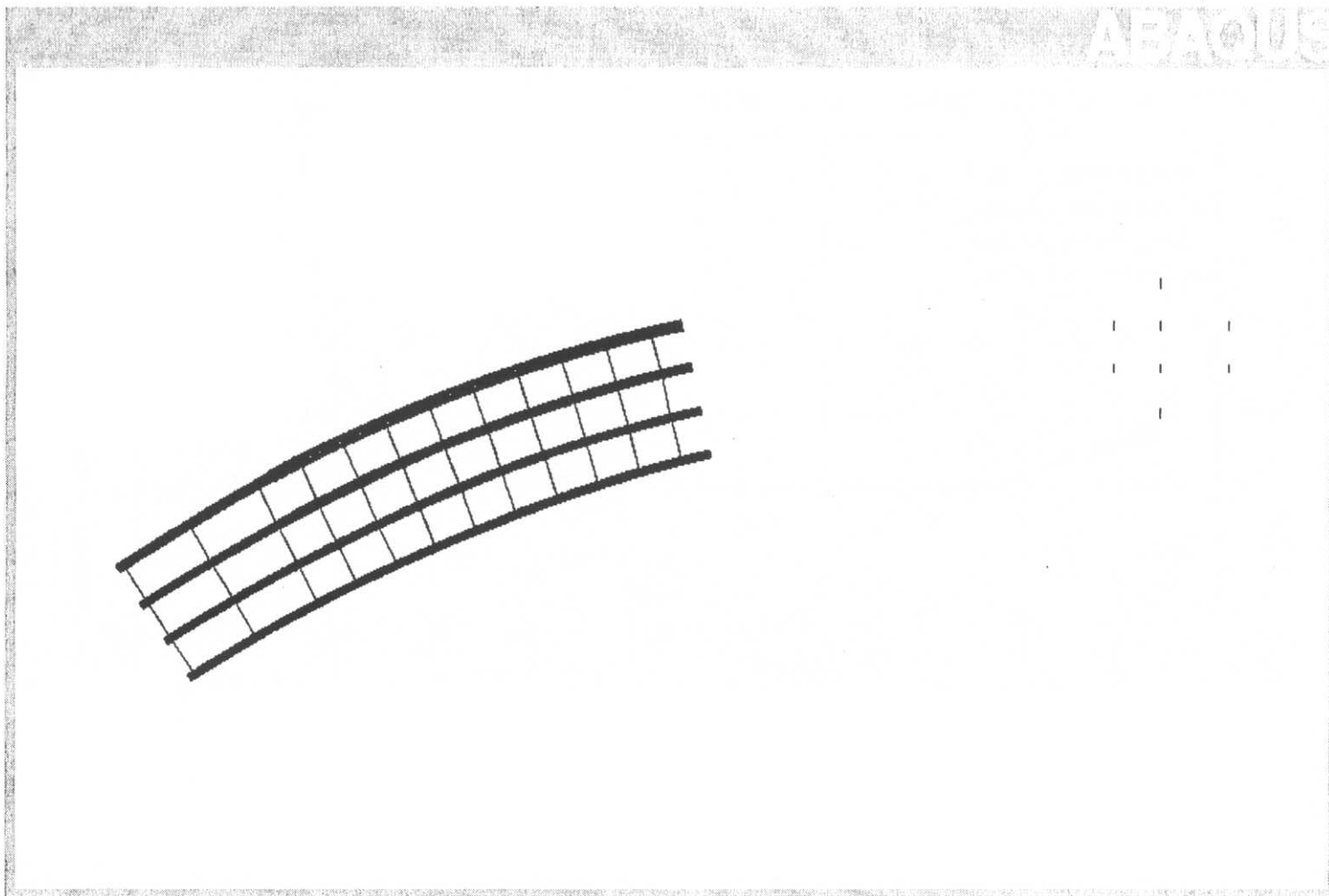


**Figure 100** Construction stage 8 - Plan view of finite element model

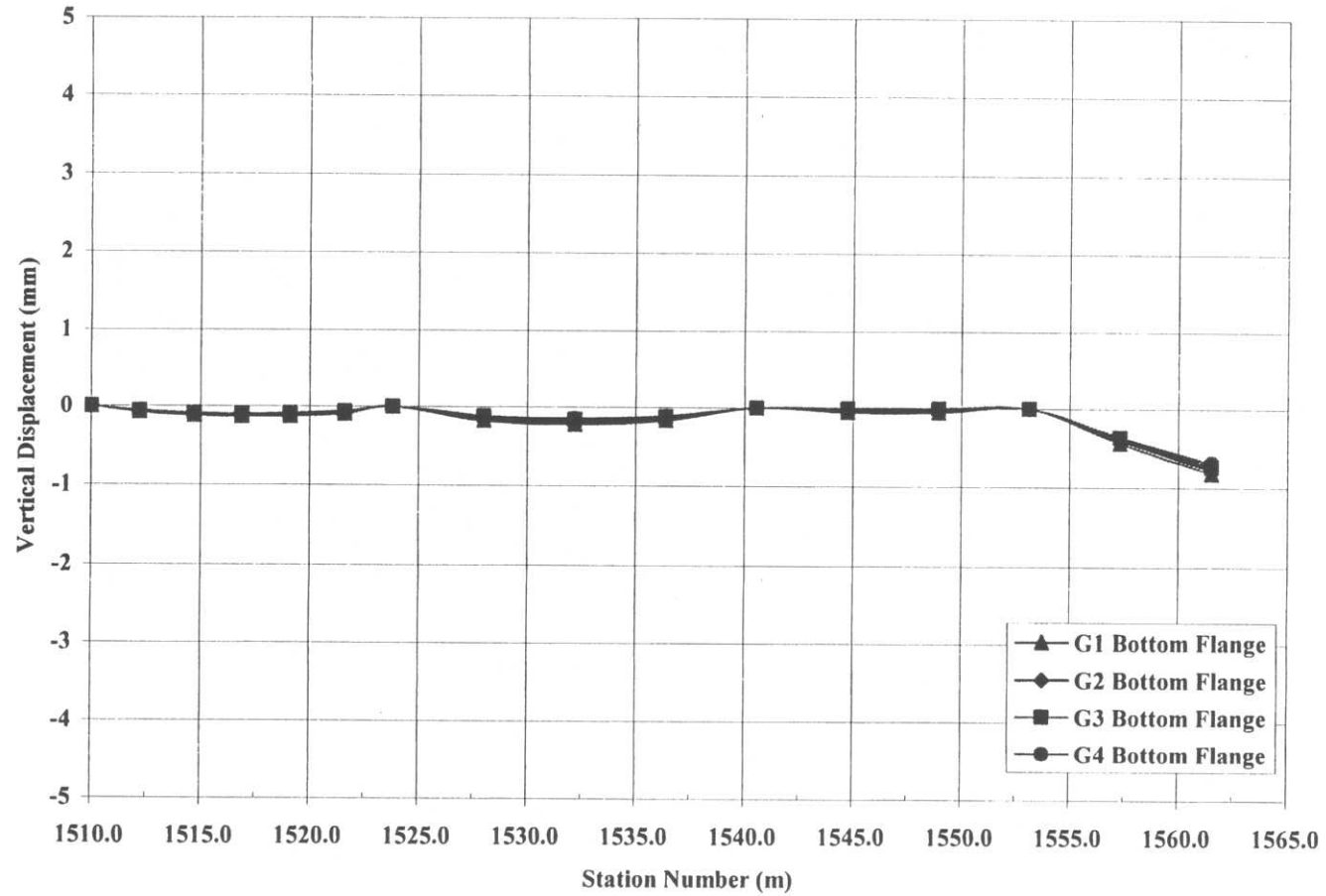


**Figure 101** Construction stage 8 – Vertical displacement, centerline of bottom flange

**Table 7** Construction stages 1 through 8 – Support reactions

		Abutment 1 (kips)				Falsework 1 (kips)				Falsework 2A (kips)				Falsework 2 (kips)			
Construction Stage	Erected Girder	G1	G2	G3	G4	G1	G2	G3	G4	G1	G2	G3	G4	G1	G2	G3	G4
1	G3-1			25				27									
2	G2-1		28	25			30	27									
3	G4-1		28	26	21		29	29	22								
4	G1-1	40	27	26	22	40	28	28	23								
5	G3-2	40	26	22	21	40	27	58	22			33				66	
6	G2-2	40	22	22	21	40	68	57	23		54	34			96	72	
7	G4-2	41	22	21	18	39	66	58	44		52	38	28		95	72	58
8	G1-2	35	22	21	18	87	69	58	44	69	54	37	27	121	102	72	57

### 7.1.5 Construction Stage 9

Bridge erection at pier 1 begins with construction stage 9, as girder G3 section 4 (G3-4) is placed over the pier. Pier brackets at pier 1, and cross-frames 26B, 27B, 27C, and 28B are used to stabilize the girder section. The north end of the girder section extends 15.6m (51.2ft) past the span 1 pier 1 bracket, and the south end is cantilevered approximately 12m (39.4ft) from the span 2 pier 1 bracket. In the field, the girder was released from the crane once the attaching cross-frames were connected and tied-down to the respective pier brackets and pier locations. Therefore, there is no stabilization via the lifting crane included in the current finite element model. Figure 102 illustrates the finite element model used for the current construction stage.

Of course, section 1 and 2 of the structure remain in the same displaced state as they were for the previous stage. However, G3-4 experiences larger vertical and out-of-plane deflections at the girder ends, as compared to the displaced position of sections 1 and 2. Figures 103 and 104 illustrate the out-of-plane (radial) displacement of the current structure. At the field-splice 3 location (north end of G3-4), the bottom flange displaces 4.75mm outward (of curve) and the top flange displaces inward (of curve) 13.9mm (0.55in). The girder deflects vertically downward 11.4mm (0.45in) at the same location, as shown in figure 105. At the south end, field-splice 4, G3-4 displaces upward 5.1mm, and the top flange centerline displaces in the out-of-plane direction by 5.2mm towards the G2 girder line. Minute out-of-plane (radial) displacement occurs at the bottom flange centerline at the south end of the G3-4.

The top flange of G3-4, near the span 1 pier 1 bracket is subjected to the largest von Mises stress of approximately 15 MPa (2.2 ksi). The von Mises stress in the top flange between the span 1 pier bracket and pier 1 is generally between 6 and 8 MPa (0.9 to 1.16 ksi).

Due to the geometric configuration of the pier bracket supports, pier 1 and the overhang dimensions of the G3-4, the girder section “lifts off” of the span 2 pier bracket support, and only the span 1 pier bracket and pier 1 have contact with the girder. The pier bracket at the cross-frame 26 location (span 1) experiences a reaction force of 36 kips (156 kN), and pier 1 is subjected to a load of 129 kips (574 kN). Vertical reactions are also evident at the cross-frame 27B and 27C tie-down locations; with a reaction force of approximately 2 kips (10 kN) at each tie-down point.

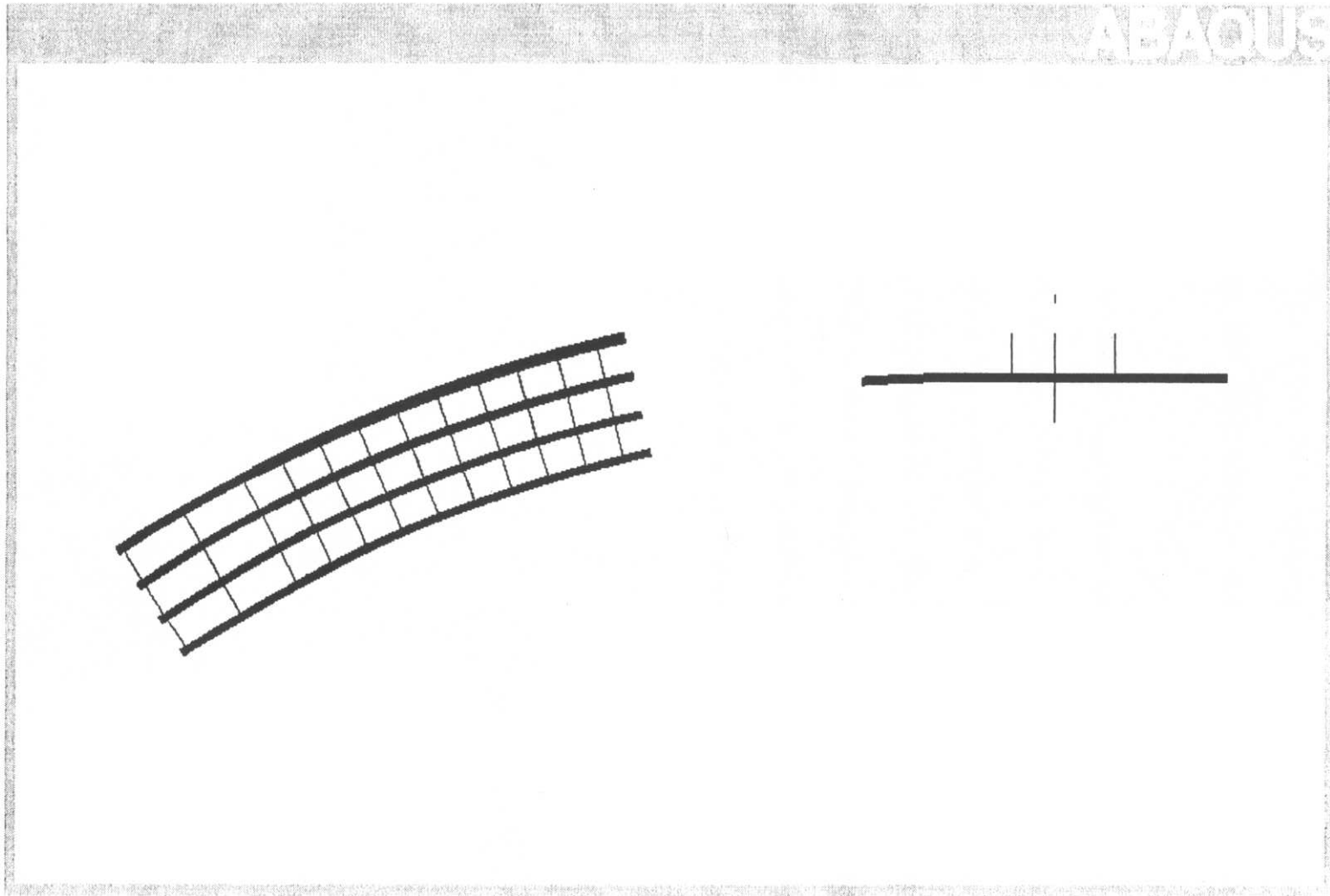
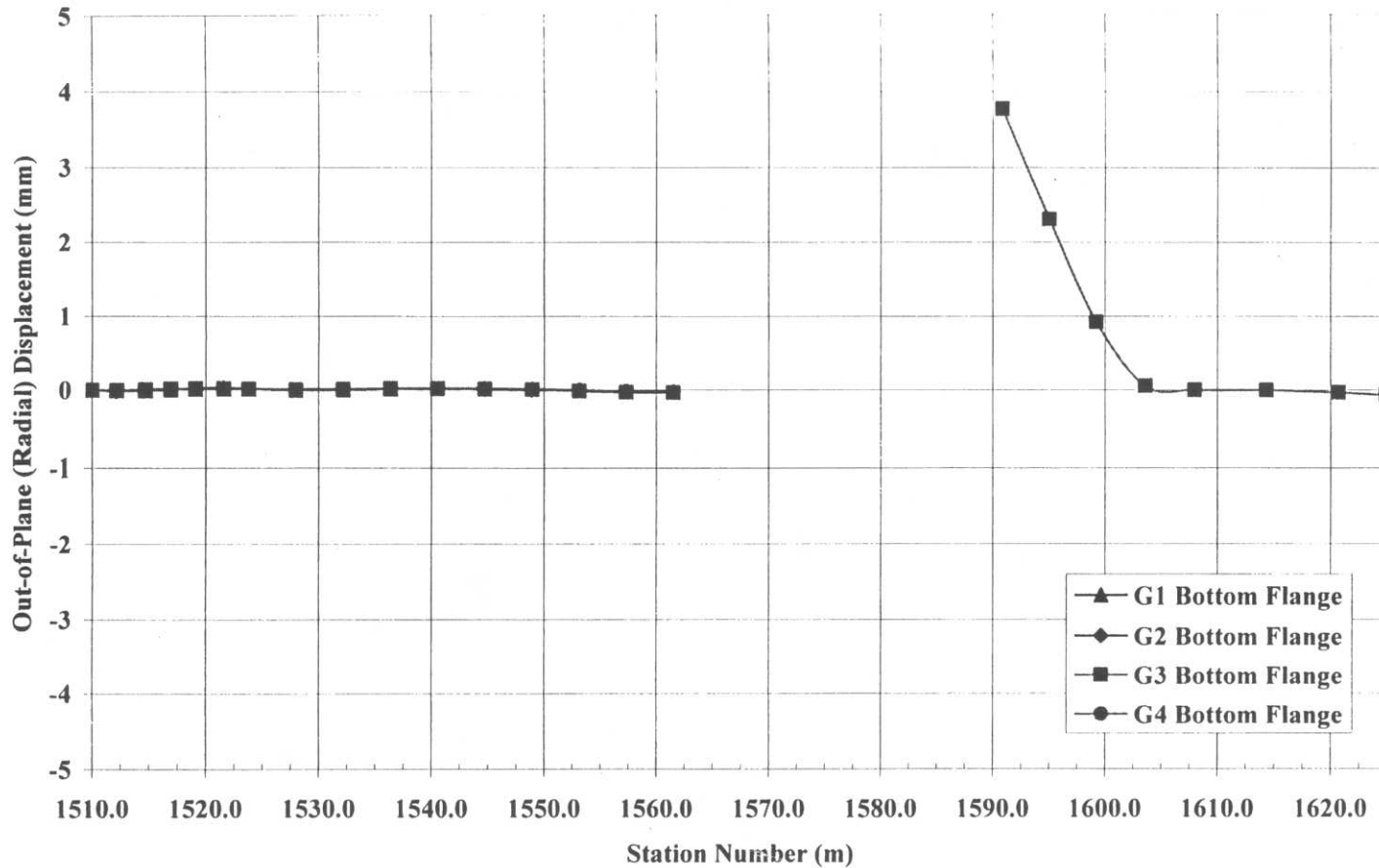
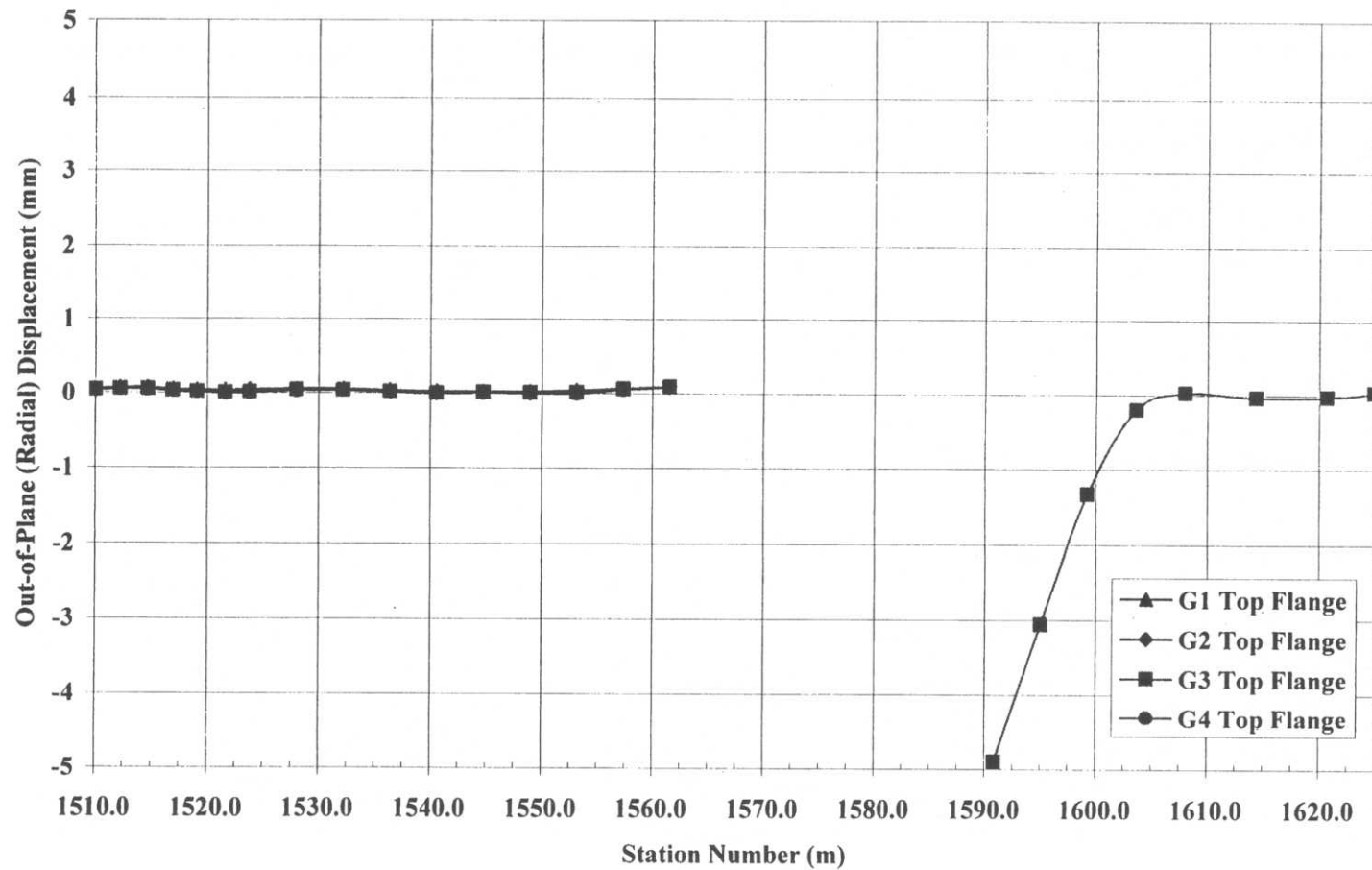


**Figure 102** Construction stage 9 – Plan view of finite element model



("-" is displacement inward of curve; "+" is displacement outward of curve)

**Figure 103** Construction stage 9 – Out-of-plane (radial) displacement, centerline of bottom flange



("-" is displacement inward of curve; "+" is displacement outward of curve)

**Figure 104** Construction stage 9 – Out-of-plane (radial) displacement, centerline of top flange

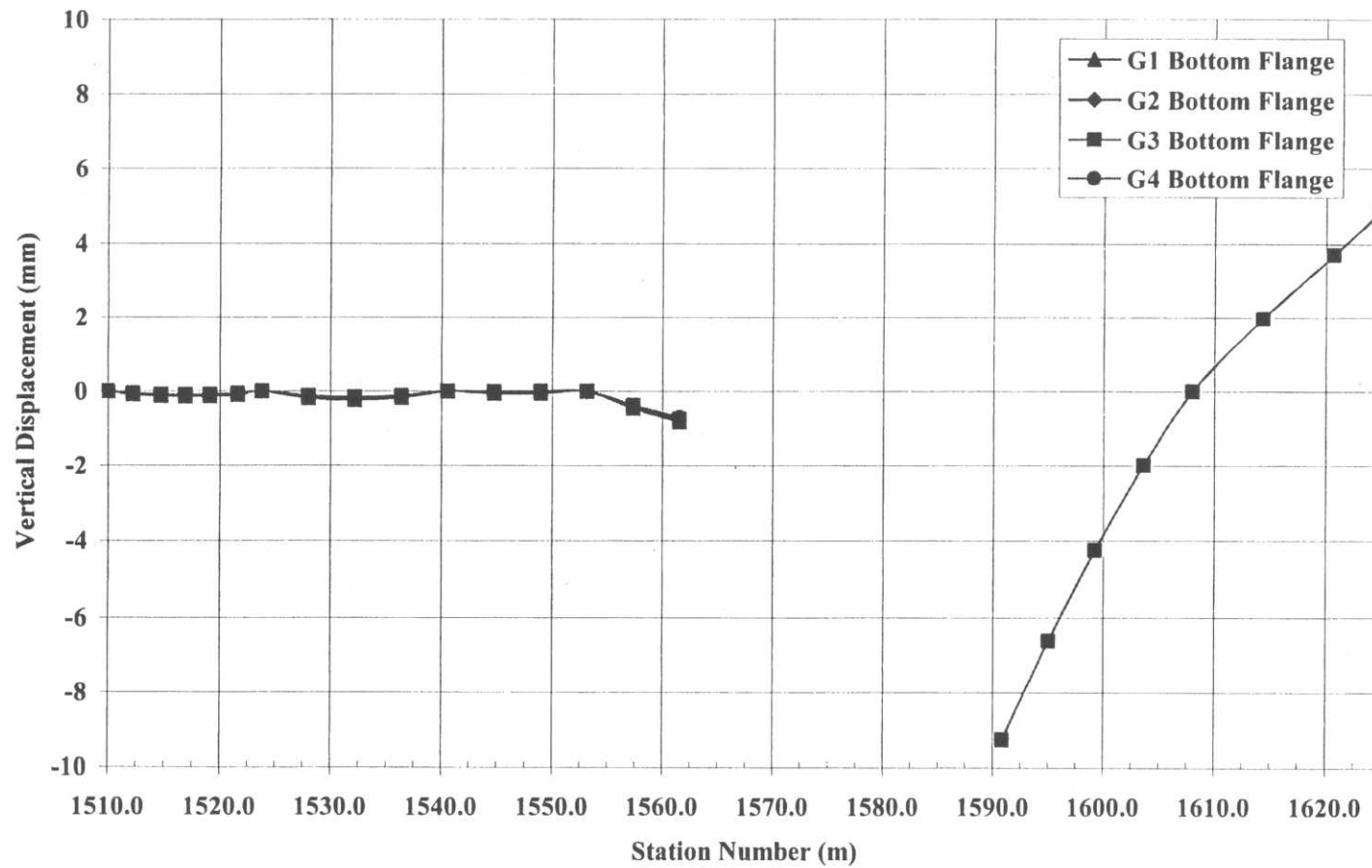


**Figure 105** Construction stage 9 – Vertical displacement, centerline of bottom flange

### 7.1.6 Construction Stage 10

Girder G2 section 4 (G2-4) and cross-frames 23B, 24B, 25B, and 29B are placed as components of construction stage 10. Pier brackets at pier 1 are used to stabilize G2-4, in the same manner as they are used to stabilize G3-4. The pier brackets are designed to support G2-4 at the cross-frame 26 and 28 positions. The north and south ends of the G2-4 are cantilevered past the pier bracket supports, just as G3-4 is. In the field, G2-4 was released from the lifting crane upon completion of the cross-frame connections with girder G3-4. The current stage finite element model, as shown in figure 106 is used to analyze the behavior once girder G2-4 is released, and therefore does not consider the influence of the lifting crane.

The addition of G2-4 to the girder system at pier 1 reduces the displacement experienced by G3-4 from the previous construction stage. Out-of-plane (radial) displacement for G3-4 is reduced to almost zero, at the top and bottom flanges. The vertical downward deflection at the field-splice 3 location of G3-4 is also reduced, from 11.4mm (0.45in) in construction stage 9, to 1.5mm. Owing to the fact that G2-4 and G3-4 act as one system, the girder out-of-plane (radial) and vertical displacements are basically the same along the length of the girders. Figure 107 illustrates the vertical displacement of the entire erected structure up to the current construction stage.

For both girders sections, the maximum von Mises stress inherent in the girders is in the top flanges between the span 1 pier bracket and pier 1. The von Mises stress at this location is approximately 9 MPa (1.3 ksi), well below the material yield stress.

As in the previous construction stage, there is no evidence of contact with the span 2 pier 1 bracket and G2-4 and G3-4, implying that girder “lift-off” occurs. Again this is due to the geometric configuration of the pier brackets, as they are designed to allow for the described “lift off.” Table 8 summarizes the support reactions at pier 1, up to the current construction stage. At the span 1 pier bracket, at the cross-frame 26 location, girder G3 has a slightly higher support reaction than G2; and at pier 1, the opposite occurs, G2 has a greater support reaction than G3. At the pier bracket, the girders are displacing down and inward (of-curve) due to the cantilevered position and curved geometry of the girders, consequently the stated support reaction distribution occurs.

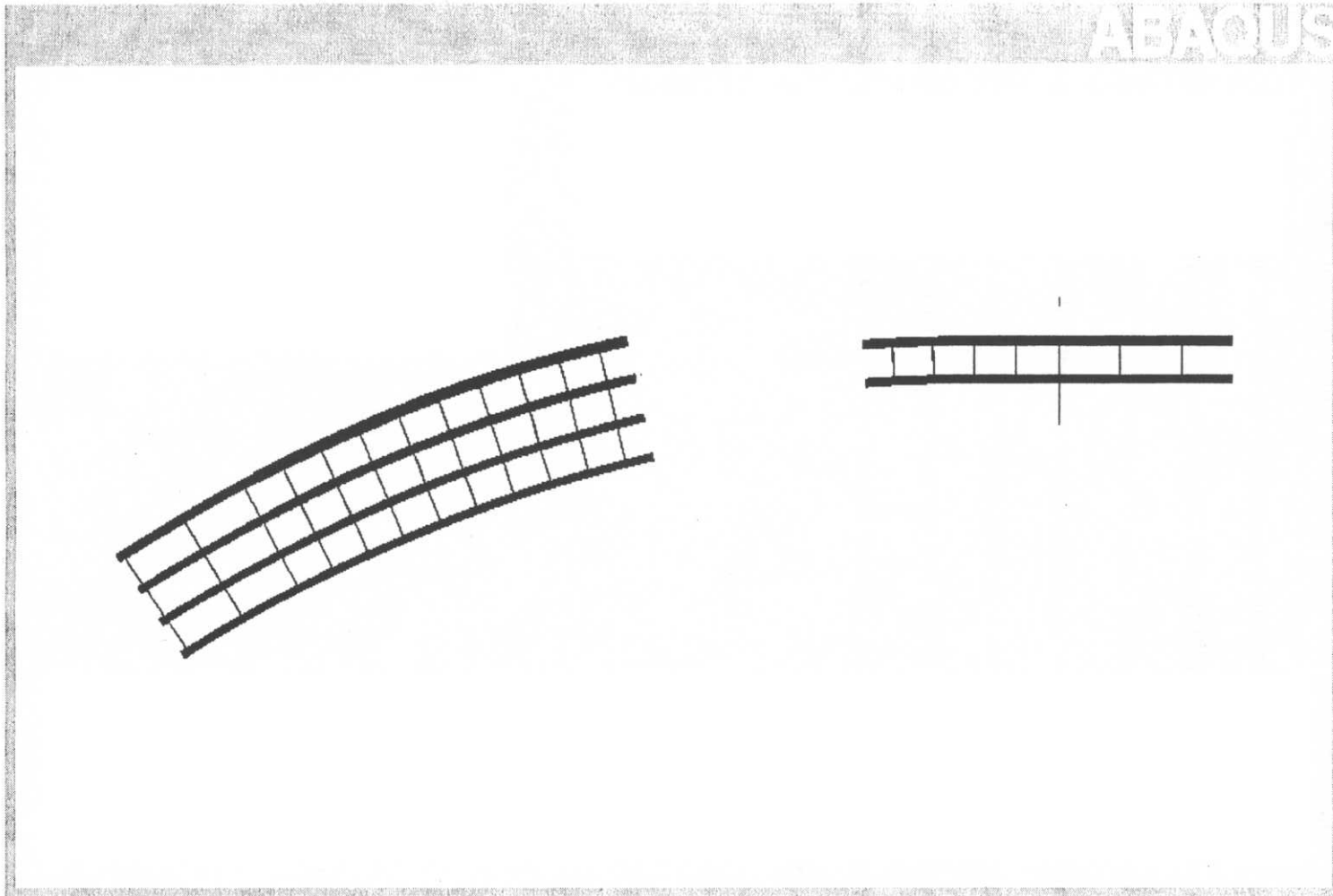


**Figure 106** Construction stage 10 – Plan view of finite element model

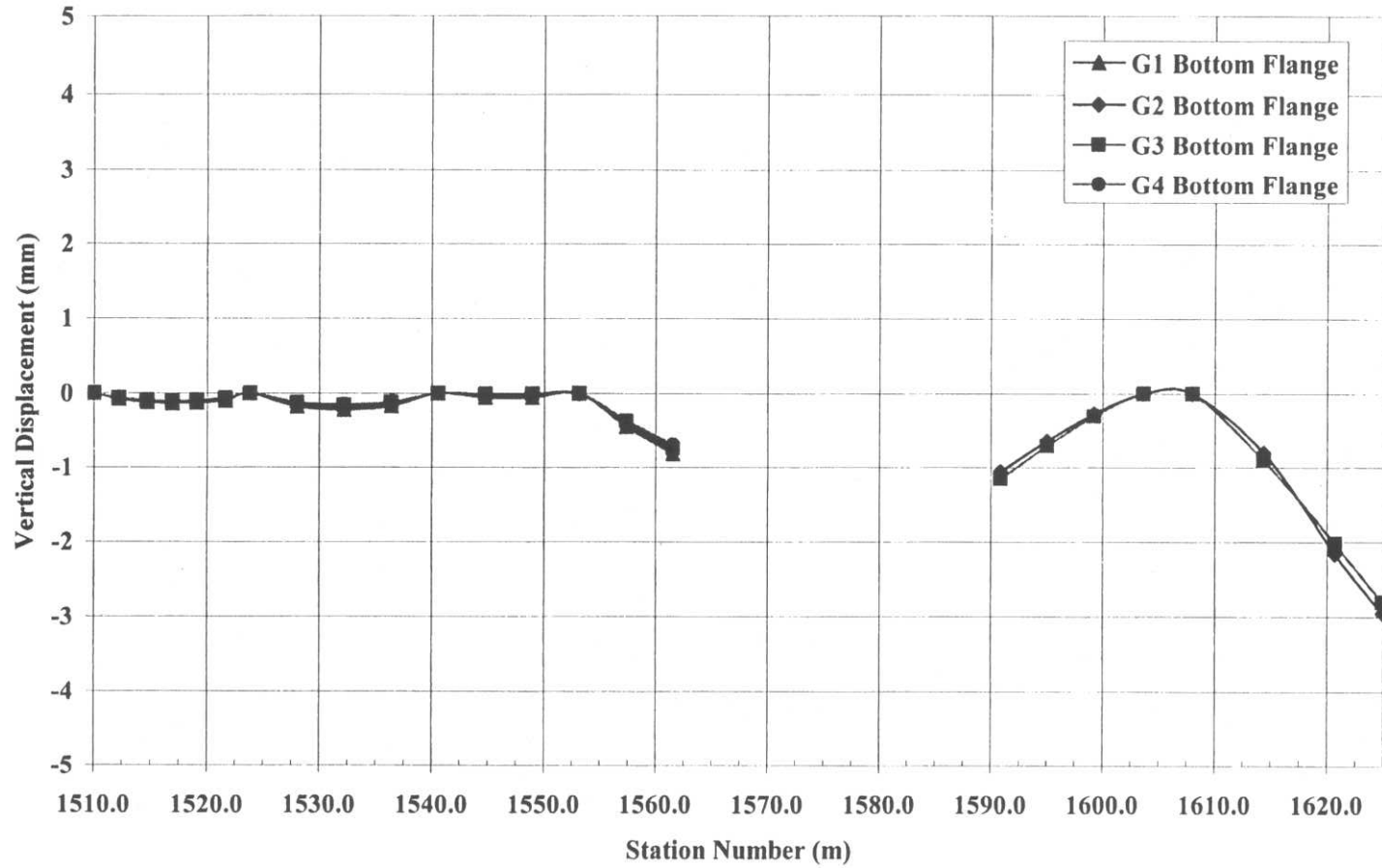


**Figure 107** Construction stage 9 – Vertical displacement, centerline of bottom flange

**Table 8** Construction stages 9 and 10 – Pier 1 support reactions

		<b>Pier 1 Bracket XF 26 (kips)</b>		<b>Pier 1 (kips)</b>			
<b>Construction Stage</b>	<b>Erected Girder</b>	G2	G3	G1	G2	G3	G4
<b>9</b>	<b>G3-4</b>		35			129	
<b>10</b>	<b>G2-4</b>	35	42		148	127	

### 7.1.7 Construction Stage 11

Construction stage 11 consists of the placement of the “drop-in” section, girder G3 section 3 (G3-3). The pier brackets at pier 1 were included, for the analysis of the current construction stage. The finite element model does not include the effects of G3-3 being held in place by a lifting crane, because, from the investigation of the actual erection sequence, it is unknown exactly where the girder was to be held in place, the crane capacities, and so on. Figure 108 shows the plan view of the finite element model of the Ford City Bridge at the current construction stage.

In comparison with the previous construction stages, greater displacements are manifest in the structure. This is due to the unsupported length of the installed G3-3 section. Maximum displacements occur at midspan of G3-3, approximately station number 1+576.0. At this location the out-of-plane (radial) displacement of the bottom flange is 8.5mm. (0.33in) inward (of curve), and the out-of-plane (radial) displacement of the top flange is 9.5mm (0.37in) outward (of curve), as shown in figure 109. The vertical

displacement at the same location is approximately 5.8mm (0.23in) downward. Figure 110 shows the vertical displacement of the entire structure at this construction stage. It should be noted, that a crane used to stabilize G3-3 in the field could prevent the displacements that occurred in the analytical model.

At the field-splice 3 location of G2-4, displacements are minimal, with a vertical downward displacement of 1.8mm. The top flange at the same location, displaces 1.3mm towards the inside portion of the curve.

Also, at the midspan of G3-3, a von Mises stress of approximately 20 MPa (2.9ksi) develops in the inside of curve edge of the top flange. The longitudinal stress at the same location is approximately 17 MPa (2.4ksi) in compression. A von Mises stress of 17 MPa (2.4 ksi) develops on the inside of curve edge of the top flange at both the cross-frame 16 and 23 locations of girder G3. A primarily constant von Mises stress of 11 MPa (1.6 ksi) is displayed on the top flanges of G2-4 and G3-4 in between the span 1 pier 1 bracket and pier 1.

In regard to the support reactions, an extremely large vertical reaction of 153 kips (682 kN) develops at the pier 1 bracket of G3, under cross-frame 26, while at the same time, the reaction at pier 1 is 48.7 kips (216.8 kN). In the field, it may be the case that the 153 kips load cannot be placed on the pier bracket, and therefore a stabilizing crane could be used to assume some of this load. Table 9 shows the support reactions at all locations for construction stage 10. Also, of note is that reactions for the inside girder, G4, begin to significantly decrease at falsework 2A from previous construction stages, showing the tendency of girder “lift-off” and “roll.”

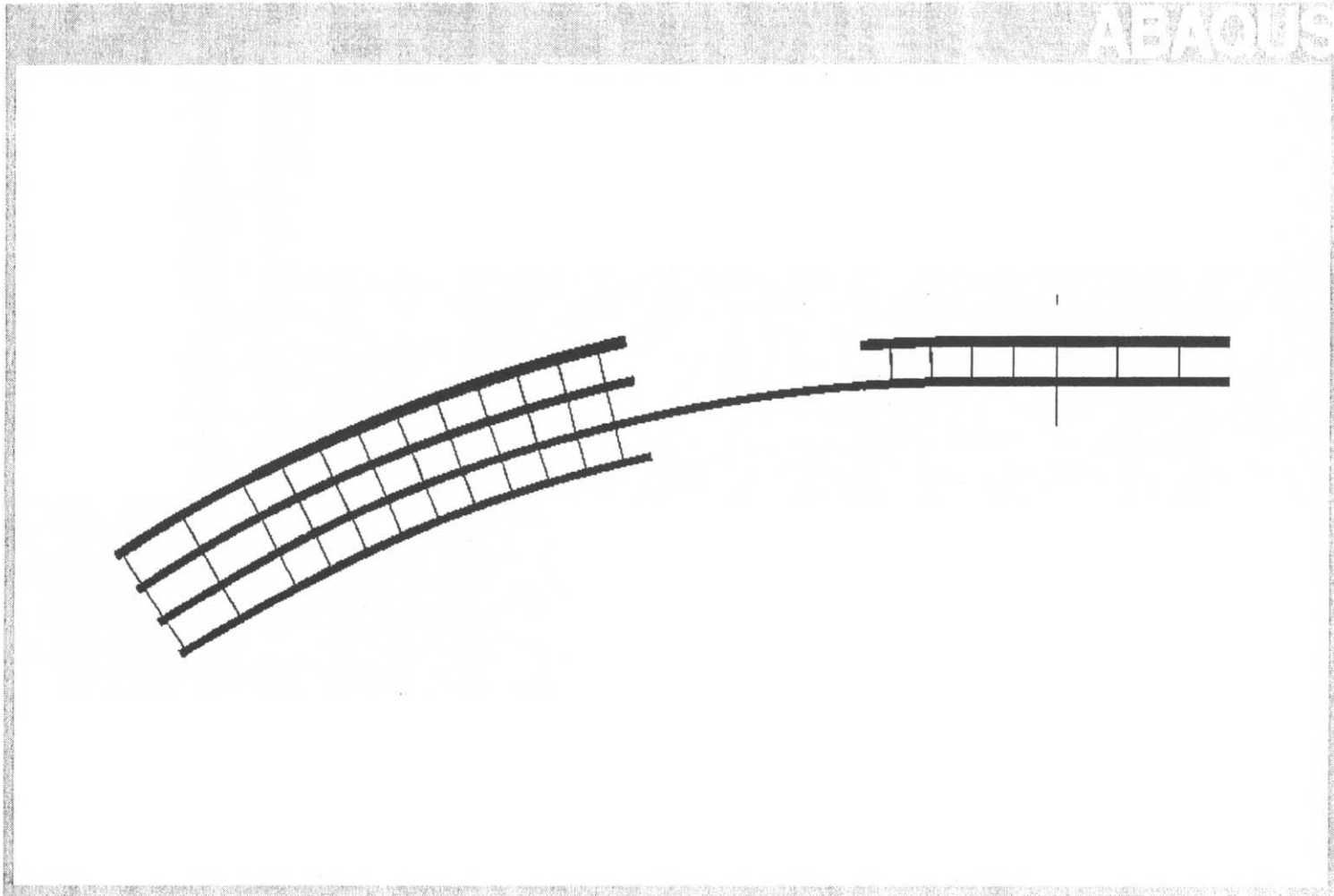
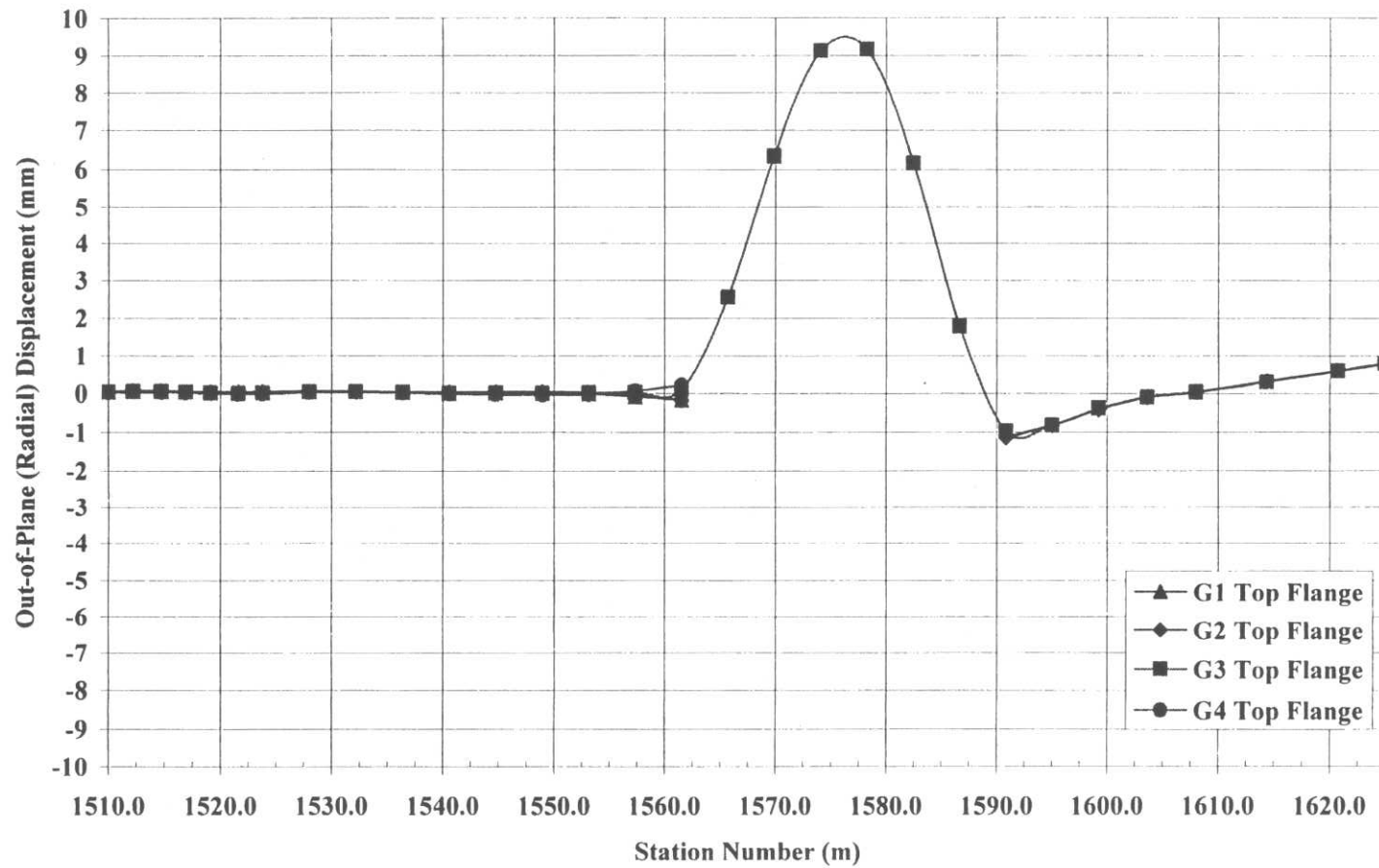


**Figure 108** Construction stage 11 – Plan view of finite element model



("-" is displacement inward of curve; "+" is displacement outward of curve)

**Figure 109** Construction stage 11 – Out-of-plane (radial) displacement, centerline of top flange

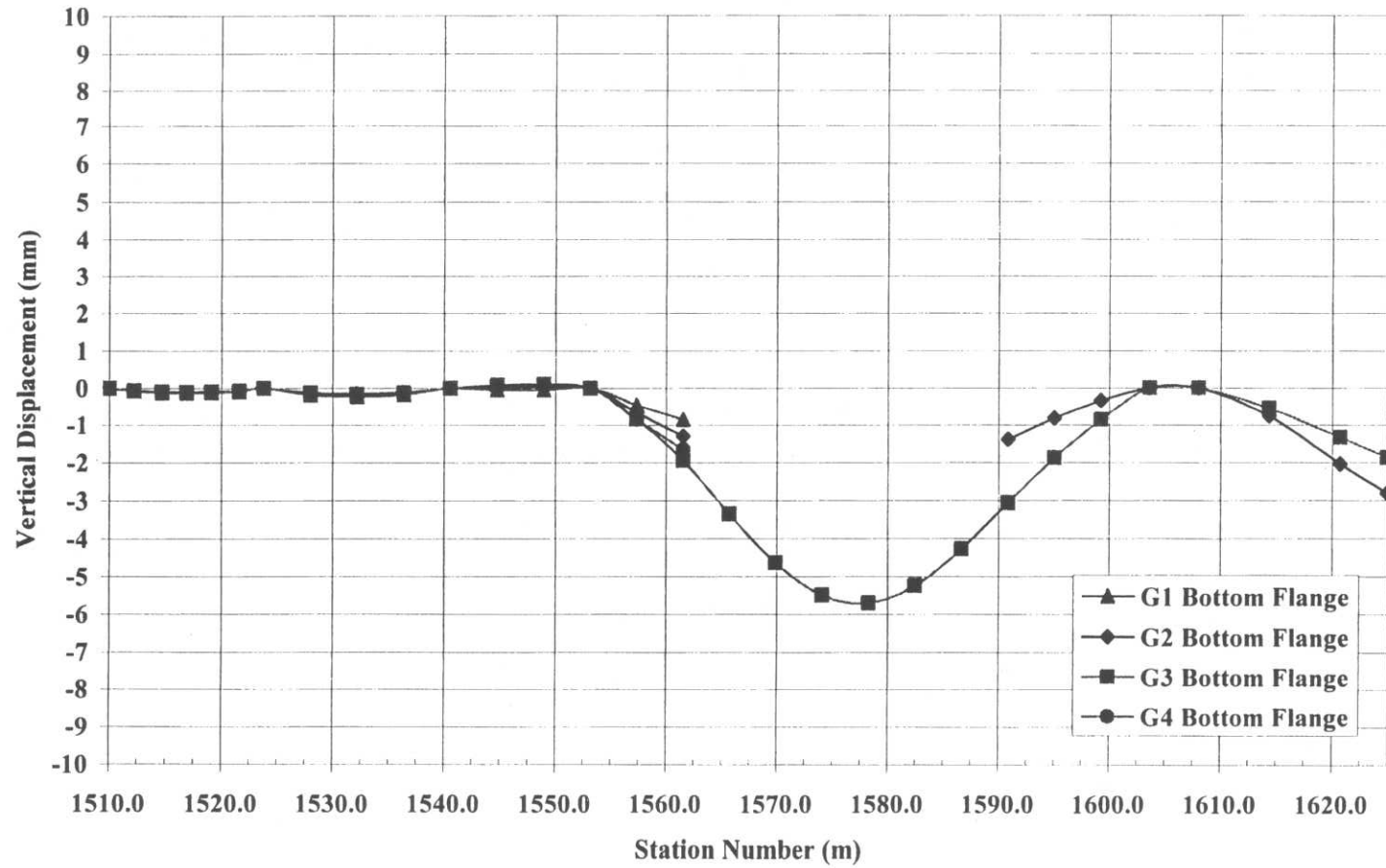


**Figure 110** Construction stage 11 – Vertical displacement, centerline of bottom flange

**Table 9** Construction stage 11 – Support reactions

	<b>Vertical Support Reactions (kips)</b>						
<b>Girder</b>	<b>Abutment 1</b>	<b>Falsework 1</b>	<b>Falsework 2A</b>	<b>Falsework 2</b>	<b>Pier Bracket at XF 26</b>	<b>Pier 1</b>	<b>Pier Bracket at XF 28</b>
G1	35.7	87.0	68.1	121.3	N/A	N/A	N/A
G2	21.8	67.3	38.1	135.4	48.1	134.4	0.0
G3	21.1	59.2	12.9	100.3	153.2	48.7	0.0
G4	18.4	44.2	9.6	101.9	N/A	N/A	N/A

### 7.1.8 Construction Stage 12

Girder G2 section 3 (G2-3) and cross-frames 17B through 22B are placed as part of construction stage 5. In the field construction, the pier brackets at pier 1 are removed upon the erection of G2-2. Therefore, the finite element model for this construction stage is the structure after the placement of G2-2 and subsequent cross-frames, and after the removal of the pier brackets. Figure 111 shows a plan view of the finite element model at the current construction stage.

Again, the unsupported length of G2-3 and G3-3 causes both out-of-plane (radial) and vertical displacements to develop near midspan of section 3, at approximately station 1+582.5. At this location, for both girders, the out-of plane (radial) displacement is almost zero at the bottom flange, but approximately 5mm outward (of curve) at the top flange. At the same location, the vertical downward displacement of G2-3 is 10.5mm (0.41in), and G3-3 is 6mm. (0.24in). Figure 112 illustrates the out-of-plane (radial) deflection of the top flange, and figure 113 shows the vertical displacement of the current structure. Also, of note, at the field-splice 2 locations of girders G1-2 and G4-2, a downward vertical displacement of approximately 2mm occurs due to the placement of G2-3.

Von Mises stresses of approximately 13 MPa (1.89 ksi) occur in the entire top flange of sections G2-3 and G3-3. Also, a von Mises stress of approximately 15 MPa (2.18 ksi) develops in the top flange of G2-2 and G3-2 above the falsework 2 locations.

The top flange longitudinal stress at the falsework 2 locations is approximately 11 MPa (1.60 ksi) in tension.

The first evidence of girder support “lift-off” occurs in the current construction stage, due to the placement of G2-3. Girders G2 and G3 “lift-off” of their supports at falsework 2A, and the subsequent reactions are redistributed to the falsework 2 and pier 1 supports. As shown in table 10, generally, a significant increase in the support reactions at falsework 2A and pier 1 occurs from construction stage 11 to 12. However, the support reactions at abutment 1 and falsework 1 basically remain unchanged.

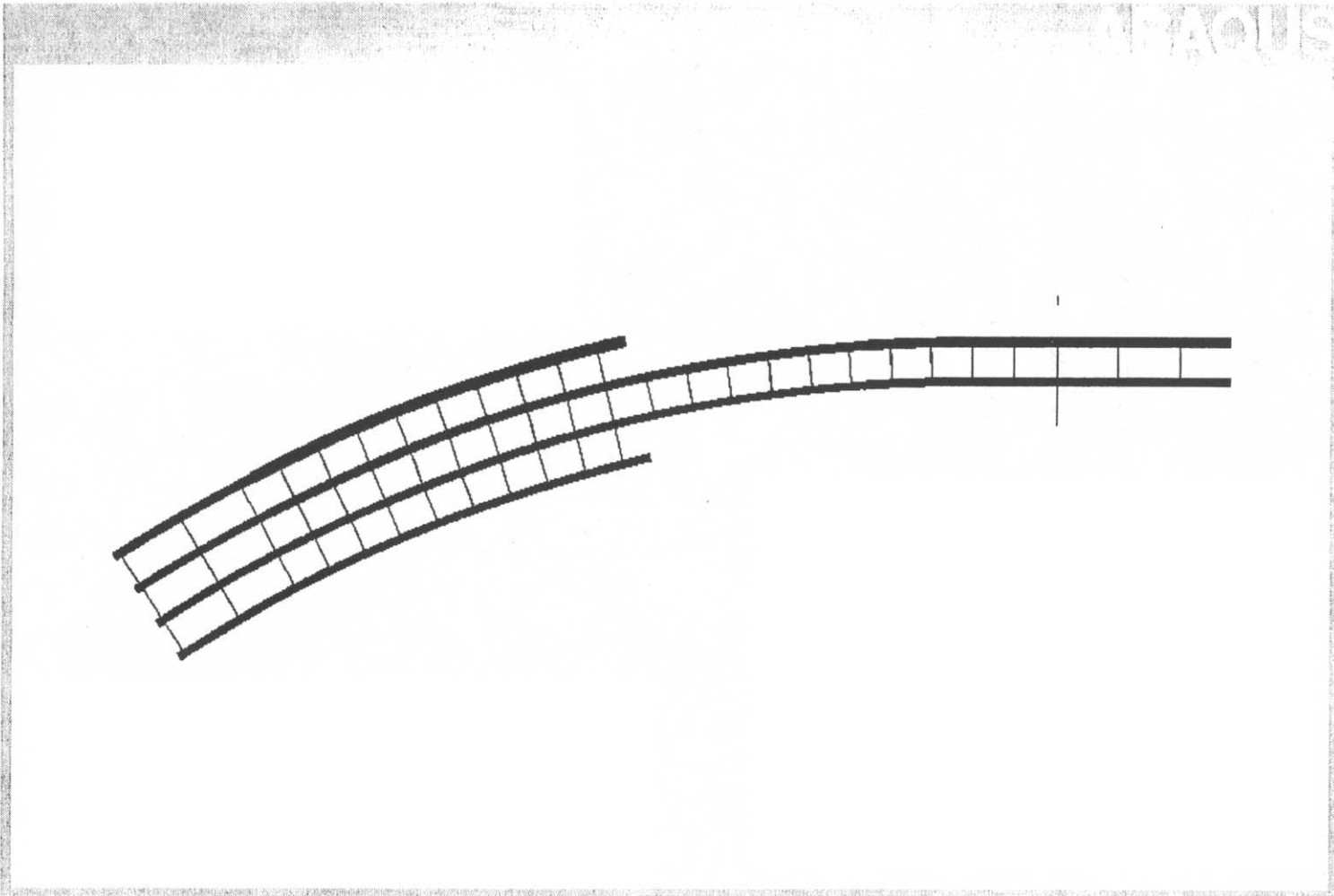
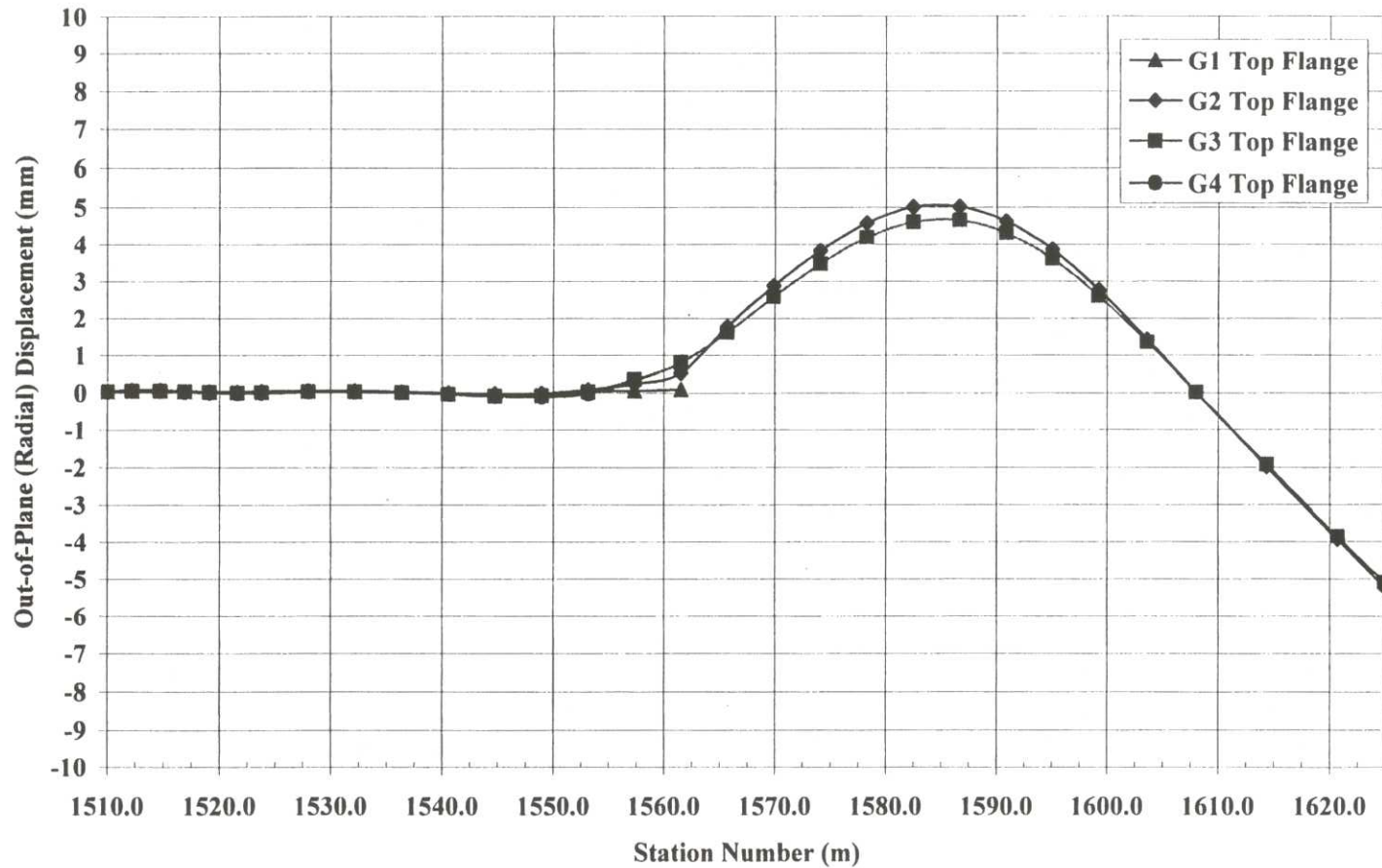


**Figure 111** Construction stage 12 – Plan view of finite element model



(“-“is displacement inward of curve; “+” is displacement outward of curve)

**Figure 112** Construction stage 12 – Out-of-plane (radial) displacement, centerline of top flange

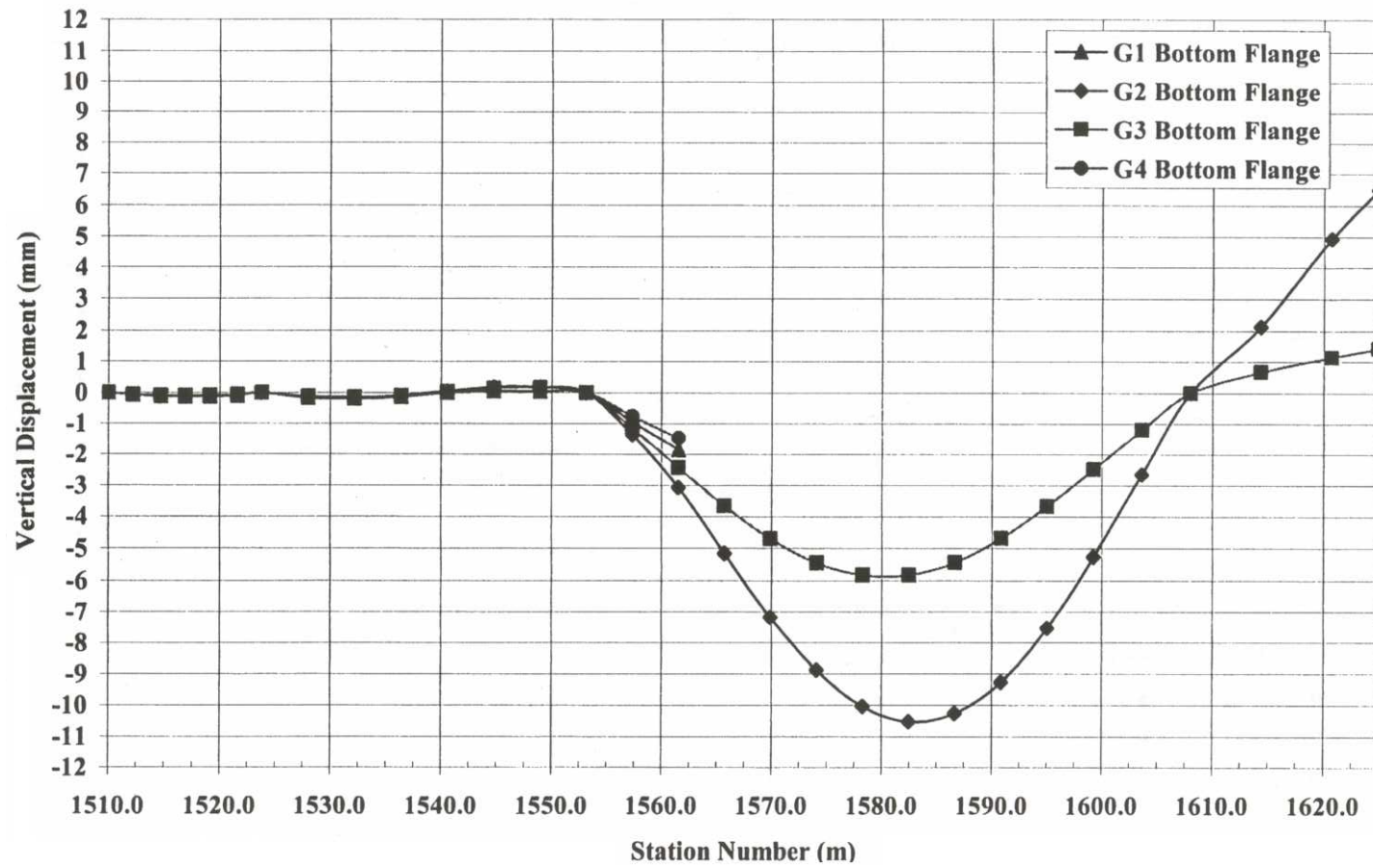


**Figure 113** Construction stage 12 – Vertical displacement, centerline of bottom flange

**Table 10** Construction stages 11 and 12 – Support reactions

		Abutment 1 (kips)				Falsework 1 (kips)				Falsework 2A (kips)			
Construction Stage	Erected Girder	G1	G2	G3	G4	G1	G2	G3	G4	G1	G2	G3	G4
11	G3-4	36	22	21	18	87	67	59	44	68	38	12	10
12	G2-4	37	22	22	18	86	67	59	44	29	0	0	13

		Falsework 2 (kips)				Pier Bracket XF 26 (kips)		Pier 1 (kips)			
Construction Stage	Erected Girder	G1	G2	G3	G4	G2	G3	G1	G2	G3	G4
11	G3-4	121	135	101	102	48	153		134	49	
12	G2-4	194	202	155	97				229	164	

### 7.1.9 Construction Stages 13 and 14

Construction stage 13 involves the placement of girder G4 section 4 (G4-4), and construction stage 14 consists of the placement of girder G1 section 4 (G1-4). Appropriate cross-frame lines are inserted into the finite element models as well. Figure 114 illustrates the finite element model for construction stage 14. This section will mainly focus on the structure after the analysis of construction stage 14.

There is no evidence of significant displacements due to the placement of G4-4, however this is not the case once G1-4 is placed into the model. At construction stage 14, the vertical displacement at the field-splice 3 location of girder G1 is 19mm (0.76in) downward; the out-of-plane (radial) displacement of the bottom flange is 2.7mm inward (of curve); and the out of-plane (radial) displacement of the top flange is 4.6mm outward (of curve). Figure 115 shows the out-of-plane (radial) displacement of the top flange, and figure 116 illustrates the vertical deflection of the current structure.

A von Mises stress of approximately 23 MPa (3.3 ksi) manifests in the top flange of girder G2 at the field-splice 3 location. Longitudinal compressive stresses are evident in the top flange of G2-3 and G3-3, ranging from 4 MPa to 22 MPa (0.58 ksi to 3.2 ksi). Also, at the falsework 2 locations of girders G2 and G3, the top flange is subjected to a von Mises stress of 17 MPa (2.5 ksi), and alternatively a tensile longitudinal stress of approximately 16 MPa (2.3 ksi).

Progressing from construction stage 12 to 14, there is no significant change in the support reactions, except for at pier 1, due to the placement of girders G1-4 and G4-4 at

the pier 1 location. Table 11 shows the change in support reactions from stage 11 to the current construction stage. Support reactions throughout the remainder of the structure generally remain unchanged.

**Table 11** Construction stages 12 through 14 – Pier 1 reactions

		<b>Pier 1 (kips)</b>			
<b>Construction Stage</b>	<b>Erected Girder</b>	<b>G1</b>	<b>G2</b>	<b>G3</b>	<b>G4</b>
12	G2-3		229	164	
13	G4-4		224	177	130
14	G1-4	184	220	179	130

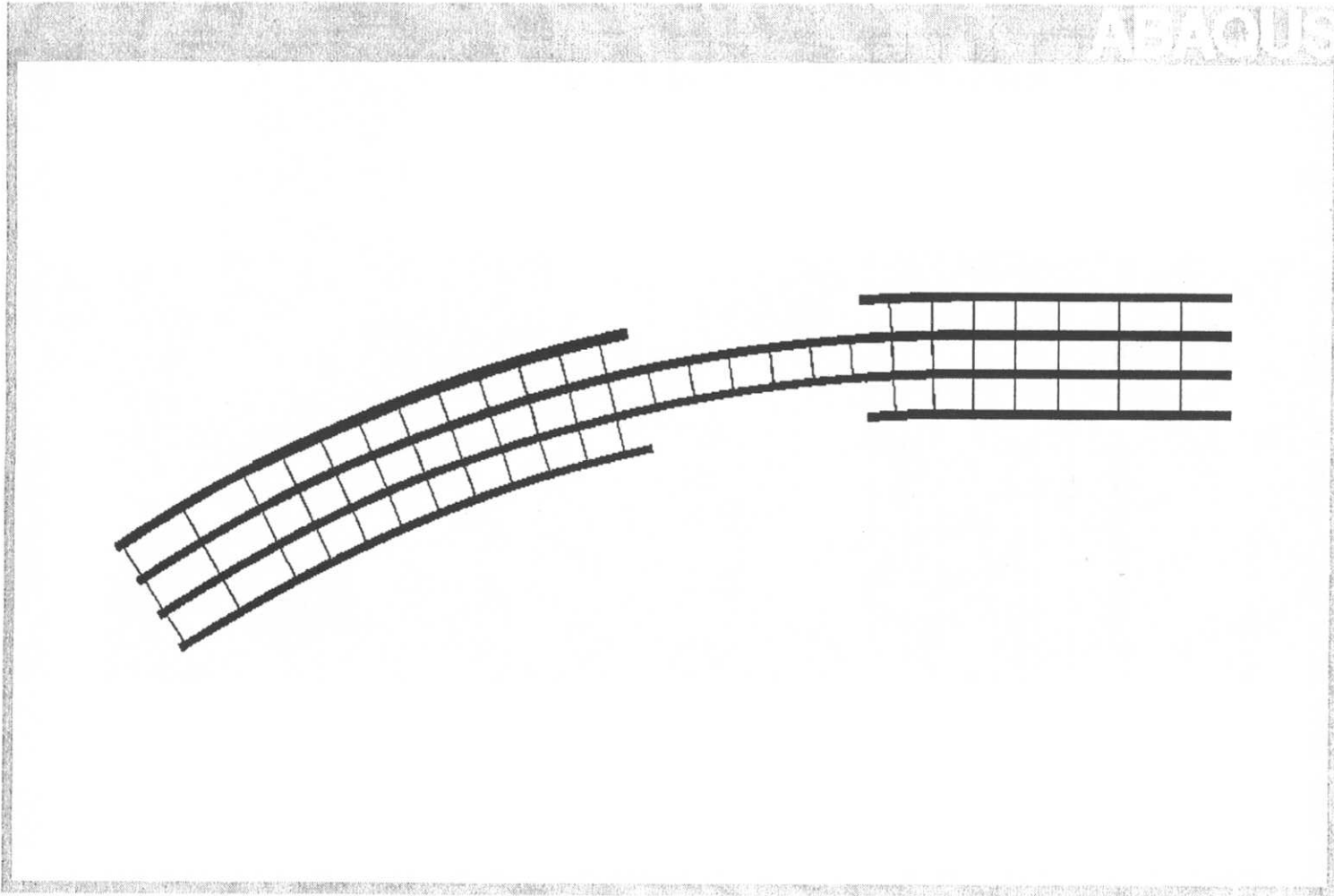
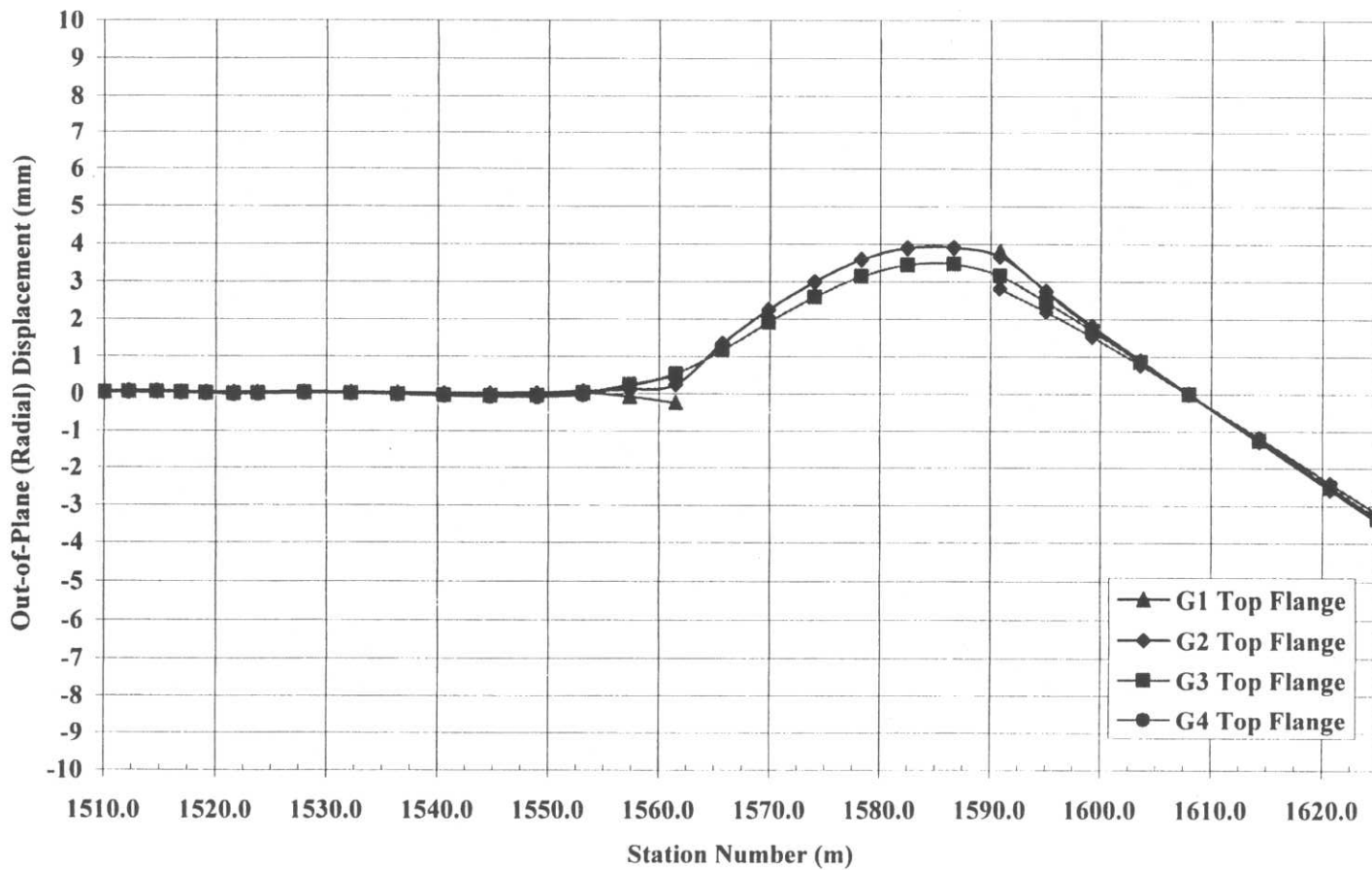


**Figure 114** Construction stage 14 – Plan view of finite element model



("-" is displacement inward of curve; "+" is displacement outward of curve)

**Figure 115** Construction stage 14 – Out-of-plane (radial) displacement, centerline of top flange

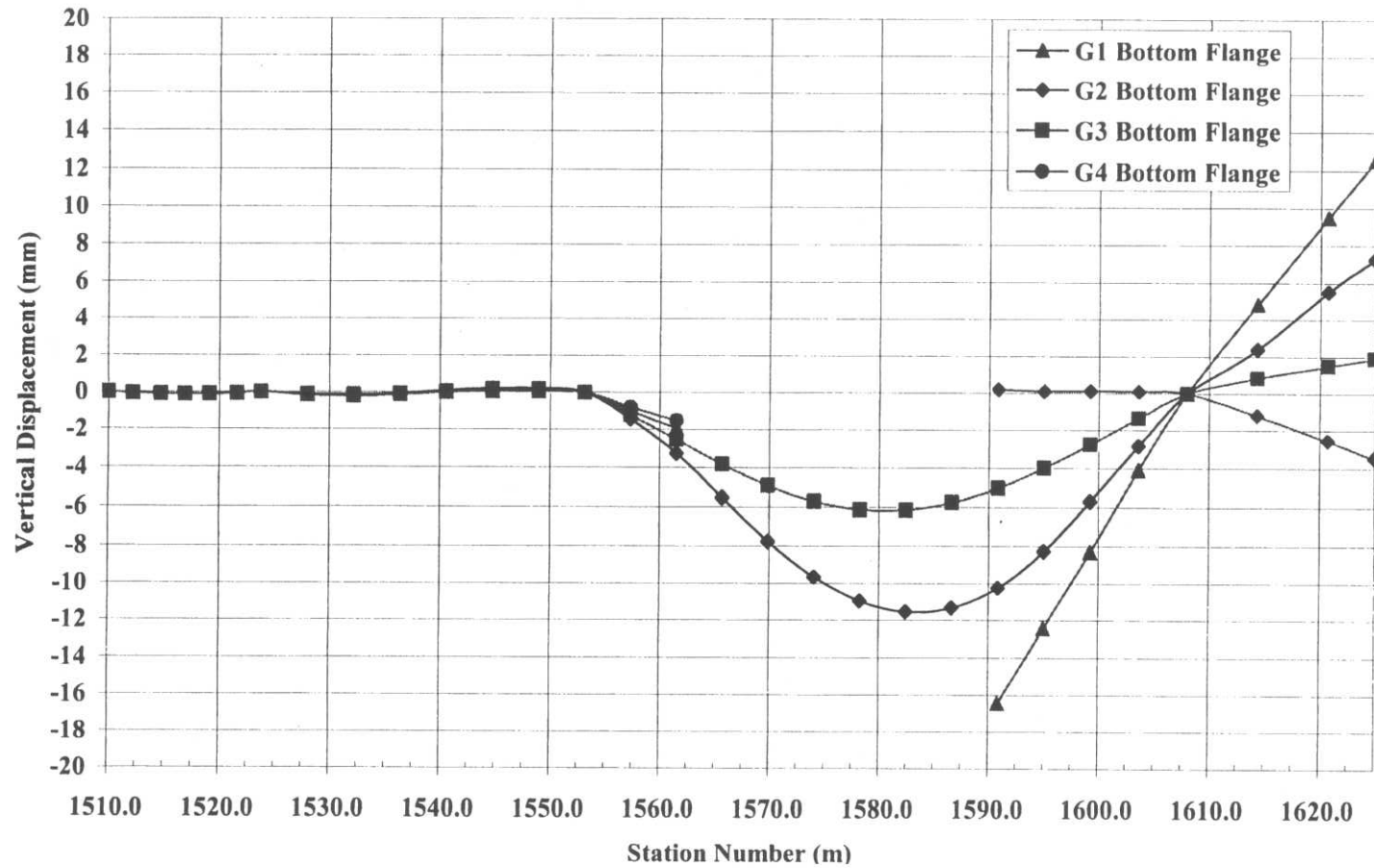


**Figure 116** Construction stage 14 – Vertical displacement, centerline of bottom flange

### 7.1.10 Construction Stage 15

Construction stage 15 entails the placement of girder G4 section 3 (G4-3) and cross-frames 17C through 22C. G4-3 is the third of the four “drop-in” sections, for section 3 of the structure. Figure 117 displays the finite element model at the current construction stage. To reiterate, the analysis is performed once the girder and all cross-frames are placed, with crane affects not being taken into consideration.

Near midspan of section 3, the out-of-plane (radial) and vertical displacements decrease slightly from construction stage 14 to 15. Due to the placement of G4-3, the structure acts more as one rigid unit, and therefore the deflections at midspan decrease. At the section 3 midspan, the maximum top flange out-of-plane (radial) displacement is 2mm for all of the girders; and the vertical deflections for girders G2, G3 and G4 are 11mm, 8mm, and 5mm, respectively. Figure 118 displays the top flange out-of-plane (radial) displacement for the current structure, and figure 119 shows the vertical displacement at construction stage 15. However, of note, is the vertical deflection at the field-splice 3 location of G1-4, which displaces 15.8mm (0.62in) downward. Additionally, at the field-splice 2 location of G1-2, the girder deflects downward 2.3mm. Certainly, if these displacements were larger, inserting the last “drop-in” section, G1-3, could prove to be difficult due to the developed misalignment at the field splices.

The maximum von Mises stress for the current structure occurs near the field-splice 3 location of girder G2, and is approximately 25 MPa (3.6 ksi). At the same location, the compressive longitudinal stress is approximately 18 MPa (2.6 ksi). Also, at

the falsework 2 location, for girders G2, G3, and G4, the von Mises stress is approximately 20 MPa (2.9 ksi) in the top flange, with a tensile longitudinal stress in the order of 16 MPa (2.3 ksi).

Somewhat significant load redistribution occurs at the falsework 2 and pier 1 supports due to the placement of G4-3. Conversely, the reactions at abutment 1 and falsework 1 generally remain unchanged from the previous construction stage. At falsework 2A, only girder G1 remains in contact with the support, as all of the other girders have “lifted off” of the support. As shown in table 12, the largest support reaction at both falsework 2 and pier 1 occurs at the G2 supports, and not the outside girder G1. This behavior can be attributed to the fact that girder G1 is not entirely complete, with section 3 not yet placed; therefore, the load is not redistributed to the outside girder.

**Table 12** Construction stage 15 – Falsework 2 and pier 1 reactions

<b>Support Location</b>	<b>Girder Reactions (kips)</b>			
	<b>G1</b>	<b>G2</b>	<b>G3</b>	<b>G4</b>
Falsework 2	189	213	175	141
Pier 1	183	223	192	139

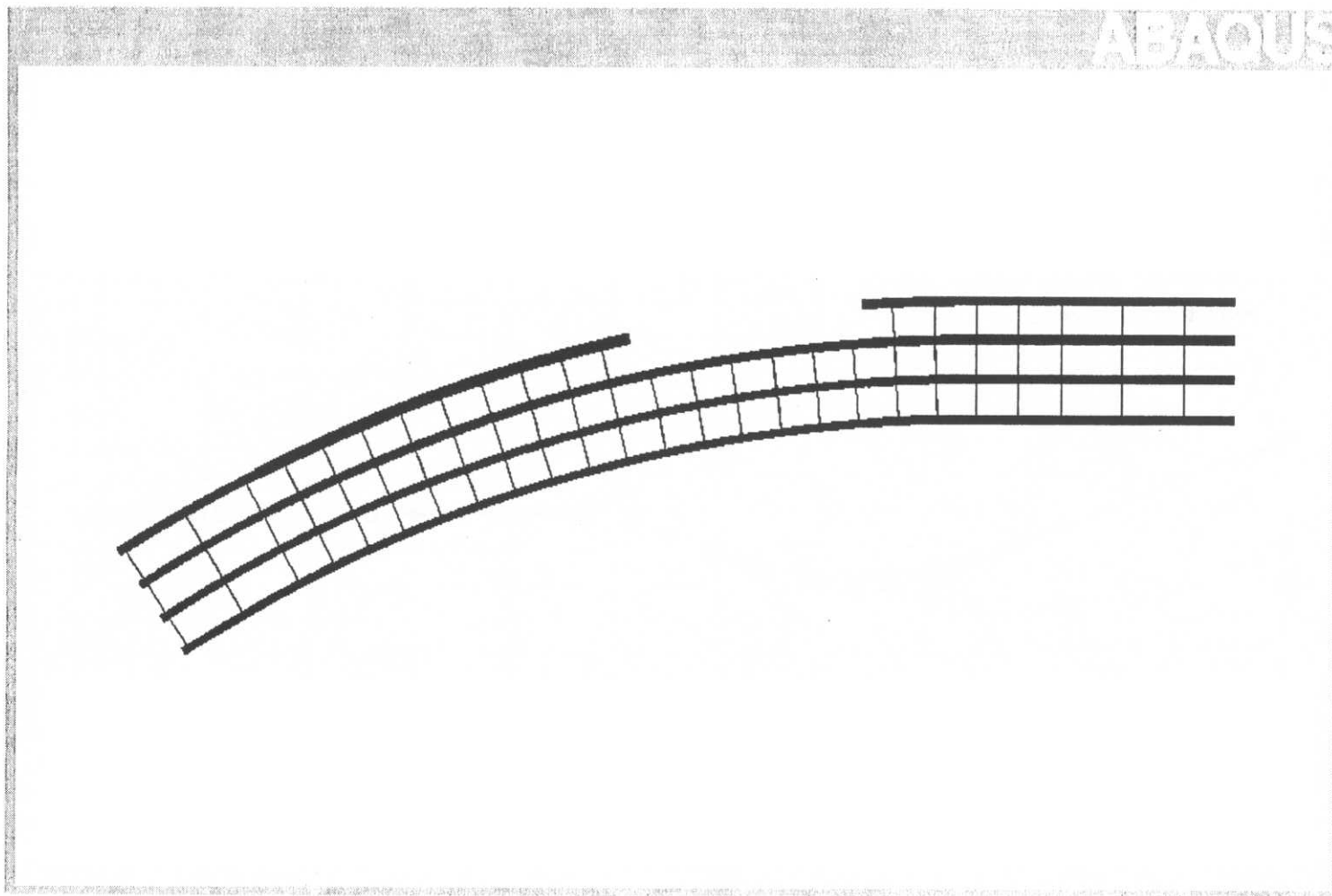
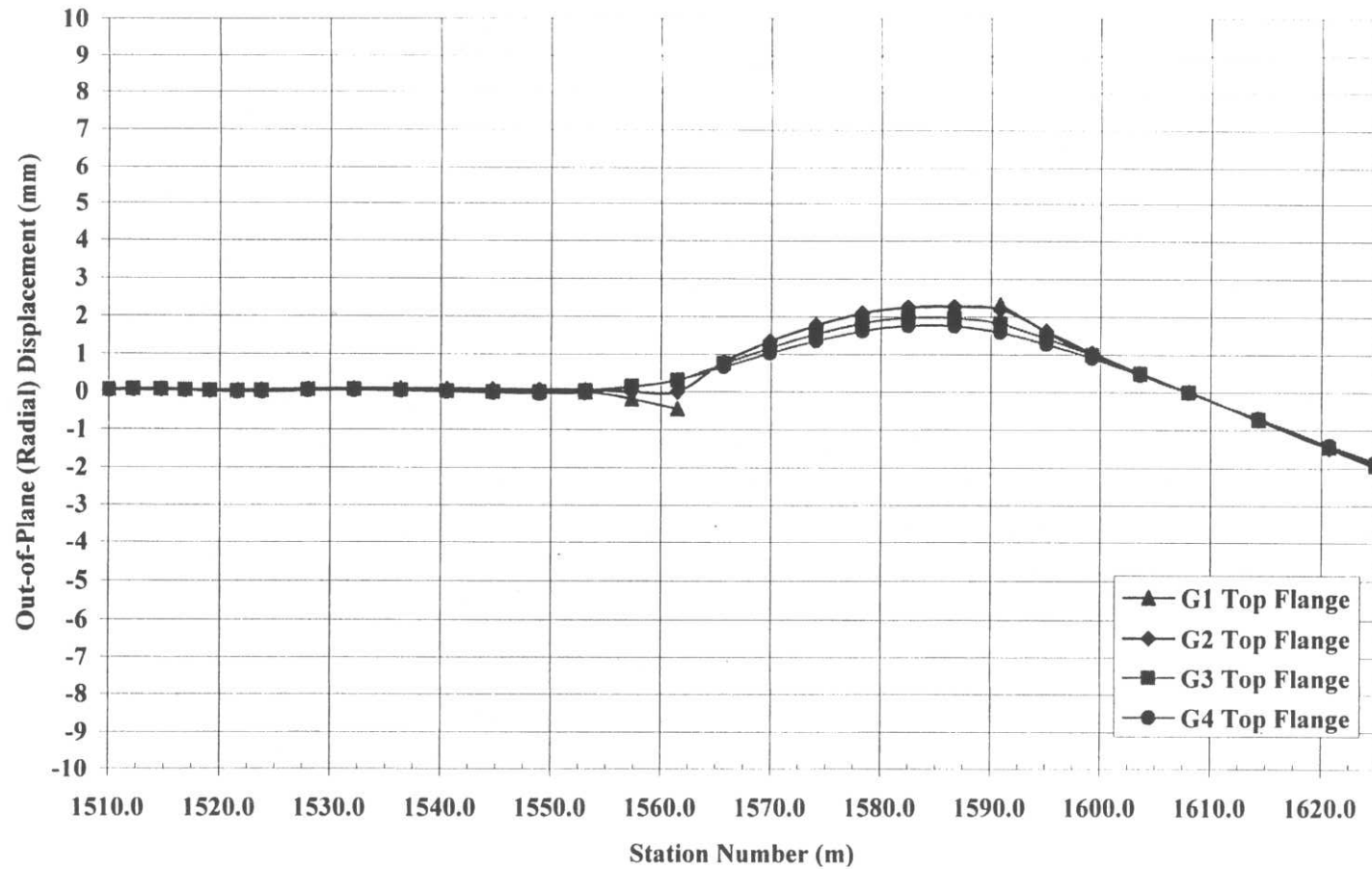


**Figure 117** Construction stage 15 – Plan view of finite element model



("-" is displacement inward of curve; "+" is displacement outward of curve)

**Figure 118** Construction stage 15 – Out-of-plane (radial) displacement, centerline of top flange

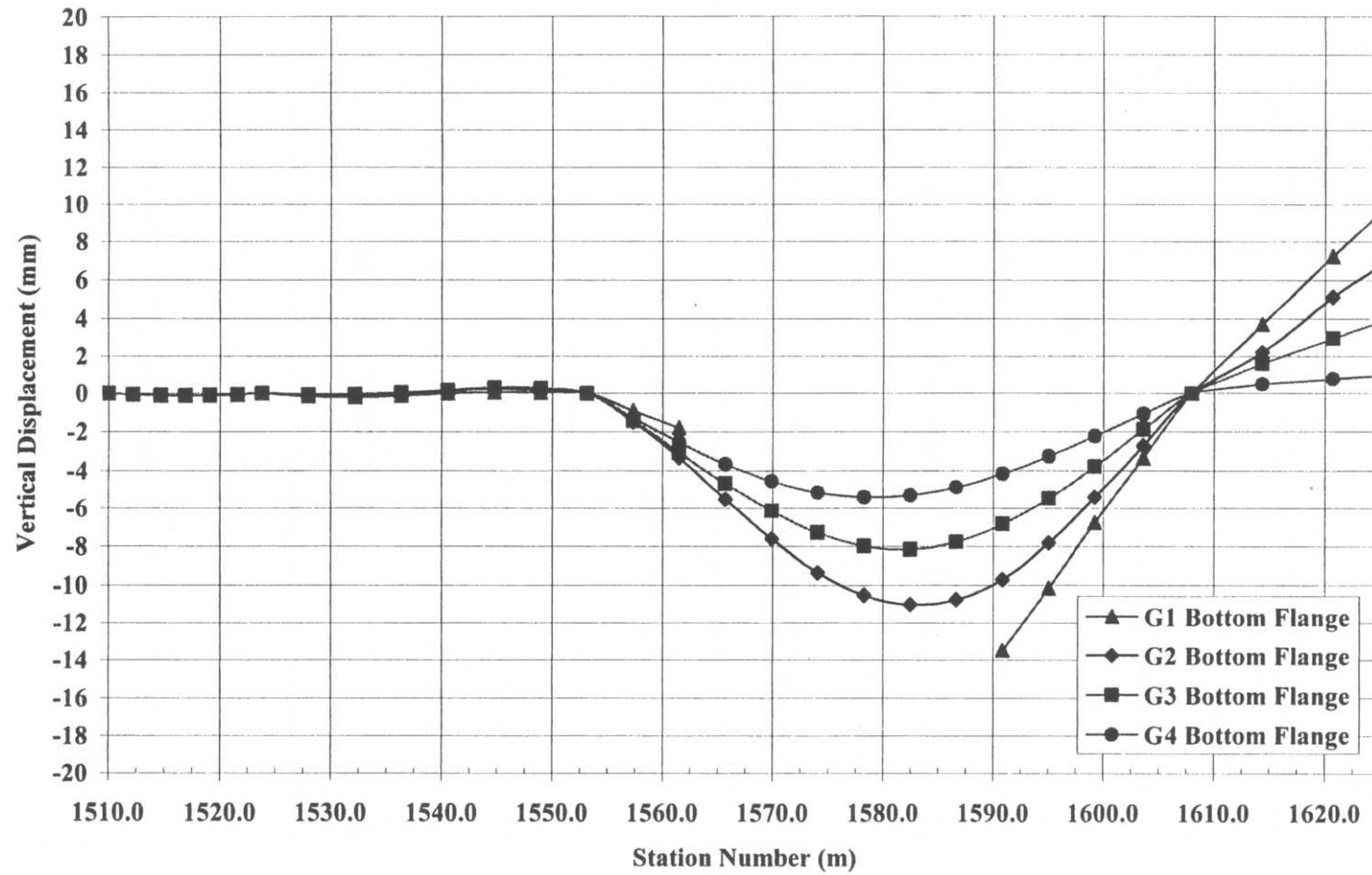


Figure 119 Construction stage 15 – Vertical displacement, centerline of bottom flange

### 7.1.11 Construction Stage 16

The final member of the curved section, girder G1 section 3 (G1-3), and cross-frames 17A through 22A, are placed as part of construction stage 16. Falsework 1, 2A and 2 remain in the finite element model for the current construction stage, given that they remained during the actual construction of the bridge. Figure 120 illustrates the plan view of the finite element model for the final construction stage.

From the previous to current construction stage, a slight decrease of the out-of-plane (radial) and vertical displacements is observed at the midspan of section 3. All of the girders at this location, are subject to a top flange out-of-plane (radial) displacement of almost 2mm outward (of curve). While the vertical deflections at the same location for girders G1, G2, G3, and G4 are approximately 12mm, 9mm, 7mm, and 5mm, (0.47in, 0.35in, 0.28in, and 0.20in) respectively. Figure 121 shows the top flange out-of-plane (radial) displacement for the current structure, and figure 122 illustrates the vertical displacement at construction stage 16.

In the proximity of the field-splice 3 location of girder G1, a von Mises stress of 28 MPa (4.1ksi) is observed in the top flange. Generally, the top and bottom flanges of girders G1-3 and G2-3 are subjected to a von Mises stress of approximately 20 MPa (2.9 ksi). The monitored longitudinal stress at the same section is approximately 14 MPa (2.03 ksi) (compression) on the top flange, and approximately 12 MPa (1.74 ksi) (tension) on the bottom flange.

The analysis demonstrates that once G1-3 and the respective cross-frames are placed, the reactions, in most cases, redistribute to the outside girders. Table 13 shows the reactions at each support for construction stage 16. All of the reactions tend to agree with engineering judgment, such that the outside girder supports receive the greatest reactions due to load redistribution. It is also shown that all of the girders, except G4, “lift off” of the falsework 2A support location.

**Table 13** Construction stage 16 – Support reactions

<b>Support Location</b>	<b>Girder Reactions (kips)</b>			
	<b>G1</b>	<b>G2</b>	<b>G3</b>	<b>G4</b>
Abutment 1	47	25	22	18
Falsework 1	60	54	55	45
Falsework 2A	0	0	0	7
Falsework 2	316	261	165	119
Pier 1	244	215	184	141

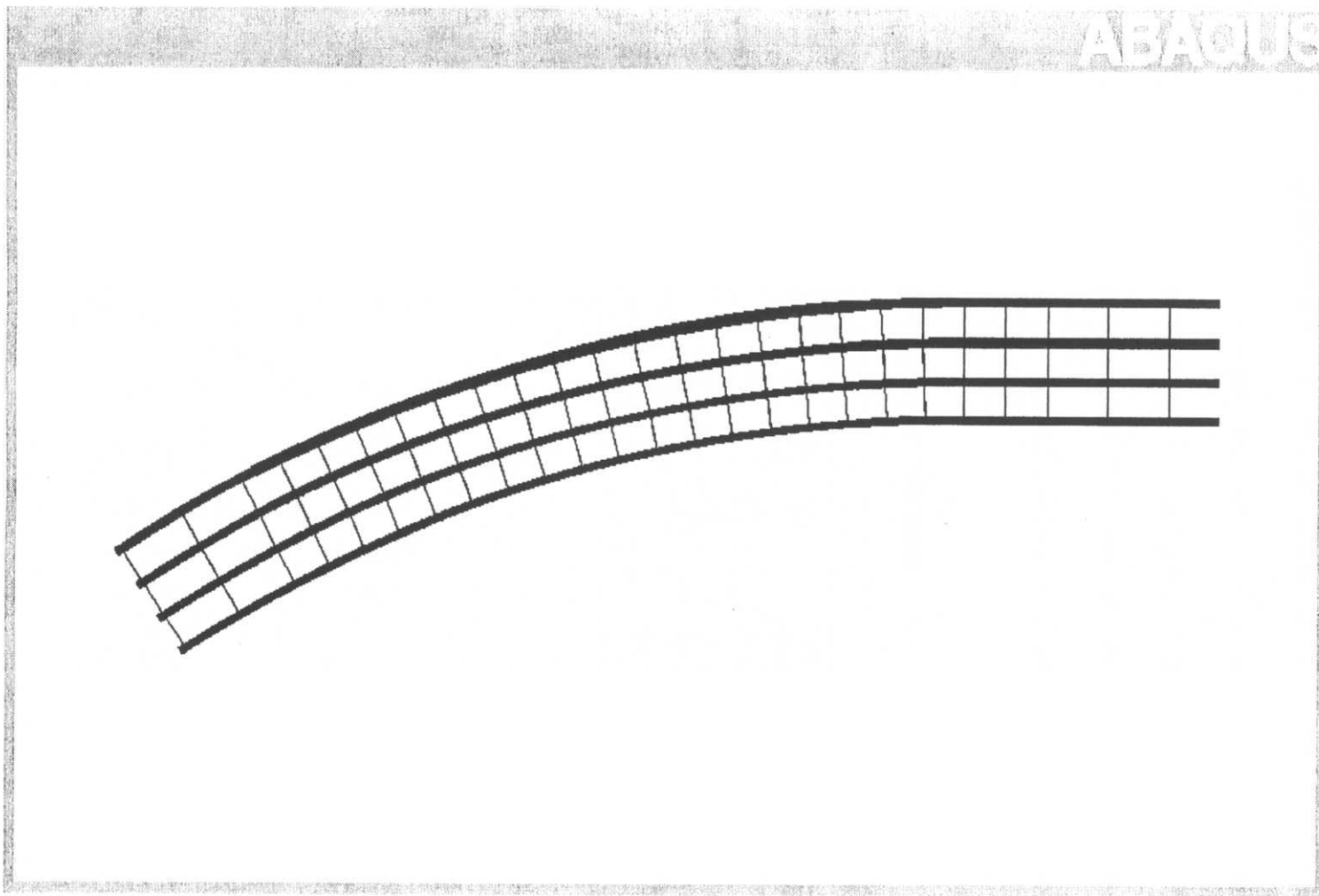
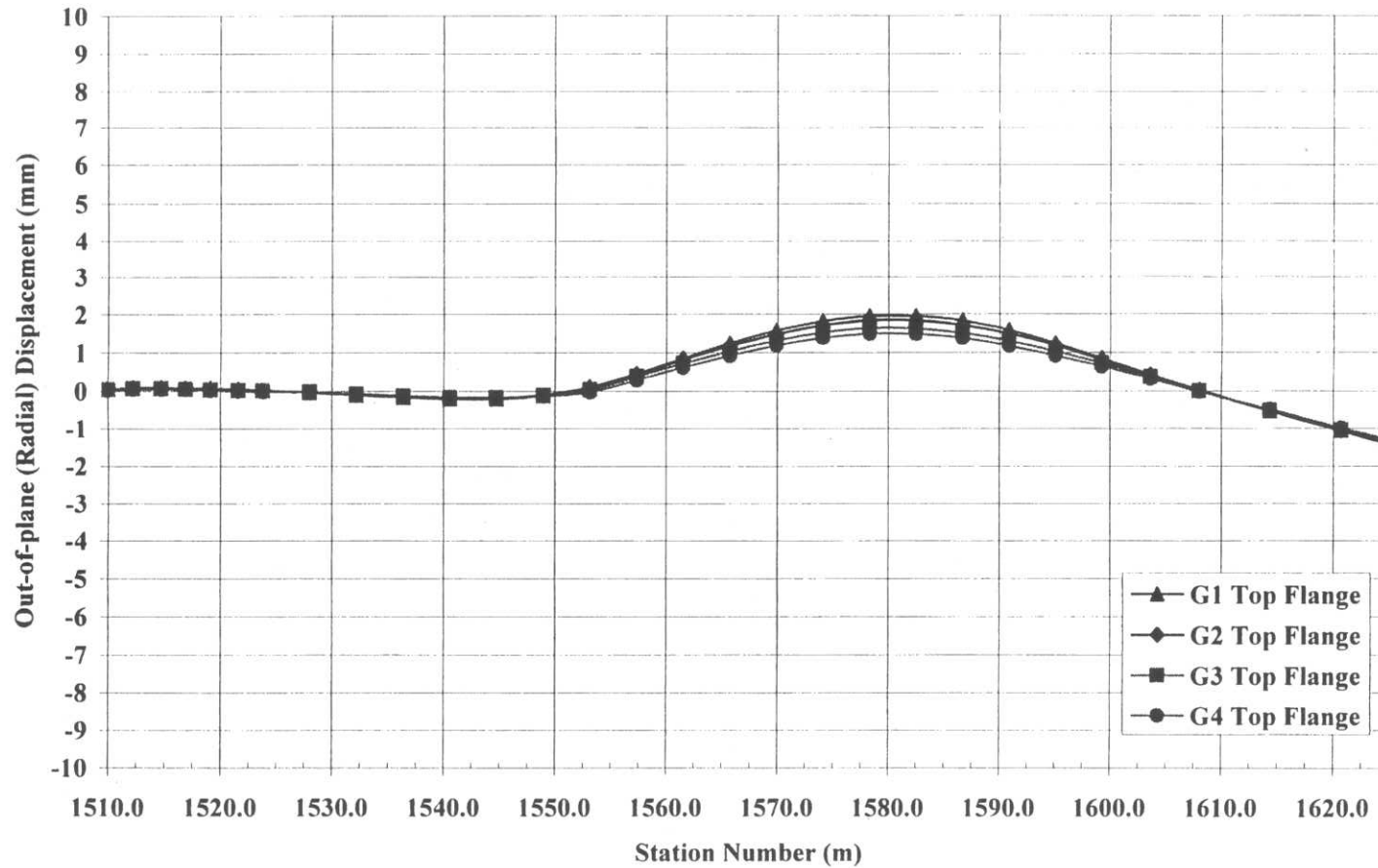


**Figure 120** Construction stage 16 – Plan view of finite element model



(“-“ is displacement inward of curve; “+” is displacement outward of curve)

**Figure 121** Construction stage 16 – Out-of-plane (radial) displacement, centerline of top flange

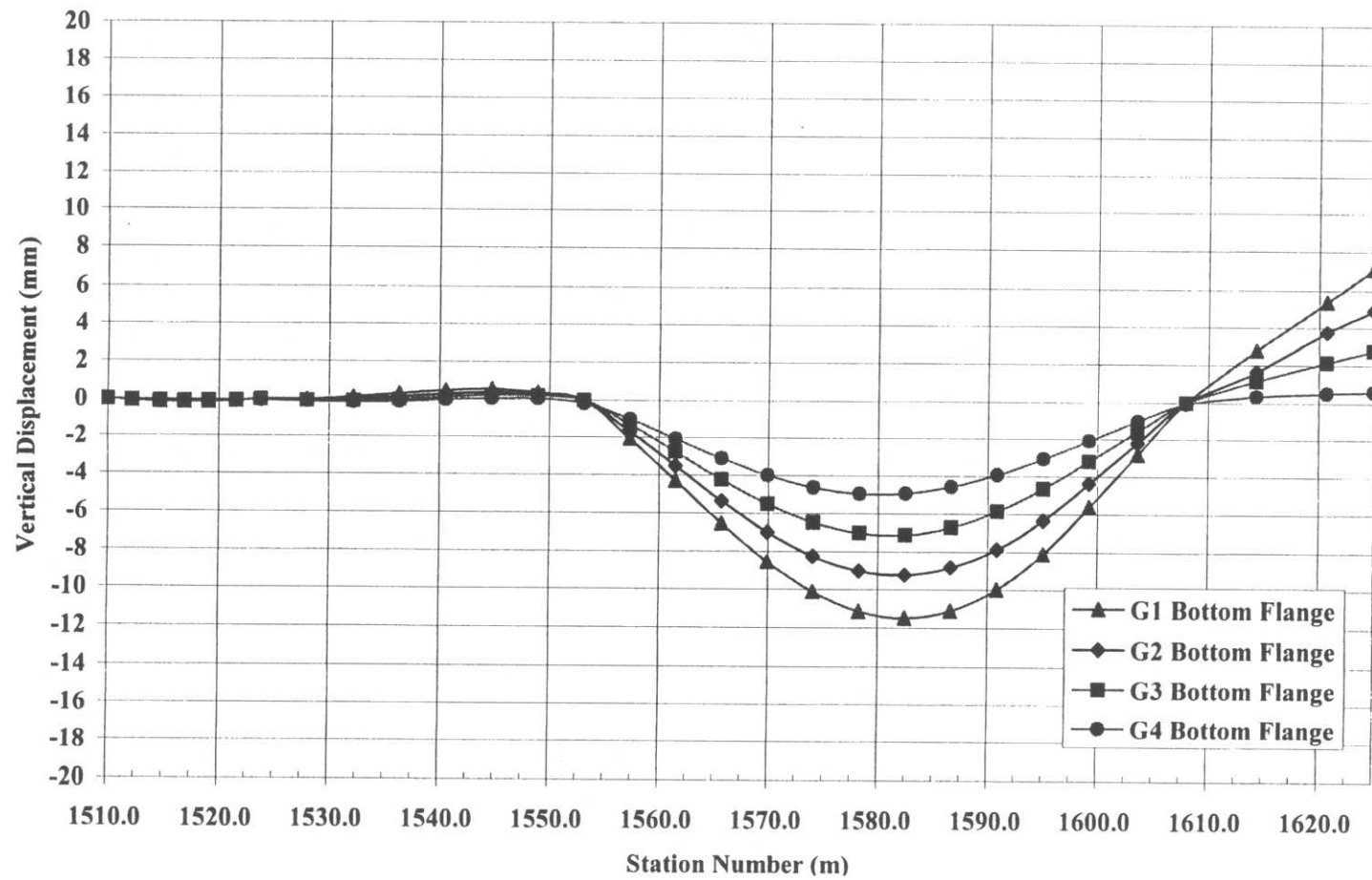


**Figure 122** Construction stage 16 – Vertical displacement, centerline of bottom flange

### 7.1.12 Removal of Falsework 1 and Falsework 2A

Upon completion of the curved span, falsework 1 and falsework 2A are removed from the finite element model. No further girder components are added to the finite element model used in construction stage 16; only boundary conditions at the subject falsework locations are removed.

As shown in figure 123, there is a slight reduction in the vertical displacements at midspan of section 3, and at all of the field-splice 4 locations for the section 4 girders, in comparison with displacements that result at the end of construction stage 16.

The removal of falsework 1 and 2A also allows for consistent load redistribution to occur at abutment 1, falsework 2, and the pier 1 supports. Table 14 illustrates the final construction reactions for the erected curved span, as the largest reaction at each support occurs at the girder G1 locations.

**Table 14** After removal of falsework 1 and 2A – Support reactions

Support Location	Girder Reactions (kips)			
	G1	G2	G3	G4
Abutment 1	97	57	51	42
Falsework 1	N/A	N/A	N/A	N/A
Falsework 2A	N/A	N/A	N/A	N/A
Falsework 2	341	288	188	144
Pier 1	238	211	183	141

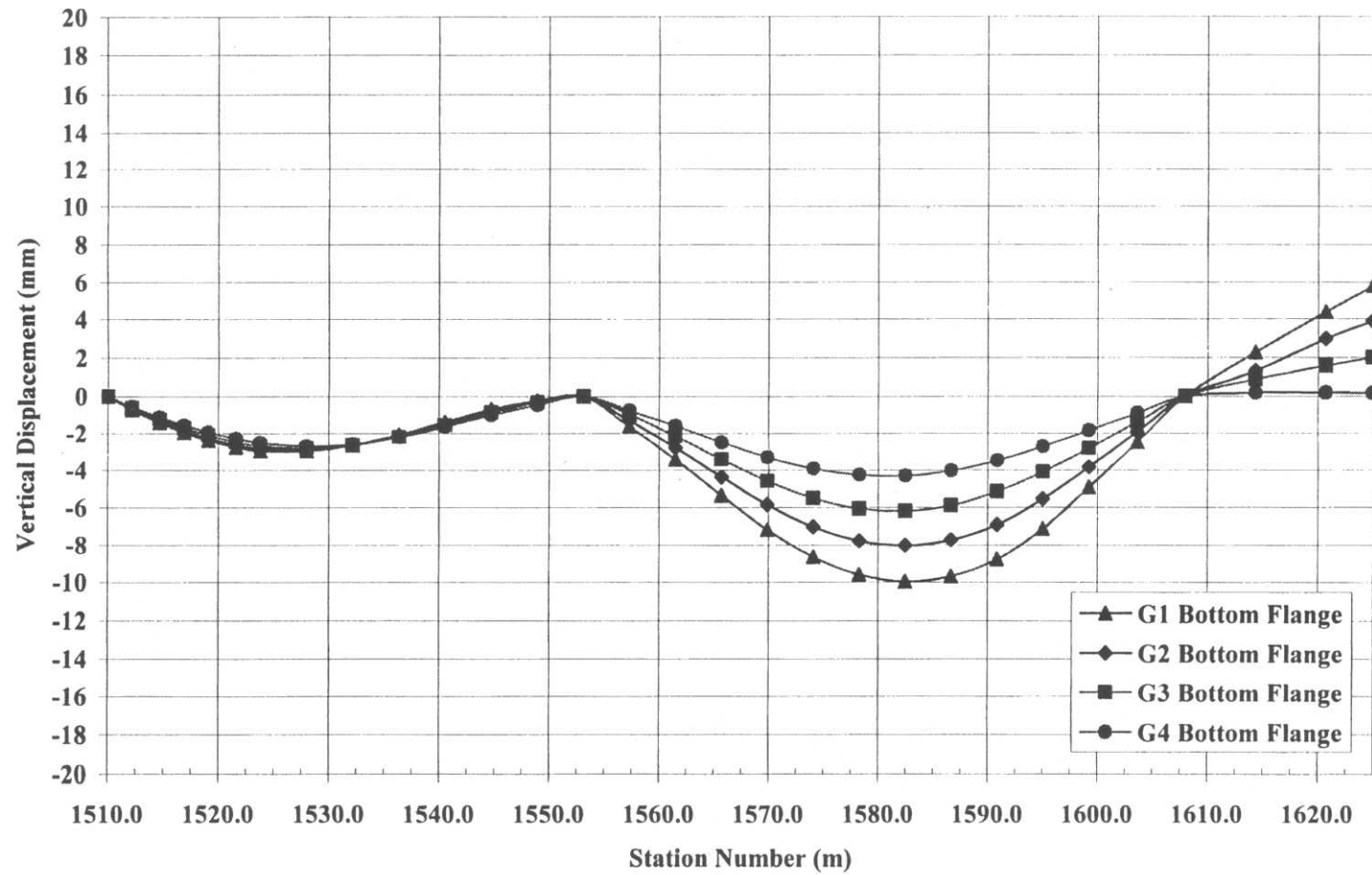


**Figure 123** After removal of falsework 1 and 2A – Vertical displacement, centerline of bottom flange

## 7.2 “Planned” Erection Sequence Analytical Studies

A slight deviation occurs between the “in field” construction of the Ford City Bridge curved span, and the “planned” erection sequence as dictated by the erection drawings (HDR 1999). Two different discrepancies are evident when comparing the erection sequences. One involves the placement of girders G3-4 and G2-4 of construction stage 9 and 10, respectively. The erection drawings direct that G2-4 is to be placed first, and then G3-4, but the actual construction placed G3-4 first, then G2-4. However, it is deemed that this discrepancy is somewhat insignificant and not germane to the current analysis.

The second discrepancy is of greater importance, and is further investigated as part of the current research. The discrepancy between the field construction and the erection drawings begins with construction stage 13. The divergence from the erection drawings dictates the creation of four alternative finite element model construction stages for stages 13, 14, 15, and 16. Table 15 illustrates the differences in the erection methodologies. The most significant difference between the erection sequences is concerned with the removal of falsework 1 and 2A, for the “planned” construction stage 13. Where as, in the field construction, the subject falsework was not removed until the curved span is completed (see section 4.0 of the current research). Another discrepancy between the construction sequences occurs in the order of placement of girders G1-4 and G4-3.

To compensate for the described construction sequence discrepancies, additional finite element analyses are carried out, and summarized as part of the current section. Comparisons in regard to support reactions and girder displacements, with particular attention given to displacements at field-splice locations, between the “in field” construction sequence (Section 7.1) and the “planned” construction sequence (current section) are presented.

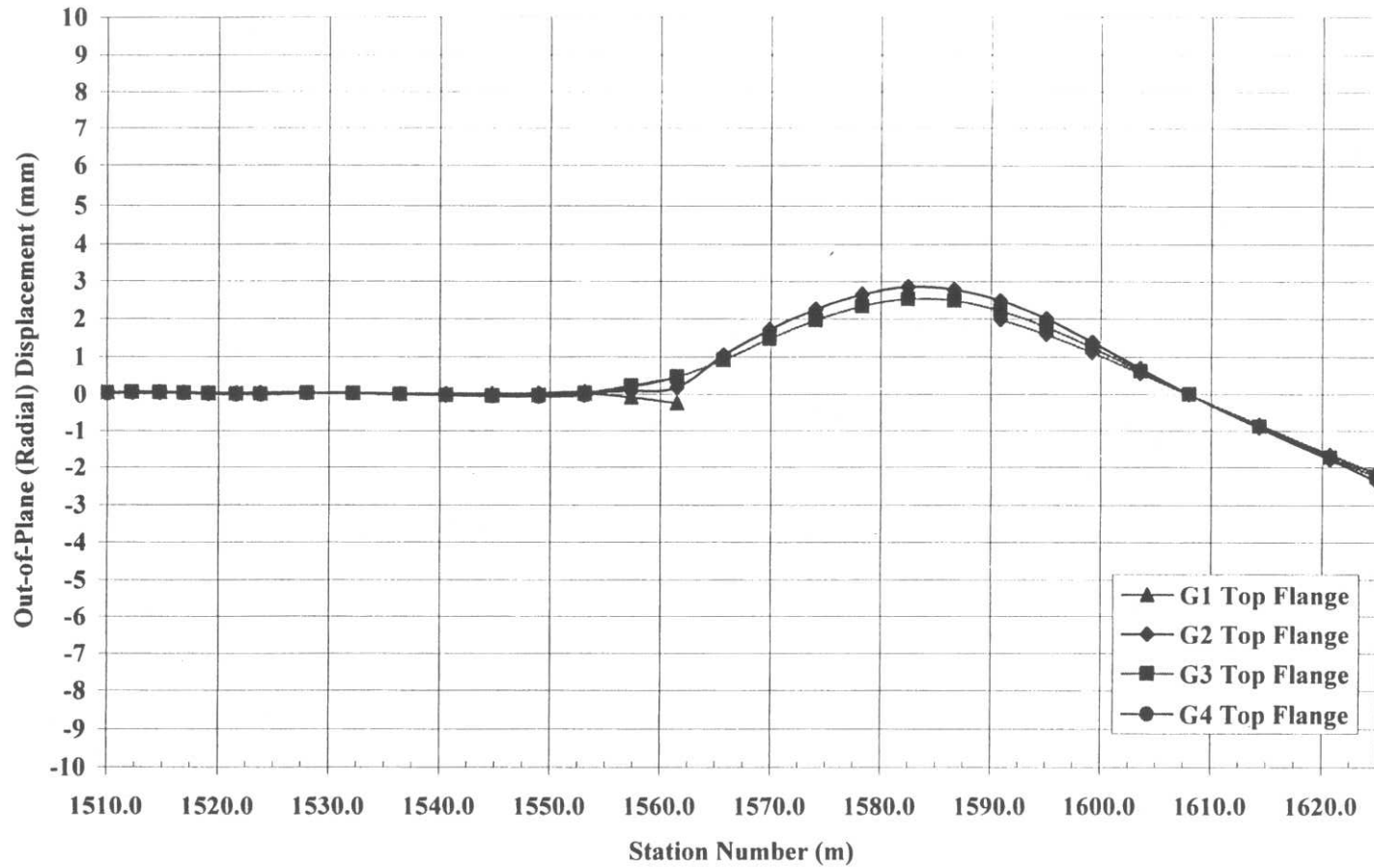
**Table 15** Difference in erection sequences

<b>Construction Stage</b>	<b>“In Field” Construction Sequence</b>	<b>“Planned” Construction Sequence</b>
12	1.) Erect Girder G2-3	1.) Erect Girder G2-3
13	1.) Remove Pier Brackets at Pier 1 2.) Erect Girder G4-4	1.) Remove Pier Brackets at Pier 1 <b>2.) Remove Falsework 1</b> <b>3.) Remove Falsework 2A</b> 4.) Erect Girder G4-4
14	<b>1.) Erect Girder G1-4</b>	<b>1.) Erect Girder G4-3</b>
15	<b>1.) Erect Girder G4-3</b>	<b>1.) Erect Girder G1-4</b>
16	1.) Erect Girder G1 -3	1.) Erect Girder G1-3
After Completion of Curved Span	<b>1.) Remove Falsework 1</b> <b>2.) Remove Falsework 2A</b>	

### 7.2.1 Construction Stage 13

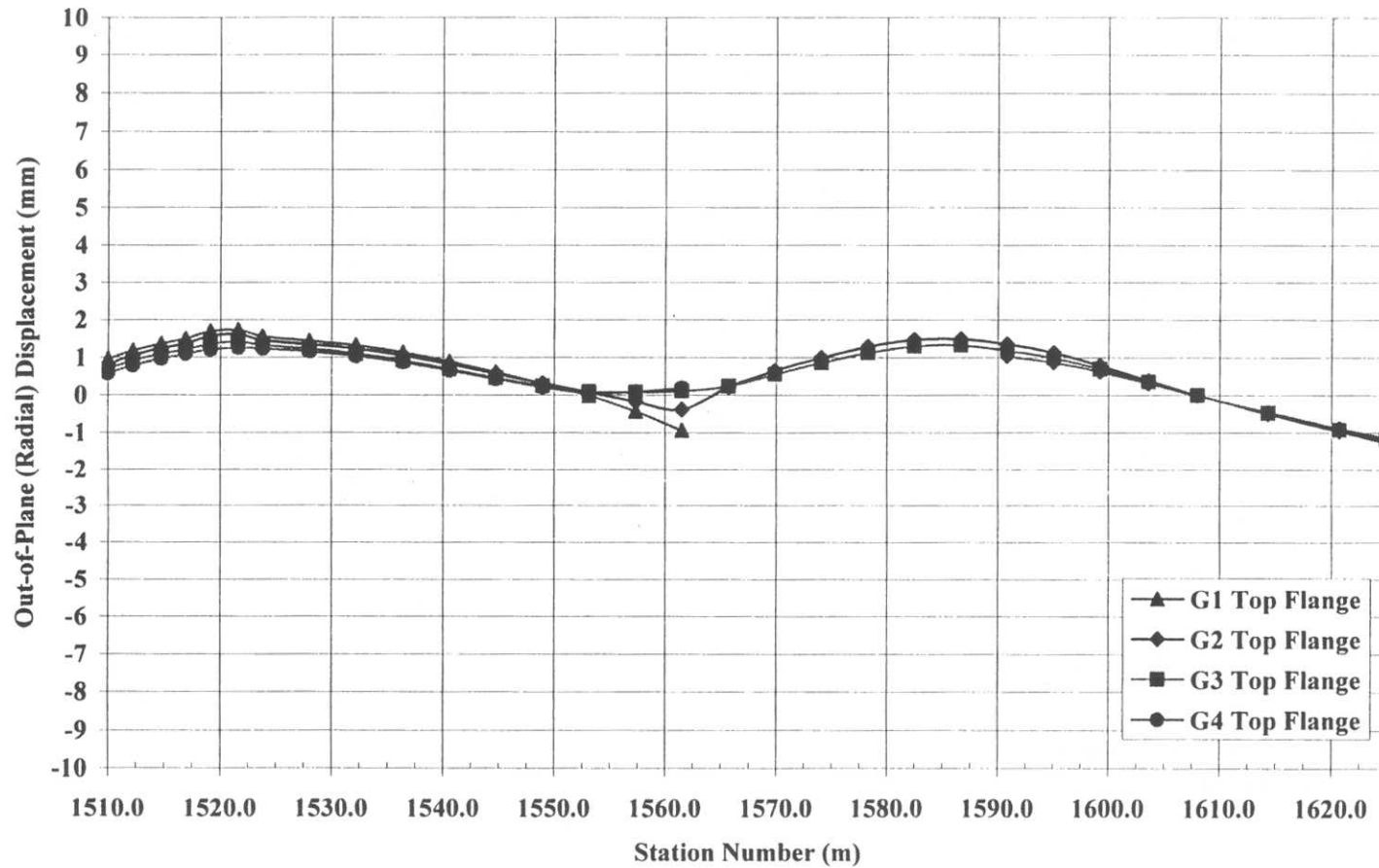
For construction stage 13, the bridge erection plans (HDR 1999) call for the removal of falsework 1 and 2A prior to the placement of girder G4 section 4 (G4-4). Therefore, the difference between the “planned” construction sequence and the “in field” construction sequence is the exclusion of falsework 1 and 2A.

Generally, the displacements throughout the current structure differ slightly between the “in field” construction, and the “planned” construction. The top flange centerline out-of-plane (radial) displacement for the “in field” construction is shown in figure 124, and likewise for the “planned” construction in figure 125. Figure 126 illustrates the vertical displacement of the system for the “in field” erection, and figure 127 shows the equivalent for the “planned” erection sequence. At midspan of section 3 a slight reduction of approximately 1mm occurs for the top flange out-of-plane (radial) displacement using the “planned” construction stage. Similarly, the vertical deflection at midspan of section 3 is 10mm (0.39in) and 6mm (0.24in) for G2 and G3, respectively, for the “in field” construction stage; while the vertical deflection at the same location for the “planned” construction stage is 7mm (0.28in) and 5mm (0.20in) for G2 and G3, respectively. Also, due to the removal of falseworks 1 and 2A, vertical displacements are observed in the section 1 and 2 girders. However, in consideration of field construction, this displacement is not of interest since the entire sections 1 and 2 are already fully completed.



(“-“ is displacement inward of curve; “+” is displacement outward of curve)

**Figure 124** “In Field” construction stage 13 – Out-of-plane (radial) displacement, centerline of top flange



(“-“ is displacement inward of curve; “+” is displacement outward of curve)

**Figure 125** “Planned” construction stage 13 – Out-of-plane (radial) displacement, centerline of top flange

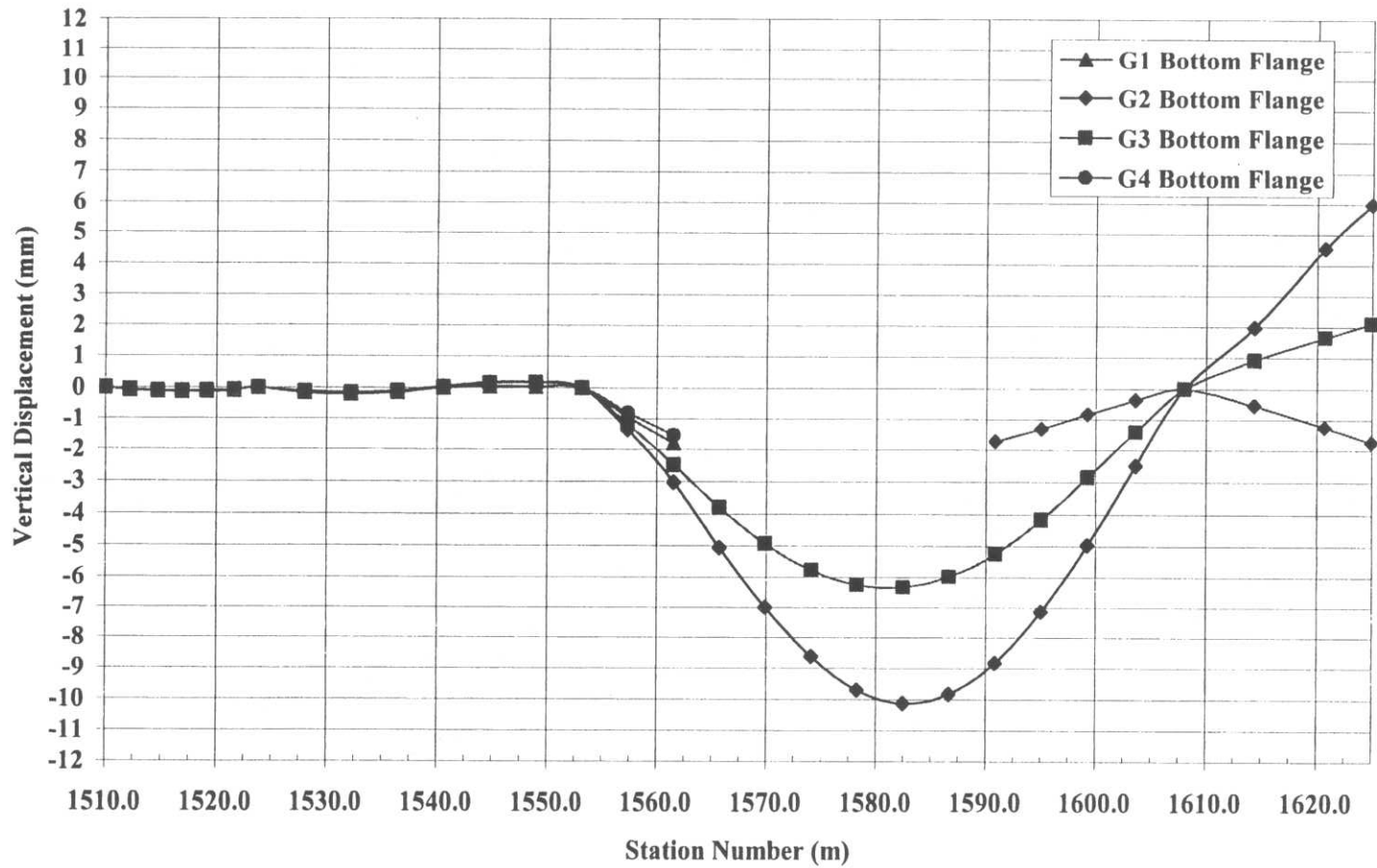


Figure 126 “In Field” construction stage 13 – Vertical displacement, centerline of bottom flange

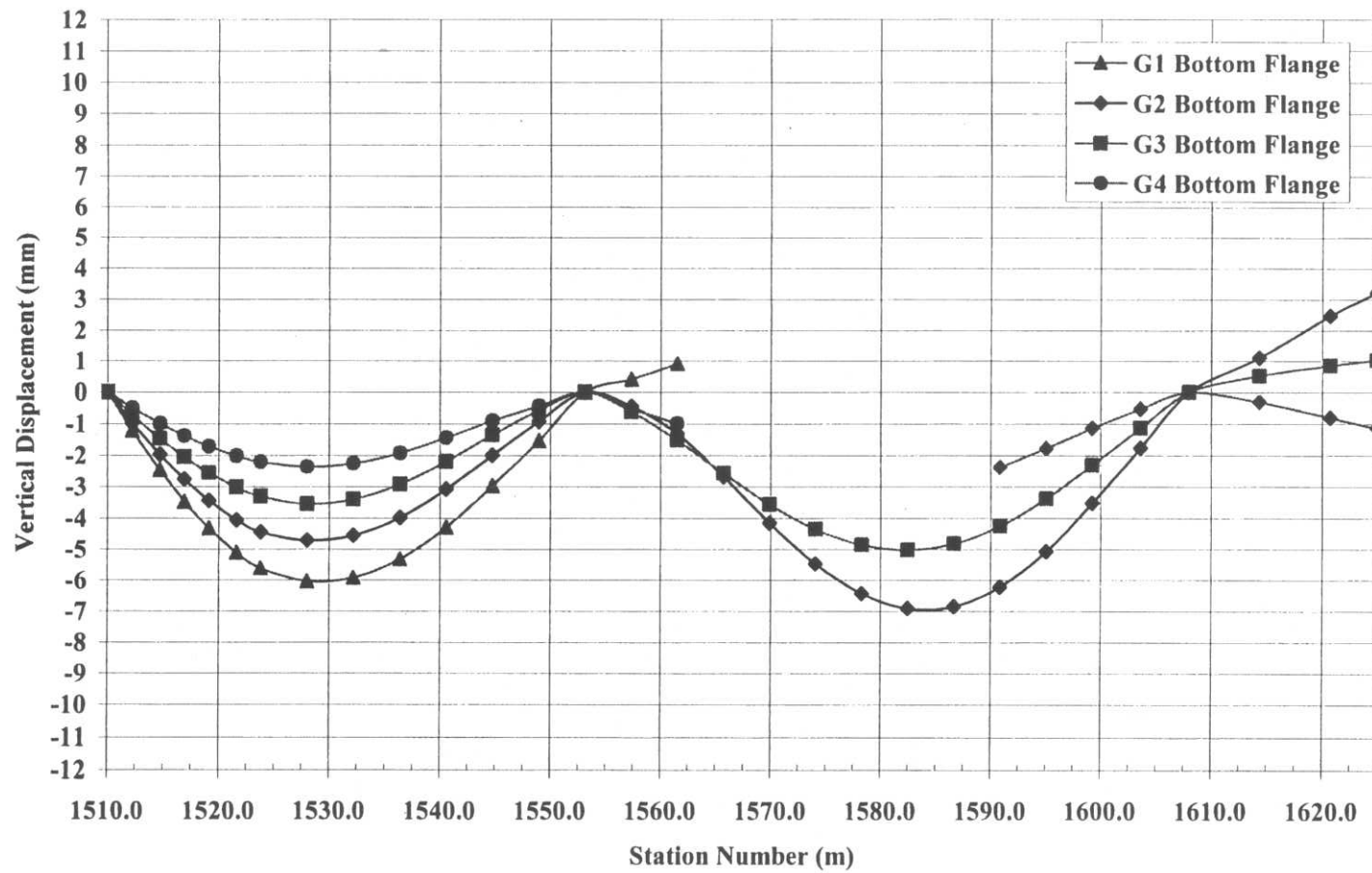


Figure 127 “Planned” construction stage 13 – Vertical displacement, centerline of bottom flange

At the field-splice 2 locations of G1-2 and G4-2 a slight improvement in the vertical displacement is evident, in comparing the “in field” erection stage to the “planned” erection stage. However, an increase in vertical displacement occurs at the field-splice 3 location of G4-4. Table 16 clarifies these changes in displacements.

**Table 16** “In Field” vs. “Planned” construction stage 13 vertical displacements

<b>Location</b>	<b>“In field” Displacement (mm)</b>	<b>“Planned” Displacement (mm)</b>
Field-Splice 2 G1-2	-2.3	1.3
Field-Splice 3 G4-2	-2.0	-1.2
Field-Splice 3 G4-4	-2.0	-2.8

Naturally, due to the removal of falseworks 1 and 2A, the support reactions at abutment 1 and falsework 2 increase significantly, as the reactions at pier 1 basically remain unchanged. As shown in table 17, the largest difference in reaction occurs for girder G1, 81.5 kips (363 kN) at abutment 1 and 59.8 kips (266 kN) at falsework 2.

**Table 17** “In Field” vs. “Planned” construction stage 13 support reactions - Section 1 and 2

<b>"In Field" Construction Stage Vertical Support Reactions (kips)</b>				
<b>Girder</b>	<b>Abutment 1</b>	<b>Falsework 1</b>	<b>Falsework 2A</b>	<b>Falsework 2</b>
<b>G1</b>	37.4	85.5	31.6	191.6
<b>G2</b>	22.2	66.7	0.0	203.0
<b>G3</b>	21.3	58.9	0.0	155.1
<b>G4</b>	18.5	44.1	10.8	99.9

<b>"Planned" Construction Stage Vertical Support Reactions (kips)</b>				
<b>Girder</b>	<b>Abutment 1</b>	<b>Falsework 1</b>	<b>Falsework 2A</b>	<b>Falsework 2</b>
<b>G1</b>	118.9	0.0	0.0	251.4
<b>G2</b>	66.5	0.0	0.0	232.9
<b>G3</b>	52.7	0.0	0.0	174.0
<b>G4</b>	36.8	0.0	0.0	121.4

### 7.2.2 Construction Stage 14

Two discrepancies exist between the “in field” construction stage 14, and the “planned” construction stage 14. Like the previous construction stage, falsework 1 and 2A are to be previously removed, per the bridge erections plans. Also, instead of placing girder G1 section 4 (G1-4) as had been done in the field construction, the bridge erection plans call for the placement of girder G4 section 3 (G4-3), completing girder G4 of the curved span. Figure 128 illustrates the finite element model used for the “in field”

construction stage 14, and figure 129 shows the plan view of the finite element model used to analyze the “planned” construction stage 14.

Similar changes in regard to displacements are monitored between the “in field” and “planned” construction stage 14 finite element models, as is shown for construction stage 13. Figures 130 and 131 illustrate the top flange out-of-plane (radial) displacement for the “in field” and “planned” construction stages, respectively. Figures 132 and 133 show the vertical displacement of the current structure for the “in field” and “planned” construction stages, respectively. At the midspan of section 3, for the top-flange of all of the current girders, an out-of-plane (radial) displacement difference of approximately 3mm is shown, with the “planned” construction stage having the smaller displacement. Likewise at the same location, the “planned” construction stage has a lesser vertical deflection, with a difference of approximately 5mm. Additionally, considerable vertical displacement occurs at the ends of G1-4 for the “in field” construction stage.

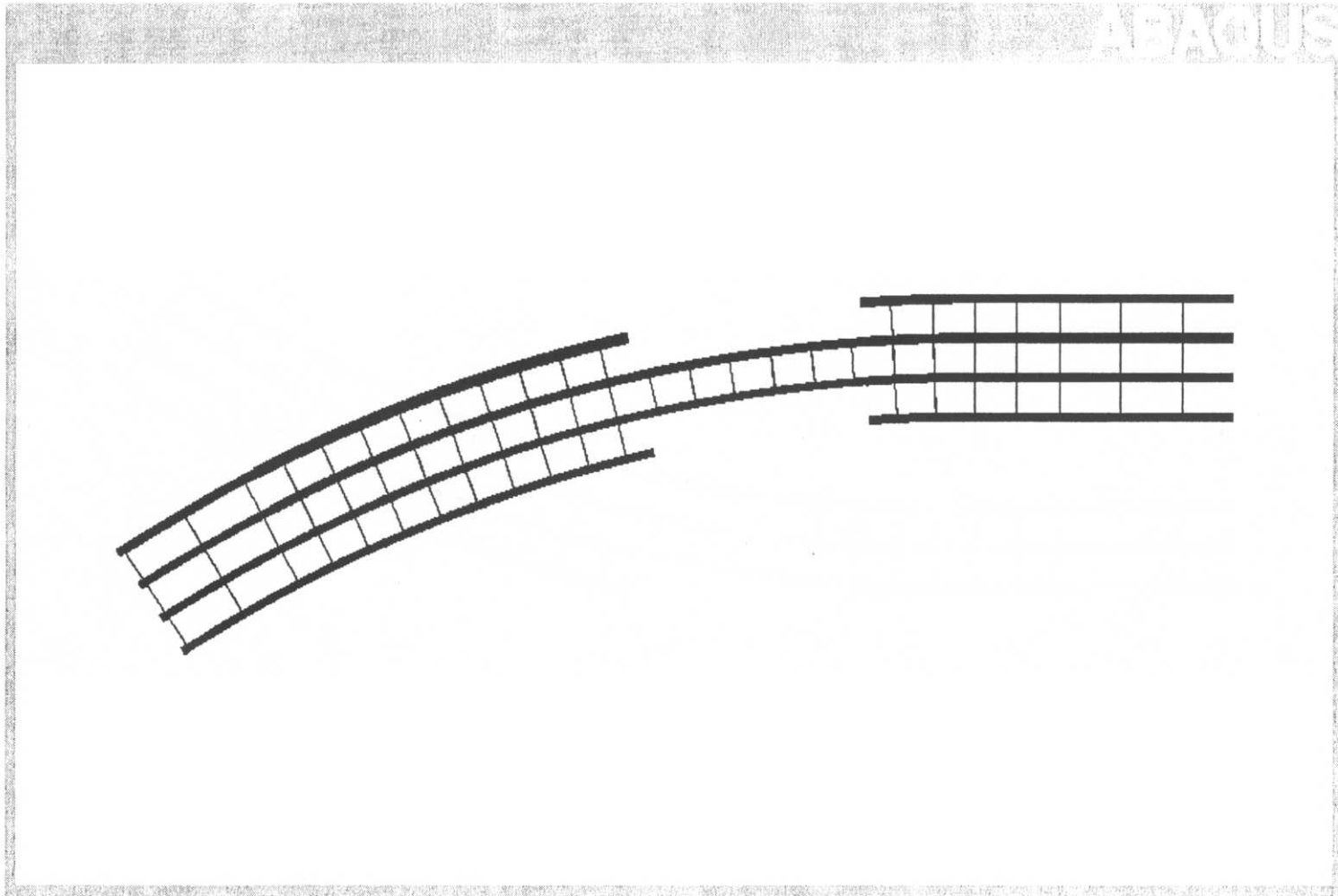


**Figure 128** “In Field” construction stage 14 – Plan view of finite element model

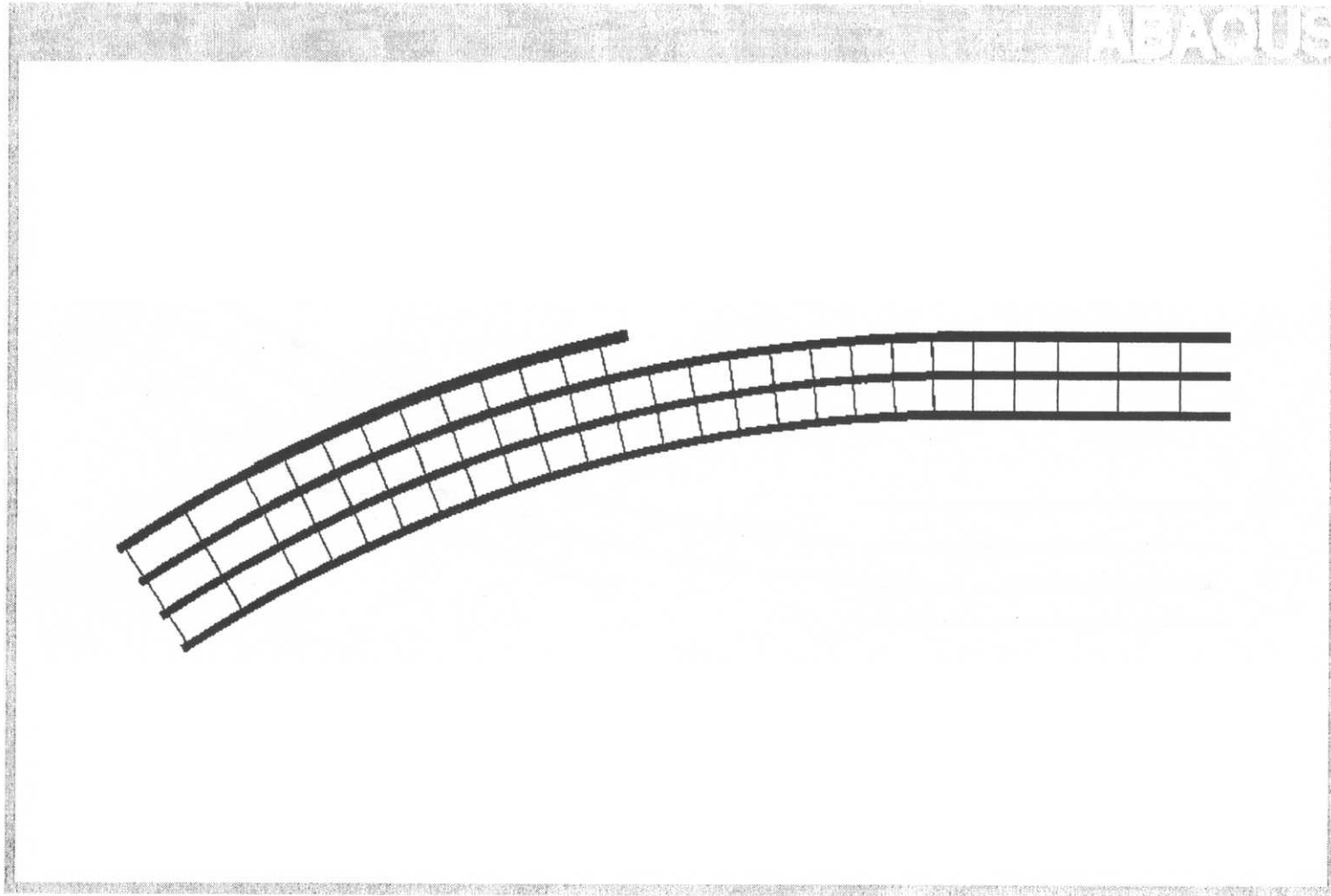
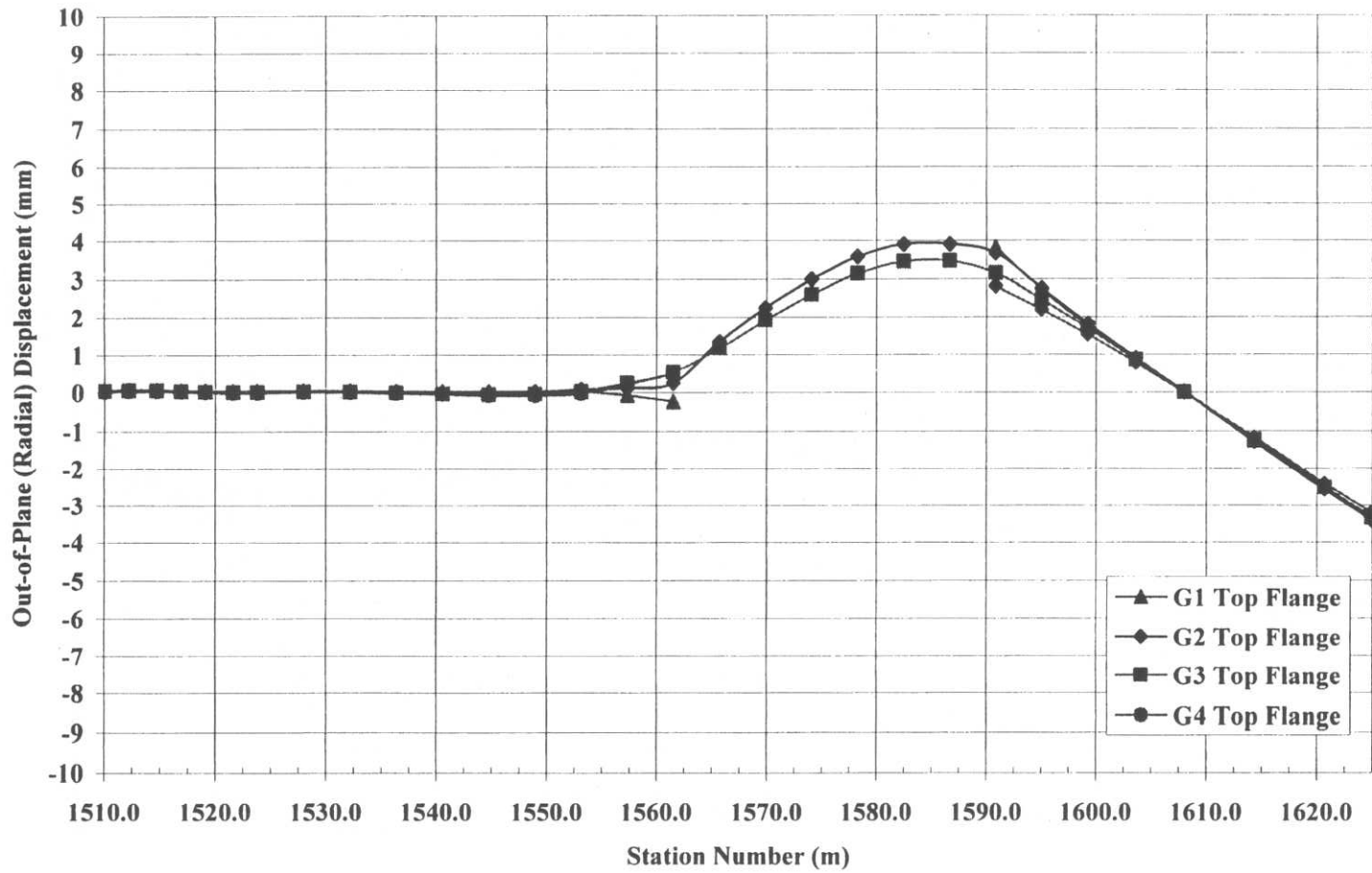
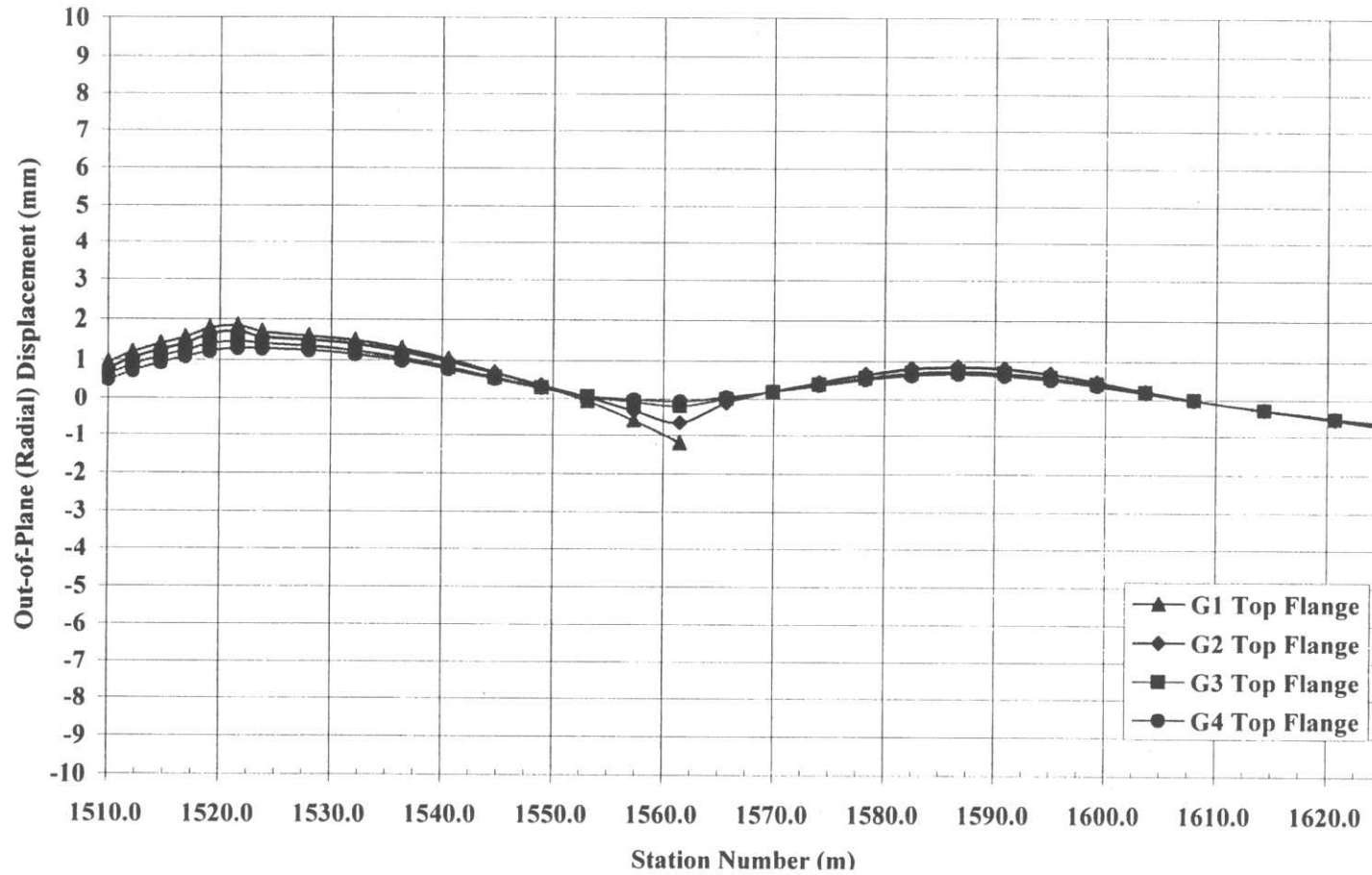


**Figure 129** “Planned” construction stage 14 – Plan view of finite element model



("-" is displacement inward of curve; "+" is displacement outward of curve)

**Figure 130** "In Field" construction stage 14 – Out-of-plane (radial) displacement, centerline of top flange



(“-“ is displacement inward of curve; “+” is displacement outward of curve)

**Figure 131** “Planned” construction stage 14 – Out-of-plane (radial) displacement, centerline of top flange

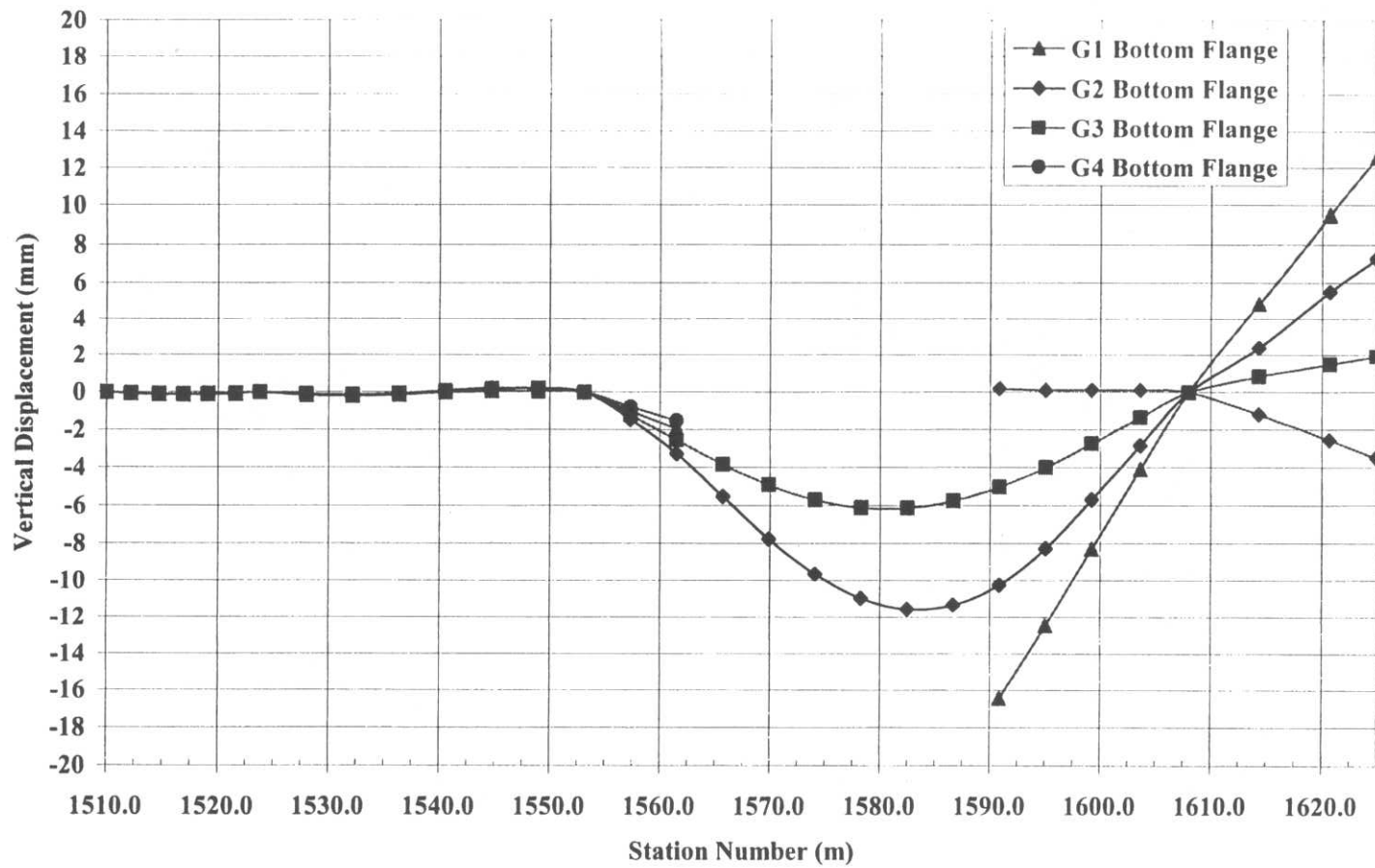
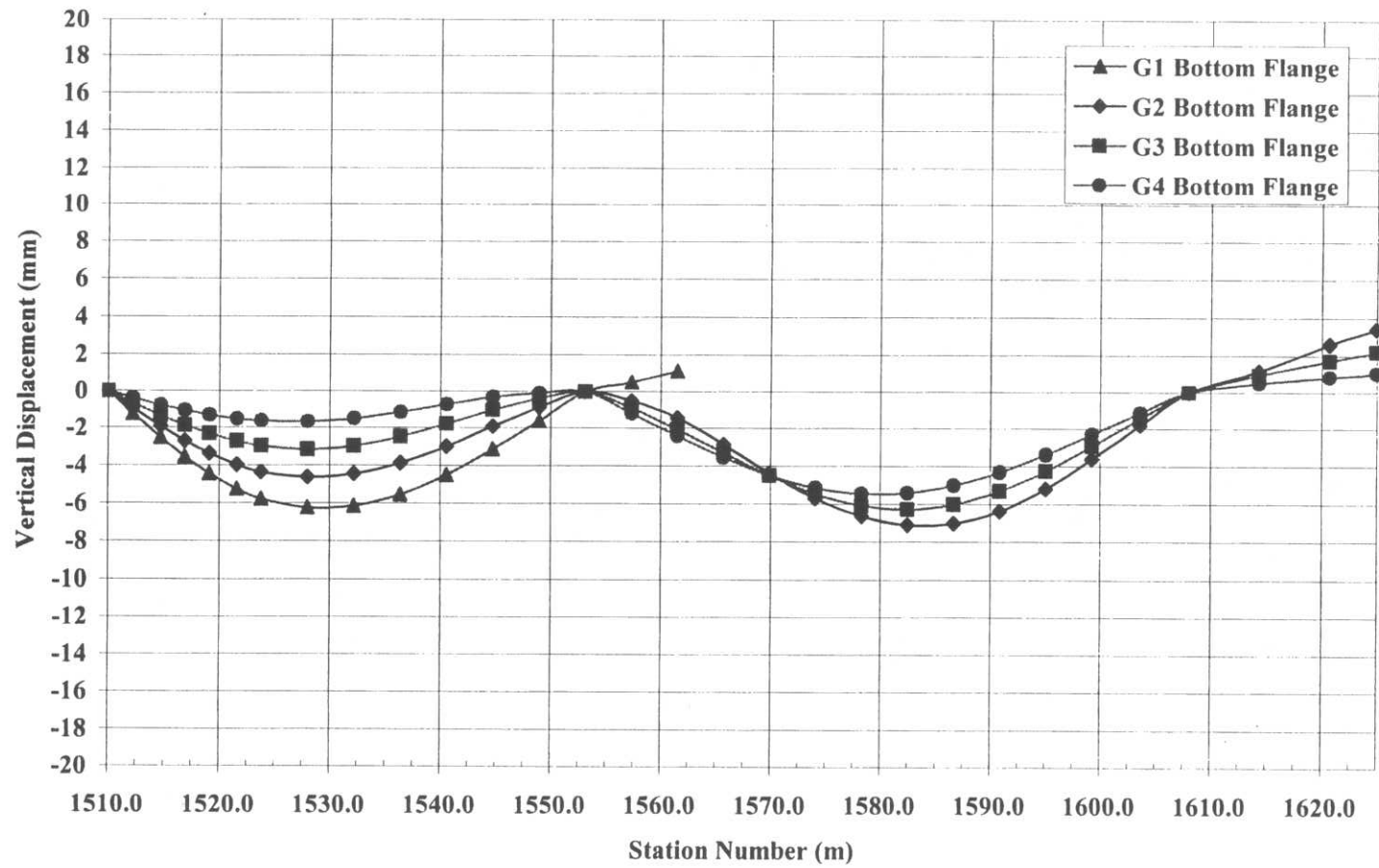


Figure 132 “In Field” construction stage 14 – Vertical displacement, centerline of bottom flange



**Figure 133** “Planned” construction stage 14 – Vertical displacement, centerline of bottom flange

Due to the erection of different girder sections, the support reactions vary between the different construction procedures, with falsework 2 and abutment 1 receiving less load at each girder location for the “in field” construction stage. Table 18 shows the differences in the support reactions for the current construction stage.

**Table 18** “In Field” vs. “Planned” construction stage 14 support reactions

<b>"In Field" Construction Stage Vertical Support Reactions (kips)</b>					
<b>Girder</b>	<b>Abutment 1</b>	<b>Falsework 1</b>	<b>Falsework 2A</b>	<b>Falsework 2</b>	<b>Pier 1</b>
<b>G1</b>	38.2	84.9	24.2	200.8	184.4
<b>G2</b>	22.5	65.8	0.0	205.9	220.4
<b>G3</b>	21.6	58.1	0.0	160.0	179.3
<b>G4</b>	18.5	43.8	10.0	99.1	129.5

<b>"Planned" Construction Stage Vertical Support Reactions (kips)</b>					
<b>Girder</b>	<b>Abutment 1</b>	<b>Falsework 1</b>	<b>Falsework 2A</b>	<b>Falsework 2</b>	<b>Pier 1</b>
<b>G1</b>	120.1	0.0	0.0	246.2	N/A
<b>G2</b>	65.4	0.0	0.0	235.6	218.1
<b>G3</b>	50.6	0.0	0.0	189.6	184.2
<b>G4</b>	33.8	0.0	0.0	156.3	144.2

### 7.2.3 Construction Stage 15

The only difference to be considered between the “in field” and “planned” construction stage 15 is the exclusion of falsework 1 and falsework 2A in the “planned” construction procedure. The “in field” construction stage places girder G4 section 3 (G4-

3), while the “planned” construction procedure calls for the erection of girder G1-4. However, analytically, the same girder components are included in the construction stage 15 finite elements models due to the placement of either girder, progressing from construction stage 14. In either finite element model, only girder G1 section 3 (G1-3) is excluded in the curved span. Therefore, the only difference in falsework supports used is considered herein.

As shown previously, the removal of falsework 1 and falsework 2A as per the erection plans slightly reduces the vertical deflection at the midspan of section 3. Also, the vertical deflection at field-splice 3 for G1-4 is 12.0mm (0.47in) downward for the “planned” construction stage, while it is 15.8mm (0.62in) for the “in field” erection procedure. At field-splice 2 for G1-2, the overall vertical displacement is reduced from 2.3mm downward for the “in field” erection, to 1.3mm upward for the “planned” erection procedure. Figures 134 and 135 show the vertical displacement of the current structure for the “in field” and “planned” erection procedures, respectively.

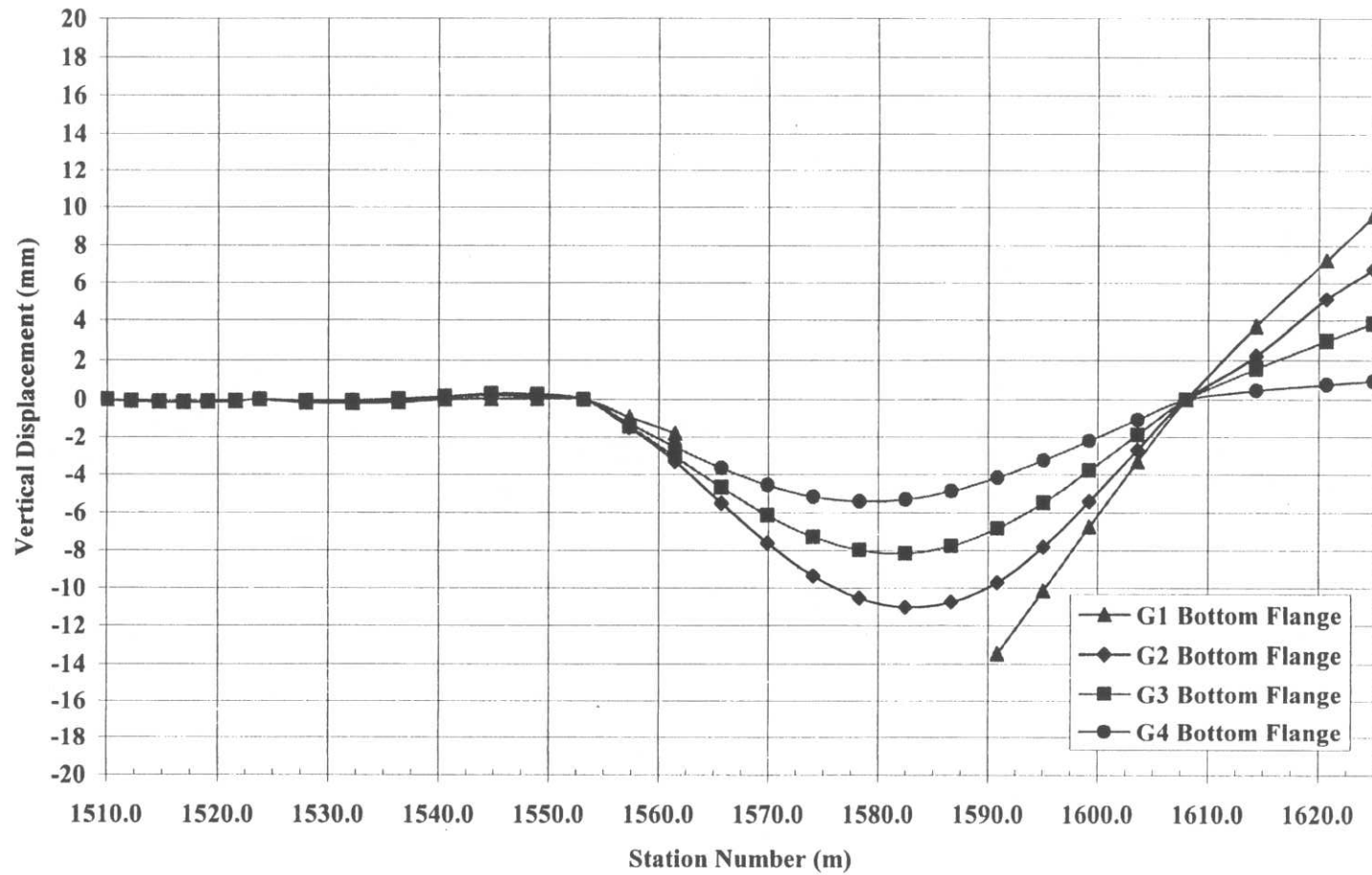


**Figure 134** “In Field” construction stage 15 – Vertical displacement, centerline of bottom flange

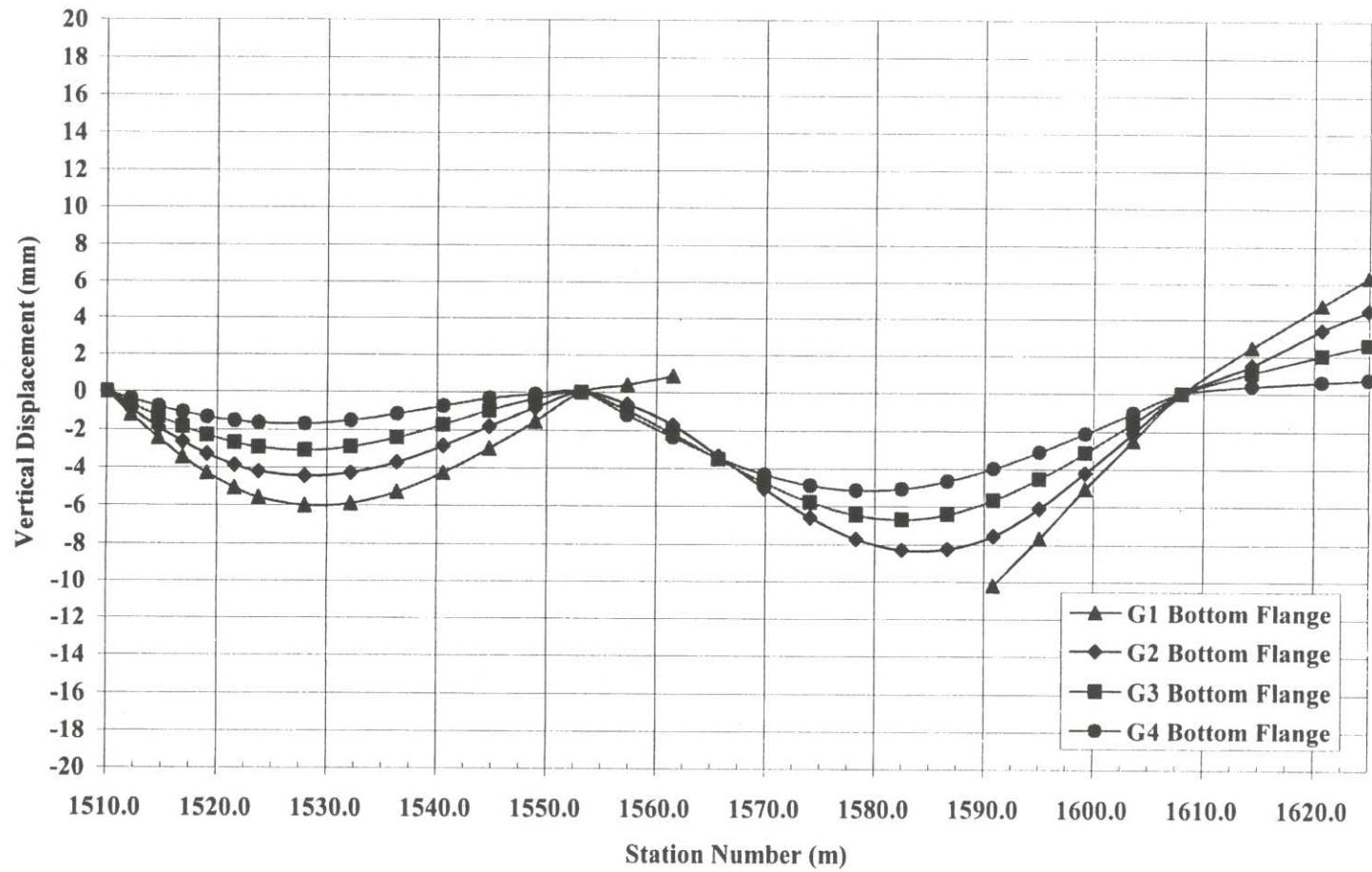


**Figure 135** “Planned” construction stage 15 – Vertical displacement, centerline of bottom flange

Table 19 shows the difference in reactions at the applicable supports for the “in field” and “planned” construction stage 15. For both of the current construction stages, girder G1 has the largest support reactions at abutment 1 and falsework 2, however not at pier 1. This behavior is owed to the fact that girder G1 is incomplete (G1-3 is yet to be placed), and therefore total load redistribution cannot occur.

**Table 19** “In Field” vs. “Planned” construction stage 15 supports reactions

<b>"In Field" Construction Stage Vertical Support Reactions (kips)</b>					
<b>Girder</b>	<b>Abutment 1</b>	<b>Falsework 1</b>	<b>Falsework 2A</b>	<b>Falsework 2</b>	<b>Pier 1</b>
<b>G1</b>	38.8	85.0	29.9	189.1	183.6
<b>G2</b>	23.0	63.8	0.0	21.3	222.6
<b>G3</b>	22.6	54.9	0.0	175.3	191.7
<b>G4</b>	19.9	39.2	0.0	141.3	139.3

<b>"Planned" Construction Stage Vertical Support Reactions (kips)</b>					
<b>Girder</b>	<b>Abutment 1</b>	<b>Falsework 1</b>	<b>Falsework 2A</b>	<b>Falsework 2</b>	<b>Pier 1</b>
<b>G1</b>	118.9	0.0	0.0	249.3	182.6
<b>G2</b>	64.8	0.0	0.0	238.9	216.5
<b>G3</b>	50.4	0.0	0.0	191.9	189.4
<b>G4</b>	34.0	0.0	0.0	155.7	140.7

#### **7.2.4 Construction Stage 16**

Analytically, there are no differences between the girder components used in the finite element models for construction stage 16. However, the use of falsework 1 and 2A is different between the “in field” and “planned” erection procedures. This difference can be seen in sections 7.1.11 and 7.1.12 of the current research. Section 7.1.11 describes the behavior of construction stage 16 in which the “in field” falsework support 1 and 2A are being utilized. Section 7.1.12 describes the same structure, but with falseworks 1 and 2A being removed.

### **7.3 Comparison of Construction Reactions for the Ford City Bridge With Incorrectly Detailed Cross-Frames and Cross-Frames Detailed for No-Load Case**

The previous construction stage analyses (section 7.1 and 7.2) utilized cross-frames that are detailed for the girder web-plumb at no-load condition. However, due to a fabrication error in the real bridge, the cross-frames in the actual structure are detailed for web-plumbness at the application of the concrete deck load. In both cases, the girders themselves were detailed for the web-plumb, no-load condition. The bridge erection plans for the Ford City Bridge (HDR 1999), are developed for this bridge with cross-frames detailed for the concrete load case. Utilizing the same construction procedure, the support reactions in the bridge erection plans are compared with the support reactions obtained from the current analytical studies with cross-frames detailed for the web-plumb position at no-load. Table 20 shows the support reactions for the erection sequence with the incorrectly detailed cross-frames, and for the erection sequence with cross-frames detailed for the web-plumb position at no-load. It should be noted that the total steel dead weight applied to the analytical model for the bridge erection plans is increased by 10% to 15% to account for welding material, bolts, field-splice plates, and etc. This increase is larger than that assumed in the finite element model previously described (Section 6.0)

This section will highlight some of the differences in support reactions between the erection sequence of the bridge using the incorrectly detailed cross-frames (Case 1), and the erection sequence using cross-frames detailed for the girder web-plumb at no-load condition (Case 2).

**Table 20** Erection sequence support reactions for bridge with incorrectly detailed cross-frames (Case 1) and cross-frames detailed for the web-plumb, no load case (Case 2)

Construction Stage	Erected Girder	Abutment 1 (kips)				Falsework 1 (kips)				Falsework 2A (kips)				Falsework 2 (kips)				Pier Brackets (Span 1) (kips)		Pier 1 (kips)			
		G1	G2	G3	G4	G1	G2	G3	G4	G1	G2	G3	G4	G1	G2	G3	G4	G2	G3	G1	G2	G3	G4
1	G3-1			27				35															
				25				27															
2	G2-1		23	27			35	31															
			28	25			30	27															
3	G4-1		21	30	17		37	27	26														
			28	26	21		29	29	22														
4	G1-1	35	21	31	18	44	43	24	26														
		40	27	26	22	40	28	28	23														
5	G3-2	35	20	25	17	44	43	57	26			36				79							
		40	26	22	21	40	27	58	22			33				66							
6	G2-2	35	17	24	17	43	74	59	26		59	28			107	97							
		40	22	22	21	40	68	57	23		54	34			96	72							
7	G4-2	35	17	23	14	43	73	64	46		56	38	24		112	89	74						
		41	22	21	18	39	66	58	44		52	38	28		95	72	58						
8	G1-2	28	17	23	14	94	73	65	47	67	54	37	25	154	130	92	72						
		35	22	21	18	87	69	58	44	69	54	37	27	121	102	72	57						
9	G2-4	28	17	23	14	94	73	65	47	67	54	37	25	154	130	92	72	62			135		
	G3-4	35	22	21	18	87	67	58	44	69	54	37	27	121	102	72	57		35			129	

10	G3-4	<b>28</b>	<b>17</b>	<b>23</b>	<b>14</b>	<b>94</b>	<b>73</b>	<b>65</b>	<b>47</b>	<b>67</b>	<b>54</b>	<b>37</b>	<b>25</b>	<b>154</b>	<b>130</b>	<b>92</b>	<b>72</b>	<b>60</b>	<b>45</b>		<b>135</b>	<b>132</b>	
	G2-4	36	22	21	18	87	67	58	44	69	54	37	27	121	102	72	57	35	42		148	127	
11	G3-3	<b>28</b>	<b>17</b>	<b>23</b>	<b>14</b>	<b>94</b>	<b>73</b>	<b>65</b>	<b>47</b>	<b>67</b>	<b>54</b>	<b>37</b>	<b>25</b>	<b>154</b>	<b>130</b>	<b>92</b>	<b>72</b>				<b>194</b>	<b>164</b>	
		36	22	21	18	87	67	59	44	68	38	12	10	121	135	101	102	48	153		134	49	
12	G2-3	<b>18</b>	<b>14</b>	<b>23</b>	<b>17</b>	<b>129</b>	<b>89</b>	<b>66</b>	<b>38</b>					<b>210</b>	<b>264</b>	<b>122</b>	<b>142</b>				<b>267</b>	<b>150</b>	
		33	21	21	18	100	74	63	47						207	205	157	100				229	164
13	G4-4	<b>113</b>	<b>65</b>	<b>59</b>	<b>36</b>									<b>362</b>	<b>146</b>	<b>214</b>	<b>154</b>				<b>235</b>	<b>161</b>	<b>153</b>
		119	67	53	37										251	233	174	121				216	177
14	G4-3	<b>114</b>	<b>64</b>	<b>57</b>	<b>33</b>									<b>355</b>	<b>154</b>	<b>228</b>	<b>188</b>				<b>236</b>	<b>174</b>	<b>163</b>
		120	66	51	34										246	236	190	157				218	184
15	G1-4	<b>109</b>	<b>62</b>	<b>56</b>	<b>33</b>									<b>364</b>	<b>161</b>	<b>234</b>	<b>186</b>			<b>182</b>	<b>261</b>	<b>181</b>	<b>151</b>
		119	65	50	34										249	239	192	157			183	217	189
16	G1-3	<b>92</b>	<b>55</b>	<b>57</b>	<b>40</b>									<b>462</b>	<b>206</b>	<b>224</b>	<b>171</b>			<b>256</b>	<b>242</b>	<b>172</b>	<b>159</b>
		97	57	51	42										341	288	188	144			238	211	183

\*\*\*\* Bold Values are for the Bridge with Incorrectly Detailed Cross-Frames (Case 1 Reactions from HDR 1999)

### **7.3.1 Construction Stage 4 Support Reaction Comparisons**

With the completion of construction stage 4, all of the section 1 girders are placed, and supported at abutment 1 and falsework 1. The reaction distribution differs slightly between the structure using the incorrectly detailed cross-frames (Case 1) and the structure with the no-load detailed cross-frames (Case 2).

The most noticeable inconsistency occurs at both supports of girder G2. The support reactions for Case 1 are 21 kips and 43 kips, at abutment 1 and falsework 1, respectively. The support reactions for Case 2 are 27 kips and 28 kips, at abutment 1 and falsework 1, respectively. It is shown that due to the use of the incorrectly detailed cross-frames, the support reactions for G2 shift to the falsework 1 support.

Also, it is apparent that the use of incorrect cross-frame detailing does not allow for uniform load redistribution to the outside girder, as is typical in curved I-girder bridges. The utilization of cross-frames detailed to the no-load condition allows for this general load redistribution to occur.

### **7.3.2 Construction Stage 8 Support Reaction Comparisons**

Construction stage 8 consists of the erection of girder G1-2, and completes section 2 of the structure. The current structure is supported at abutment 1, falsework 1, falsework 2A and falsework 2.

Generally at abutment 1, the support reactions for Case 1 are less than the support reactions for Case 2, even though additional load (10% to 15% for miscellaneous weights) is applied to the analytical model used for case 1. Additionally, at falsework 2, the support reactions for the erection sequence utilizing the incorrectly detailed cross-frames are much larger (approximately 15 to 30 kips) than the support reactions for the structure employing cross-frames detailed for the no-load case. It seems that the use of incorrect cross-frames leads to a greater shift in load to falsework 2, than with the use of the no-load detailed cross-frames.

With the exception of the reactions at abutment 1, load redistribution to the outside girders seems to be evident in both cases of detailed cross-frames.

### **7.3.3 Construction Stage 12 Support Reaction Comparisons**

Girder G2 section 3 (G2-3) is placed as part of construction stage 12, therefore completing girder G2 and G3 of the curved span. Falsework 1, falsework 2, and abutment 1 and pier 1 support the structure, as falsework 2A is removed.

At the falsework 2 location, there is evidence of a moderately large discrepancy in the reactions for the three inside girders, G2, G3, and G4. The use of the incorrectly detailed cross-frames results in nonuniform load redistribution at falsework 2. Girder G2 has the highest reaction force of 264 kips, followed by G1, G4, and then G3 (in order of magnitude). On the whole, the reaction forces at falsework 2 for Case 1 differ greatly from the reactions resulting from Case 2. Case 2 shows uniform load distribution at the

falsework, taking into account that girder G1 is not fully complete, and therefore the reaction of G1 at falsework 2 is not much larger than the reaction of G2 at the same location. It is obvious that the inconsistency in the cross-frame detailing causes a large discrepancy in the measured reactions at the falsework 2 location.

The reaction forces at abutment 1 for Case 1 also do not show distinct load redistribution to the outside girder, with G3 subjected to the largest reaction. However, as shown in table 20 this behavior is not the case for the structure using cross-frames detailed for the no-load case.

#### **7.3.4 Construction Stage 14 Support Reaction Comparisons**

Construction stage 14 completes girder line G4 of the curved span. Abutment 1, falsework 2, and pier 1 support the structure at the current construction stage.

A considerable difference in support reactions is realized at falsework 2 due the inconsistency concerning the detailing of the cross-frames. The reactions for Case 1 are nonuniformly distributed, as shown in table 20, with the girder G2 support receiving the smallest load. The use of the incorrectly detailed cross-frames also leads to large variation in the G1 reaction at pier 1, as a difference of slightly more than 100 kips is observed, with the larger reaction resulting from Case 1.

Also, the reactions at pier 1 differ slightly between the two cases. While for Case 1, a larger reaction is evident at the G2 and G4 supports than what is observed in Case 2; a smaller reaction is produced at the G3 support than what is shown for Case 2.

### 7.3.5 Construction Stage 16 Support Reactions Comparisons

Construction stage 16 is the final stage in the erection sequence of the curved span of the Ford City Bridge. All of girder sections 1 through 4 are in position, and falsework 2 is the only temporary support in place.

The abutment 1 and pier 1 reactions match fairly closely between the two detailing cases. However, discrepancies are evident at the falsework 2 location between reactions observed for Case 1 and Case 2. The girder G2 support for Case 1 is subjected to a reaction force 120 kips more than the reaction experienced in Case 2 in which the cross-frames are detailed for the web-plumb at no-load case. Also, nonuniform load distribution at falsework 2 is evident, such that the reaction at G2 is less than the reaction at G3. It seems that the error in detailing has the most effect on the support reactions for the inside girders G2 and G3.

#### 7.4 Summary of Ford City Bridge Erection Sequence Analytical Studies

The verified finite element model of the Ford City Bridge is used to recreate the “as-built” erection sequence of the bridge. The analytical models used for the studies contained in this section utilize cross-frames detailed for the theoretical no-load case.

It is observed that throughout the analyses of the “as-built” erection sequence, out-of-plane (radial) and vertical displacements remain minimal, with displacements usually less than 25mm (1in). Displacements are monitored at the bottom and top flanges along each girder line, with particular attention given to displacements at the field-splice locations. The largest displacement often occurs at the field-splice 3 locations of the section 4 girders due to the substantial unsupported length. The maximum out-of-plane (radial) and vertical displacement at non field-splice locations occurs at midspan of the section 3 girders.

Monitored von Mises stresses and longitudinal stresses are largest in the top and bottom flanges for each erection stage. These stresses remain well below the yield stress of the steel (Grade 50 and HPS70W) used in the structure. A maximum von Mises stress of 28 MPa (4.1 ksi) occurs in construction stage 16, in the top flange of G1 near the field-splice 3 location.

Generally, reactions throughout the analytical bridge erection sequence are consistent with engineering judgment, in which the load is often transferred to the outside girders. Beginning with construction stage 12 and the placement of G2-3, girders G2 and G3 tend to “lift off” of the support at falsework 2A.

As stated previously, a slight deviation occurs between the “in field” construction of the curved span, and the “planned” erection sequence as dictated by the erection plans (HDR 1999). The differences in erection procedures begin with construction stage 13, with the major alteration being the removal of falsework 1 and falsework 2A. For all variations, it is shown that the displacements at the midspan of section 3 and at most field-splice locations are less for the “planned” construction stages. Also, the load redistribution after each construction stage is much more uniform for the “planned” bridge erection sequence.

The issue of incorrect cross-frame detailing, and its relation to support reactions during construction is also explored as part of the current section. The reactions provided in the bridge erection plans (HDR 1999) are for the structure with the incorrectly detailed cross-frames (detailed for the web-plumb position at the concrete deck load case). These reactions are compared to reactions for the erection sequence using the structure with cross-frames detailed for the web-plumb position at the no-load condition. The use of the incorrect cross-frames has a greater effect on the support reactions of the structure during the later stages of construction. A higher degree of uniform load redistribution at each construction stage is shown to exist for the structure erected with the cross-frames detailed for the web-plumb position at the no-load condition. In some cases for the structure with the incorrectly detailed cross-frames, the maximum support reactions are not at the outside girder, G1, contrary to engineering judgment.

## 8.0 INCONSISTENT DETAILING OF CROSS-FRAME MEMBERS

Construction difficulties can result from inconsistent detailing of cross-frame members, which are primary load carrying members in curved steel I-girder bridges. The fabrication of curved steel I-girders to one load condition and the cross-frames to another load condition will induce additional stresses and displacements unaccounted for in the original design. Additionally, if girders and cross-frames are not detailed consistently, very significant forces will need to be applied to the structure during erection to bring bridge components into alignment.

In most cases of inconsistent detailing, girders are detailed to have their webs plumb at the beginning of construction, and cross-frames are fabricated so that the webs of the girders are plumb after steel erection, or concrete deck placement. Given that horizontally curved I-girders displace vertically and horizontally upon loading, the webs of the girders cannot remain plumb both before and after application of load (steel self-weight, and/or concrete load). Essentially, the girder webs can be plumb at only one stage of the bridge erection. Currently there is no guidance given in design specifications or in the literature for bridge engineers or bridge detailers, concerning the issue of inconsistent detailing of cross-frame members in curved steel I-girder bridges.

This section will describe two different detailing procedures that are often mistakenly interchanged when detailing cross-frames in curved steel I-girder bridges. Additionally, the analytical model of the entire Ford City Bridge (curved and non-curved

spans) is used to illustrate that a substantial difference in cross-frame member lengths results from the application of inconsistent detailing methods.

Another, but similar detailing inconsistency occurs in the fabrication of the cross-frames for the Ford City Bridge. The cross-frames are incorrectly fabricated for the web-plumb condition at application of the concrete deck load instead of the web-plumb condition at no-load. The girders of the bridge are fabricated to the web-plumb condition at no-load, in which the webs of the girders are plumb at the beginning of construction. It should be noted, that the cross-frames were intended to be designed for the application of steel self-weight only, however, apparently an error occurred during fabrication, and the incorrect data (concrete deck load case) was used to detail the cross-frames. Nevertheless, detailing the cross-frames for the web-plumb condition at the application of concrete deck weight only, and the girders to the web-plumb condition at no-load, also creates an inconsistency.

This section also will explore the difference in cross-frame member lengths detailed for web-plumb at application of concrete deck load, and those detailed for the web-plumb position at no-load. The finite element model of the Ford City Bridge is used to demonstrate the difference in detailing methods. Furthermore, the final steel elevations prior to deck placement resulting from the analytical model using cross-frames detailed for the web-plumb at no-load condition will be compared with field-surveyed elevations of the structure upon completion of the steel erection (i.e. the inconsistently detailed case).

## 8.1 Typical Inconsistent Detailing of Cross-Frames in Curved Steel I-Girder Bridges

Horizontally curved steel I-girders displace vertically, horizontally, and rotate upon load application as a direct result of their curved geometry. The horizontal displacement and rotation is caused by the eccentricity of the load being applied to the girder, whether it is self-weight or a service load. This eccentricity is due to the fact the center of gravity (COG) of curved I-girders is not located in the plane of the girder web. As shown in figure 136, the center of gravity is offset (X) from a chord line drawn between the girder ends.

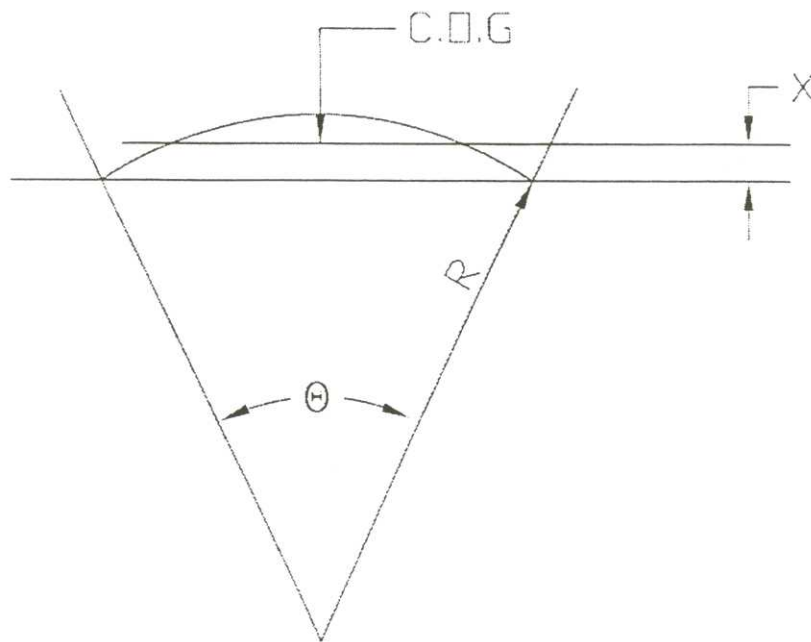


**Figure 136** Curved I-girder center of gravity

To illustrate the behavior of a curved I-girder bridge, figures 137, 138, 139, 140, and 141 are provided. All of the figures give details about the displacement of the analytical model of the entire Ford City Bridge (curved and straight spans, see Figure 90) when it is subjected to the steel self-weight load only. The cross-frames used in the finite element model are detailed for the web-plumb condition at no-load (see section 8.1.1 for further information). Figure 137 illustrates the displaced finite element model due to steel self-weight loading, as viewed from abutment 1 (the displacement is magnified by a factor of 10). Figure 138 shows the monitored vertical displacement of each girder; figure 139 illustrates the out-of-plane (radial) displacement that occurs at the bottom flange of each girder; and figure 140 displays the out-of-plane (radial) displacement that occurs at the top flange of each girder. The out-of-plane displacements at the bottom and top flanges are related to the girder web rotation, which is shown in figure 141.

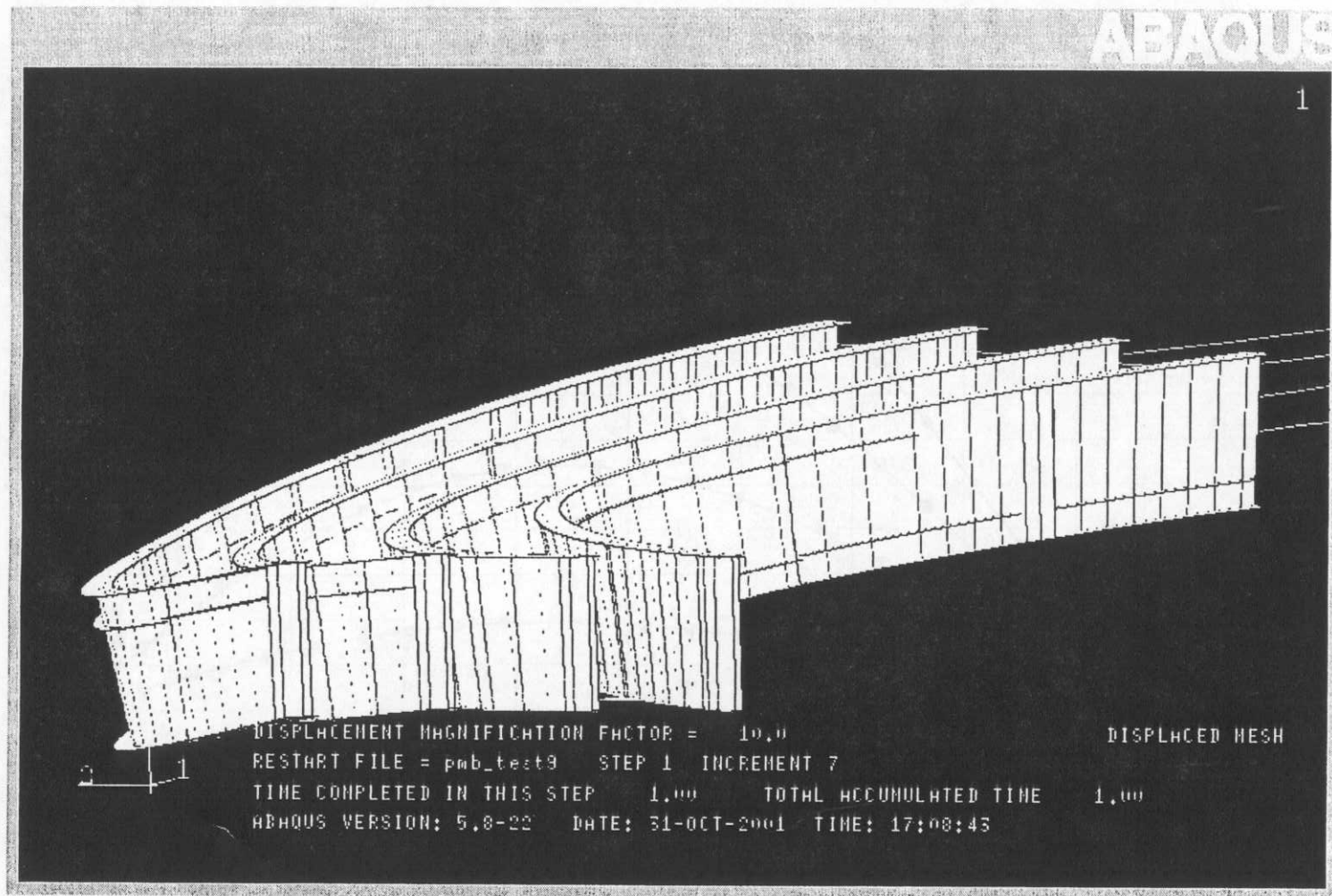


**Figure 137** Displacement of finite element model – Displacement magnified by a factor of 10 (displaced structure is colored white, original structure is darker shade)

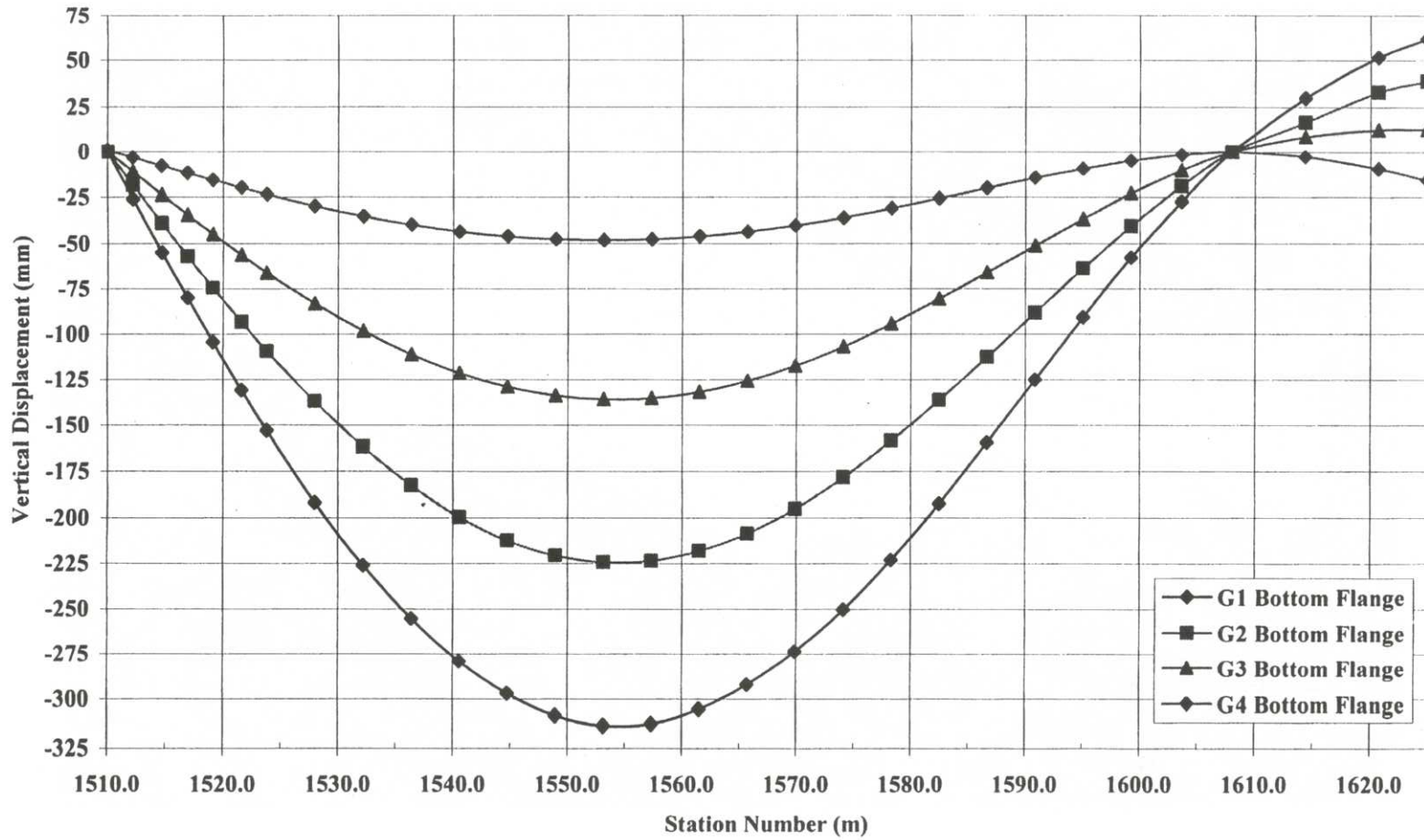


**Figure 138** Vertical displacement using the entire Ford City Bridge finite element model – curved span shown

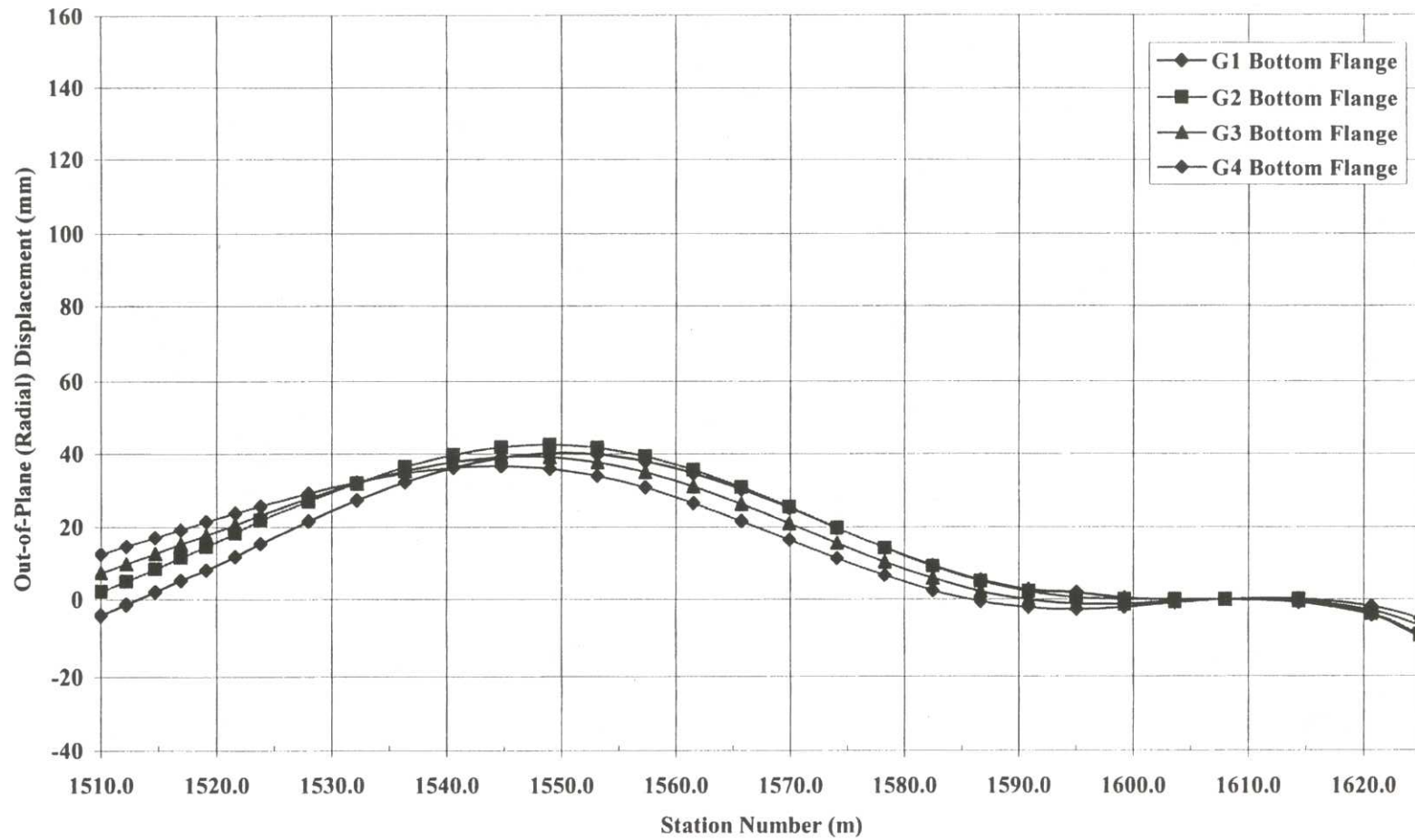


**Figure 139** Out-of-plane (radial) displacement at the bottom flange using the entire Ford City Bridge finite element model – curved span shown

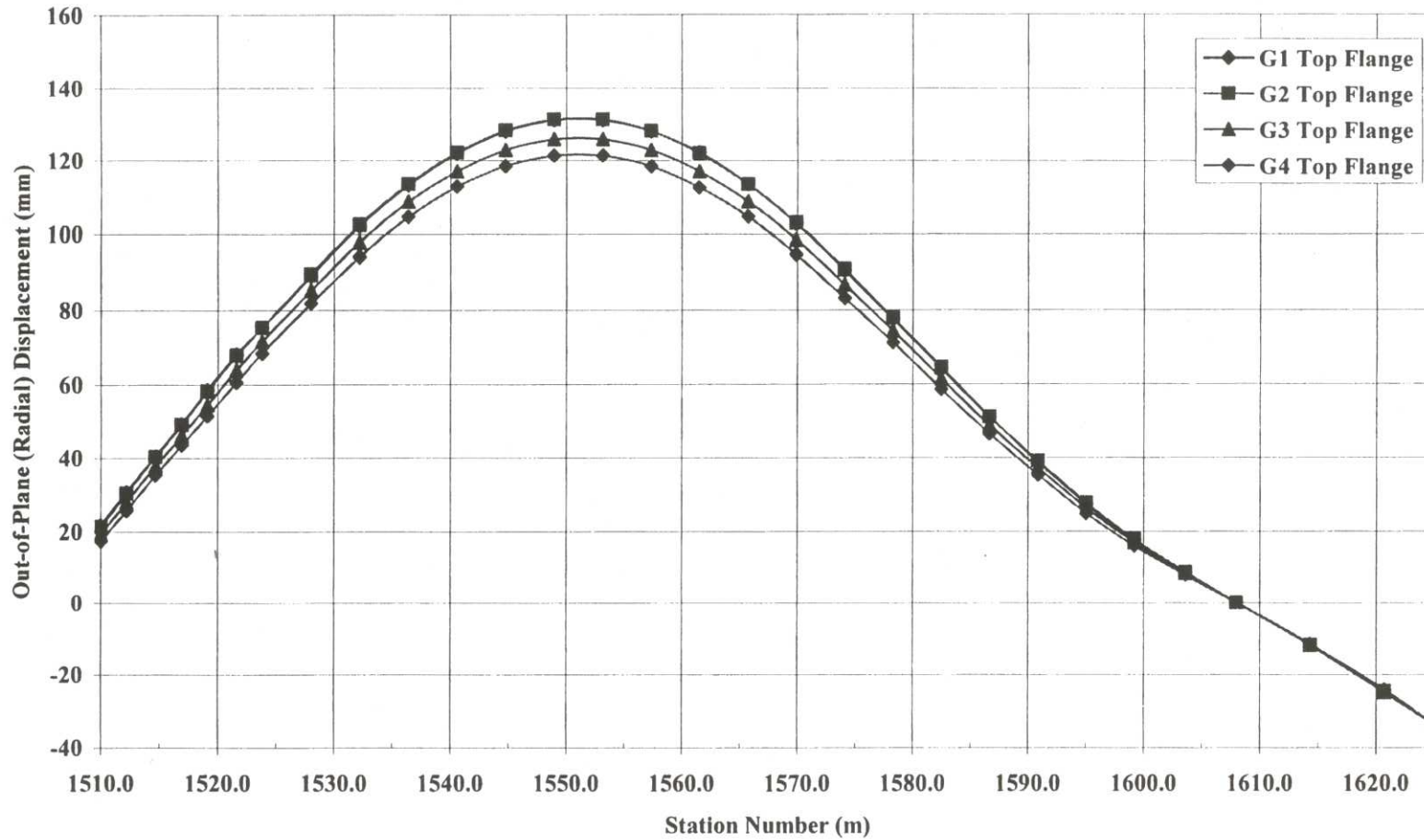


**Figure 140** Out-of-plane (radial) displacement at the top of the flange using the entire Ford City Bridge finite element model – curved span shown

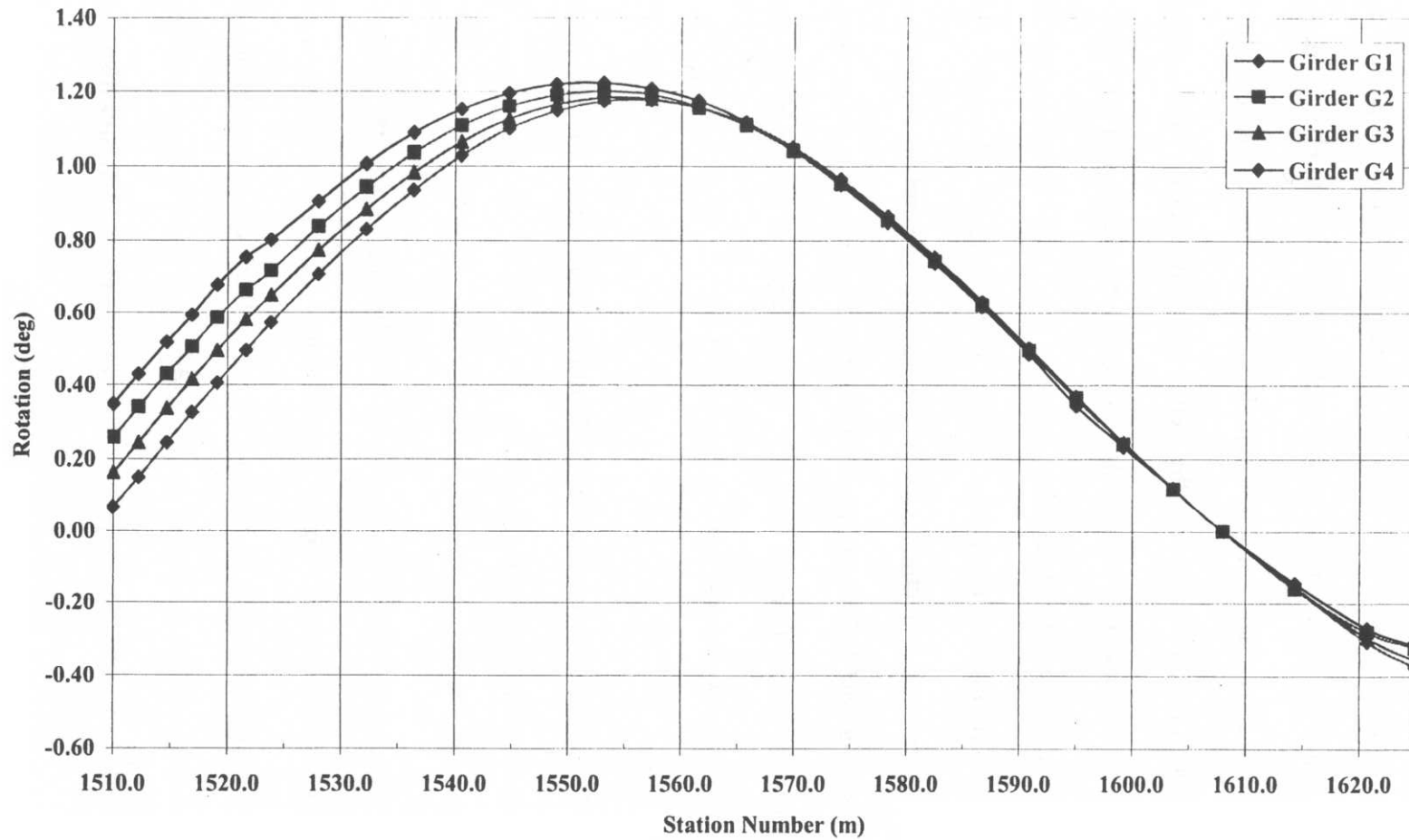


**Figure 141** Girder web rotation using the entire Ford City Bridge finite element model – curved span shown

Given this tendency to displace and rotate upon load application, the webs of the girders cannot remain plumb both before and after load is applied. An inconsistency occurs when the I-girders of a curved bridge are detailed to one geometric condition and the cross-frames to another. For example, if the girders are fabricated to fit cross-frames in a no-load condition in which the webs are plumb but the cross-frames are detailed to connect to girders in a web-plumb position after load application, steel self-weight for instance, an inconsistency develops. Simply put, the girder webs can only be vertically plumb at one instance during the erection of the bridge. Therefore, only two distinct, non-interchangeable methods should be used to determine the cross-frame member lengths in curved I-girder bridges: 1.) Construction begins at the no-load condition with girder webs plumb (section 8.1.1); or 2.) Construction begins at the no-load condition with the girder webs out-of-plumb (section 8.1.2).

### **8.1.1 Detailing of Cross-Frames to Girder Web-Plumb Condition at the Beginning of Construction (No-Load Condition)**

The girders and cross-frames can be fabricated so that the girder webs are plumb at the no-load condition. Figure 142 illustrates a cross-sectional view of the Ford City Bridge at cross-frame 14, in the no-load, web-plumb condition. In this case, in order to simulate the no-load condition during bridge construction, temporary supports, such as falsework bents, may be required. Excess girder rotation and displacement must be

prevented by the placement of the temporary supports; otherwise problems during erection would still develop.

To detail a bridge using this approach, only the geometric positions of the girders are required. The geometric positions of the girders are calculated using the camber diagram in the bridge plans, and using any change in elevations for the structure. Once the positions of the girders are known, cross-frame dimensions for each individual cross-frame can simply be calculated using typical bracing formulae or other geometric calculations. Since the girder webs are vertically plumb, the determination of cross-frame dimensions is much simplified as compared to detailing with girder webs-out-of-plumb at the no-load condition.

Upon removal of the temporary supports, the steel structure will deflect due to self-weight (and concrete deck weight if placed prior to support removal), and the girder webs will no longer remain vertically plumb. Figure 143 illustrates the cross-sectional view at cross-frame 14 of the girder rotation and displacement that occurs in the analytical model of the Ford City Bridge due to the application of steel self-weight only. The application of steel self-weight is commonly referred to as the “gravity-on” condition. Figures 144 and 145 show views of the analytical model in the displaced position, from the abutment 1 location (for figure 145 the displacement is magnified by a factor of five). Depending on serviceability requirements of the given bridge, the subsequent girder rotation and displacement may or may not be acceptable.

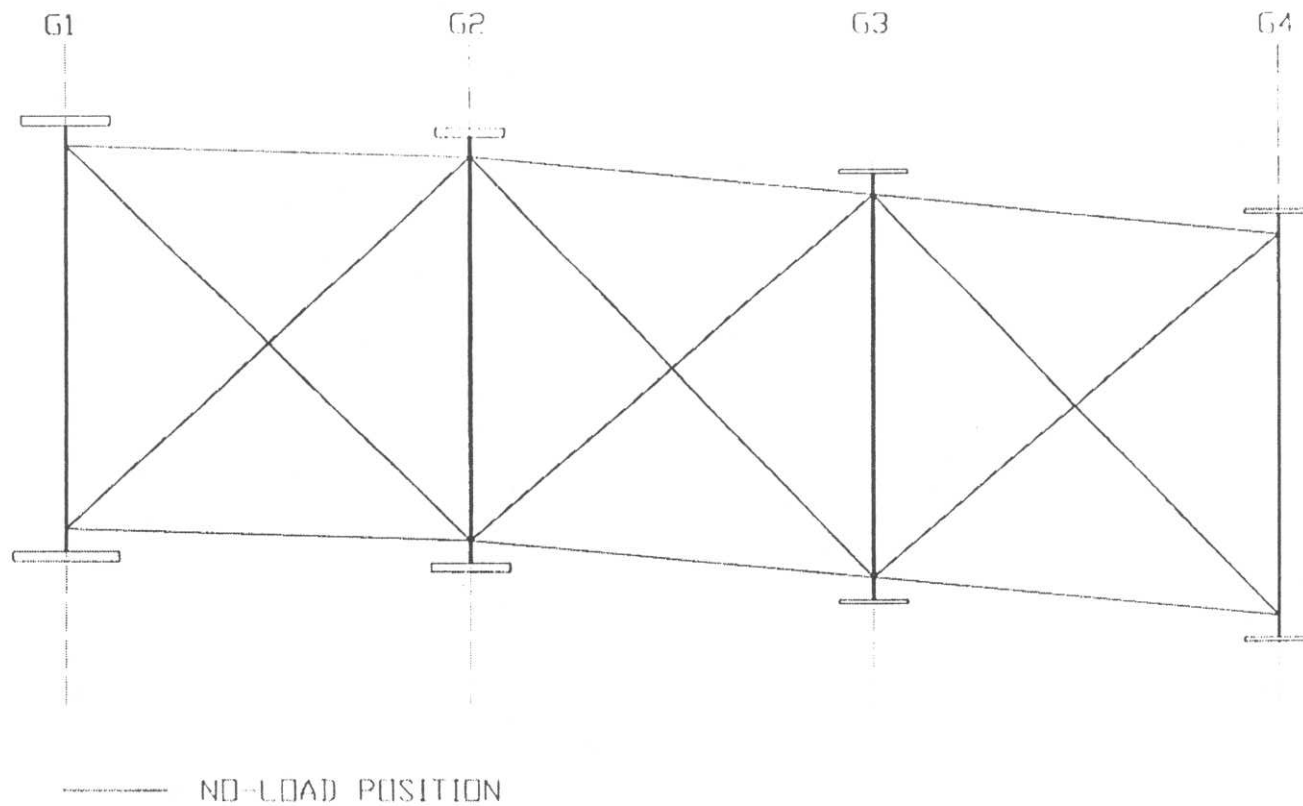


**Figure 142** Cross-sectional view of bridge at cross-frame 14 – Undeformed structure with cross-frames detailed for the no-load , web-plumb condition.

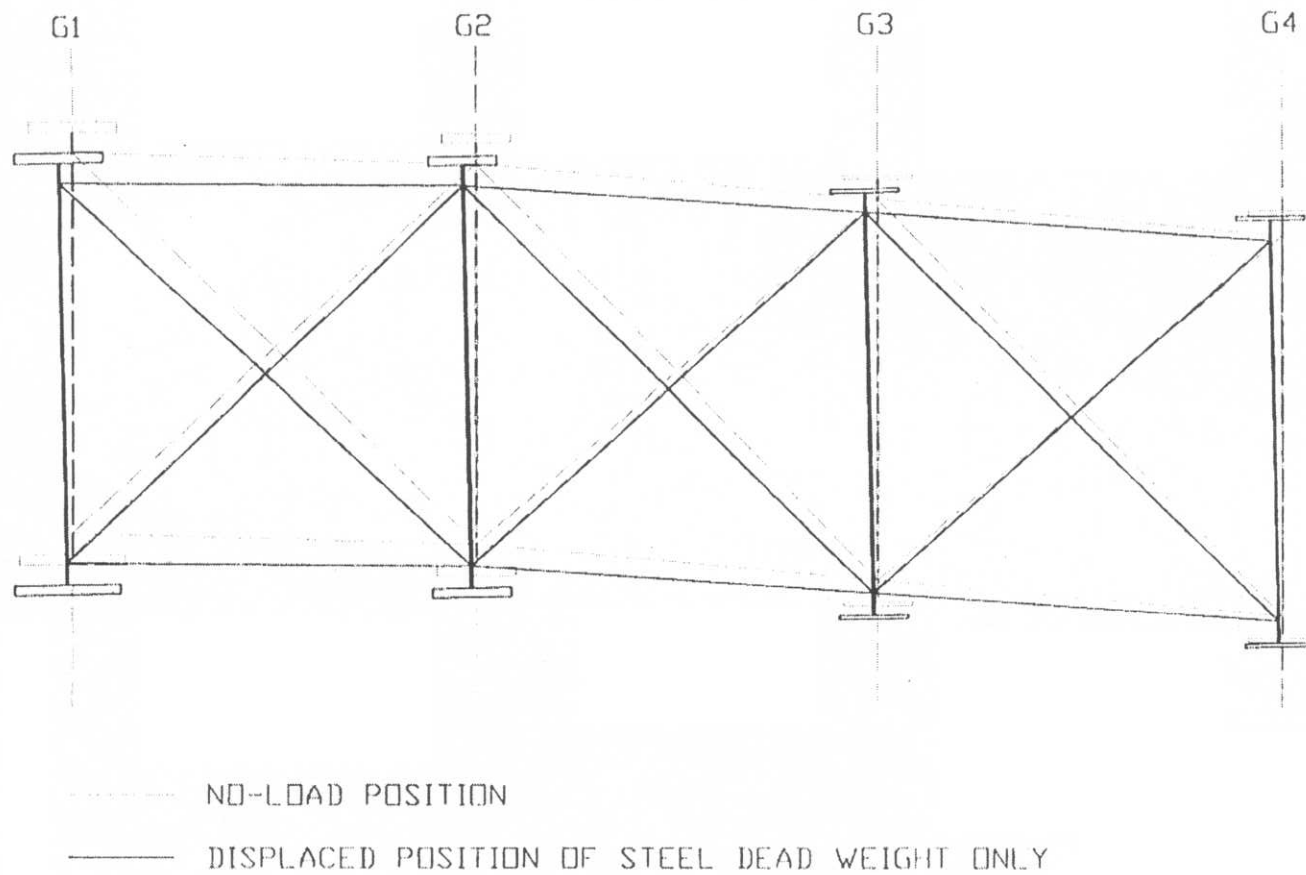


**Figure 143** Cross-sectional view of bridge at cross-frame 14 – Deformed structure due to steel self-weight with cross-frames detailed for the no-load, web-plumb condition

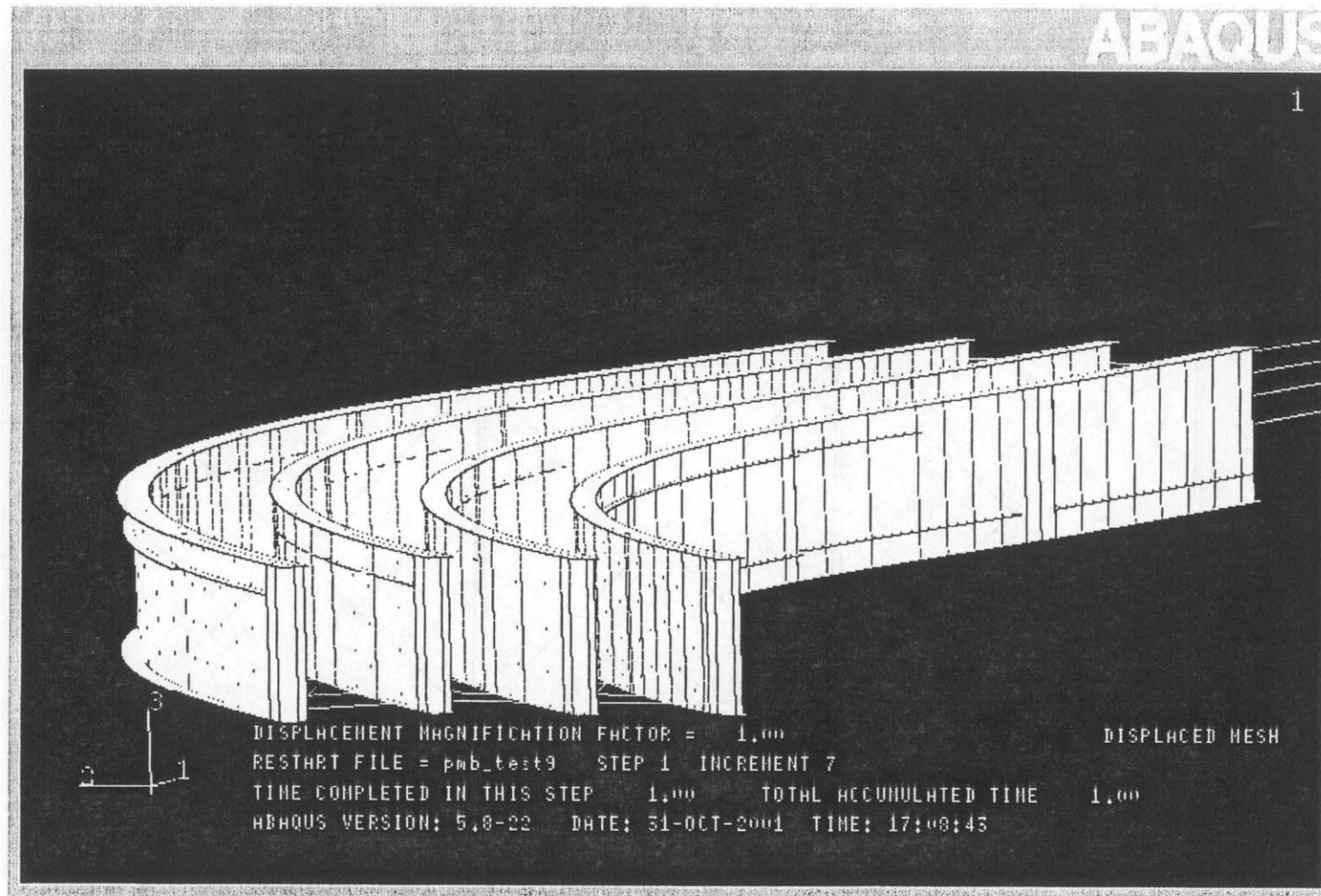


**Figure 144** Displacement of finite element model with cross-frames detailed for the no-load, web-plumb condition (displaced structure is colored white, original structure is darker shade)

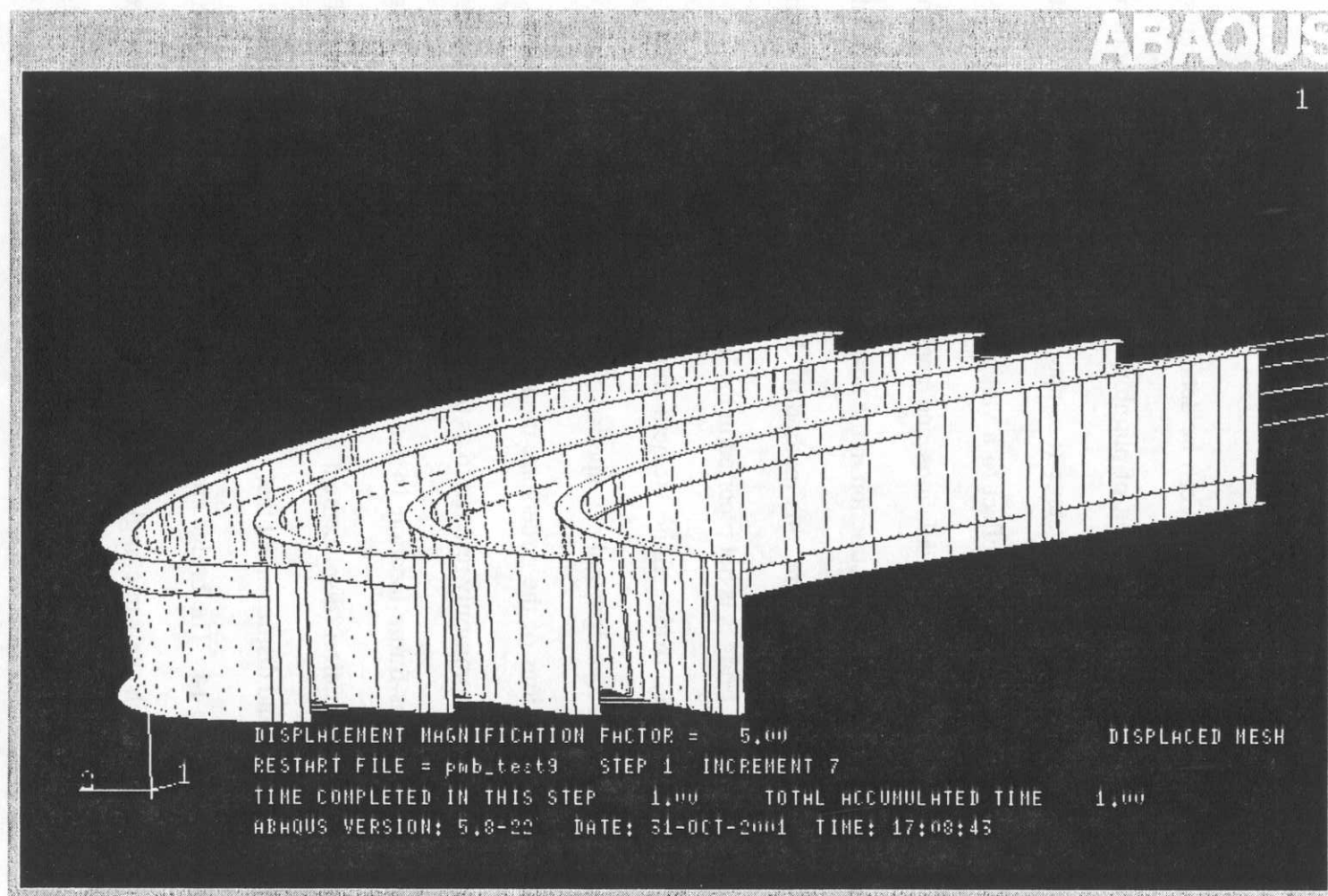


**Figure 145** Displacement of finite element model with cross-frames detailed for the no-load, web-plumb condition – Displacement magnified by a factor of 5 (displaced structure is colored white, original structure is darker shade)

### **8.1.2 Detailing of Cross-Frames to Girder Web Out-of-Plumb Condition at the Beginning of Construction (No-Load Condition)**

The girders and cross-frames can be detailed and erected in a web out-of-plumb position, so that the girder webs, out-of-plumb at the beginning of construction, end up plumb at some later construction stage (i.e. upon load application, such as steel self-weight, the girder webs would deflect to a vertically plumb position). This method of detailing requires additional calculations and analysis, as opposed to detailing cross-frames and girders to begin construction in the no-load, web-plumb position, as described in section 8.1.2. Furthermore, this method of detailing and erection for horizontally curved steel I-girders is not reported in the literature.

The Ford City Bridge finite element model is used to illustrate this detailing technique. Steel self-weight only is applied to the analytical bridge model, and the rotations and deflections of the girders are monitored at each cross-frame location. This loading condition is commonly referred to as the “gravity-on” condition. The girders and cross-frames at cross-frame location 14 are used for illustrative purposes. Figure 146 illustrates an exaggeration (displacement and rotation magnified by a factor of five) of the girder rotation and displacement that occurs due to the application of steel self-weight only, at cross-frame 14. The bridge cross section rotates as a rigid body, such that each girder rotates through the same angle about each girder’s individual vertical axis. The vertical displacements are different for each girder, due to the innate behavior of a curved

I-girder bridge. Load and deflection is distributed to the outside girders, and therefore they deflect more than the inside girders.

To determine the cross-frame member length for girder web-plumbness after load application, the following geometric manipulations must be accomplished. Using a sufficient analysis, the displaced and rotated position due to steel self-weight (gravity-on) is determined, and then the girder webs are geometrically rotated back to a vertically plumb position, as shown in figure 147. New cross-frame lengths are then determined, using a compatibility condition of girder web-plumbness, in the presence of vertical displacement. This condition is shown in figure 148.

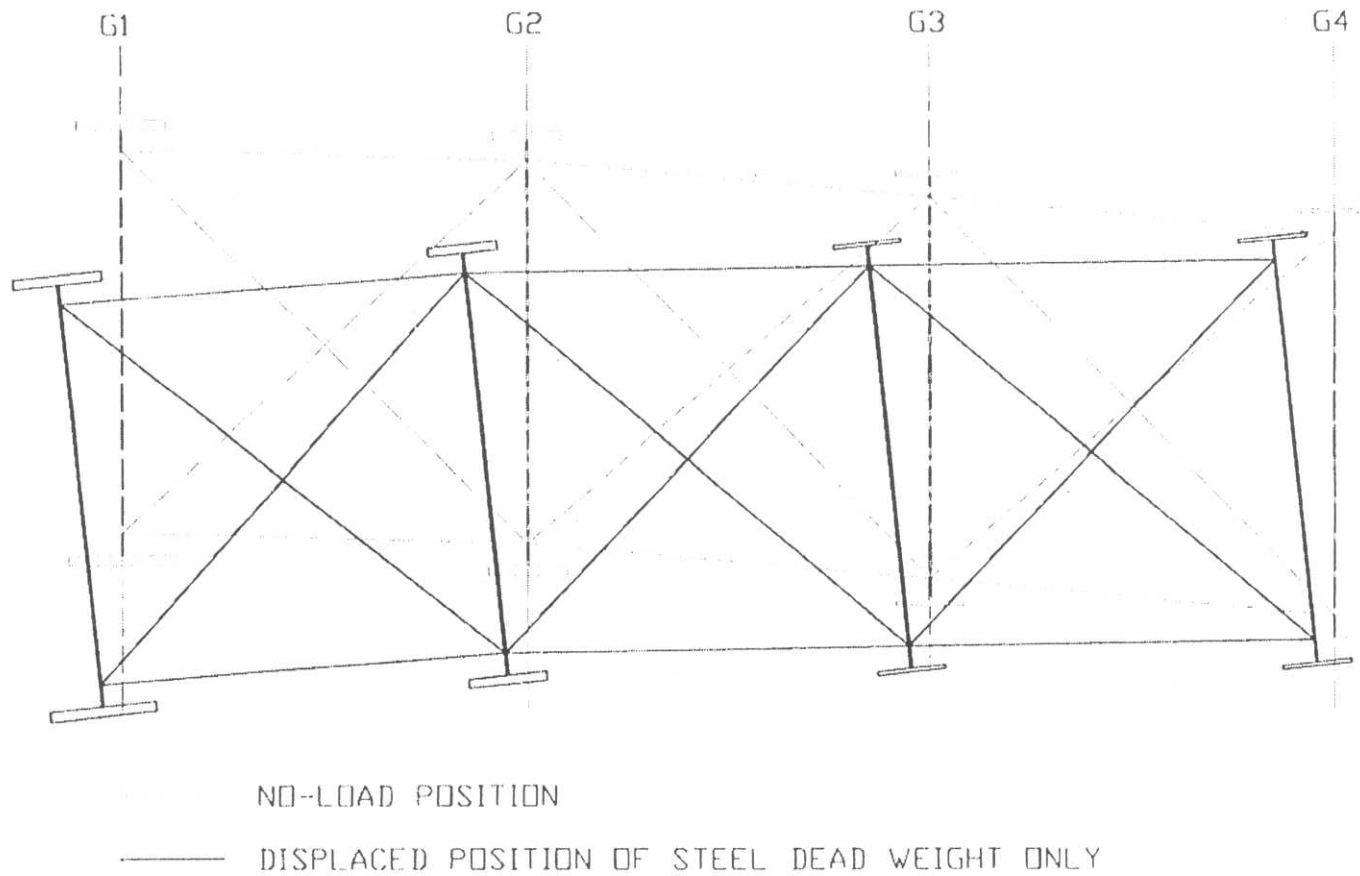


**Figure 146** Cross-sectional view of bridge at cross-frame 14 – Deformed structure due to steel self-weight with cross-frames detailed for the no-load, web-plumb condition (Displacement magnified by a factor of 5)

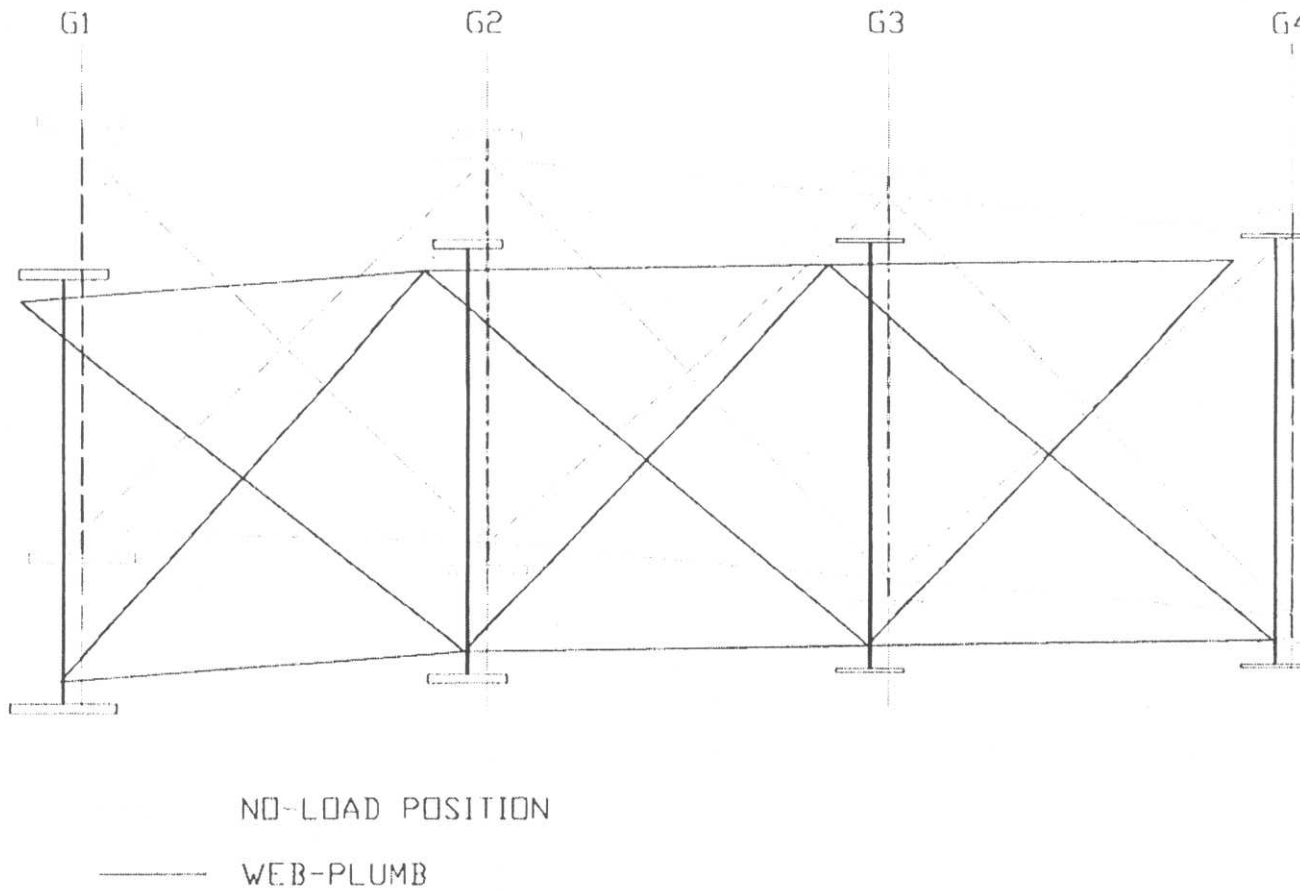


**Figure 147** Cross-sectional view of bridge at cross-frame 14 – Girder webs rotated back to web-plumb position (Displacement magnified by a factor of 5)

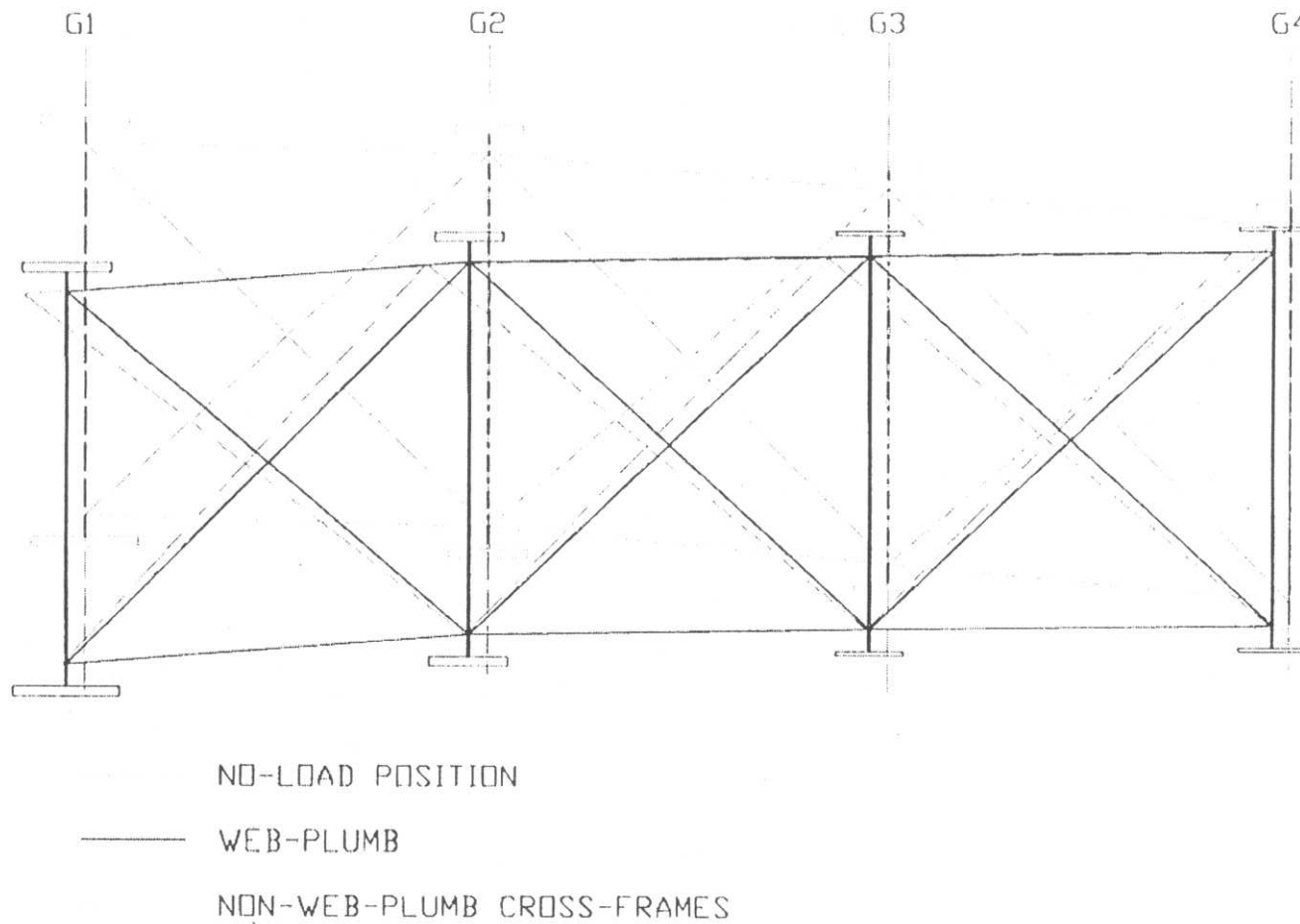


**Figure 148** Cross-sectional view of bridge at cross-frame 14 – Girder webs rotated back to web-plumb position and new cross-frame members are inserted (Displacement magnified by a factor of 5)

The bridge cross section is then rotated back by the same angle it deflected due to the application of steel self-weight (gravity-on). The vertical and horizontal displacements due to application of steel self-weight are also “reversed,” such that the midpoint of the bottom of each girder bottom flange is in the same location as it is in the no-load, web-plumb position. This stage is illustrated in figure 149, and can be referred to as “gravity-off.”

Figure 149 illustrates the starting point of bridge erection for girders and cross-frames detailed so that girder webs are vertically plumb after application of steel self-weight. Temporary supports would be required to ensure that girders remain in the “twisted position” during bridge erection and to ensure cross-frame connections are easily made. Once the temporary supports are removed, the girders will displace and rotate as a rigid body to the desired web verticality, in this case, after application of steel self-weight.

The same method can be utilized for steel self-weight combined with concrete deck weight, if it is desired to have the girder webs vertically plumb after application of steel self-weight and concrete deck load. Of course, in consideration of concrete deck weight application, issues arise concerning the composite / non-composite cross section, if the temporary supports are removed before the concrete is fully cured.

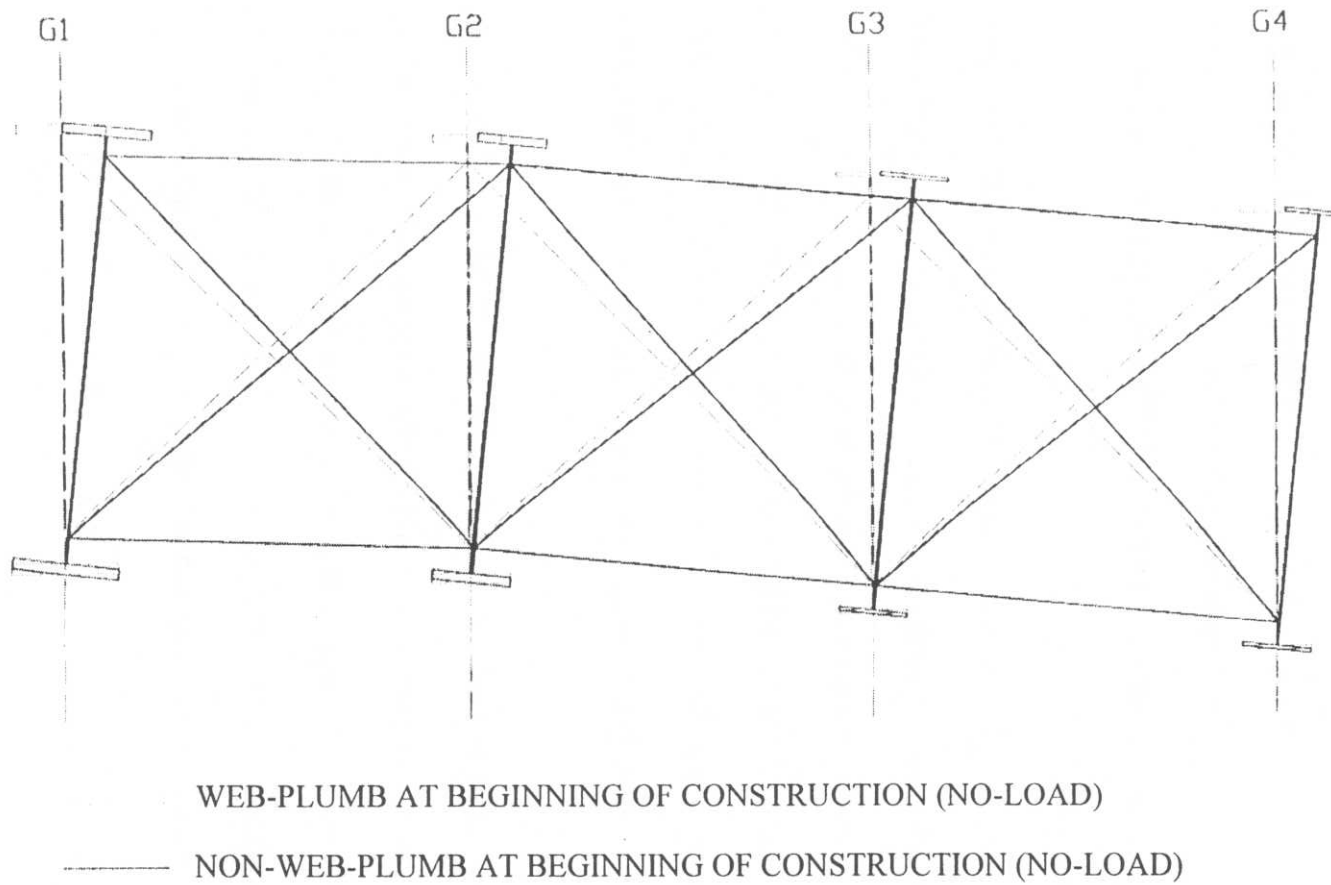


**Figure 149** Cross-sectional view of bridge at cross-frame 14 – Web-plumb versus non-web-plumb at beginning of construction (Displacement magnified by a factor of 5)

### 8.1.3 Difference in Cross-Frame Member Lengths Due Inconsistent Detailing

#### Procedures

**8.1.3.1 Analysis and Results.** The detailing inconsistency results from the fact that the steel detailer is only given the vertical camber (reverse of vertical deflection) in the design drawings. The detailer (possibly per engineering or owner guidelines) will then fabricate the girders to the specified camber, but in some cases, will geometrically apply the steel-load vertical deflection (reverse of camber) to the girders and determine cross-frame lengths for the bridge girders in the vertically deflected position. Therefore applying the detail technique shown in section 8.1.1 (Web-plumb at no-load) to the girders, and applying a component of (vertical displacement only) the detailing method of section 8.1.2 (Web-non-plumb at no-load) to the cross-frames will result in an inconsistency. This discrepancy often occurs when the bridge engineer or owner desires to have the girder webs vertically plumb after construction

In some situations, this inconsistency can be quite large, therefore causing the need for additional forces to be applied to the structure via cranes and/or jacking devices in order to bring components into alignment and make the necessary connections. If the bridge designer and/or steel detailer do not eliminate this inconsistency, additional cranes and jacking equipment may be needed at the bridge erection site, which is unaccounted for in the original cost estimates of the bridge.

The analytical model of the Ford City Bridge is used to illustrate that a substantial difference in cross-frame member lengths is observed to result from inconsistent cross-

frame detailing procedures. The cross-frames in the Ford City Bridge finite element model are calculated using both techniques in turn and the lengths compared; (1) girder webs plumb at the beginning of construction, and (2) girder webs plumb at some point during the construction (i.e. after application of steel self-weight). Figure 150 shows the naming convention of the cross-frame members to be used in this section, and for later sections as well.

As shown in figure 151, there is a considerable difference in the cross-frame member lengths between those detailed to allow for the girders to be plumb at no-load, and those which are detailed for the non-web-plumb girders at no-load. The largest difference is in the diagonal members 'F' and 'M,' in which member 'F' increases in length and member 'M' decreases. There is only minimal disparity in member lengths for the top and bottom chords of the cross-frames. Table 21 displays the calculated cross-frame member lengths for both detailing conditions, for cross-frames 10A through 20A. The cross-frame member dimensions for all cross-frames can be found in Appendix D of the current research.

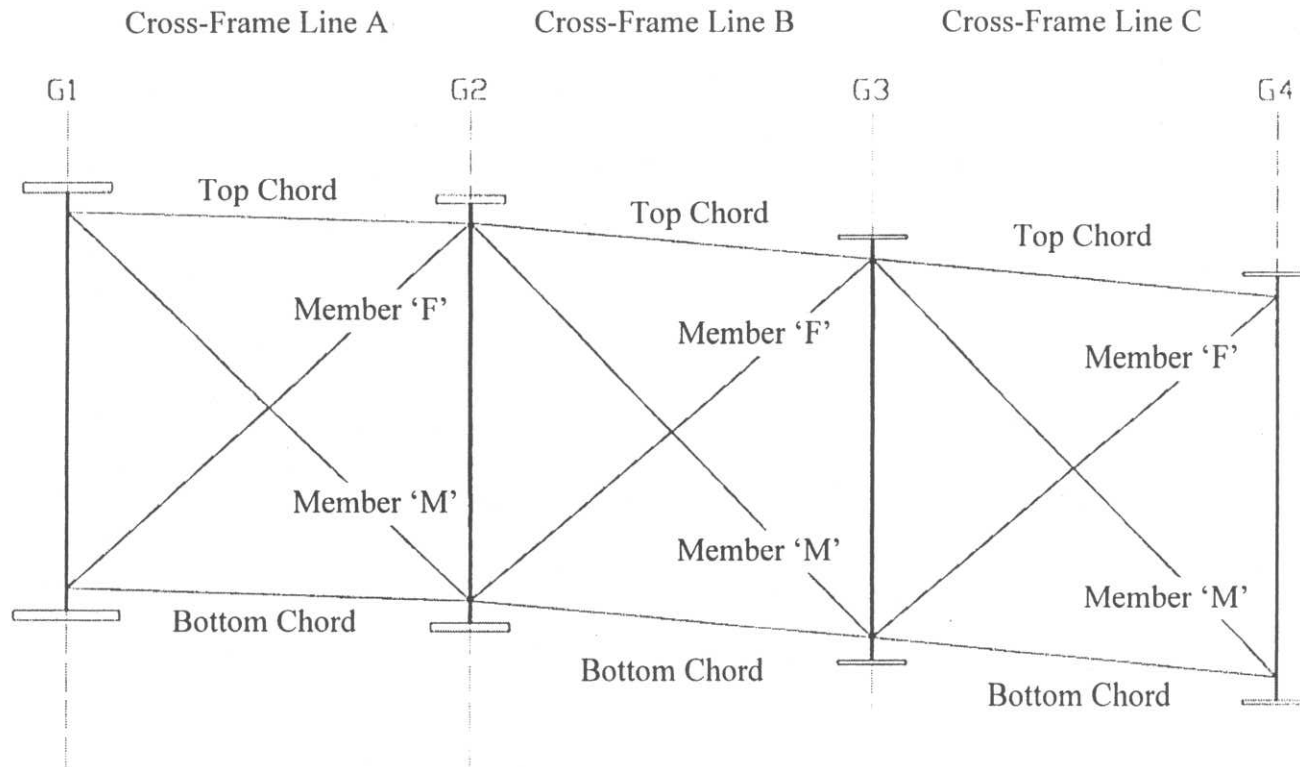


**Figure 150** Inconsistent detailing – naming convention for cross-frame members

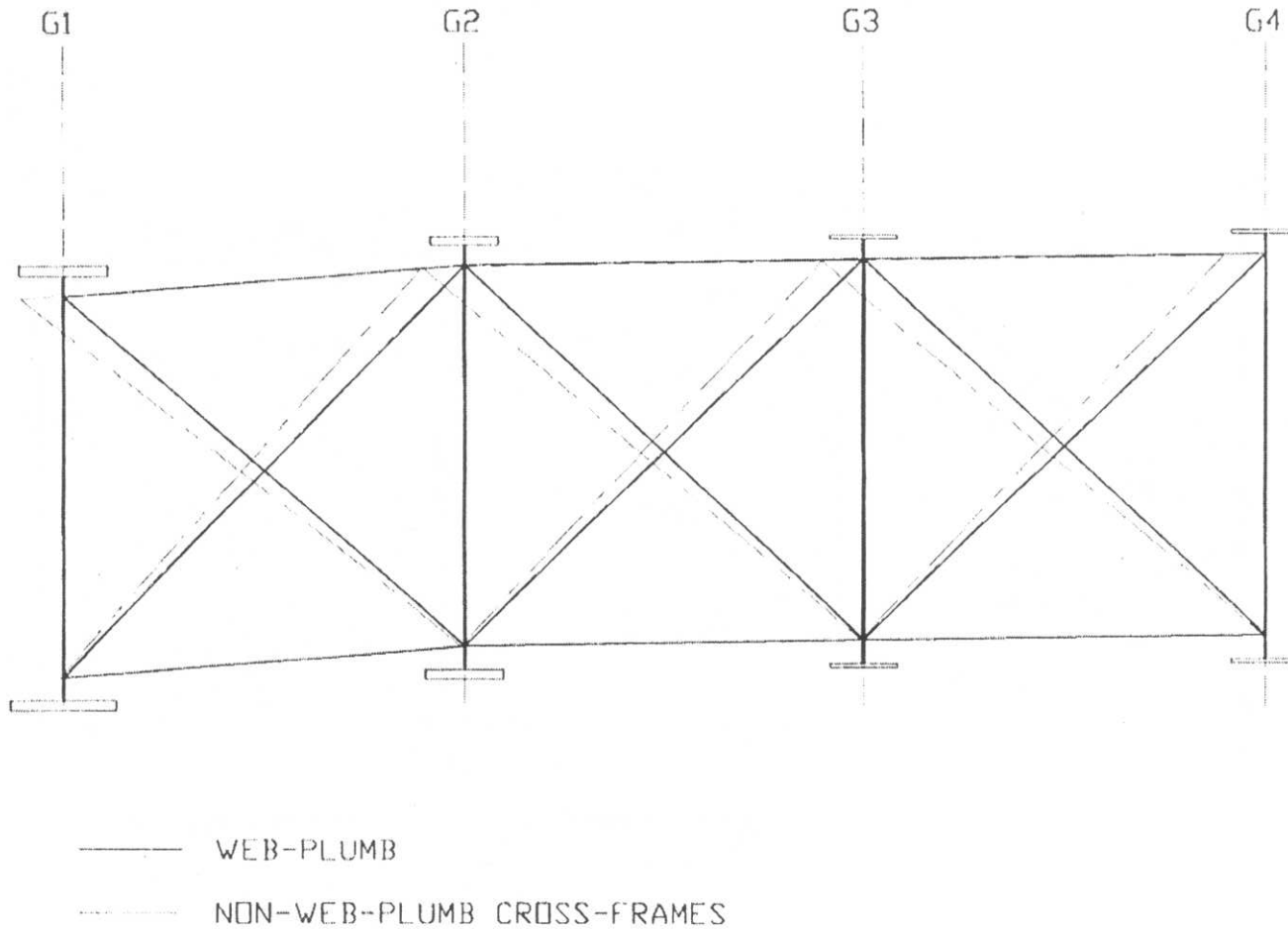


**Figure 151** Cross-sectional view of bridge at cross-frame 14 – Difference in cross-frame member lengths between web-plumb and non-web-plumb girders at no-load (Displacement magnified by a factor of 5)  
(No-load condition not shown for clarity)

**Table 21** Cross-frames 10A - 20A - Dimensions for web-plumb at no-load condition versus web-non-plumb at no-load condition

		<b>Cross-Frame Member Lengths (mm)</b>			
<b>Cross-Frame</b>	<b>Detailed Condition</b>	<b>F</b>	<b>M</b>	<b>Top Chord</b>	<b>Bottom Chord</b>
<b>10A</b>	Web-Plumb at No-Load	5574.43	5660.82	4100.49	4100.49
	Web-Non-Plumb at No-Load	5620.89	5607.89	4095.83	4095.83
<b>11A</b>	Web-Plumb at No-Load	5565.76	5669.67	4100.70	4100.70
	Web-Non-Plumb at No-Load	5617.22	5612.44	4096.43	4096.43
<b>12A</b>	Web-Plumb at No-Load	5558.67	5676.91	4100.91	4100.91
	Web-Non-Plumb at No-Load	5613.98	5616.57	4097.04	4097.04
<b>13A</b>	Web-Plumb at No-Load	5553.18	5682.55	4101.09	4101.09
	Web-Non-Plumb at No-Load	5611.17	5620.25	4097.64	4097.64
<b>14A</b>	Web-Plumb at No-Load	5549.28	5686.55	4101.23	4101.23
	Web-Non-Plumb at No-Load	5608.64	5623.57	4098.18	4098.18
<b>15A</b>	Web-Plumb at No-Load	5546.96	5688.94	4101.32	4101.32
	Web-Non-Plumb at No-Load	5606.51	5626.42	4098.68	4098.68
<b>16A</b>	Web-Plumb at No-Load	5546.20	5689.72	4101.34	4101.34
	Web-Non-Plumb at No-Load	5604.76	5628.81	4099.13	4099.13
<b>17A</b>	Web-Plumb at No-Load	5546.96	5688.93	4101.32	4101.32
	Web-Non-Plumb at No-Load	5603.29	5630.85	4099.52	4099.52
<b>18A</b>	Web-Plumb at No-Load	5549.22	5686.61	4101.23	4101.23
	Web-Non-Plumb at No-Load	5602.30	5632.24	4099.80	4099.80
<b>19A</b>	Web-Plumb at No-Load	5552.92	5682.81	4101.10	4101.10
	Web-Non-Plumb at No-Load	5601.77	5633.10	4100.02	4100.02
<b>20A</b>	Web-Plumb at No-Load	5557.98	5677.62	4100.93	4100.93
	Web-Non-Plumb at No-Load	5601.88	5633.19	4100.16	4100.16

Figures 17, 18, 19 and 20 clearly illustrate the inconsistency in cross-frame member lengths throughout the curved span of the Ford City Bridge. Figure 152 shows that the maximum length difference of member 'F' occurs at midspan of the curved section, at approximately station 1+555, which is the cross-frame 14 location. At the same location, cross-frame 14, the length difference of member 'M' is greatest, as shown in figure 153. The maximum difference in length for members 'F' and 'M' of cross-frame 14 is +/- 60mm (2.36in), respectively. The length of member 'F' increases as one changes from web-plumb at no-load detailing to non-web-plumb at no-load detailing; while length of member 'M' decreases as one changes from web-plumb no-load detailing to non-web-plumb at no-load detailing.

Demonstrated by means of figures 152 and 153, the increase of member 'F' lengths, and decrease of member 'M' lengths, follows a constant curved shape centered about the midspan of the curved section along the length of the bridge. Owing to the rigid body rotation of the bridge cross-section, the member length differences of 'F' and 'M' are basically the same for each cross-frame line (A, B, or C).

Figures 154 and 155 illustrate the fact that the top and bottom chord members do not experience the same drastic change in length between detailing methods. This is due to the fact the girders displace out-of-plane (laterally) in a uniform behavior with little variation from girder to girder.

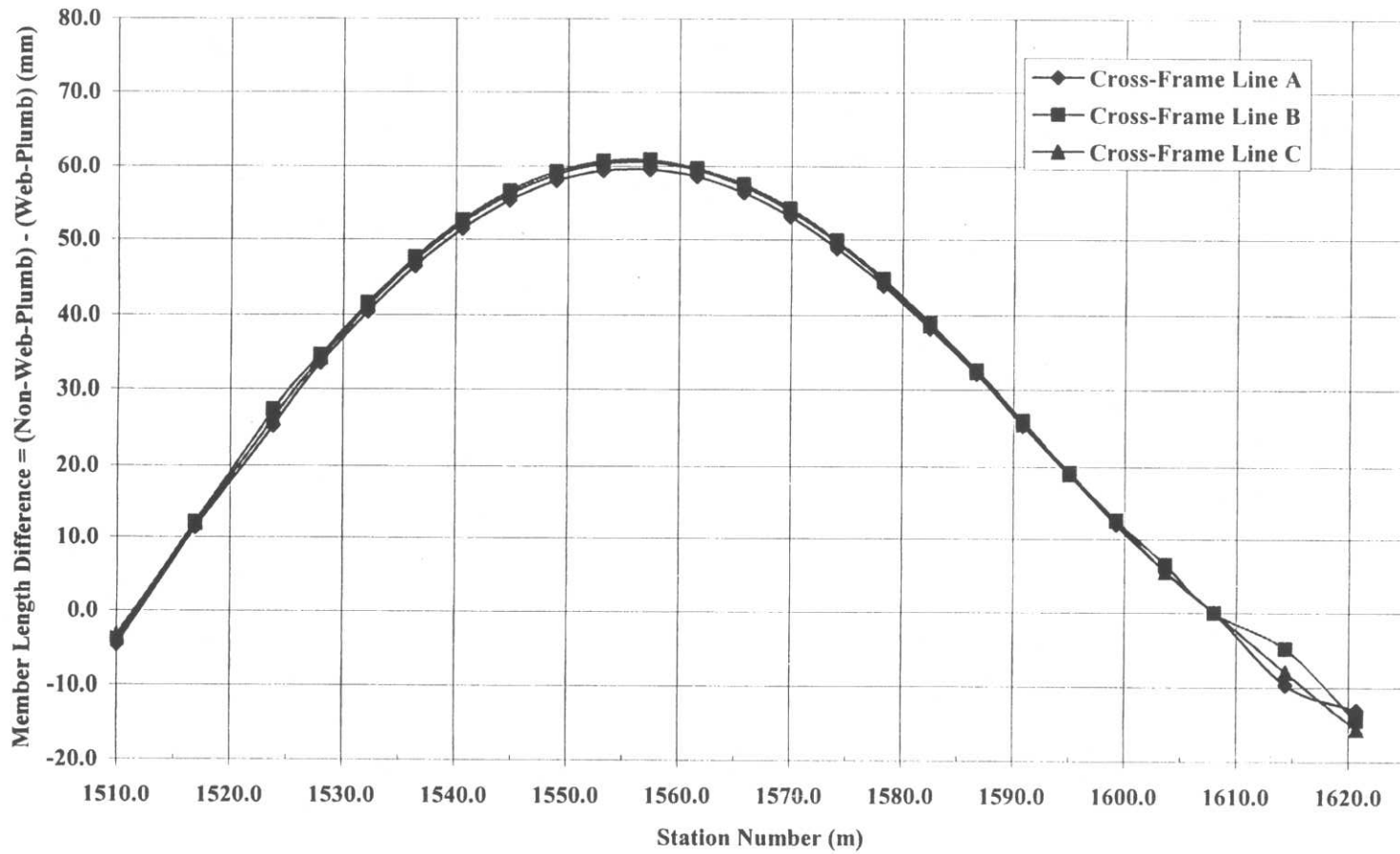


**Figure 152** Cross-frame member 'F' – Non-web-plumb detail vs. web-plumb detail length difference

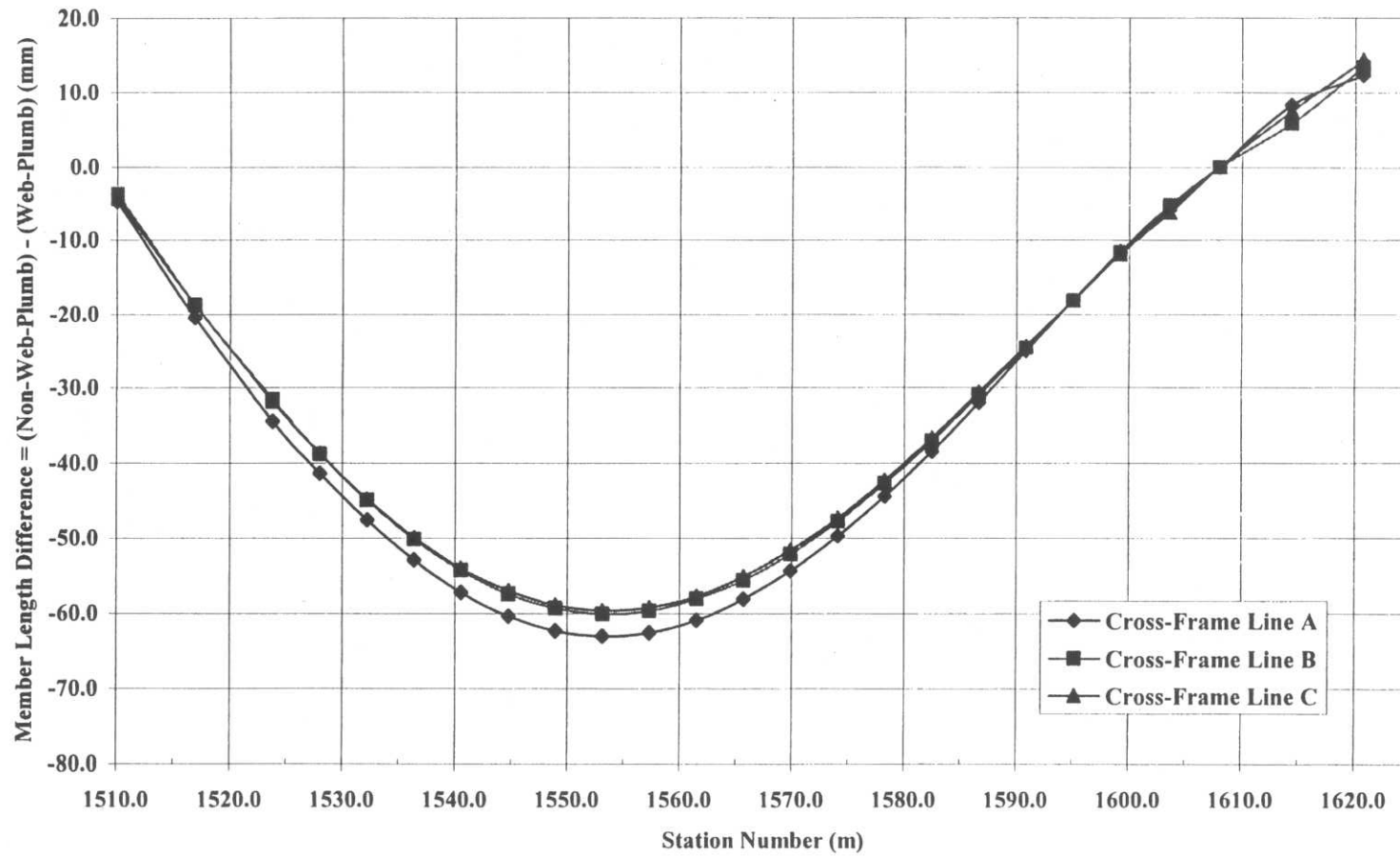


**Figure 153** Cross-frame member 'M' – Non-web-plumb detail vs. web-plumb detail length difference

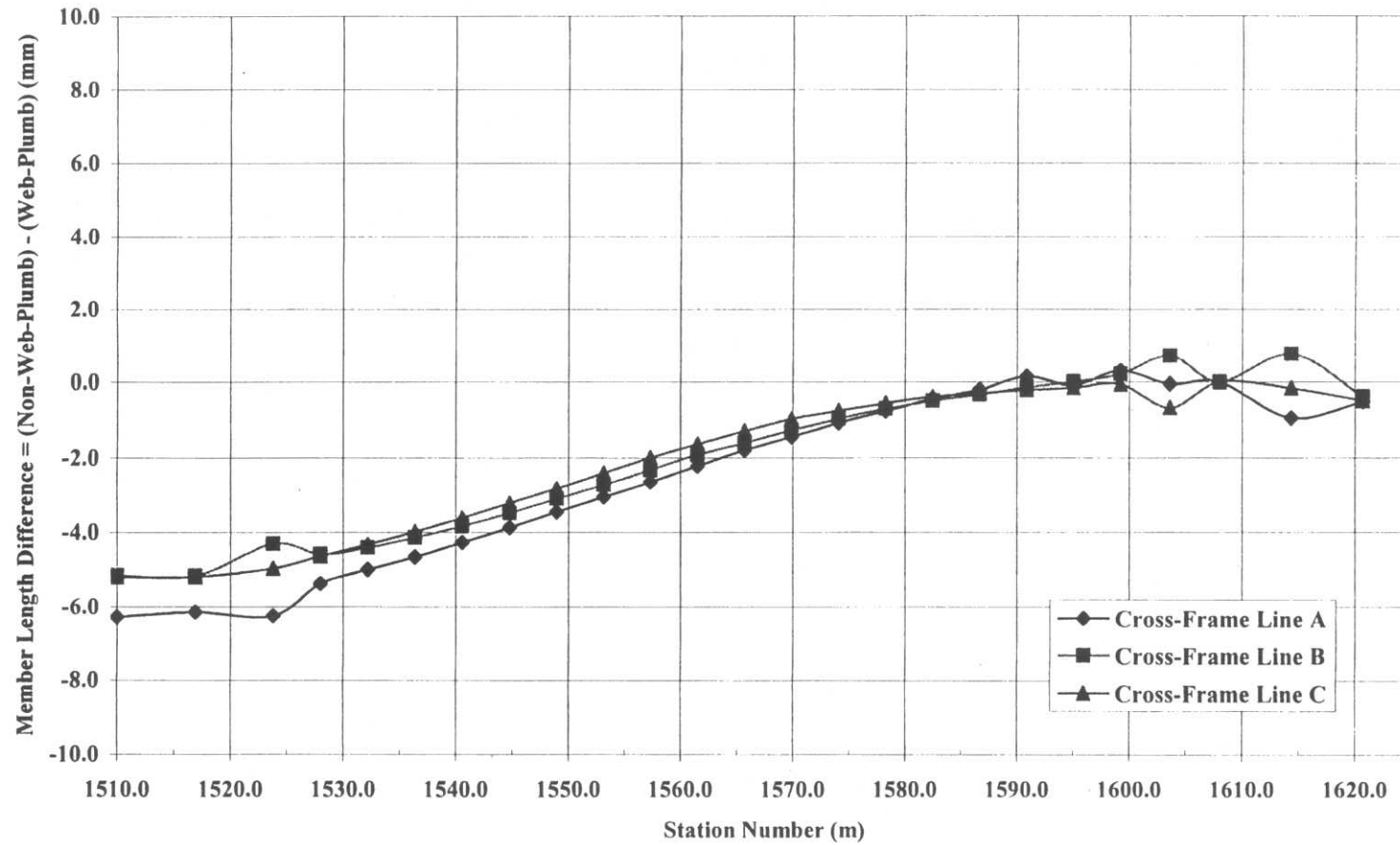


**Figure 154** Cross-frame top chord – Non-web plumb detail vs. web-plumb detail length difference

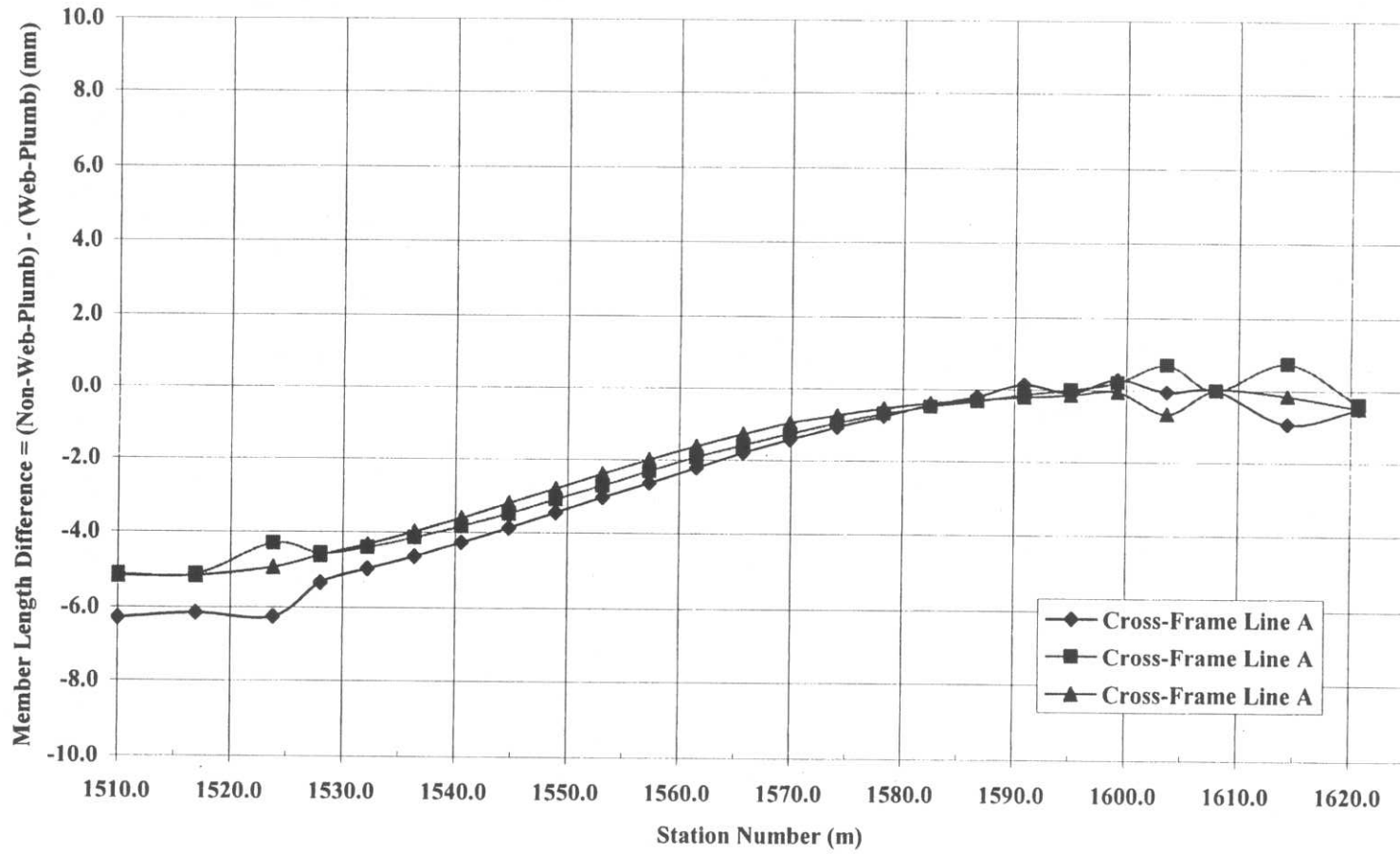


Figure 155 Cross-frame bottom chord – Non-web-plumb detail vs. web-plumb detail length difference

**8.1.3.2 Consequences of Results.** The use of inconsistent detailing results in large discrepancies concerning the length of the diagonal cross-frame members. By designing/detailing the girders and the cross-frames in the same no-load position, so that the girder webs are vertically plumb during the steel erection (using temporary supports), detailing inconsistencies do not develop.

However, if the girders are fabricated for the web-plumb position at no-load, and the cross-frames are detailed to fit girders in a non-web-plumb position at no-load, a detailing inconsistency occurs. Using the Ford City Bridge analytical model, the largest cross-frame connection gap that must be made up during erection is approximately 60mm (2.4in) due to either shorter or longer cross-frames. Therefore, due to the inconsistent detailing, the girders and the cross-frames would have to be forced into place during the steel erection of the bridge, since the girders are fabricated for one condition, and the cross-frames for another. Additional external forces would need to be applied during steel erection of the structure in order to bring the cross-frames and girders into alignment. In some cases, the additional forces to fit components may be acceptable, but in other cases the erection of the bridge may become complicated, or even impossible.

For a curved I-girder bridge fabricated inconsistently, it may be necessary to acquire larger capacity cranes to bring components into alignments, and/or additional jacking frames and temporary supports may be required. Predetermined construction costs assumed for a consistently detailed bridge, will increase in proportion to problems resulting from inconsistent detailing. In addition to increased steel erection costs, the girder elevations after steel erection may not be in the designed location, resulting in

design changes in the concrete deck thickness and haunch at each girder. As steel curved I-girder bridges are designed for smaller radii, deeper webs, longer spans, and so on; the problems emanating from inconsistent detailing will increase accordingly. It is very important the for bridge engineer pay very close attention to the issue of consistent detailing when designing curved I-girder bridges.

## **8.2 Ford City Bridge – Cross-Frames Incorrectly Detailed For Girder Web-Plumb Condition After Application of Concrete Deck Load Only**

The cross-frames of the Ford City Bridge were intended to be designed for the web-plumb condition after application of steel self-weight only, with the girders detailed for the web-plumb condition at no-load. This would have created the inconsistency in detailing that is presented in the previous section (section 8.1). However, a different discrepancy resulted because of an error during the fabrication of the cross-frames, in which incorrect data was used to detail the cross-frames. The vertical displacement due to concrete deck load only was used to calculate the cross-frame dimensions, instead of the vertical displacement due to steel self-weight only. Nonetheless, detailing the cross-frames for the web-plumb condition at application of concrete deck weight only, and the girders for the web-plumb condition at no-load, also creates a detailing inconsistency.

Using the finite element model of the entire Ford City Bridge, this section will examine the difference in cross-frame member lengths detailed for the concrete deck load case, and those detailed for girder web-plumbness at no-load. Additionally, the steel

elevations prior to concrete deck placement using the analytical model with cross-frames detailed for the web-plumb condition at no-load will be compared with the actual field-survey elevations of the Ford City Bridge.

### **8.2.1 Difference in Cross-Frame Member Lengths Due to Incorrect Detailing**

The incorrectly detailed cross-frames are detailed using the same basic technique as described in Section 8.1.2 (Cross-frames detailed for girder web-out-of-plumb at the no-load condition), but with two exceptions. First, the concrete deck load weight is applied to the structure in order to obtain the displaced position (instead of the steel self-weight). In other words the concrete deck “gravity is turned on,” and the steel self-weight “gravity is turned off.” The second difference is the typical inconsistency detailing discrepancy; in which the girders are designed to be at the web-plumb position at the no-load condition, while cross-frames are detailed for a different load condition other than no-load.

To show that a considerable difference in cross-frame member lengths exists for this current detailing inconsistency, the cross-frame dimensions in the Ford City Bridge analytical model are compared for: (1) girder webs are plumb at the no-load condition (at the beginning of construction); (2) girder webs are plumb when the concrete deck load is theoretically applied. Table 22 displays the calculated cross-frame member lengths for both detailing techniques, for cross-frames 10A through 20A. The cross-frame member dimensions for all cross-frames can be found in Appendix D of the current research.

**Table 22** Cross-frames 10A - 20A - Dimensions for web-plumb at no-load and web-plumb for concrete deck load

Cross-Frame	Detailed Condition	Cross-Frame Member Lengths (mm)			
		F	M	Top Chord	Bottom Chord
10A	Web-Plumb at No-Load	5574.43	5660.82	4100.49	4100.49
	Web-Non-Plumb at No-Load	5599.21	5632.30	4097.73	4097.73
11A	Web-Plumb at No-Load	5565.76	5669.67	4100.70	4100.70
	Web-Non-Plumb at No-Load	5593.14	5638.96	4098.17	4098.17
12A	Web-Plumb at No-Load	5558.67	5676.91	4100.91	4100.91
	Web-Non-Plumb at No-Load	5588.10	5644.57	4098.59	4098.59
13A	Web-Plumb at No-Load	5553.18	5682.55	4101.09	4101.09
	Web-Non-Plumb at No-Load	5583.98	5649.25	4099.01	4099.01
14A	Web-Plumb at No-Load	5549.28	5686.55	4101.23	4101.23
	Web-Non-Plumb at No-Load	5580.76	5652.98	4099.38	4099.38
15A	Web-Plumb at No-Load	5546.96	5688.94	4101.32	4101.32
	Web-Non-Plumb at No-Load	5578.49	5655.69	4099.71	4099.71
16A	Web-Plumb at No-Load	5546.20	5689.72	4101.34	4101.34
	Web-Non-Plumb at No-Load	5577.04	5657.55	4100.00	4100.00
17A	Web-Plumb at No-Load	5646.96	5688.93	4101.32	4101.32
	Web-Non-Plumb at No-Load	5576.62	5658.31	4100.24	4100.24
18A	Web-Plumb at No-Load	5549.22	5686.61	4101.23	4101.23
	Web-Non-Plumb at No-Load	5549.22	5686.61	4101.23	4101.23
19A	Web-Plumb at No-Load	5552.92	5682.81	4101.10	4101.10
	Web-Non-Plumb at No-Load	5578.55	5656.75	4100.48	4100.48
20A	Web-Plumb at No-Load	5557.98	5677.62	4100.93	4100.93
	Web-Non-Plumb at No-Load	5580.94	5654.46	4100.52	4100.52

The difference in cross-frame lengths due to detailing the cross-frames for web-plumbness at concrete deck load only, and for detailing the cross-frames for web-plumbness at the no-load condition is proportional to the difference in cross-frame lengths due to detailing the cross-frames for web-plumbness; at steel self-weight only, and detailing for web-plumbness at the no-load condition (section 8.1.2). Figure 156 shows a representation of the difference in cross-frame member lengths that occurs due to the concrete deck load application (figure 21 is actually for steel self-weight only application). Again the diagonal members 'F' and 'M' have the largest difference in length, in which typically member 'F' increases in length and member 'M' decreases in length from web-plumbness at no-load to web-plumbness at concrete deck load.

Figures 157, 158, 159 and 160 show the measured differences in cross-frame member lengths throughout the curved span of the Ford City Bridge. Figure 157 shows that the maximum length difference of member 'F' occurs at midspan of the curved section, at approximately station 1+555, which is at cross-frame 14; this is the identical location in which the largest difference for the web-plumb at steel self-weight condition versus web-plumb at no-load condition occurs. As shown in figure 158, the largest difference in length of member 'M' is at the midspan of the curved section as well. The maximum difference in length of members 'F' and 'M' of cross-frame 14 is +/- 32mm (1.25in), respectively. Detailing the cross-frames to the web-plumb condition at application of concrete deck load, instead of detailing to the web-plumb condition at no-load, increases the length of member 'F' by 32mm (1.25in); while the length of member 'M' decreases by 32mm (1.25in).

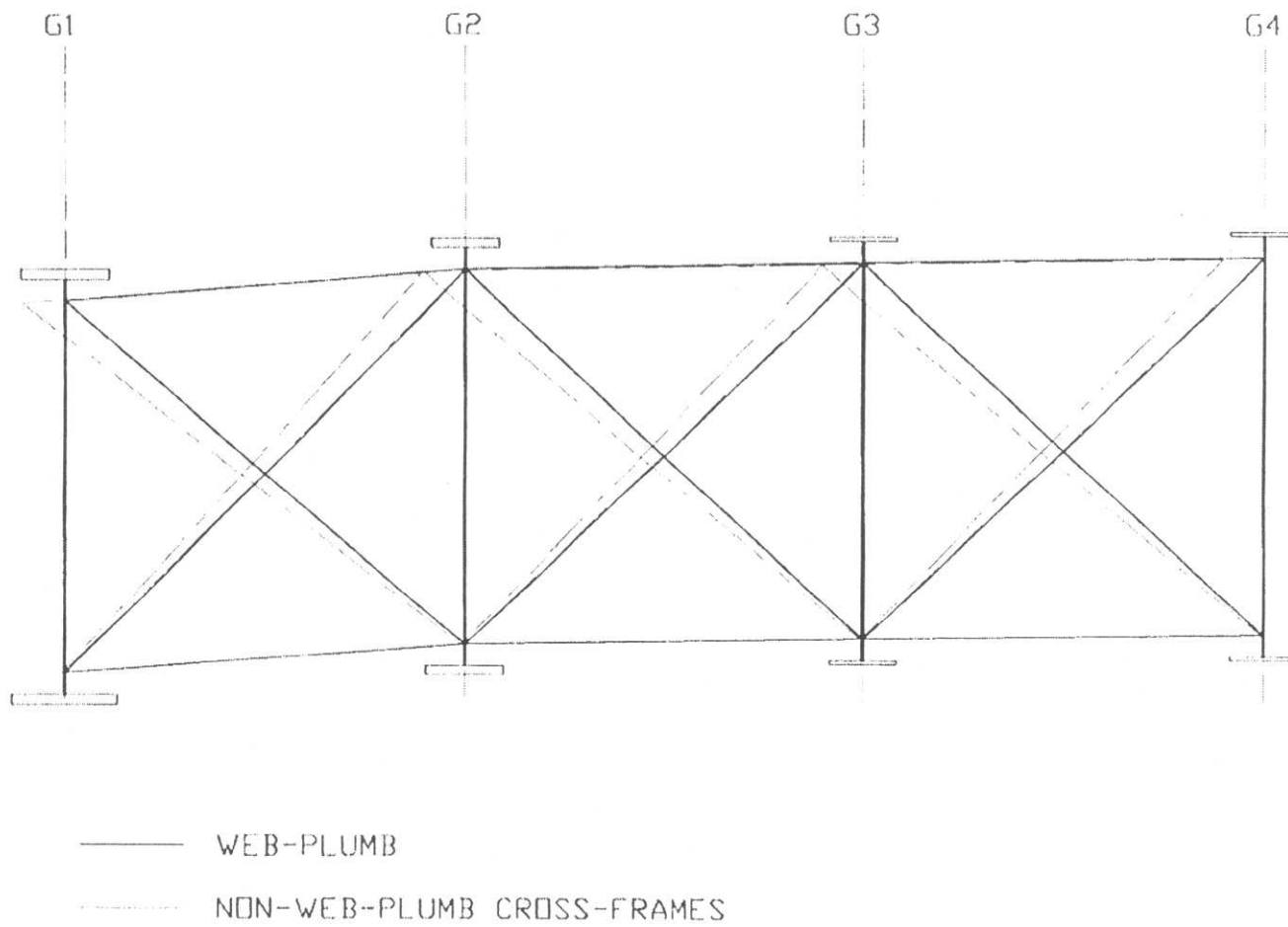


**Figure 156** Representative cross-frame member length difference due to incorrect detailing (application of course concrete deck load)

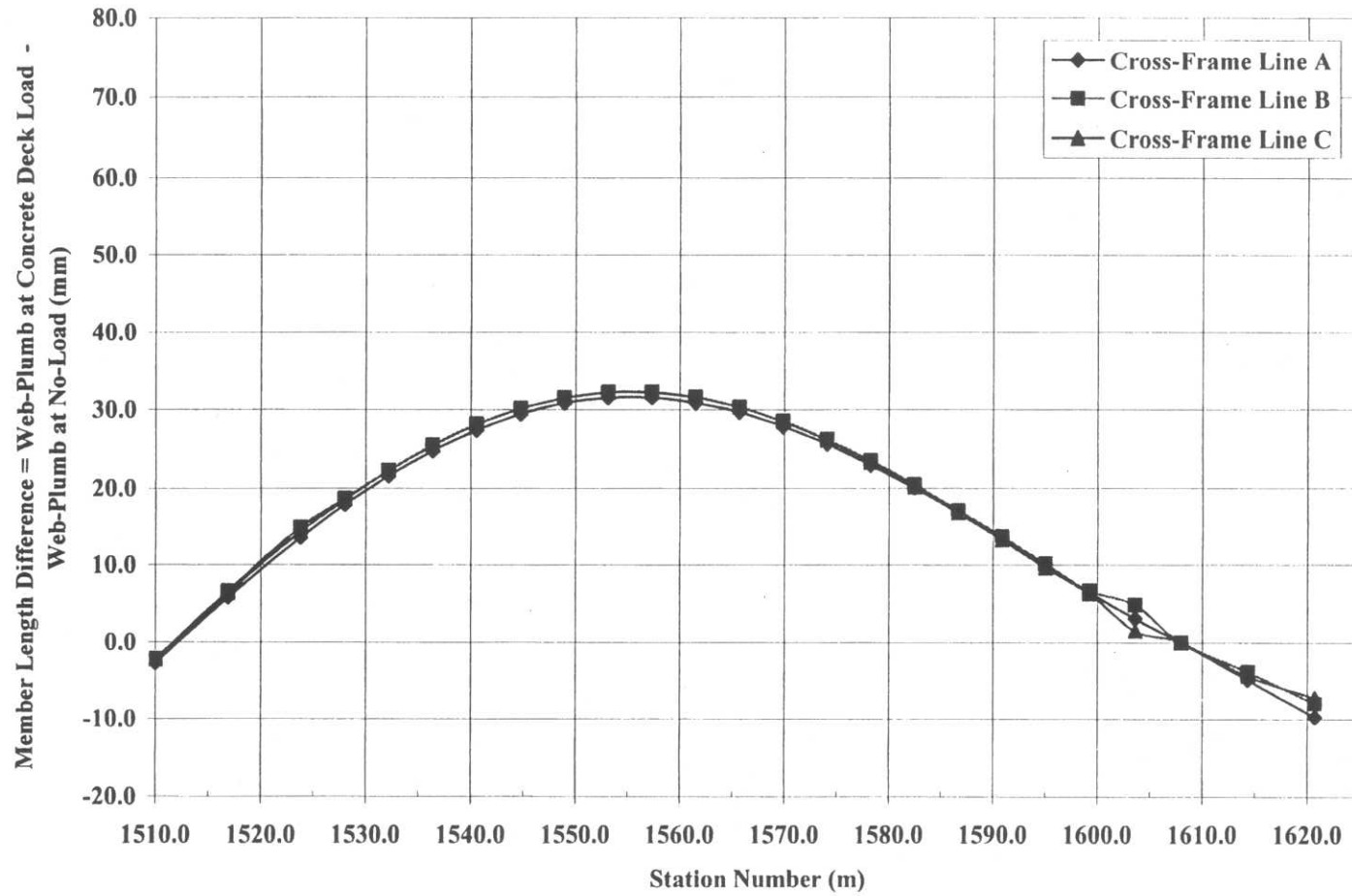


**Figure 157** Cross-frame member 'F' – Web-plumb at concrete deck load detail vs. web-plumb at no-plumb at no-load detail length difference

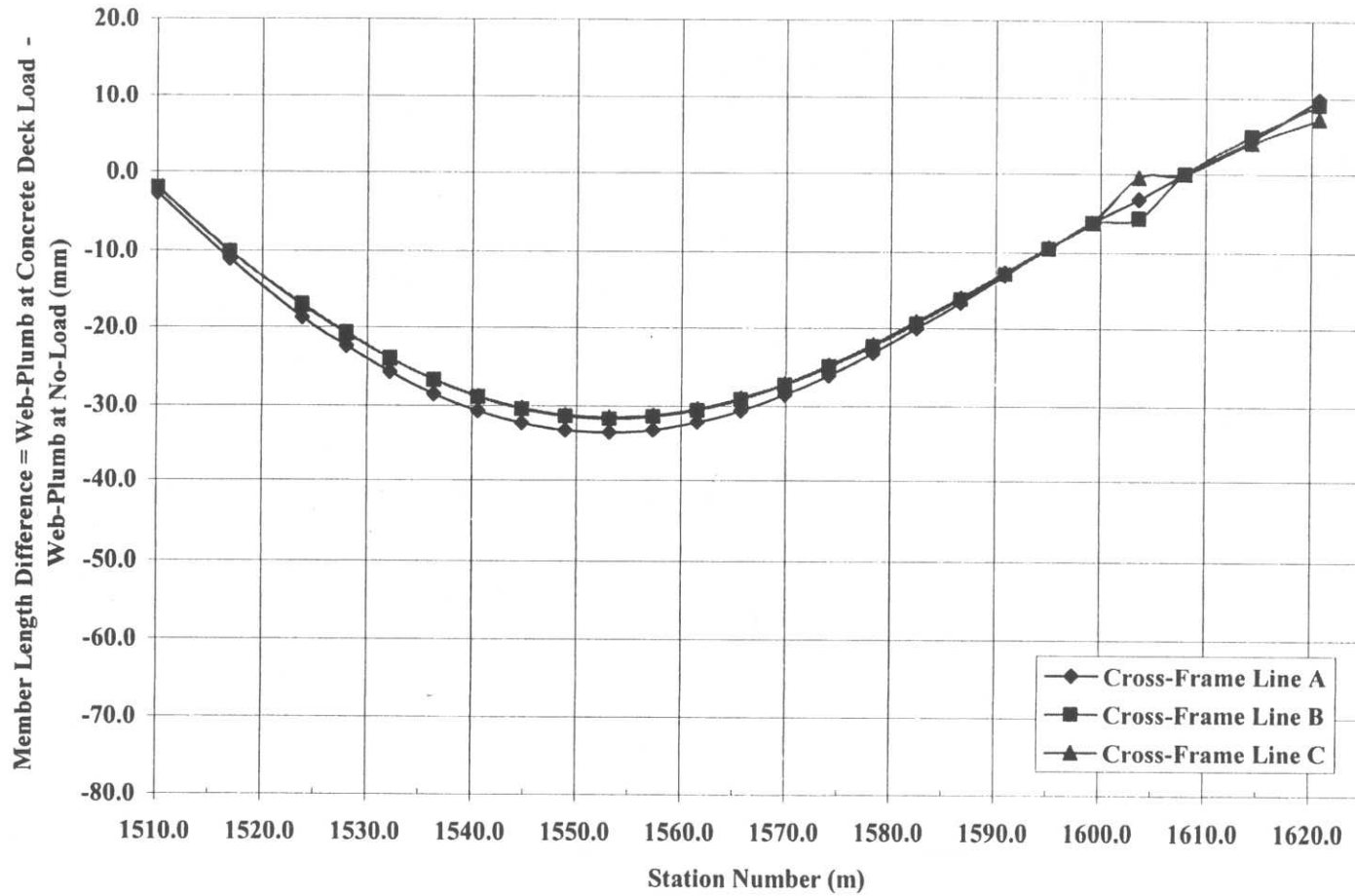


**Figure 158** Cross-frame member 'M' – Web-plumb at concrete deck load detail vs. web-plumb at no-load detail length difference

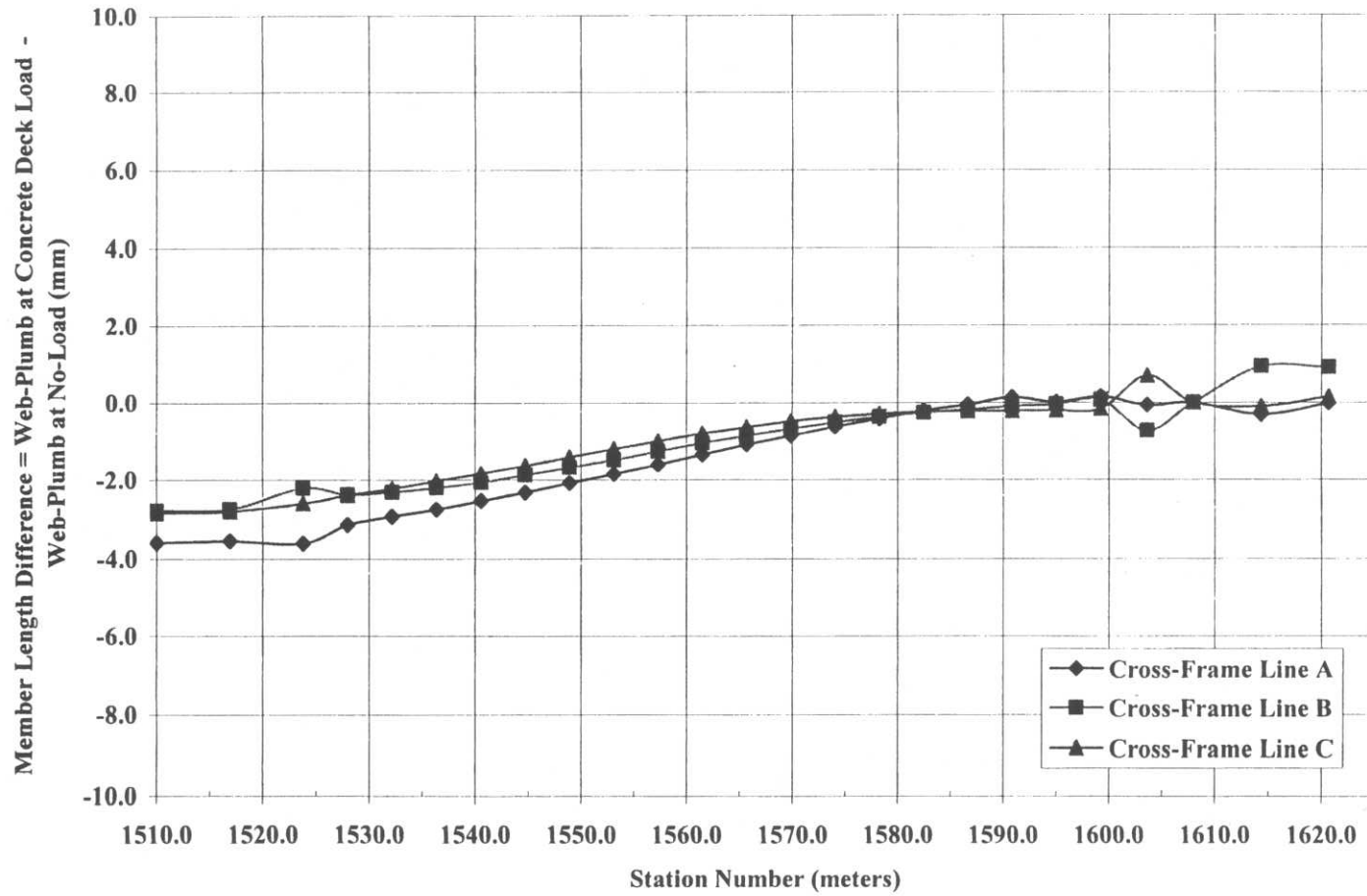


**Figure 159** Cross-frame top chord – Web-plumb at concrete deck load detail vs. web-plumb at no-load detail length difference

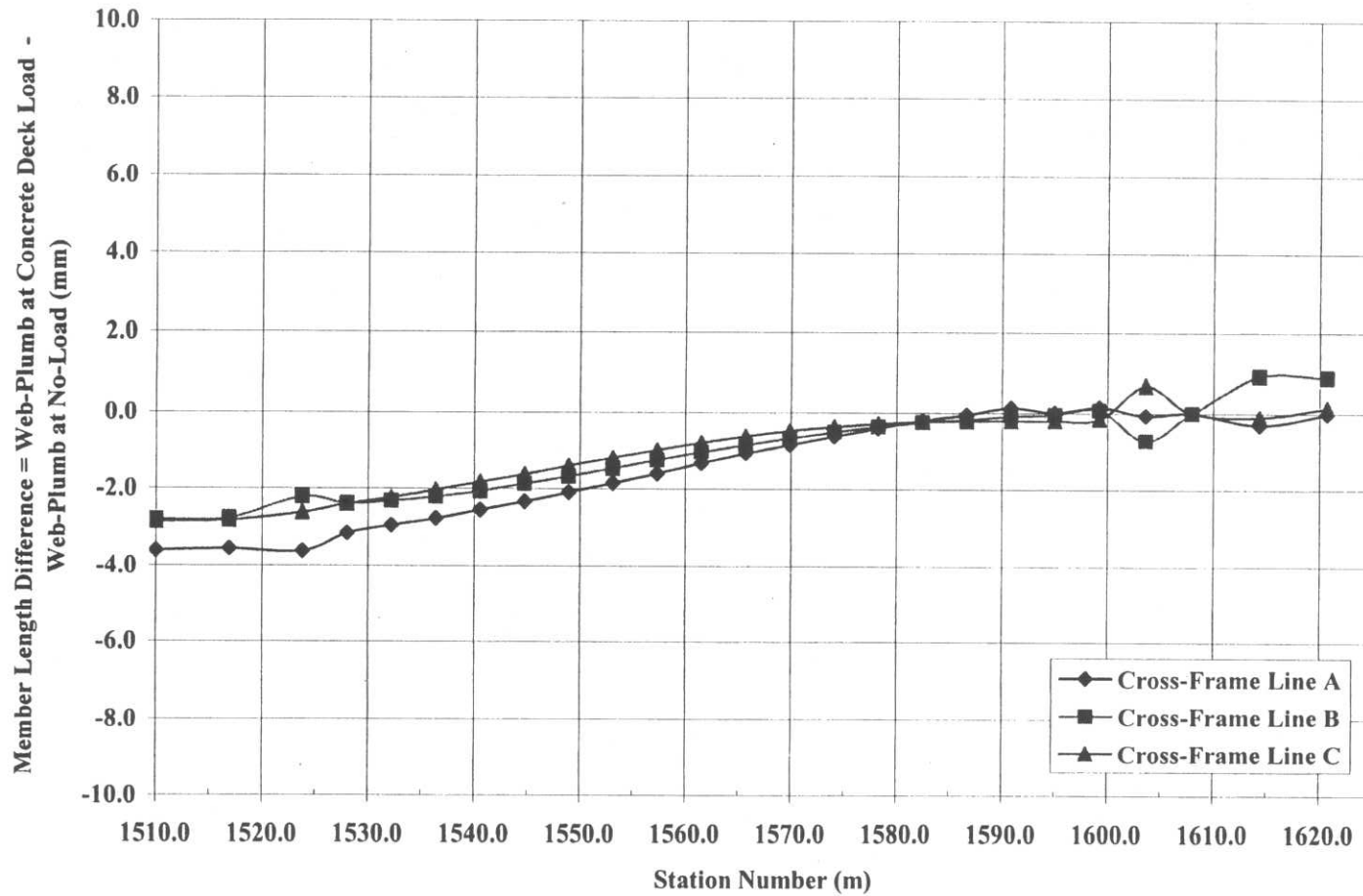


**Figure 160** Cross-frame bottom chord – Web-plumb at concrete deck load detail vs. web-plumb at no-load detail length difference

As shown in figures 159 and 160, the change in length for the top and bottom chords, respectively, are minimal due to the constant out-of-plane (lateral) displacement of the bridge cross-section.

The use of the incorrect load case to detail the cross-frames of the Ford City Bridge results in somewhat large differences in diagonal member lengths. According to the field record of construction, difficulties did arise during the erection of the bridge, related to girder misalignments (see section 4.0 of the current study, which details the “as-built” bridge erection sequence). This gives evidence to the fact that construction difficulties in curved steel I-girder bridges can result from incorrectly detailing, and/or inconsistently detailing girders and cross-frames.

However, the noted “as-built” construction difficulties could have been worse, given the fact the cross-frames were incorrectly detailed to the web-plumb condition at concrete deck load, instead of being inconsistently detailed to the web-plumb condition at the application of steel self-weight only. From the preceding analysis, 32mm (1.25in) cross-frame misfits, instead of 60mm (2.4 in) misfits due to detailing to web-plumbness at steel self-weight only, are predicted. This corroborates data obtained from interviews conducted as part of the current study (see Appendix A), in which 38mm cross-frame misfits were recorded in the field during bridge erection.

### **8.2.2 Comparison of Field Surveyed Elevations of Steel Superstructure Prior to Concrete Deck Placement with Finite Element Model Predictions**

To further illustrate the fact that incorrect detailing can result in bridge erection problems, the steel elevations prior to concrete deck placement using the analytical model with cross-frames detailed for the web-plumb condition at no-load will be compared with the actual field-survey elevations of the Ford City Bridge. The cross-frame for the actual Ford City Bridge are incorrectly detailed so that they fit the girders in a web-plumb position after the theoretical application of the concrete deck load. However, the girders are detailed for the web-plumb condition at the no-load stress state.

Differences in the predicted elevations via the finite element model and the field-surveyed elevations are observed. Elevation profiles for each girder are provided in Appendix D of the current study. The largest difference for each girder occurs near the midspan of the curved section, at approximately station 1+553. The following discrepancies are noted at this location:

1. Girder G1 – Field-surveyed elevation is approximately 25mm (1in) higher than the predicted elevation using the finite element model.
2. Girder G2 – Field-surveyed elevation is approximately 25mm (1in) higher than the predicted elevation using the finite element model.
3. Girder G3 – Field-surveyed elevation is approximately 76mm (3in) higher than the predicted elevation using the finite element model.

4. Girder G4 – Field-surveyed elevation is approximately 100mm (4in) higher than the predicted elevation using the finite element model (shown in figure 161).

Once again, these discrepancies show that incorrectly detailing cross-frame members can lead to further problems in the constructed bridge. Due to the fact that the girders are higher than what is predicted in the design of the bridge, design changes concerning the concrete deck and haunch would be required in order to provide the required deck thickness. Of course, if the cross-frames were detailed for the web-plumb condition after application of steel self-weight only, the deck placement conditions could have been worse due to previously discussed increased cross-frame misfit dimensions. Cross-frame misfits for the concrete load application detailing are only 32mm (1.25in), instead of 60mm (2.4in) for detailing with steel self-weight. These cross-frame misalignments due to inconsistent, and/or incorrect detailing are avoidable by using consistent detailing techniques, i.e.: (1) detail the girders and cross-frames to be in the web-plumb condition at the no-load stress state and permit the bridge to rotate to an out-of-plumb position after load application; or (2) detail the girders and cross-frames such that the girder webs are out-of-plumb at the no-load condition, and rotate to a vertically plumb position after application of steel self-weight (after removal of temporary supports).

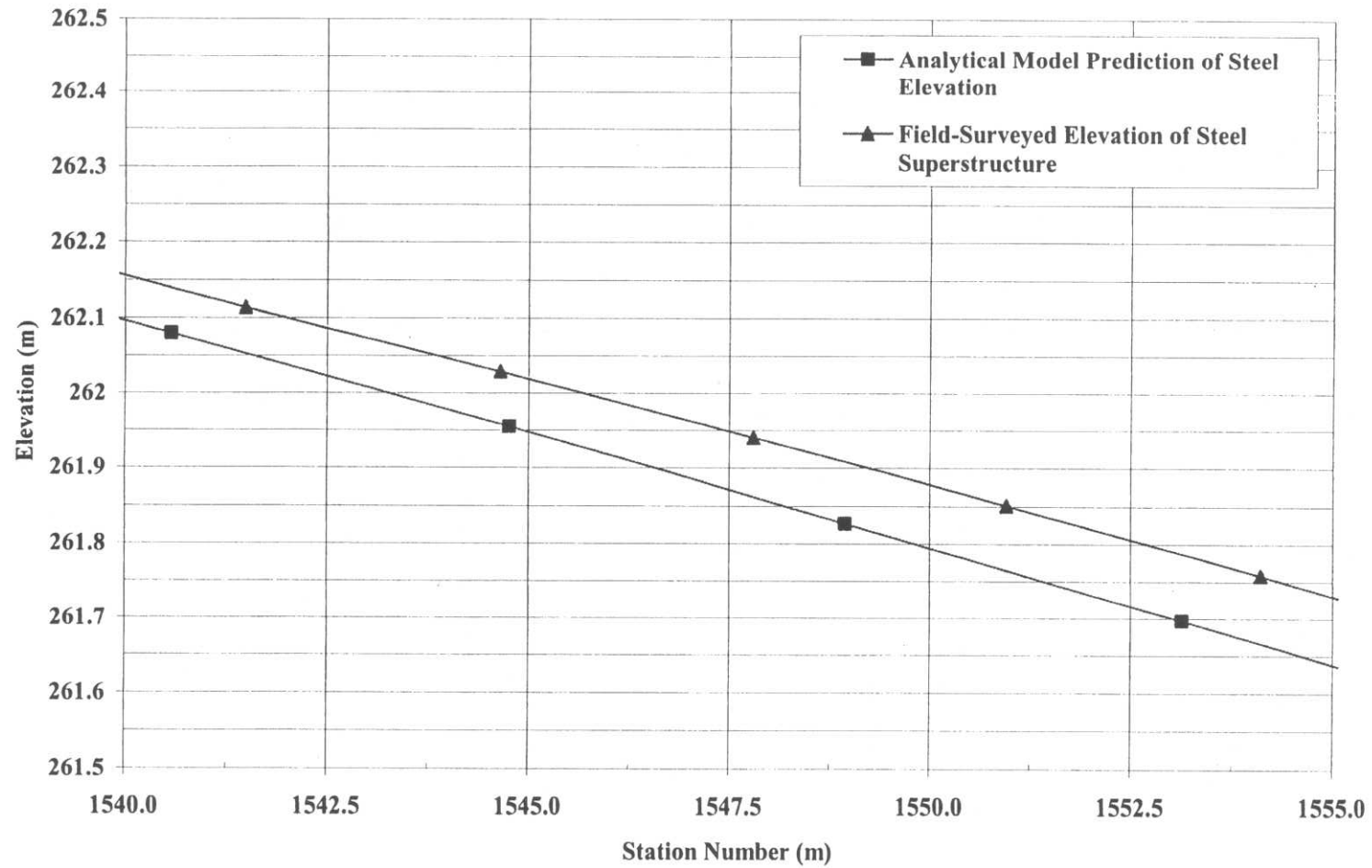


**Figure 161** G4 – Elevation profile, STA 1+540 to 1+555; Analytical model versus field-surveyed data

## 9.0 CONCLUSIONS

This study has presented examples of difficulties that often occur during the construction of horizontally curved steel I-girder bridges. These problems can result from unwanted displacements, stresses, and temporary support reactions, which are unaccounted for by the designer. Additional construction difficulties can result from the inconsistent detailing of cross-frame members which occurs when the design engineer, the bridge erector, or the owner desires to have the girder webs vertically plumb before an after bridge erection. A verified nonlinear finite element model of the Ford City Veterans Bridge is created to investigate these horizontally curved steel I-girder construction issues.

The concept of inconsistent cross-frame detailing has been shown to be an extremely critical issue in relation to erection of curved I-girder bridges. If the girders are fabricated to fit cross-frames in a girder web-plumb position at the no-load condition; but the cross-frames are detailed to connect girders in a web-plumb position after load application, steel self-weight for instance, an inconsistency develops. In the case of the Ford City Bridge, it is shown that if this concept of inconsistent detailing had occurred, some cross-frame members would be too long or too short by more than two inches. This length difference can lead to extreme problems with girder and cross-frame alignments, resulting in the need for additional, and sometimes significant, forces to be applied to the structure to in order to bring components into alignment. Therefore, due to this detailing inconsistency, additional construction costs would be incurred for larger capacity cranes,

additional shoring, and/or additional jacking devices. In some cases, the additional forces to fit components may be acceptable, but the erection of the bridge might also become extremely complicated, or even impossible. Currently there is no guidance given in design specifications or in the literature for bridge engineers or bridge detailers concerning the issue of consistent detailing of cross-frame members in curved I-girder bridges.

In order to prevent the problem of inconsistent detailing, two distinct, non-interchangeable methods are presented in order to determine cross-frame member lengths in curved I-girder bridges:

1. The girders and cross-frames can be fabricated to the girder web-plumb position, at the no-load condition. In order to maintain the no-load condition, temporary supports (falsework) may be required during the bridge erection, in order to prevent unwanted displacements, rotations, stresses, and support reactions. Upon the removal of the temporary supports, the steel structure will deflect, and will no longer remain in the web-plumb position. The amount of rotation and displacement that occurs after the support removal is a serviceability issue that must be addressed by the design engineer or the bridge owner.
2. The girders and cross-frames can be detailed such that the girder webs are out-of-plumb at the no-load condition (at the beginning of construction). Again temporary supports would be required as in the previous detailing technique. Once the temporary supports are removed the bridge girders will rotate as a rigid body to a vertically web-plumb position due the application of the structure's self-

weight. However, this method of erection and analysis for horizontally curved I-girders is not reported in the literature, and it would require additional camber information be shown in the design drawings of the structure.

The cross-frames for the actual Ford City Bridge were detailed incorrectly. The cross-frames were detailed so that the girder webs were plumb after the application of concrete deck load, which is never a possibility in the erection of a bridge, due to the obvious effects of the self-weight of the steel structure. Detailing the cross-frames for the web-plumb condition at application of concrete deck weight only, and the girders for the web-plumb condition at no-load creates a significant inconsistency. The current study provides comparisons relating cross-frame lengths detailed for the actual bridge with cross-frame lengths determined for the web-plumb position at the no-load condition versus other, inconsistent cases. Using the finite element model of the Ford City Bridge it was shown that cross-frame misfits in the order of 32mm could be expected (38mm from actual field records); in some cases support reactions do not follow typical load distribution; and final steel elevations could deviate significantly from intended values, thus causing design changes related to the concrete deck and haunch thicknesses.

The “as-built” and “planned” erection sequences are recreated using the finite element model of the Ford City Bridge, employing cross-frames detailed for the web-plumb position at the no-load condition. It is analytically shown that, as a result of consistent detailing, girder displacements and stresses during construction are minimal, and support reactions often follow a typical load distribution path. From the field record

of the construction of the Ford City Bridge (and interviews conducted as part of this study), which employed the incorrectly detailed cross-frames, it was apparent that girder misalignment problems, and unwanted displacements occurred, which required additional forces that were not considered in the design of the structure. This demonstrates the fact that inconsistent detailing can lead to extreme problems during construction.

This study has shown that bridge engineers must pay very close attention to the issue of consistent detailing when designing horizontally curved steel I-girder bridges. One of the objectives of this research has been to promote awareness of the issue of consistent/inconsistent/incorrect cross-frame and girder detailing as it relates to the design and erection of curved I-girder bridges.

### **9.1 Recommended Future Research**

One of the main goals in any future research endeavor in the area of horizontally curved steel I-girder construction, should be to determine at what stage of construction it is most advantageous to have the girder webs vertically plumb (i.e. at no-load, at steel self-weight load, or at steel self-weight load plus concrete deck load).

Further research is required with regard to detailing the girders and cross-frames such that the girder webs are out-of-plumb at the no-load condition, and rotate to the vertically web-plumb position upon load application (removal of temporary supports). Currently this method of erection and analysis for horizontally curved I-girders is not reported in the literature, and it would require that further design analyses be

accomplished, and require that additional camber information be provided in the design drawings of the structure. Further analytical, and possibly experimental investigations concerning these detailing and erection methods need to be carried out.

The additional forces required to bring girder and cross-frame components into alignment when inconsistent detailing occurs needs to be investigated further.

Further studies of erection sequences for bridges of different radii, span lengths, girder spacing, girder depth, and cross-frame spacing could prove to be very useful, and possibly evolve into codified guidelines for the erection of horizontally curved I-girder bridges. Also, further “in-field” construction studies of curved I-girder bridges could be useful so that other difficulties and problems might be recorded, and subsequently used to aid in the erection of future bridges of this type.

## **APPENDIX A**

## APPENDIX A

### A.1 NOTES FROM PERSONAL MEETING WITH MICHAEL BAKER ENGINEERS CONCERNING DESIGN AND CONSTRUCTION – AUGUST 22, 2000

#### A.1.1 Michael Baker Engineers

Mr. William Hess, P.E.; Structural Engineer

Mr. Michael Bonkovich, P.E.; Senior Structural Engineer

#### A.1.2 Cambering

- The dimension from top of girder web to top of deck is always fixed.
- Cambering is designed for completed bridge, not for any certain erection stages.
- Decking – camber is not for segmental deck pour, but for monolithic deck pour.
- Per DM4 Manual, camber is to be based on a monolithic deck pour.
- Steel elevations before deck placement were not achieved as planned.

#### A.1.3 Steel Erection

- Assumed a fully supported (no load) case.
- HDR came to Michael Baker with an erection sequence, Baker performed the “number crunching.”

#### A.1.4 Fabrication

- Cross-frames were to be detailed for full load case, not for any particular erection sequence, or the no load case.
- “No load” condition used for girder fabrication, due to the use of falsework.
- For curved girders, maximum out-of plumbness (after load application) is obtained when “no-load” condition is used to detail the girders and cross-frames.
- Ford City Bridge
  - No slotted holes were to be used in the curved section, standard sized holes only.

- No industry standards exist for detailing of X-Frames.
- Inconsistencies exist between what is designed, and what can actually be fabricated.
- Cross-frames should be detailed so as to be installed in a stress free state.
- Pre-twisting of girder web can not be built into fabrication, too much work and time required.
- In regard to detailing; what is easiest for erection, is worst case for fabrication.

#### **A.1.5 Detailing**

- Detail for entire assembled bridge cross section (all 4 girders), not just one or two girders erected at a time.
- Twisting of girders is always overlooked.
- In order to design individual cross-frames for twisting – would lead to more erection problems and more litigation, since all cross-frames would need to be somewhat different.
- 38min misfits with cross-frames in some cases were recorded in the Ford City Bridge erection.
- Cross-frames were actually detailed for concrete and misc. loads for Ford City Bridge, instead of the steel dead load only.

#### **A.1.6 Lateral Bracing**

- Detail and cost nightmare for fabricator.
- “Beef” up the flange or have deck provide all lateral bracing restraint, in order to not have to use lateral bracing.
- Lateral bracing was implemented in the finite element model Mr. Bill Hess used.
- Lateral bracing had the most impact in span 3.

#### **A.1.7 Reactions in Field**

- Can be measured in the field using load cells.

#### **A.1.8 Thermal Conditions**

- 68-70 degrees – was the assumed temperature used for design.

**A.1.9 Finite Element Modeling**

- Webs - 4 noded shell elements.
- Flanges – 2 noded beam elements.
- Both linear and geometric non-linear analysis accomplished; material non-linearity was ignored.
- Residual stresses were not accounted for.

**A.1.10 Miscellaneous Data**

- Curve cut girder flanges.
- No pick points were specified for the girders.

## **A.2 Notes from Meeting with Pennsylvania Department of Transportation PennDOT Personnel For Field Construction – December 15<sup>th</sup>, 2000**

### **A.2.1 PennDOT Personnel**

Mr. Steve Guidel

### **A.2.2 Curved Section “Drop-In” Section (Section #3)**

- At field splice #2 had problems with connecting “drop-in” girders G2 and G3. Problem was not due to the previously placed cantilever section girders rotating (section #2), but due to possible vertical deflection of cantilevered section #2. There was a problem of closure at the bottom of the girders at field splice #2, for both “drop-in” girders G2 and G3.
- In the field when field splice #3 was being accomplished, also had problems making connections of the lower flanges. It is possible that the use-of “built-up” plates, due to flange transition in thickness at the field splice, also aided in causing the fit-up problems. There were actually four plates in which pins must be placed through, at field splice #3, for section #4 girders.
- Two cranes were used to hold the first drop-in girder, G3, until the second drop in girder, G2, was erected and connected to G3 via the cross frames.

### **A.2.3 Entire Curved Section of Bridge**

- The two center girders, G2 and G3, always were completely tightened at their connections (field splices and cross-frame connections), before fascia girders, G1 and G4, were erected and connected to the center girders.
- Field splices were always completely tightened before another girder was erected, for any girder line.
- After construction was completed, it was determined that girders were possibly 3 to 4 inches higher than the expected final elevations.

### **A.2.4 Lateral Bracing**

- Was placed after all girders and cross-frames were connected in the entire bridge.

**A.2.5 Curved Girder Pick Points Used For Lifting**

- Used lifting lugs and clamps to lift girders.
- Lifting lug locations were already predetermined, and drilled and installed, upon arrival to construction site.
- Clamps used for lifting girders of section #1, and the drop-in section, section #3.
- Lifting lugs used for lifting girders of section #2 and section #4.

**A.2.6 Miscellaneous Details**

- There were no major problems installing the cross frames for the curved section.
- Falsework #2A was the first falsework that was removed.
- Future guideline possibility – what stage of construction to have the girder webs vertical.
- Valuable information was received concerning final steel elevations, prior to placement of the concrete deck, and photos taken during steel erection.

## **APPENDIX B**

## APPENDIX B

### B.1 ABAQUS FINITE ELEMENT MODELING TERMINOLOGY (ABAQUS 2001)

#### B.1.1 ELEMENTS

**B.1.1.1 S4R Element.** The ABAQUS S4R element is a 4-node doubly curved general-purpose shell element, with reduced integration, that is shear deformable. These elements are used for the flanges, webs, longitudinal stiffeners, and transverse stiffeners in the Ford City Bridge finite element model. Each element set of S4R elements are given its respective properties, such as shell thickness and material properties using the \*SHELL SECTION option.

**B.1.1.2 B32 Element.** The ABAQUS B32 element is a 3 node quadratic beam in space, and allows for transverse shear deformation. These elements are used to model the straight spans of the Ford City Bridge. Using the \*BEAM GENERAL SECTION option, the cross-sectional area, and the moments of inertia  $I_{xx}$  and  $I_{yy}$  for each girder section are input into the finite element model.

**B.1.1.3 B31 Element.** The ABAQUS B31 element is a 2 node linear beam in space, and allows for transverse shear deformation. These elements are used to model the cross-frame members of the Ford City Bridge. Using the \*BEAM GENERAL SECTION option, the cross-sectional area, and the moments of inertia  $I_{xx}$  and  $I_{yy}$  for each girder section are input into the finite element model.

**B.1.1.4 RB3D2 Element.** The ABAQUS RB3D2 element is a three dimensional, 2 node rigid beam. The \*RIGID BODY option is used to assign a unit area to the RB3D2 elements. These elements are placed along the flange and web edges of the section 4 girders, which are modeled with shell elements. This location is where the beam elements of the straight span girders attach to the neutral axis of the girders at the end of the curved span. Mesh conformity at the inter element boundary between the shell and beam elements is accomplished via the plane section hypothesis being enforced at the transition interface using the RB3D2 elements.

**B.1.1.5 GAPUNI Gap Elements.** The ABAQUS GAPUNI element is a unidirectional gap element which models contact between two nodes when the contact direction is fixed in space. This gap element allows for the nodes to be in contact or separated with respect to the specified direction of the gap element. The gap element is defined by specifying the two nodes forming the gap and an initial length of the space between the nodes. In the Ford City Bridge finite element model, the unidirectional GAP elements are used at

all of the support locations, which in turn permit the girders to “lift-off” of their supports during the analysis.

### B.1.2 Additional ABAQUS Terminology

**B.1.2.1 MPC TIE.** The multi-point constraint (MPC) TIE is used in order to make all active degrees of freedom equal at the two nodes specified. The MPC TIE constraint is used to enforce on a slave node all translations and rotations of the master node. The use of the MPC TIE constraint is a simplified approach to modeling the field-splices and the cross-frame/girder connections in the finite element model of the Ford City Bridge.

**B.1.2.2 MPC LINEAR.** The MPC LINEAR option constrains each degree of freedom of one node,  $p$ , to be linearly interpolated from the corresponding degrees of freedom at two nodes,  $a$  and  $b$ , of a different mesh. See figure B-1 for details. The LINEAR constraint is used to simplify the modeling of the field-splice, and cross-frame/girder connections.

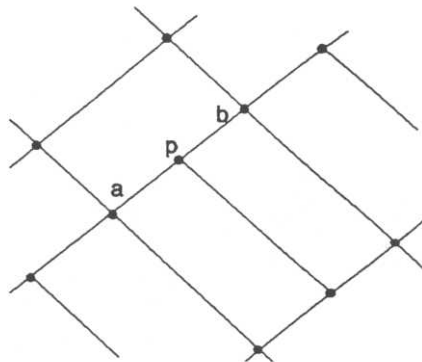


**Figure B-1 MPC LINEAR constraint (ABAQUS 2001)**

**B.1.2.3 MODEL CHANGE.** The ABAQUS MODEL CHANGE command allows for the removal and reactivation of elements during an analysis. The MODEL CHANGE command is used in the Ford City Bridge finite element model in order deactivate the girders that are yet to be erected for each erection stage.

## **APPENDIX C**

## APPENDIX C

### C.1 “As-built” Erection Sequence Analytical Results

Results are presented for the “as-built” (“in-field”) erection sequence analytical studies, construction stages 1 through 16, and the removal of Falseworks 1 and 2A upon completion of the curved span. For each construction stage the following five figures are included:

1. Figure ‘1’ - Plan view of finite element model.
2. Figure ‘2’ - Field-splice location deflections and support reactions summary.
3. Figure ‘3’ - Out-of-plane (radial) displacement, centerline of bottom flange.
4. Figure ‘4’ - Out-of-plane (radial) displacement, centerline of top flange.
5. Figure ‘5’ - Vertical displacement, centerline of bottom flange.

For figures ‘3’ and ‘4,’ “-“ (negative) is displacement inward of curve, and “+” (positive) is displacement outward of curve.

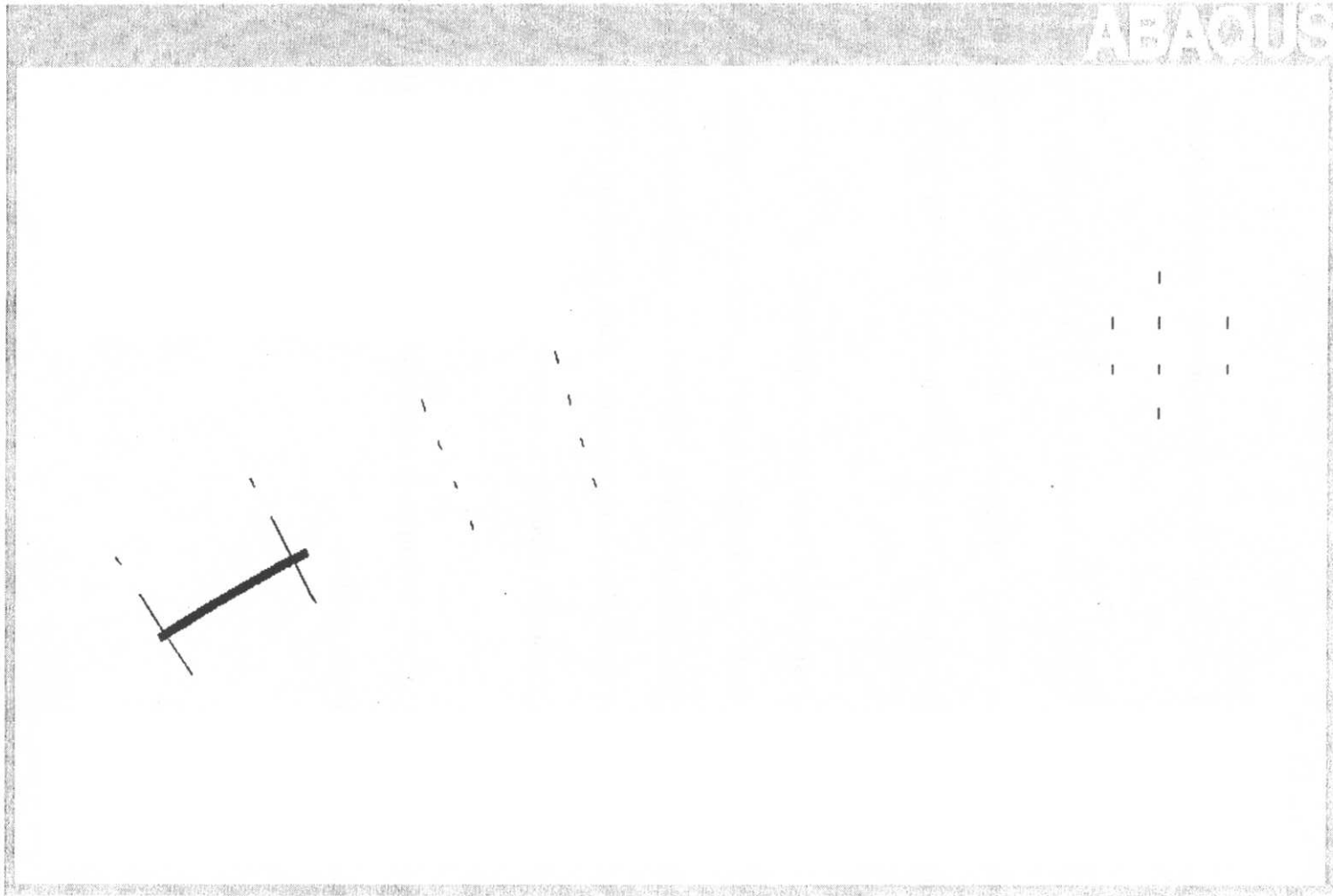


**Figure C-1** Construction stage 1 - Plan view of finite element model

**Deflections - Out-of-Plane (Radial) (mm)**

	Abutment 1	Field Splice 1 Section 1	Field Splice 1 Section 2	Field Splice 2 Section 2	Field Splice 2 Section 3	Field Splice 3 Section 3	Field Splice 3 Section 4	Field Splice 4 Section 4
G1- Bottom Flange								
G1- Top Flange								
G2 - Bottom Flange								
G2 - Top Flange								
G3 - Bottom Flange	0.0528	0.2296						
G3 - Top Flange	-0.0402	-0.2268						

G4 - Bottom flange  
G4 - Top Flange

**Deflections - Vertical (mm)**

	Abutment 1	Field Splice 1 Section 1	Field Splice 1 Section 2	Field Splice 2 Section 2	Field Splice 2 Section 3	Field Splice 3 Section 3	Field Splice 3 Section 4	Field Splice 4 Section 4
G1- Bottom Flange								
G1- Top Flange								
G2 - Bottom Flange								
G2 - Top Flange								
G3 - Bottom Flange	0.0081	0.0208						
G3 - Top Flange	-0.0056	0.0180						

G4 - Bottom flange  
G4 - Top Flange

**Vertical - Support Reactions (kN)**

	Abutment 1	Falsework 1	Falsework 2A	Falsework 2	Pier Bracket at XF 26	Pier 1	Pier Bracket at XF 28
G1							
G2							
G3	112.3	119.7					
G4							

**Vertical Support Reactions (kips)**

	Abutment 1	Falsework 1	Falsework 2A	Falsework 2	Pier Bracket at XF 26	Pier 1	Pier Bracket at XF 28
G1							
G2							
G3	25.2	26.9					
G4							

**Cross-frame Vertical Reactions**

	(kN)	(kip)
XF 1B (outside)	3.249	0.7304
XF 1C (inside)	1.533	0.3446
XF 7B (outside)	3.779	0.8496
XF 7C (inside)	2.161	0.4858

**Figure C - 2** Construction stage 1 – Field-splice location deflections and support reactions summary

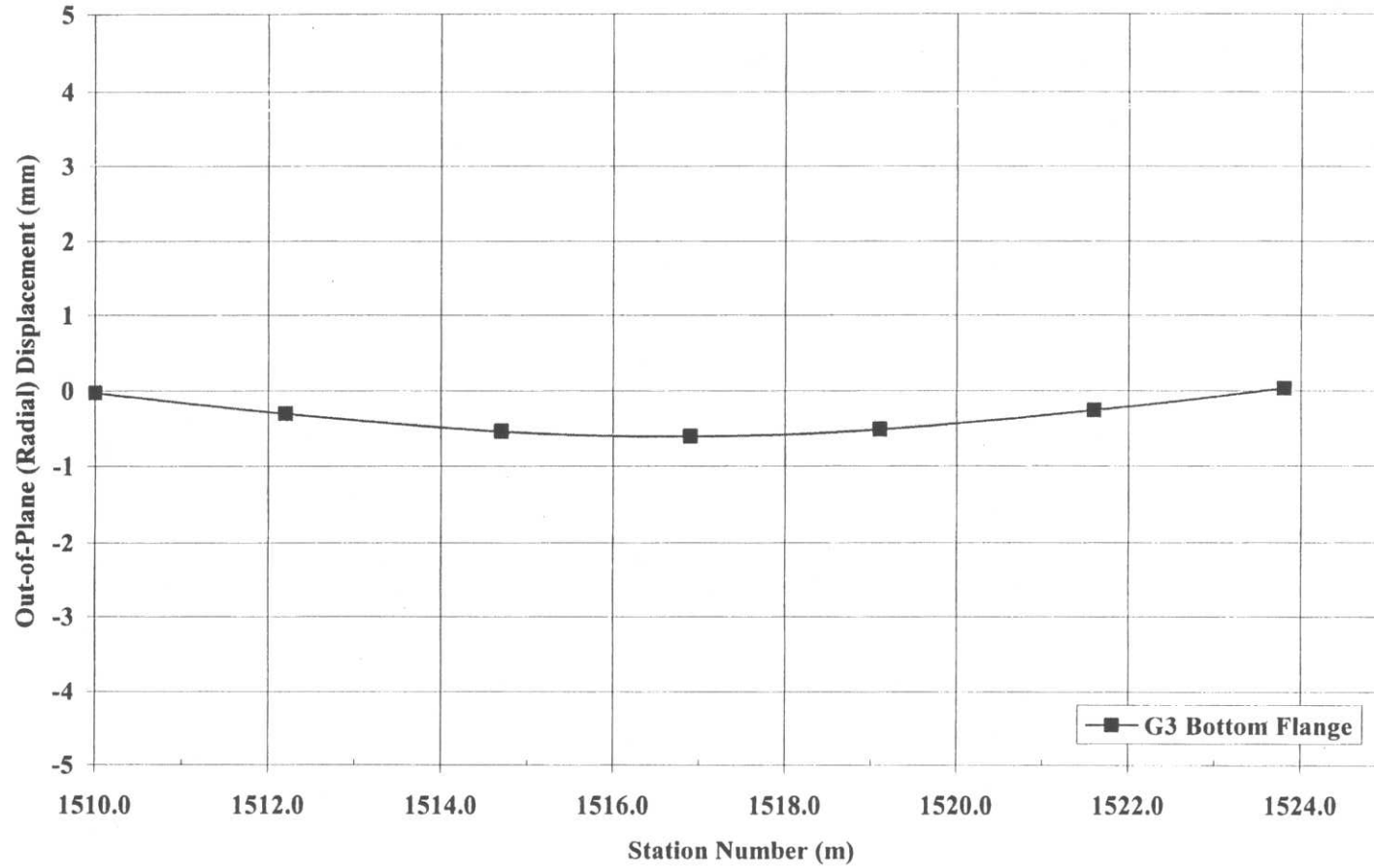


**Figure C - 3** Construction stage 1 – Out-of-plane (radial) displacement, centerline of bottom flange

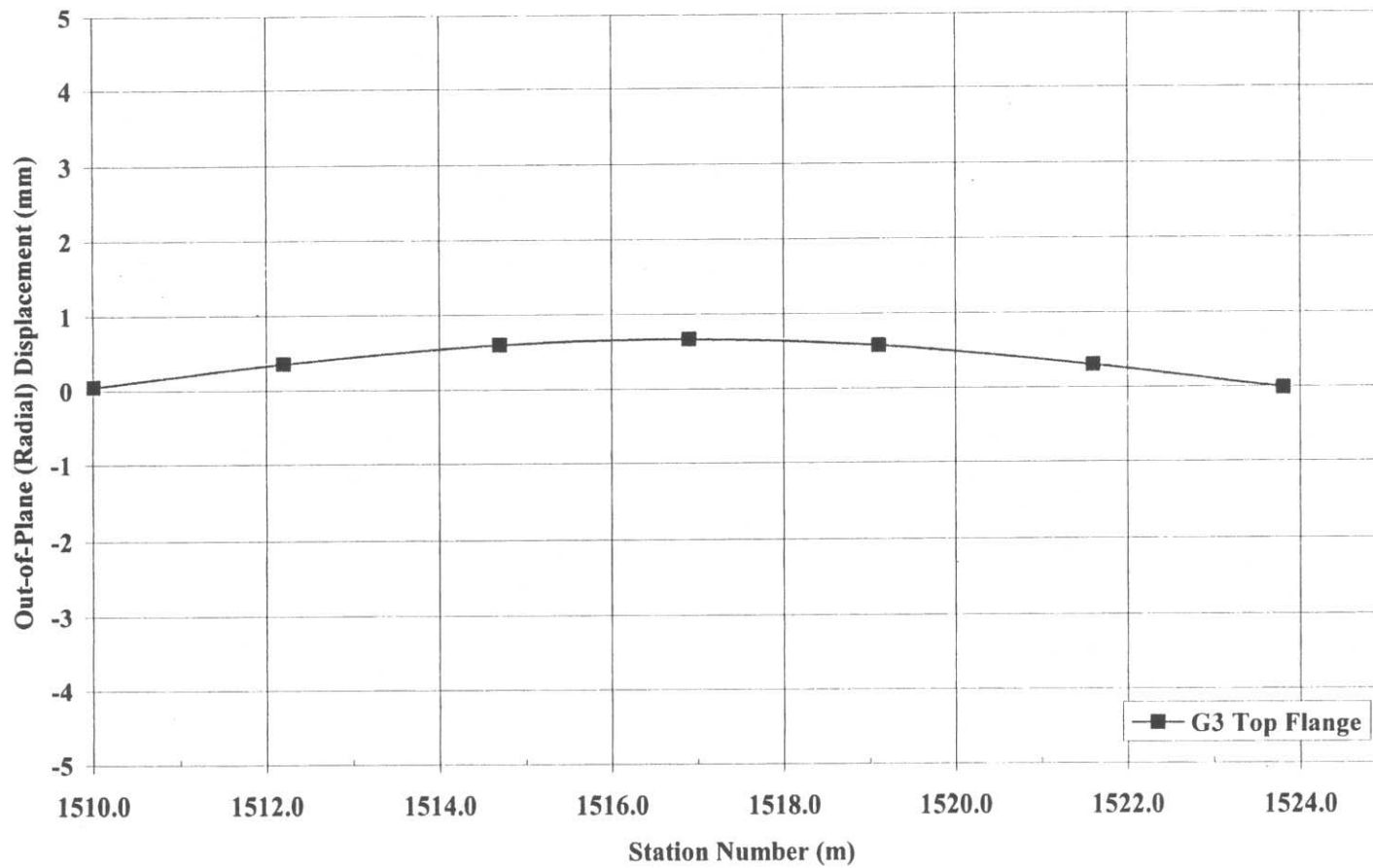


**Figure C- 4** Construction stage 1 – Out-of-plane (radial) displacement, centerline of top flange

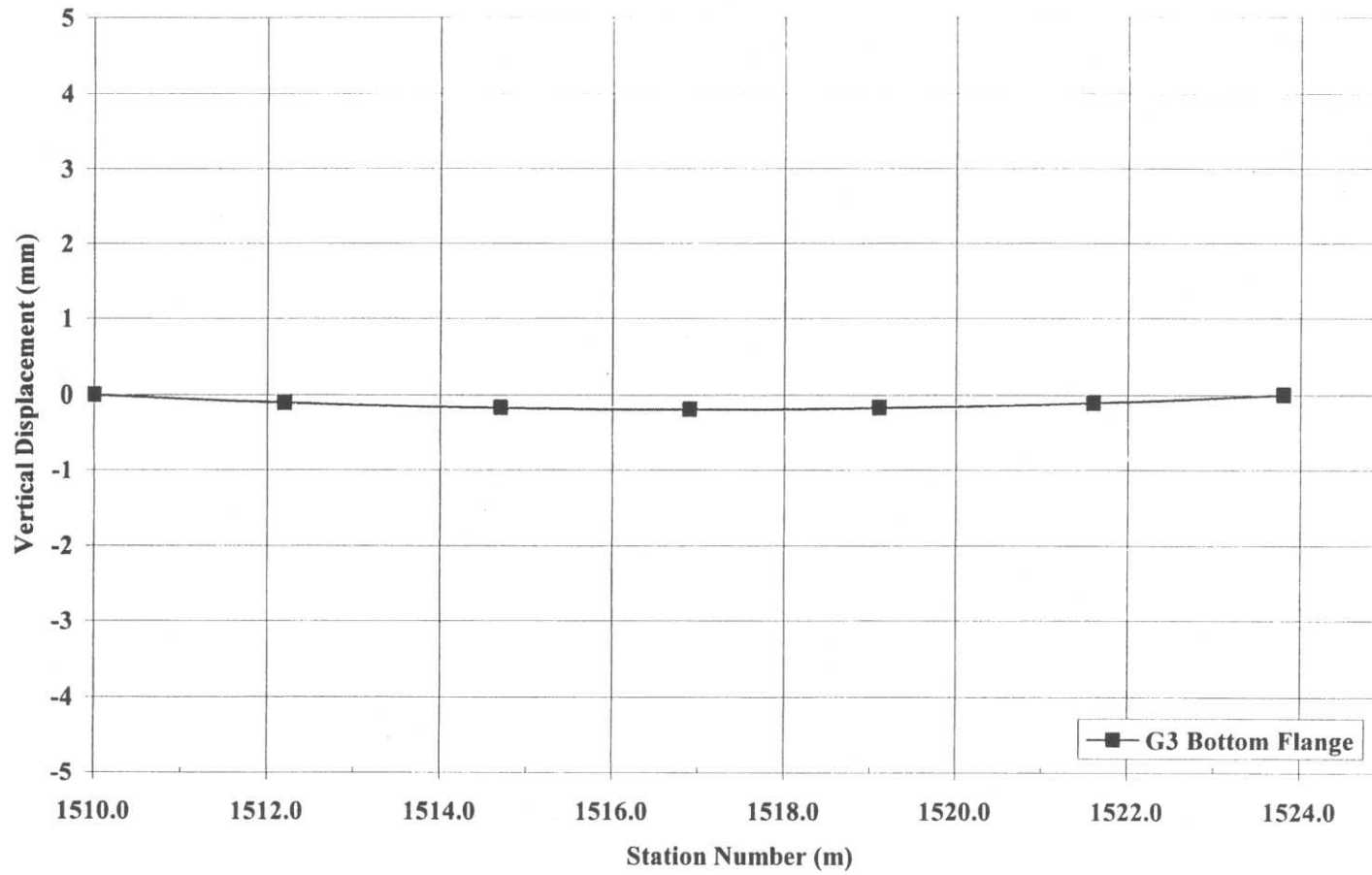


**Figure C-5** Construction stage 1 - Vertical displacement, centerline of bottom flange

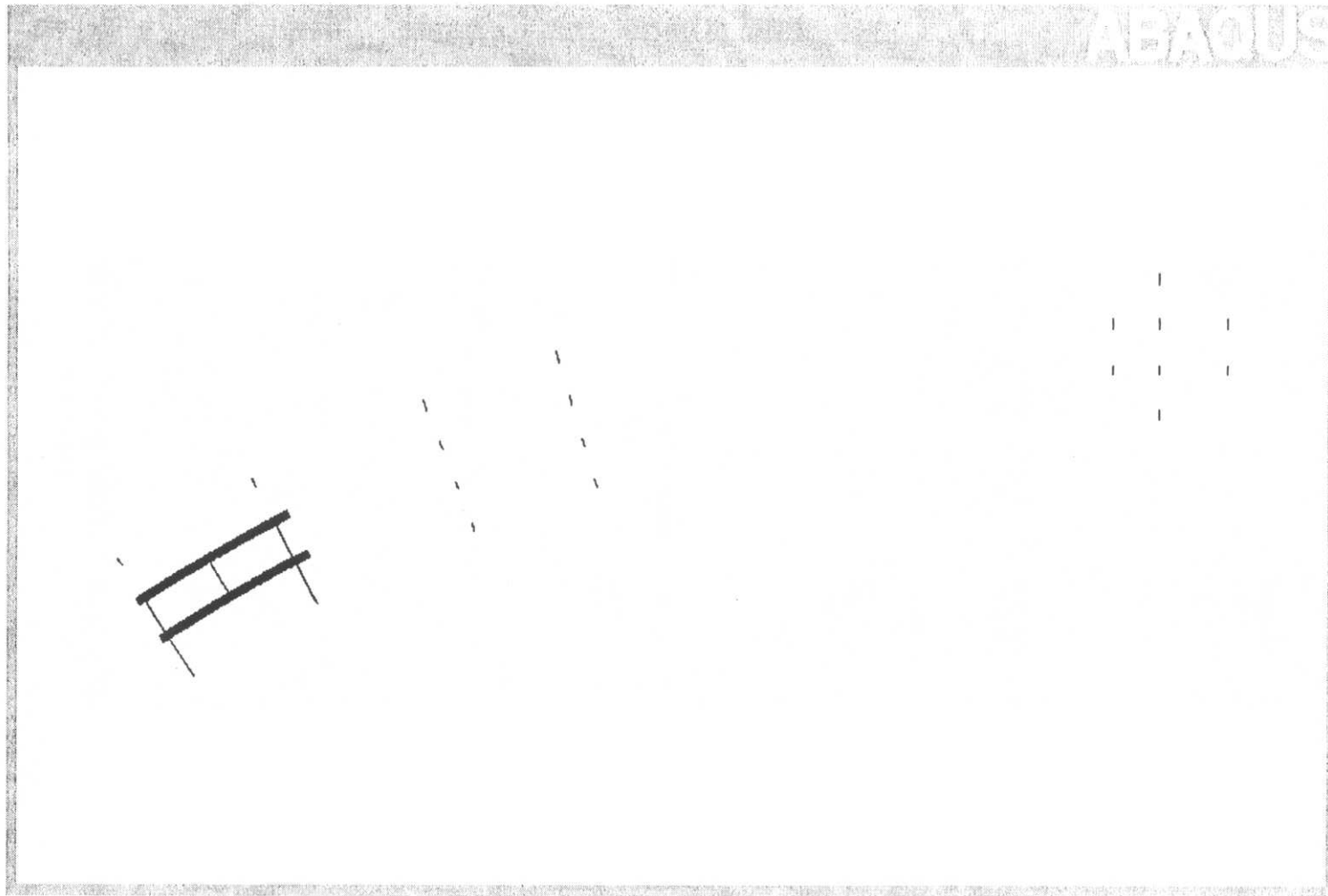


**Figure C - 6** Construction stage 2 - Plan view of finite element model

**Deflections - Out-of-Plane (Radial) (mm)**

	Abutment 1	Field Splice 1 Section 1	Field Splice 1 Section 2	Field Splice 2 Section 2	Field Splice 2 Section 3	Field Splice 3 Section 3	Field Splice 3 Section 4	Field Splice 4 Section 4
G1- Bottom Flange								
G1- Top Flange								
G2 - Bottom Flange	-0.0169	-0.0581						
G2 - Top Flange	0.0320	-0.0068						
G3 - Bottom Flange	-0.0162	0.0335						
G3 - Top Flange	0.0239	-0.0072						

G4 - Bottom flange  
G4 - Top Flange

**Deflections - Vertical (mm)**

	Abutment 1	Field Splice 1 Section 1	Field Splice 1 Section 2	Field Splice 2 Section 2	Field Splice 2 Section 3	Field Splice 3 Section 3	Field Splice 3 Section 4	Field Splice 4 Section 4
G1- Bottom Flange								
G1- Top Flange								
G2 - Bottom Flange	0.0028	0.0103						
G2 - Top Flange	-0.0131	0.0073						
G3 - Bottom Flange	0.0021	0.0060						
G3 - Top Flange	-0.0114	0.0030						

G4 - Bottom flange  
G4 - Top Flange

**Vertical - Support Reactions (kN)**

	Abutment 1	Falsework 1	Falsework 2A	Falsework 2	Pier Bracket at XF 26	Pier 1	Pier Bracket at XF 28
G1							
G2	127.4	131.9					
G3	110.2	121.6					

G4

**Vertical Support Reactions (kips)**

	Abutment 1	Falsework 1	Falsework 2A	Falsework 2	Pier Bracket at XF 26	Pier 1	Pier Bracket at XF 28
G1							
G2	28.6	29.6					
G3	24.8	27.3					

G4

**Cross-frame Vertical Reactions**

	(kN)	(kip)
XF 1B (outside)	0.000	0.0000
XF 1C (inside)	1.266	0.2846
XF 7B (outside)	0.000	0.0000
XF 7C (inside)	-0.026	-0.0058

**Figure C-7** Construction stage 2 – Field-splice location deflections and support reactions summary

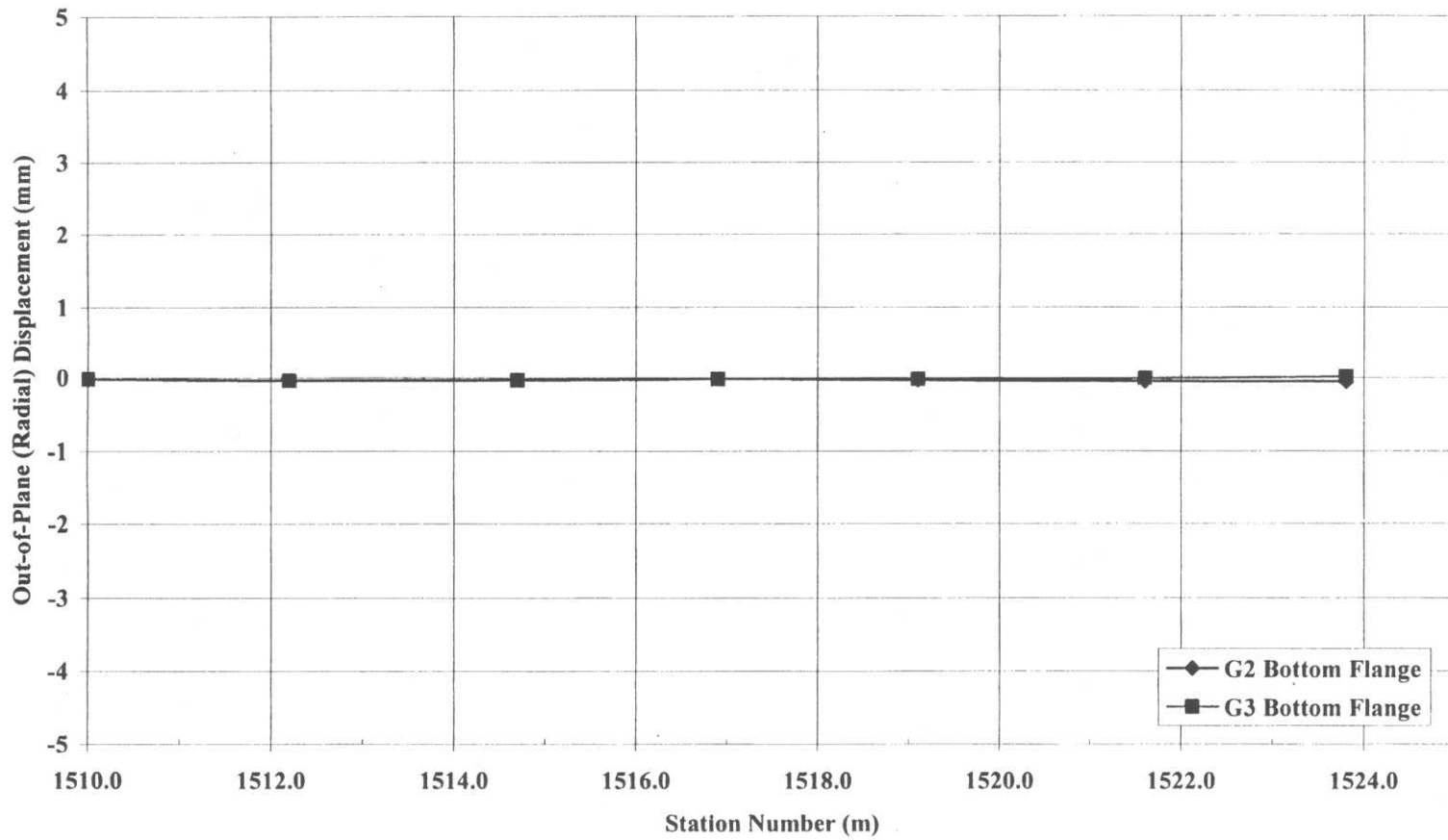


Figure C-8 Construction stage 2 – Out-of-plane (radial) displacement, centerline of bottom of flange

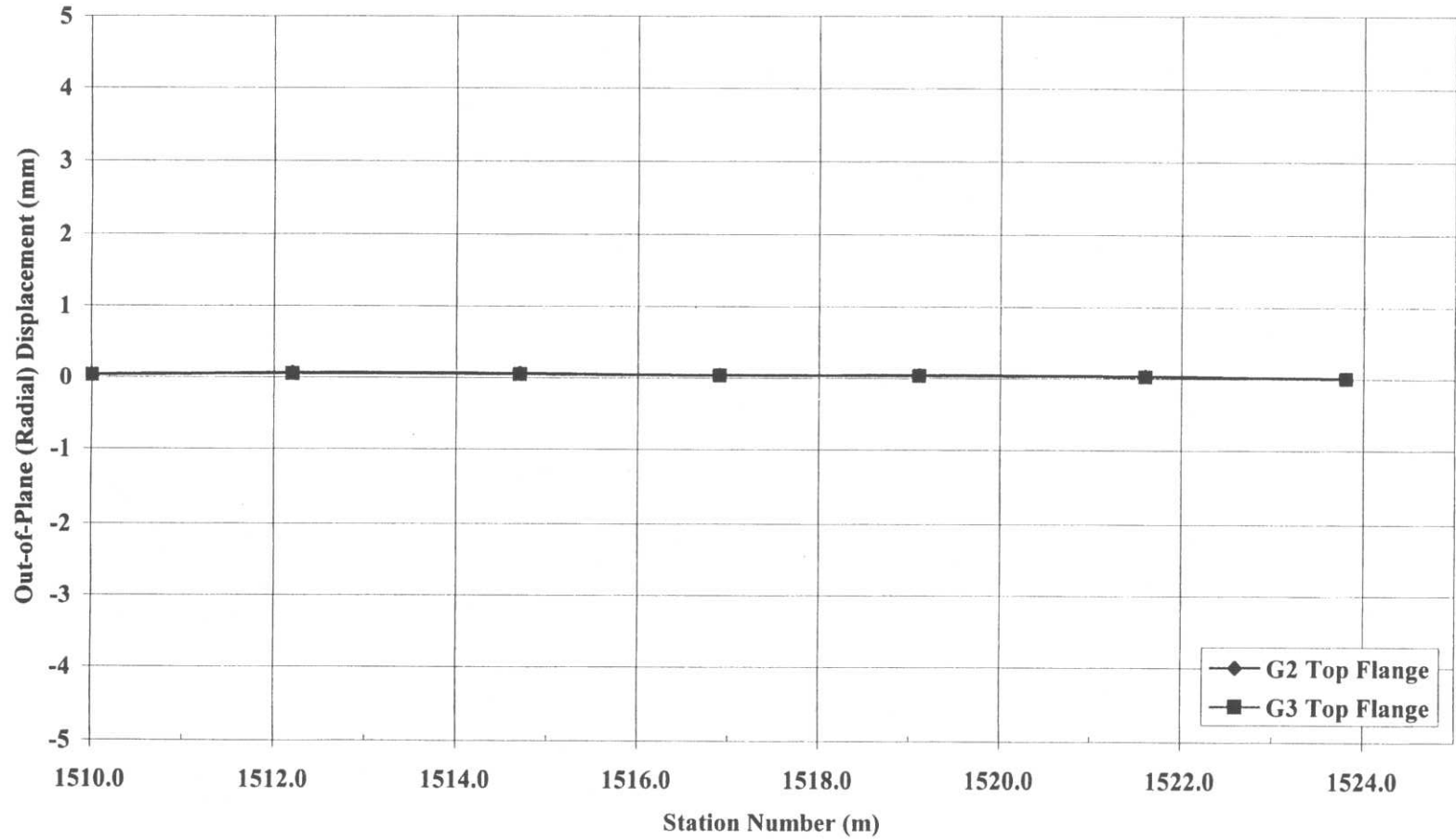


Figure C-9 Construction stage 2 – Out-pf-plane (radial) displacement, centerline of top flange

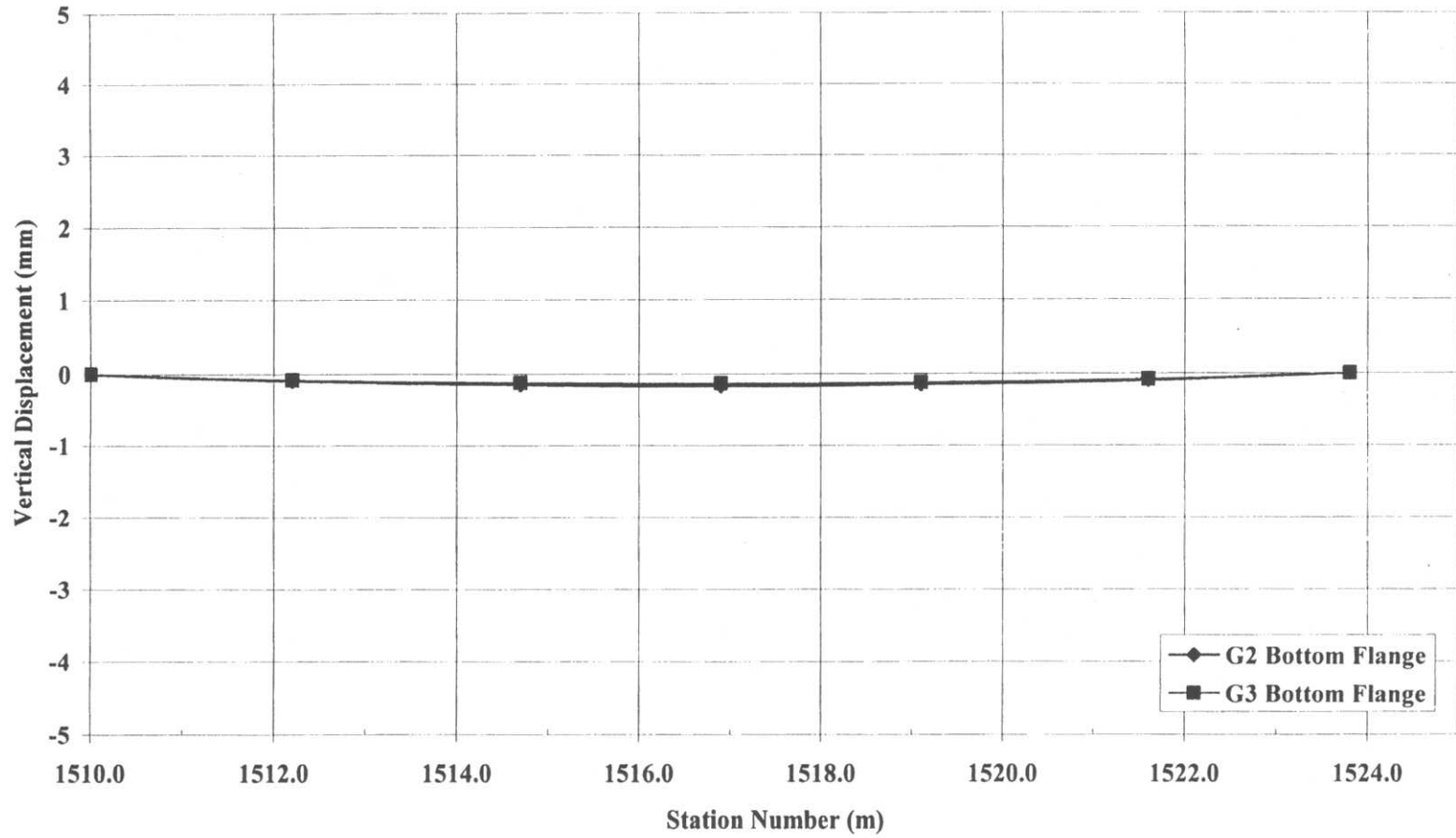
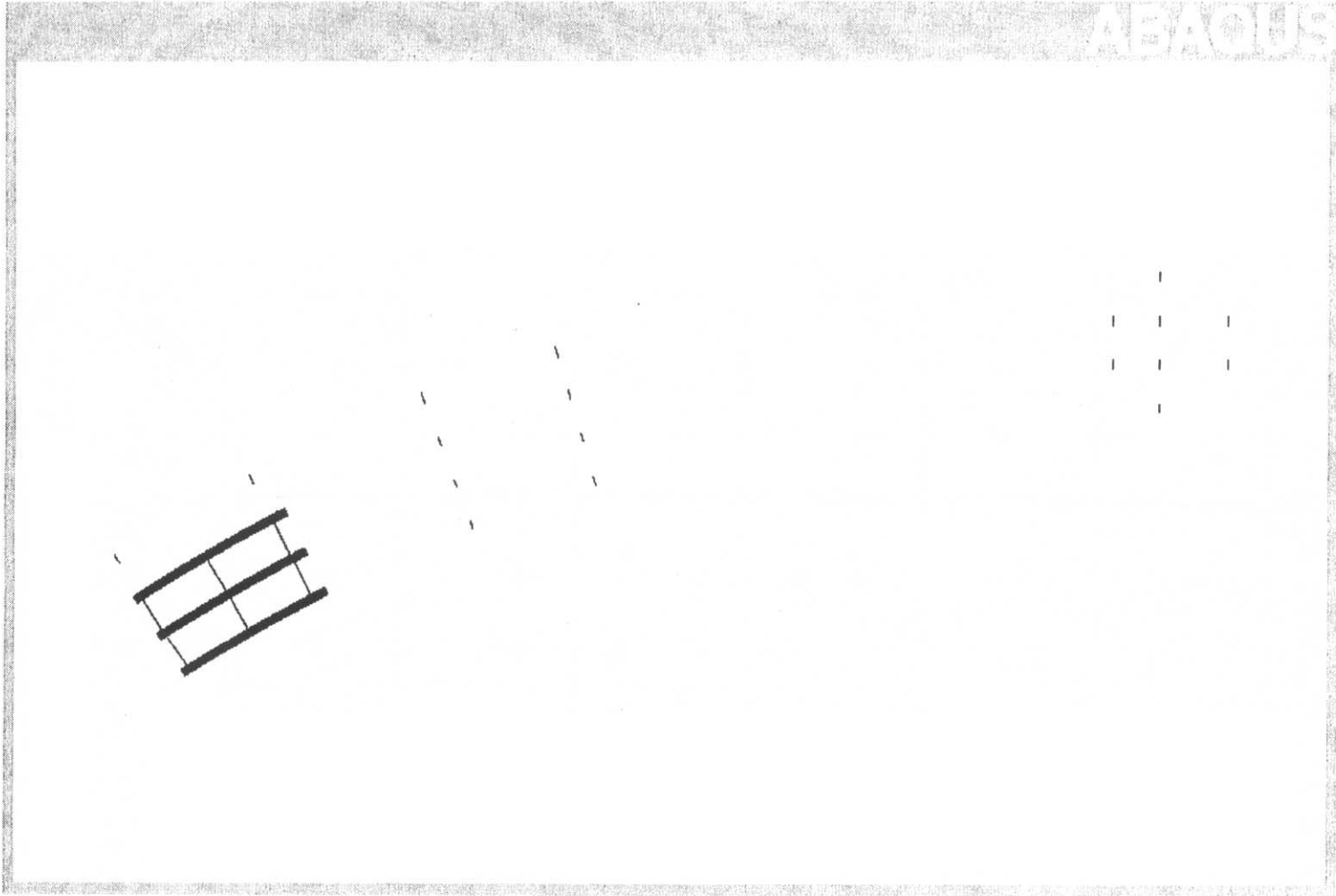


Figure C-10 Construction stage 2 - Vertical displacement, centerline of bottom flange



**Figure C-11** Construction stage 3 - Plan view of finite element model

**Deflections - Out-of-Plane (Radial) (mm)**

	Abutment 1	Field Splice 1 Section 1	Field Splice 1 Section 2	Field Splice 2 Section 2	Field Splice 2 Section 3	Field Splice 3 Section 3	Field Splice 3 Section 4	Field Splice 4 Section 4
G1- Bottom Flange								
G1- Top Flange								
G2 - Bottom Flange	0.0078	-0.0518						
G2 - Top Flange	0.0527	-0.0013						
G3 - Bottom Flange	0.0002	0.0527						
G3 - Top Flange	0.0431	-0.0111						
G4 - Bottom Flange	0.0081	0.0422						
G4 - Top Flange	0.0357	-0.0137						

**Deflections - Vertical (mm)**

	Abutment 1	Field Splice 1 Section 1	Field Splice 1 Section 2	Field Splice 2 Section 2	Field Splice 2 Section 3	Field Splice 3 Section 3	Field Splice 3 Section 4	Field Splice 4 Section 4
G1- Bottom Flange								
G1- Top Flange								
G2 - Bottom Flange	0.0026	0.0101						
G2 - Top Flange	-0.0130	0.0072						
G3 - Bottom Flange	0.0021	0.0066						
G3 - Top Flange	-0.0119	0.0036						
G4 - Bottom flange	0.0010	-0.0067						
G4 - Top Flange	-0.0128	-0.0095						

**Vertical - Support Reactions (kN)**

	Abutment 1	Falsework 1	Falsework 2A	Falsework 2	Pier Bracket at XF 26	Pier 1	Pier Bracket at XF 28
G1							
G2	125.3	128.9					
G3	116.3	128.1					
G4	96.5	98.3					

**Vertical Support Reactions (kips)**

	Abutment 1	Falsework 1	Falsework 2A	Falsework 2	Pier Bracket at XF 26	Pier 1	Pier Bracket at XF 28
G1							
G2	28.2	29.0					
G3	26.2	28.8					
G4	21.7	22.1					

**Cross-frame Vertical Reactions**

	(kN)	(kips)
XF 1B (outside)	0.000	0.000
XF 1C (inside)	0.000	0.000
XF 7B (outside)	0.000	0.000
XF 7C (inside)	0.000	0.000

**Figure C-12** Construction stage 3 – Field-splice location deflections and support reactions summary

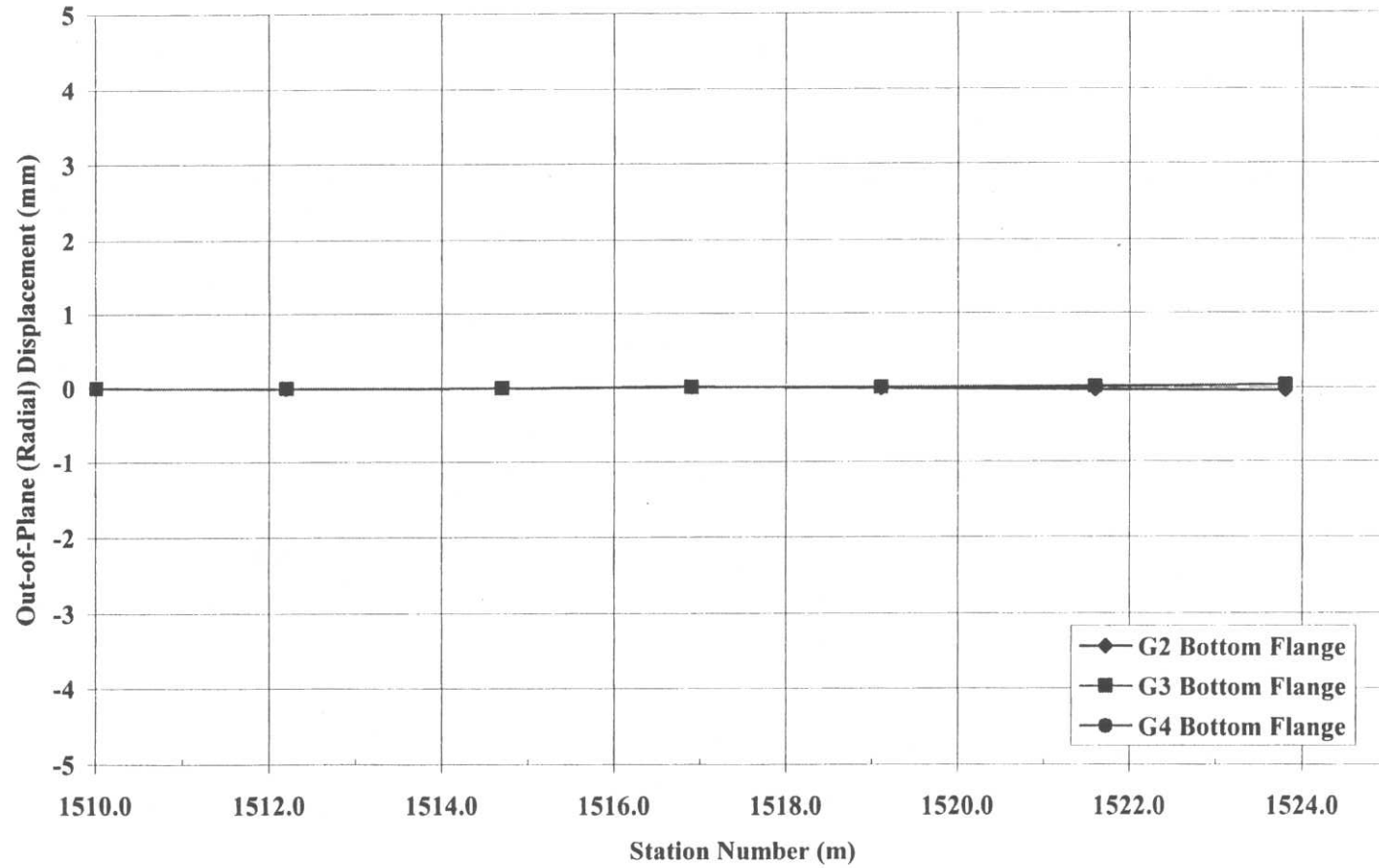


**Figure C-13** Construction stage 3 – Out-of-plane (radial) displacement, centerline of bottom flange

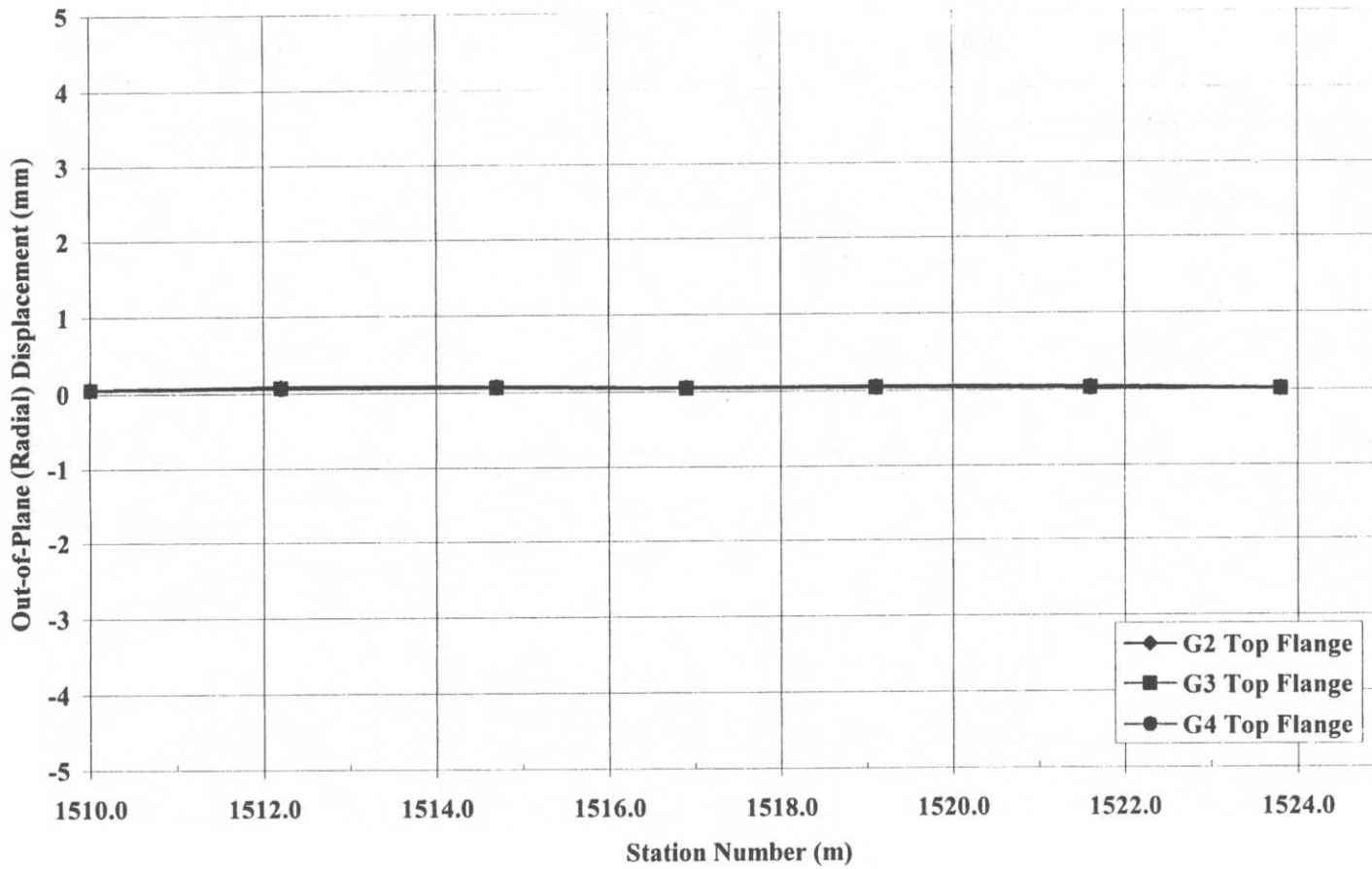


**Figure C-14** Construction stage 3 – Out-of-plane (radial) displacement, centerline of top flange

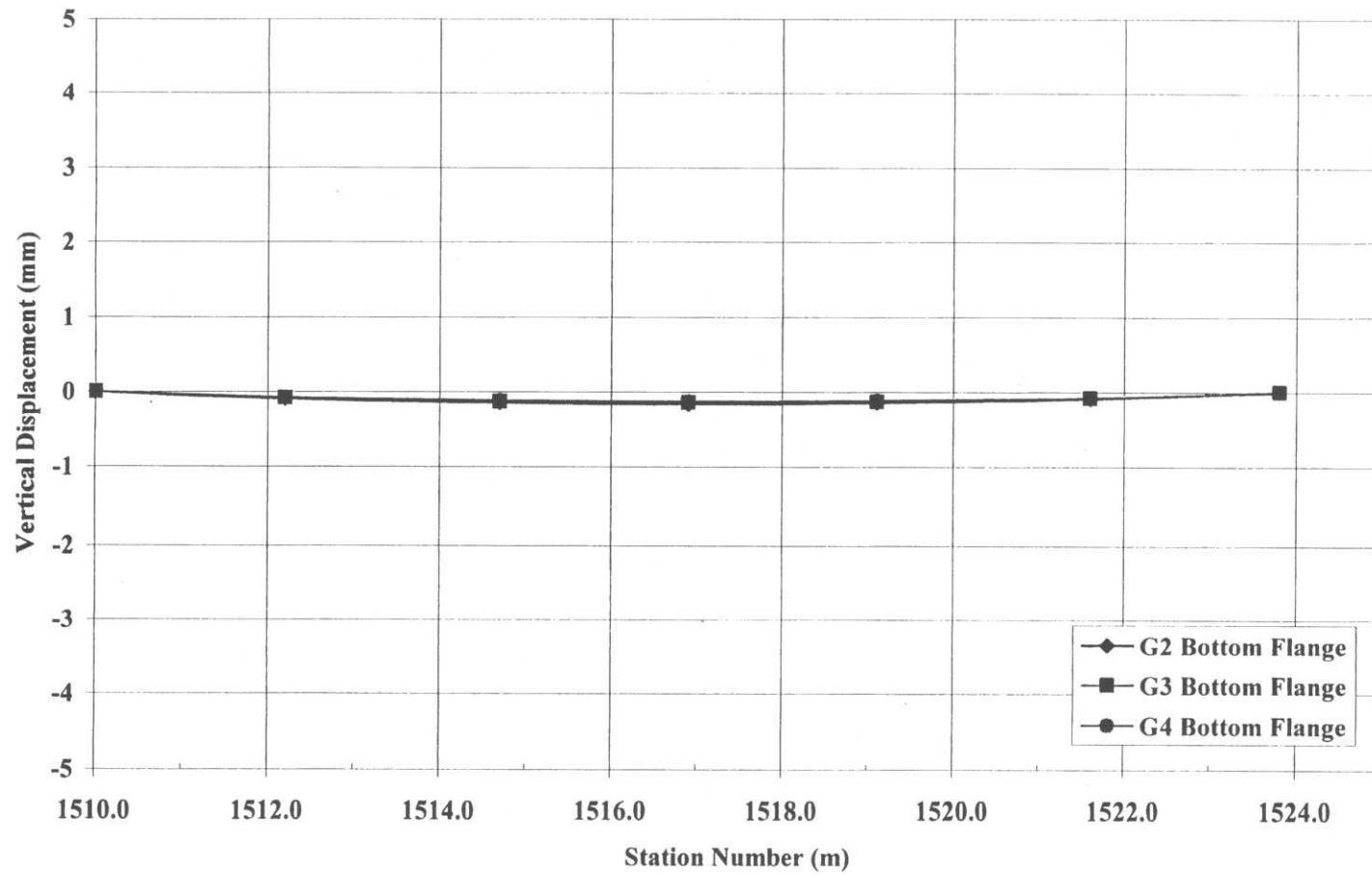


**Figure C-15** Construction stage 3 – Vertical displacement, centerline of bottom flange

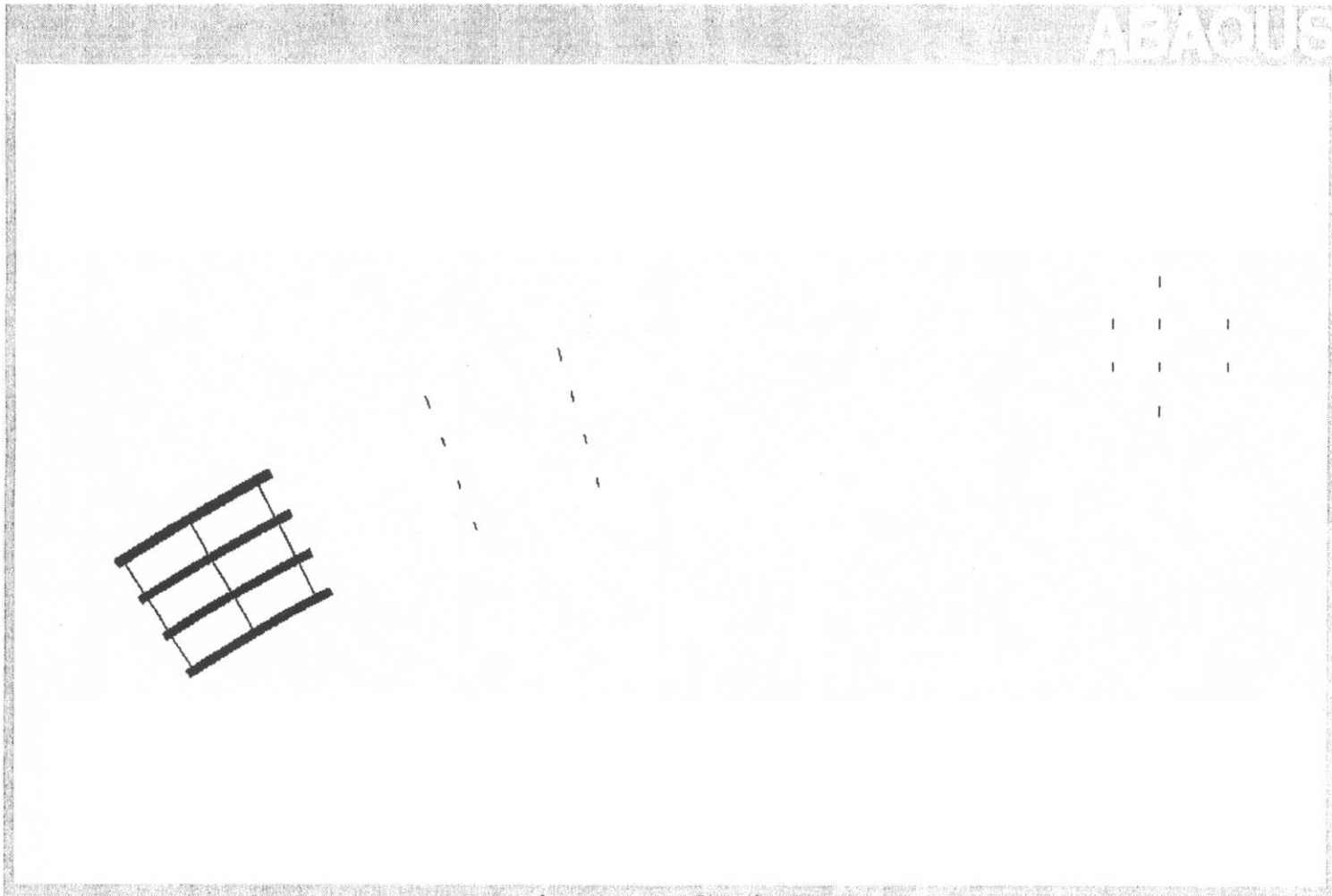


**Figure C-16** Construction stage 4 - Plan view of finite element model

**Deflections - Out-of-Plane (Radial) (mm)**

	Abutment 1	Field Splice 1 Section 1	Field Splice 1 Section 2	Field Splice 2 Section 2	Field Splice 2 Section 3	Field Splice 3 Section 3	Field Splice 3 Section 4	Field Splice 4 Section 4
G1 - Bottom Flange	0.0138	0.0520						
G1 - Top Flange	0.0577	0.0048						
G2 - Bottom Flange	0.0062	-0.0438						
G2 - Top Flange	0.0473	0.0047						
G3 - Bottom Flange	0.0002	0.0517						
G3 - Top Flange	0.0421	0.0011						
G4 - Bottom Flange	0.0089	0.0488						
G4 - Top Flange	0.0324	-0.3351						

**Deflections - Vertical (mm)**

	Abutment 1	Field Splice 1 Section 1	Field Splice 1 Section 2	Field Splice 2 Section 2	Field Splice 2 Section 3	Field Splice 3 Section 3	Field Splice 3 Section 4	Field Splice 4 Section 4
G1 - Bottom Flange	0.0002	-0.0066						
G1 - Top Flange	-0.0157	-0.0096						
G2 - Bottom Flange	0.0024	0.0095						
G2 - Top Flange	-0.0121	0.0067						
G3 - Bottom Flange	0.0021	0.0066						
G3 - Top Flange	-0.0119	0.0036						
G4 - Bottom flange	0.0012	-0.0140						
G4 - Top Flange	-0.0127	-0.0184						

**Vertical - Support Reactions (kN)**

	Abutment 1	Falsework 1	Falsework 2A	Falsework 2	Pier Bracket at XF 26	Pier 1	Pier Bracket at XF 28
G1	176.3	179.1					
G2	120.5	123.7					
G3	116.2	125.1					
G4	97.1	100.1					

**Vertical Support Reactions (kN)**

	Abutment 1	Falsework 1	Falsework 2A	Falsework 2	Pier Bracket at XF 26	Pier 1	Pier Bracket at XF 28
G1	39.6	40.3					
G2	27.1	27.8					
G3	26.1	28.1					
G4	21.8	22.5					

**Cross-frame Vertical Reactions**

	(kN)	(kips)
XF 1B (outside)	0.000	0.000
XF 1C (inside)	0.000	0.000
XF 7B (outside)	0.000	0.000
XF 7C (inside)	0.000	0.000

**Figure C-17** Construction stage 4 – Field-splice location deflections and support Reactions summary

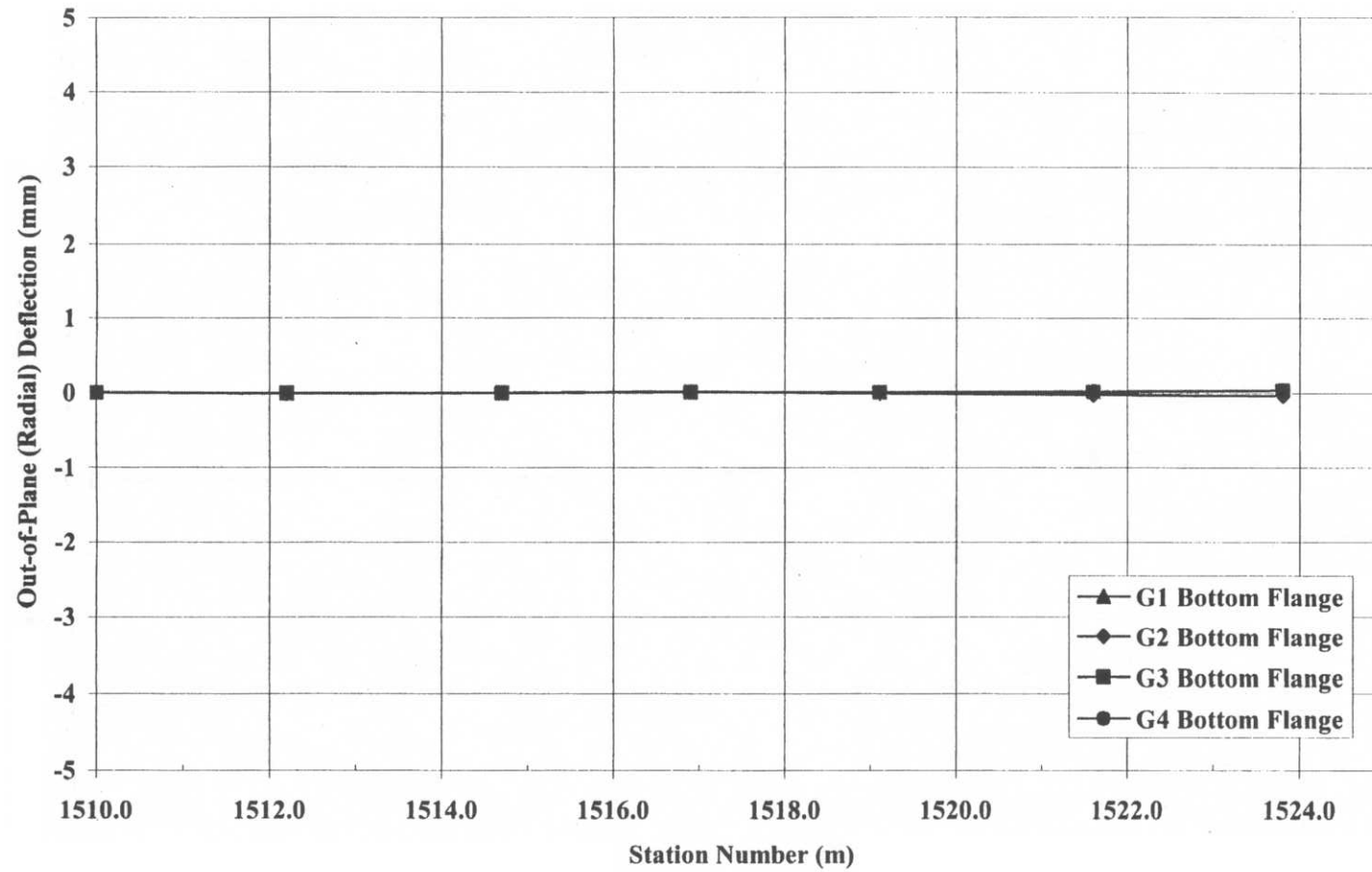


**Figure C-18** Construction stage 4 – Out-of-plane (radial) displacement, centerline of bottom flange

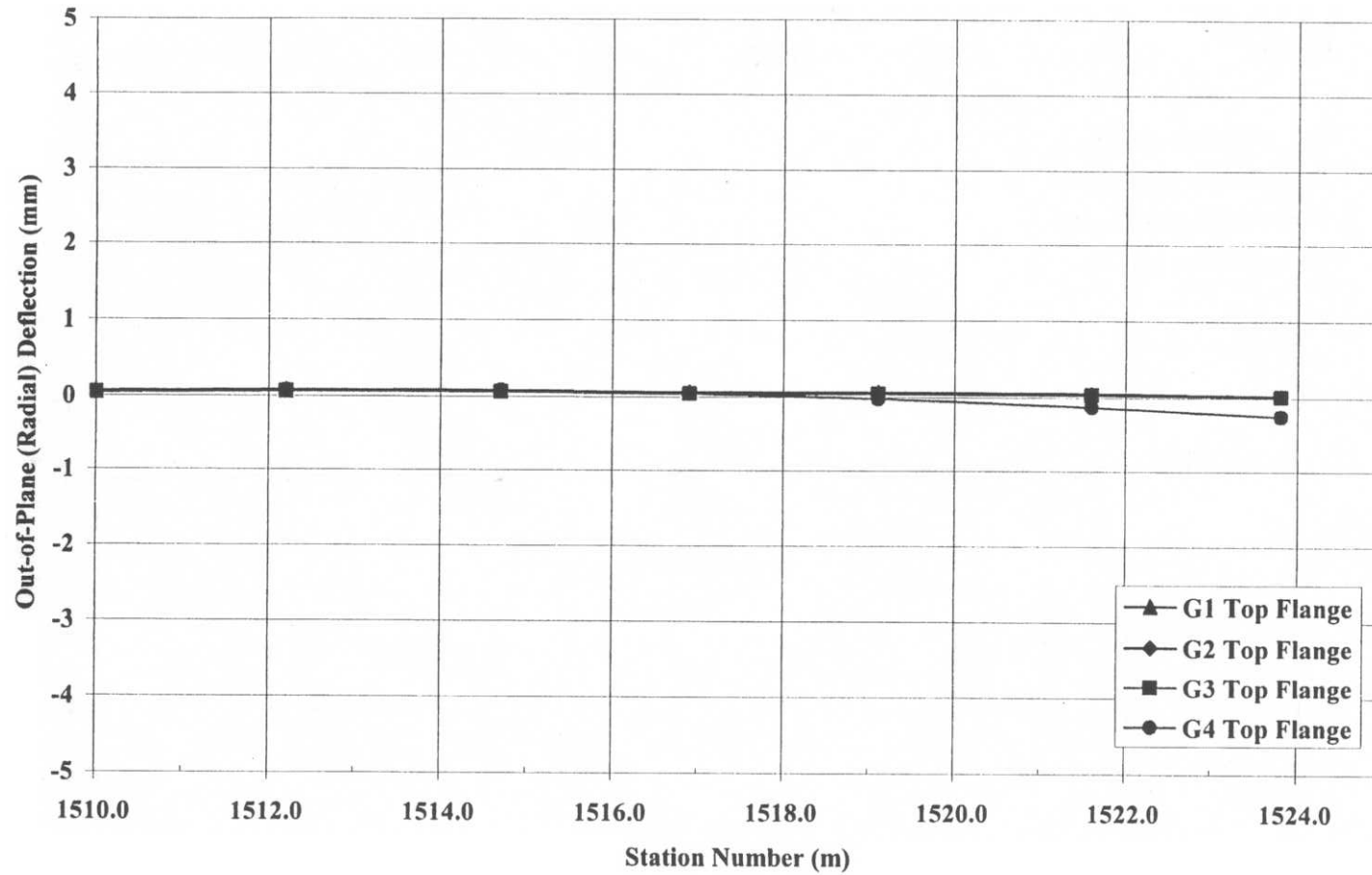


**Figure C-19** Construction stage 4 – Out-of-plane (radial) displacement, centerline of top flange

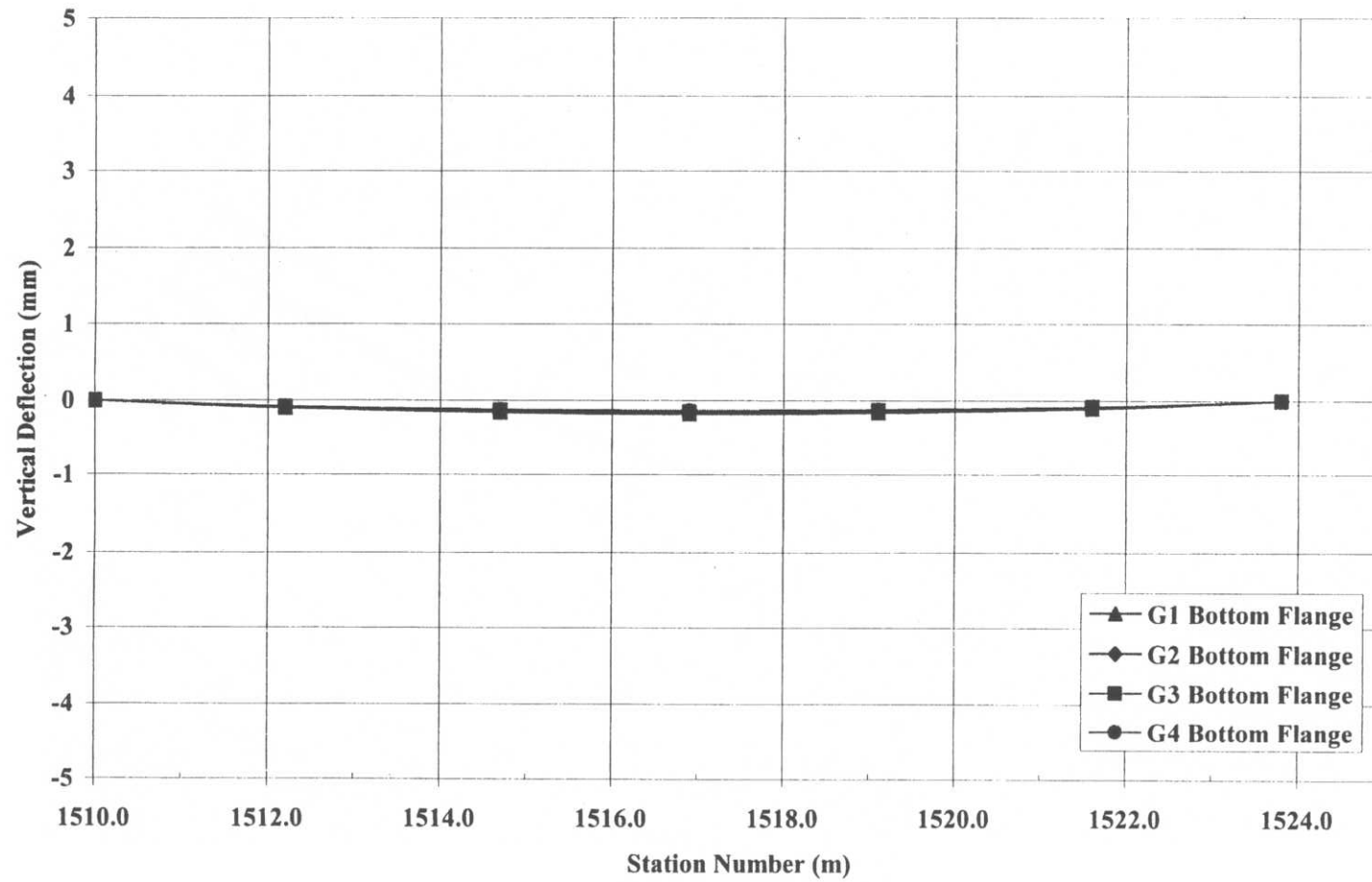


**Figure C-20** Construction stage 4 - Vertical displacement, centerline of bottom flange

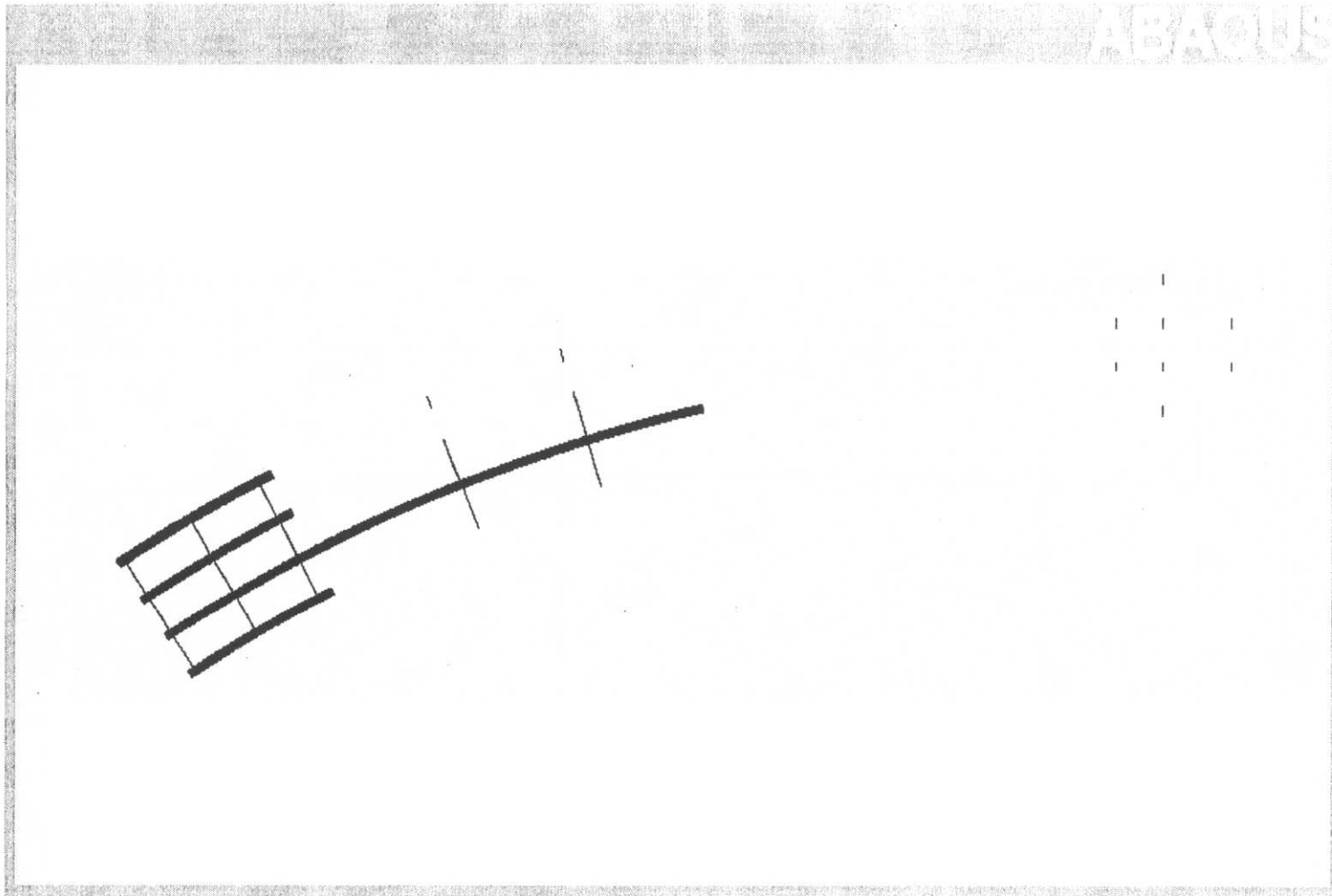


**Figure C-21** Construction stage 5 - Plan view of finite element model

**Deflections - Out-of-Plane (Radial) (mm)**

	Abutment 1	Field Splice 1 Section 1	Field Splice 1 Section 2	Field Splice 2 Section 2	Field Splice 2 Section 3	Field Splice 3 Section 3	Field Splice 3 Section 4	Field Splice 4 Section 4
G1- Bottom Flange	0.0158	0.0506						
G1- Top Flange	0.0592	-0.0065						
G2 - Bottom Flange	0.0076	-0.0457						
G2 - Top Flange	0.0462	0.0057						
G3 - Bottom Flange	0.0002	-0.0486	-0.0486	1.7060				
G3 - Top Flange	0.0301	0.0790	0.0790	-1.9490				
G4 - Bottom Flange	-0.0029	0.0214						
G4 - Top Flange	0.0251	-0.0185						

**Deflections - Vertical (mm)**

	Abutment 1	Field Splice 1 Section 1	Field Splice 1 Section 2	Field Splice 2 Section 2	Field Splice 2 Section 3	Field Splice 3 Section 3	Field Splice 3 Section 4	Field Splice 4 Section 4
G1- Bottom Flange	-0.0001	-0.0065						
G1- Top Flange	-0.0157	-0.0095						
G2 - Bottom Flange	0.0022	0.0084						
G2 - Top Flange	-0.0120	0.0056						
G3 - Bottom Flange	0.0014	-0.0693	-0.0693	-1.1250				
G3 - Top Flange	-0.0102	-0.0739	-0.0739	-1.1270				
G4 - Bottom Flange	0.0008	-0.0073						
G4 - Top Flange	-0.0128	-0.0101						

**Vertical - Support Reactions (kN)**

	Abutment 1	Falsework 1	Falsework 2A	Falsework 2	Pier Bracket at XF 26	Pier 1	Pier Bracket at XF 28
G1	178.1	178.7					
G2	116.9	121.5					
G3	96.2	261.7	145.5	293.5			
G4	95.0	99.6					

**Vertical Support Reactions (kips)**

	Abutment 1	Falsework 1	Falsework 2A	Falsework 2	Pier Bracket at XF 26	Pier 1	Pier Bracket at XF 28
G1	40.0	40.2					
G2	26.3	27.3					
G3	21.6	58.8	32.7	66.0			
G4	21.4	22.4					

**Cross-frame Vertical Reactions**

	(kN)	(kips)
XF 11B (outside)	2.784	0.6259
XF 11C (inside)	4.359	0.9799
XF 14B (outside)	0.884	0.1987
XF 14C (inside)	13.067	2.9376

**Figure C-22** Construction stage 5 – Field-splice location deflections and support reaction summary

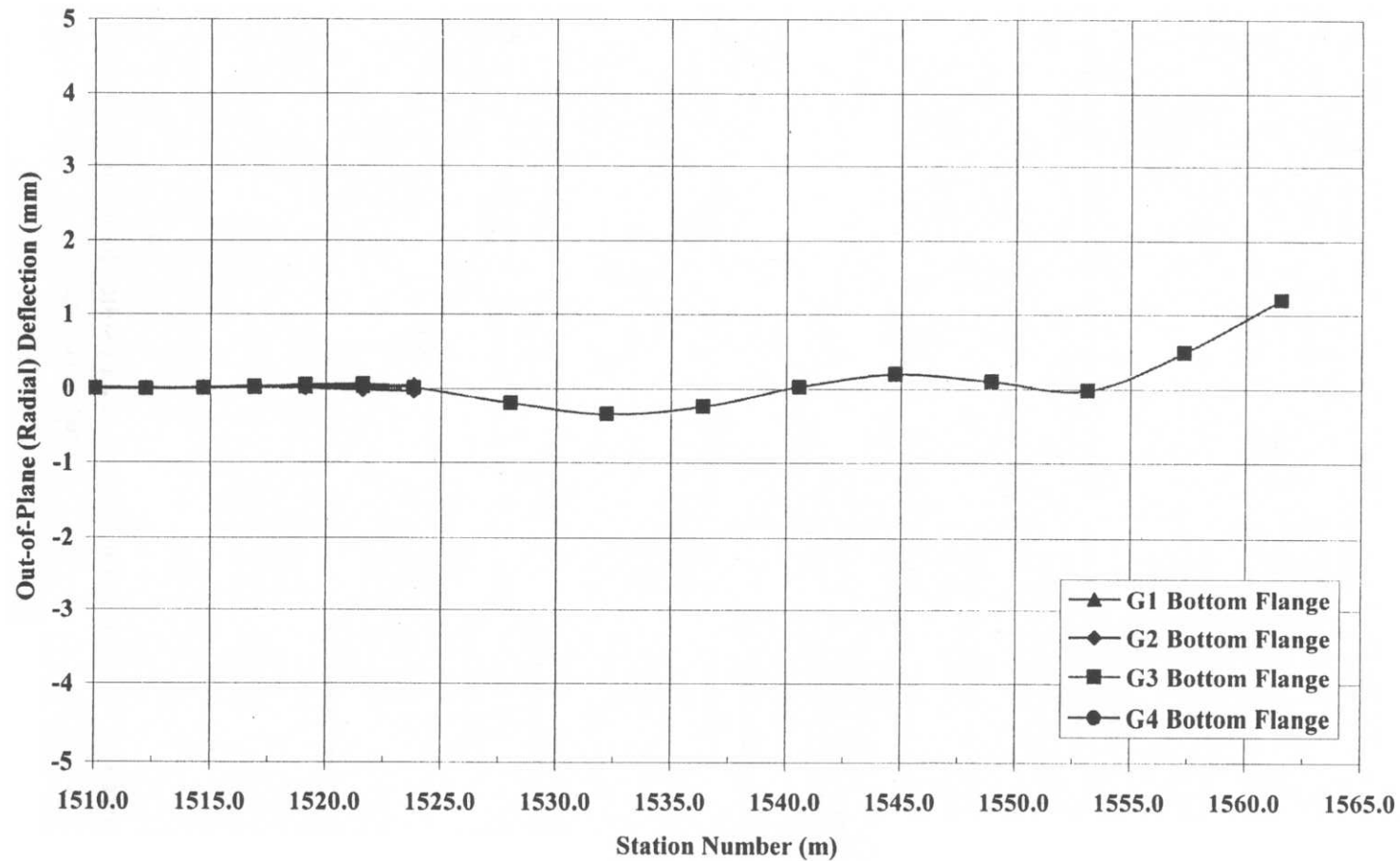


Figure C-23 Construction stage 5 – Out-of-plane (radial) displacement, centerline of bottom Flange

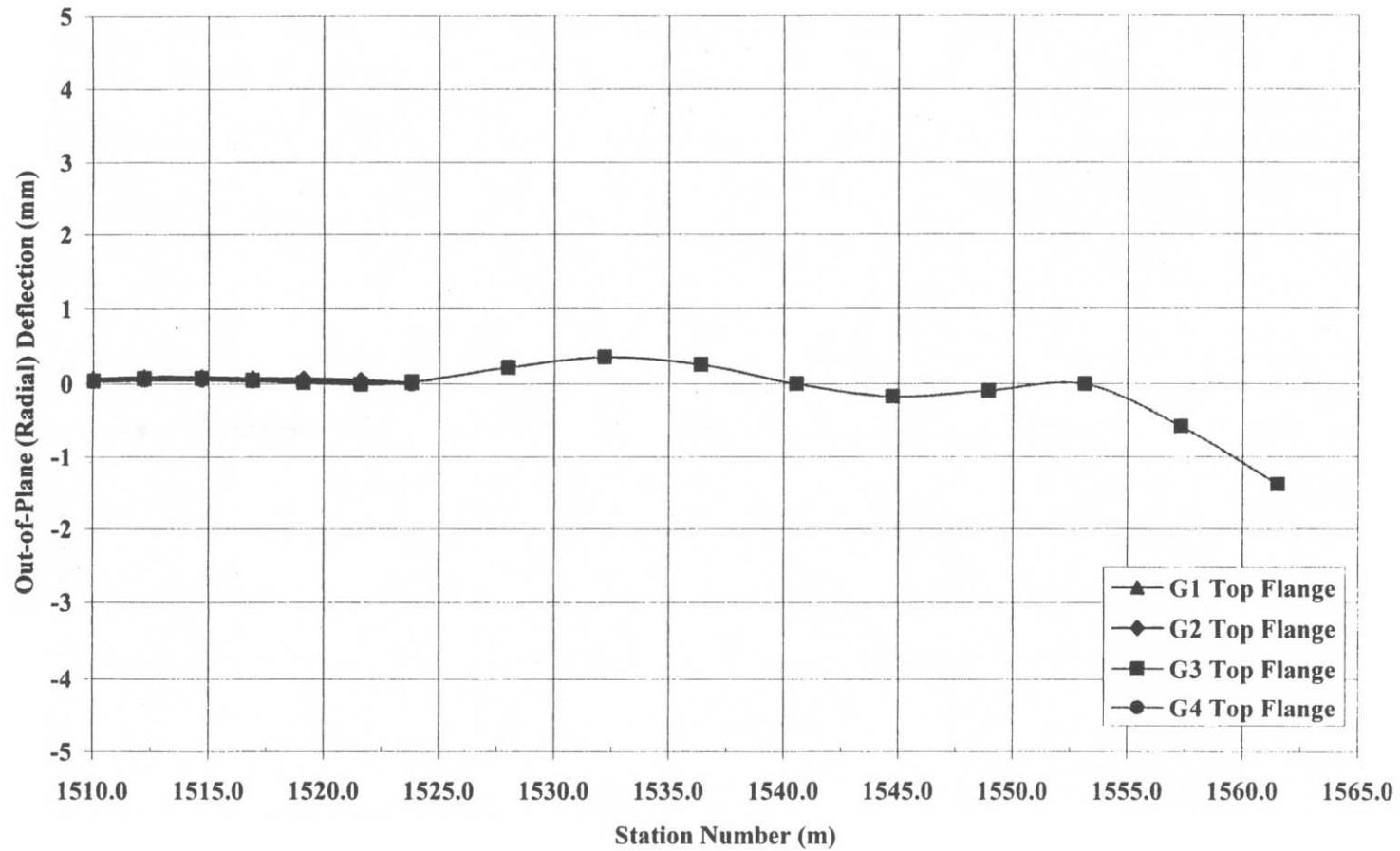


Figure C-24 Construction stage 5 – Out-of-plane (radial) displacement, centerline of top flange

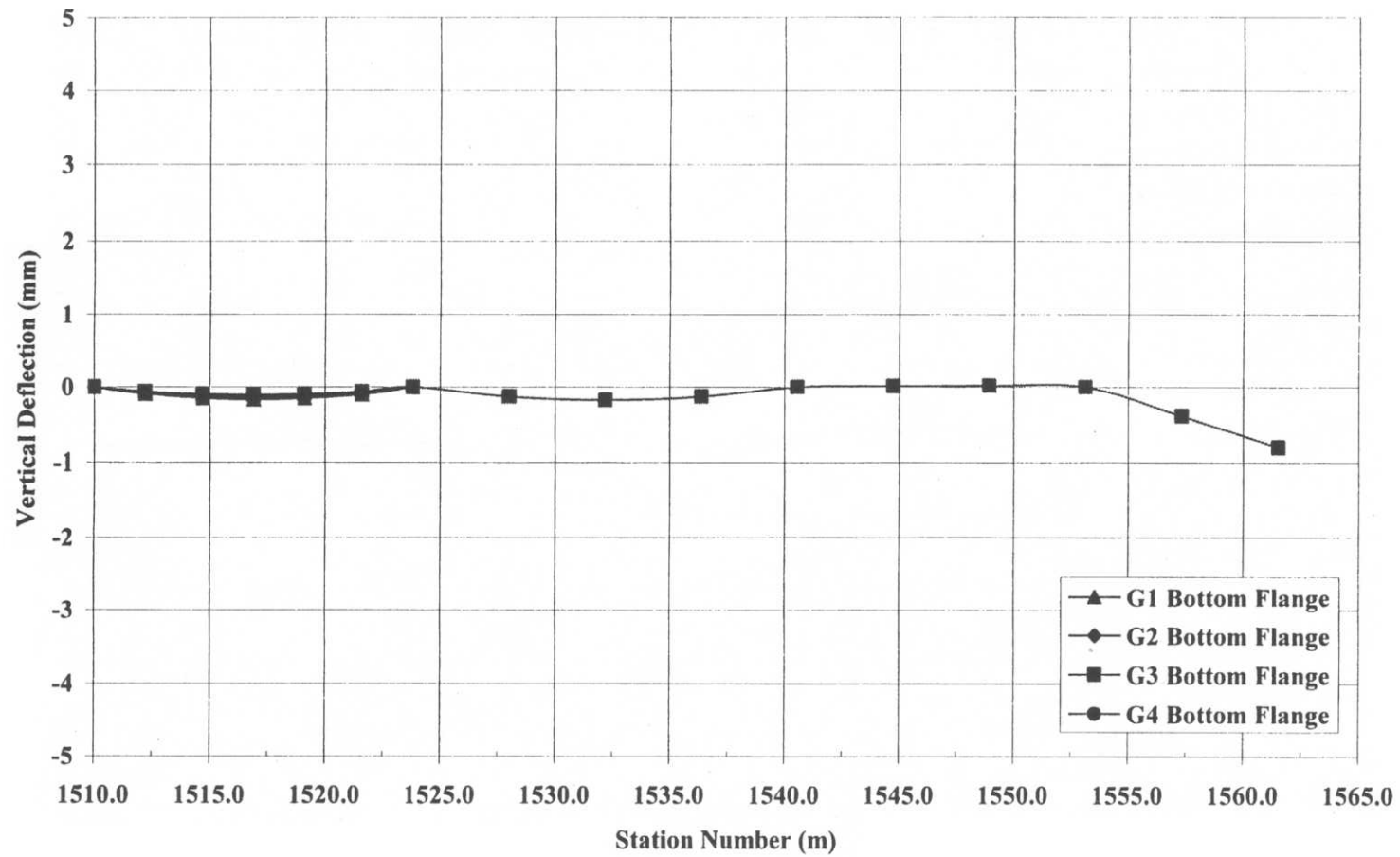
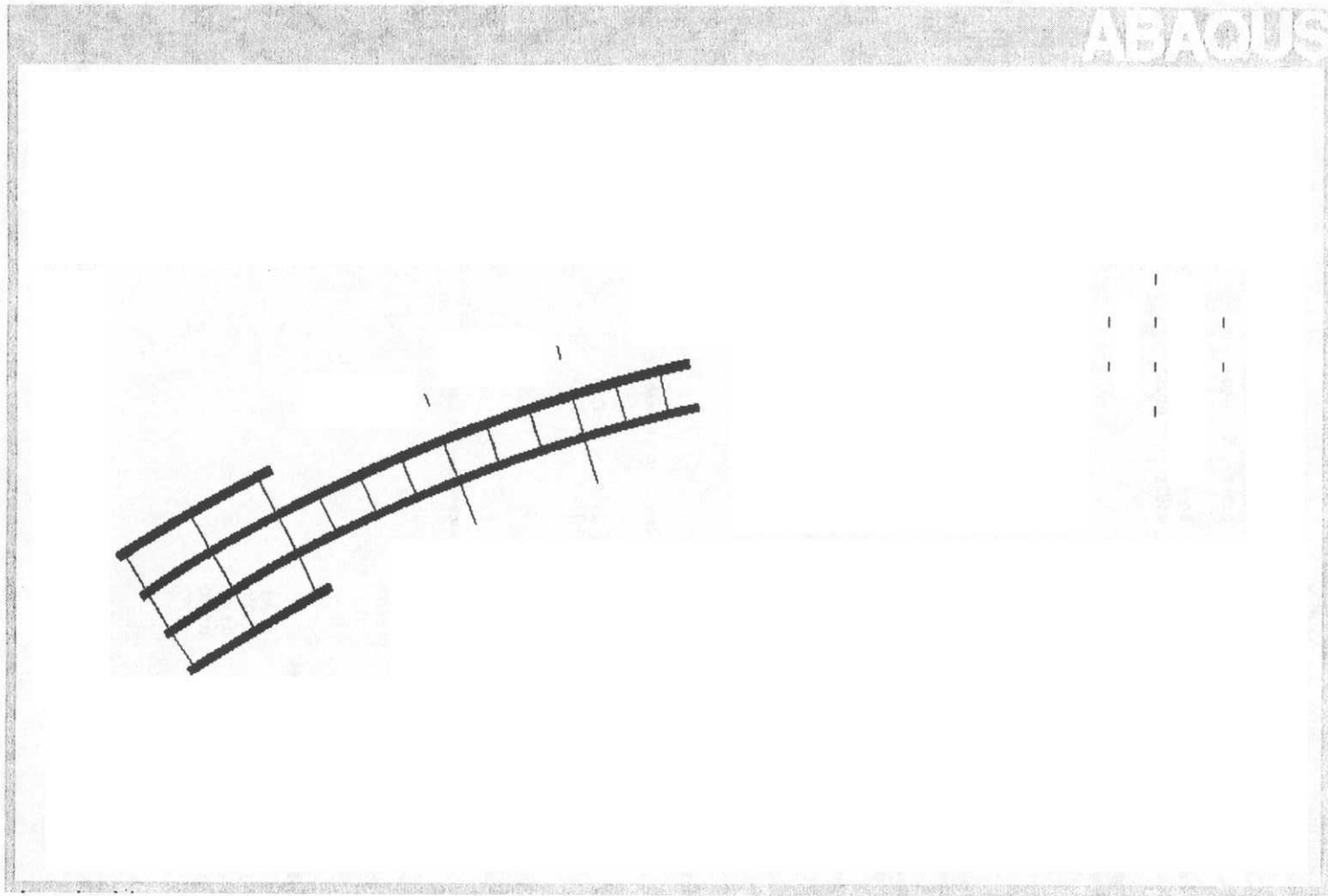


Figure C-25 Construction stage 5 - Vertical displacement, centerline of bottom flange



**Figure C-26** Construction stage 6 - Plan view of finite element model

**Deflections - Out-of-Plane (Radial) (mm)**

	Abutment 1	Field Splice 1 Section 1	Field Splice 1 Section 2	Field Splice 2 Section 2	Field Splice 2 Section 3	Field Splice 3 Section 3	Field Splice 3 Section 4	Field Splice 4 Section 4
G1- Bottom Flange	0.0063	0.0576						
G1- Top Flange	0.0473	-0.0038						
G2 - Bottom Flange	0.0073	0.0102	0.0102	-0.0250				
G2 - Top Flange	0.0360	0.0408	0.0408	0.0246				
G3 - Bottom Flange	0.0002	0.0031	0.0031	-0.0342				
G3 - Top Flange	0.0312	0.0278	0.0278	0.0252				
G4 - Bottom Flange	-0.0020	0.0210						
G4 - Top Flange	0.0265	-0.0211						

**Deflections - Vertical (mm)**

	Abutment 1	Field Splice 1 Section 1	Field Splice 1 Section 2	Field Splice 2 Section 2	Field Splice 2 Section 3	Field Splice 3 Section 3	Field Splice 3 Section 4	Field Splice 4 Section 4
G1- Bottom Flange	-0.0008	-0.0063						
G1- Top Flange	-0.0156	-0.0091						
G2 - Bottom Flange	0.0017	-0.0827	-0.0827	-0.9781				
G2 - Top Flange	-0.0101	-0.0877	-0.0877	-0.9773				
G3 - Bottom Flange	0.0013	-0.0628	-0.0628	-1.0250				
G3 - Top Flange	-0.0103	-0.0671	-0.0671	-1.0260				
G4 - Bottom Flange	0.0009	-0.0075						
G4 - Top Flange	-0.0129	-0.0103						

**Vertical - Support Reactions (kN)**

	Abutment 1	Falsework 1	Falsework 2A	Falsework 2	Pier Bracket at XF 26	Pier 1	Pier Bracket at XF 28
G1	178.0	175.9					
G2	97.8	299.0	241.4	426.4			
G3	95.8	251.8	149.7	321.4			
G4	95.7	100.7					

**Vertical Support Reactions (kips)**

	Abutment 1	Falsework 1	Falsework 2A	Falsework 2	Pier Bracket at XF 26	Pier 1	Pier Bracket at XF 28
G1	40.0	39.6					
G2	22.0	67.3	54.3	96.0			
G3	21.5	56.7	33.7	72.3			
G4	21.5	22.7					

**Cross-frame Vertical Reactions**

	(kN)	(kips)
XF 11B (outside)	0.000	0.0000
XF 11C (inside)	2.360	0.5305
XF 14B (outside)	0.000	0.0000
XF 14C (inside)	7.906	1.7773

**Figure C-27** Construction stage 6 – Field-splice location deflections and support reactions summary

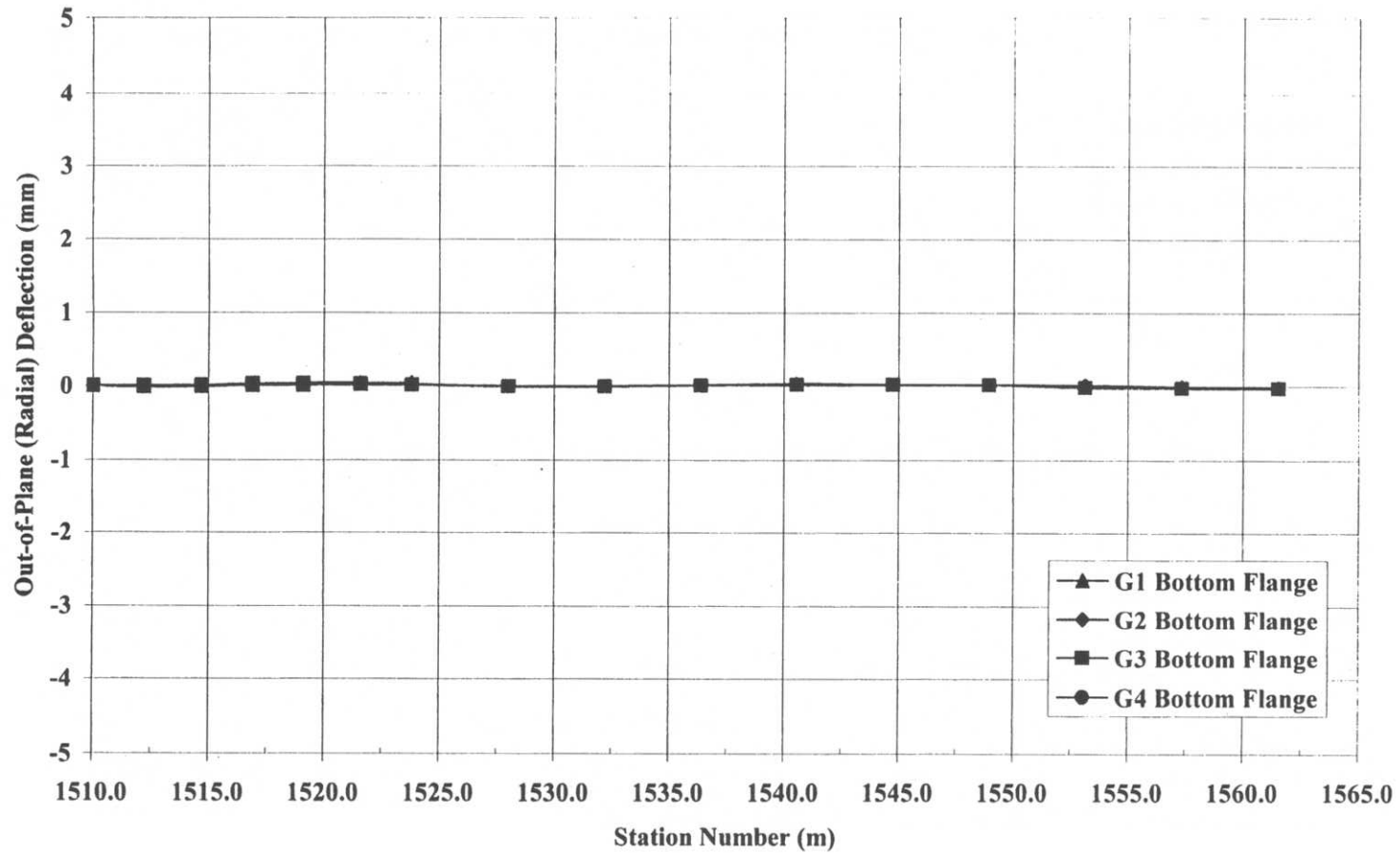


**Figure C-28** Construction stage 6 – Out-of-plane (radial) displacement, centerline of bottom flange

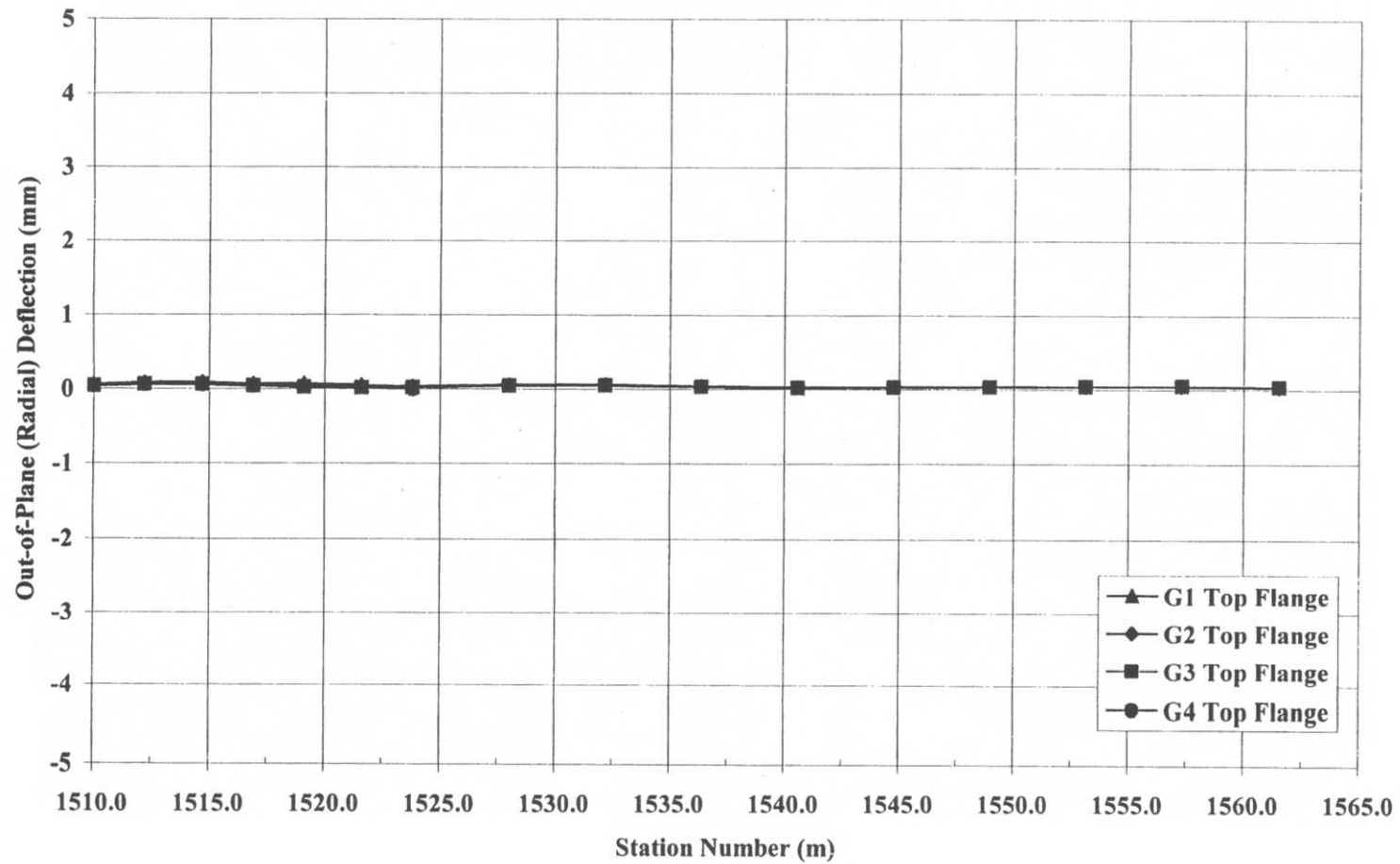


Figure C-29 Construction stage 6 – Out-of-plane (radial) displacement, centerline of top flange

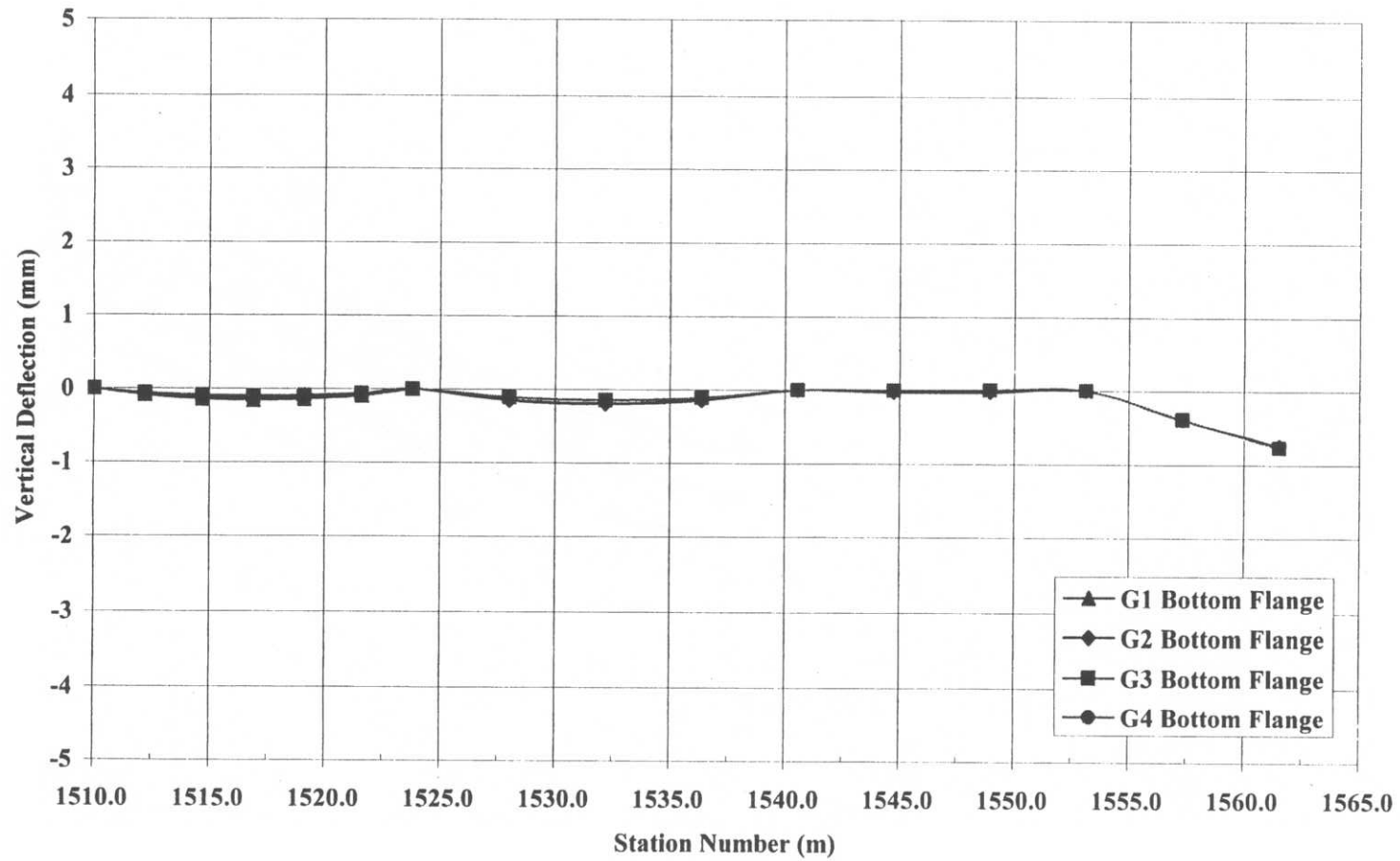
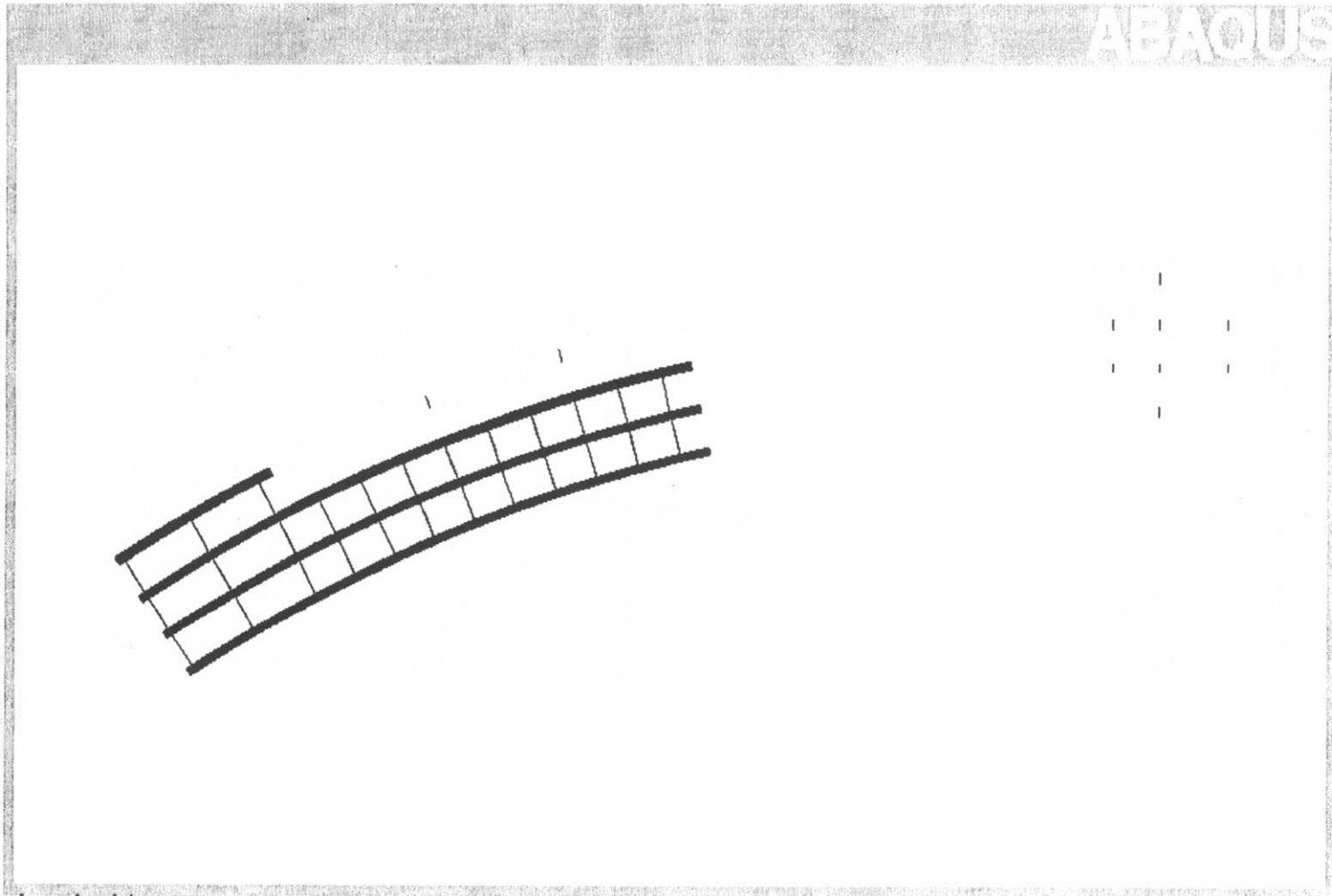


Figure C-30 Construction stage 6 - Vertical displacement, centerline of bottom flange



**Figure C-31** Construction stage 7 - Plan view of finite element model

**Deflections - Out-of-Plane (Radial) (mm)**

	Abutment 1	Field Splice 1 Section 1	Field Splice 1 Section 2	Field Splice 2 Section 2	Field Splice 2 Section 3	Field Splice 3 Section 3	Field Splice 3 Section 4	Field Splice 4 Section 4
G1 - Bottom Flange	0.0091 0.0503	0.0549 -0.0084						
G1 - Top Flange								
G2 - Bottom Flange	0.0088 0.0378	0.0080 0.0297	0.0080 0.0297	-0.0730 0.0397				
G2 - Top Flange								
G3 - Bottom Flange	0.0002 0.0312	0.0022 0.0140	0.0022 0.0140	-0.0852 0.0364				
G3 - Top Flange								
G4 - Bottom Flange	-0.0030 0.0233	0.0032 -0.0036	0.0032 -0.0036	-0.0894 0.0302				
G4 - Top Flange								

**Deflections - Vertical (mm)**

	Abutment 1	Field Splice 1 Section 1	Field Splice 1 Section 2	Field Splice 2 Section 2	Field Splice 2 Section 3	Field Splice 3 Section 3	Field Splice 3 Section 4	Field Splice 4 Section 4
G1 - Bottom Flange	-0.0016 -0.0157	-0.0062 -0.0090						
G1 - Top Flange								
G2 - Bottom Flange	0.0017 -0.0101	-0.0810 -0.0859	-0.0810 -0.0859	-0.9886 -0.9878				
G2 - Top Flange								
G3 - Bottom Flange	0.0012 -0.0102	-0.0666 -0.0709	-0.0666 -0.0709	-0.9838 -0.9841				
G3 - Top Flange								
G4 - Bottom Flange	0.0014 -0.0103	-0.0745 -0.0787	-0.0745 -0.0787	-0.9213 -0.9209				
G4 - Top Flange								

**Vertical - Support Reactions (kN)**

	Abutment 1	Falsework 1	Falsework 2A	Falsework 2	Pier Bracket at XF 26	Pier 1	Pier Bracket at XF 28
G1	182.2	175.3					
G2	98.1	294.6	231.5	420.7			
G3	93.7	260.0	166.8	322.0			
G4	81.4	194.7	122.3	257.6			

**Vertical Support Reactions (kips)**

	Abutment 1	Falsework 1	Falsework 2A	Falsework 2	Pier Bracket at XF 26	Pier 1	Pier Bracket at XF 28
G1	41.0	39.4					
G2	22.1	66.2	52.0	94.6			
G3	21.1	58.4	37.5	72.4			
G4	18.3	43.8	27.5	57.9			

**Cross-frame Vertical Reactions**

	(kN)	(kip)
XF 11B (outside)	0.000	0.000
XF 11C (inside)	0.000	0.000
XF 14B (outside)	0.000	0.000
XF 14C (inside)	0.000	0.000

**Figure C-32** Construction stage 7 – Field-splice location deflections and support reactions summary

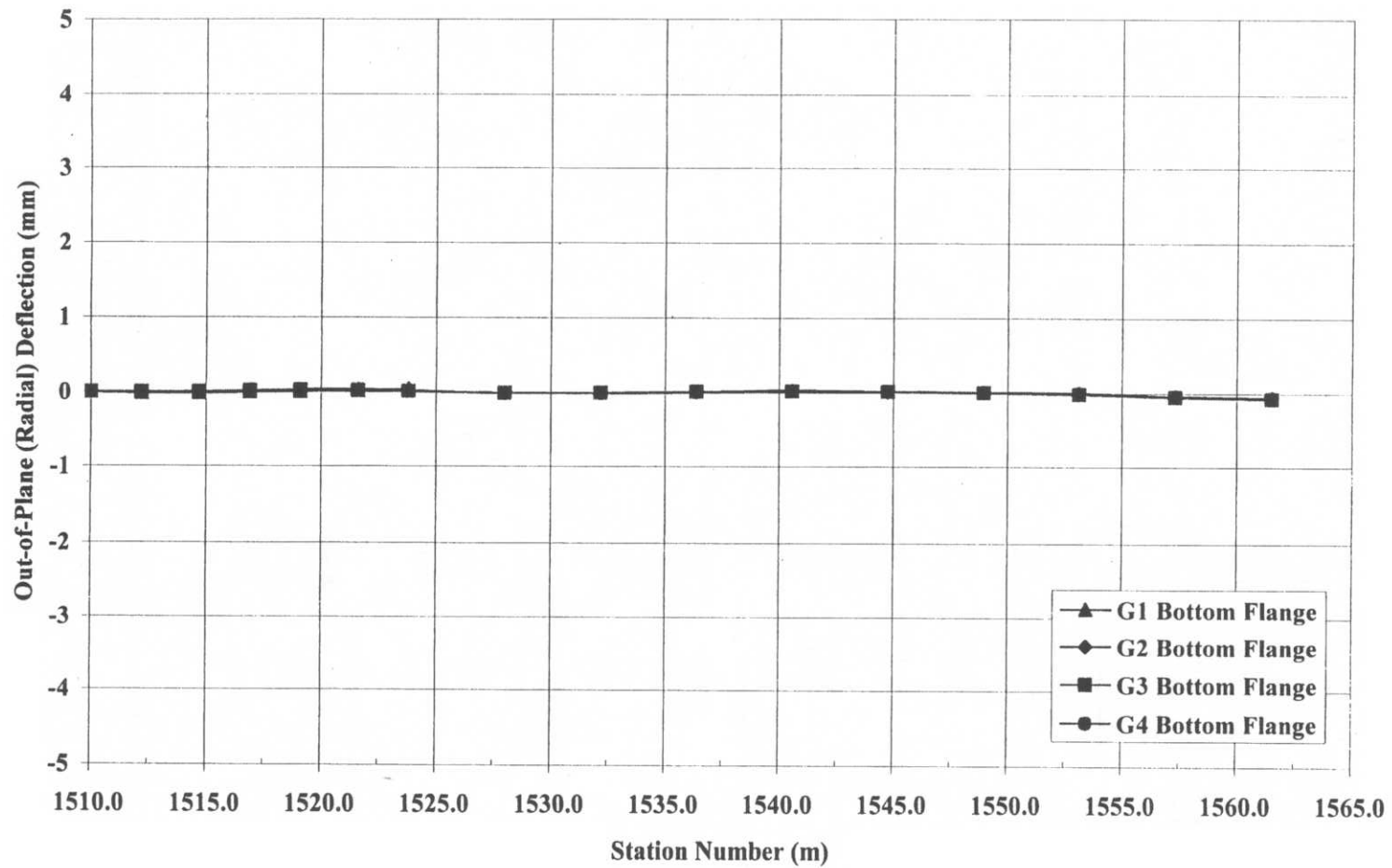


Figure C- 33 Construction stage 7 – Out-of-plane (radial) displacement, centerline of bottom flange

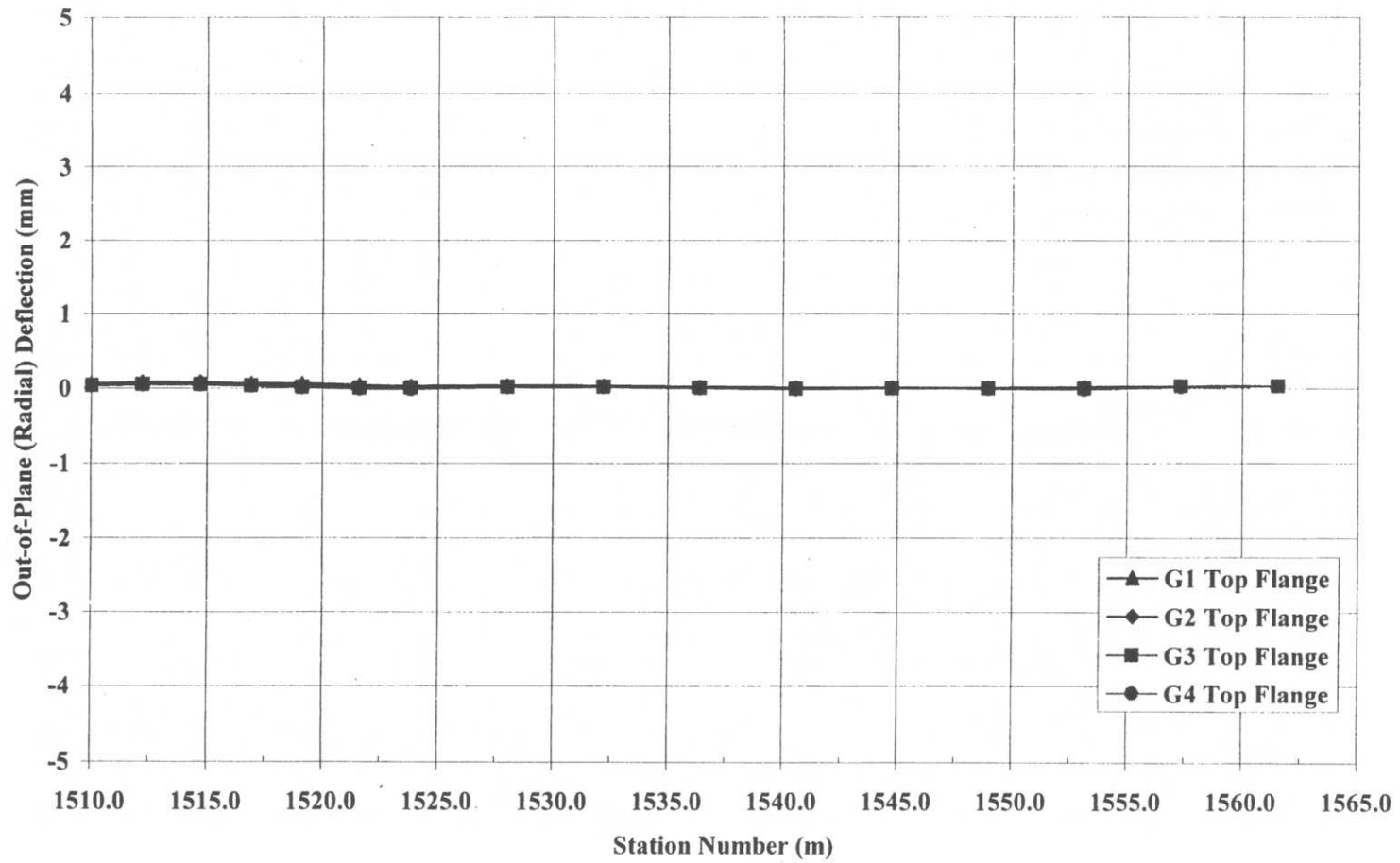


Figure C-34 Construction stage 7 – Out-of-plane (radial) displacement, centerline of top flange

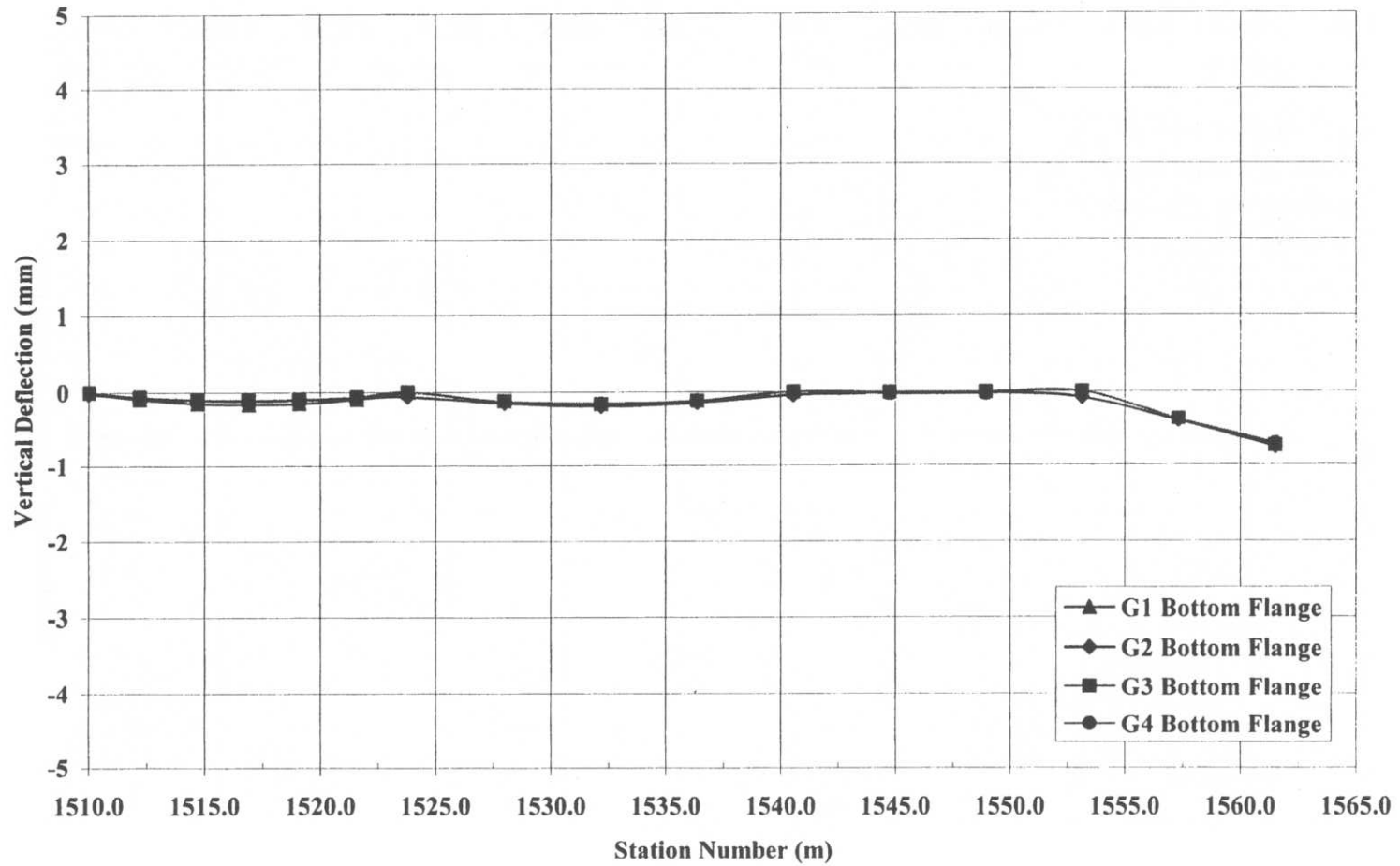
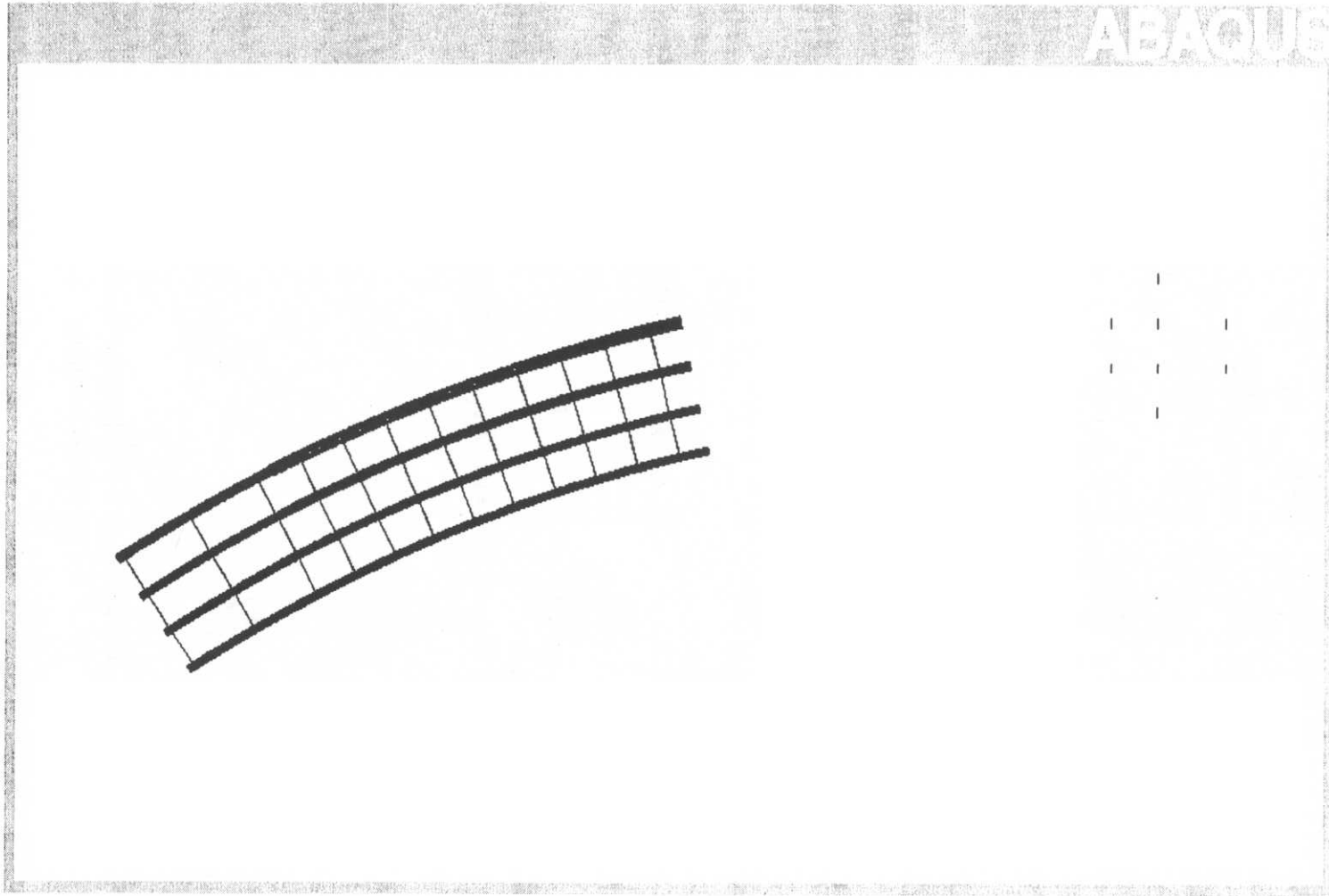


Figure C-35 Construction stage 7 – Vertical displacement, centerline of bottom flange



**Figure C-36** Construction stage 8 – Plan view of finite element model

**Deflections - Out-of-Plane (Radial) (mm)**

	Abutment 1	Field Splice 1 Section 1	Field Splice 1 Section 2	Field Splice 2 Section 2	Field Splice 2 Section 3	Field Splice 3 Section 3	Field Splice 3 Section 4	Field Splice 4 Section 4
G1- Bottom Flange	0.0046	0.0037	0.0037	-0.0283				
G1- Top Flange	0.0429	0.0482	0.0482	0.1112				
G2 - Bottom Flange	0.0061	0.0070	0.0070	-0.0248				
G2 - Top Flange	0.0353	0.0391	0.0391	0.1046				
G3 - Bottom Flange	0.0002	0.0069	0.0069	-0.0369				
G3 - Top Flange	0.0316	0.0209	0.0209	0.1016				
G4 - Bottom Flange	0.0002	0.0107	0.0107	-0.0395				
G4 - Top Flange	0.0263	0.0048	0.0048	0.0952				

**Deflections - Vertical (mm)**

	Abutment 1	Field Splice 1 Section 1	Field Splice 1 Section 2	Field Splice 2 Section 2	Field Splice 2 Section 3	Field Splice 3 Section 3	Field Splice 3 Section 4	Field Splice 4 Section 4
G1- Bottom Flange	-0.0018	-0.1071	-0.1071	-1.0550				
G1- Top Flange	-0.0121	-0.1144	-0.1144	-1.0540				
G2 - Bottom Flange	0.0016	-0.0806	-0.0806	-1.0110				
G2 - Top Flange	-0.0101	-0.0855	-0.0855	-1.0110				
G3 - Bottom Flange	0.0012	-0.0660	-0.0660	-0.9869				
G3 - Top Flange	-0.0102	-0.0704	-0.0704	-0.9872				
G4 - Bottom Flange	0.0014	-0.0743	-0.0743	-0.9094				
G4 - Top Flange	-0.0103	-0.0784	-0.0784	-0.9090				

**Vertical - Support Reactions (kN)**

	Abutment 1	Falsework 1	Falsework 2A	Falsework 2	Pier Bracket at XF 26	Pier 1	Pier Bracket at XF 28
G1	155.1	387.2	307.6	538.1			
G2	97.0	297.0	240.3	454.5			
G3	94.3	258.5	164.6	320.7			
G4	82.0	194.4	121.0	253.0			

**Vertical Support Reactions (kips)**

	Abutment 1	Falsework 1	Falsework 2A	Falsework 2	Pier Bracket at XF 26	Pier 1	Pier Bracket at XF 28
G1	34.9	87.0	69.2	121.0			
G2	21.8	66.8	54.0	102.2			
G3	21.2	58.1	37.0	72.1			
G4	18.4	43.7	27.2	56.9			

**Cross-frame Vertical Reactions**

	(kN)	(kip)
XF 11B (outside)	0.000	0.000
XF 11C (inside)	0.000	0.000
XF 14B (outside)	0.000	0.000
XF 14C (inside)	0.000	0.000

**Figure C-37** Construction stage 8 – Field-splice location deflections and support reactions summary

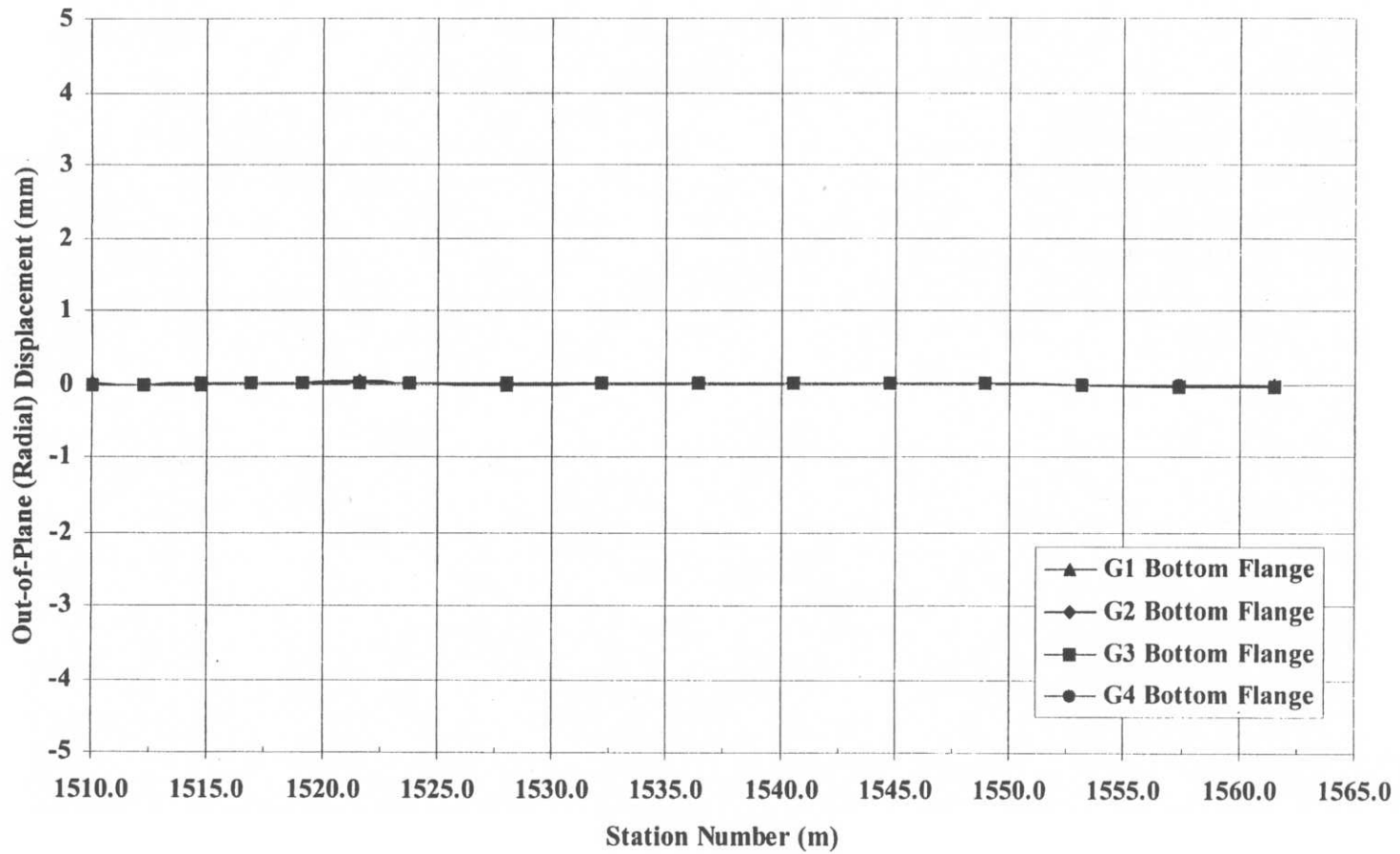


**Figure C-38** Construction stage 8 – Out-of-plane (radial) displacement, centerline of bottom flange

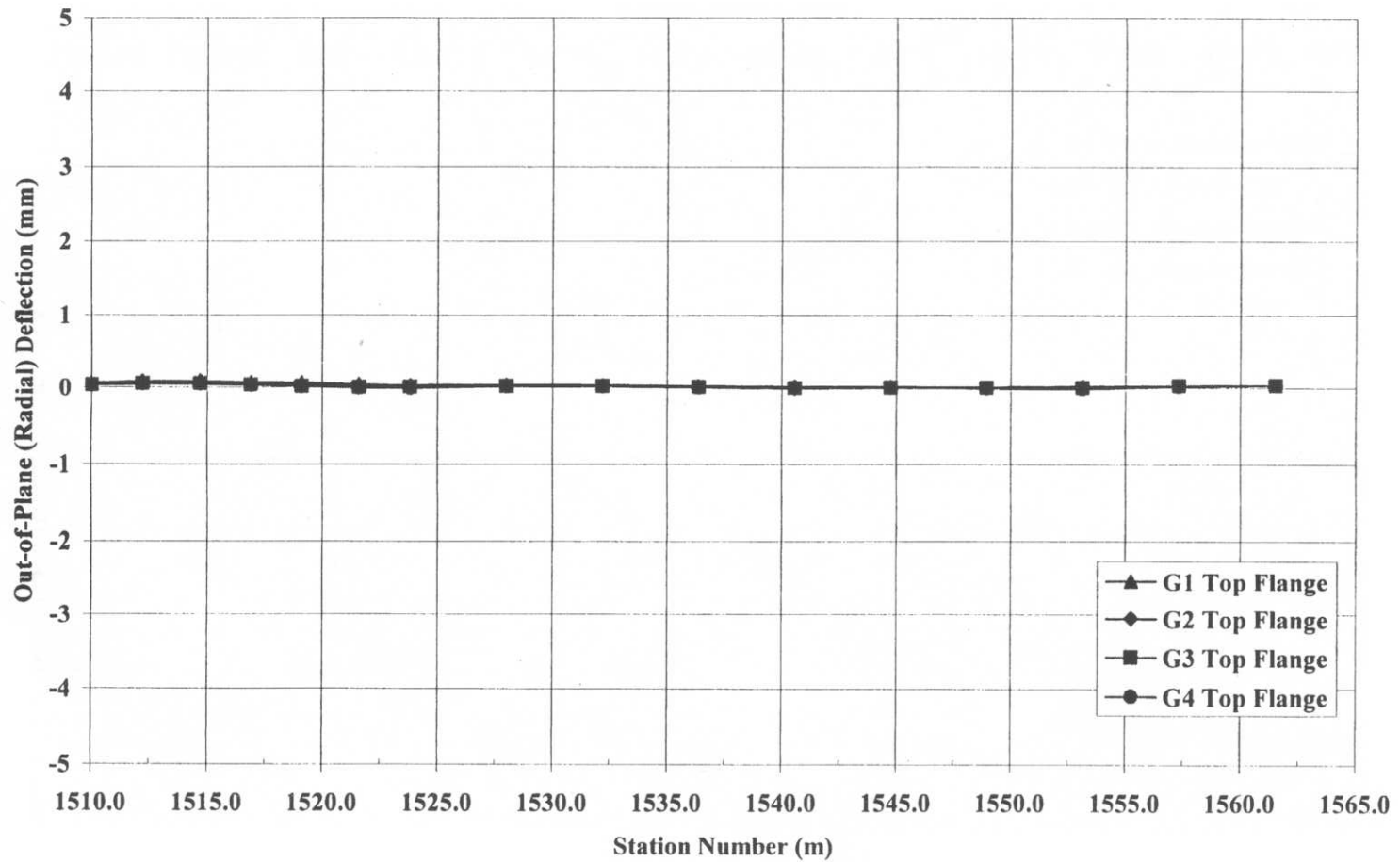


**Figure C-39** Construction stage 8 – Out-of-plane (radial) displacement, centerline of top flange

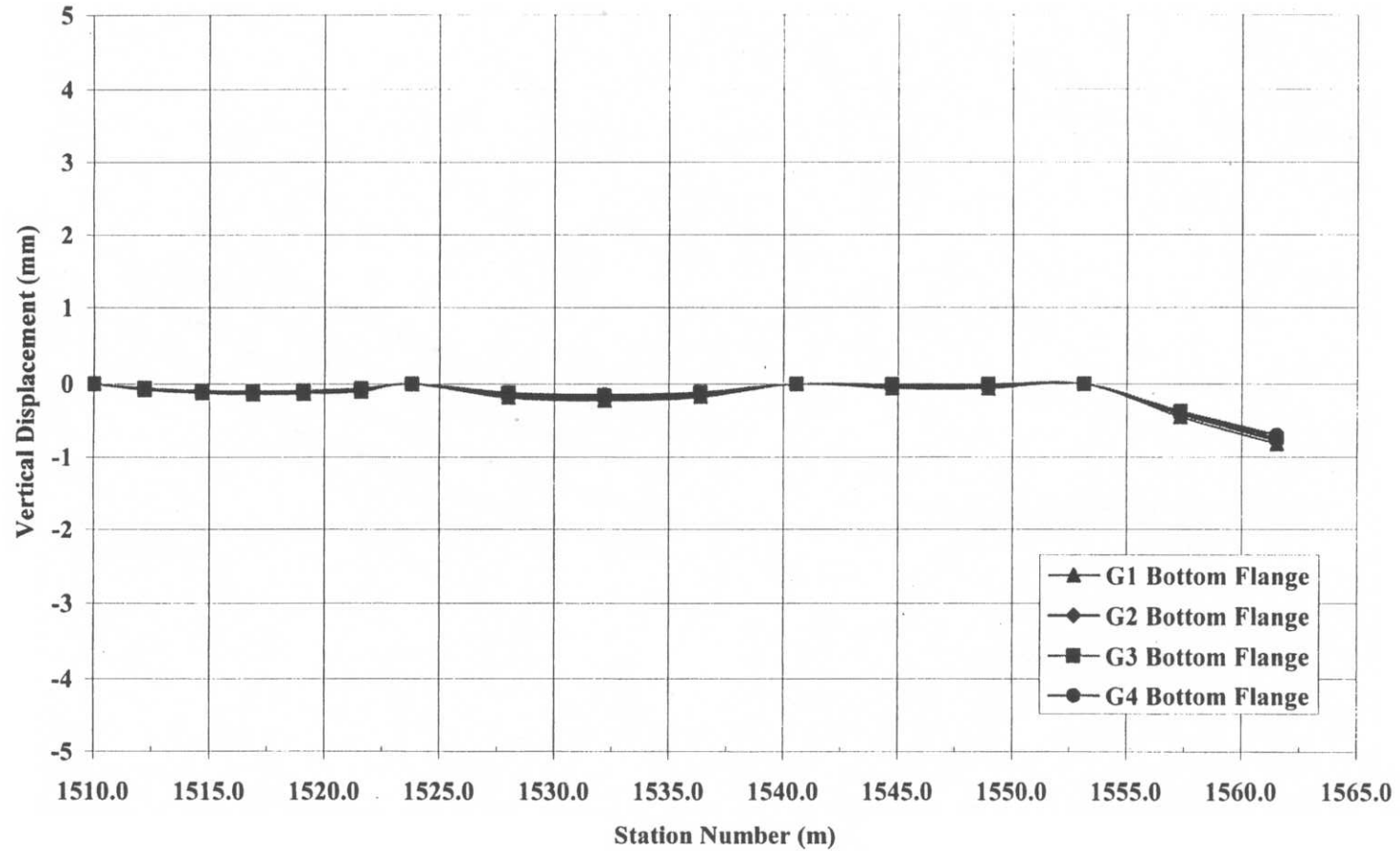


**Figure C-40** Construction stage 8 - Vertical displacement, centerline of bottom flange

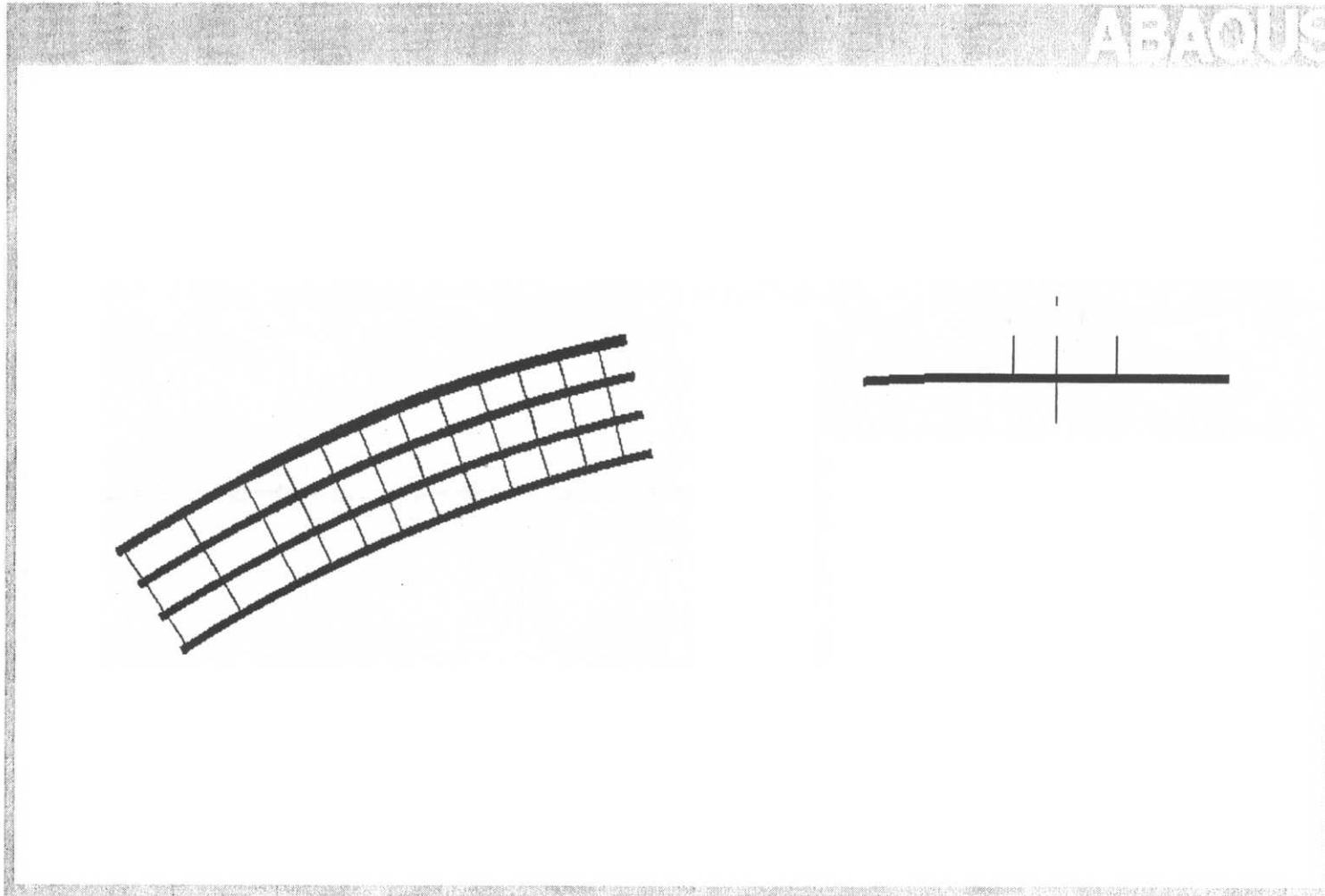


**Figure C-41** Construction stage 9 - Plan view of finite element model

**Deflections - Out-of-Plane (Radial) (mm)**

	Abutment 1	Field Splice 1 Section 1	Field Splice 1 Section 2	Field Splice 2 Section 2	Field Splice 2 Section 3	Field Splice 3 Section 3	Field Splice 3 Section 4	Field Splice 4 Section 4
G1- Bottom Flange	0.0047	0.0038	0.0038	-0.0283				
G1- Top Flange	0.0429	0.0482	0.0482	0.1112				
G2 - Bottom Flange	0.0061	0.0070	0.0070	-0.0248				
G2 - Top Flange	0.0353	0.0391	0.0391	0.1046				
G3 - Bottom Flange	0.0002	0.0069	0.0069	-0.0369			4.7510	-0.5151
G3 - Top Flange	0.0316	0.0209	0.0209	0.1046			-13.8500	5.1580
G4 - Bottom Flange	0.0002	0.0107	0.0107	-0.0359				
G4 - Top Flange	0.0263	0.0048	0.0048	0.0952				

**Deflections - Vertical (mm)**

	Abutment 1	Field Splice 1 Section 1	Field Splice 1 Section 2	Field Splice 2 Section 2	Field Splice 2 Section 3	Field Splice 3 Section 3	Field Splice 3 Section 4	Field Splice 4 Section 4
G1- Bottom Flange	-0.0021	-0.1071	-0.1071	-1.0550				
G1- Top Flange	-0.0121	-0.1144	-0.1144	-1.0540				
G2 - Bottom Flange	0.0016	-0.0806	-0.0806	-1.0110				
G2 - Top Flange	-0.0101	-0.0855	-0.0855	-1.0110				
G3 - Bottom Flange	0.0012	-0.0660	-0.0660	-0.9869			-11.3800	5.1310
G3 - Top Flange	-0.0102	-0.0704	-0.0704	-0.9872			-11.4200	5.1270
G4 - Bottom Flange	0.0015	-0.0743	-0.0743	-0.9094				
G4 - Top Flange	-0.0103	-0.0784	-0.0784	-0.9090				

**Vertical - Support Reactions (kN)**

	Abutment 1	Falsework 1	Falsework 2A	Falsework 2	Pier Bracket at XF 26	Pier 1	Pier Bracket at XF 28
G1	157.0	387.2	307.6	538.1			
G2	97.0	297.0	240.3	454.5			
G3	94.3	258.5	164.6	320.7	155.8	573.7	0.0
G4	82.0	194.4	121.0	253.0			

**Vertical Support Reactions (kips)**

	Abutment 1	Falsework 1	Falsework 2A	Falsework 2	Pier Bracket at XF 26	Pier 1	Pier Bracket at XF 28
G1	35.3	87.0	69.2	121.0			
G2	21.8	66.8	54.0	102.2			
G3	21.2	58.1	37.0	72.1	35.0	129.0	0.0
G4	18.4	43.7	27.2	56.9			

**Cross-frame Vertical Reactions**

	(kN)	(kips)
XF 26B (outside)	-1.888	-0.4244
XF 27B (outside)	9.342	2.1002
XF 27C (inside)	10.135	2.2784
XF 28B (outside)	2.699	0.6068

**Figure C-42** Construction stage 9 – Field-splice location deflections and support reactions summary

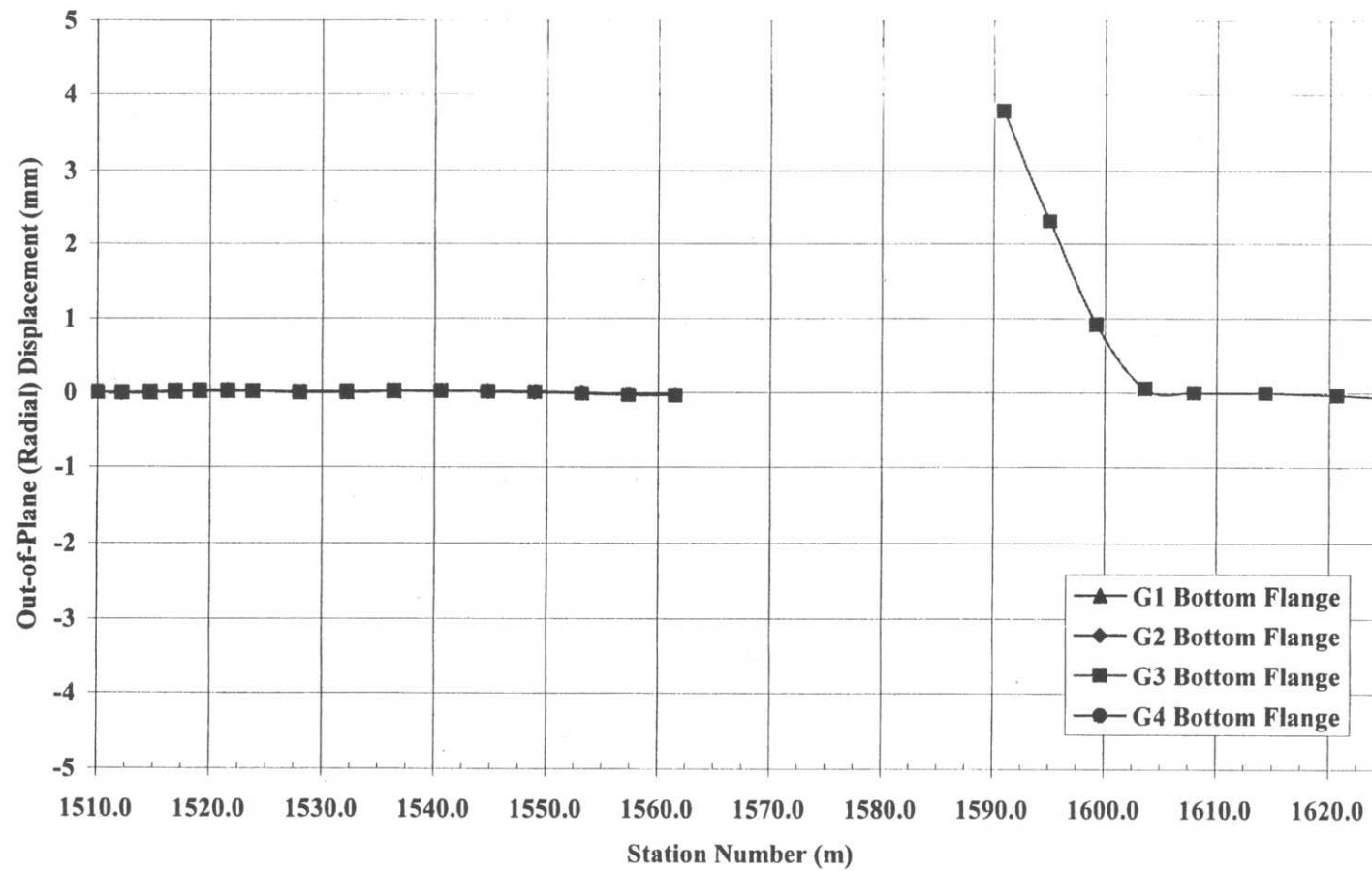
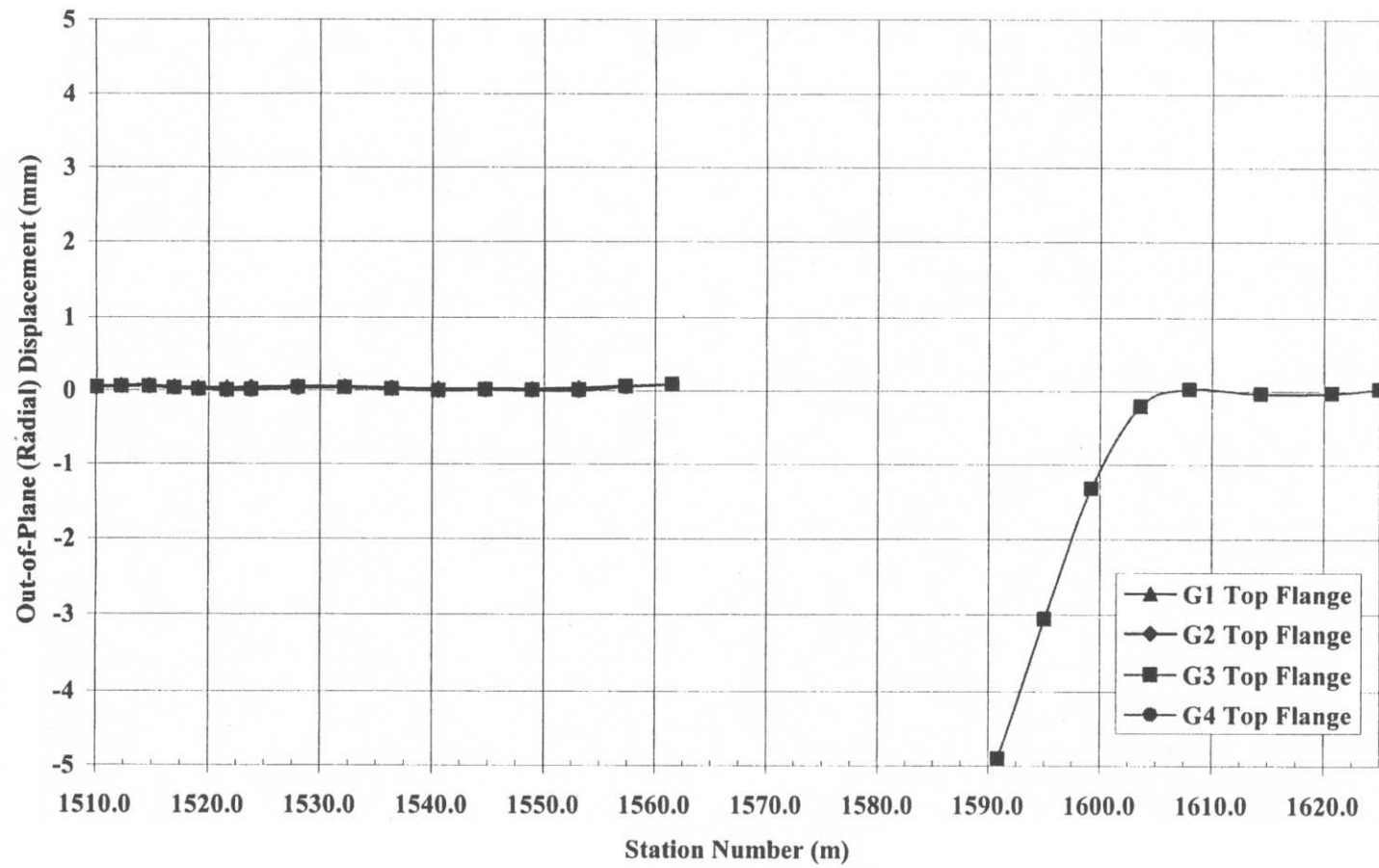


Figure C-43 Construction stage 9 – Out-of-plane (radial) displacement, centerline of bottom flange



**Figure C-44** Construction stage 9 – Out-of-plane (radial) displacement, centerline of top flange

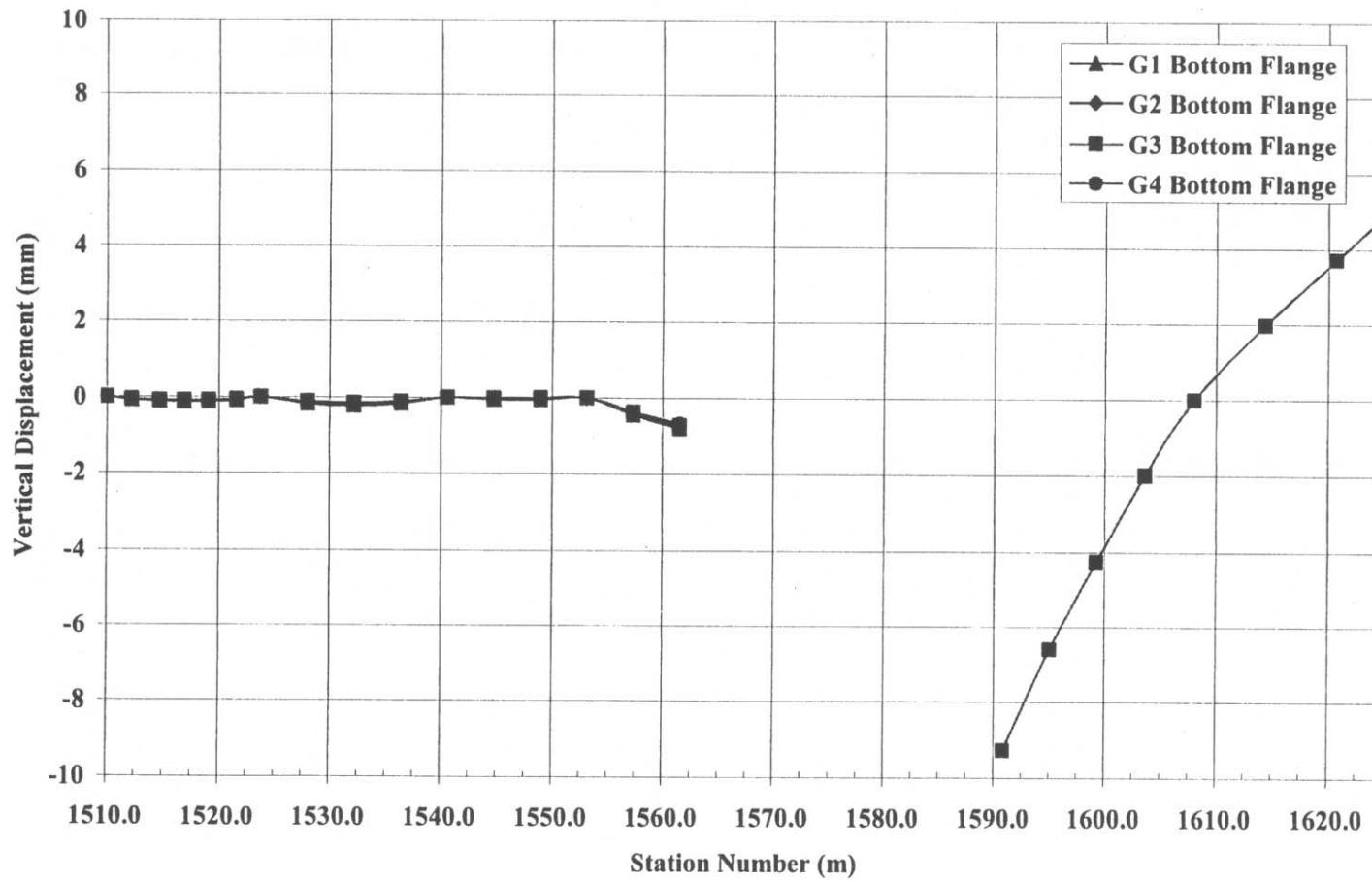
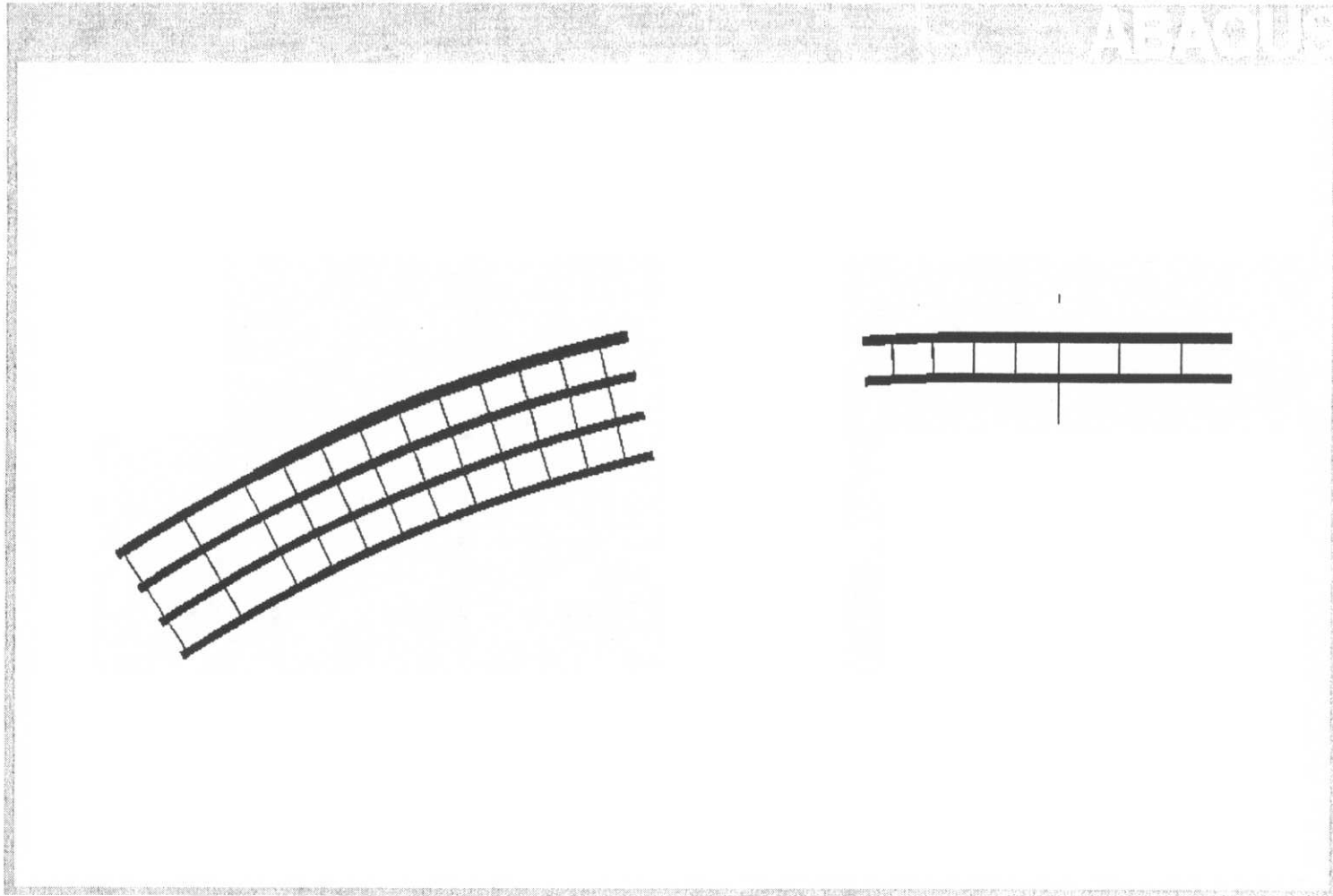


Figure C-45 Construction stage 9 - Vertical displacement, centerline of bottom flange



**Figure C-46** Construction stage 10 - Plan view of finite element model

**Deflections - Out-of-Plane (Radial) (mm)**

	Abutment 1	Field Splice 1	Field Splice 1	Field Splice 2	Field Splice 2	Field Splice 3	Field Splice 3	Field Splice 4
		Section 1	Section 2	Section 2	Section 3	Section 3	Section 4	Section 4
G1- Bottom Flange	0.0048	0.0038	0.0038	-0.0283				
G1- Top Flange	0.0429	0.0482	0.0482	0.1112				
G2 - Bottom Flange	0.0061	0.0070	0.0070	-0.0248			0.0557	-0.0133
G2 - Top Flange	0.0353	0.0391	0.0391	0.1046			-0.0793	0.1469
G3 - Bottom Flange	0.0002	0.0069	0.0069	-0.0369			0.0675	-0.0232
G3 - Top Flange	0.0316	0.0209	0.0209	0.1016			-0.0757	0.1945
G4 - Bottom Flange	0.0002	0.0107	0.0107	-0.0395				
G4 - Top Flange	0.0263	0.0048	0.0048	0.0952				

**Deflections - Vertical (mm)**

	Abutment 1	Field Splice 1	Field Splice 1	Field Splice 2	Field Splice 2	Field Splice 3	Field Splice 3	Field Splice 4
		Section 1	Section 2	Section 2	Section 3	Section 3	Section 4	Section 4
G1- Bottom Flange	-0.0026	-0.1071	-0.1071	-1.0550				
G1- Top Flange	-0.0122	-0.1144	-0.1144	-1.0540				
G2 - Bottom Flange	0.0016	-0.0806	-0.0806	-1.0110			-1.3440	-3.1490
G2 - Top Flange	-0.0101	-0.0855	-0.0855	-1.0110			-1.3450	-3.1480
G3 - Bottom Flange	0.0012	-0.0660	-0.0660	-0.9869			-1.4690	-2.9830
G3 - Top Flange	-0.0102	-0.0704	-0.0704	-0.9872			-1.4690	-2.9830
G4 - Bottom Flange	0.0015	-0.0743	-0.0743	-0.9094				
G4 - Top Flange	-0.0103	-0.0784	-0.0784	-0.9090				

**Vertical - Support Reactions (kN)**

	Abutment 1	Falsework 1	Falsework 2A	Falsework 2	Pier Bracket at XF 26	Pier 1	Pier Bracket at XF 28
G1	158.0	387.1	307.6	538.1			
G2	97.0	297.0	240.3	454.5	156.7	658.3	0.0
G3	94.3	258.5	164.6	320.7	185.4	562.5	0.0
G4	82.0	194.4	121.0	253.0			

**Vertical Support Reactions (kips)**

	Abutment 1	Falsework 1	Falsework 2A	Falsework 2	Pier Bracket at XF 26	Pier 1	Pier Bracket at XF 28
G1	35.7	87.0	69.2	121.0			
G2	21.8	66.8	54.0	102.2	35.2	148.0	0.0
G3	21.2	58.1	37.0	72.1	41.7	126.5	0.0
G4	18.4	43.7	27.2	56.9			

**Cross-frame Vertical Reactions**

	(kN)	(kips)
XF 26B (outside)	0.000	0.0000
XF 27B (outside)	0.000	0.0000
XF 27C (inside)	8.311	1.8684
XF 28B (outside)	0.000	0.0000

**Figure C-47** Construction stage 10 – Field-splice location deflections and support reactions summary

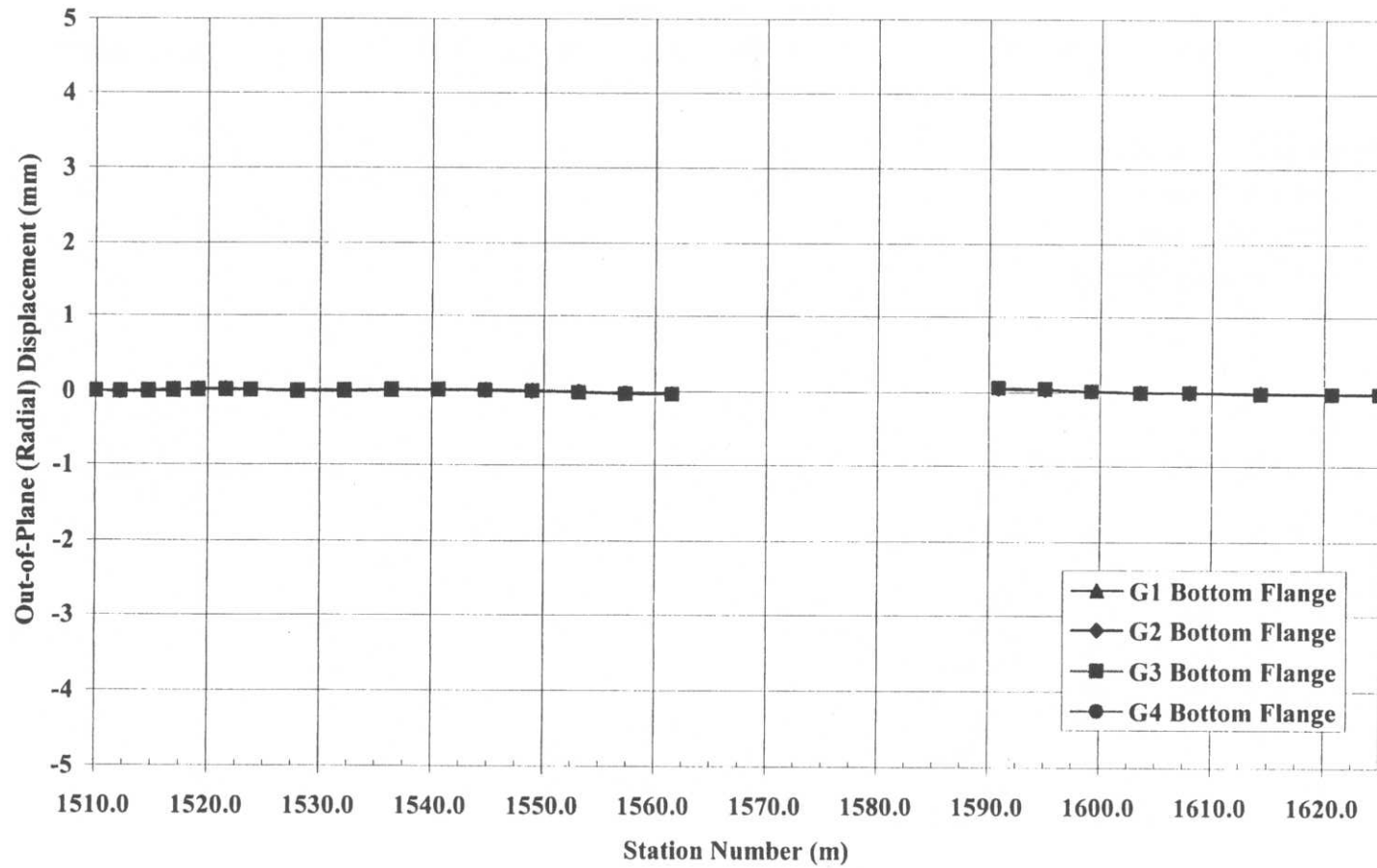


**Figure C-48** Construction stage 10 – Out-of-plane (radial) displacement, centerline of bottom flange

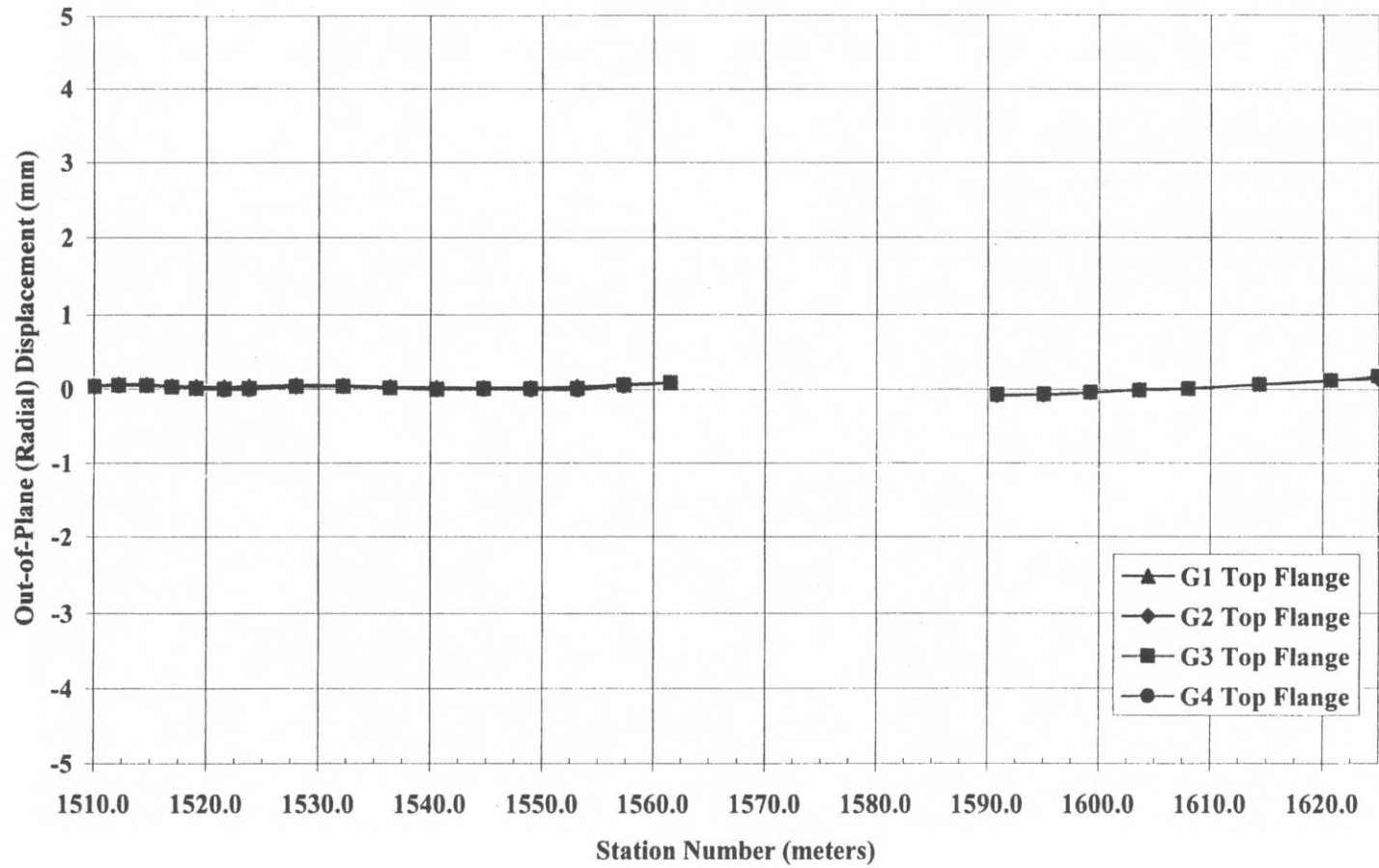


**Figure C-49** Construction stage 10 – Out-of-plane (radial) displacement, centerline of top flange

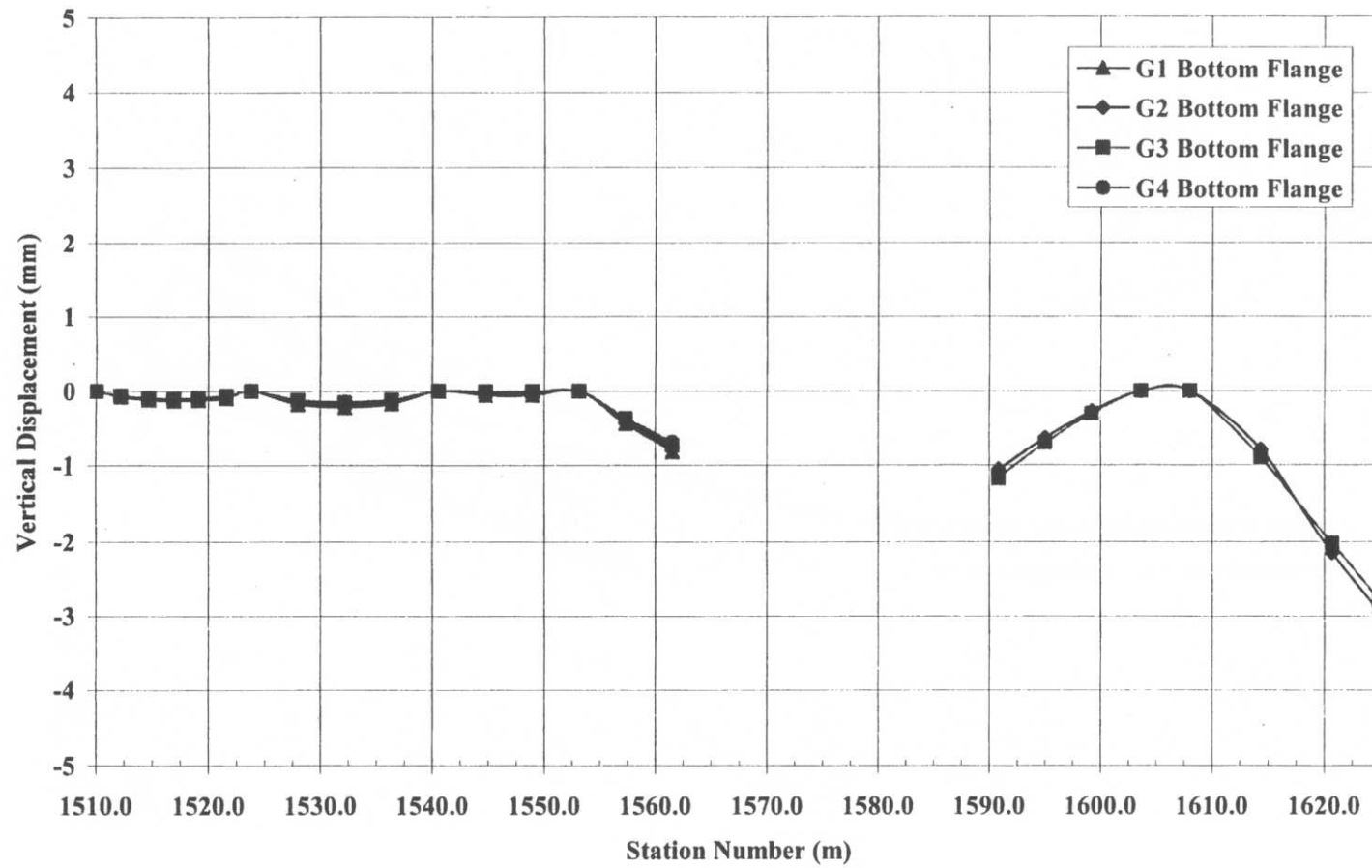
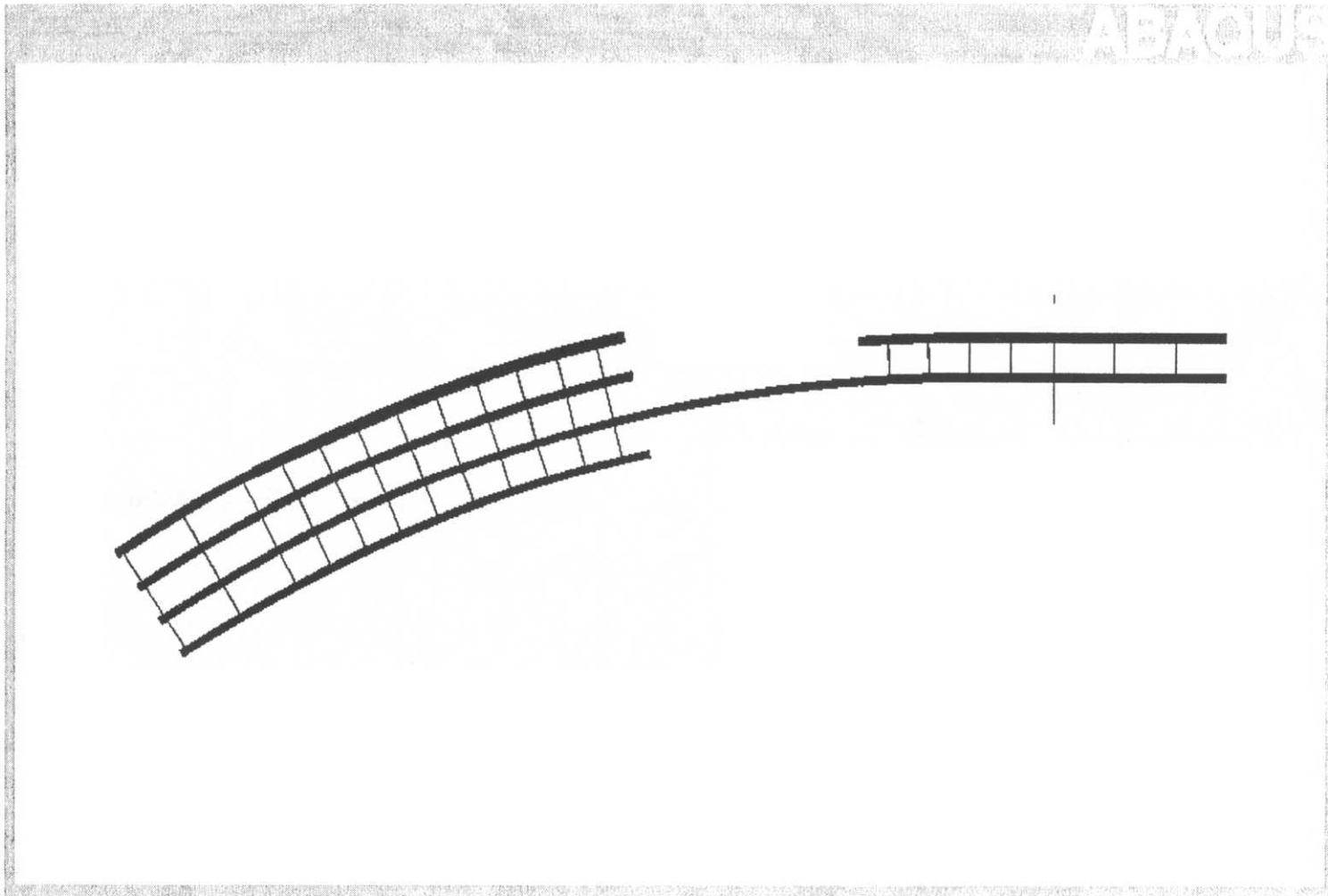


Figure C-50 Construction stage 10 - Vertical displacement, centerline of bottom flange



**Figure C - 51** Construction 11 – Plane view of finite element model

**Deflections - Out-of-Plane (Radial) (mm)**

	Abutment 1	Field Splice 1 Section 1	Field Splice 1 Section 2	Field Splice 2 Section 2	Field Splice 2 Section 3	Field Splice 3 Section 3	Field Splice 3 Section 4	Field Splice 4 Section 4
G1 - Bottom Flange	-0.0016	0.0007	0.0007	0.3342				
G1 - Top Flange	0.0365	0.0443	0.0443	-0.2131				
G2 - Bottom Flange	0.0015	0.0052	0.0052	0.3306			0.6572	-0.1805
G2 - Top Flange	0.0307	0.0368	0.0368	-0.1704			-1.3350	0.8125
G3 - Bottom Flange	0.0002	0.0071	0.0071	-1.4150	-1.4150	-0.7894	-0.7894	-0.2163
G3 - Top Flange	0.0319	0.0222	0.0222	1.5320	1.5320	0.6908	0.6908	0.8428
G4 - Bottom Flange	-0.0090	0.0042	0.0042	-0.1192				
G4 - Top Flange	0.0173	-0.0010	-0.0010	0.3200				

**Deflections - Vertical (mm)**

	Abutment 1	Field Splice 1 Section 1	Field Splice 1 Section 2	Field Splice 2 Section 2	Field Splice 2 Section 3	Field Splice 3 Section 3	Field Splice 3 Section 4	Field Splice 4 Section 4
G1 - Bottom Flange	-0.0026	-0.1070	-0.1070	-1.1010				
G1 - Top Flange	-0.0122	-0.1142	-0.1142	-1.1000				
G2 - Bottom Flange	0.0016	-0.0813	-0.0813	-1.7250			-1.8000	-2.9980
G2 - Top Flange	-0.0101	-0.0863	-0.0863	-1.7240			-1.8010	-2.9970
G3 - Bottom Flange	0.0013	-0.0680	-0.0680	-2.9080	-2.9080	-3.9240	-3.9240	-2.0140
G3 - Top Flange	-0.0101	-0.0725	-0.0725	-2.9060	-2.9060	-3.9260	-3.9260	-2.0140
G4 - Bottom Flange	0.0015	-0.0752	-0.0752	-2.1590				
G4 - Top Flange	-0.0103	-0.0793	-0.0793	-2.1580				

**Vertical - Support Reactions (kN)**

	Abutment 1	Falsework 1	Falsework 2A	Falsework 2	Pier Bracket at XF 26	Pier 1	Pier Bracket at XF 28
G1	158.7	386.9	302.7	539.5			
G2	97.0	299.3	169.6	602.1	213.7	597.8	0.0
G3	93.9	263.2	57.5	446.4	681.6	216.8	0.0
G4	82.1	196.6	42.6	453.3			

**Vertical Support Reactions (kips)**

	Abutment 1	Falsework 1	Falsework 2A	Falsework 2	Pier Bracket at XF 26	Pier 1	Pier Bracket at XF 28
G1	35.7	87.0	68.1	121.3			
G2	21.8	67.3	38.1	135.4	48.1	134.4	0.0
G3	21.1	59.2	12.9	100.3	153.2	48.7	0.0
G4	18.4	44.2	9.6	101.9			

**Cross-frame Vertical Reactions**

	(kN)	(kips)
XF 26B (outside)	0.000	0.0000
XF 27B (outside)	0.000	0.0000
XF 27C (inside)	-1.113	-0.2502
XF 28B (outside)	0.000	0.0000

**Figure C-52** Construction stage 11 – Field-splice location deflections and support reactions summary

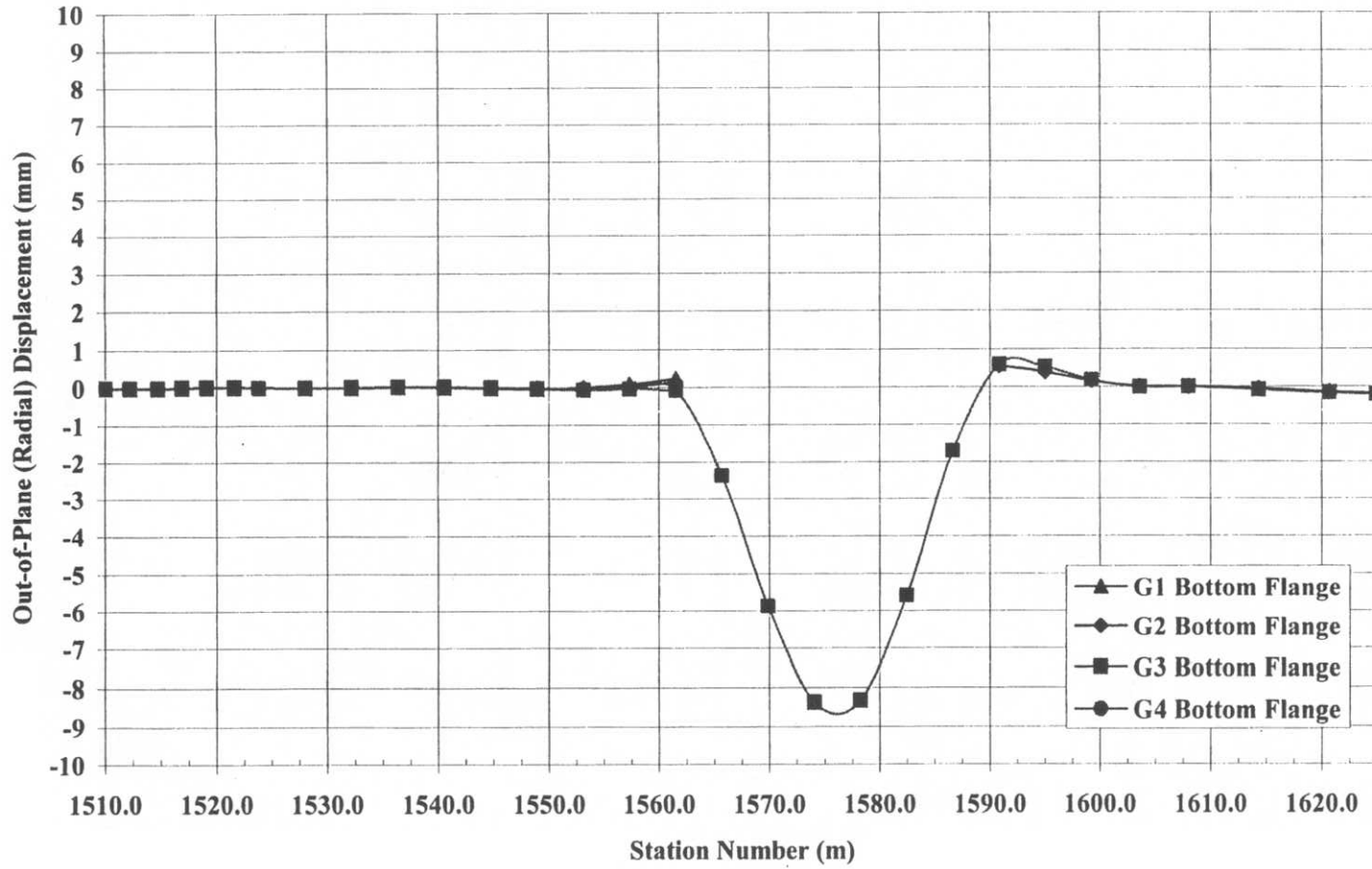


**Figure C-53** Construction stage 11 – Out-of-plane (radial) displacement, centerline of bottom flange

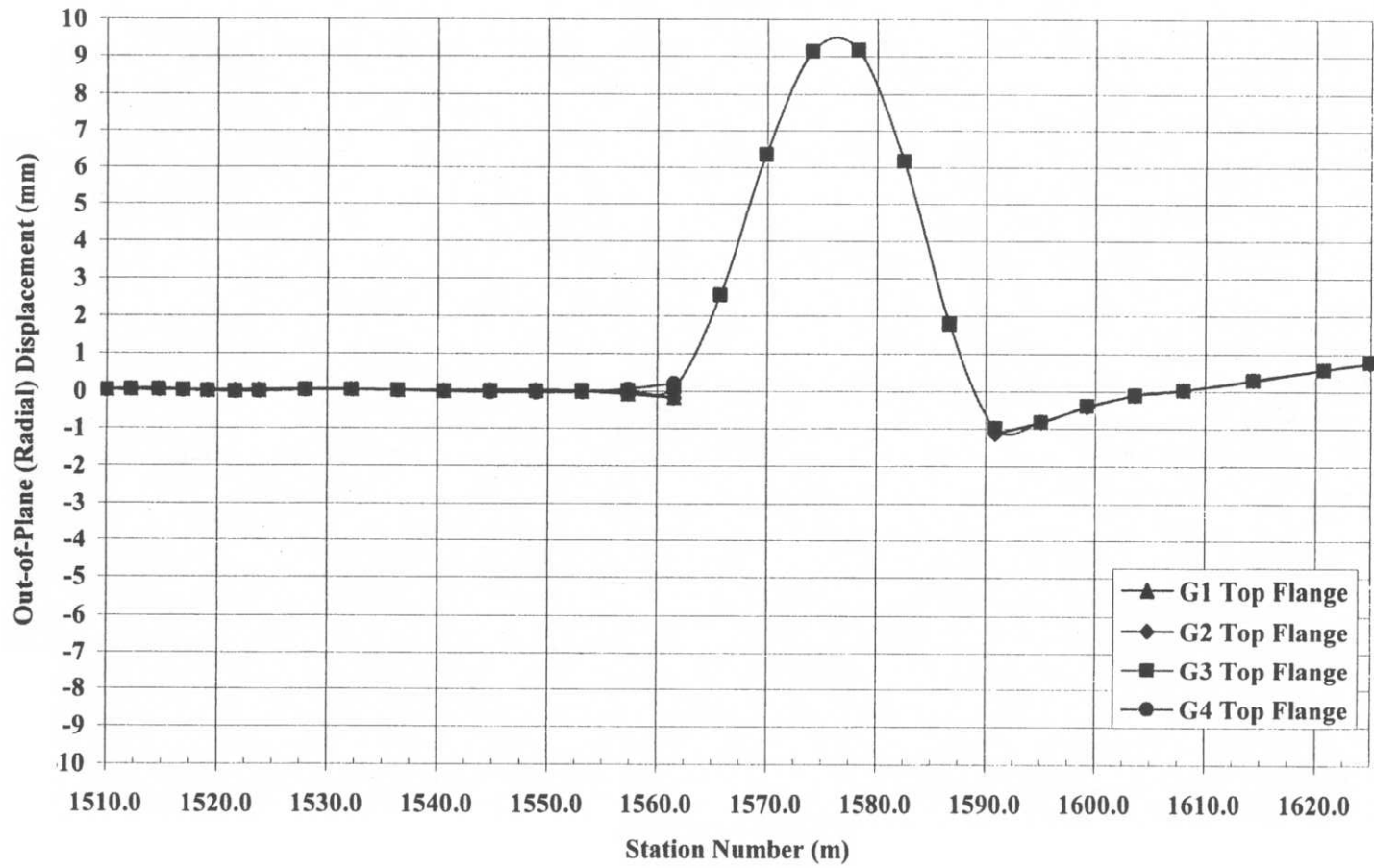


Figure C-54 Construction stage 11 – Out-of-plane (radial) displacement, centerline of top flange

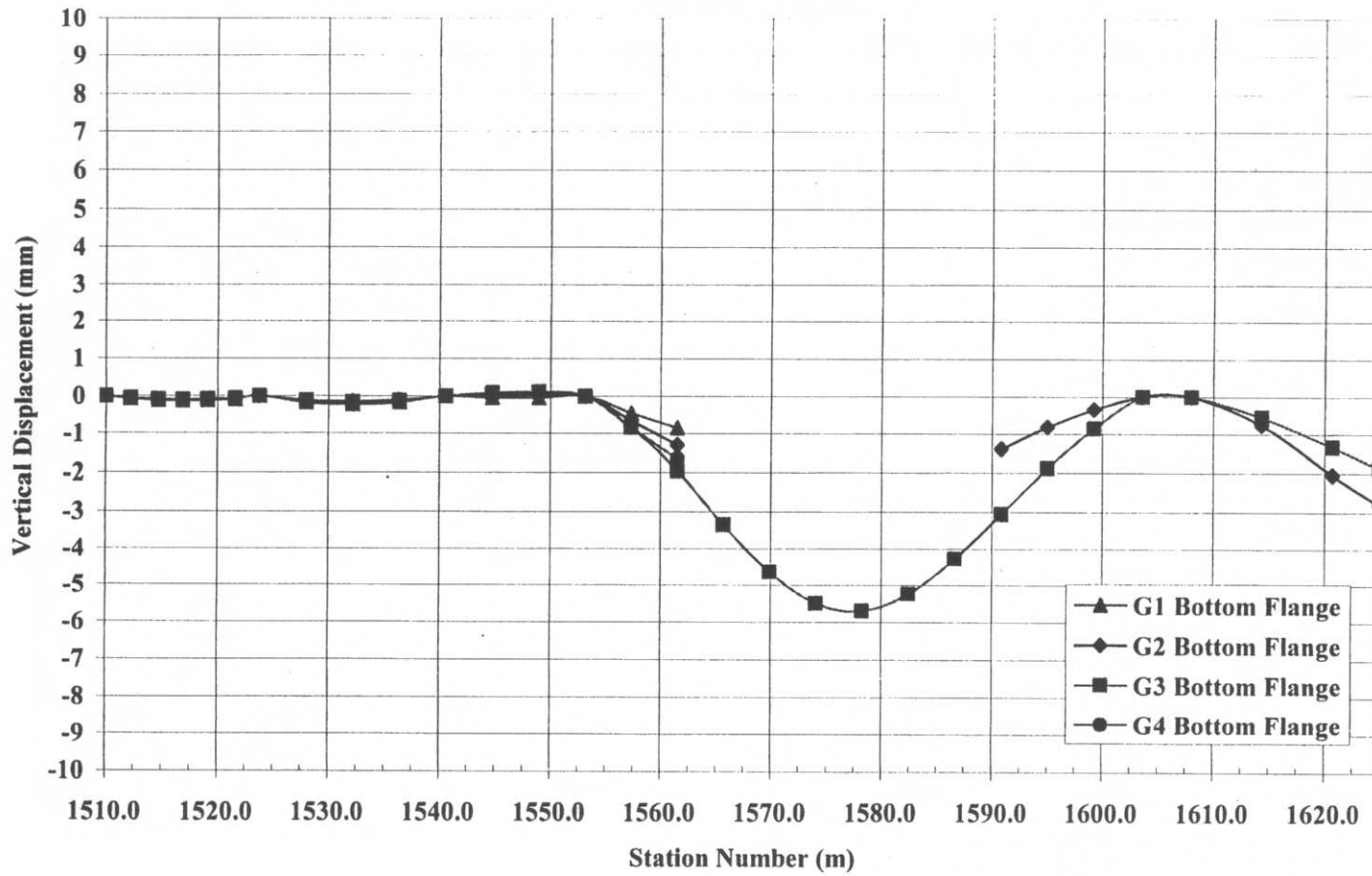
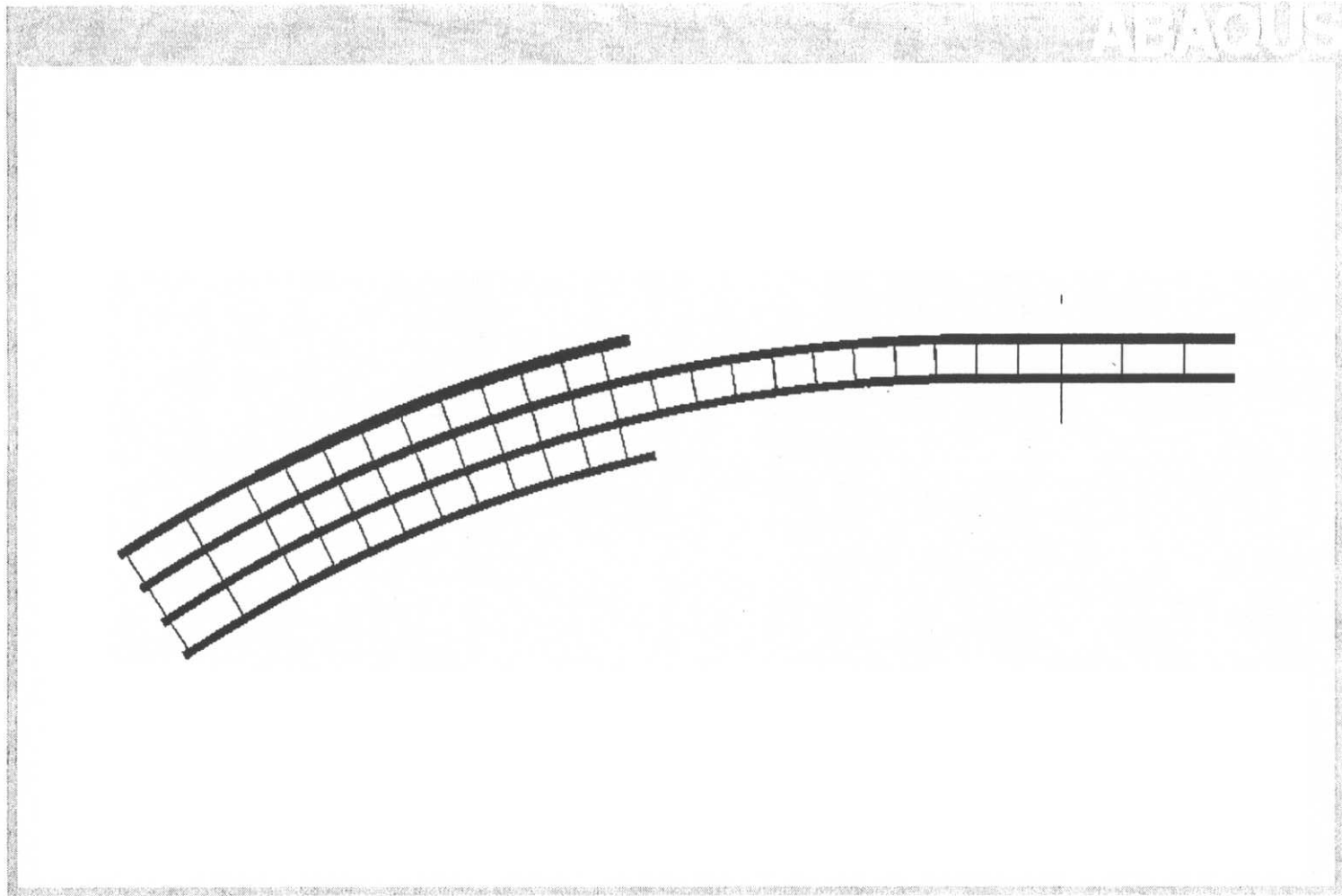


Figure C-55 Construction stage 11 - Vertical displacement, centerline of bottom flange



**Figure C-56** Construction stage 12 – Plan view of finite element model

**Deflections - Out-of-Plane (Radial) (mm)**

	Abutment 1	Field Splice 1	Field Splice 1	Field Splice 2	Field Splice 2	Field Splice 3	Field Splice 3	Field Splice 4
		Section 1	Section 2	Section 2	Section 3	Section 3	Section 4	Section 4
G1 - Bottom Flange	0.0004	0.0057	0.0057	0.9542				
G1 - Top Flange	0.0390	0.0463	0.0463	0.1162				
G2 - Bottom Flange	0.0136	0.0199	0.0199	0.0940	0.0940	-0.1987	-0.1987	-0.1064
G2 - Top Flange	0.0437	0.0467	0.0467	1.3430	1.3430	4.9320	4.9320	-5.5460
G3 - Bottom Flange	0.0001	0.0056	0.0056	-0.1009	-0.1009	-0.4795	-0.4795	0.0951
G3 - Top Flange	0.0282	0.0193	0.0193	1.3320	1.3320	4.5900	4.5900	-5.4020
G4 - Bottom Flange	-0.0117	0.0041	0.0041	-0.2183				
G4 - Top Flange	0.0147	-0.0019	-0.0019	1.0750				

**Deflections - Vertical (mm)**

	Abutment 1	Field Splice 1	Field Splice 1	Field Splice 2	Field Splice 2	Field Splice 3	Field Splice 3	Field Splice 4
		Section 1	Section 2	Section 2	Section 3	Section 3	Section 4	Section 4
G1 - Bottom Flange	-0.0031	-0.1030	-0.1030	-2.3850				
G1 - Top Flange	-0.0124	-0.1101	-0.1101	-2.3860				
G2 - Bottom Flange	0.0017	-0.0778	-0.0778	-4.4940	-4.4940	-10.0600	-10.0600	6.8890
G2 - Top Flange	-0.0102	-0.0826	-0.0826	-4.4870	-4.4870	-10.0600	-10.0600	6.8860
G3 - Bottom Flange	-0.0006	-0.0664	-0.0664	-3.2870	-3.2870	-5.2460	-5.2460	1.5020
G3 - Top Flange	-0.0109	-0.0703	-0.0703	-3.2850	-3.2850	-5.2490	-5.2490	1.4990
G4 - Bottom Flange	0.0015	-0.0748	-0.0748	-1.9020				
G4 - Top Flange	-0.0103	-0.0790	-0.0790	-1.9020				

**Vertical - Support Reactions (kN)**

	Abutment 1	Falsework 1	Falsework 2A	Falsework 2	Pier Bracket at XF 26	Pier 1	Pier Bracket at XF 28
G1	163.5	380.3	133.1	864.2			
G2	98.6	296.2	0.0	896.5	0.0	1020.5	0.0
G3	96.8	260.0	0.0	690.7	0.0	730.8	0.0
G4	82.0	195.6	55.4	430.3			

**Vertical Support Reactions (kips)**

	Abutment 1	Falsework 1	Falsework 2A	Falsework 2	Pier Bracket at XF 26	Pier 1	Pier Bracket at XF 28
G1	36.8	85.5	29.9	194.3			
G2	22.2	66.6	0.0	201.6	0.0	229.4	0.0
G3	21.8	58.5	0.0	155.3	0.0	164.3	0.0
G4	18.4	44.0	12.5	96.7			

**Cross-frame Vertical Reactions**

	(kN)	(kip)
XF 26B (outside)	0.000	0.0000
XF 27B (outside)	0.000	0.0000
XF 27C (inside)	9.965	2.2402
XF 28B (outside)	0.000	0.0000

**Figure C-57** Construction stage 12 – Field-splice location deflections and support reactions summary

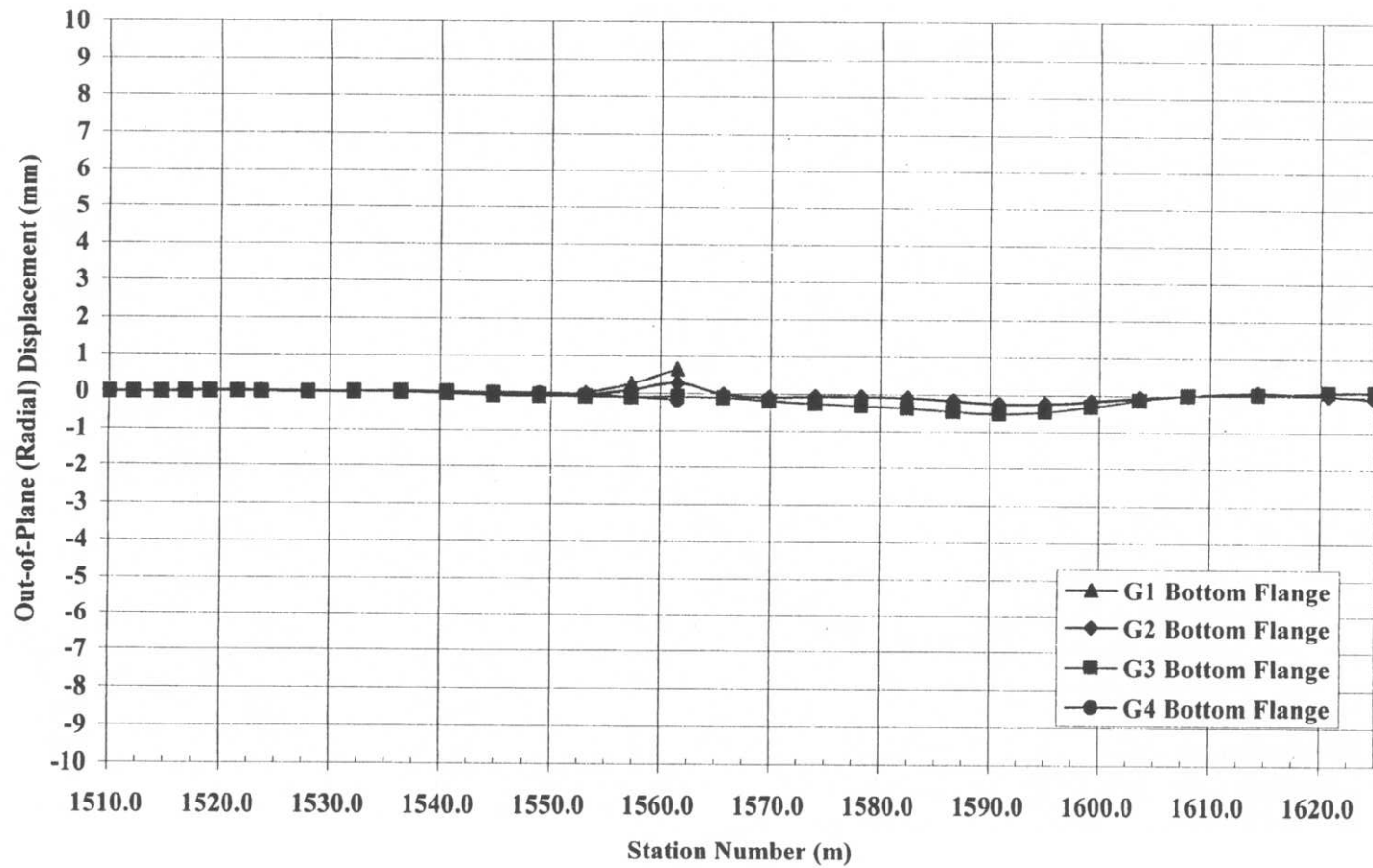


**Figure C-58** Construction stage 12 – Out-of-plane (radial) displacement, centerline of bottom flange

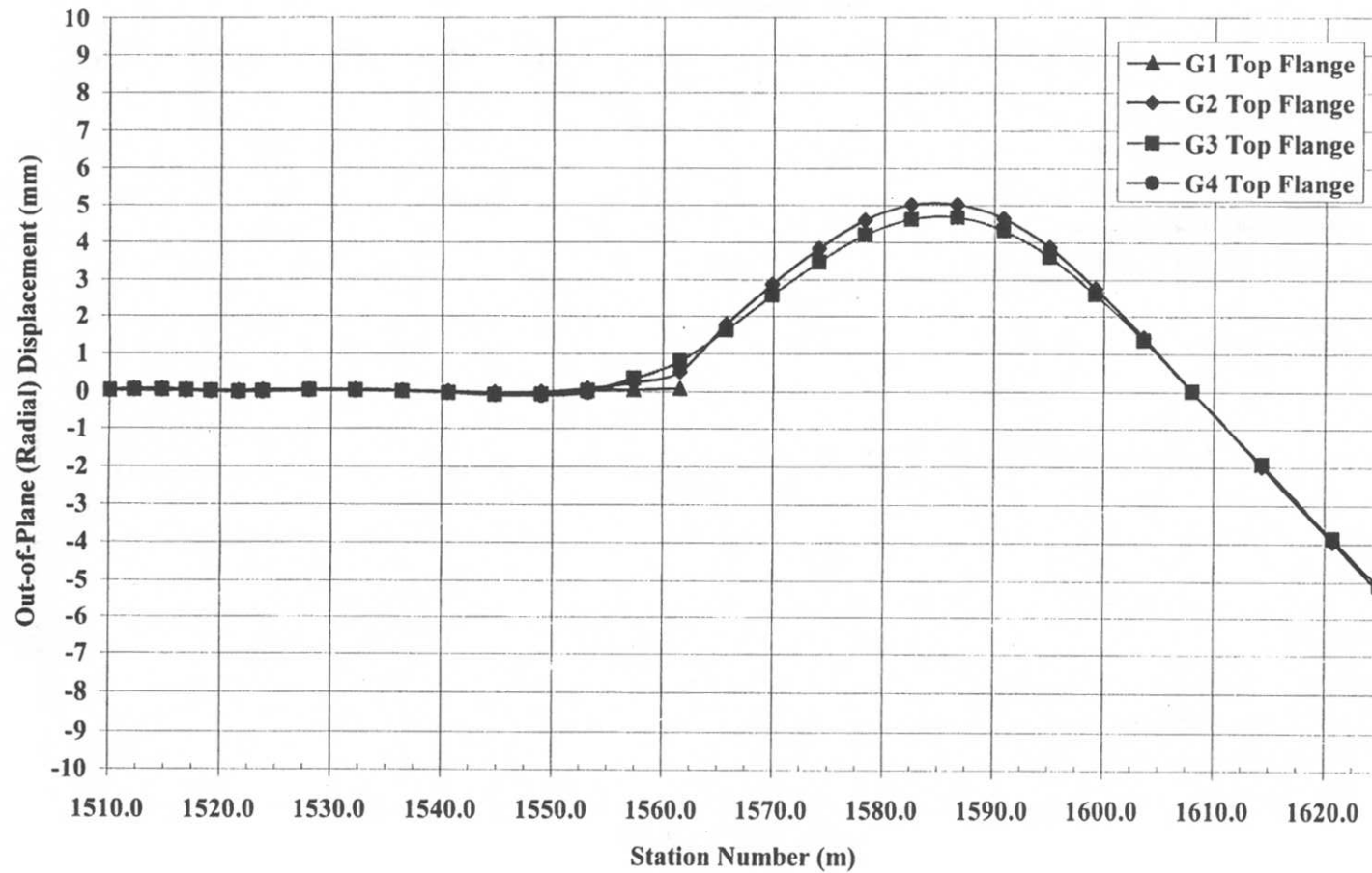


**Figure C-59** Construction stage 12 – Out-of-plane (radial) displacement, centerline of top flange

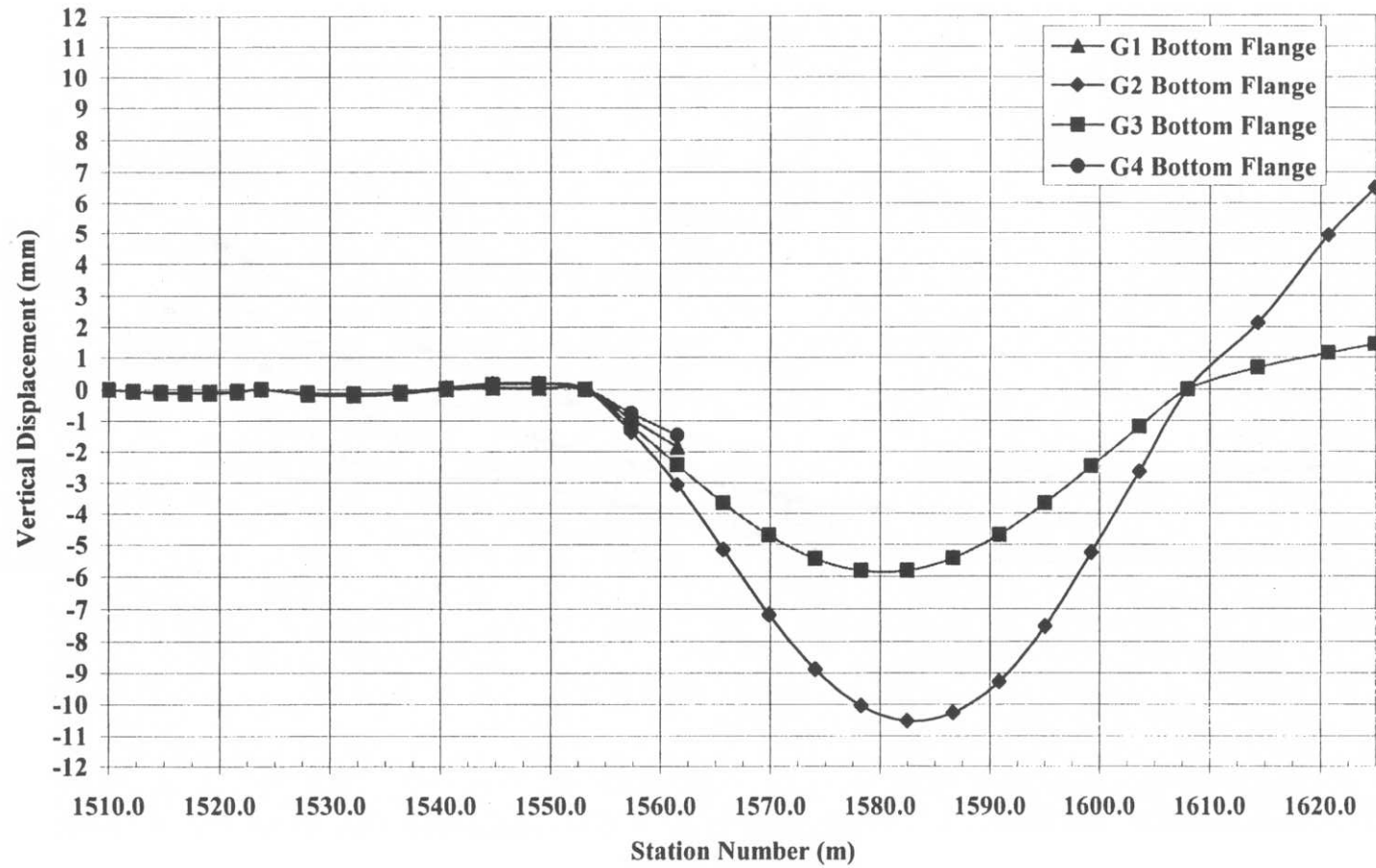
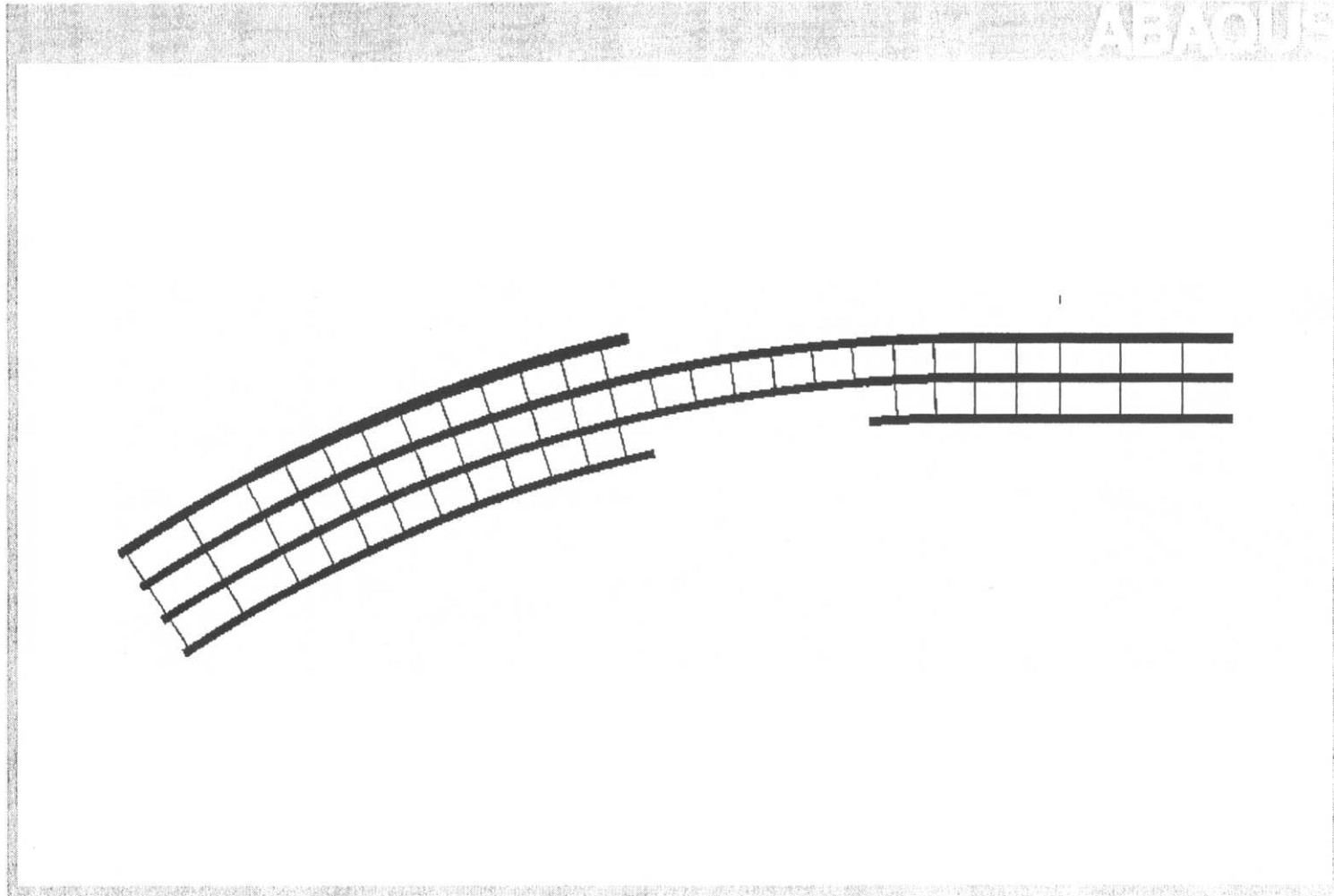


Figure C-60 Construction stage 12 - Vertical displacement, centerline of bottom flange



**Figure C-61** Construction stage 13 – Plan view of finite element model

**Deflections - Out-of-Plane (Radial) (mm)**

	Abutment 1	Field Splice 1 Section 1	Field Splice 1 Section 2	Field Splice 2 Section 2	Field Splice 2 Section 3	Field Splice 3 Section 3	Field Splice 3 Section 4	Field Splice 4 Section 4
G1 - Bottom Flange	0.0031	0.0034	0.0034	0.5214				
G1 - Top Flange	0.0416	0.0441	0.0441	-0.3534				
G2 - Bottom Flange	0.0082	0.0112	0.0112	-0.3376	-0.3376	-1.3610	-1.3610	1.6580
G2 - Top Flange	0.0384	0.0380	0.0380	0.7398	0.7398	2.7120	2.7120	-2.5040
G3 - Bottom Flange	0.0002	0.0075	0.0075	-0.5220	-0.5220	-1.5720	-1.5720	1.8070
G3 - Top Flange	0.0320	0.0195	0.0195	0.7592	0.7592	2.4390	2.4390	-2.3770
G4 - Bottom Flange	-0.0118	0.0005	0.0005	-0.6535			-1.8950	1.8920
G4 - Top Flange	0.0145	-0.0061	-0.0061	0.6101			2.2410	-2.2890

**Deflections - Vertical (mm)**

	Abutment 1	Field Splice 1 Section 1	Field Splice 1 Section 2	Field Splice 2 Section 2	Field Splice 2 Section 3	Field Splice 3 Section 3	Field Splice 3 Section 4	Field Splice 4 Section 4
G1 - Bottom Flange	-0.0036	-0.1032	-0.1032	-2.3360				
G1 - Top Flange	-0.0125	-0.1103	-0.1103	-2.3370				
G2 - Bottom Flange	0.0017	-0.0779	-0.0779	-4.4160	-4.4160	-9.6110	-9.6110	6.3340
G2 - Top Flange	-0.0102	-0.0828	-0.0828	-4.4090	-4.4090	-9.6110	-9.6110	6.3320
G3 - Bottom Flange	0.0013	-0.0664	-0.0664	-3.3970	-3.3970	-5.8080	-5.8080	2.2190
G3 - Top Flange	-0.0102	-0.0707	-0.0707	-3.3950	-3.3950	-5.8100	-5.8100	2.2180
G4 - Bottom Flange	0.0015	-0.0748	-0.0748	-1.9940			-1.9580	-1.8590
G4 - Top Flange	-0.0103	-0.0790	-0.0790	-1.9940			-1.9610	-1.8610

**Vertical - Support Reactions (kN)**

	Abutment 1	Falsework 1	Falsework 2A	Falsework 2	Pier Bracket at XF 26	Pier 1	Pier Bracket at XF 28
G1	166.1	380.5	140.6	852.2			
G2	98.7	296.5	0.0	902.8	n/a	997.0	n/a
G3	94.9	261.8	0.0	689.8	n/a	788.9	n/a
G4	82.2	196.1	48.2	444.4	n/a	578.3	n/a

**Vertical Support Reactions (kips)**

	Abutment 1	Falsework 1	Falsework 2A	Falsework 2	Pier Bracket at XF 26	Pier 1	Pier Bracket at XF 28
G1	37.4	85.5	31.6	191.6			
G2	22.2	66.7	0.0	203.0	n/a	224.1	n/a
G3	21.3	58.9	0.0	155.1	n/a	177.4	n/a
G4	18.5	44.1	10.8	99.9	n/a	130.0	n/a

**Cross-frame Vertical Reactions**

	(kN)	(kips)
XF 26B (outside)	0.000	0.000
XF 27B (outside)	0.000	0.000
XF 27C (inside)	0.000	0.000
XF 28B (outside)	0.000	0.000

**Figure C-62** Construction stage 13 – Field-splice location deflections and support reactions summary

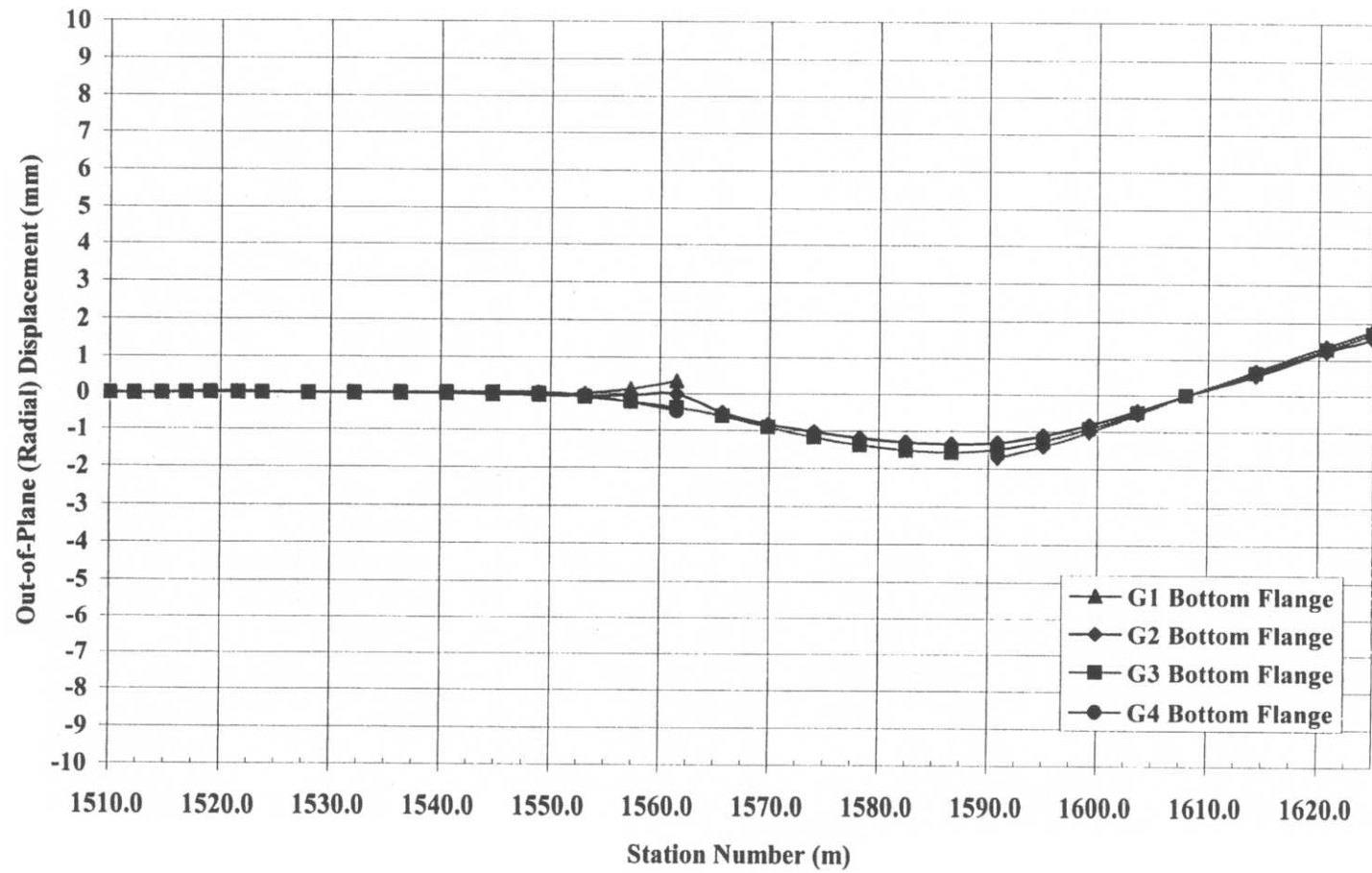


**Figure C-63** Construction stage 13 – Out-of-plane (radial) displacement, centerline of bottom flange

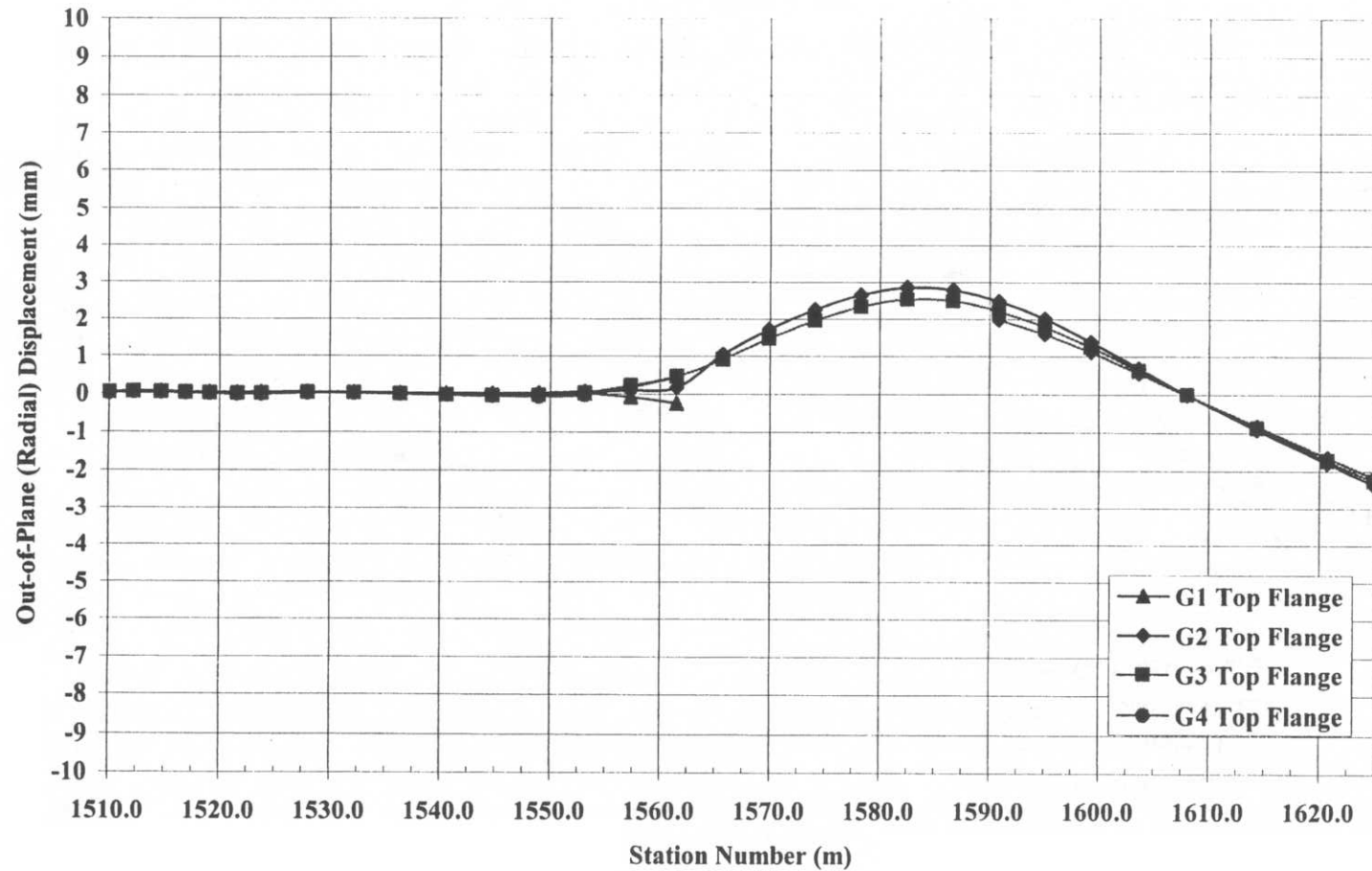


**Figure C-64** Construction stage 13 – Out-of-plane (radial) displacement, centerline of top flange

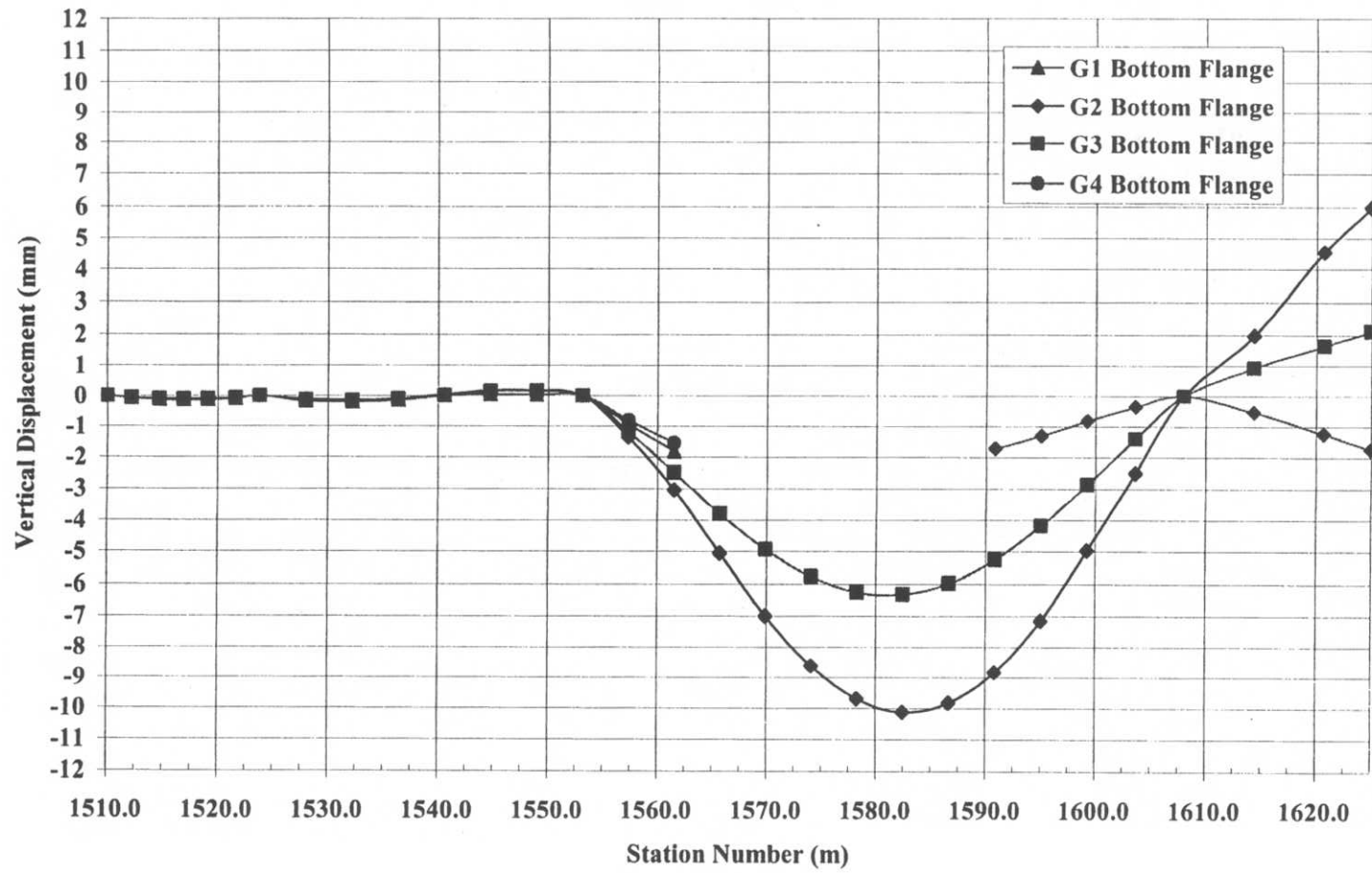
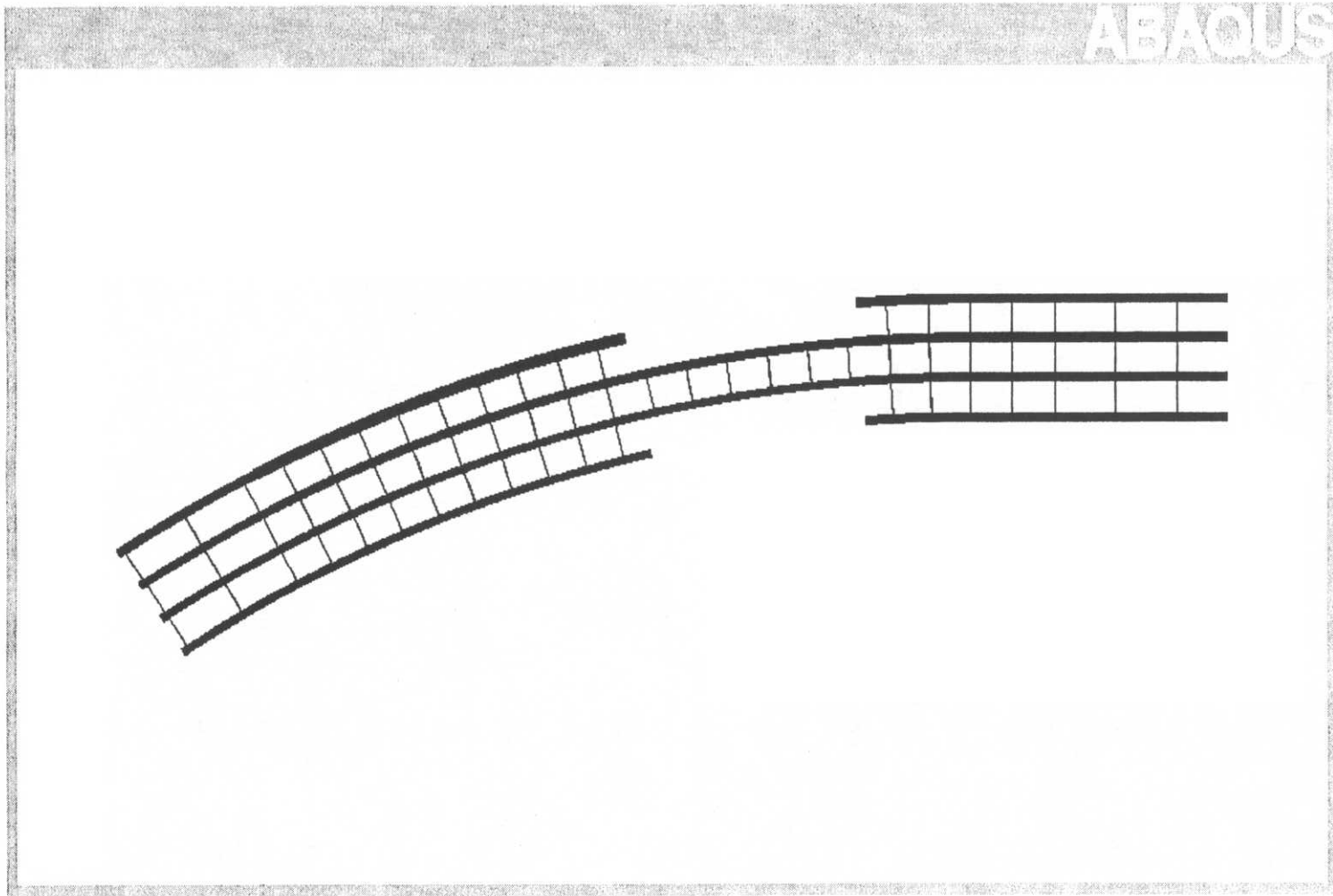


Figure C-65 Construction stage 13 - Vertical displacement, centerline of bottom flange



**Figure C-66** Construction stage 14 – Plan view of finite element model

**Deflections - Out-of-Plane (Radial) (mm)**

	Abutment 1	Field Splice 1 Section 1	Field Splice 1 Section 2	Field Splice 2 Section 2	Field Splice 2 Section 3	Field Splice 3 Section 3	Field Splice 3 Section 4	Field Splice 4 Section 4
G1- Bottom Flange	0.0117	0.0098	0.0098	0.5745			-2.7450	2.2970
G1- Top Flange	0.0504	0.0507	0.0507	-0.3426			4.5810	-3.5490
G2 - Bottom Flange	0.0152	0.0181	0.0181	-0.4490	-0.4490	-2.1770	-2.1770	2.1010
G2 - Top Flange	0.0461	0.0422	0.0422	0.9566	0.9566	3.8760	3.8760	-3.6340
G3 - Bottom Flange	0.0002	0.0086	0.0086	-0.6559	-0.6559	-2.4380	-2.4380	2.3320
G3 - Top Flange	0.0325	0.0178	0.0178	0.9417	0.9417	3.4210	3.4210	-3.5080
G4 - Bottom Flange	-0.0145	-0.0015	-0.0015	-0.7153			-3.0570	2.4680
G4 - Top Flange	0.0117	-0.0095	-0.0095	0.6828			3.2480	-3.3930

**Deflections - Vertical (mm)**

	Abutment 1	Field Splice 1 Section 1	Field Splice 1 Section 2	Field Splice 2 Section 2	Field Splice 2 Section 3	Field Splice 3 Section 3	Field Splice 3 Section 4	Field Splice 4 Section 4
G1- Bottom Flange	-0.0042	-0.1016	-0.1016	-2.5130			-19.2100	13.3200
G1- Top Flange	-0.0126	-0.1087	-0.1087	-2.5140			-19.2200	13.3200
G2 - Bottom Flange	0.0018	-0.0748	-0.0748	-4.8220	-4.8220	-11.1100	-11.1100	7.7110
G2 - Top Flange	-0.0103	-0.0796	-0.0796	-4.8140	-4.8140	-11.1100	-11.1100	7.7080
G3 - Bottom Flange	0.0013	-0.0639	-0.0639	-3.4480	-3.4480	-5.5950	-5.5950	1.9990
G3 - Top Flange	-0.0103	-0.0682	-0.0682	-3.4470	-3.4470	-5.5990	-5.5990	1.9950
G4 - Bottom Flange	0.0015	-0.0739	-0.0739	-1.9580			0.3381	-3.7170
G4 - Top Flange	-0.0104	-0.0780	-0.0780	-1.9570			0.3331	-3.7200

**Vertical - Support Reactions (kN)**

	Abutment 1	Falsework 1	Falsework 2A	Falsework 2	Pier Bracket at XF 26	Pier 1	Pier Bracket at XF 28
G1	170.0	377.5	107.5	893.3	n/a	820.1	n/a
G2	99.9	292.7	0.0	915.8	n/a	980.4	n/a
G3	95.9	258.6	0.0	711.8	n/a	797.5	n/a
G4	82.4	194.8	44.5	440.9	n/a	576.1	n/a

**Vertical Support Reactions (kips)**

	Abutment 1	Falsework 1	Falsework 2A	Falsework 2	Pier Bracket at XF 26	Pier 1	Pier Bracket at XF 28
G1	38.2	84.9	24.2	200.8	n/a	184.4	n/a
G2	22.5	65.8	0.0	205.9	n/a	220.4	n/a
G3	21.6	58.1	0.0	160.0	n/a	179.3	n/a
G4	18.5	43.8	10.0	99.1	n/a	129.5	n/a

**Cross-frame Vertical Reactions**

	(kN)	(kips)
XF 26B (outside)	0.000	0.000
XF 27B (outside)	0.000	0.000
XF 27C (inside)	0.000	0.000
XF 28B (outside)	0.000	0.000

**Figure C-67** Construction stage 14 – Field-splice location deflections and support reactions summary

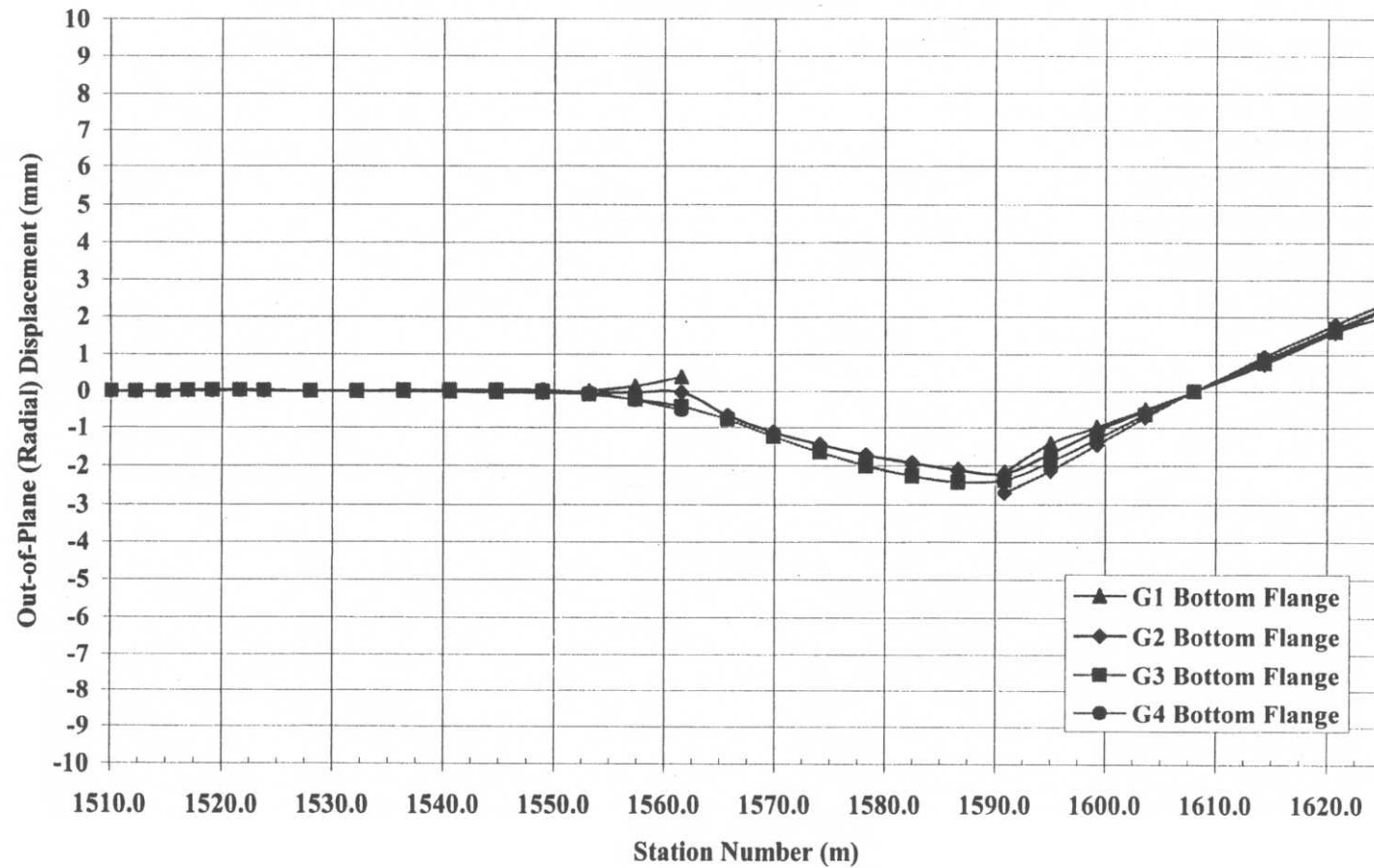
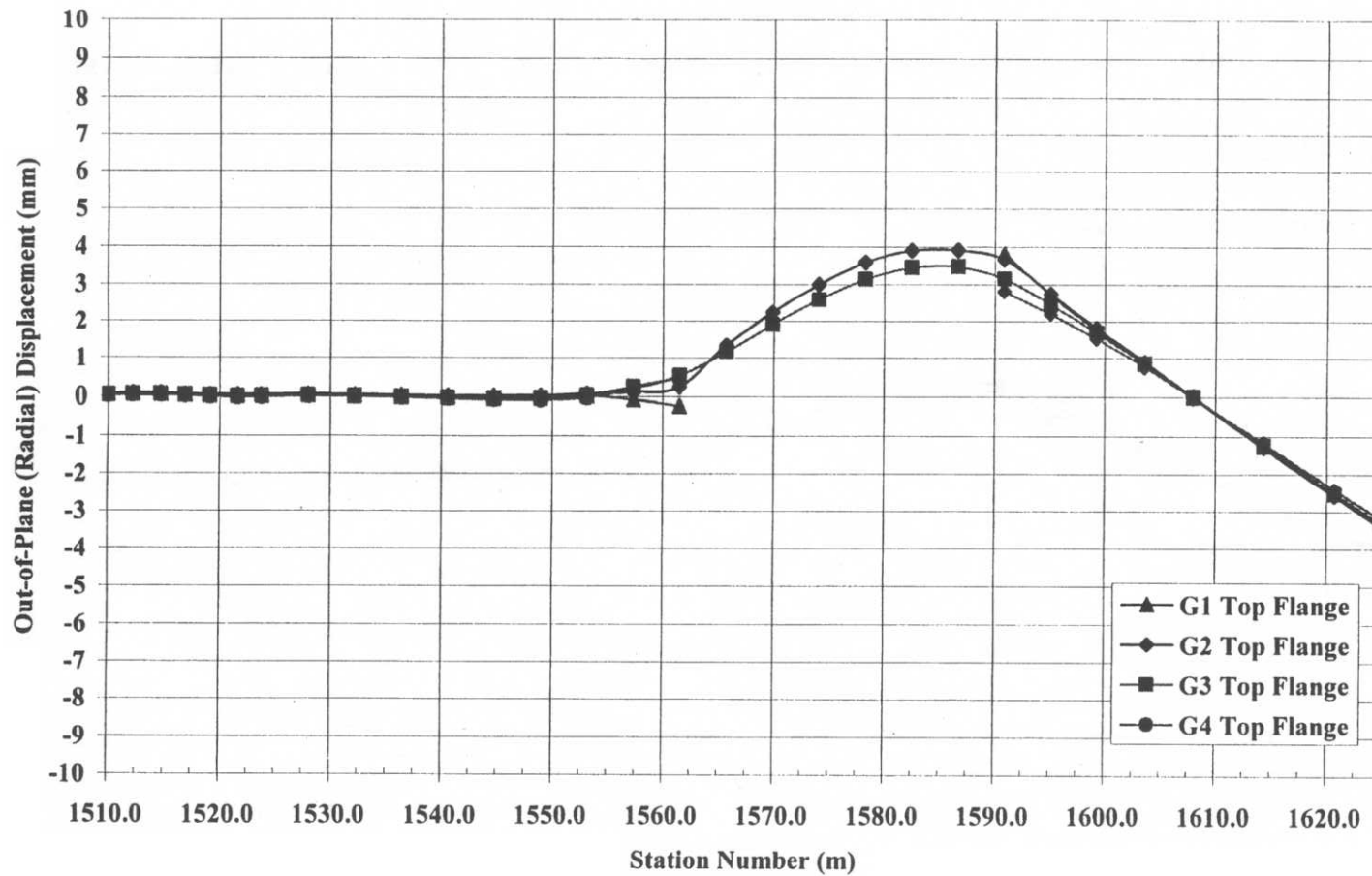
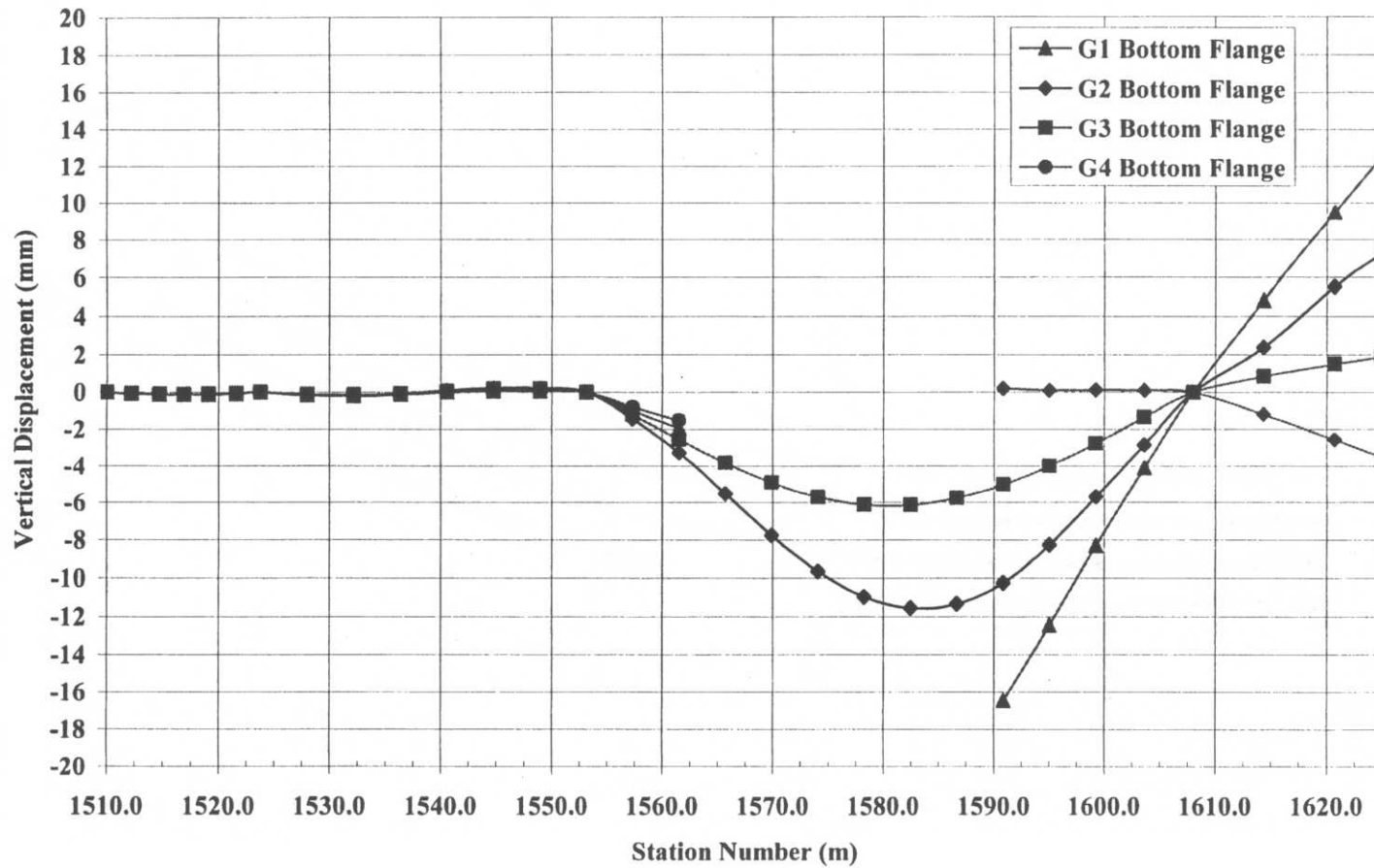


Figure C-68 Construction stage 14 – Out-of-plane (radial) displacement, centerline of bottom flange



**Figure C-69** Construction stage 14 – Out-of-plane (radial) displacement, centerline of top flange



**Figure C-70** Construction stage 14 - Vertical displacement, centerline of bottom flange

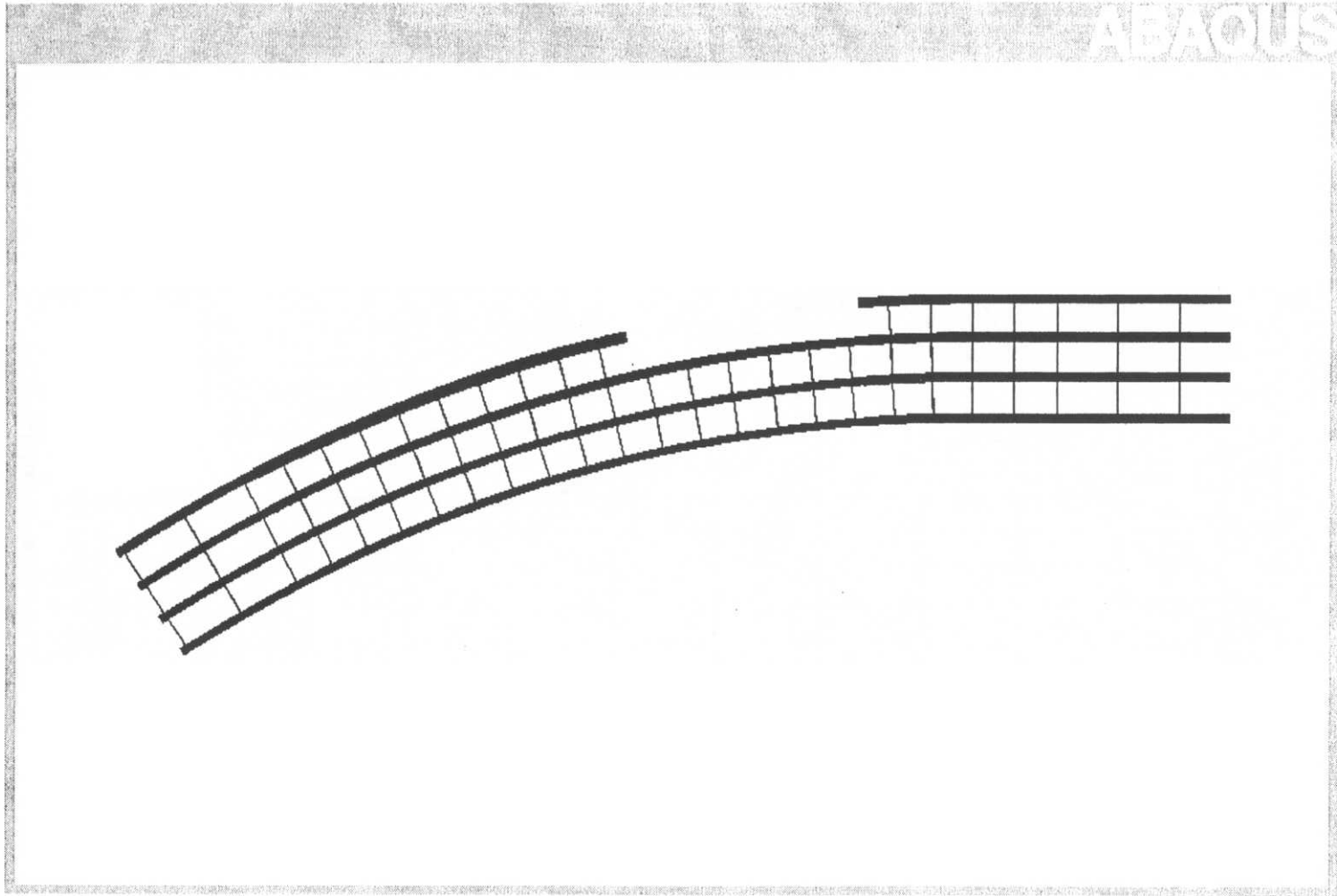


**Figure C-71** Construction stage 15 – Plan view of finite element model

**Deflections - Out-of-Plane (Radial) (mm)**

	Abutment 1	Field Splice 1	Field Splice 1	Field Splice 2	Field Splice 2	Field Splice 3	Field Splice 3	Field Splice 4
		Section 1	Section 2	Section 2	Section 3	Section 3	Section 4	Section 4
G1- Bottom Flange	0.0041	0.0055	0.0055	0.6528			-1.5610	1.0690
G1- Top Flange	0.0428	0.0527	0.0527	-0.6218			2.8430	-2.0570
G2 - Bottom Flange	0.0069	0.0163	0.0163	-0.2341	-0.2341	-1.1030	-1.1030	0.9646
G2 - Top Flange	0.0389	0.0413	0.0413	0.5160	0.5160	2.2710	2.2710	-2.1040
G3 - Bottom Flange	0.0002	0.0165	0.0165	-0.4285	-0.4285	-1.1690	-1.1690	1.0930
G3 - Top Flange	0.0348	0.0221	0.0221	0.5983	0.5983	1.9540	1.9540	-2.0180
G4 - Bottom Flange	-0.0137	0.0068	0.0068	-0.4968	-0.4968	-1.3280	-1.3280	1.1640
G4 - Top Flange	0.0135	-0.0056	-0.0056	0.5484	0.5484	1.7300	1.7300	-1.9570

**Deflections - Vertical (mm)**

	Abutment 1	Field Splice 1	Field Splice 1	Field Splice 2	Field Splice 2	Field Splice 3	Field Splice 3	Field Splice 4
		Section 1	Section 2	Section 2	Section 3	Section 3	Section 4	Section 4
G1- Bottom Flange	-0.0048	-0.1021	-0.1021	-2.3340			-15.7700	10.1200
G1- Top Flange	-0.0127	-0.1092	-0.1092	-2.3350			-15.7800	10.1200
G2 - Bottom Flange	0.0019	-0.0689	-0.0689	-4.8170	-4.8170	-10.5200	-10.5200	7.1350
G2 - Top Flange	-0.0104	-0.0736	-0.0736	-4.8090	-4.8090	-10.5200	-10.5200	7.1340
G3 - Bottom Flange	0.0016	-0.0531	-0.0531	-4.1800	-4.1800	-7.5360	-7.5360	4.0710
G3 - Top Flange	-0.0106	-0.0572	-0.0572	-4.1770	-4.1770	-7.5380	-7.5380	4.0700
G4 - Bottom Flange	0.0015	-0.0558	-0.0558	-3.3280	-3.3280	-4.6950	-4.6950	1.0050
G4 - Top Flange	-0.0112	-0.0595	-0.0595	-3.3250	-3.3250	-4.6970	-4.6970	1.0050

**Vertical - Support Reactions (kN)**

	Abutment 1	Falsework 1	Falsework 2A	Falsework 2	Pier Bracket at XF 26	Pier 1	Pier Bracket at XF 28
G1	172.4	377.9	133.0	841.0	n/a	816.8	n/a
G2	102.1	284.0	0.0	949.0	n/a	990.0	n/a
G3	100.4	244.4	0.0	779.0	n/a	852.5	n/a
G4	88.3	174.2	0.0	628.7	n/a	619.5	n/a

**Vertical Support Reactions (kips)**

	Abutment 1	Falsework 1	Falsework 2A	Falsework 2	Pier Bracket at XF 26	Pier 1	Pier Bracket at XF 28
G1	38.8	85.0	29.9	189.1	n/a	183.6	n/a
G2	23.0	63.8	0.0	213.3	n/a	222.6	n/a
G3	22.6	54.9	0.0	175.3	n/a	191.7	n/a
G4	19.9	39.2	0.0	141.3	n/a	139.3	n/a

**Cross-frame Vertical Reactions**

	(kN)	(kips)
XF 26B (outside)	0.000	0.000
XF 27B (outside)	0.000	0.000
XF 27C (inside)	0.000	0.000
XF 28B (outside)	0.000	0.000

**Figure C-72** Construction stage 15–Field-splice location deflections and support reactions summary

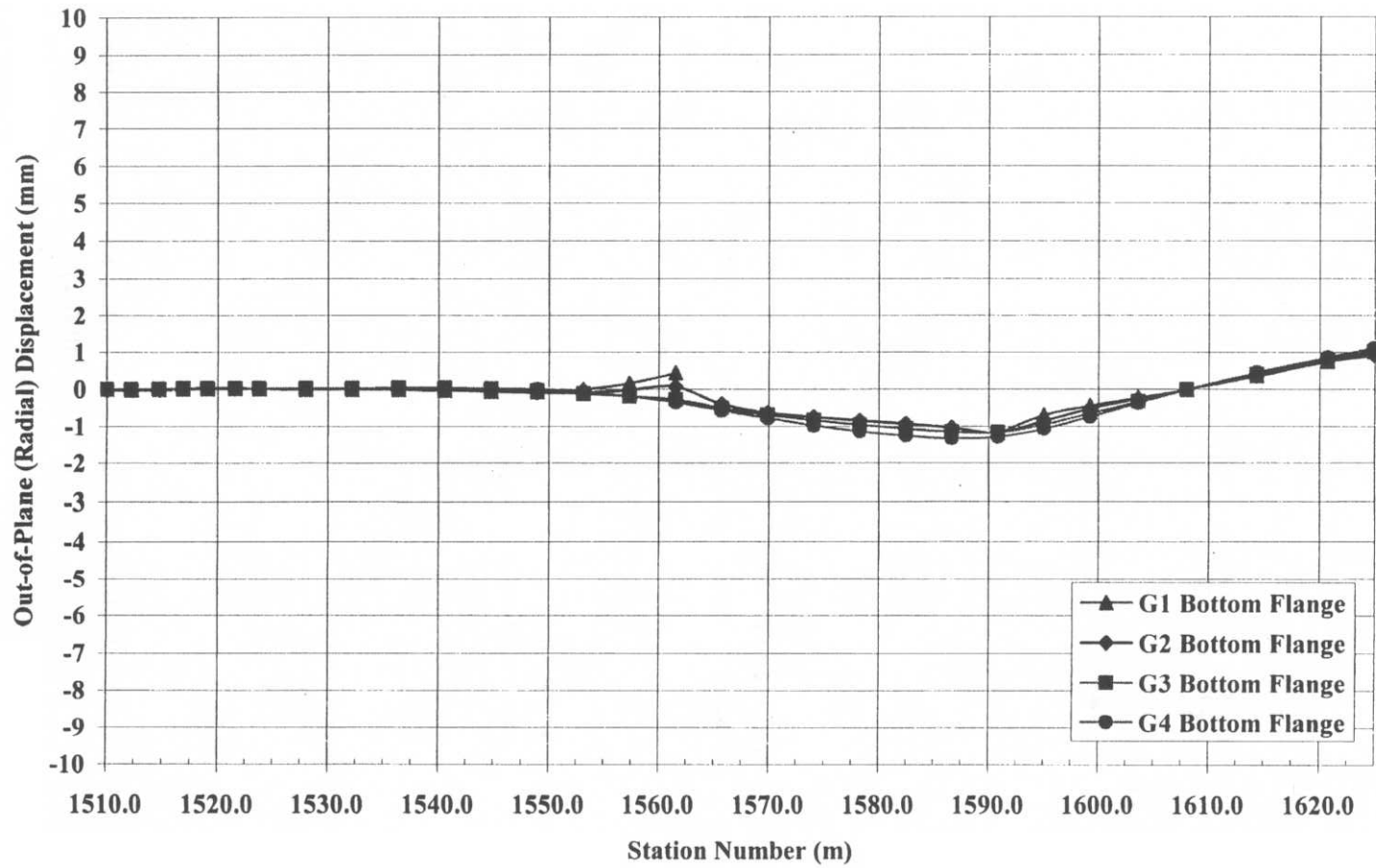


**Figure C-73** Construction stage 15 – Out-of-plane (radial) displacement, centerline of bottom flange

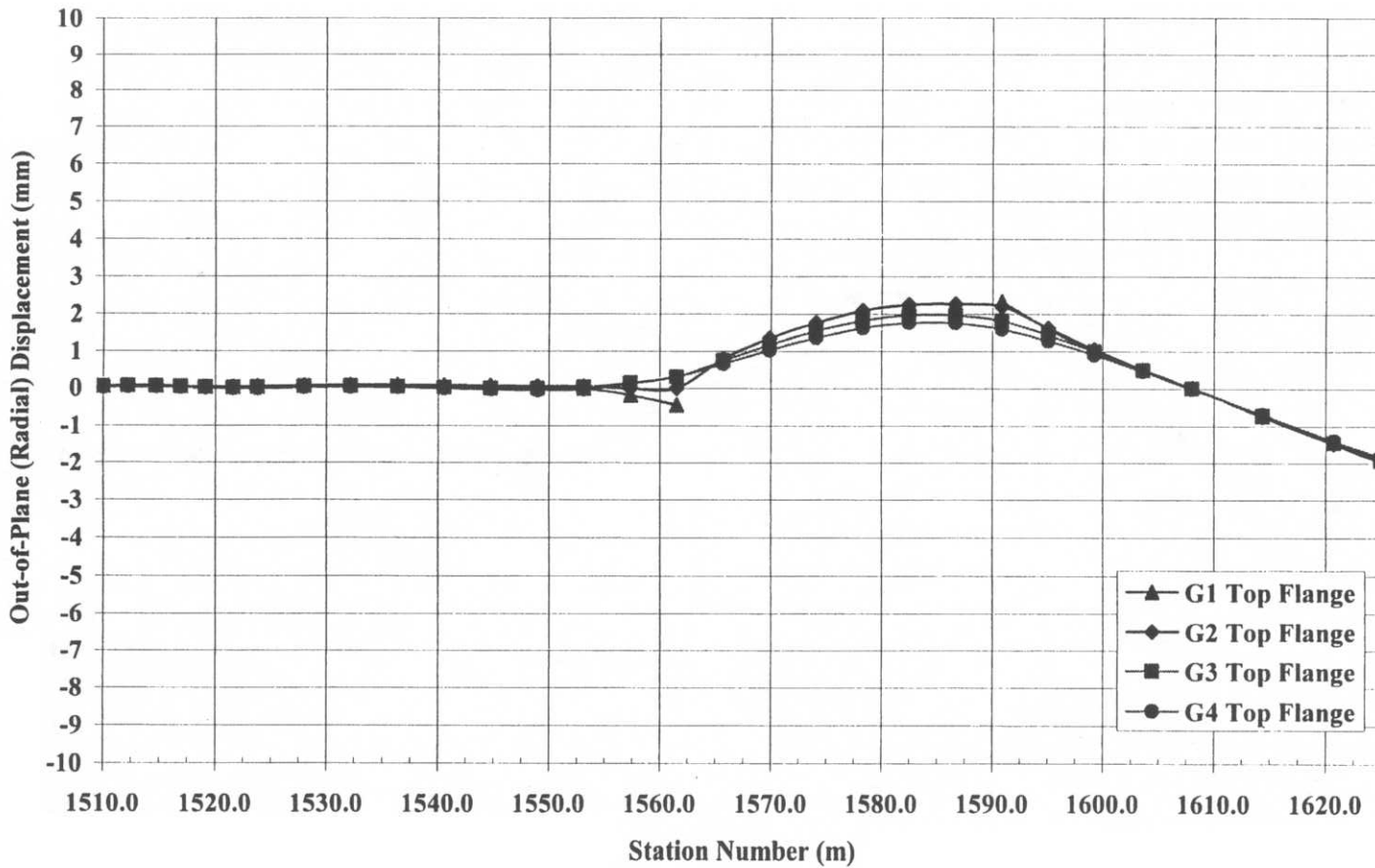


**Figure C-74** Construction stage 15 – Out-of-plane (radial) displacement, centerline of top flange

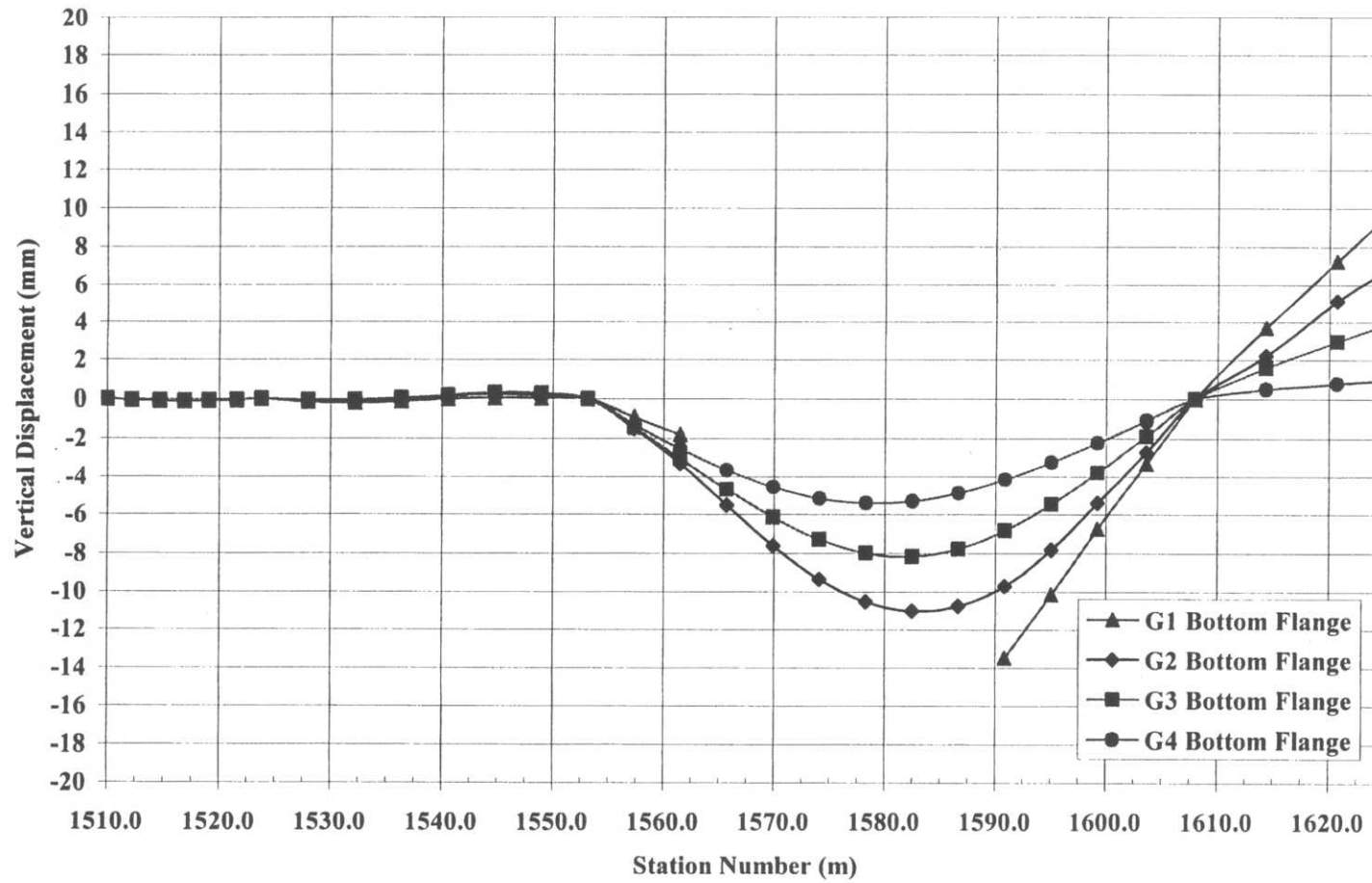
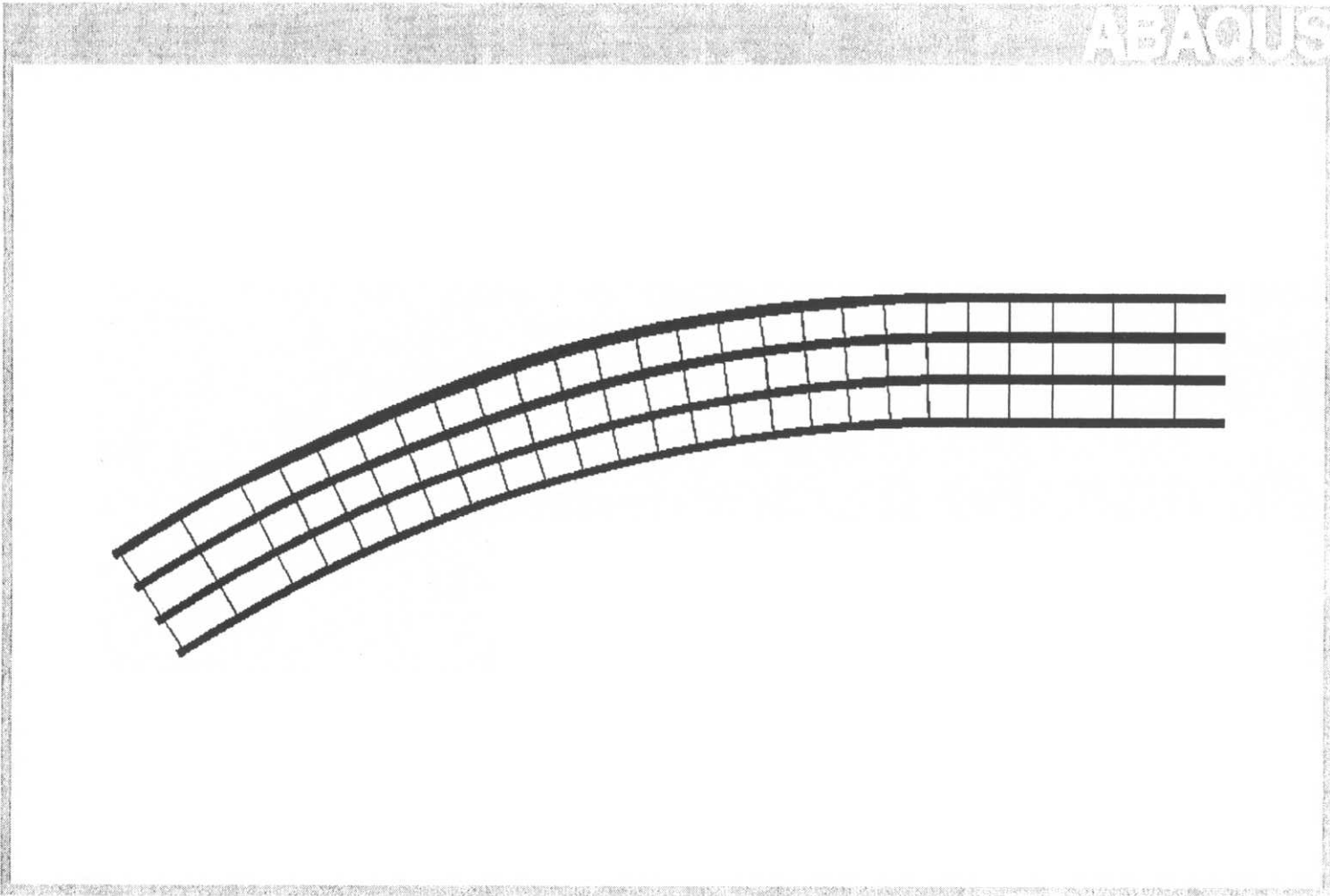


Figure C-75 Construction stage 15 - Vertical displacement, centerline of bottom flange



**Figure C-76** Construction stage 16 - Plane view of finite element model

**Deflections - Out-of-Plane (Radial) (mm)**

	Abutment 1	Field Splice 1 Section 1	Field Splice 1 Section 2	Field Splice 2 Section 2	Field Splice 2 Section 3	Field Splice 3 Section 3	Field Splice 3 Section 4	Field Splice 4 Section 4
G1 - Bottom Flange	0.0087	0.0301	0.0301	-0.3808	-0.3808	-0.7460	-0.7460	0.9065
G1 - Top Flange	0.0537	0.0025	0.0025	1.1300	1.1300	1.7940	1.7940	-1.5010
G2 - Bottom Flange	-0.0001	0.0219	0.0219	-0.3518	-0.3518	-0.6805	-0.6805	0.8155
G2 - Top Flange	0.0357	-0.0013	-0.0013	1.0700	1.0700	1.6550	1.6550	-1.5260
G3 - Bottom Flange	0.0002	0.0148	0.0148	-0.3991	-0.3991	-0.7617	-0.7617	0.8919
G3 - Top Flange	0.0339	-0.0013	-0.0013	0.9456	0.9456	1.4690	1.4690	-1.4250
G4 - Bottom Flange	-0.0083	0.0036	0.0036	-0.4203	-0.4203	-0.9025	-0.9025	0.9345
G4 - Top Flange	0.0177	-0.0167	-0.0167	0.8264	0.8264	1.3290	1.3290	-1.3680

**Deflections - Vertical (mm)**

	Abutment 1	Field Splice 1 Section 1	Field Splice 1 Section 2	Field Splice 2 Section 2	Field Splice 2 Section 3	Field Splice 3 Section 3	Field Splice 3 Section 4	Field Splice 4 Section 4
G1 - Bottom Flange	-0.0052	-0.0362	-0.0362	-5.8380	-5.8380	-10.8700	-10.8700	7.5280
G1 - Top Flange	-0.0157	-0.0407	-0.0407	-5.8290	-5.8290	-10.8700	-10.8700	7.5280
G2 - Bottom Flange	0.0024	-0.0426	-0.0426	-4.7900	-4.7900	-8.6150	-8.6150	5.2100
G2 - Top Flange	-0.0110	-0.0466	-0.0466	-4.7840	-4.7840	-8.6130	-8.6130	5.2090
G3 - Bottom Flange	0.0016	-0.0539	-0.0539	-3.7800	-3.7800	-6.5020	-6.5020	2.9050
G3 - Top Flange	-0.0105	-0.0580	-0.0580	-3.7770	-3.7770	-6.5020	-6.5020	2.9050
G4 - Bottom Flange	0.0016	-0.0785	-0.0785	-2.7960	-2.7960	-4.4190	-4.4190	0.6459
G4 - Top Flange	-0.0101	-0.0827	-0.0827	-2.7930	-2.7930	-4.4210	-4.4210	0.6457

**Vertical - Support Reactions (kN)**

	Abutment 1	Falsework 1	Falsework 2A	Falsework 2	Pier Bracket at XF 26	Pier 1	Pier Bracket at XF 28
G1	206.9	270.1	0.0	1403.9	n/a	1086.9	n/a
G2	110.9	241.6	0.0	1158.9	n/a	956.2	n/a
G3	99.9	244.2	0.0	735.9	n/a	819.1	n/a
G4	81.3	201.8	29.6	528.4	n/a	626.2	n/a

**Vertical Support Reactions (kips)**

	Abutment 1	Falsework 1	Falsework 2A	Falsework 2	Pier Bracket at XF 26	Pier 1	Pier Bracket at XF 28
G1	46.5	60.7	0.0	315.6	n/a	244.3	n/a
G2	24.9	54.3	0.0	260.5	n/a	215.0	n/a
G3	22.4	54.9	0.0	165.4	n/a	184.1	n/a
G4	18.3	45.4	6.7	118.8	n/a	140.8	n/a

**Cross-frame Vertical Reactions**

	(kN)	(kips)
XF 26B (outside)	0.000	0.000
XF 27B (outside)	0.000	0.000
XF 27C (inside)	0.000	0.000
XF 28B (outside)	0.000	0.000

**Figure C-77** Construction stage 16 – Field-splice location deflections and support reactions summary

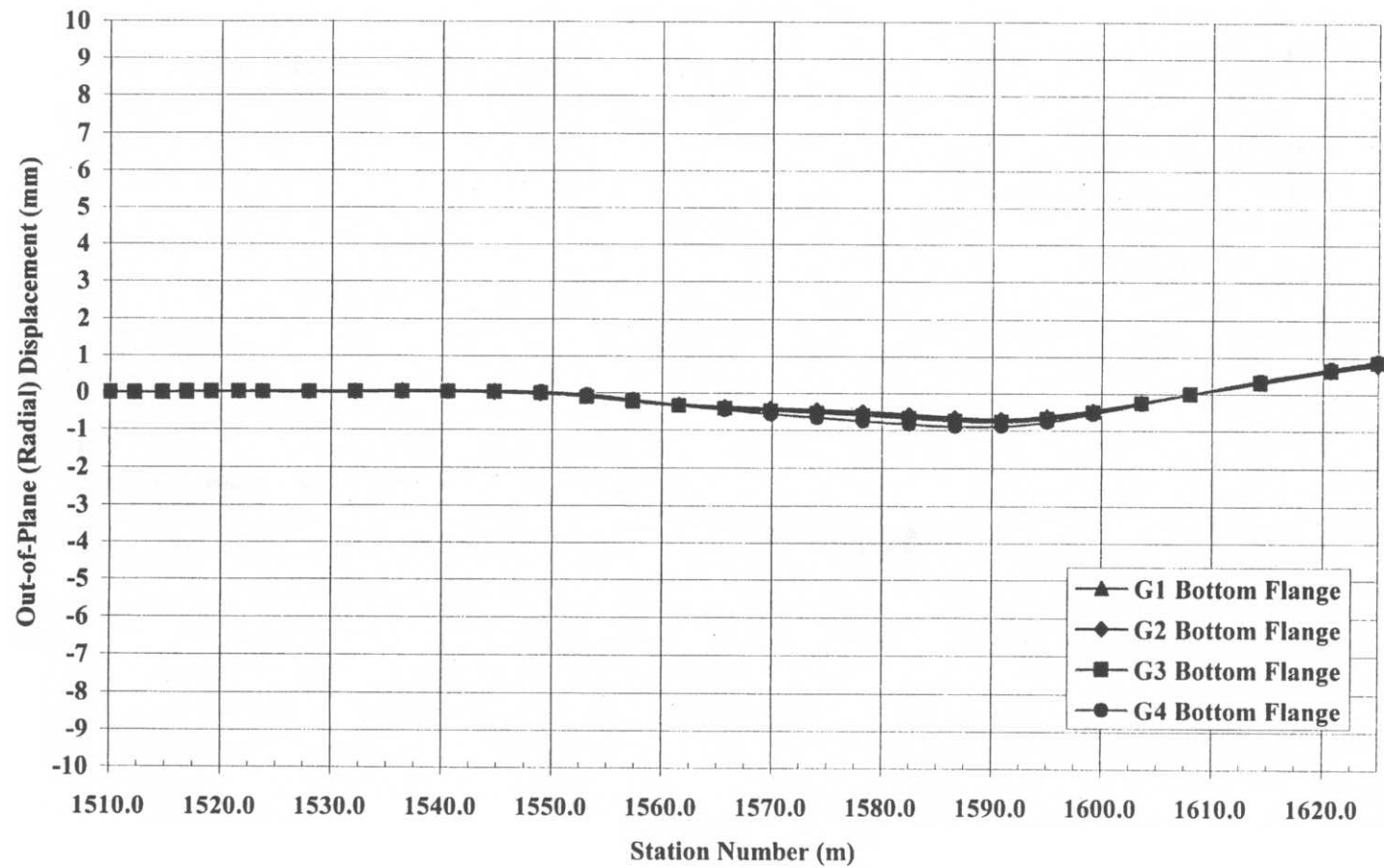


**Figure C-78** Construction stage 16 – Out-of-plane (radial) displacement, centerline of bottom flange

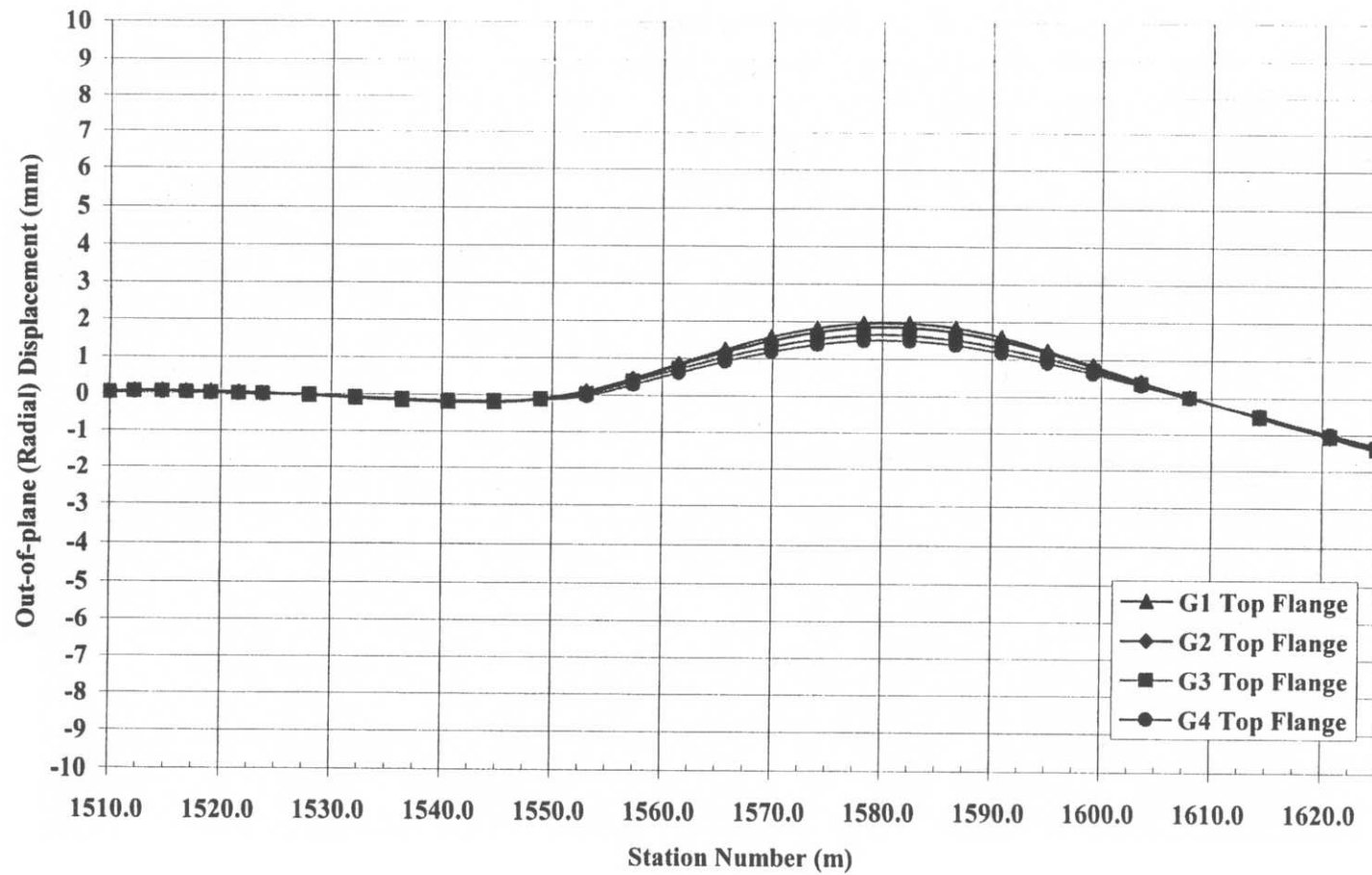
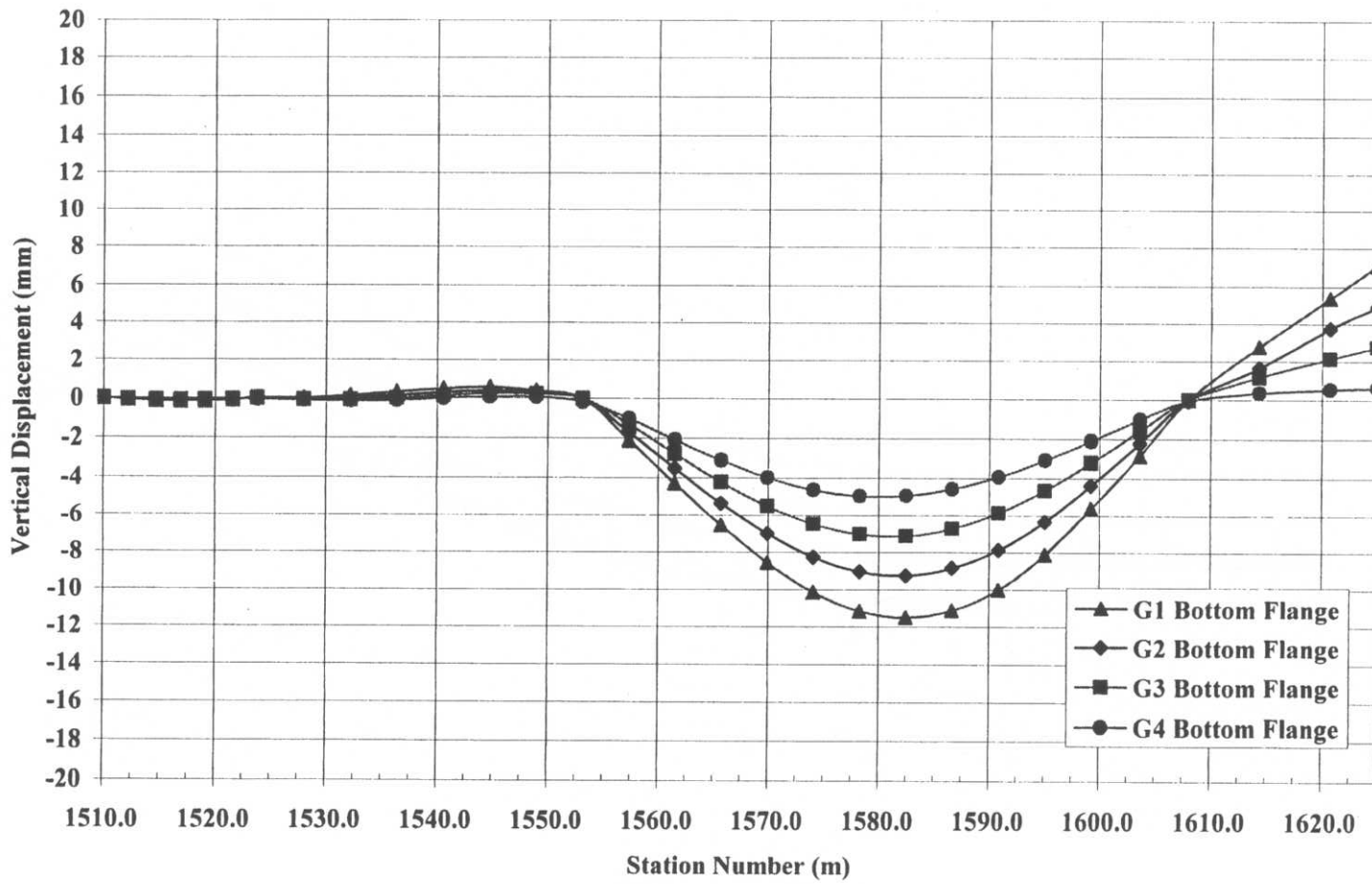
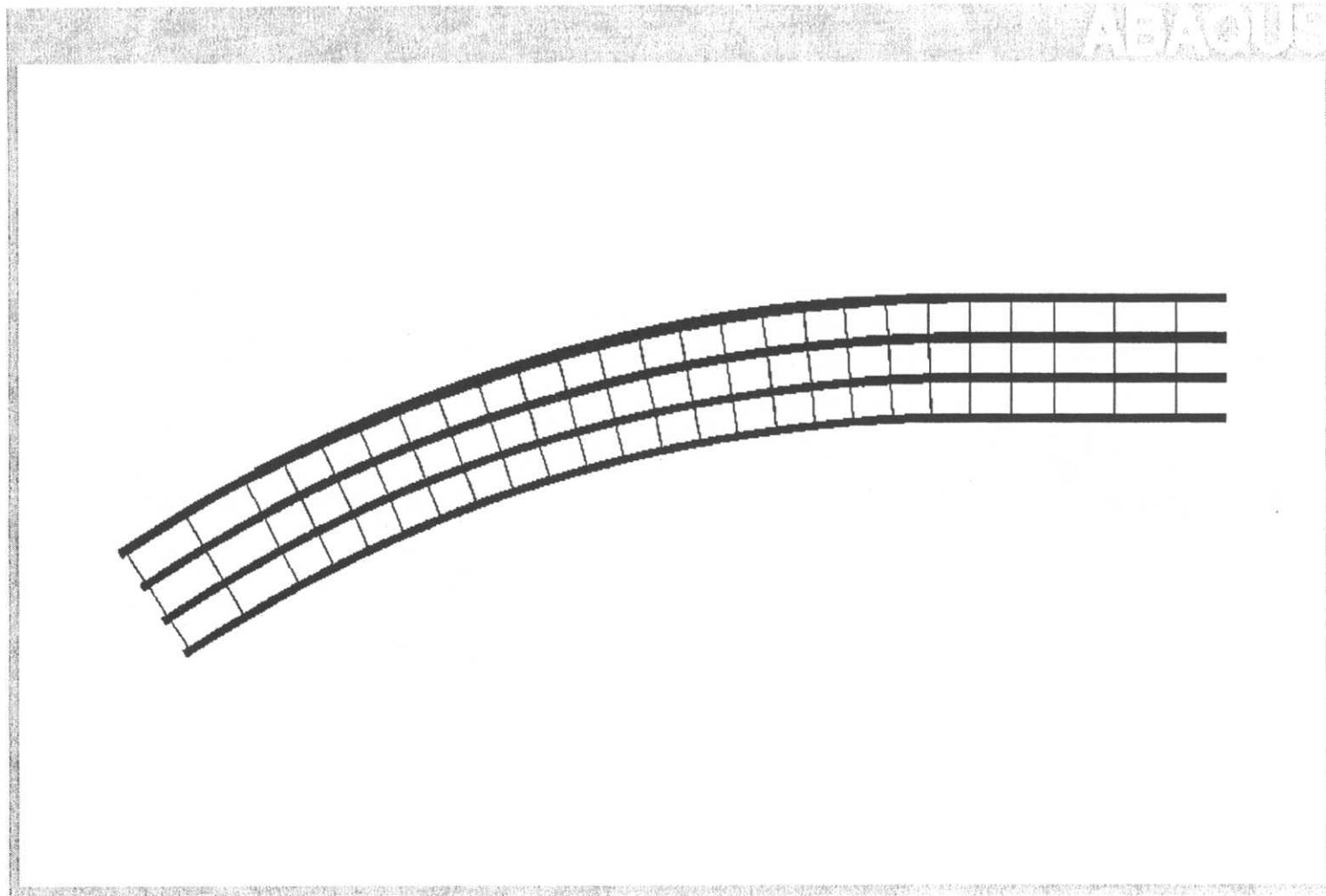


Figure C-79 Construction stage 16 – Out-of-plane (radial) displacement, centerline of top flange



**Figure C-80** Construction stage 16 - Vertical displacement, centerline of bottom flange



**Figure C-81** Removal of Falsework 1 and Falsework 2A – Plan view of finite element model  
(Note: only change from construction stage 16 is the boundary condition due to falsework removal)

**Deflections - Out-of-Plane (Radial) (mm)**

	Abutment 1	Field Splice 1 Section 1	Field Splice 1 Section 2	Field Splice 2 Section 2	Field Splice 2 Section 3	Field Splice 3 Section 3	Field Splice 3 Section 4	Field Splice 4 Section 4
G1- Bottom Flange	0.0296	0.2761	0.2761	-0.2303	-0.2303	-0.6449	-0.6449	0.7825
G1- Top Flange	0.6138	0.5539	0.5539	0.9994	0.9994	1.5690	1.5690	-1.3090
G2 - Bottom Flange	-0.0130	0.3154	0.3154	-0.2185	-0.2185	-0.5826	-0.5826	0.7031
G2 - Top Flange	0.5633	0.5213	0.5213	0.9587	0.9587	1.4460	1.4460	-1.3310
G3 - Bottom Flange	0.0019	0.2641	0.2641	-0.2665	-0.2665	-0.6564	-0.6564	0.7692
G3 - Top Flange	0.5450	0.5403	0.5403	0.8567	0.8567	1.2830	1.2830	-1.2370
G4 - Bottom Flange	0.0204	0.1994	0.1994	-0.2775	-0.2775	-0.7810	-0.7810	0.8049
G4 - Top Flange	0.5065	0.5538	0.5538	0.7500	0.7500	1.1630	1.1630	-1.1870

**Deflections - Vertical (mm)**

	Abutment 1	Field Splice 1 Section 1	Field Splice 1 Section 2	Field Splice 2 Section 2	Field Splice 2 Section 3	Field Splice 3 Section 3	Field Splice 3 Section 4	Field Splice 4 Section 4
G1- Bottom Flange	0.1243	-3.0010	-3.0010	-4.7580	-4.7580	-9.4920	-9.4920	6.1300
G1- Top Flange	0.0921	-2.9950	-2.9950	-4.7490	-4.7490	-9.4930	-9.4930	6.1300
G2 - Bottom Flange	0.1354	-2.8780	-2.8780	-3.8820	-3.8820	-7.5370	-7.5370	4.1180
G2 - Top Flange	0.1047	-2.8770	-2.8770	-3.8760	-3.8760	-7.5360	-7.5360	4.1180
G3 - Bottom Flange	0.1298	-2.7700	-2.7700	-3.0250	-3.0250	-5.7090	-5.7090	2.1160
G3 - Top Flange	0.1028	-2.7700	-2.7700	-3.0220	-3.0220	-5.7100	-5.7100	2.1160
G4 - Bottom Flange	0.1186	-2.6060	-2.6060	-2.2030	-2.2030	-3.9020	-3.9020	0.1569
G4 - Top Flange	0.0924	-2.6060	-2.6060	-2.1990	-2.1990	-3.9030	-3.9030	0.1568

**Vertical - Support Reactions (kN)**

	Abutment 1	Falsework 1	Falsework 2A	Falsework 2	Pier Bracket at XF 26	Pier 1	Pier Bracket at XF 28
G1	431.5	0.0	0.0	1517.2	n/a	1059.3	n/a
G2	253.8	0.0	0.0	1279.0	n/a	939.9	n/a
G3	224.7	0.0	0.0	835.4	n/a	812.7	n/a
G4	184.4	0.0	0.0	638.2	n/a	625.5	n/a

**Vertical Support Reactions (kips)**

	Abutment 1	Falsework 1	Falsework 2A	Falsework 2	Pier Bracket at XF 26	Pier 1	Pier Bracket at XF 28
G1	97.0	0.0	0.0	341.1	n/a	238.1	n/a
G2	57.1	0.0	0.0	287.5	n/a	211.3	n/a
G3	50.5	0.0	0.0	187.8	n/a	182.7	n/a
G4	41.5	0.0	0.0	143.5	n/a	140.6	n/a

**Cross-frame Vertical Reactions**

	(kN)	(kips)
XF 26B (outside)	0.000	0.0000
XF 27B (outside)	0.000	0.0000
XF 27C (inside)	0.000	0.0000
XF 28B (outside)	0.000	0.0000

**Figure C-82** Removal of Falsework 1 and 2A – Field-splice location deflections and support reactions summary

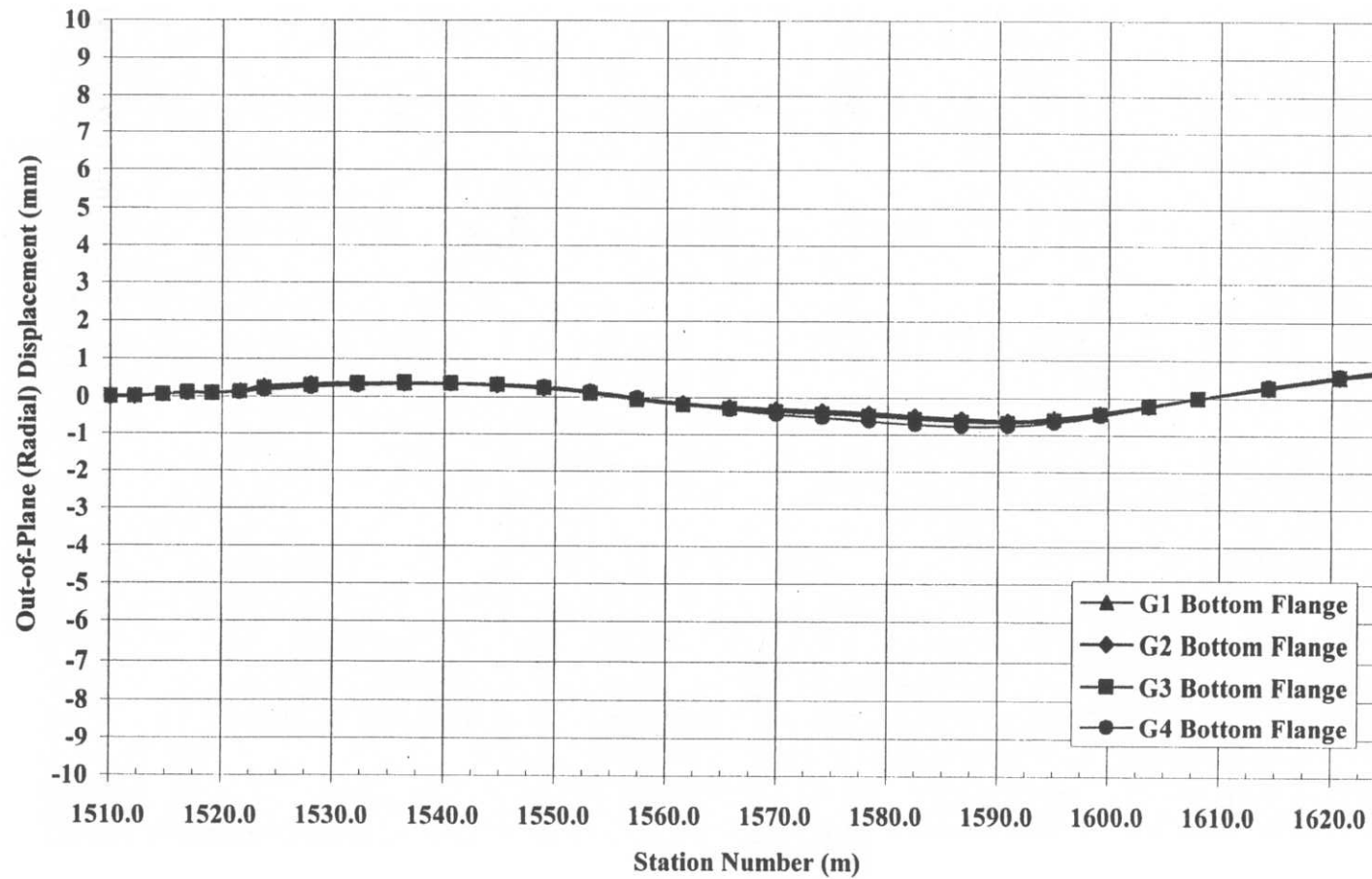
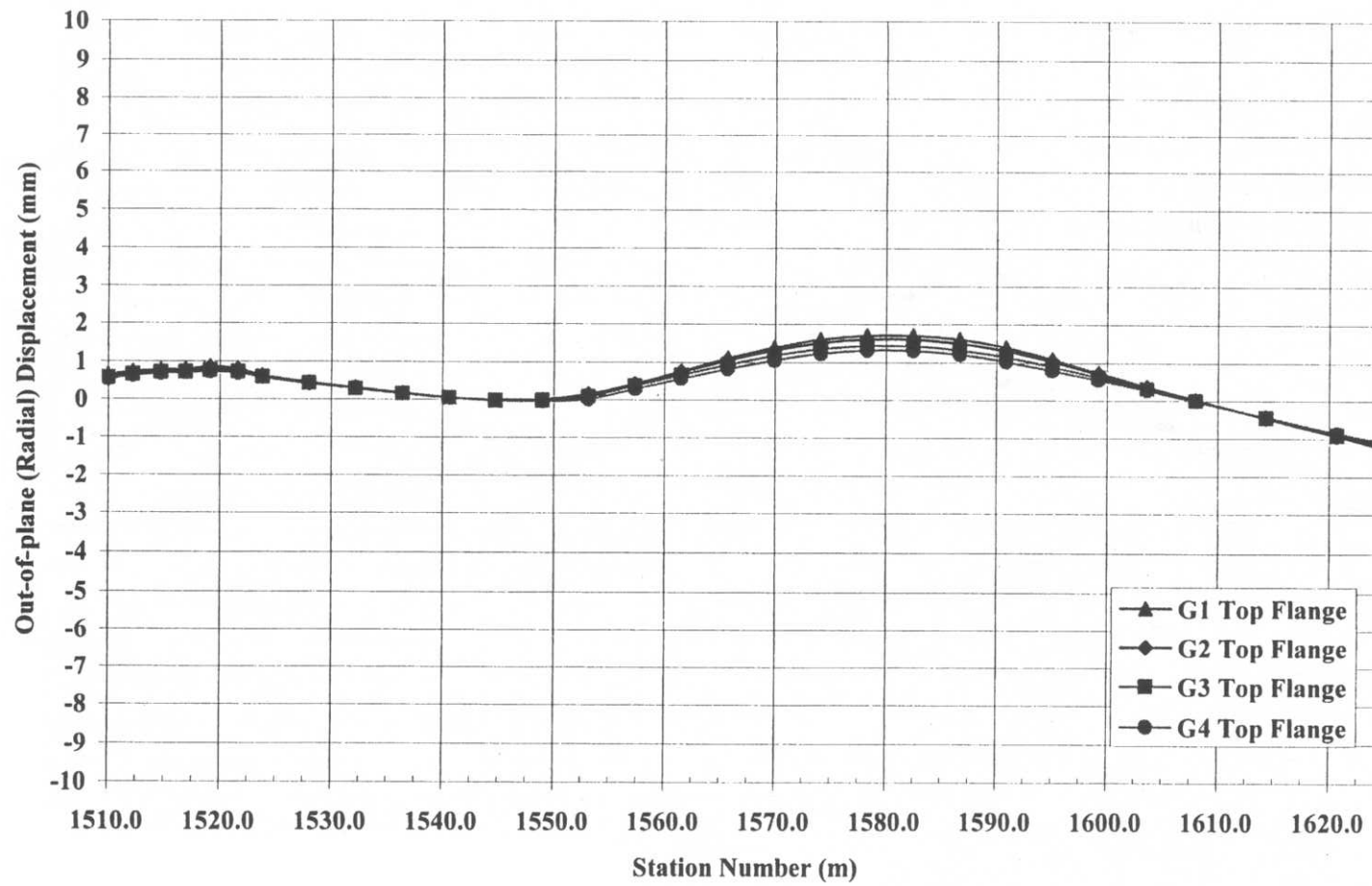
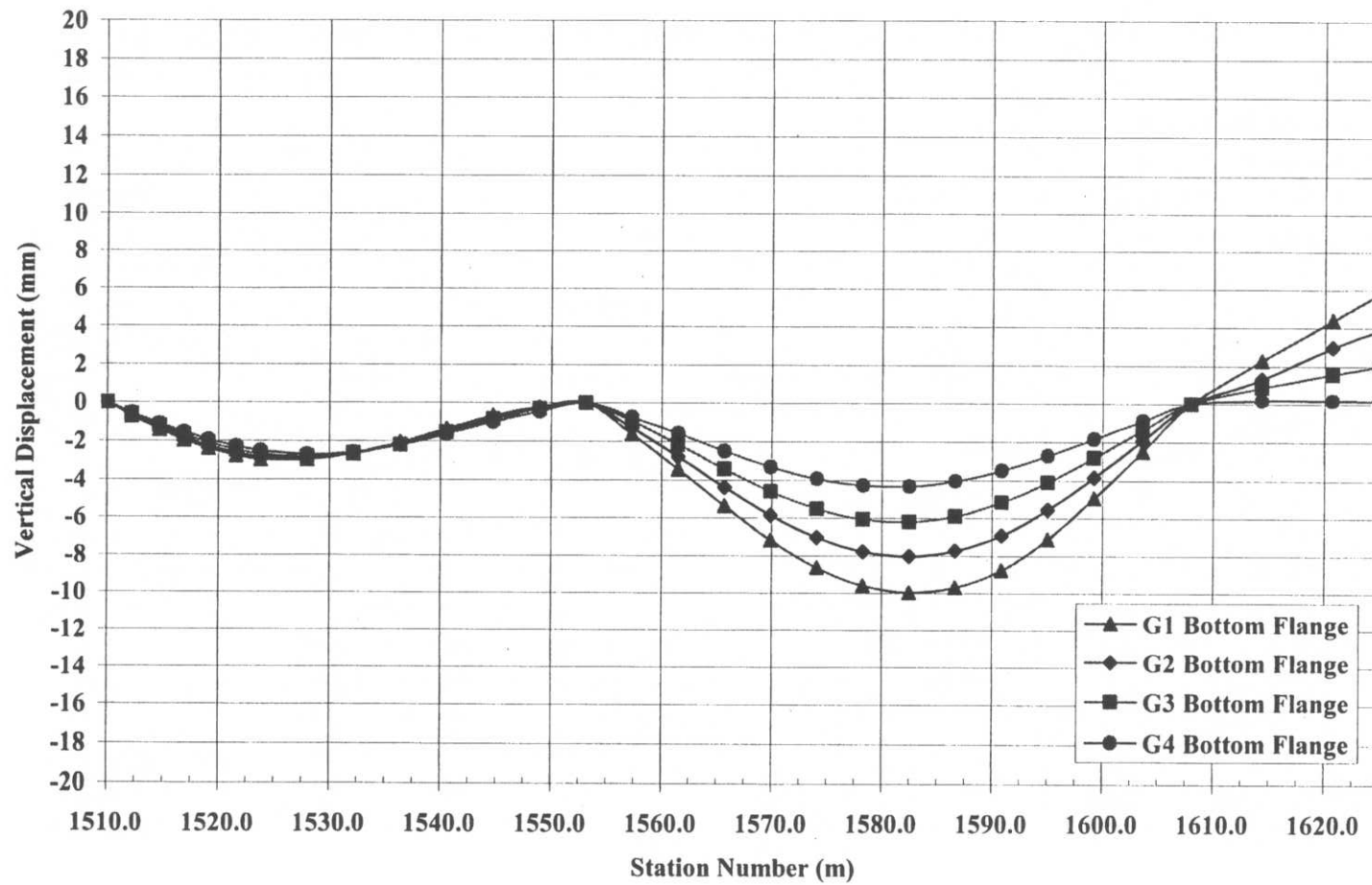


Figure C-83 Removal of Falsework 1 and 2A – Out-of-plane (radial) displacement, centerline of bottom flange



**Figure C-84** Removal of Falsework 1 and 2A – Out-of-plane (radial) displacement, centerline of top flange



**Figure C-85** Removal of Falsework 1 and 2A - Vertical displacement, centerline of bottom flange

### **Appendix C.2 “Planned” Erection Sequence Analytical Results**

Results are presented for the “planned” erection sequence analytical studies, construction stages 13 through 16. For each construction stage the following five figures are included:

1. Figure ‘1’ - Plan view of finite element model.
2. Figure ‘2’ - Field-splice location deflections and support reactions summary.
3. Figure ‘3’ - Out-of-plane (radial) displacement, centerline of bottom flange.
4. Figure ‘4’ - Out-of-plane (radial) displacement, centerline of top flange.
5. Figure ‘5’ - Vertical displacement, centerline of bottom flange.

For figures ‘3’ and ‘4,’ “-“ (negative) is displacement inward of curve, and “+” (positive) is displacement outward of curve

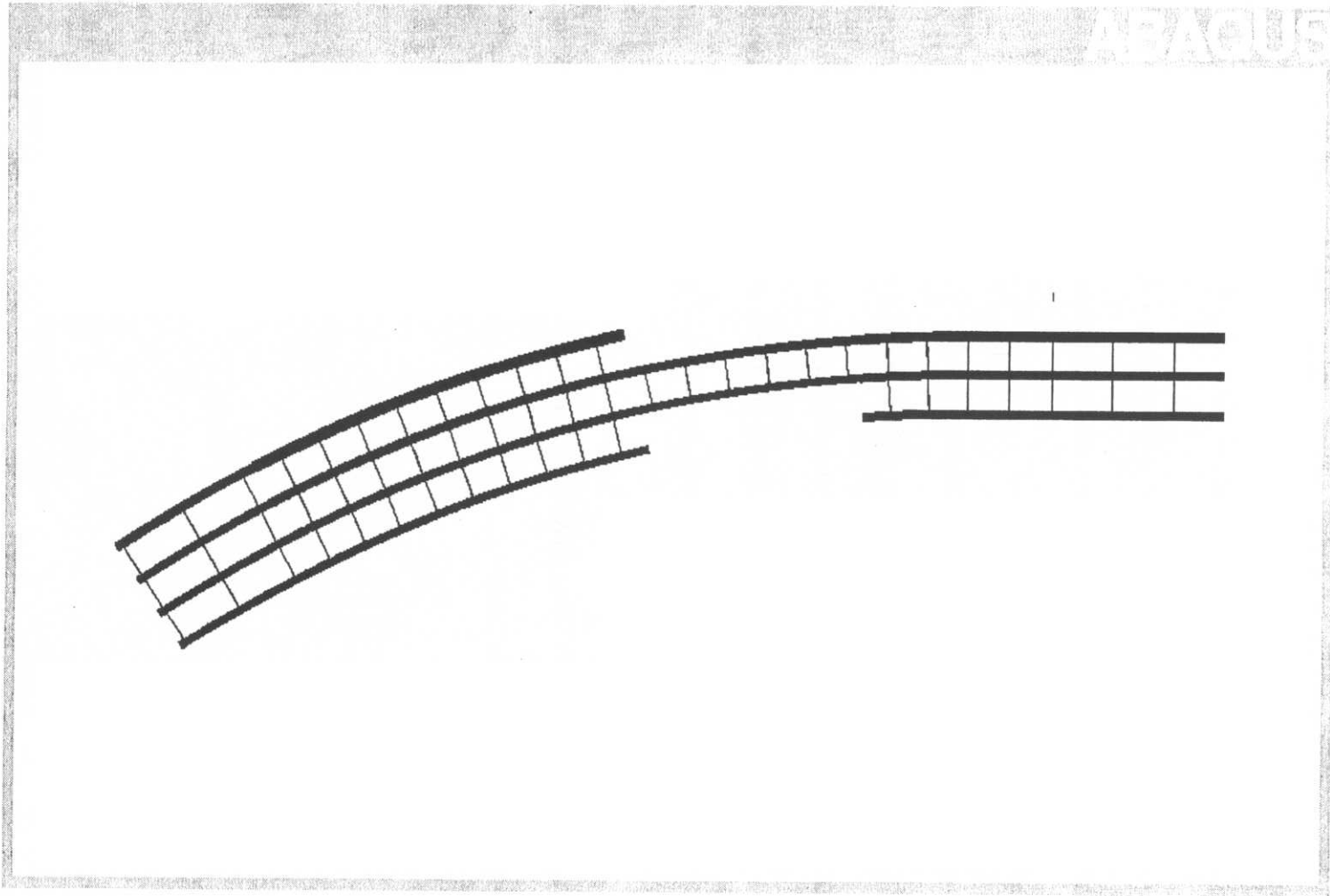


**Figure C-86** “Planned” construction stage 13 – Plan view of finite element model  
(Note: only change from “in-field” construction stage 13 is the boundary condition due to falsework 1 and 2 removal)

**Deflections - Out-of-Plane (Radial) (mm)**

	Abutment 1	Field Splice 1 Section 1	Field Splice 1 Section 2	Field Splice 2 Section 2	Field Splice 2 Section 3	Field Splice 3 Section 3	Field Splice 3 Section 4	Field Splice 4 Section 4
G1- Bottom Flange	-0.1257	-0.0422	-0.0422	1.1590				
G1- Top Flange	0.8923	1.4970	1.4970	-1.2840				
G2 - Bottom Flange	-0.0903	0.0879	0.0879	0.1677	0.1677	-0.7824	-0.7824	1.0140
G2 - Top Flange	0.7471	1.4040	1.4040	-0.0093	-0.0093	1.4560	1.4560	-1.3450
G3 - Bottom Flange	0.0023	0.0220	0.0220	-0.0209	-0.0209	-0.8818	-0.8818	1.0970
G3 - Top Flange	0.6355	1.3000	1.3000	0.1712	0.1712	1.2950	1.2950	-1.2510
G4 - Bottom Flange	0.1126	-0.0375	-0.0375	-0.2871			-1.0100	1.1400
G4 - Top Flange	0.5077	1.2130	1.2130	0.2402			1.1410	-1.1980

**Deflections - Vertical (mm)**

	Abutment 1	Field Splice 1 Section 1	Field Splice 1 Section 2	Field Splice 2 Section 2	Field Splice 2 Section 3	Field Splice 3 Section 3	Field Splice 3 Section 4	Field Splice 4 Section 4
G1- Bottom Flange	0.2436	-5.8210	-5.8210	1.3130				
G1- Top Flange	0.1994	-5.8120	-5.8120	1.3110				
G2 - Bottom Flange	0.2110	-4.5810	-4.5810	-2.2300	-2.2300	-6.7230	-6.7230	3.4090
G2 - Top Flange	0.1751	-4.5780	-4.5780	-2.2230	-2.2230	-6.7230	-6.7230	3.4090
G3 - Bottom Flange	0.1607	-3.4320	-3.4320	-2.2360	-2.2360	-4.6790	-4.6790	1.0790
G3 - Top Flange	0.1325	-3.4320	-3.4320	-2.2330	-2.2330	-4.6790	-4.6790	1.0790
G4 - Bottom Flange	0.1062	-2.2890	-2.2890	-1.2450			-2.7620	-1.2180
G4 - Top Flange	0.0831	-2.2900	-2.2900	-1.2450			-2.7630	-1.2180

**Vertical - Support Reactions (kN)**

	Abutment 1	Falsework 1	Falsework 2A	Falsework 2	Pier Bracket at XF 26	Pier 1	Pier Bracket at XF 28
G1	529.0	0.0	0.0	1118.3			
G2	295.8	0.0	0.0	1036.2	0.0	958.5	0.0
G3	234.4	0.0	0.0	774.1	0.0	787.5	0.0
G4	163.5	0.0	0.0	540.1	0.0	581.8	0.0

**Vertical Support Reactions (kN)**

	Abutment 1	Falsework 1	Falsework 2A	Falsework 2	Pier Bracket at XF 26	Pier 1	Pier Bracket at XF 28
G1	118.9	0.0	0.0	251.4			
G2	66.5	0.0	0.0	232.9	0.0	215.5	0.0
G3	52.7	0.0	0.0	174.0	0.0	177.0	0.0
G4	36.8	0.0	0.0	121.4	0.0	130.8	0.0

**Cross-frame Vertical Reactions**

	(kN)	(kips)
XF 26B (outside)	0.000	0.000
XF 27B (outside)	0.000	0.000
XF 27C (inside)	0.000	0.000
XF 28B (outside)	0.000	0.000

**Figure C-87** “Planned” construction stage 13 – Field-splice location deflections and support reactions summary

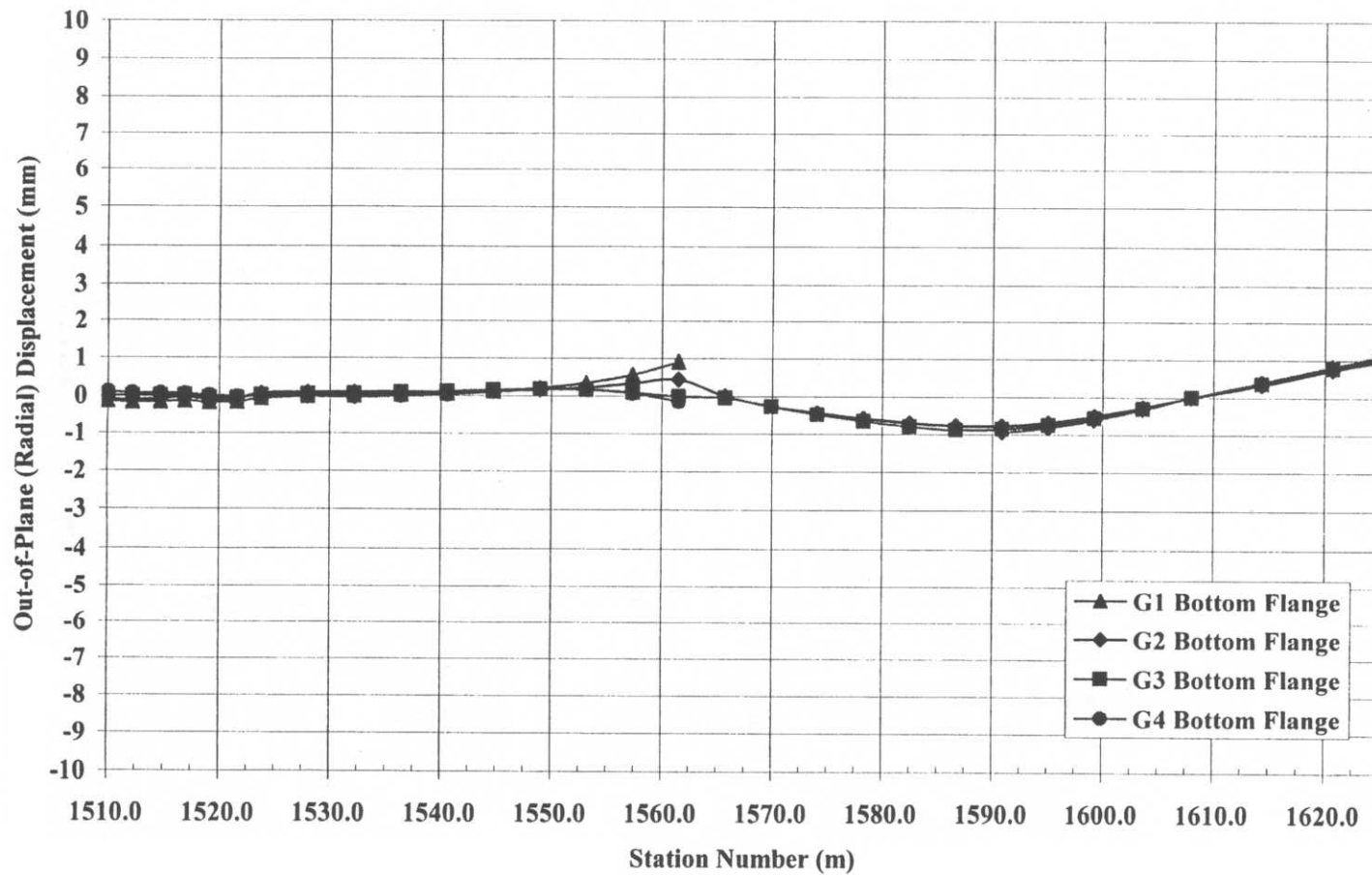


**Figure C-88** “Planned” construction stage 13 – Out-of-plane (radial) displacement, centerline of bottom flange

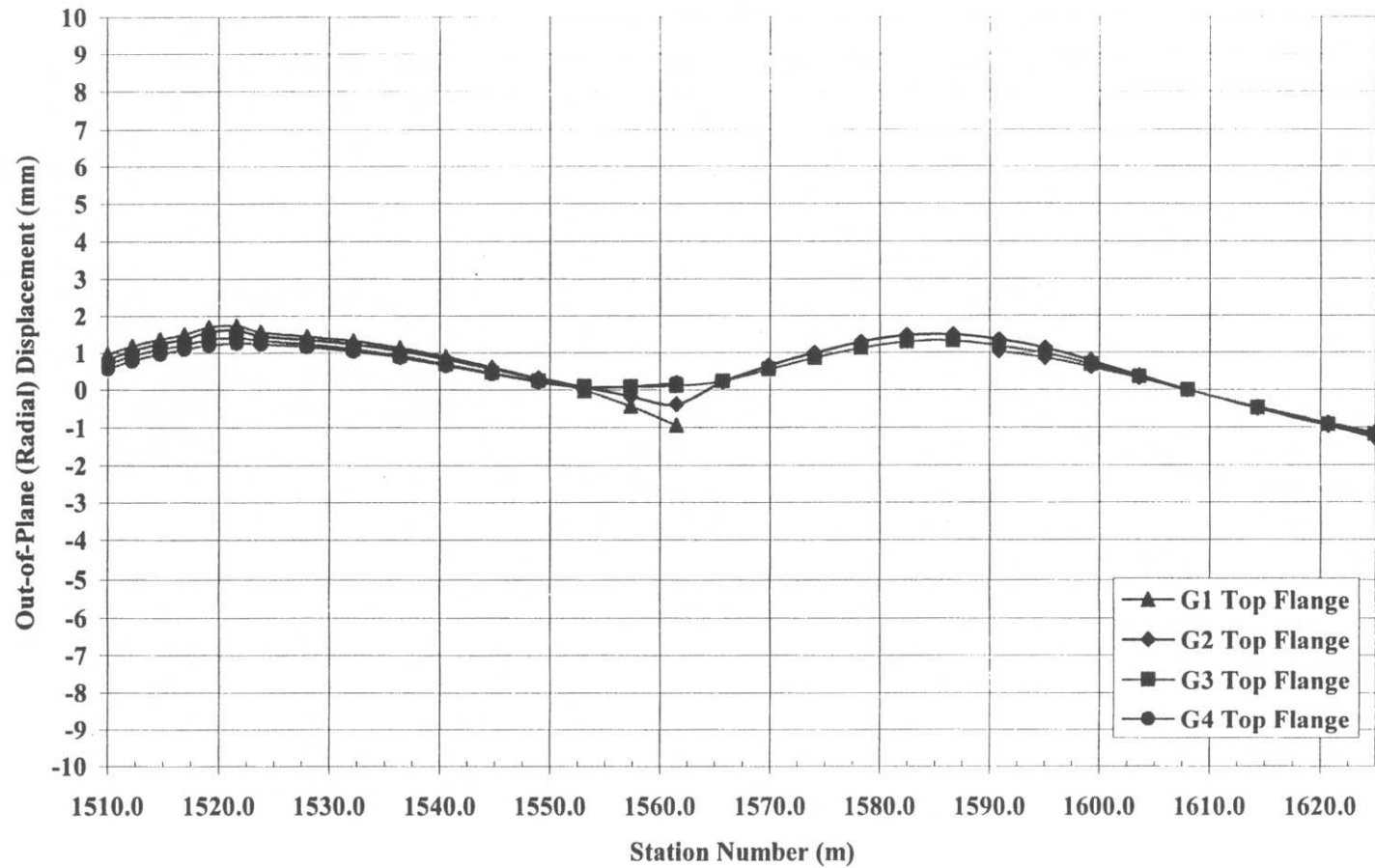


Figure C-89 “Planned” construction stage 13 – Out-of-plane (radial) displacement, centerline to top flange

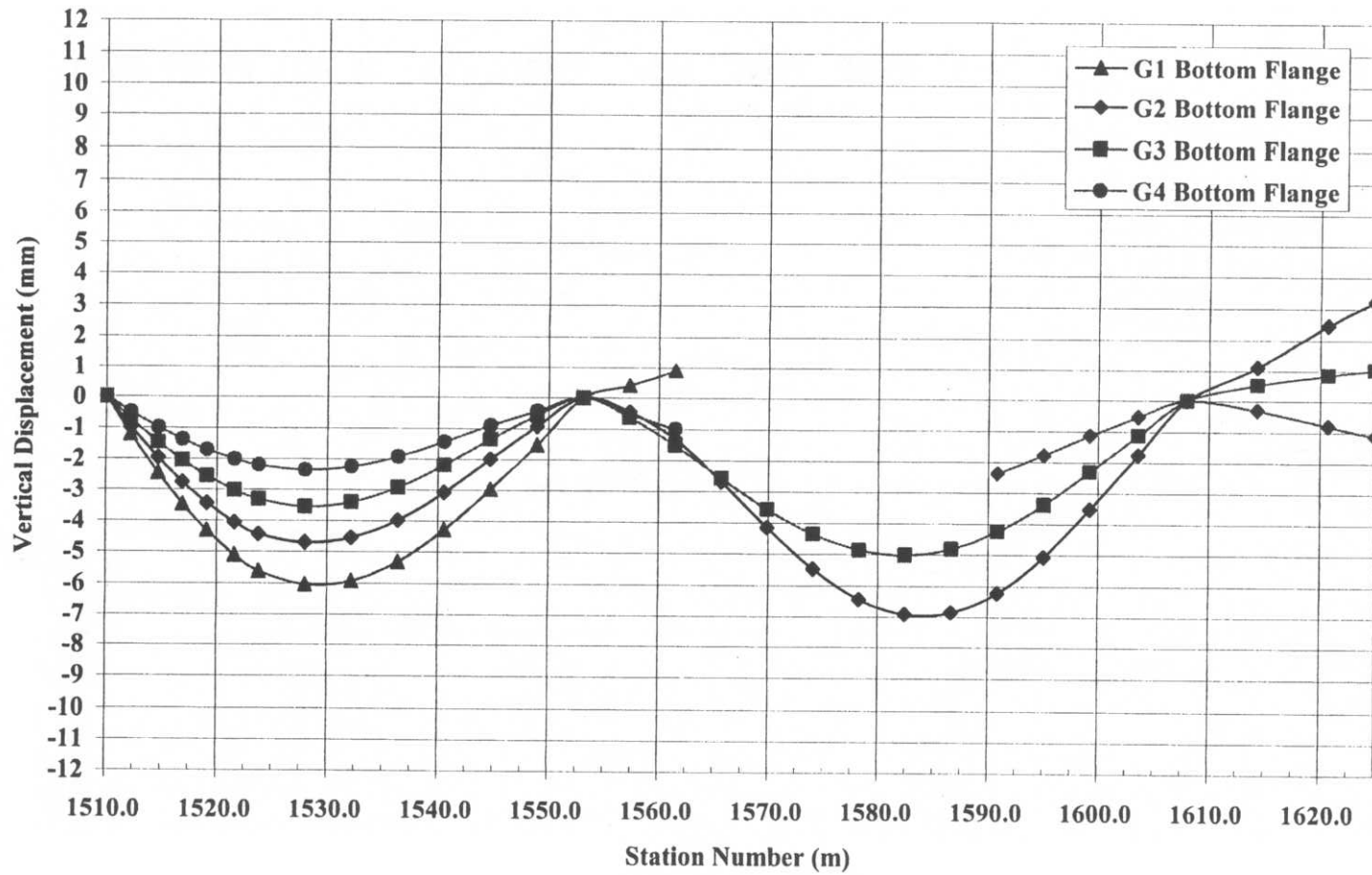
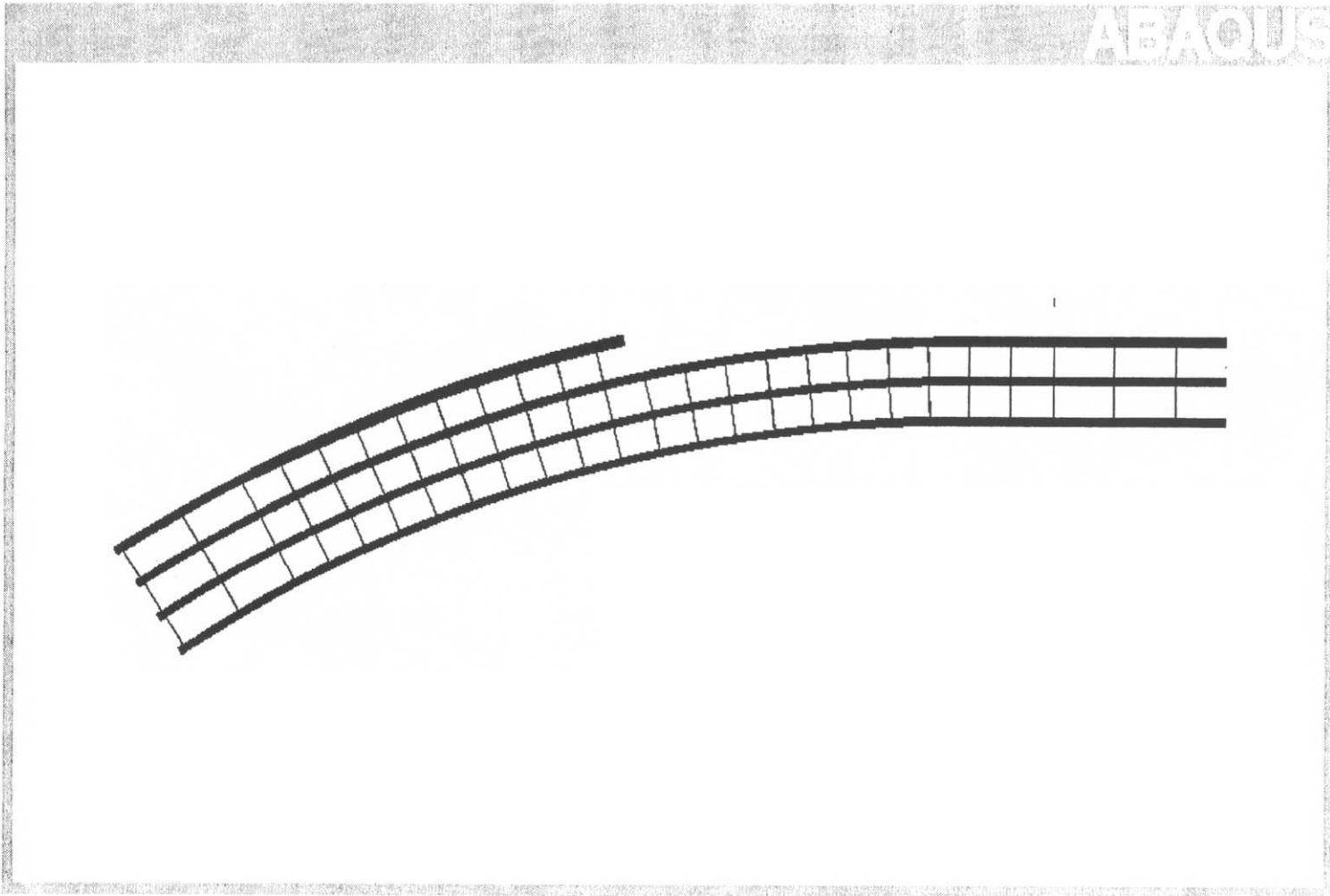


Figure C-90 “Planned” construction stage 13 – Vertical displacement, centerline of bottom flange



**Figure C-91** “Planned” construction stage 14 – Plan view of finite element model  
(Note: change from “in-field” construction stage 14 is the boundary conditions due to falsework 1 and 2 removal and different girder placement)

**Deflections - Out-of-Plane (Radial) (mm)**

	Abutment 1	Field Splice 1 Section 1	Field Splice 1 Section 2	Field Splice 2 Section 2	Field Splice 2 Section 3	Field Splice 3 Section 3	Field Splice 3 Section 4	Field Splice 4 Section 4
G1 - Bottom Flange	-0.1708	-0.1705	-0.1705	1.3440				
G1 - Top Flange	0.8689	1.6350	1.6350	-1.6340				
G2 - Bottom Flange	-0.1140	-0.0260	-0.0260	0.3339	0.3339	-0.3597	-0.3597	0.5053
G2 - Top Flange	0.6998	1.5300	1.5300	-0.3180	-0.3180	0.8476	0.8476	-0.7747
G3 - Bottom Flange	0.0021	-0.0869	-0.0869	0.1672	0.1672	-0.3843	-0.3843	0.5505
G3 - Top Flange	0.5708	1.3980	1.3980	-0.0810	-0.0810	0.7427	0.7427	-0.6981
G4 - Bottom Flange	0.1354	-0.1399	-0.1399	0.1315	0.1315	-0.4557	-0.4557	0.5680
G4 - Top Flange	0.4195	1.2810	1.2810	0.0017	0.0017	0.6728	0.6728	-0.6670

**Deflections - Vertical (mm)**

	Abutment 1	Field Splice 1 Section 1	Field Splice 1 Section 2	Field Splice 2 Section 2	Field Splice 2 Section 3	Field Splice 3 Section 3	Field Splice 3 Section 4	Field Splice 4 Section 4
G1 - Bottom Flange	0.2510	-6.0070	-6.0070	1.5940				
G1 - Top Flange	0.2071	-5.9980	-5.9980	1.5920				
G2 - Bottom Flange	0.2077	-4.4940	-4.4940	-2.4010	-2.4010	-6.8970	-6.8970	3.5900
G2 - Top Flange	0.1724	-4.4920	-4.4920	-2.3930	-2.3930	-6.8960	-6.8960	3.5900
G3 - Bottom Flange	0.1460	-3.0810	-3.0810	-2.9220	-2.9220	-5.8480	-5.8480	2.3250
G3 - Top Flange	0.1189	-3.0810	-3.0810	-2.9190	-2.9190	-5.8480	-5.8480	2.3250
G4 - Bottom flange	0.0805	-1.6810	-1.6810	-3.2070	-3.2070	-4.4320	-4.4320	1.0940
G4 - Top Flange	0.0592	-1.6820	-1.6820	-3.2040	-3.2040	-4.8330	-4.8330	1.0940

**Vertical - Support Reactions (kN)**

	Abutment 1	Falsework 1	Falsework 2A	Falsework 2	Pier Bracket at XF 26	Pier 1	Pier Bracket at XF 28
G1	534.4	0.0	0.0	1095.2			
G2	291.1	0.0	0.0	1048.2	0.0	970.0	0.0
G3	225.1	0.0	0.0	843.2	0.0	819.3	0.0
G4	150.3	0.0	0.0	695.1	0.0	641.1	0.0

**Vertical Support Reactions (kips)**

	Abutment 1	Falsework 1	Falsework 2A	Falsework 2	Pier Bracket at XF 26	Pier 1	Pier Bracket at XF 28
G1	120.1	0.0	0.0	246.2			
G2	65.4	0.0	0.0	235.6	0.0	218.1	0.0
G3	50.6	0.0	0.0	189.6	0.0	184.2	0.0
G4	33.8	0.0	0.0	156.3	0.0	144.1	0.0

**Cross-frame Vertical Reactions**

	(kN)	(kips)
XF 26B (outside)	0.000	0.000
XF 27B (outside)	0.000	0.000
XF 27C (inside)	0.000	0.000
XF 28B (outside)	0.000	0.000

**Figure C-92** “Planned” construction stage 14 – Field-splice location deflections and support reactions summary

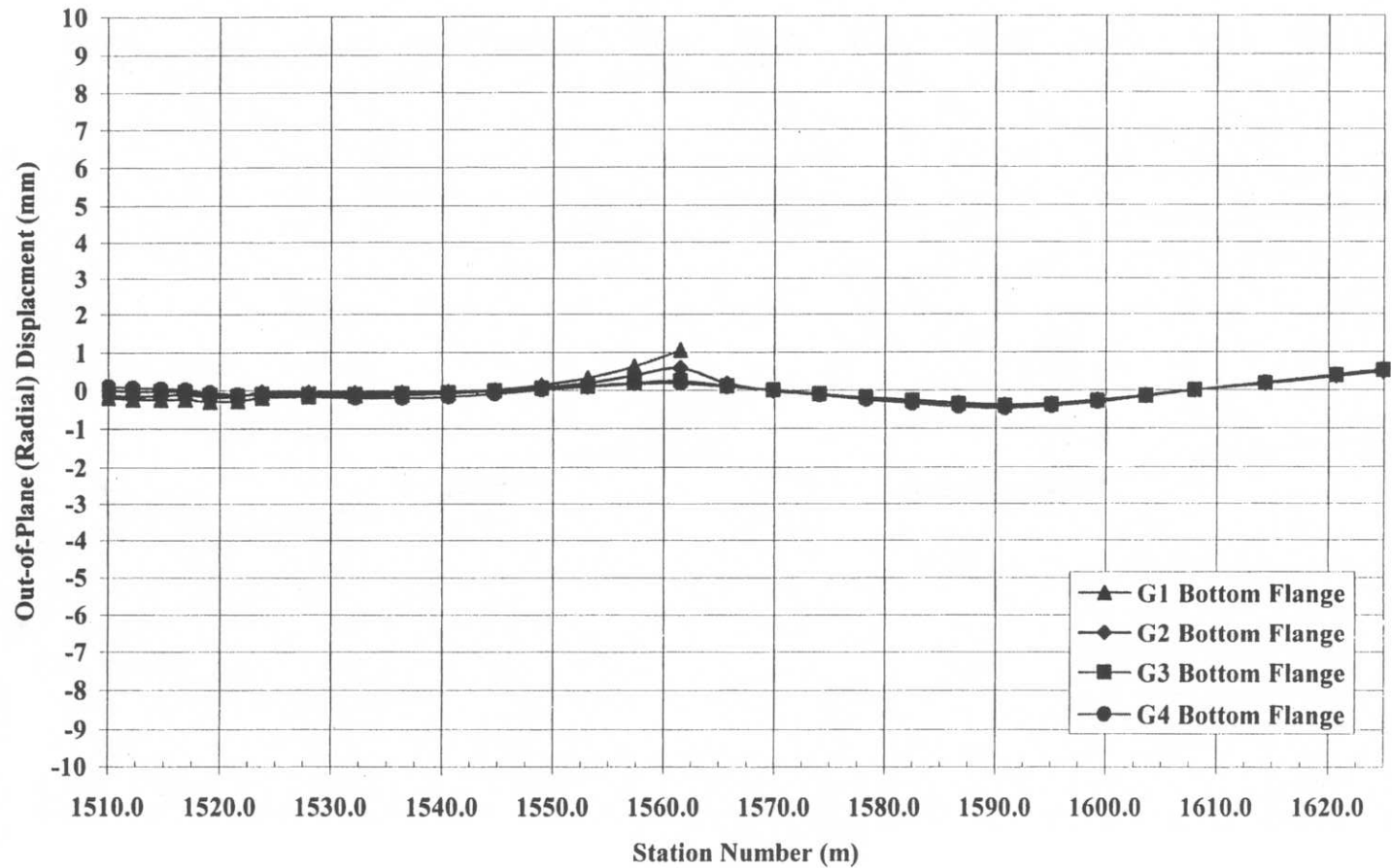


Figure C-93 “Planned” construction stage 14 – Out-of-plane (radial) displacement, centerline of bottom flange

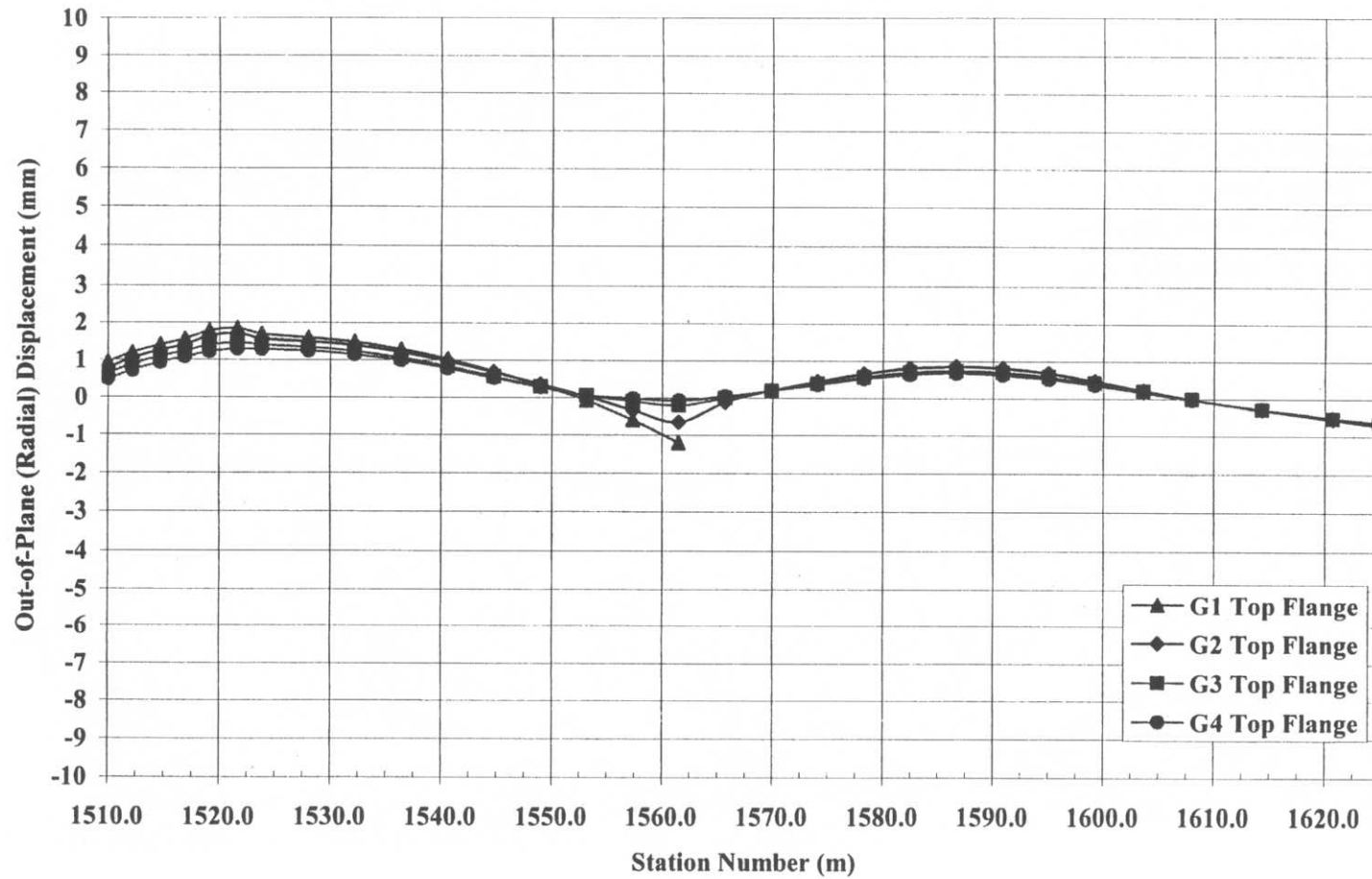


Figure C-94 “Planned” construction stage 14 – Out-of-plane (radial) displacement, centerline of top flange

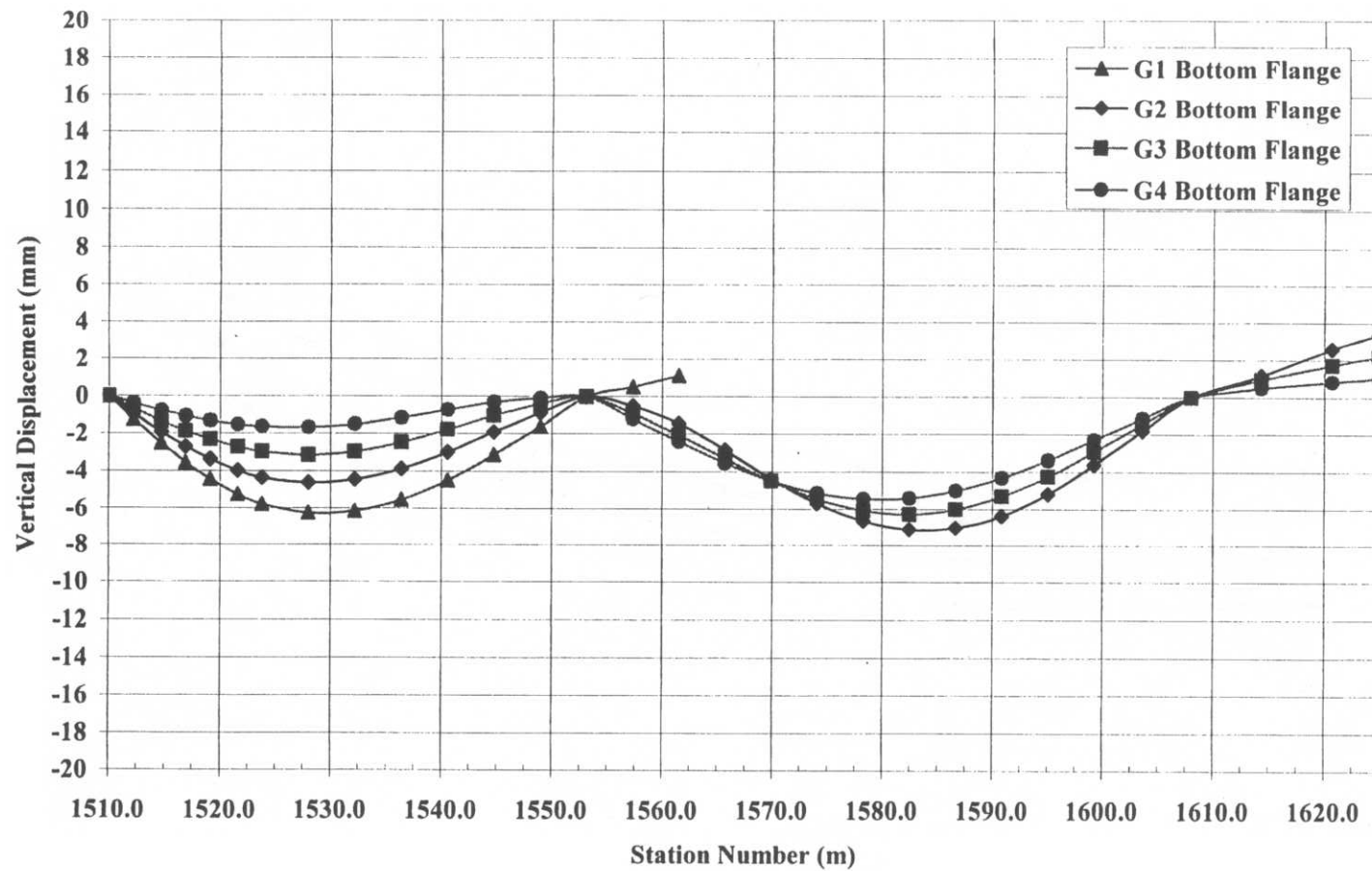
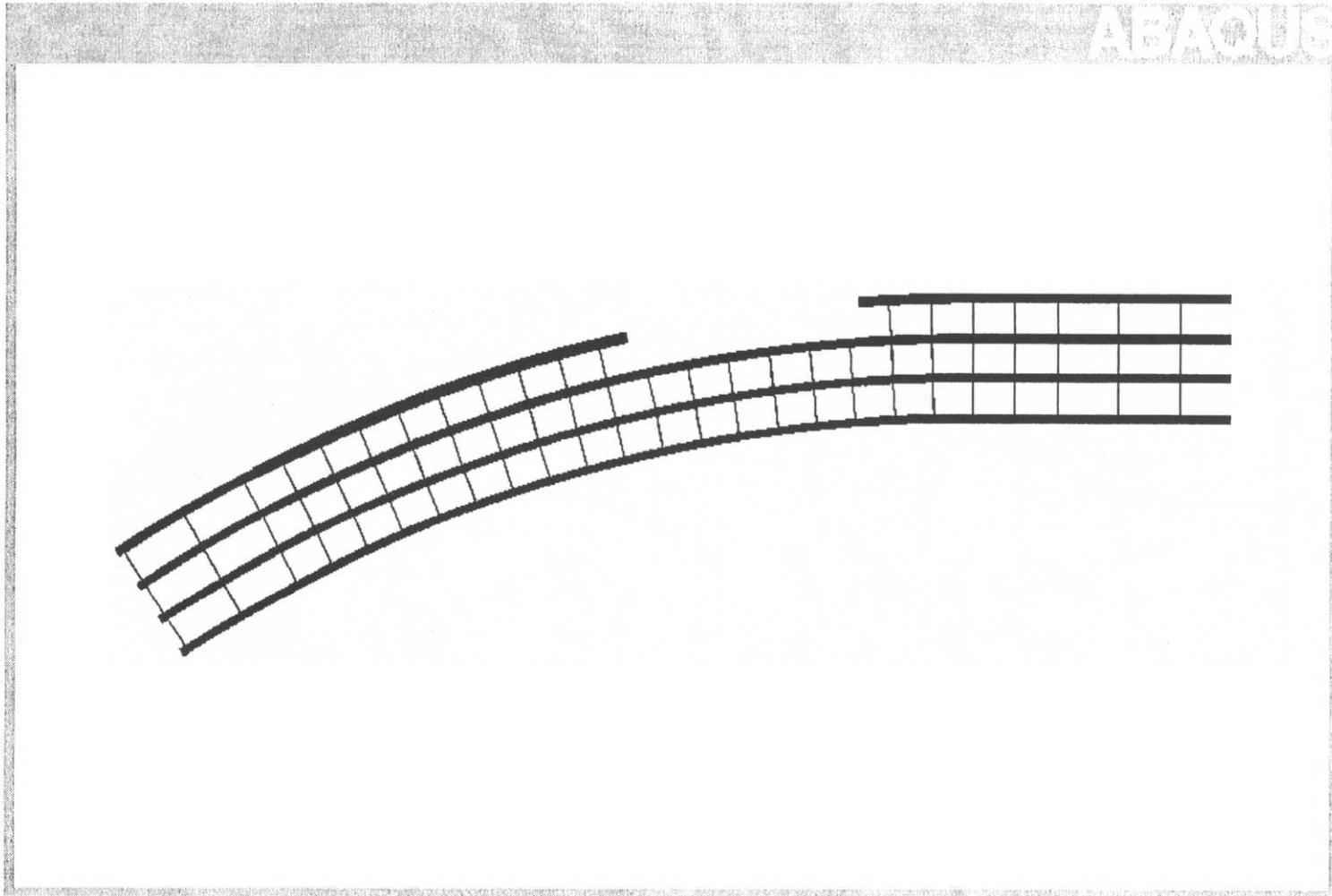


Figure C-95 “Planned” construction stage 14 – Vertical displacement, centerline of bottom flange



**Figure C-96** “Planned” construction stage 15 – Plan view of finite element model  
(Note: change from “in-field” construction stage 15 is the boundary conditions due to falsework 1 and 2 removal)

**Deflections - Out-of-Plane (Radial) (mm)**

	Abutment 1	Field Splice 1 Section 1	Field Splice 1 Section 2	Field Splice 2 Section 2	Field Splice 2 Section 3	Field Splice 3 Section 3	Field Splice 3 Section 4	Field Splice 4 Section 4
G1- Bottom Flange	-0.1570	-0.1587	-0.1587	1.3640			-1.1430	0.6833
G1- Top Flange	0.8488	1.5550	1.5550	-1.5710			1.9580	-1.3420
G2 - Bottom Flange	-0.1047	-0.0188	-0.0188	0.2622	0.2622	-0.7300	-0.7300	0.6158
G2 - Top Flange	0.6879	1.4540	1.4540	-0.1455	-0.1455	1.4600	1.4600	-1.3730
G3 - Bottom Flange	0.0020	-0.0804	-0.0804	0.0689	0.0689	-0.7357	-0.7357	0.7001
G3 - Top Flange	0.5625	1.3280	1.3280	0.0790	0.0790	1.2250	1.2250	-1.3010
G4 - Bottom Flange	0.1261	-0.1362	-0.1362	0.0203	0.0203	-0.8267	-0.8267	0.7429
G4 - Top Flange	0.4148	1.2170	1.2170	0.1357	0.1357	1.0780	1.0780	-1.2590

**Deflections - Vertical (mm)**

	Abutment 1	Field Splice 1 Section 1	Field Splice 1 Section 2	Field Splice 2 Section 2	Field Splice 2 Section 3	Field Splice 3 Section 3	Field Splice 3 Section 4	Field Splice 4 Section 4
G1- Bottom Flange	0.2413	-5.7890	-5.7890	1.2760			-11.9500	6.6750
G1- Top Flange	0.1987	-5.7800	-5.7800	1.2740			-11.9600	6.6750
G2 - Bottom Flange	0.2016	-4.3540	-4.3540	-2.8090	-2.8090	-8.0870	-8.0870	4.7480
G2 - Top Flange	0.1666	-4.3520	-4.3520	-2.8010	-2.8010	-8.0850	-8.0850	4.7480
G3 - Bottom Flange	0.1432	-3.0190	-3.0190	-3.0930	-3.0930	-6.2300	-6.2300	2.7600
G3 - Top Flange	0.1162	-3.0190	-3.0190	-3.0900	-3.0900	-6.2300	-6.2300	2.7590
G4 - Bottom Flange	0.0809	-1.6930	-1.6930	-3.1150	-3.1150	-4.4940	-4.4940	0.7786
G4 - Top Flange	0.0595	-1.6930	-1.6930	-3.1120	-3.1120	-4.4960	-4.4960	0.7786

**Vertical - Support Reactions (kN)**

	Abutment 1	Falsework 1	Falsework 2A	Falsework 2	Pier Bracket at XF 26	Pier 1	Pier Bracket at XF 28
G1	528.9	0.0	0.0	1108.8	0.0	812.2	0.0
G2	288.0	0.0	0.0	1062.5	0.0	963.1	0.0
G3	224.4	0.0	0.0	853.8	0.0	842.4	0.0
G4	151.4	0.0	0.0	692.6	0.0	626.1	0.0

**Vertical Support Reactions (kips)**

	Abutment 1	Falsework 1	Falsework 2A	Falsework 2	Pier Bracket at XF 26	Pier 1	Pier Bracket at XF 28
G1	118.9	0.0	0.0	249.3	0.0	182.6	0.0
G2	64.8	0.0	0.0	238.9	0.0	216.5	0.0
G3	50.4	0.0	0.0	191.9	0.0	189.4	0.0
G4	34.00	0.0	0.0	155.7	0.0	140.7	0.0

**Cross-frame Vertical Reactions**

	(kN)	(kips)
XF 26B (outside)	0.000	0.0000
XF 27B (outside)	0.000	0.0000
XF 27C (inside)	0.000	0.0000
XF 28B (outside)	0.000	0.0000

**Figure C-97** “Planned” construction stage 15 – Field-splice location deflections and support reactions summary

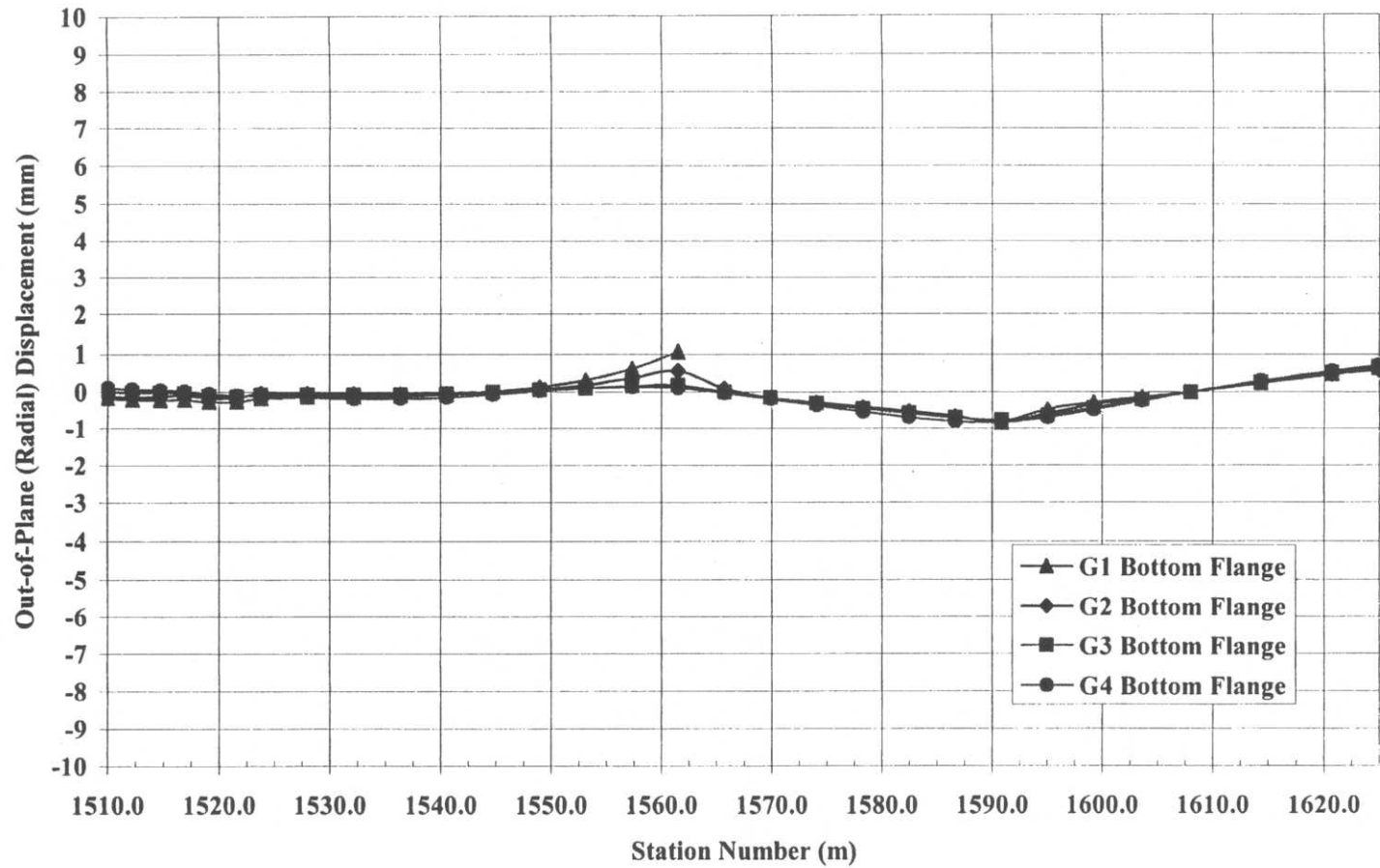


Figure C-98 “Planned” construction stage 15 – Out-of-plane (radial) displacement, centerline of bottom flange

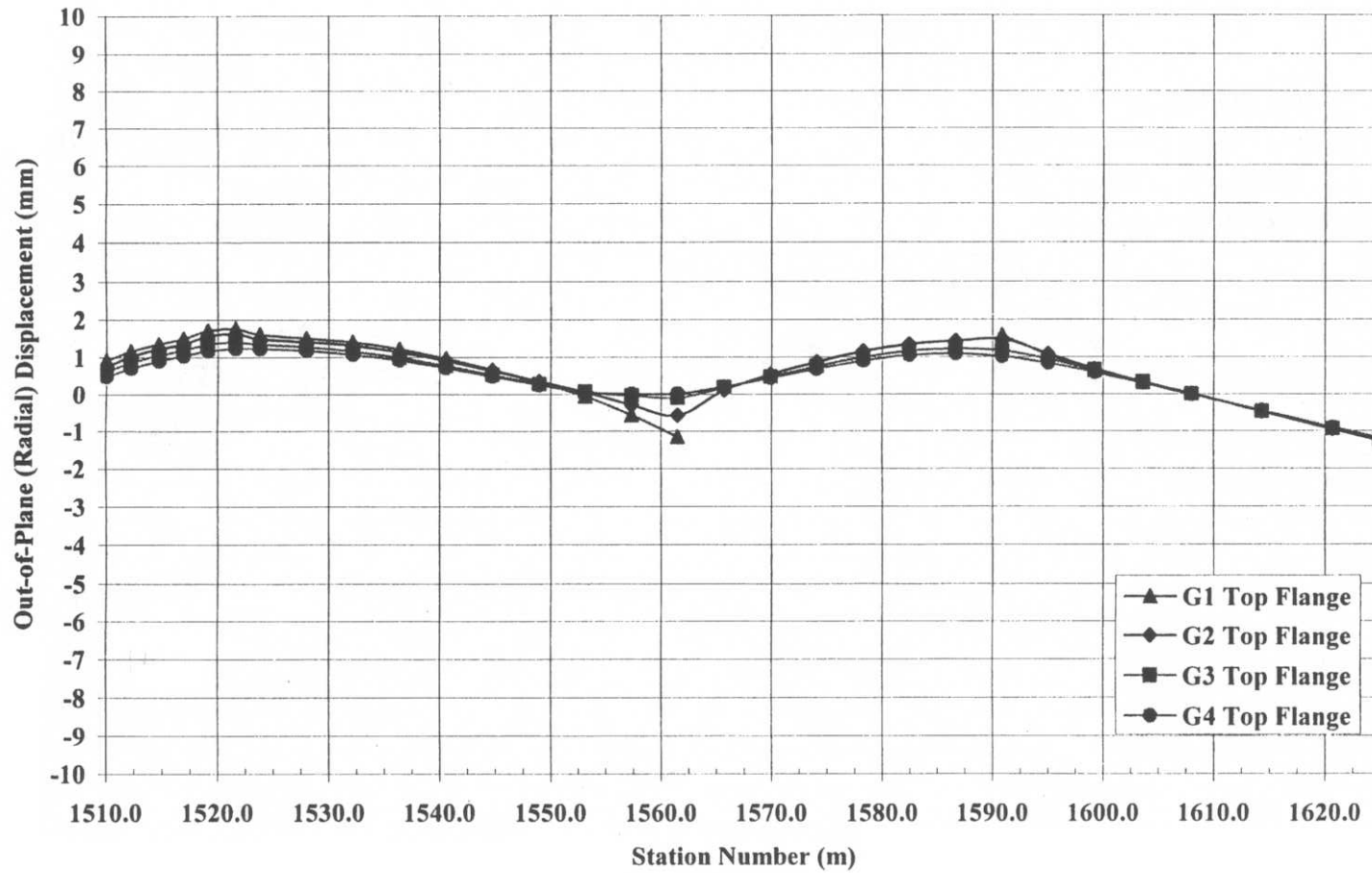


Figure C-99 “Planned” construction stage 15 – Out-of-plane (radial) displacement, centerline to top flange

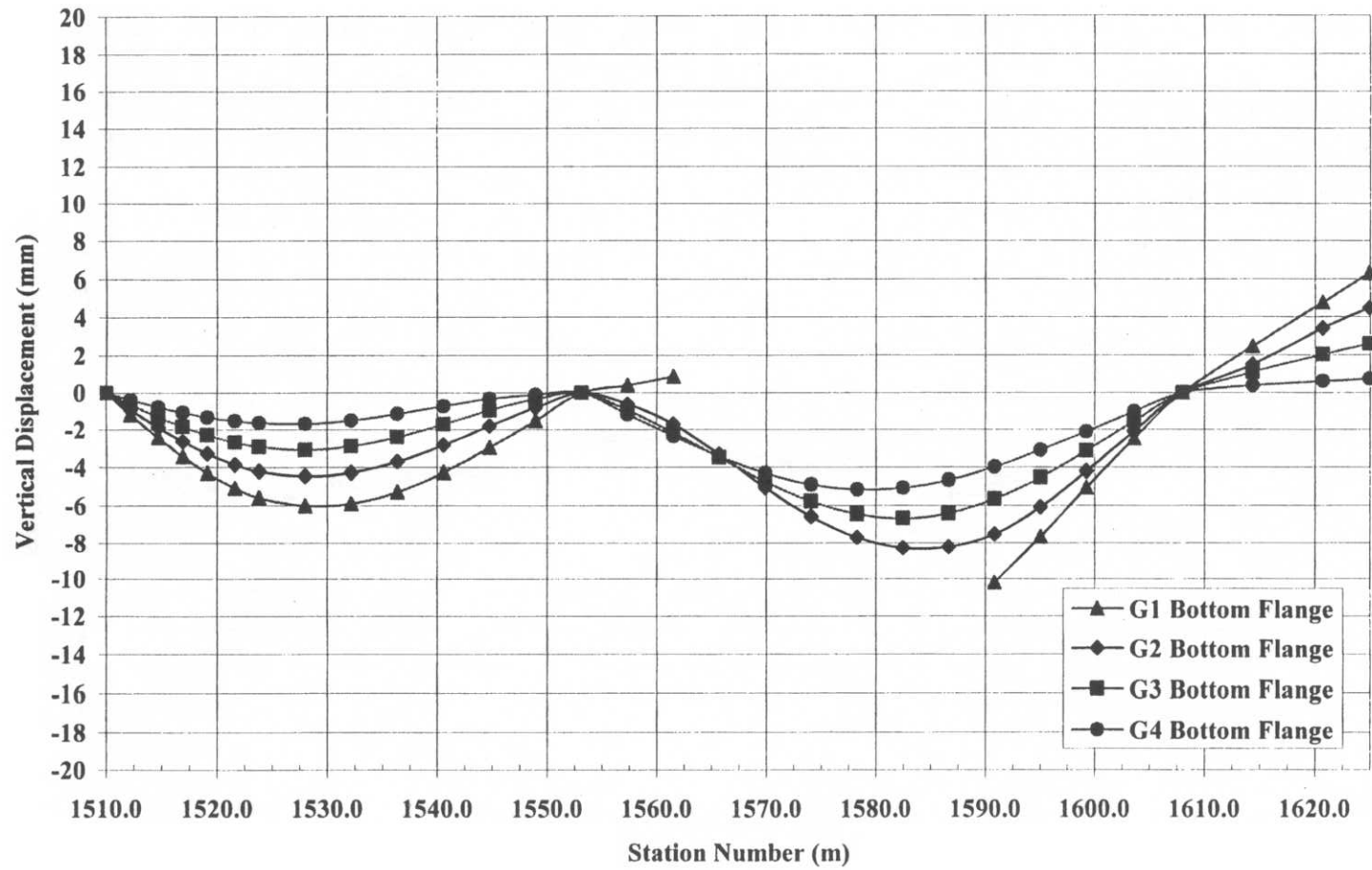
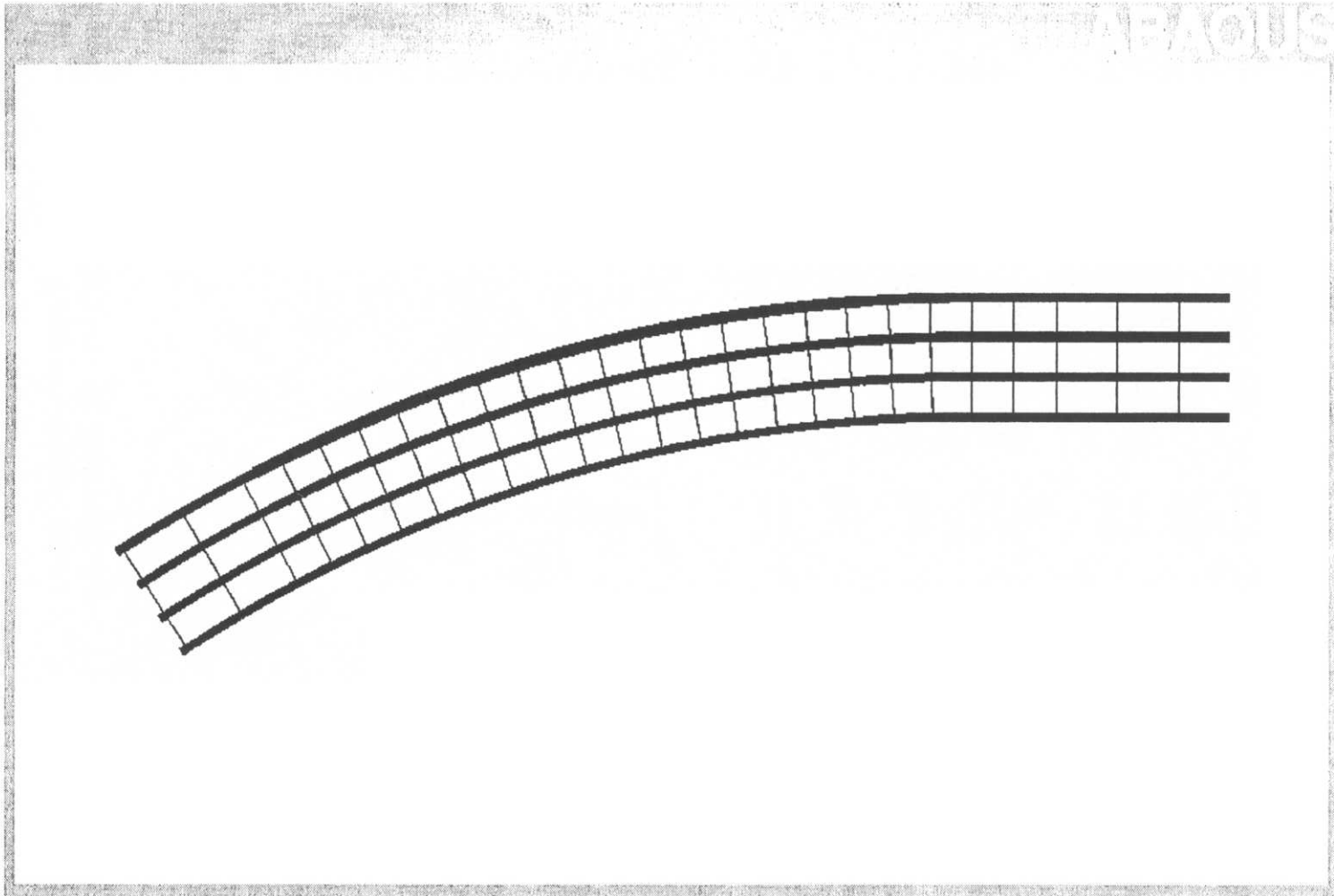


Figure C-100 “Planned” construction stage 15 – Vertical displacement, centerline of bottom flange



**Figure C-101** “Planned” construction stage 16 – Plan view of finite element model  
(Note: change from “in-field” construction stage 16 is the boundary conditions due to falsework 1 and 2 removal)

**Deflections - Out-of-Plane (Radial) (mm)**

	Abutment 1	Field Splice 1 Section 1	Field Splice 1 Section 2	Field Splice 2 Section 2	Field Splice 2 Section 3	Field Splice 3 Section 3	Field Splice 3 Section 4	Field Splice 4 Section 4
G1- Bottom Flange	0.0296	0.2761	0.2761	-0.2303	-0.2303	-0.6449	-0.6449	0.7825
G1- Top Flange	0.6138	0.5539	0.5539	0.9994	0.9994	1.5690	1.5690	-1.3090
G2 - Bottom Flange	-0.0130	0.3154	0.3154	-0.2185	-0.2185	-0.5856	-0.5856	0.7031
G2 - Top Flange	0.5633	0.5213	0.5213	0.9587	0.9587	1.4460	1.4460	-1.3310
G3 - Bottom Flange	0.0019	0.2641	0.2641	-0.2665	-0.2665	-0.6564	-0.6564	0.7692
G3 - Top Flange	0.5450	0.5403	0.5403	0.8567	0.8567	1.2830	1.2830	-1.2370
G4 - Bottom Flange	0.0204	0.1994	0.1994	-0.2775	-0.2775	-0.7810	-0.7810	0.8049
G4 - Top Flange	0.5065	0.5538	0.5538	0.7500	0.7500	1.1630	1.1630	-1.1870

**Deflections - Vertical (mm)**

	Abutment 1	Field Splice 1 Section 1	Field Splice 1 Section 2	Field Splice 2 Section 2	Field Splice 2 Section 3	Field Splice 3 Section 3	Field Splice 3 Section 4	Field Splice 4 Section 4
G1- Bottom Flange	0.1243	-3.0010	-3.0010	-4.7580	-4.7580	-9.4920	-9.4920	6.1300
G1- Top Flange	0.0921	-2.9950	-2.9950	-4.7490	-4.7490	-9.4930	-9.4930	6.1300
G2 - Bottom Flange	0.1354	-2.8780	-2.8780	-3.8820	-3.8820	-7.5370	-7.5370	4.1180
G2 - Top Flange	0.1047	-2.8770	-2.8770	-3.8760	-3.8760	-7.5360	-7.5360	4.1180
G3 - Bottom Flange	0.1298	-2.7700	-2.7700	-3.0250	-3.0250	-5.7090	-5.7090	2.1160
G3 - Top Flange	0.1028	-2.7700	-2.7700	-3.0220	-3.0220	-5.7100	-5.7100	2.1160
G4 - Bottom Flange	0.1186	-2.6060	-2.6060	-2.2030	-2.2030	-3.9020	-3.9020	0.1569
G4 - Top Flange	0.0924	-2.6060	-2.6060	-2.1990	-2.1990	-3.9030	-3.9030	0.1568

**Vertical - Support Reactions (kN)**

	Abutment 1	Falsework 1	Falsework 2A	Falsework 2	Pier Bracket at XF 26	Pier 1	Pier Bracket at XF 28
G1	431.5	0.0	0.0	1517.2	n/a	1059.3	n/a
G2	253.8	0.0	0.0	1279.0	n/a	939.9	n/a
G3	224.7	0.0	0.0	835.4	n/a	812.7	n/a
G4	184.4	0.0	0.0	638.2	n/a	625.5	n/a

**Vertical Support Reactions (kips)**

	Abutment 1	Falsework 1	Falsework 2A	Falsework 2	Pier Bracket at XF 26	Pier 1	Pier Bracket at XF 28
G1	97.0	0.0	0.0	341.1	n/a	238.1	n/a
G2	57.1	0.0	0.0	287.5	n/a	211.3	n/a
G3	50.5	0.0	0.0	187.8	n/a	182.7	n/a
G4	41.5	0.0	0.0	143.5	n/a	140.6	n/a

**Cross-frame Vertical Reactions**

	(kN)	(kips)
XF 26B (outside)	0.000	0.0000
XF 27B (outside)	0.000	0.0000
XF 27C (inside)	0.000	0.0000
XF 28B (outside)	0.000	0.0000

**Figure C-102** “Planned” construction stage 16 – Field-splice location deflections and support reaction summary

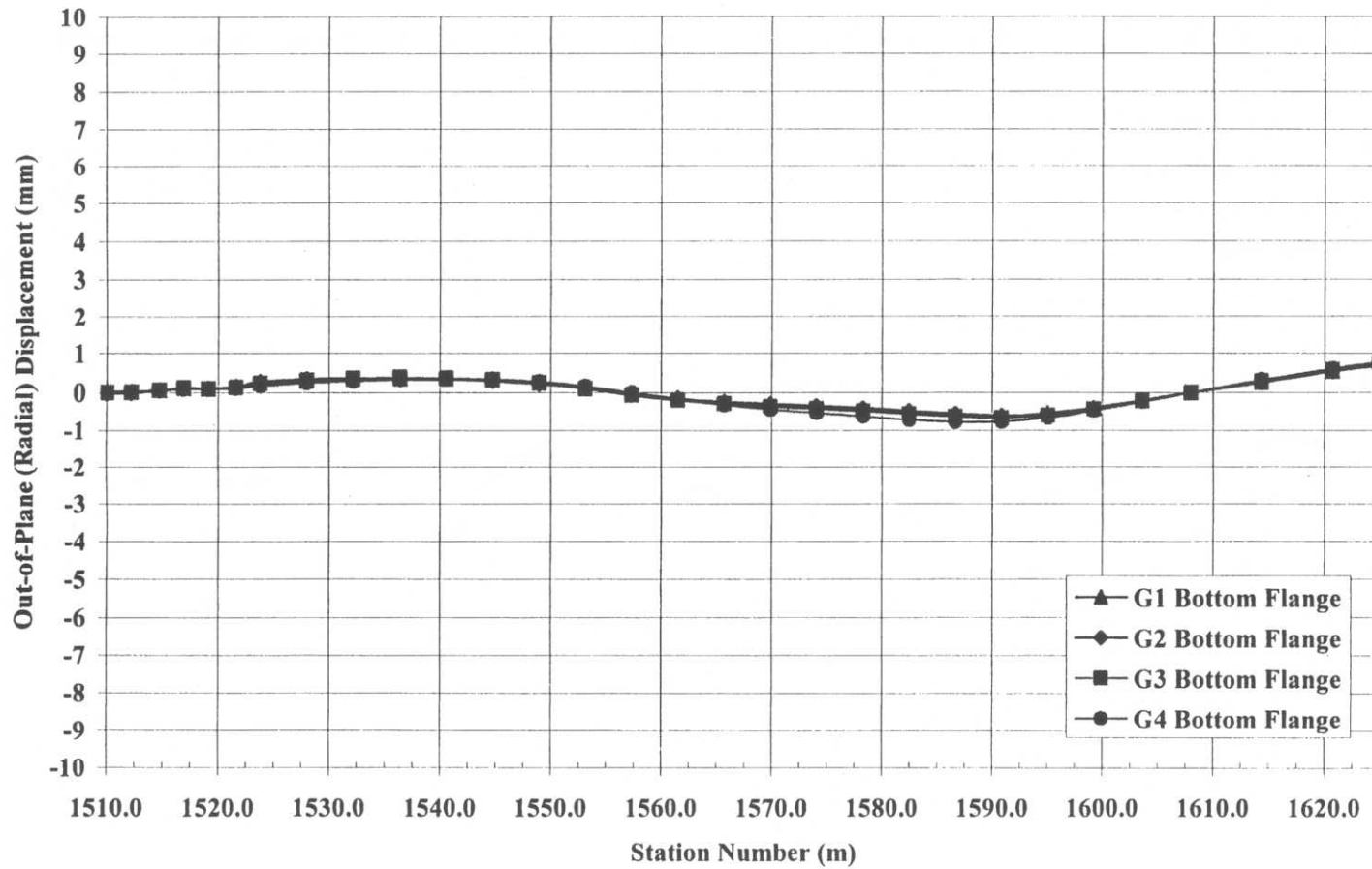
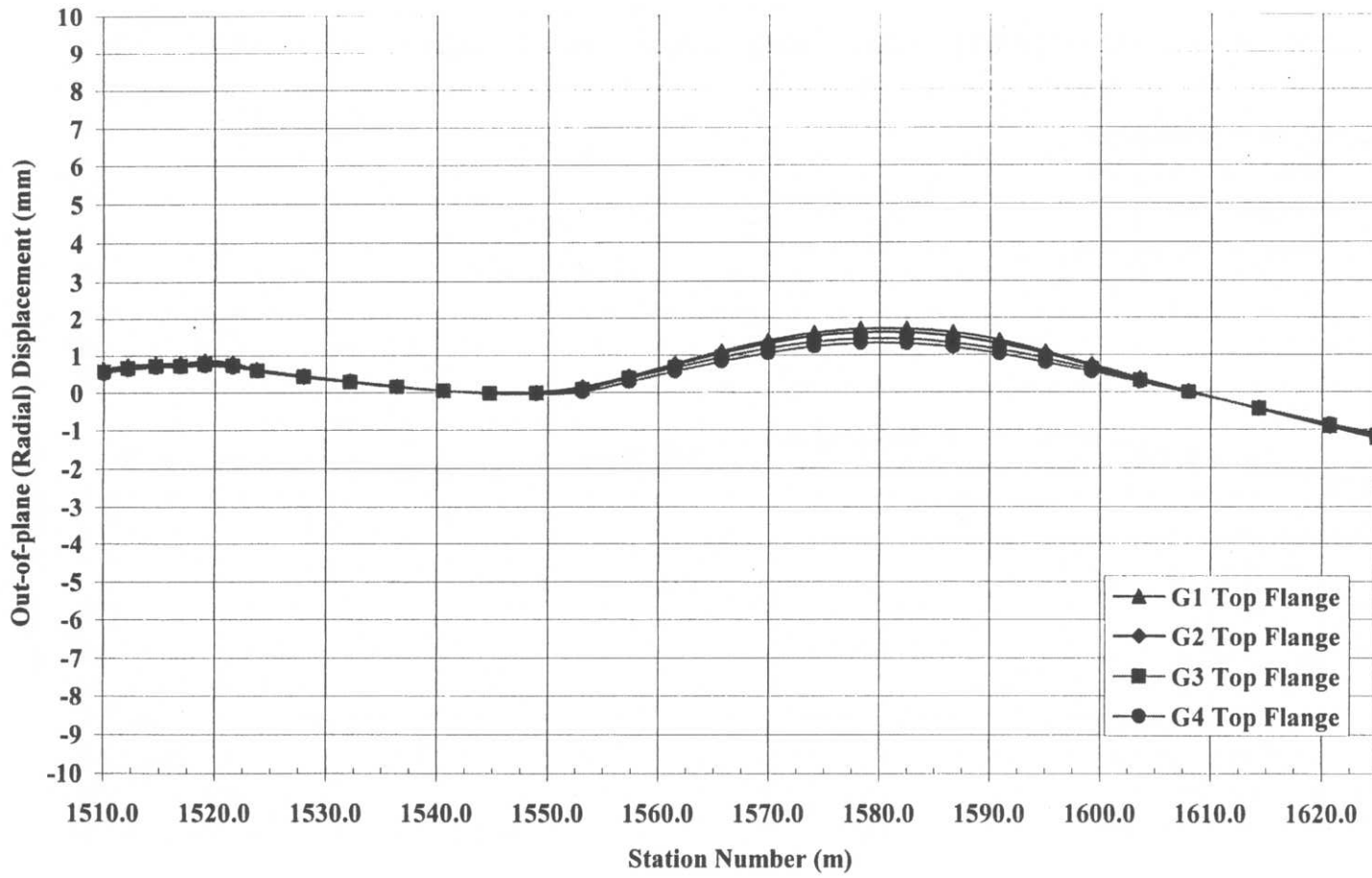


Figure C-103 “Planned” construction stage 16 – Out-of-plane (radial) displacement, centerline of bottom flange



**Figure C-104** “Planned” construction stage16 – Out-of-plane (radial) displacement, centerline of top flange

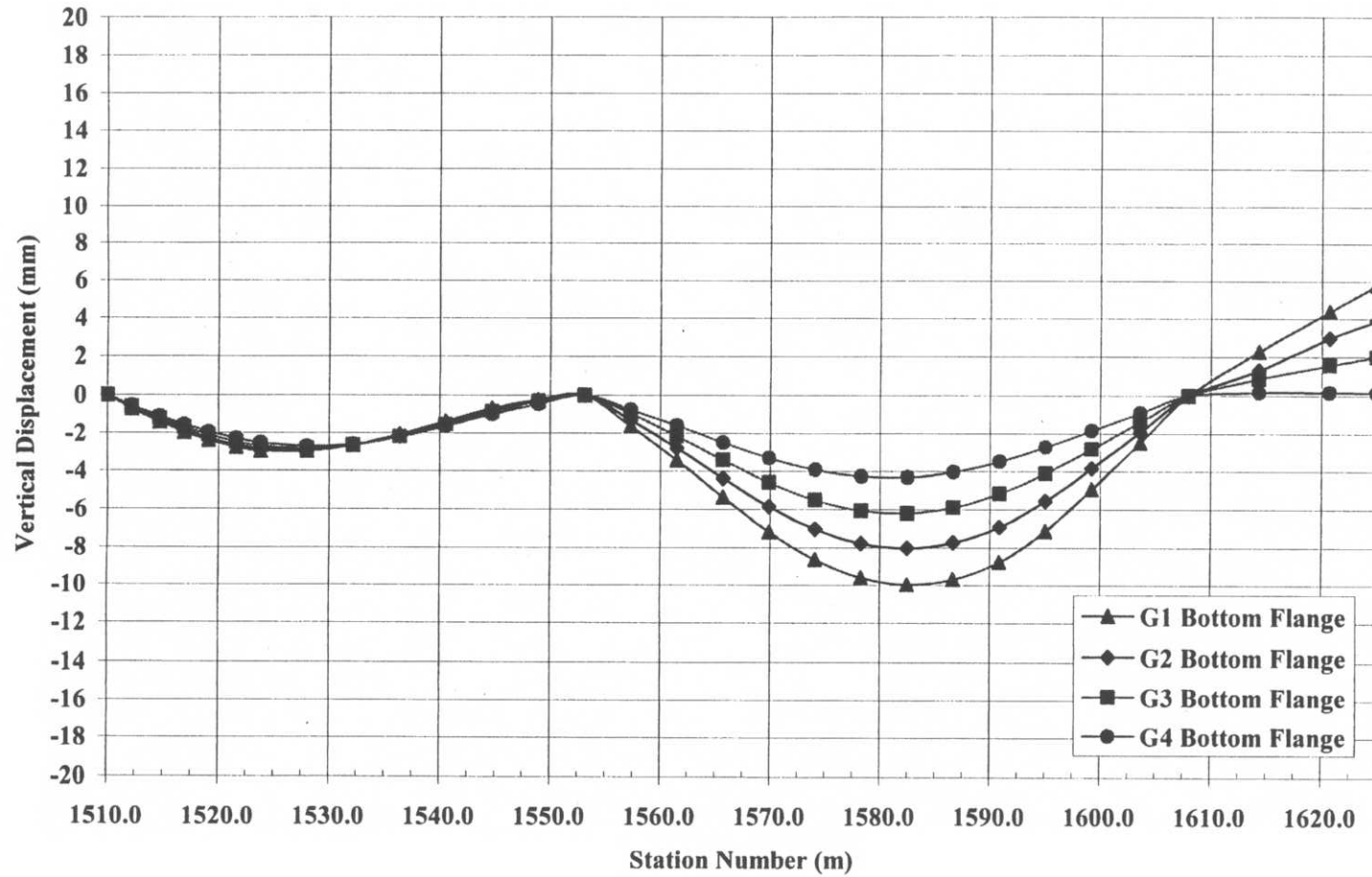


Figure C-105 “Planned” construction stage 16 – Vertical displacement, centerline of bottom flange

## **APPENDIX D**

## APPENDIX D

### **D.1 Cross-Frame Member Dimensions for Girder Web-Plumb Position at the No-load Condition Versus Web-Non-Plumb Position at No-load Condition**

This section of Appendix D consists of tables showing the cross-frame member lengths for each cross-frame in the Ford City Bridge. A dimension is given for the two detailing methods:

1. Web-Plumb at No-Load – The girders and cross-frames are detailed such that the girder webs are plumb at the no-load (fully supported) condition. Once temporary supports are removed, the girder webs displace to an out-of-plumb position.
2. Web-Non-Plumb at No-Load – the girders and cross-frames are detailed such that the girder webs are out-of-plumb at the no-load (fully supported) condition. Once temporary supports are removed, the girder webs displace to a vertically plumb position.

Following the tables, graphs are presented which illustrate the difference in cross-frame member dimensions as a function of station number due to the inconsistent detailing of the cross-frames and girders.

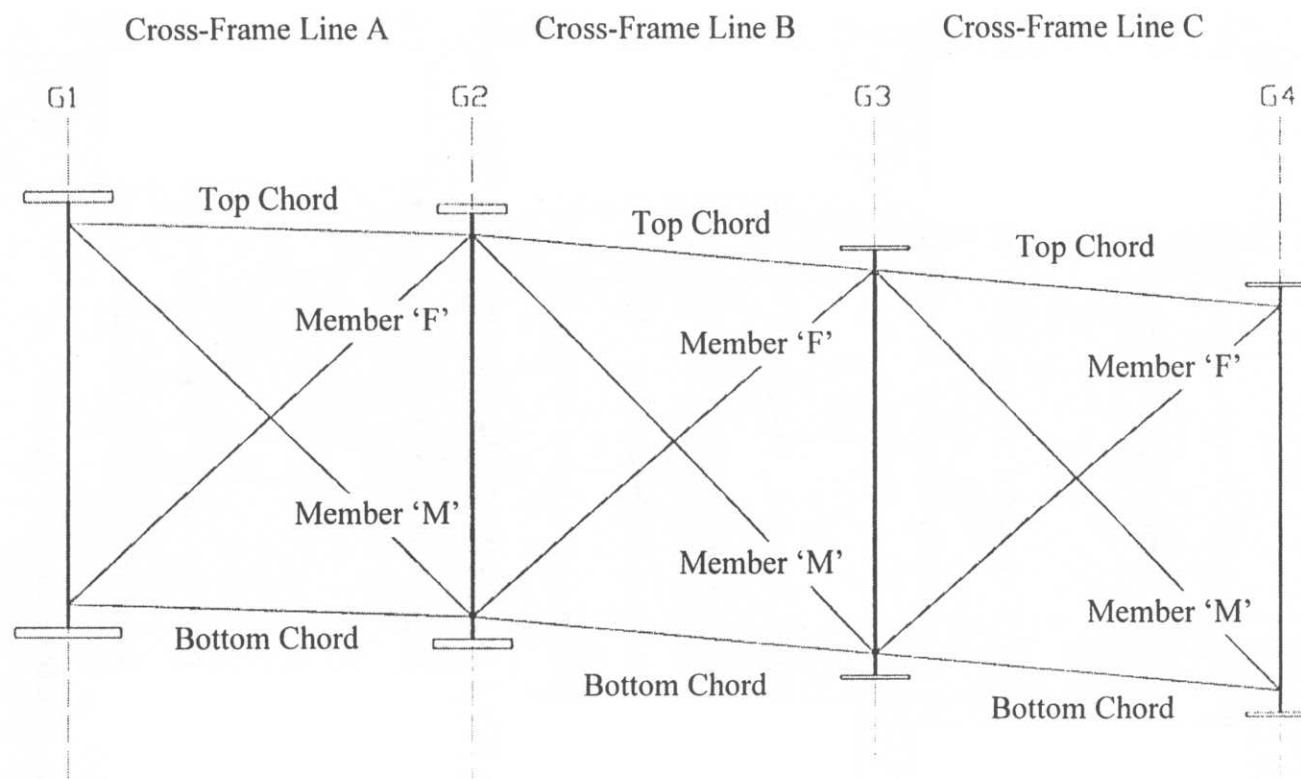


**Figure D-1** Inconsistent detailing – naming convention for cross-frame members

**Table D-1** Cross-frames 1 through 8 – Detailing dimensions for web-plumb position at no-load condition versus web-non-plumb position at no-load condition

		<b>Cross-Frame Member Lengths (mm)</b>			
<b>Cross-Frame</b>	<b>Detailed Condition</b>	<b>F</b>	<b>M</b>	<b>Top Chord</b>	<b>Bottom Chord</b>
<b>1A</b>	Web-Plumb at No-Load	5530.73	5441.70	4100.55	4100.55
	Web-Non-Plumb at No-Load	5526.07	5436.96	4094.26	4094.26
<b>1B</b>	Web-Plumb at No-Load	5334.02	5643.48	4106.62	4106.62
	Web-Non-Plumb at No-Load	5330.06	5639.74	4101.47	4101.47
<b>1D</b>	Web-Plumb at No-Load	5364.85	5610.61	4104.17	4104.17
	Web-Non-Plumb at No-Load	5361.48	5606.25	4098.99	4098.99
<b>4A</b>	Web-Plumb at No-Load	5634.77	5600.16	4100.08	4100.08
	Web-Non-Plumb at No-Load	5646.10	5579.71	4093.93	4093.93
<b>4B</b>	Web-Plumb at No-Load	5436.78	5804.98	4108.85	4108.85
	Web-Non-Plumb at No-Load	5448.91	5786.29	4103.70	4103.70
<b>4C</b>	Web-Plumb at No-Load	5466.12	5773.56	4106.17	4106.17
	Web-Non-Plumb at No-Load	5478.02	5754.89	4100.99	4100.99
<b>7A</b>	Web-Plumb at No-Load	5609.74	5625.14	4100.02	4100.02
	Web-Non-Plumb at No-Load	5635.04	5590.66	4093.77	4093.77
<b>7B</b>	Web-Plumb at No-Load	5417.47	5825.89	4110.89	4110.89
	Web-Non-Plumb at No-Load	5444.75	5794.30	4106.58	4106.58
<b>7C</b>	Web-Plumb at No-Load	5444.12	5797.09	4108.13	4108.13
	Web-Non-Plumb at No-Load	5470.36	5765.28	4103.17	4103.17
<b>8A</b>	Web-Plumb at No-Load	5596.46	5638.51	4100.12	4100.12
	Web-Non-Plumb at No-Load	5629.96	5597.21	4094.75	4094.75
<b>8B</b>	Web-Plumb at No-Load	5407.85	5836.36	4111.98	4111.98
	Web-Non-Plumb at No-Load	5442.48	5797.59	4107.40	4107.40
<b>8C</b>	Web-Plumb at No-Load	5432.86	5809.22	4109.24	4109.24
	Web-Non-Plumb at No-Load	5467.00	5770.51	4104.61	4104.61

**Table D-2** Cross-frames 9 through 12 – Detailing dimensions for web-plumb position at no-load condition versus web-non-plumb position at no-load condition

		<b>Cross-Frame Member Lengths (mm)</b>			
<b>Cross-Frame</b>	<b>Detailed Condition</b>	<b>F</b>	<b>M</b>	<b>Top Chord</b>	<b>Bottom Chord</b>
<b>9A</b>	Web-Plumb at No-Load	5584.67	5650.42	4100.28	4100.28
	Web-Non-Plumb at No-Load	5625.15	5602.84	4095.29	4095.29
<b>9B</b>	Web-Plumb at No-Load	5399.74	5845.23	4112.95	4112.95
	Web-Non-Plumb at No-Load	5441.30	5800.32	4108.54	4108.54
<b>9C</b>	Web-Plumb at No-Load	5423.10	5819.77	4110.27	4110.27
	Web-Non-Plumb at No-Load	5467.89	5771.13	4105.64	4105.64
<b>10A</b>	Web-Plumb at No-Load	5574.43	5660.82	4100.49	4100.49
	Web-Non-Plumb at No-Load	5620.89	5607.89	4095.83	4095.83
<b>10B</b>	Web-Plumb at No-Load	5393.06	5852.56	4113.78	4113.78
	Web-Non-Plumb at No-Load	5440.68	5802.46	4109.64	4109.64
<b>10C</b>	Web-Plumb at No-Load	5414.81	5828.78	4111.18	4111.18
	Web-Non-Plumb at No-Load	5462.06	5778.87	4107.20	4107.20
<b>11A</b>	Web-Plumb at No-Load	5565.76	5669.67	4100.70	4100.70
	Web-Non-Plumb at No-Load	5617.22	5612.44	4096.43	4096.43
<b>11B</b>	Web-Plumb at No-Load	5387.77	5858.37	4114.45	4114.45
	Web-Non-Plumb at No-Load	5440.40	5804.11	4110.62	4110.62
<b>11C</b>	Web-Plumb at No-Load	5407.94	5836.26	4111.97	4111.97
	Web-Non-Plumb at No-Load	5460.22	5782.24	4108.36	4108.36
<b>12A</b>	Web-Plumb at No-Load	5558.67	5676.91	4100.91	4100.91
	Web-Non-Plumb at No-Load	5613.98	5616.57	4097.04	4097.04
<b>12B</b>	Web-Plumb at No-Load	5383.83	5862.72	4114.97	4114.97
	Web-Non-Plumb at No-Load	5440.42	5805.30	4111.48	4111.48
<b>12C</b>	Web-Plumb at No-Load	5402.48	5842.24	4112.62	4112.62
	Web-Non-Plumb at No-Load	5458.63	5785.25	4109.41	4109.41

**Table D-3** Cross-frames 13 through 16 – Detailing dimensions for web-plumb position at no-load condition versus web-non-plumb position at no-load condition

Cross-Frame	Detailed Condition	Cross-Frame Member Lengths (mm)			
		F	M	Top Chord	Bottom Chord
13A	Web-Plumb at No-Load	5553.18	5682.55	4101.09	4101.09
	Web-Non-Plumb at No-Load	5611.17	5620.25	4097.64	4097.64
13B	Web-Plumb at No-Load	5381.22	5865.60	4115.31	4115.31
	Web-Non-Plumb at No-Load	5440.46	5806.31	4112.21	4112.21
13C	Web-Plumb at No-Load	5398.39	5846.71	4113.12	4113.12
	Web-Non-Plumb at No-Load	5457.22	5787.84	4110.30	4110.30
14A	Web-Plumb at No-Load	5549.28	5686.55	4101.23	4101.23
	Web-Non-Plumb at No-Load	5608.64	5623.57	4098.18	4098.18
14B	Web-Plumb at No-Load	5379.92	5867.04	4115.49	4115.49
	Web-Non-Plumb at No-Load	5440.59	5806.97	4112.77	4112.77
14C	Web-Plumb at No-Load	5395.66	5849.70	4113.45	4113.45
	Web-Non-Plumb at No-Load	5455.96	5790.10	4111.06	4111.06
15A	Web-Plumb at No-Load	5546.96	5688.94	4101.32	4101.32
	Web-Non-Plumb at No-Load	5606.51	5626.42	4098.68	4098.68
15B	Web-Plumb at No-Load	5379.94	5867.02	4115.48	4115.48
	Web-Non-Plumb at No-Load	5440.78	5807.78	4113.17	4113.17
15C	Web-Plumb at No-Load	5394.30	5851.20	4113.62	4113.62
	Web-Non-Plumb at No-Load	5454.81	5792.00	4111.63	4111.63
16A	Web-Plumb at No-Load	5546.20	5689.72	4101.34	4101.34
	Web-Non-Plumb at No-Load	5604.76	5628.81	4099.13	4099.13
16B	Web-Plumb at No-Load	5381.29	5865.53	4115.30	4115.30
	Web-Non-Plumb at No-Load	5441.00	5807.46	4113.38	4113.38
16C	Web-Plumb at No-Load	5394.29	5851.20	4113.62	4113.62
	Web-Non-Plumb at No-Load	5453.80	5793.48	4112.00	4112.00

**Table D-4** Cross-frames 17 through 20 – Detailing dimensions for web-plumb position at no-load condition versus web-non-plumb position at no-load condition

Cross-Frame	Detailed Condition	Cross-Frame Member Lengths (mm)			
		F	M	Top Chord	Bottom Chord
17A	Web-Plumb at No-Load	5546.96	5688.93	4101.32	4101.32
	Web-Non-Plumb at No-Load	5603.29	5630.85	4099.52	4099.52
17B	Web-Plumb at No-Load	5384.00	5862.53	4114.94	4114.94
	Web-Non-Plumb at No-Load	5441.53	5806.92	4113.35	4113.35
17C	Web-Plumb at No-Load	5395.66	5849.71	4113.45	4113.45
	Web-Non-Plumb at No-Load	5452.86	5794.60	4112.17	4112.17
18A	Web-Plumb at No-Load	5549.22	5686.61	4101.23	4101.23
	Web-Non-Plumb at No-Load	5602.30	5632.24	4099.80	4099.80
18B	Web-Plumb at No-Load	5388.11	5858.00	4114.41	4114.41
	Web-Non-Plumb at No-Load	5442.32	5805.88	4113.15	4113.15
18C	Web-Plumb at No-Load	5398.40	5846.70	4113.11	4113.11
	Web-Non-Plumb at No-Load	5452.28	5795.10	4112.14	4112.14
19A	Web-Plumb at No-Load	5552.92	5682.81	4101.10	4101.10
	Web-Non-Plumb at No-Load	5601.77	5633.10	4100.02	4100.02
19B	Web-Plumb at No-Load	5393.68	5851.88	4113.70	4113.70
	Web-Non-Plumb at No-Load	5443.55	5804.15	4112.74	4112.74
19C	Web-Plumb at No-Load	5402.56	5842.14	4112.61	4112.61
	Web-Non-Plumb at No-Load	5452.17	5794.81	4111.86	4111.86
20A	Web-Plumb at No-Load	5557.98	5677.62	4100.93	4100.93
	Web-Non-Plumb at No-Load	5601.88	5633.19	4100.16	4100.16
20B	Web-Plumb at No-Load	5400.78	5844.10	4112.83	4112.83
	Web-Non-Plumb at No-Load	5445.55	5801.40	4112.12	4112.12
20C	Web-Plumb at No-Load	5408.17	5836.01	4111.95	4111.95
	Web-Non-Plumb at No-Load	5452.62	5793.72	4111.39	4111.39

**Table D-5** Cross-frames 21 through 24 – Detailing dimensions for web-plumb position at no-load condition versus web-non-plumb position at no-load condition

		<b>Cross-Frame Member Lengths (mm)</b>			
<b>Cross-Frame</b>	<b>Detailed Condition</b>	<b>F</b>	<b>M</b>	<b>Top Chord</b>	<b>Bottom Chord</b>
<b>21A</b>	Web-Plumb at No-Load	5564.35	5671.10	4100.74	4100.74
	Web-Non-Plumb at No-Load	5602.60	5632.66	4100.30	4100.30
<b>21B</b>	Web-Plumb at No-Load	5409.48	5834.59	4111.79	4111.79
	Web-Non-Plumb at No-Load	5448.46	5797.50	4111.30	4111.30
<b>21C</b>	Web-Plumb at No-Load	5415.27	5828.28	4111.13	4111.13
	Web-Non-Plumb at No-Load	5453.89	5791.60	4110.74	4110.74
<b>22A</b>	Web-Plumb at No-Load	5571.93	5663.37	4100.55	4100.55
	Web-Non-Plumb at No-Load	5604.01	5631.33	4100.35	4100.35
<b>22B</b>	Web-Plumb at No-Load	5419.88	5823.26	4110.62	4110.62
	Web-Non-Plumb at No-Load	5452.45	5792.31	4110.29	4110.29
<b>22C</b>	Web-Plumb at No-Load	5423.91	5818.89	4110.18	4110.18
	Web-Non-Plumb at No-Load	5456.18	5788.24	4109.89	4109.89
<b>23A</b>	Web-Plumb at No-Load	5580.63	5654.52	4100.36	4100.36
	Web-Non-Plumb at No-Load	5606.09	5629.50	4100.51	4100.51
<b>23B</b>	Web-Plumb at No-Load	5432.01	5810.13	4109.33	4109.33
	Web-Non-Plumb at No-Load	5458.01	5785.52	4109.19	4109.19
<b>23C</b>	Web-Plumb at No-Load	5434.21	5807.76	4109.11	4109.11
	Web-Non-Plumb at No-Load	5459.84	5783.38	4108.90	4108.90
<b>24A</b>	Web-Plumb at No-Load	5459.60	5780.51	4106.72	4106.72
	Web-Non-Plumb at No-Load	5478.51	5762.47	4106.64	4106.64
<b>24B</b>	Web-Plumb at No-Load	5446.03	5795.03	4107.95	4107.95
	Web-Non-Plumb at No-Load	5465.24	5776.93	4107.95	4107.95
<b>24C</b>	Web-Plumb at No-Load	5446.19	5794.86	4107.93	4107.93
	Web-Non-Plumb at No-Load	5465.12	5776.81	4107.79	4107.79

**Table D-6** Cross-frames 25 through 28 – Detailing dimensions for web-plumb position at no-load condition versus web-non-plumb position at no-load condition

		<b>Cross-Frame Member Lengths (mm)</b>			
<b>Cross-Frame</b>	<b>Detailed Condition</b>	<b>F</b>	<b>M</b>	<b>Top Chord</b>	<b>Bottom Chord</b>
<b>25A</b>	Web-Plumb at No-Load	5600.94	5633.99	4100.07	4100.07
	Web-Non-Plumb at No-Load	5612.95	5622.47	4100.37	4100.37
<b>25B</b>	Web-Plumb at No-Load	5462.14	5777.79	4106.50	4106.50
	Web-Non-Plumb at No-Load	5474.75	5766.16	4106.72	4106.72
<b>25C</b>	Web-Plumb at No-Load	5459.92	5780.17	4106.69	4106.69
	Web-Non-Plumb at No-Load	5472.39	5768.28	4106.63	4106.63
<b>26A</b>	Web-Plumb at No-Load	5609.12	5625.77	4100.02	4100.02
	Web-Non-Plumb at No-Load	5614.80	5620.03	4099.96	4099.96
<b>26B</b>	Web-Plumb at No-Load	5478.40	5760.52	4105.19	4105.19
	Web-Non-Plumb at No-Load	5484.97	5755.28	4105.91	4105.91
<b>26C</b>	Web-Plumb at No-Load	5473.90	5765.28	4105.54	4105.54
	Web-Non-Plumb at No-Load	5479.50	5759.00	4104.86	4104.86
<b>27A</b>	Web-Plumb at No-Load	5597.43	5596.52	4100.00	4100.00
	Web-Non-Plumb at No-Load	5597.43	5596.52	4100.00	4100.00
<b>27B</b>	Web-Plumb at No-Load	5477.47	5719.51	4103.85	4103.85
	Web-Non-Plumb at No-Load	5477.47	5719.51	4103.85	4103.85
<b>27C</b>	Web-Plumb at No-Load	5470.46	5726.88	4104.33	4104.33
	Web-Non-Plumb at No-Load	5470.46	5726.88	4104.33	4104.33
<b>28A</b>	Web-Plumb at No-Load	5618.67	5582.15	4100.09	4100.09
	Web-Non-Plumb at No-Load	5608.98	5590.49	4099.14	4099.14
<b>28B</b>	Web-Plumb at No-Load	5505.80	5696.84	4102.40	4102.40
	Web-Non-Plumb at No-Load	5500.86	5702.70	4103.16	4103.16
<b>28C</b>	Web-Plumb at No-Load	5503.38	5699.36	4102.52	4102.52
	Web-Non-Plumb at No-Load	5495.35	5706.87	4102.36	4102.36

**Table D-7** Cross-frames 29 – Detailing dimensions for web-plumb position at no-load condition versus web-non-plumb position at no-load condition

		<b>Cross-Frame Member Lengths (mm)</b>			
<b>Cross-Frame</b>	<b>Detailed Condition</b>	<b>F</b>	<b>M</b>	<b>Top Chord</b>	<b>Bottom Chord</b>
<b>29A</b>	Web-Plumb at No-Load	5636.61	5564.42	4100.34	4100.34
	Web-Non-Plumb at No-Load	5623.58	5576.82	4099.83	4099.83
<b>29B</b>	Web-Plumb at No-Load	5541.70	5659.77	4100.92	4100.92
	Web-Non-Plumb at No-Load	5527.35	5673.24	4100.54	4100.54
<b>29C</b>	Web-Plumb at No-Load	5531.41	5670.34	4101.27	4101.27
	Web-Non-Plumb at No-Load	5515.86	5684.75	4100.77	4100.77

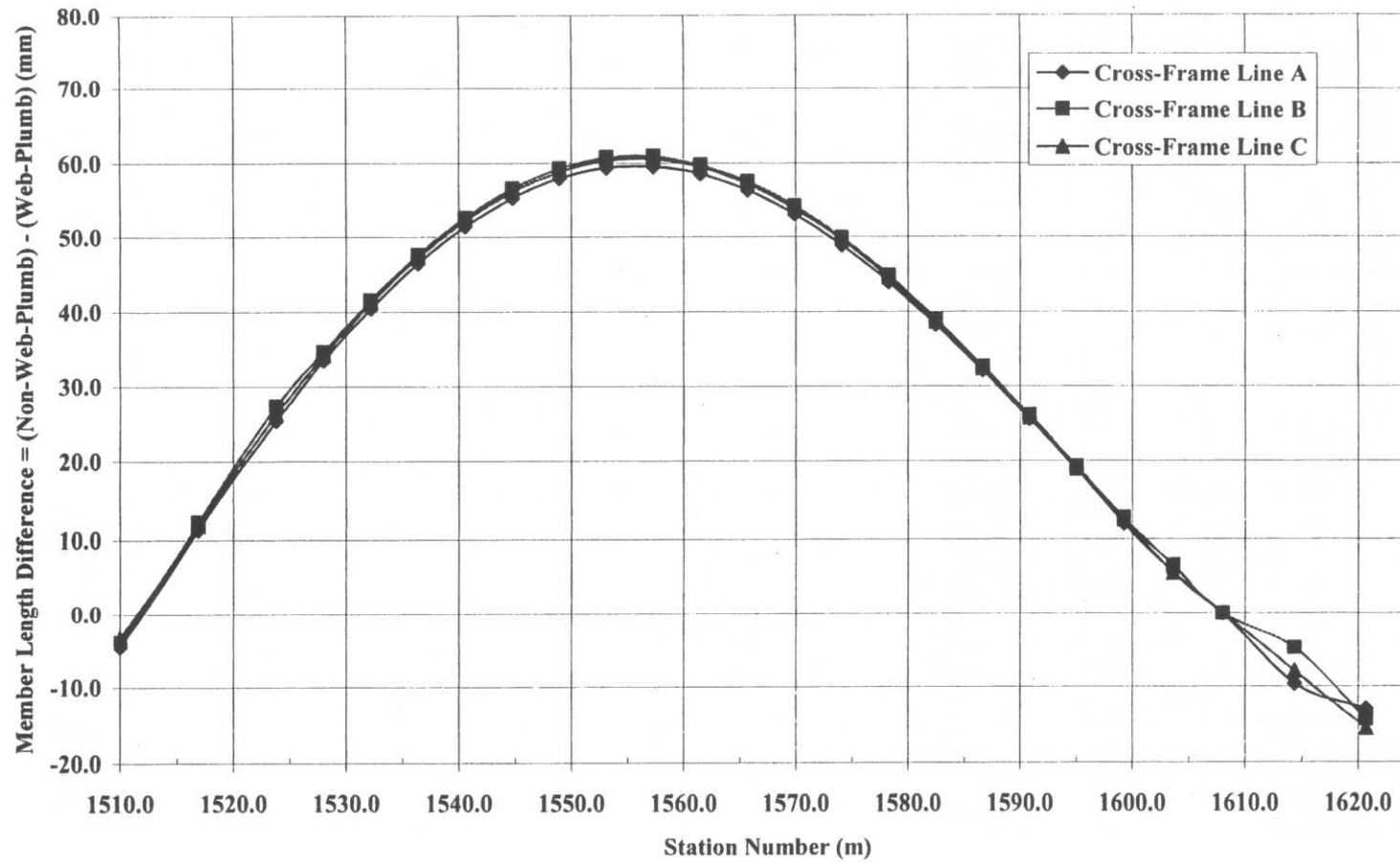
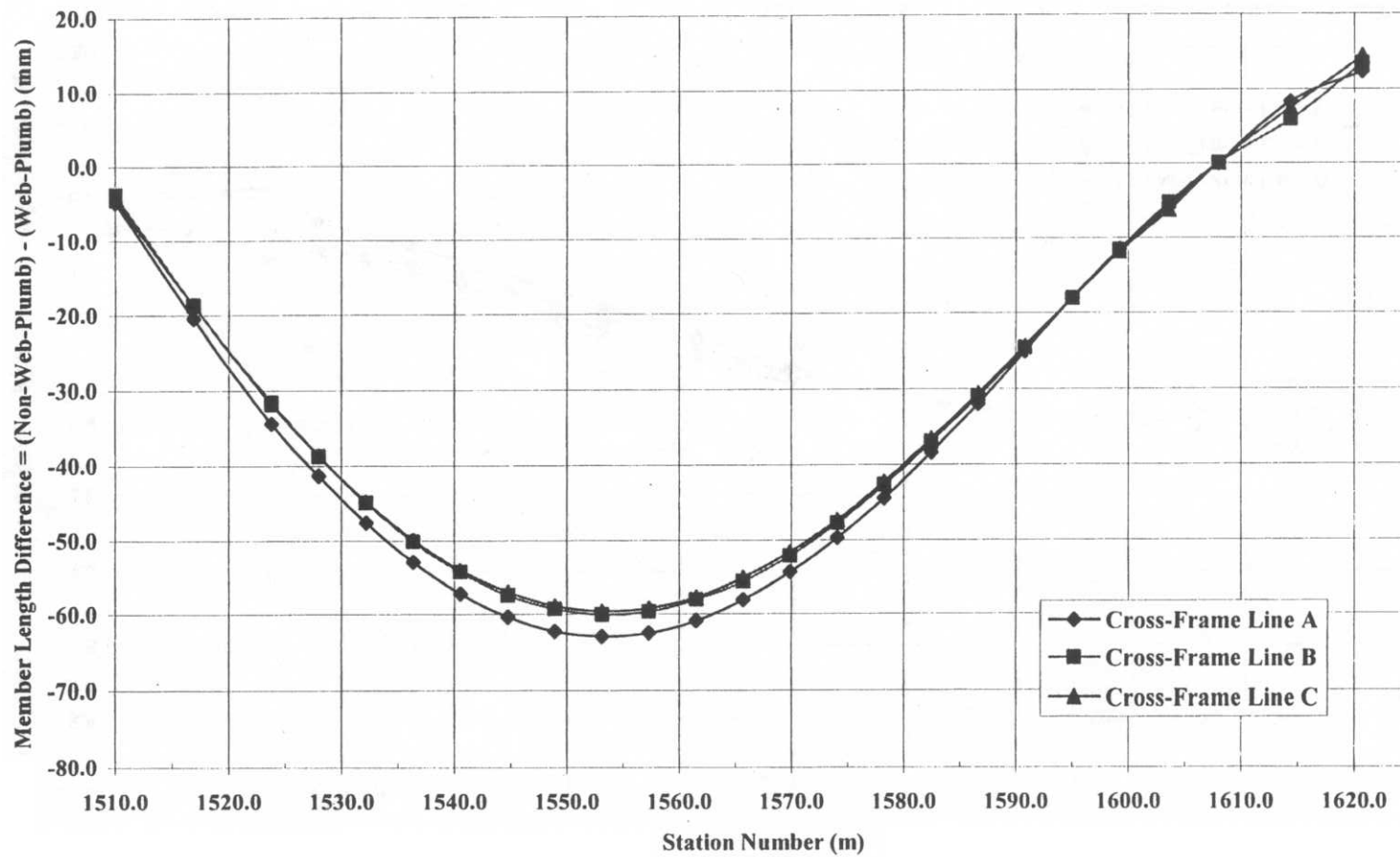
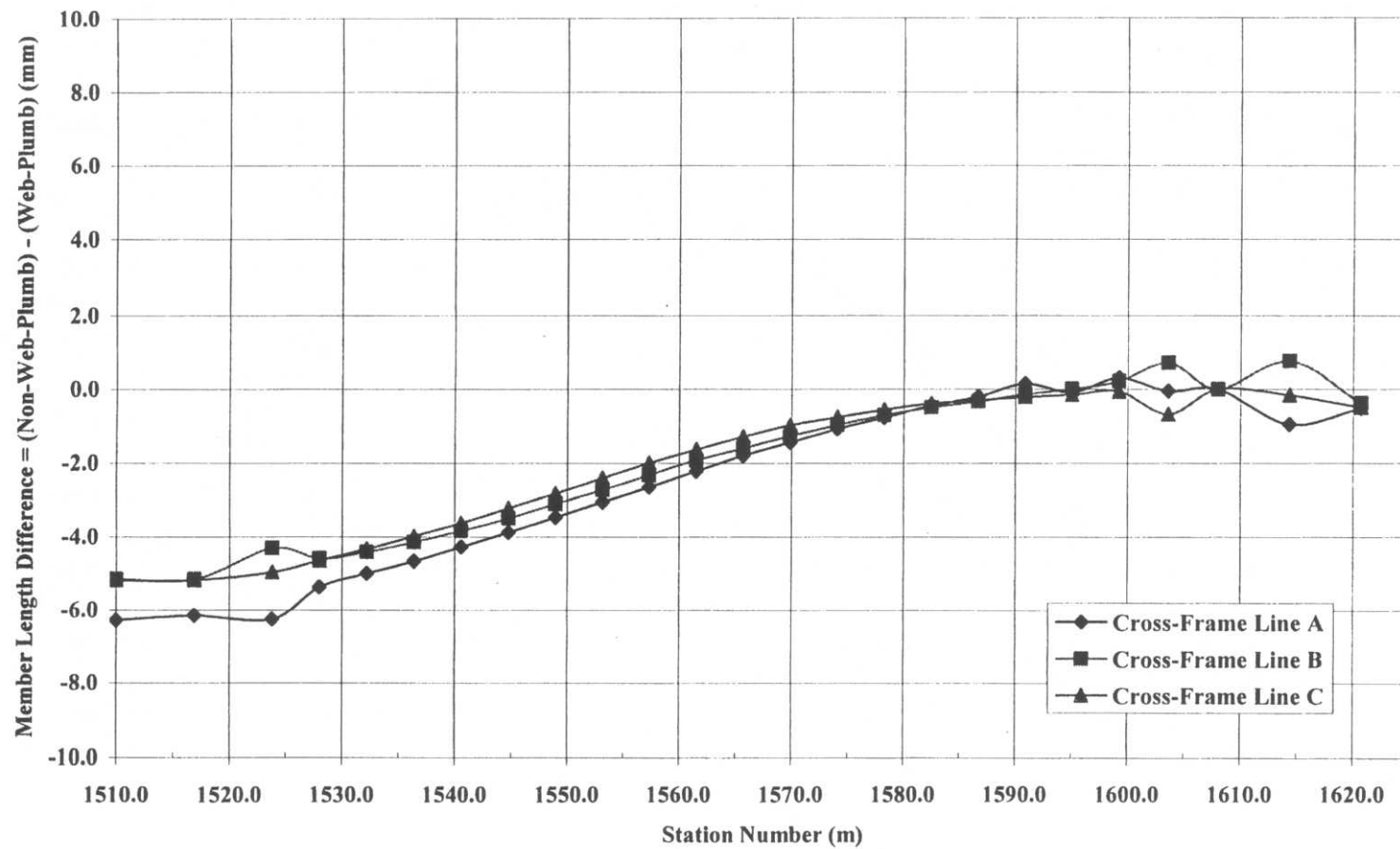


Figure D-2 Cross-frame member 'F' – Non-web-plumb vs. web-plumb detail length difference



**Figure D-3** Cross-frame member 'M' – Non-web-plumb detail vs. web-plumb detail length difference



**Figure D-4** Cross-frame top chord – Non-web-plumb detail vs. web-plumb detail length difference

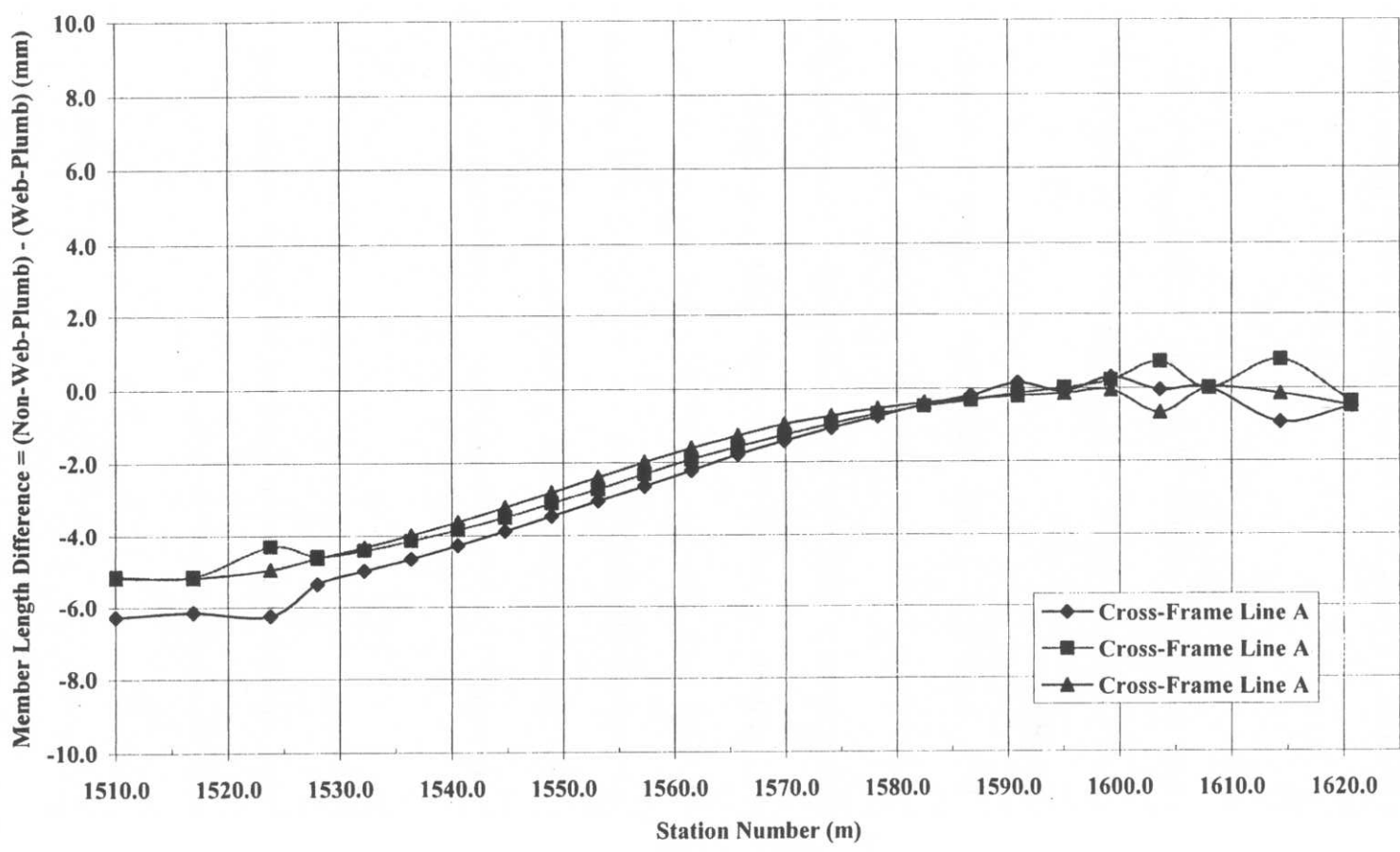


Figure D-5 Cross-frame bottom chord – Non-web-plumb detail vs. web-plumb detail length difference

## **D.2 Cross-Frame Member Dimensions for Girder Web-Plumb Position at the No-load Condition Versus Web-Plumb Position After Application of Concrete Deck Load Only**

This section of Appendix D consists of tables showing the cross-frame member lengths for each cross-frame in the Ford City Bridge. A dimension is given for the two detailing methods:

1. Web-Plumb at No-Load – The girders and cross-frames are detailed such that the girder webs are plumb at the no-load (fully supported) condition. Once temporary supports are removed, the girder webs displace to an out-of-plumb position.
2. Web-Plumb at Concrete Deck Load Only – the girders and cross-frames are detailed such that the girder webs are out-of-plumb at the no-load (fully supported) condition; but the webs are plumb after application of the concrete deck load only. This is never a possibility in the erection of the actual structure due to the self-weight of the steel used in the structure.

Following the tables, graphs are presented which illustrate the difference in cross-frame member dimensions as a function of station number due to the inconsistent detailing of the cross-frames and girders.

**Table D-8** Cross-frames 1 through 8 – Detailing dimensions for web-plumb position at no-load condition versus web-plumb position after application of concrete deck load

Cross-Frame	Detailed Condition	Cross-Frame Member Lengths (mm)			
		F	M	Top Chord	Bottom Chord
1A	Web-Plumb at No-Load	5530.73	5441.70	4100.55	4100.55
	Web-Plumb at Concrete Deck Load	5528.06	5438.99	4096.95	4096.95
1B	Web-Plumb at No-Load	5334.02	5643.48	4106.62	4106.62
	Web-Plumb at Concrete Deck Load	5331.87	5641.46	4103.83	4103.83
1C	Web-Plumb at No-Load	5364.85	5610.61	4104.17	4104.17
	Web-Plumb at Concrete Deck Load	5362.67	5608.53	4101.33	4101.33
4A	Web-Plumb at No-Load	5634.77	5600.16	4100.08	4100.08
	Web-Plumb at Concrete Deck Load	5640.61	5589.08	4096.53	4096.53
4B	Web-Plumb at No-Load	5436.78	5804.98	4108.85	4108.85
	Web-Plumb at Concrete Deck Load	5443.42	5794.87	4106.10	4106.10
4C	Web-Plumb at No-Load	5466.12	5773.56	4106.17	4106.17
	Web-Plumb at Concrete Deck Load	5472.51	5763.51	4103.37	4103.37
7A	Web-Plumb at No-Load	5609.74	5625.14	4100.02	4100.02
	Web-Plumb at Concrete Deck Load	5623.23	5606.38	4096.40	4096.40
7B	Web-Plumb at No-Load	5417.47	5825.89	4110.89	4110.89
	Web-Plumb at Concrete Deck Load	5432.31	5808.92	4108.68	4108.68
7C	Web-Plumb at No-Load	5444.12	5797.09	4108.13	4108.13
	Web-Plumb at Concrete Deck Load	5458.40	5779.95	4105.53	4105.53
8A	Web-Plumb at No-Load	5596.46	5638.51	4100.12	4100.12
	Web-Plumb at Concrete Deck Load	5614.34	5616.11	4096.97	4096.97
8B	Web-Plumb at No-Load	5407.85	5836.36	4111.98	4111.98
	Web-Plumb at Concrete Deck Load	5426.52	5815.65	4109.60	4109.60
8C	Web-Plumb at No-Load	5432.86	5809.22	4109.24	4109.24
	Web-Plumb at Concrete Deck Load	5451.39	5788.43	4106.85	4106.85

**Table D-9** Cross-frames 9 through 12 – Detailing dimensions for web-plumb position at no-load condition versus web-plumb position after application of concrete deck load

Cross-Frame	Detailed Condition	Cross-Frame Member Lengths (mm)			
		F	M	Top Chord	Bottom Chord
9A	Web-Plumb at No-Load	5584.67	5650.42	4100.28	4100.28
	Web-Plumb at Concrete Deck Load	5606.27	5624.72	4097.35	4097.35
9B	Web-Plumb at No-Load	5399.74	5845.23	4112.95	4112.95
	Web-Plumb at Concrete Deck Load	5422.02	5821.30	4110.63	4110.63
9C	Web-Plumb at No-Load	5423.10	5819.77	4110.27	4110.27
	Web-Plumb at Concrete Deck Load	5445.36	5795.80	4108.04	4108.04
10A	Web-Plumb at No-Load	5574.43	5660.82	4100.49	4100.49
	Web-Plumb at Concrete Deck Load	5599.21	5632.30	4097.73	4097.73
10B	Web-Plumb at No-Load	5393.06	5852.56	4113.78	4113.78
	Web-Plumb at Concrete Deck Load	5418.55	5825.86	4111.58	4111.58
10C	Web-Plumb at No-Load	5414.81	5828.78	4111.18	4111.18
	Web-Plumb at Concrete Deck Load	5440.27	5802.15	4109.16	4109.16
11A	Web-Plumb at No-Load	5565.76	5669.67	4100.70	4100.70
	Web-Plumb at Concrete Deck Load	5593.14	5638.96	4098.17	4098.17
11B	Web-Plumb at No-Load	5387.77	5858.37	4114.45	4114.45
	Web-Plumb at No-Load	5415.90	5829.47	4112.39	4112.39
11C	Web-Plumb at No-Load	5407.94	5836.26	4111.97	4111.97
	Web-Plumb at Concrete Deck Load	5436.04	5807.51	4110.14	4110.14
12A	Web-Plumb at No-Load	5558.67	5676.91	4100.91	4100.91
	Web-Plumb at Concrete Deck Load	5588.10	5644.57	4098.59	4098.59
12B	Web-Plumb at No-Load	5383.83	5862.72	4114.97	4114.97
	Web-Plumb at Concrete Deck Load	5413.99	5832.24	4113.10	4113.10
12C	Web-Plumb at No-Load	5402.48	5842.24	4112.62	4112.62
	Web-Plumb at Concrete Deck Load	5432.58	5811.95	4110.99	4110.99

**Table D-10** Cross-frames 13 through 16 – Detailing dimensions for web-plumb position at no-load condition versus web-plumb position after application of concrete deck load

Cross-Frame	Detailed Condition	Cross-Frame Member Lengths (mm)			
		F	M	Top Chord	Bottom Chord
13A	Web-Plumb at No-Load	5553.18	5682.55	4101.09	4101.09
	Web-Plumb at Concrete Deck Load	5583.98	5649.25	4099.01	4099.01
13B	Web-Plumb at No-Load	5381.22	5865.60	4115.31	4115.31
	Web-Plumb at Concrete Deck Load	5412.70	5834.20	4113.63	4113.63
13C	Web-Plumb at No-Load	5398.39	5846.71	4113.12	4113.12
	Web-Plumb at Concrete Deck Load	5429.86	5815.50	4111.71	4111.71
14A	Web-Plumb at No-Load	5549.28	5686.55	4101.23	4101.23
	Web-Plumb at Concrete Deck Load	5580.76	5652.98	4099.38	4099.38
14B	Web-Plumb at No-Load	5379.92	5867.04	4115.49	4115.49
	Web-Plumb at Concrete Deck Load	5412.10	5835.28	4114.01	4114.01
14C	Web-Plumb at No-Load	5395.66	5849.70	4113.45	4113.45
	Web-Plumb at Concrete Deck Load	5427.82	5818.18	4112.25	4112.25
15A	Web-Plumb at No-Load	5546.96	5688.94	4101.32	4101.32
	Web-Plumb at Concrete Deck Load	5578.49	5655.69	4099.71	4099.71
15B	Web-Plumb at No-Load	5379.94	5867.02	4115.48	4115.48
	Web-Plumb at Concrete Deck Load	5412.11	5835.58	4114.22	4114.22
15C	Web-Plumb at No-Load	5394.30	5851.20	4113.62	4113.62
	Web-Plumb at Concrete Deck Load	5426.48	5819.96	4112.63	4112.63
16A	Web-Plumb at No-Load	5546.20	5689.72	4101.34	4101.34
	Web-Plumb at Concrete Deck Load	5577.04	5657.55	4100.00	4100.00
16B	Web-Plumb at No-Load	5381.29	5865.53	4115.30	4115.30
	Web-Plumb at Concrete Deck Load	5412.84	5834.94	4114.26	4114.26
16C	Web-Plumb at No-Load	5394.29	5851.20	4113.62	4113.62
	Web-Plumb at Concrete Deck Load	5425.86	5820.83	4112.83	4112.83

**Table D-11** Cross-frames 17 through 20 – Detailing dimensions for web-plumb position at no-load condition versus web-plumb position after application of concrete deck load

Cross-Frame	Detailed Condition	Cross-Frame Member Lengths (mm)			
		F	M	Top Chord	Bottom Chord
17A	Web-Plumb at No-Load	5546.96	5688.93	4101.32	4101.32
	Web-Plumb at Concrete Deck Load	5576.62	5658.31	4100.24	4100.24
17B	Web-Plumb at No-Load	5384.00	5862.53	4114.94	4114.94
	Web-Plumb at Concrete Deck Load	5414.29	5833.37	4114.09	4114.09
17C-	Web-Plumb at No- Load	5395.66	5849.71	4113.45	4113.45
	Web-Plumb at Concrete Deck Load	5425.95	5820.73	4112.83	4112.83
18A	Web-Plumb at No-Load	5549.22	5686.61	4101.23	4101.23
	Web-Plumb at Concrete Deck Load	5577.03	5658.10	4100.38	4100.38
18B	Web-Plumb at No-Load	5388.11	5858.00	4114.41	4114.41
	Web-Plumb at Concrete Deck Load	5416.61	5830.71	4113.74	4113.74
18C	Web-Plumb at No-Load	5398.40	5846.70	4113.11	4113.11
	Web-Plumb at Concrete Deck Load	5426.87	5819.62	4112.64	4112.64
19A	Web-Plumb at No-Load	5552.92	5682.81	4101.10	4101.10
	Web-Plumb at Concrete Deck Load	5578.55	5656.75	4100.48	4100.48
19B	Web-Plumb at No-Load	5393.68	5851.88	4113.70	4113.70
	Web-Plumb at Concrete Deck Load	5419.87	5826.91	4113.19	4113.19
19C	Web-Plumb at No-Load	5402.56	5842.14	4112.61	4112.61
	Web-Plumb at Concrete Deck Load	5428.68	5817.37	4112.24	4112.24
20A	Web-Plumb at No-Load	5557.98	5677.62	4100.93	4100.93
	Web-Plumb at Concrete Deck Load	5580.94	5654.46	4100.52	4100.52
20B	Web-Plumb at No-Load	5400.78	5844.10	4112.83	4112.83
	Web-Plumb at Concrete Deck Load	5424.28	5821.77	4112.45	4112.45
20C	Web-Plumb at No-Load	5408.17	5836.01	4111.95	4111.95
	Web-Plumb at Concrete Deck Load	5431.48	5813.92	4111.66	4111.66

**Table D-12** Cross-frames 21 through 24 – Detailing dimensions for web-plumb position at no-load condition versus web-plumb position after application of concrete deck load

Cross-Frame	Detailed Condition	Cross-Frame Member Lengths (mm)			
		F	M	Top Chord	Bottom Chord
21A	Web-Plumb at No-Load	5564.35	5671.10	4100.74	4100.74
	Web-Plumb at Concrete Deck Load	5584.38	5651.08	4100.54	4100.54
21B	Web-Plumb at No-Load	5409.48	5834.59	4111.79	4111.79
	Web-Plumb at Concrete Deck Load	5429.95	5815.17	4111.53	4111.53
21C	Web-Plumb at No-Load	5415.27	5828.28	4111.13	4111.13
	Web-Plumb at Concrete Deck Load	5435.43	5809.15	4110.89	4110.89
22A	Web-Plumb at No-Load	5571.27	5663.37	4100.55	4100.55
	Web-Plumb at Concrete Deck Load	5588.78	5646.66	4100.49	4100.49
22B	Web-Plumb at No-Load	5419.88	5823.26	4110.62	4110.62
	Web-Plumb at Concrete Deck Load	5436.97	5807.05	4110.43	4110.43
22C	Web-Plumb at No-Load	5423.91	5818.89	4100.18	4100.18
	Web-Plumb at Concrete Deck Load	5440.64	5802.94	4109.96	4109.96
23A	Web-Plumb at No-Load	5580.63	5654.52	4100.36	4100.36
	Web-Plumb at Concrete Deck Load	5593.99	5641.50	4100.49	4100.49
23B	Web-Plumb at No-Load	5432.01	5810.13	4109.33	4109.33
	Web-Plumb at Concrete Deck Load	5445.64	5797.23	4109.24	4109.24
23C	Web-Plumb at No-Load	5434.21	5807.76	4109.11	4109.11
	Web-Plumb at Concrete Deck Load	5447.39	5795.10	4108.89	4108.89
24A	Web-Plumb at No-Load	5459.60	5780.51	4106.72	4106.72
	Web-Plumb at Concrete Deck Load	5469.60	5771.07	4106.73	4106.73
24B	Web-Plumb at No-Load	5446.03	5795.03	4107.95	4107.95
	Web-Plumb at Concrete Deck Load	5456.12	5785.47	4107.90	4107.90
24C	Web-Plumb at No-Load	5446.19	5794.86	4107.93	4107.93
	Web-Plumb at Concrete Deck Load	5455.82	5785.50	4107.72	4107.72

**Table D-13** Cross-frames 25 through 28 - Detailing dimensions for web-plumb position at no-load condition versus web-plumb position after application of concrete deck load

Cross-Frame	Detailed Condition	Cross-Frame Member Lengths (mm)			
		F	M	Top Chord	Bottom Chord
25A	Web-Plumb at No-Load	5600.94	5633.99	4100.07	4100.07
	Web-Plumb at Concrete Deck Load	5607.39	5627.79	4100.22	4100.22
25B	Web-Plumb at No-Load	5462.14	5777.79	4106.50	4106.50
	Web-Plumb at Concrete Deck Load	5468.84	5771.56	4106.57	4106.57
25C	Web-Plumb at No-Load	5459.92	5780.17	4106.69	4106.69
	Web-Plumb at Concrete Deck Load	5466.22	5773.96	4106.52	4106.52
26A	Web-Plumb at No-Load	5609.12	5625.77	4100.02	4100.02
	Web-Plumb at Concrete Deck Load	5612.25	5622.54	4099.95	4099.95
26B	Web-Plumb at No-Load	5478.40	5760.52	4105.19	4105.19
	Web-Plumb at Concrete Deck Load	5483.25	5754.86	4104.46	4104.46
26C	Web-Plumb at No-Load	5473.90	5765.28	4105.54	4105.54
	Web-Plumb at Concrete Deck Load	5475.41	5764.83	4106.23	4106.23
27A	Web-Plumb at No-Load	5597.43	5596.52	4100.00	4100.00
	Web-Plumb at Concrete Deck Load	5597.43	5596.52	4100.00	4100.00
27B	Web-Plumb at No-Load	5477.47	5719.51	4103.85	4103.85
	Web-Plumb at Concrete Deck Load	5477.47	5719.51	4103.85	4103.85
27C	Web-Plumb at No-Load	5470.46	5726.88	4104.33	4104.33
	Web-Plumb at Concrete Deck Load	5470.46	5726.88	4104.33	4104.33
28A	Web-Plumb at No-Load	5618.67	5582.15	4100.09	4100.09
	Web-Plumb at Concrete Deck Load	5613.79	5586.60	4099.77	4099.77
28B	Web-Plumb at No-Load	5505.80	5696.84	4102.40	4102.40
	Web-Plumb at Concrete Deck Load	5502.03	5701.81	4103.32	4103.32
28C	Web-Plumb at No-Load	5503.38	5699.36	4102.52	4102.52
	Web-Plumb at Concrete Deck Load	5499.04	5703.40	4102.42	4102.42

**Table D-14** Cross-frames 29 - Detailing dimensions for web-plumb position at no-load condition versus web-plumb position after application of concrete deck load

		<b>Cross-Frame Member Lengths (mm)</b>			
<b>Cross-Frame</b>	<b>Detailed Condition</b>	<b>F</b>	<b>M</b>	<b>Top Chord</b>	<b>Bottom Chord</b>
<b>29A</b>	Web-Plumb at No-Load	5636.61	5564.42	4100.34	4100.34
	Web-Plumb at Concrete Deck Load	5626.85	5574.26	4100.32	4100.32
<b>29B</b>	Web-Plumb at No-Load	5541.70	5659.77	4100.92	4100.92
	Web-Plumb at Concrete Deck Load	5533.70	5668.89	4101.81	4101.81
<b>29C</b>	Web-Plumb at No-Load	5531.41	5670.34	4101.27	4101.27
	Web-Plumb at Concrete Deck Load	5524.19	5677.59	4101.41	4101.41

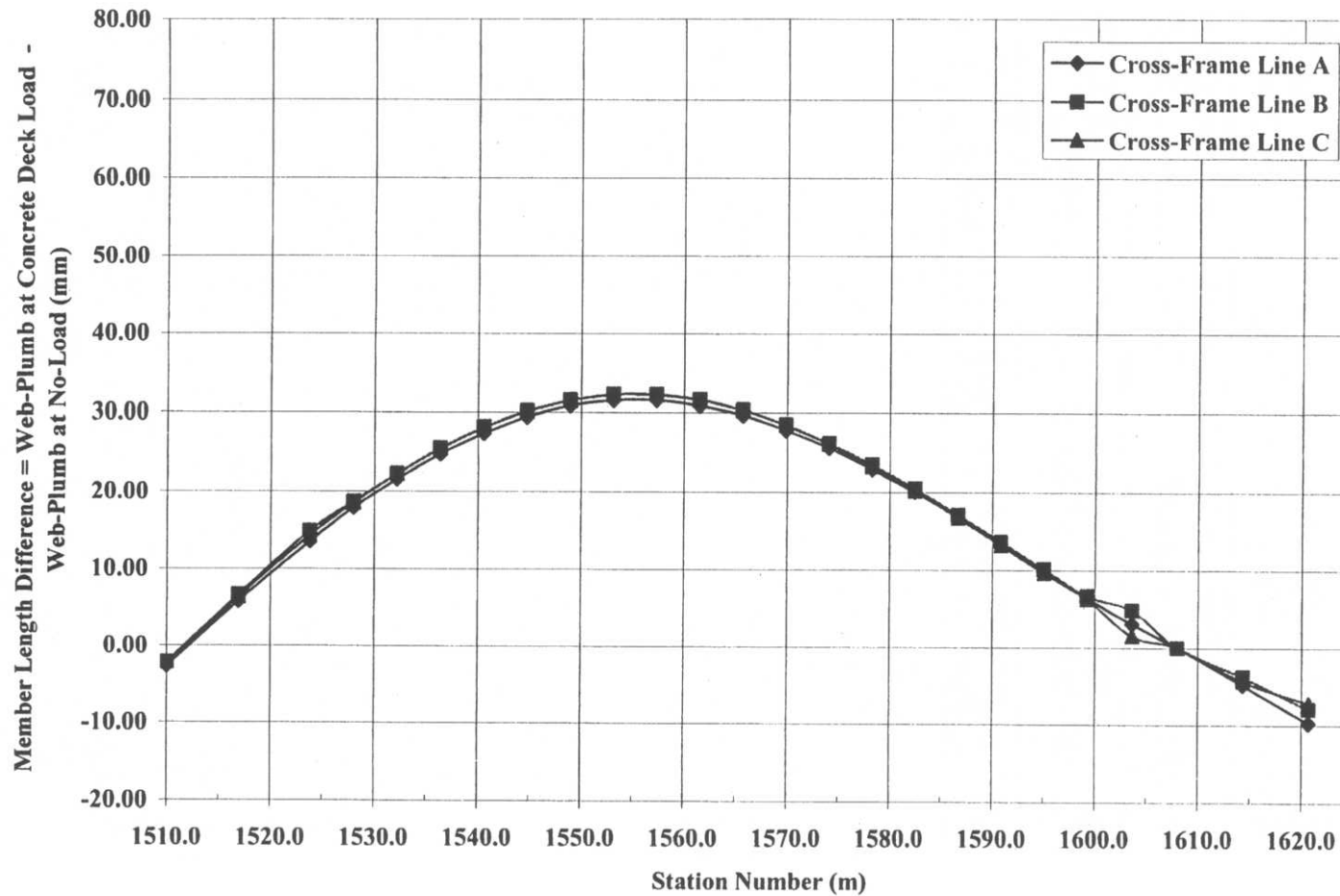


**Figure D-6** Cross-frame member 'F' – Web-plumb at concrete deck load detail vs. web-plumb at no-load detail length difference

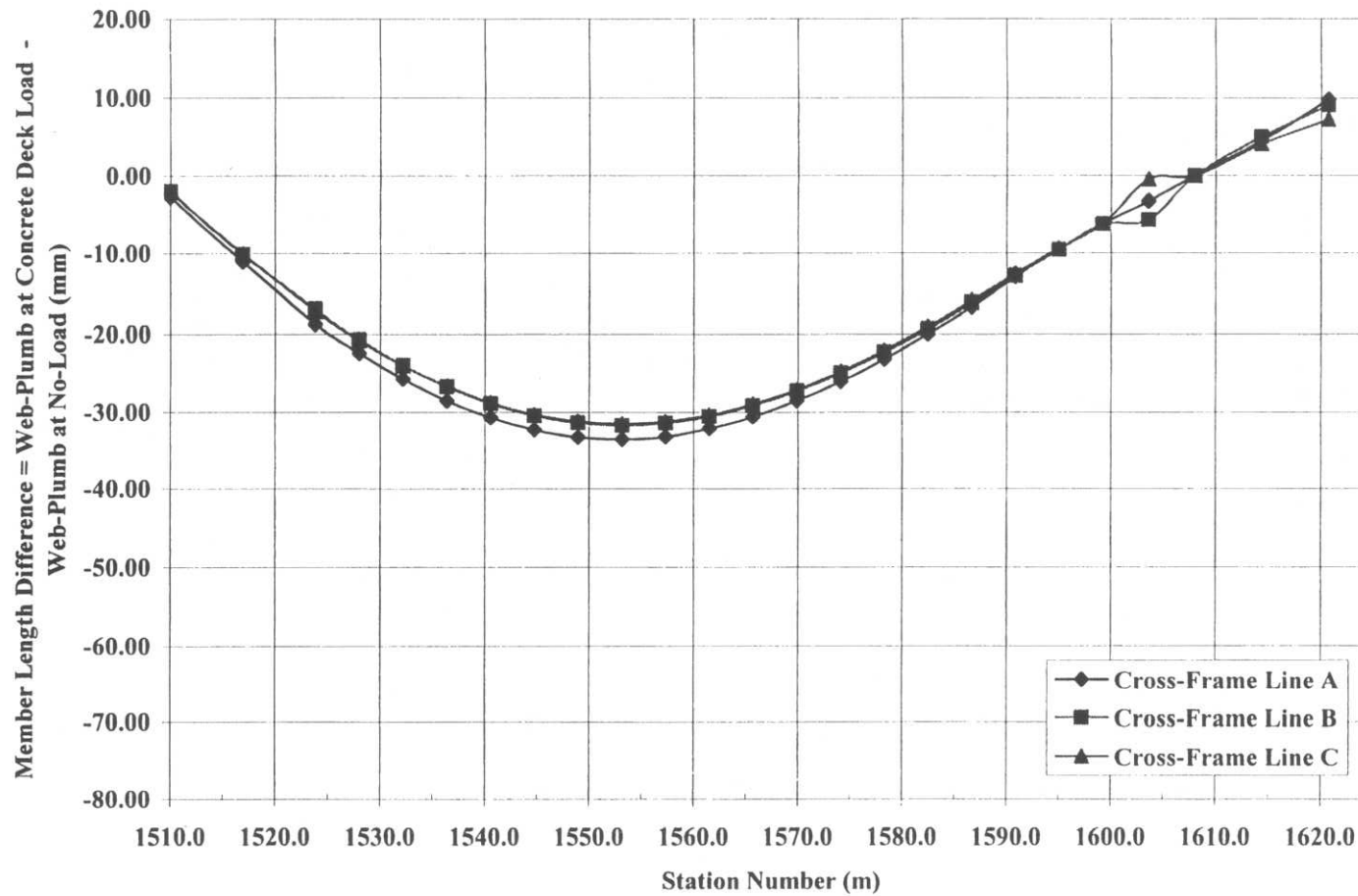


**Figure D-7** Cross-frame member 'M' – Web-plumb at concrete deck load detail vs. web-plumb at no-load detail length difference

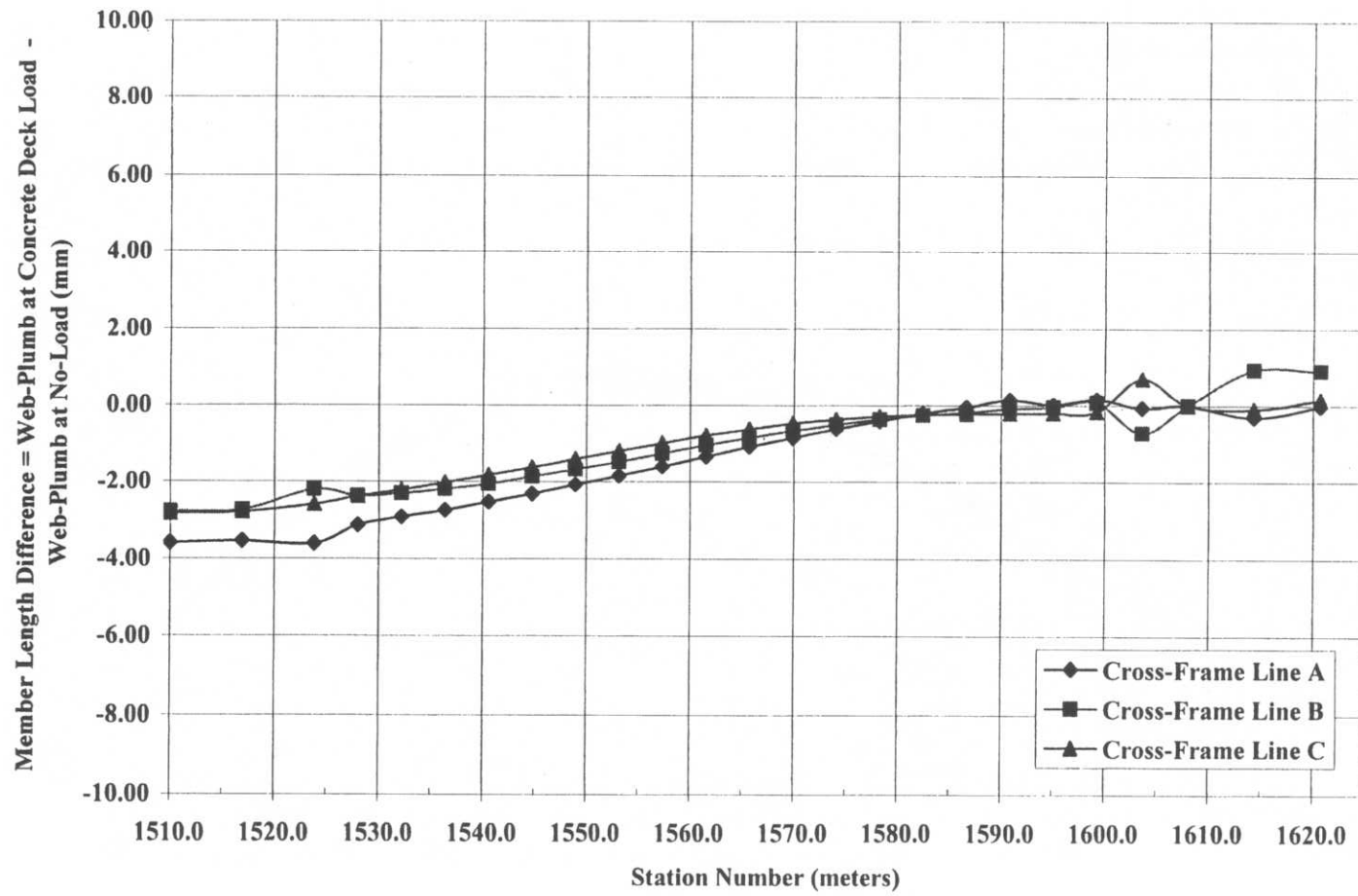


**Figure D-8** Cross-frame to chord – Web-plumb at concrete deck load detail vs. web-plumb at no-load detail length difference

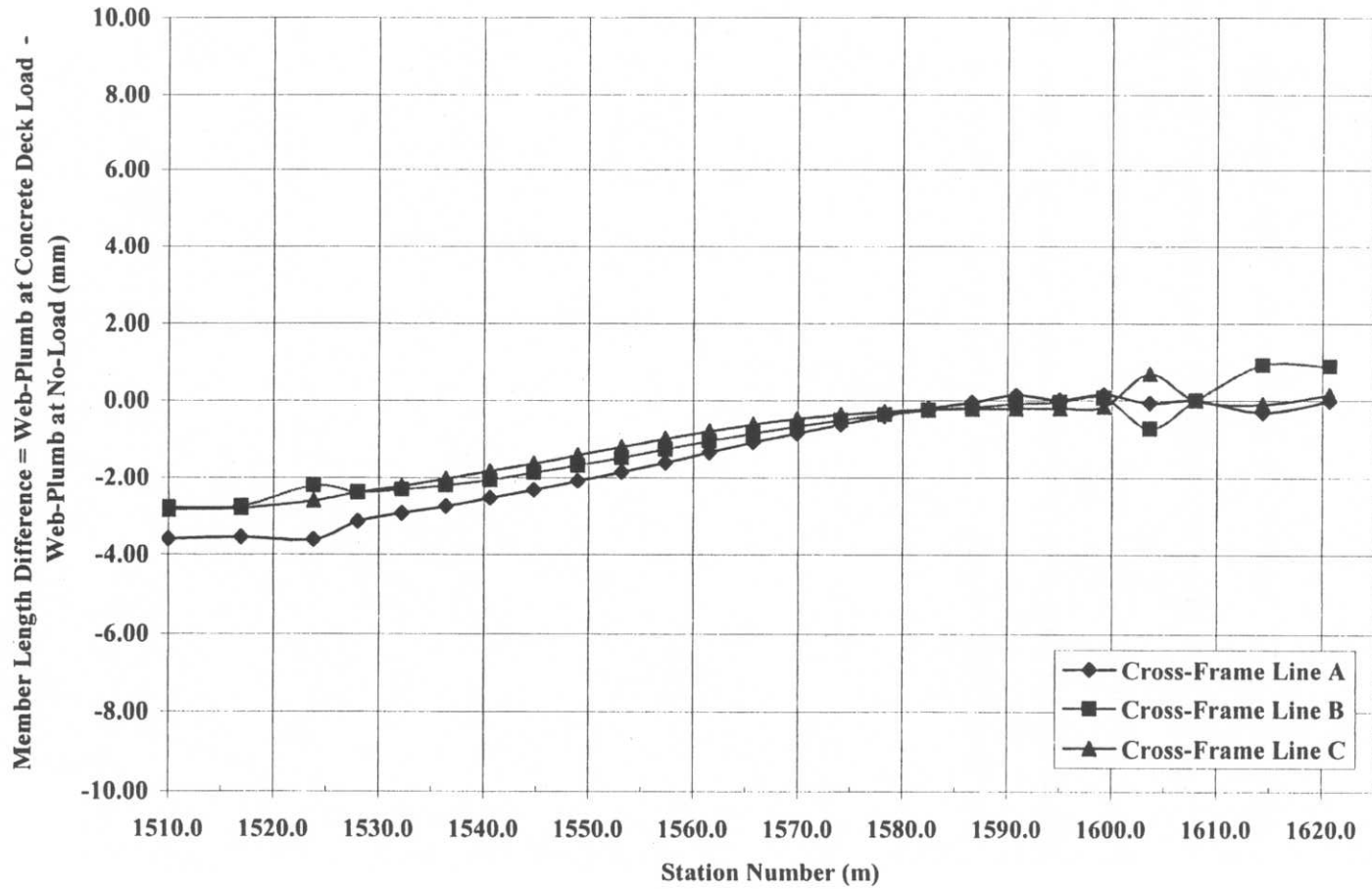


**Figure D-9** Cross-frame bottom chord – Web-plumb at concrete deck load detail vs. web-plumb at no-load detail length difference

### **D.3 Profiles of Field-Surveyed Elevations of the Steel Superstructure Prior to Concrete Deck Placement with Finite Element Model Predictions**

This section of Appendix D provides elevation profiles for the steel elevations prior to concrete deck placement using the analytical model with cross-frames detailed for the web-plumb position at no-load and actual field-surveyed elevations of the Ford City Bridge. The elevations are measured to the top of the top flange for each girder. For each girder, the elevations for both cases are shown on a series of elevation profile graphs, in station number increments of 15m, resulting in seven total graphs for each girder.

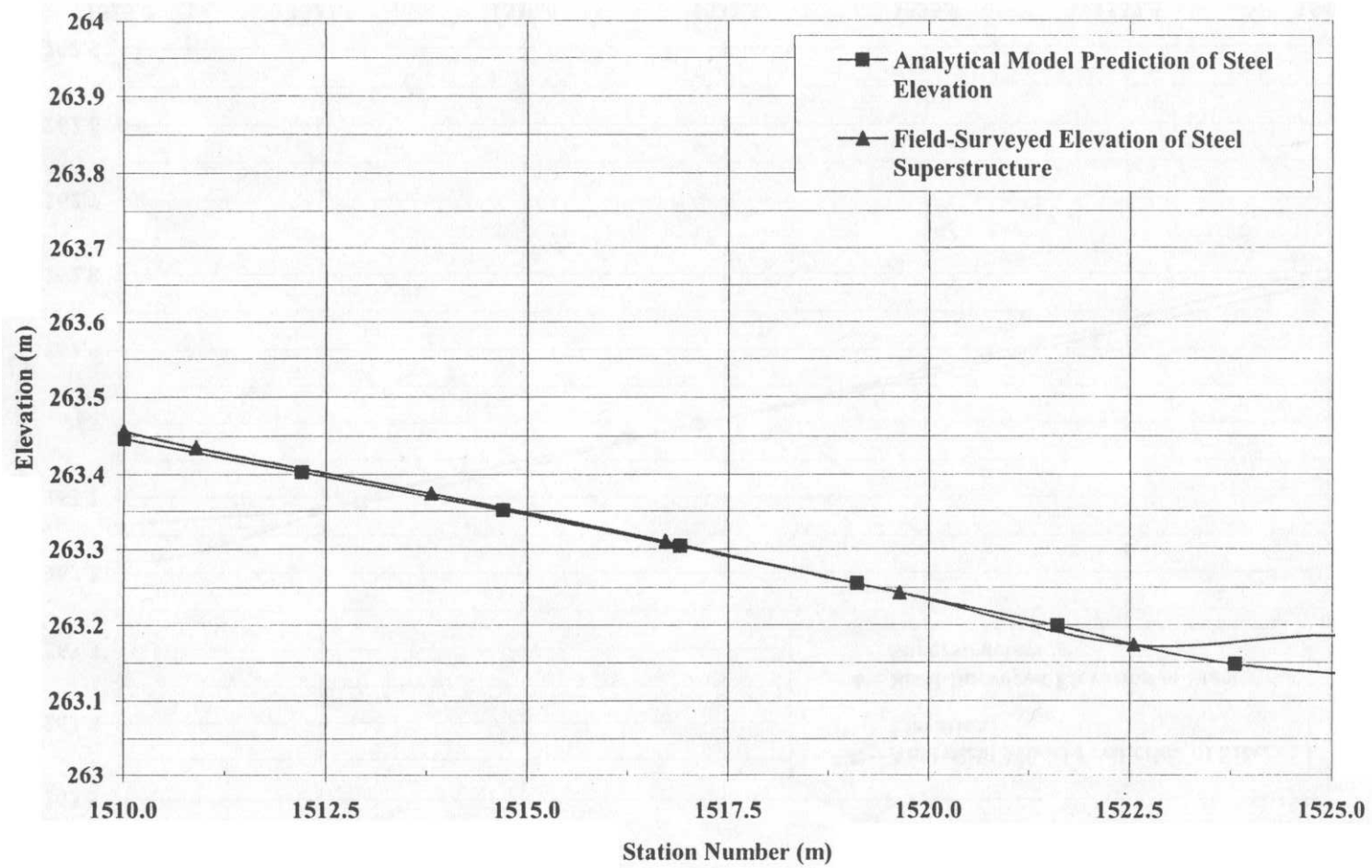


**Figure D-10** G1 – Elevation profile, STA 1+510 to 1+525; Analytical model versus field-surveyed data

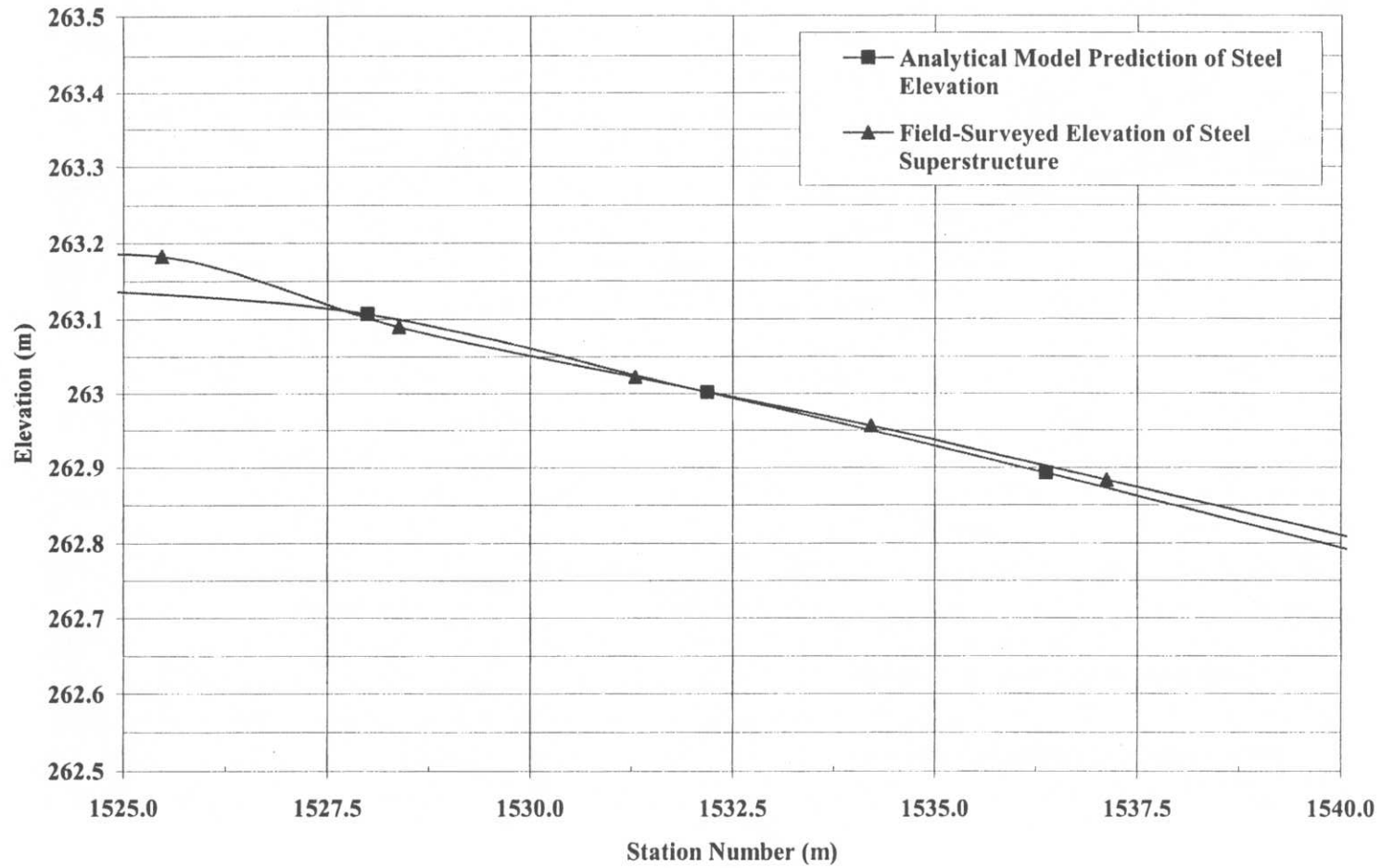


**Figure D-11 G1** – Elevation profile, STA 1+525 to 1+540; Analytical model versus field-surveyed data

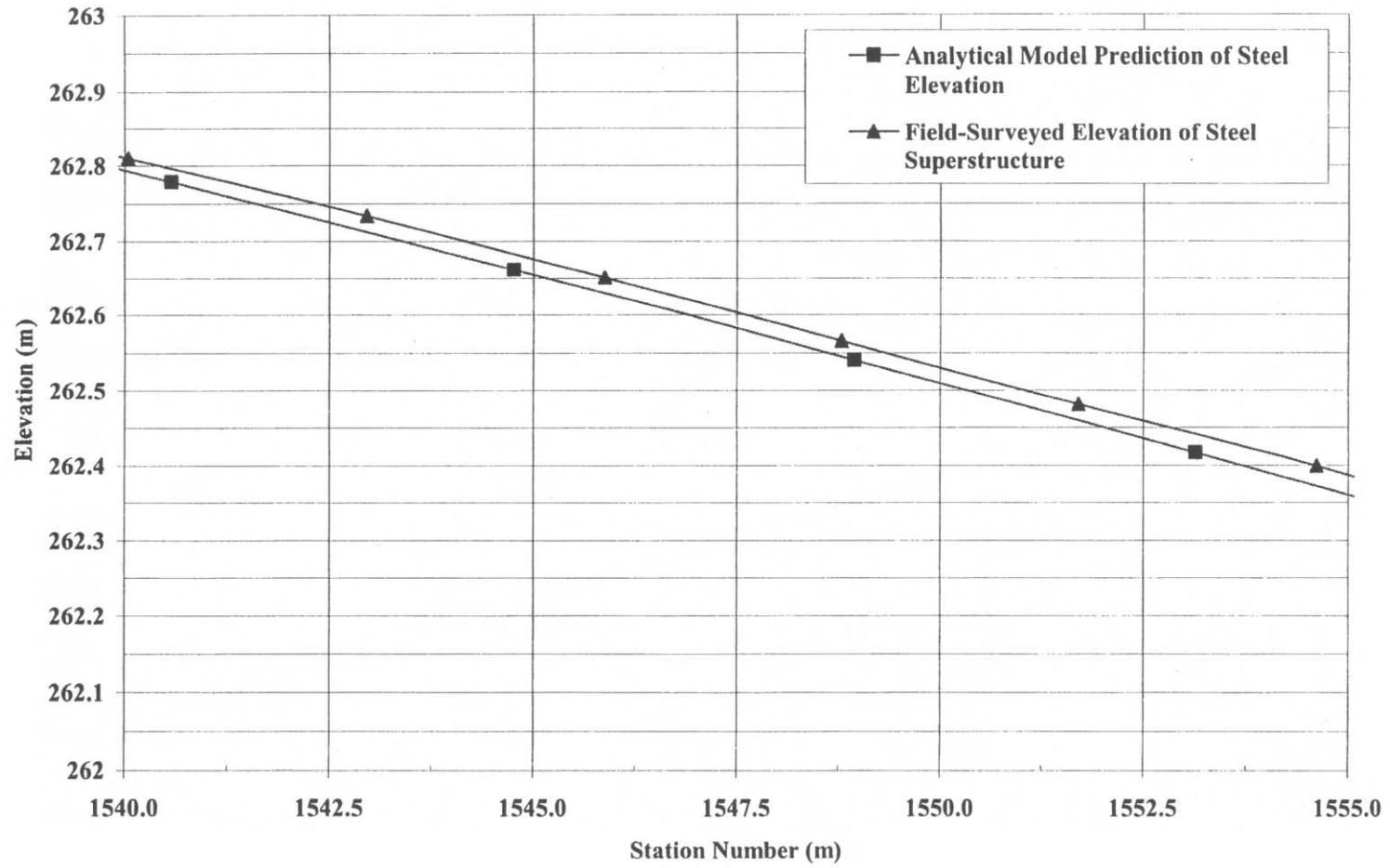
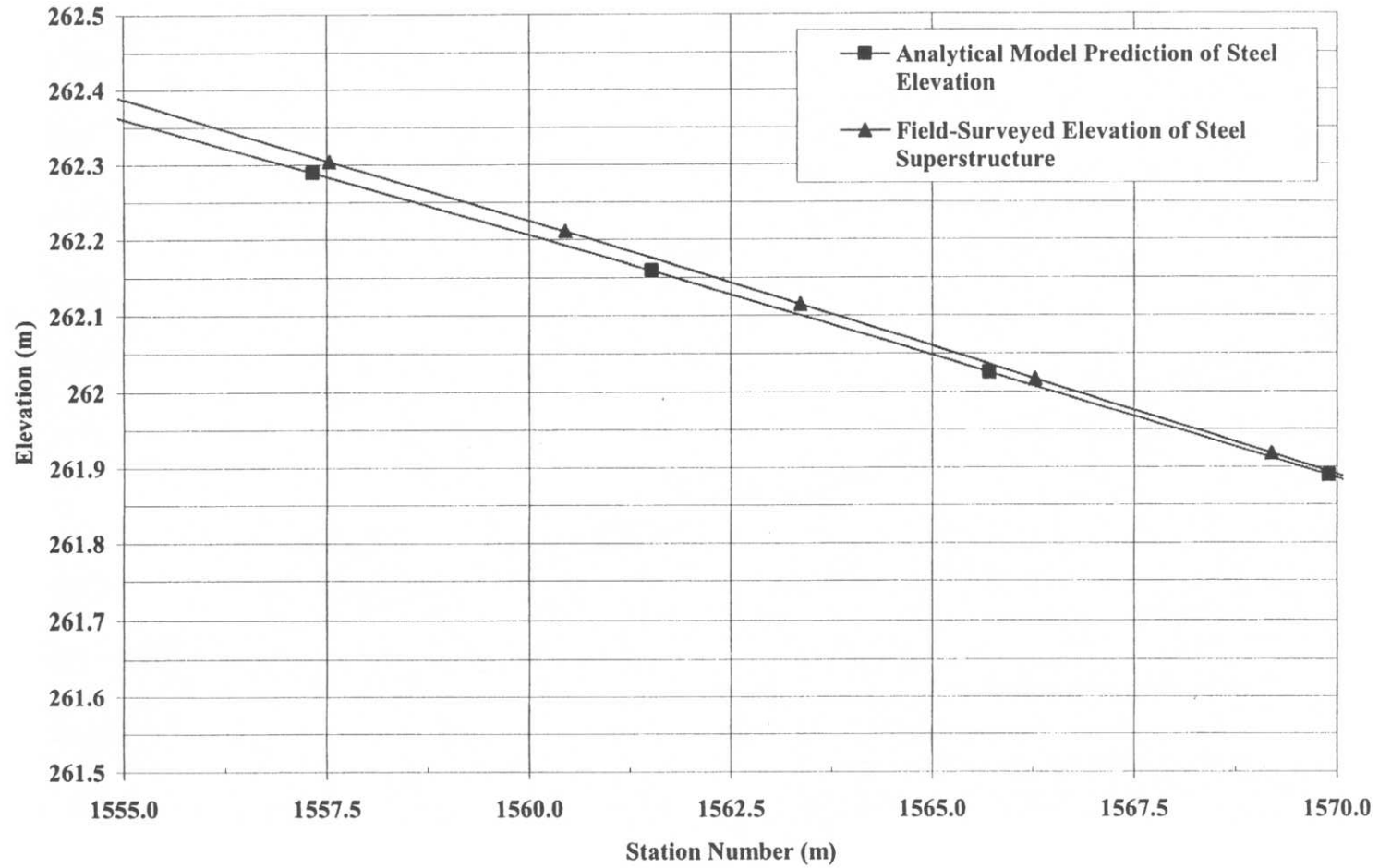
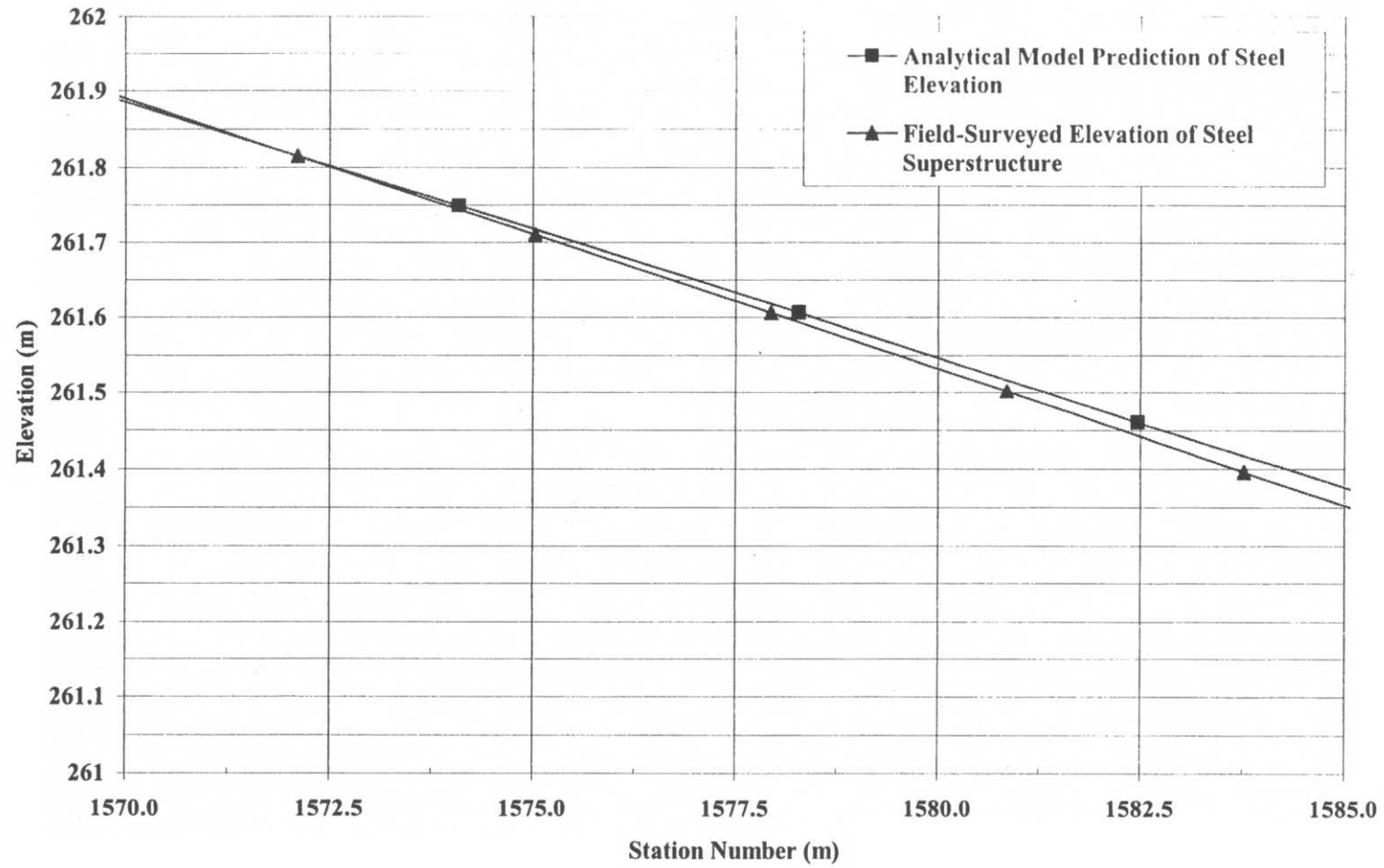


Figure D-12 G1 – Elevation profile, STA 1+540 to 1+555; Analytical model versus field-surveyed data



**Figure D-13** G1 – Elevation profile, STA 1+555 to 1+570; Analytical model versus field-surveyed data



**Figure D-14** G1 – Elevation profile, STA 1+570 to 1+585; Analytical model versus field-surveyed data

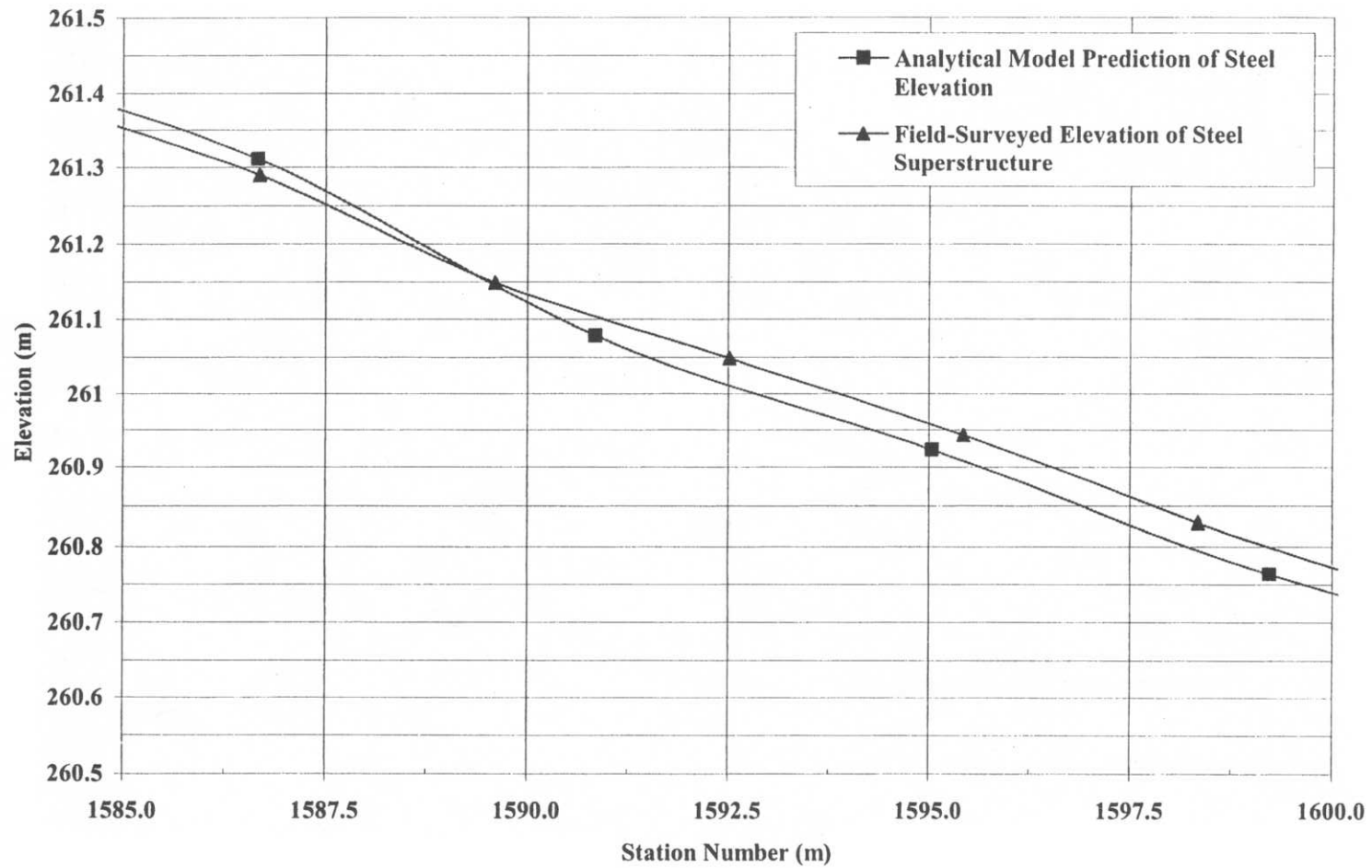


**Figure D-15** G1 – Elevation profile, STA 1+585 to 1+600; Analytical model versus field-surveyed data

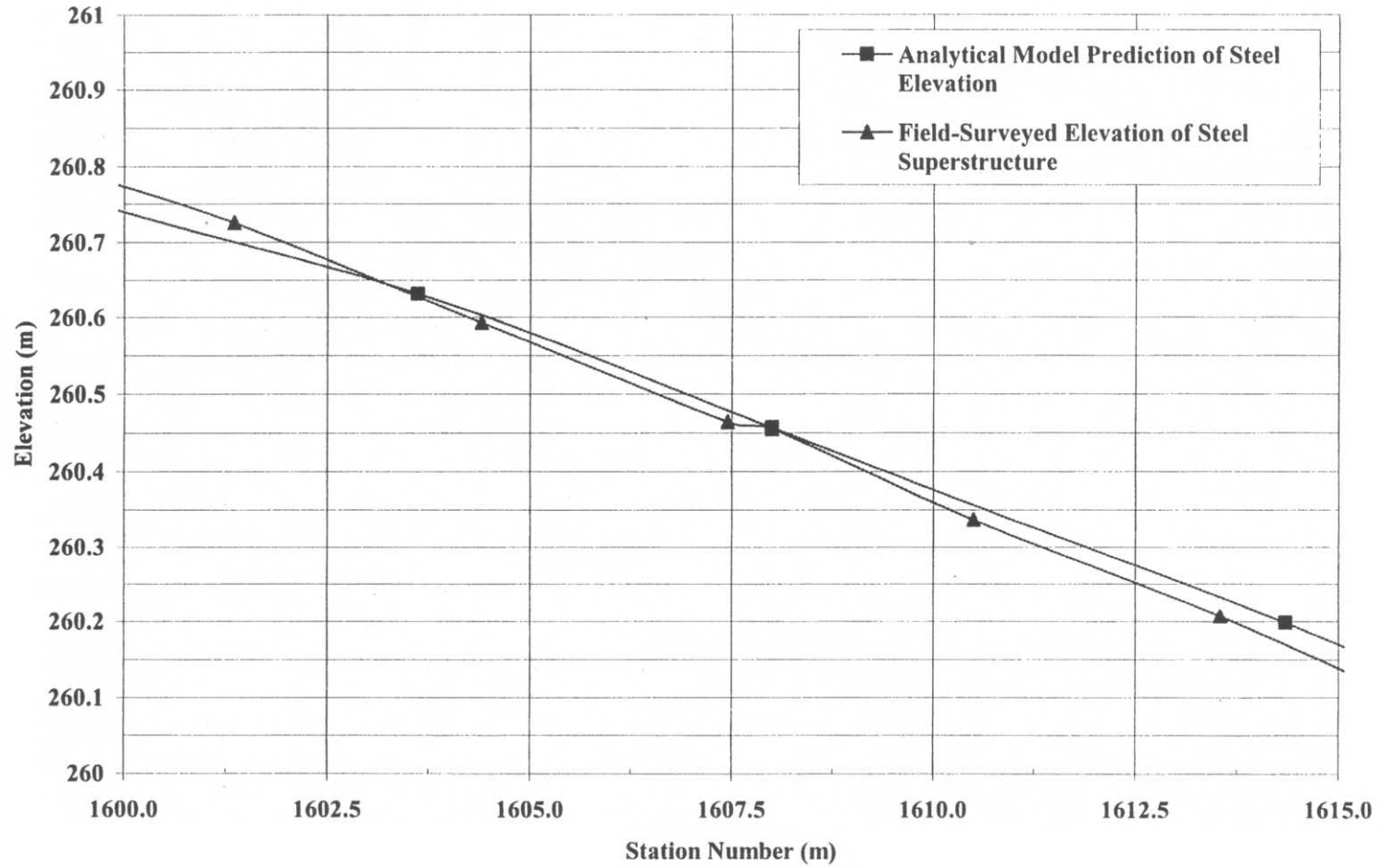


**Figure D-16** G1 – Elevation profile, STA 1+600 to 1+615; Analytical model versus field-surveyed data

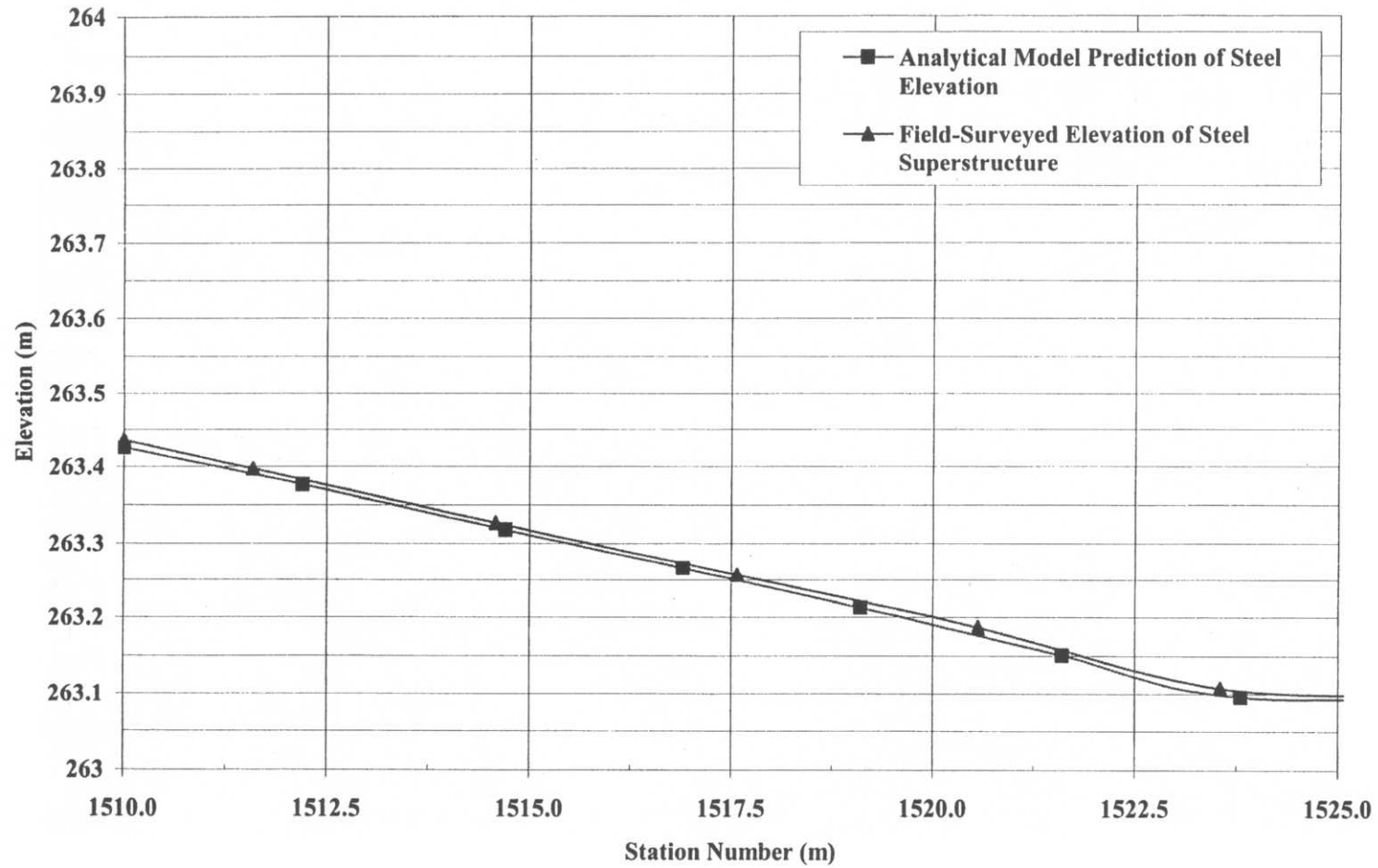


**Figure D-17** G2 – Elevation profile, STA 1+510 to 1+525; Analytical model versus field-surveyed data

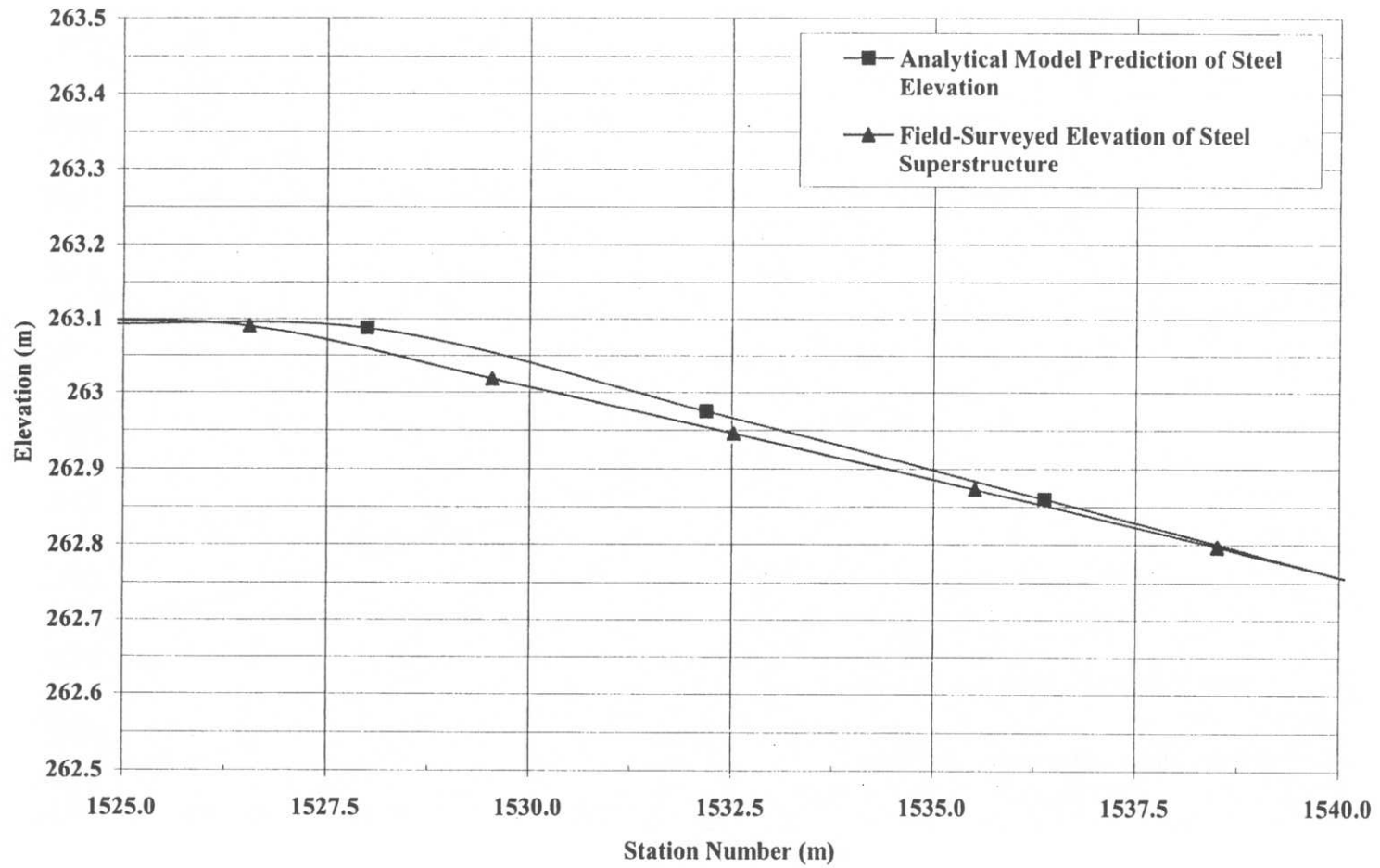


**Figure D-18** G2 – Elevation profile, STA 1+525 to 1+540; Analytical model versus field-surveyed data

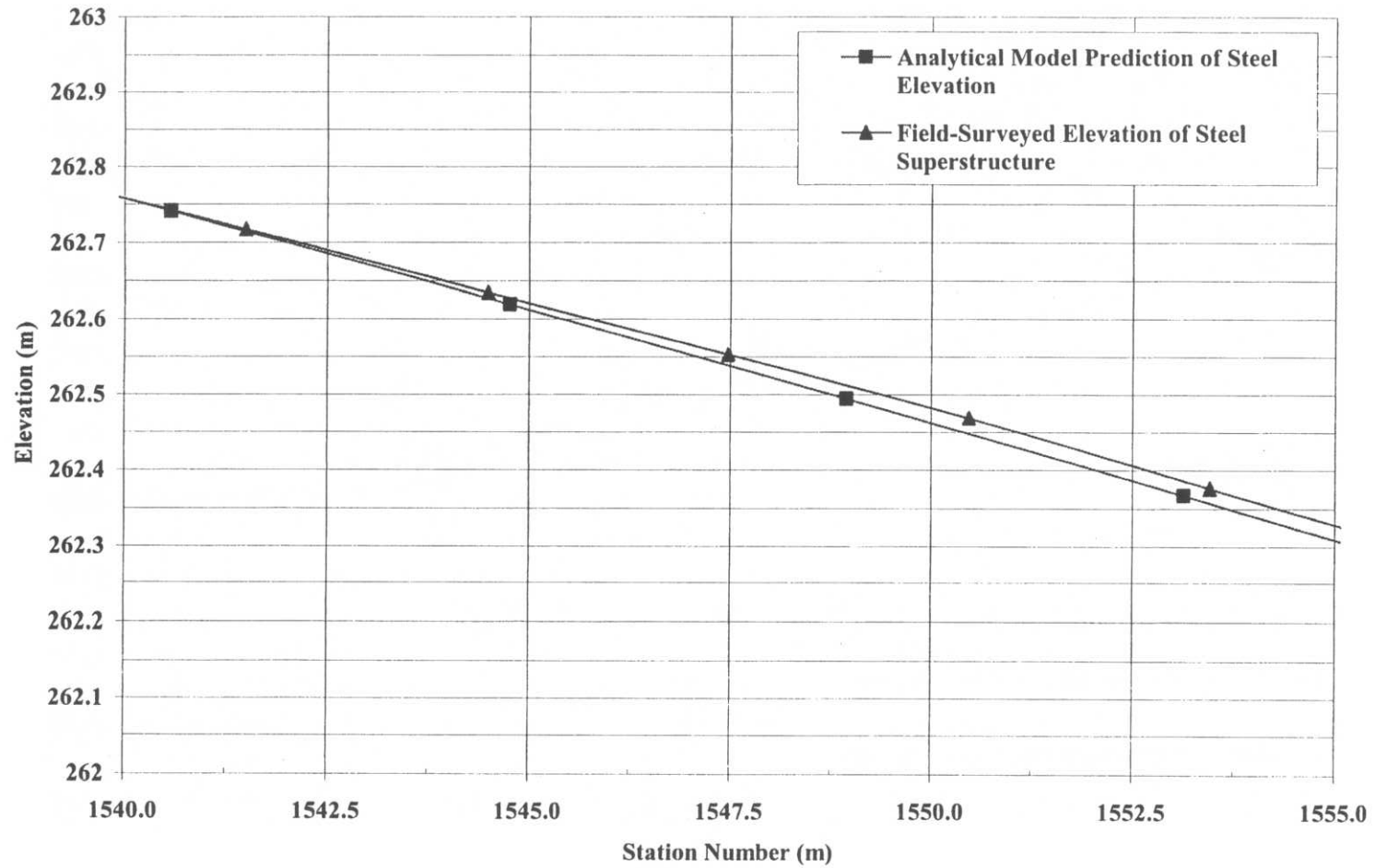


**Figure D-19** G2 – Elevation profile, STA 1+540 to 1+555; Analytical model versus field-surveyed data

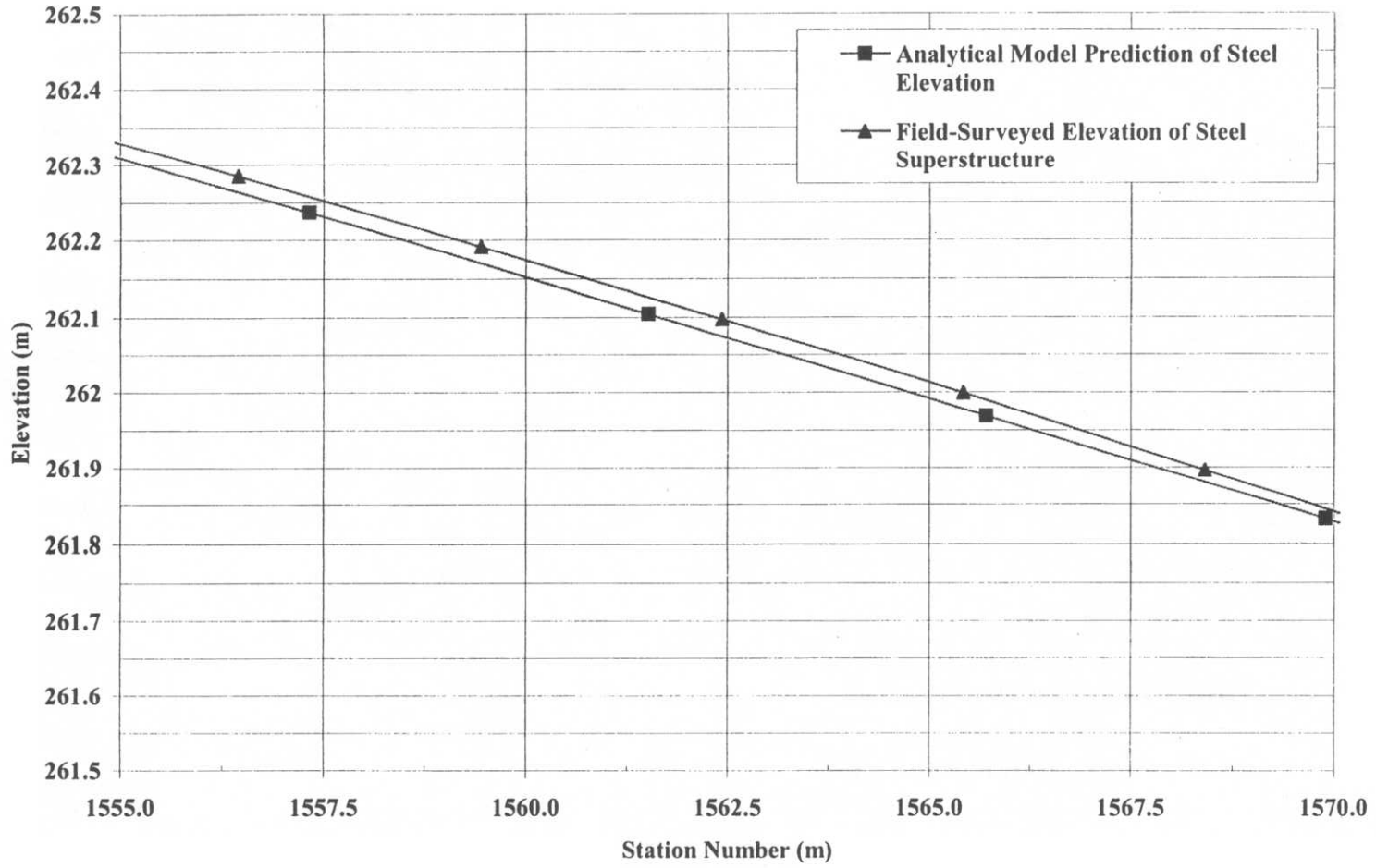


**Figure D-20** G2 – Elevation profile, STA 1+555 to 1+570; Analytical model versus field-surveyed data

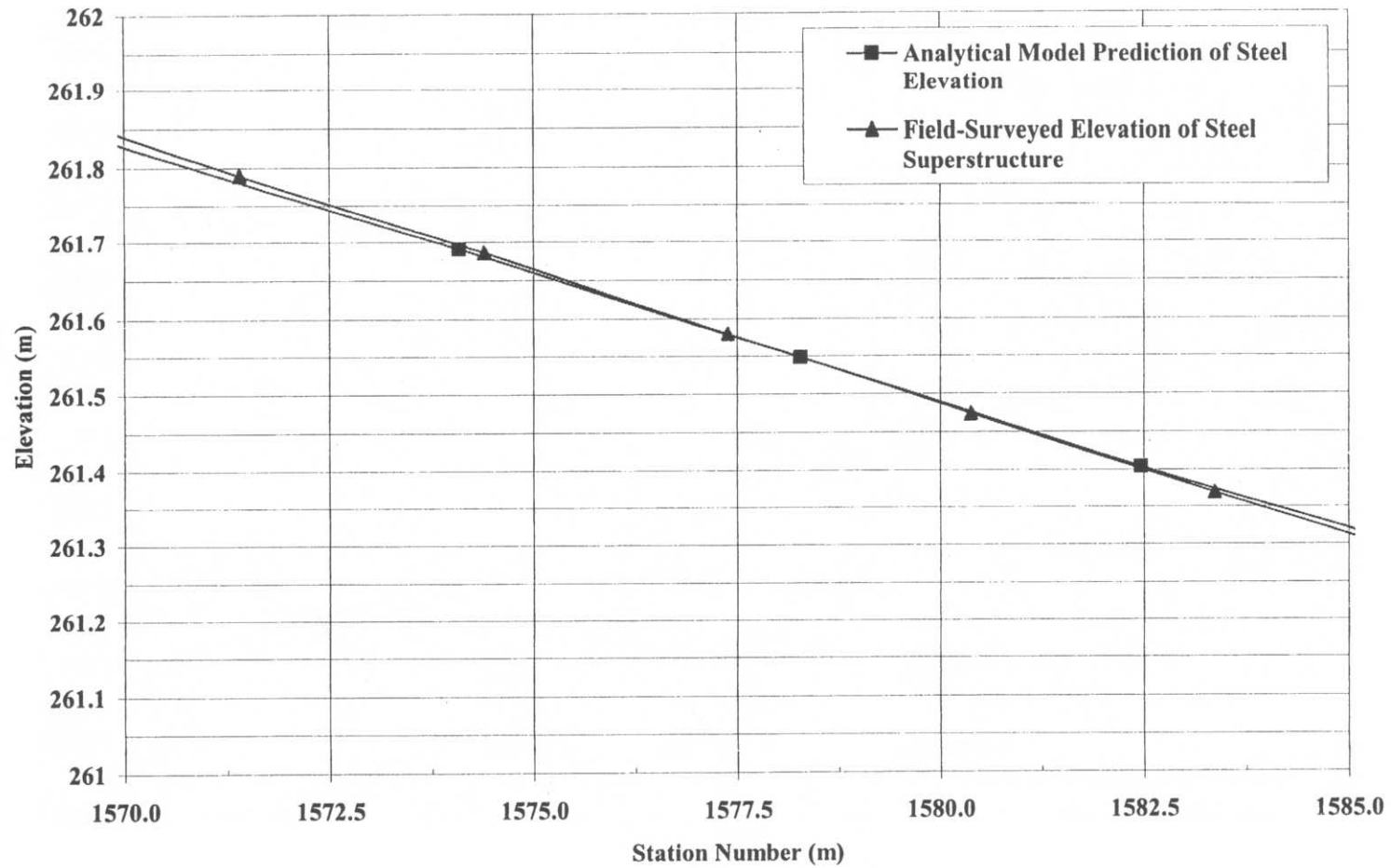


**Figure D-21** G2 – Elevation profile, STA 1+570 to 1+585; Analytical model versus field-surveyed data

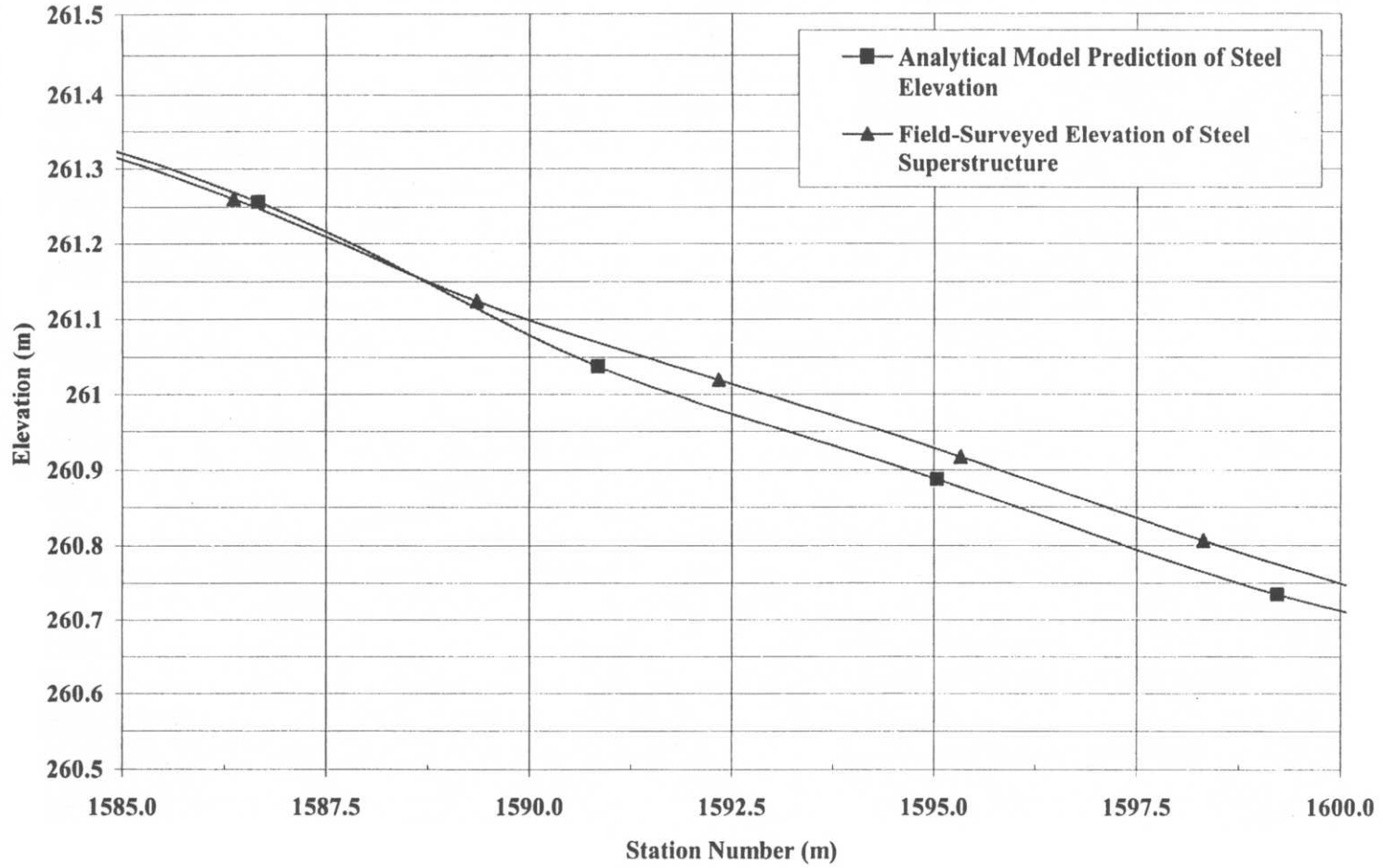


**Figure D-22** G2 – Elevation profile, STA 1+585 to 1+600; Analytical model versus field-surveyed data

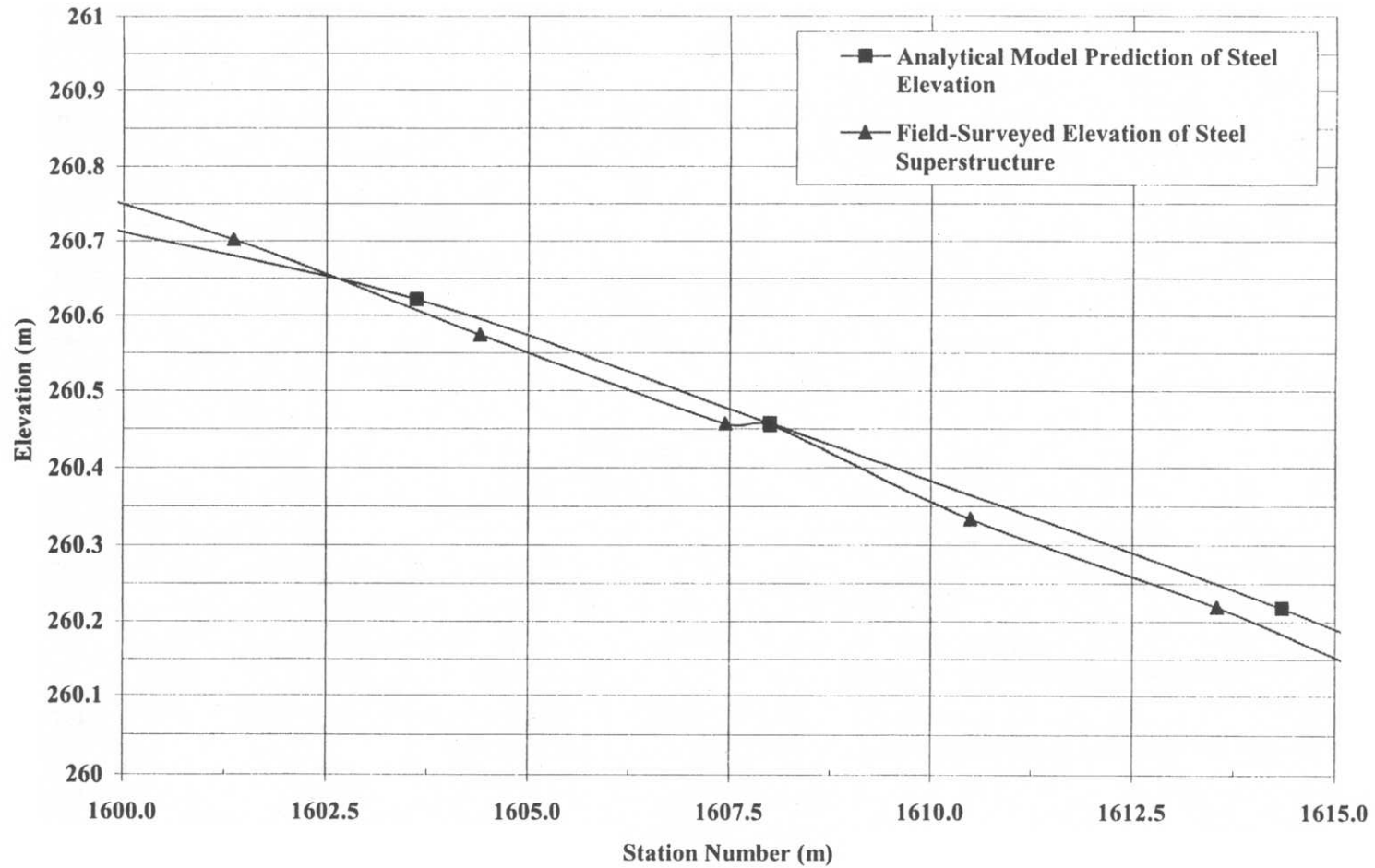


**Figure D-23** G2 – Elevation profile, STA 1+600 to 1+615; Analytical model versus field-surveyed data

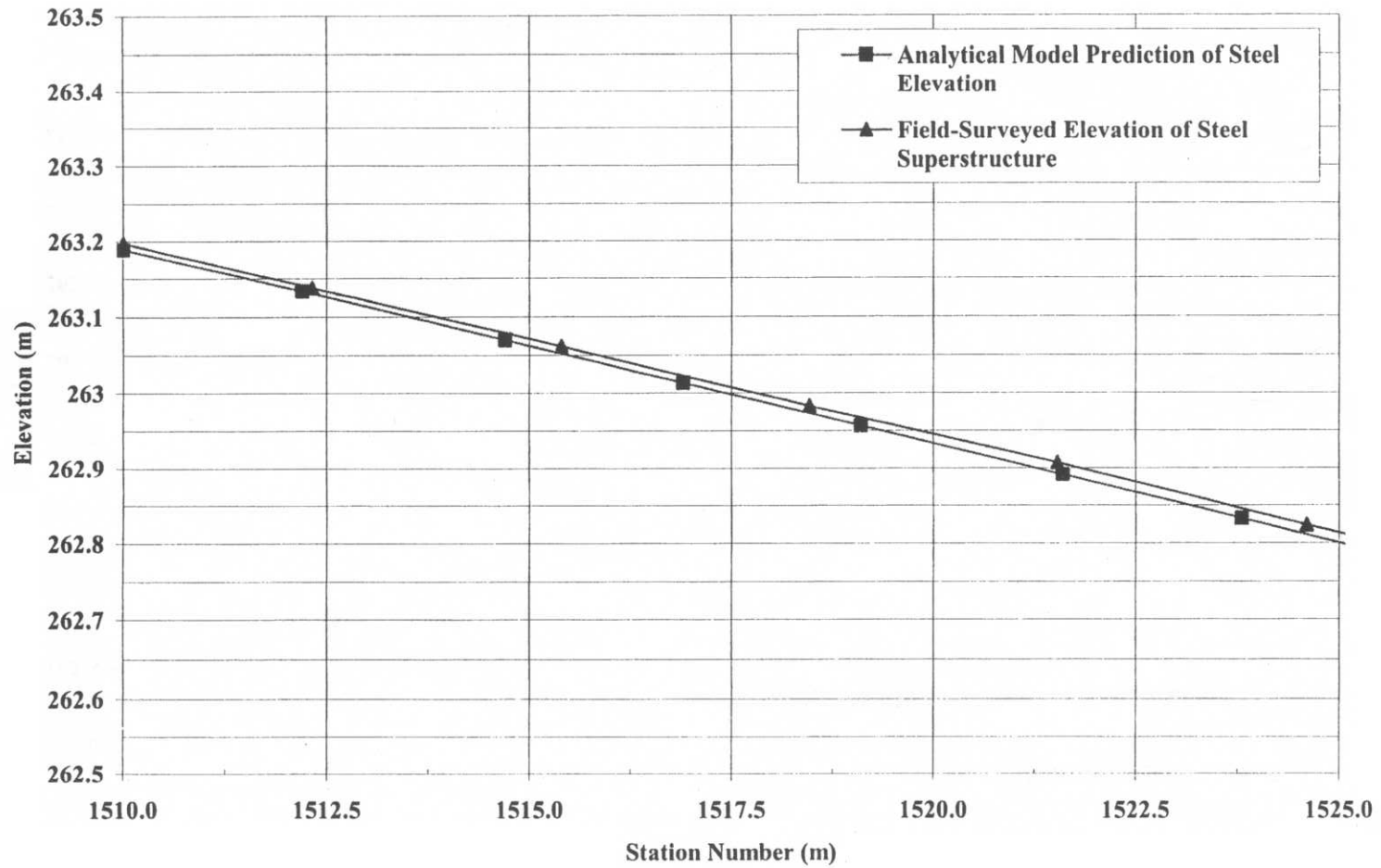


**Figure D-24** G3 – Elevation profile, STA 1+510 to 1+525; Analytical model versus field-surveyed data

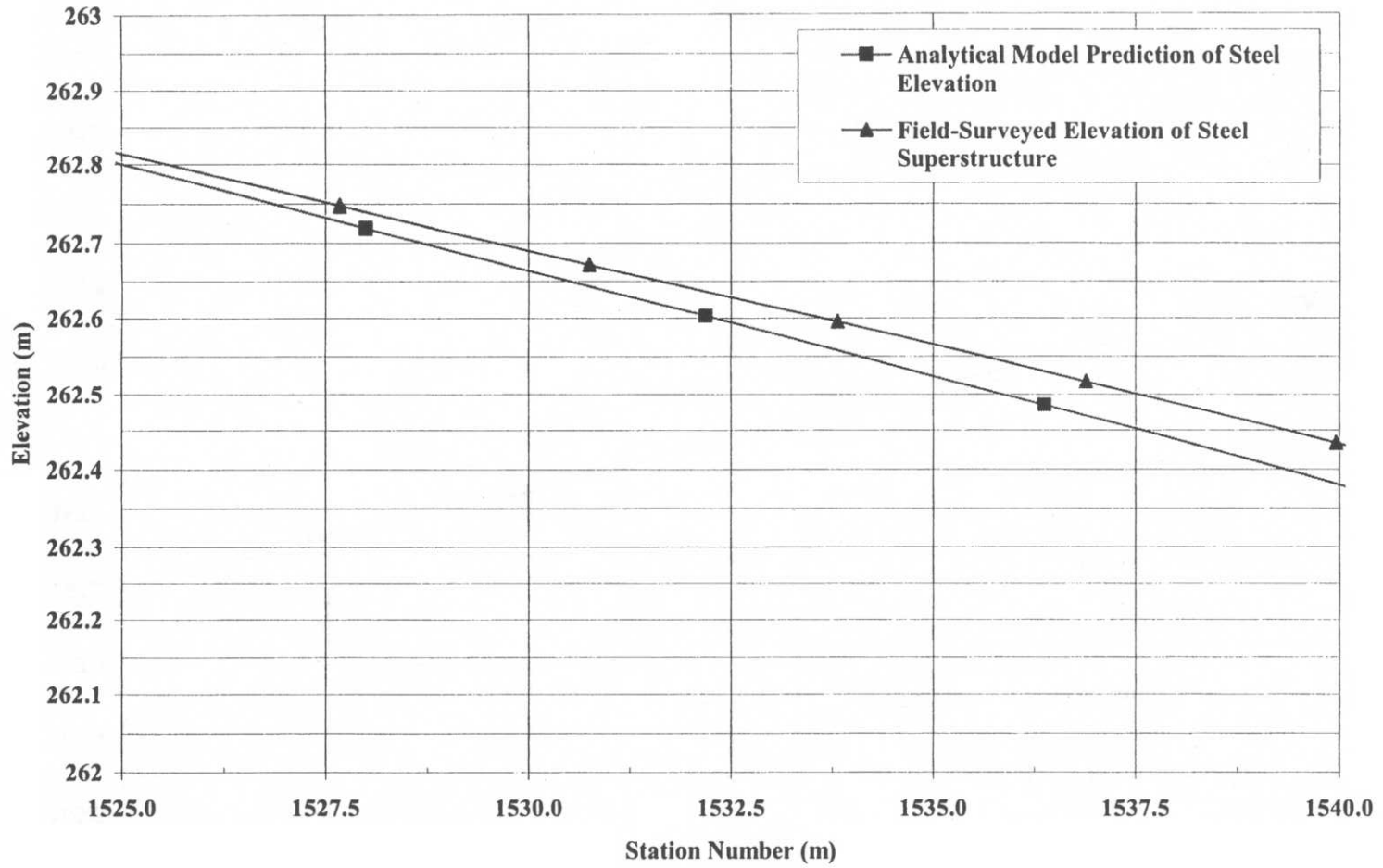


**Figure D-25** G3 – Elevation profile, STA 1+525 to 1+540; Analytical model versus field-surveyed data

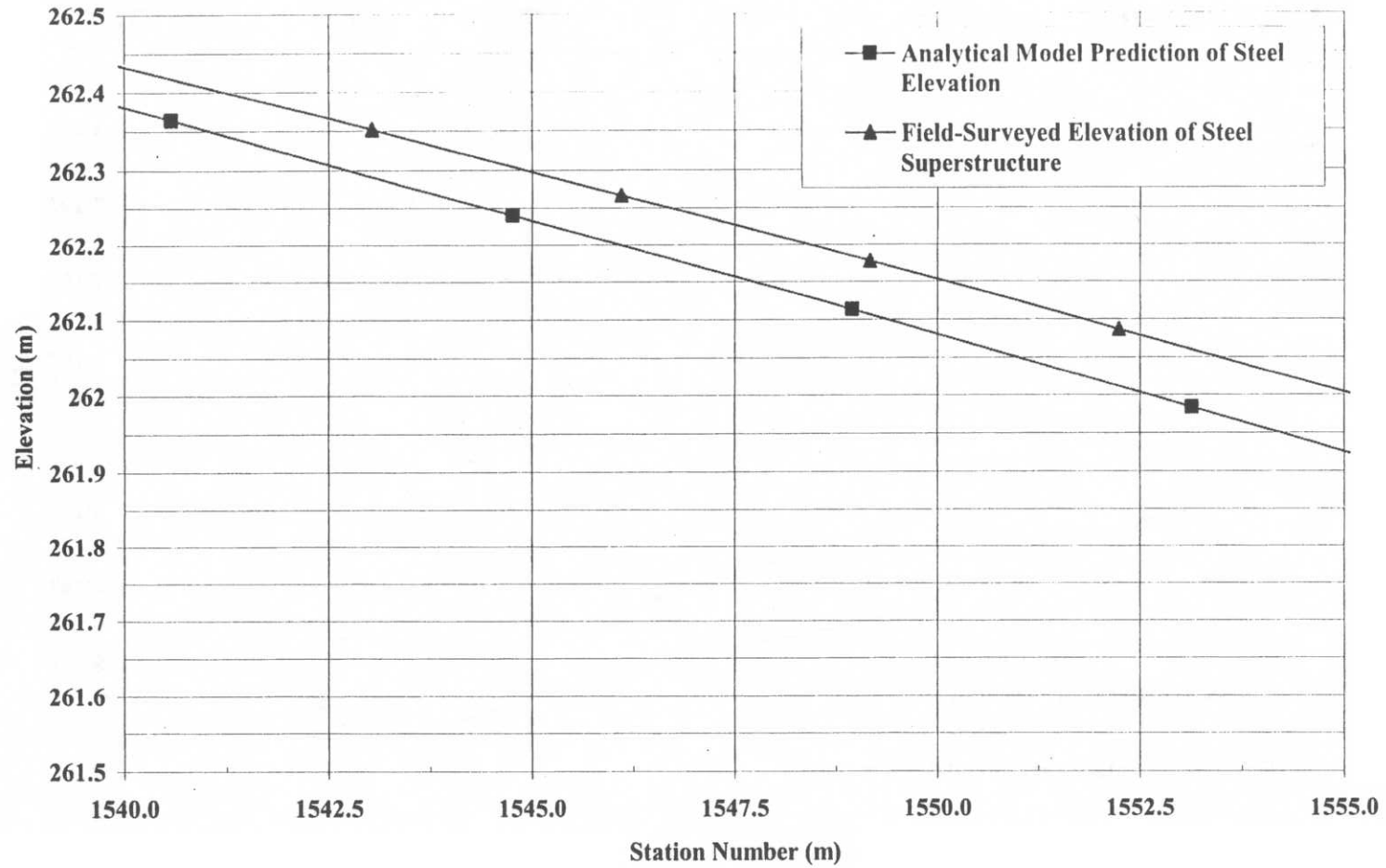


**Figure D-26** G3 – Elevation profile, STA 1+540 to 1+555; Analytical model versus field-surveyed data

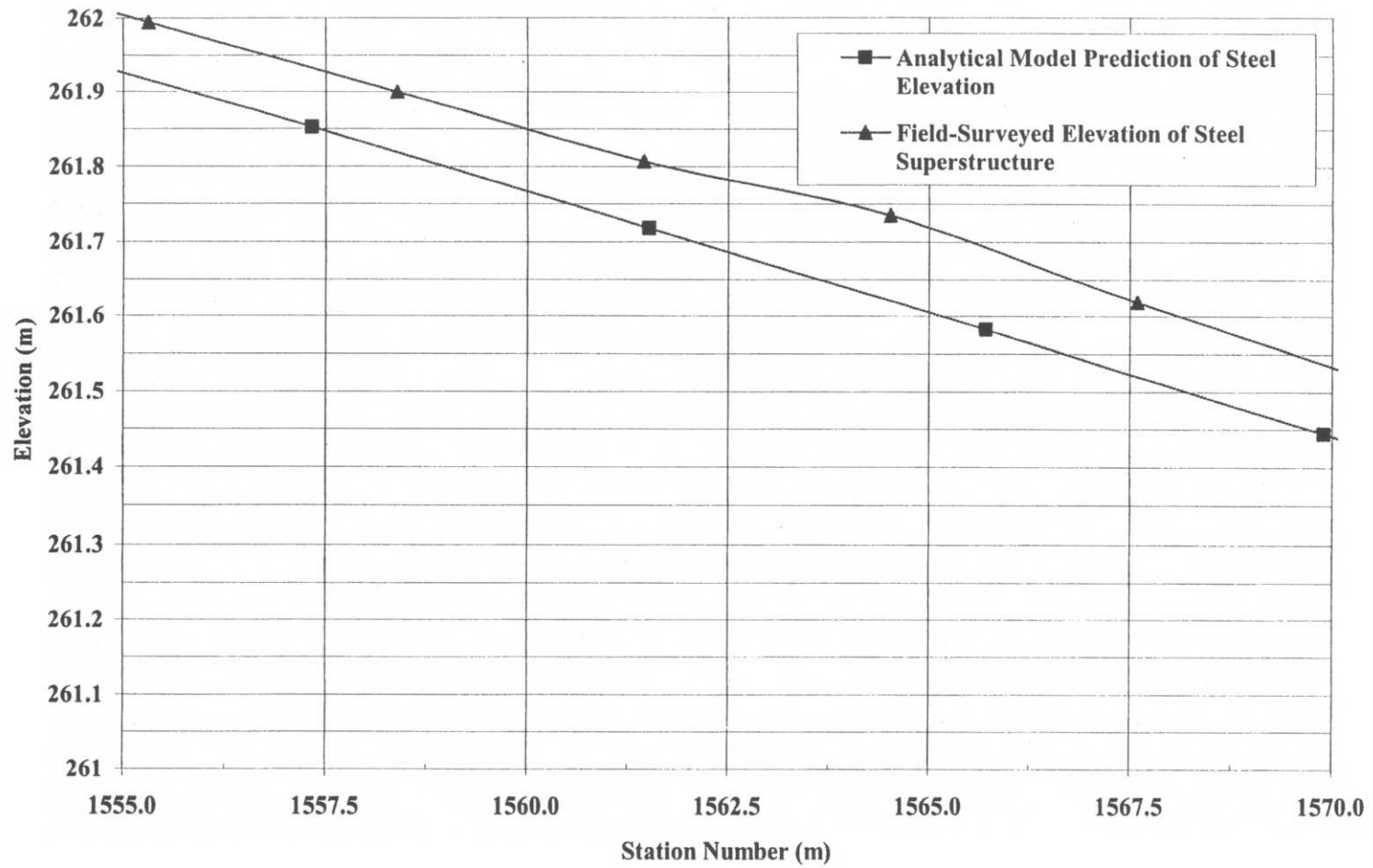


**Figure D-27** G3 – Elevation profile, STA 1+555 to 1+570; Analytical model versus field-surveyed data

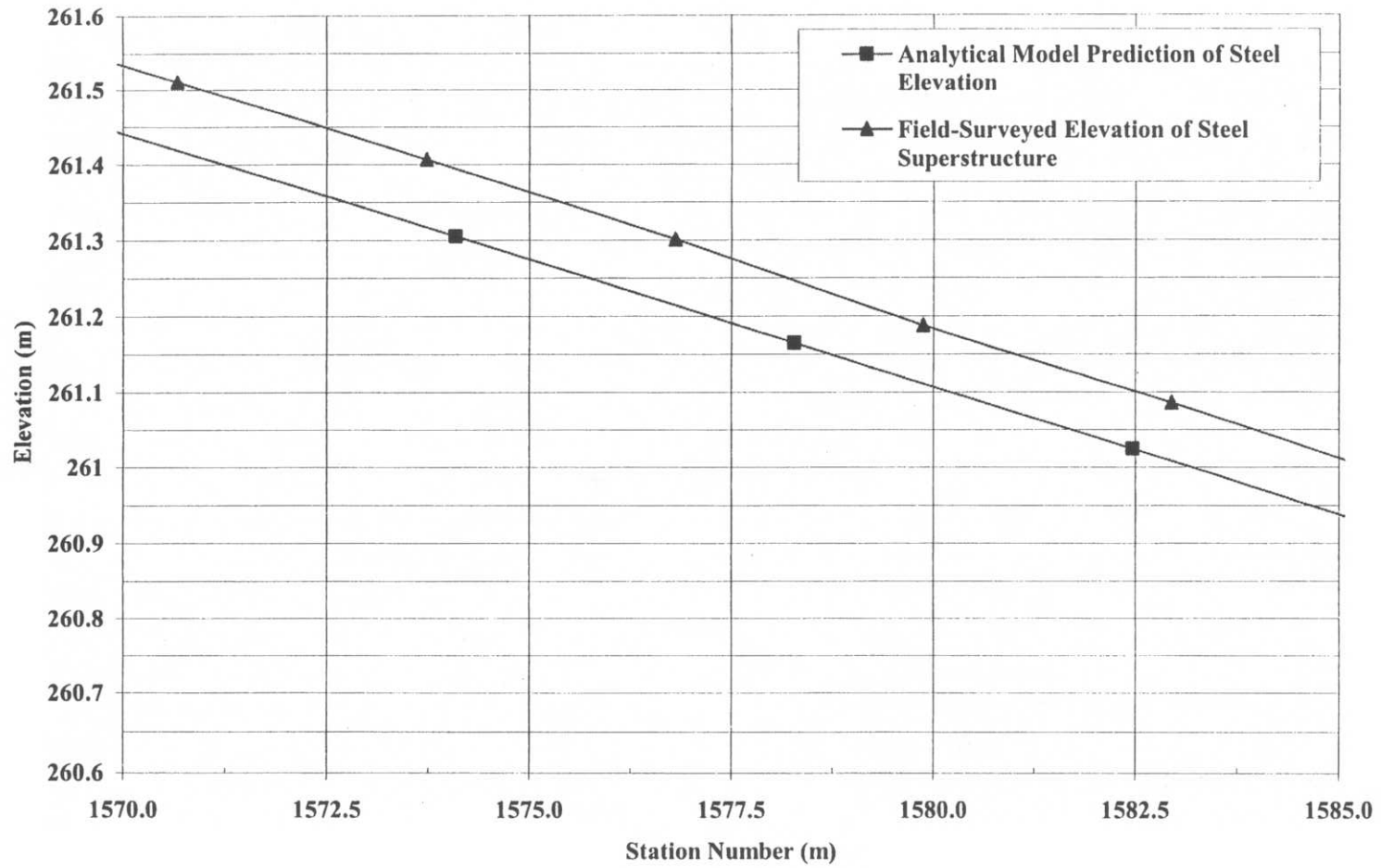


**Figure D-28** G3 – Elevation profile, STA 1+570 to 1+585; Analytical model versus field-surveyed data

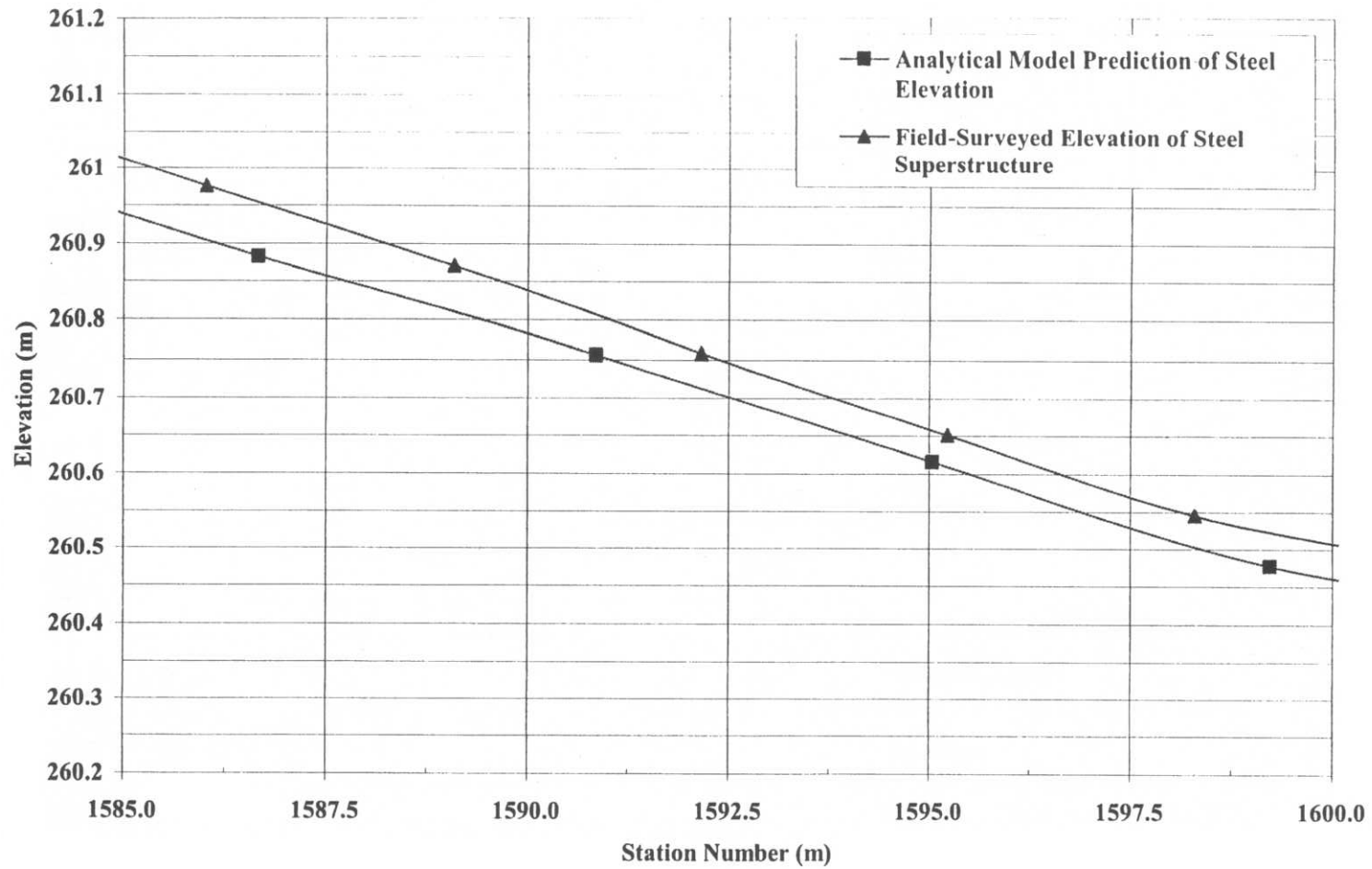


**Figure D-29** G3 – Elevation profile, STA 1+585 to 1+600; Analytical model versus field-surveyed data

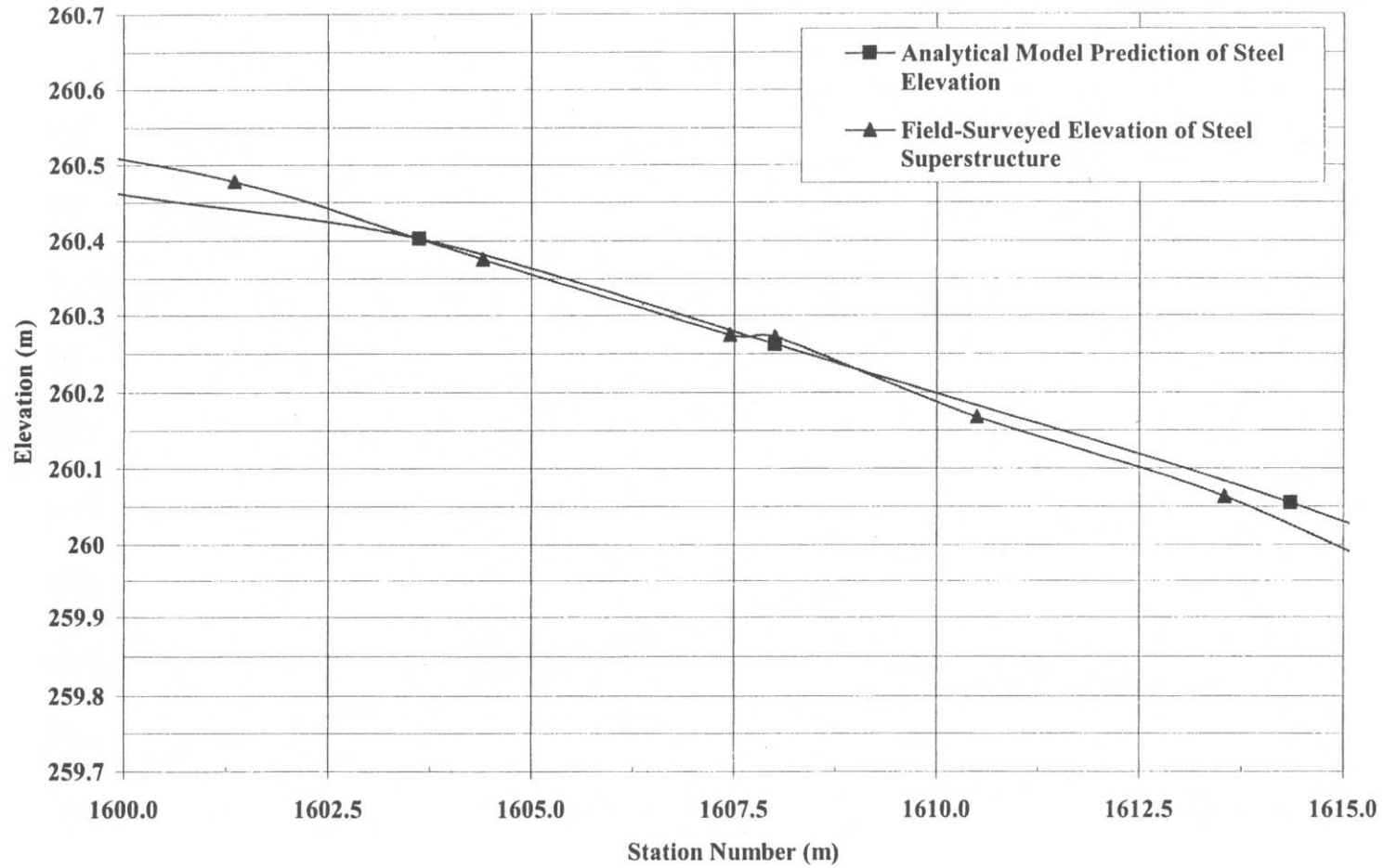


**Figure D-30** G3 – Elevation profile, STA 1+600 to 1+615; Analytical model versus field-surveyed data

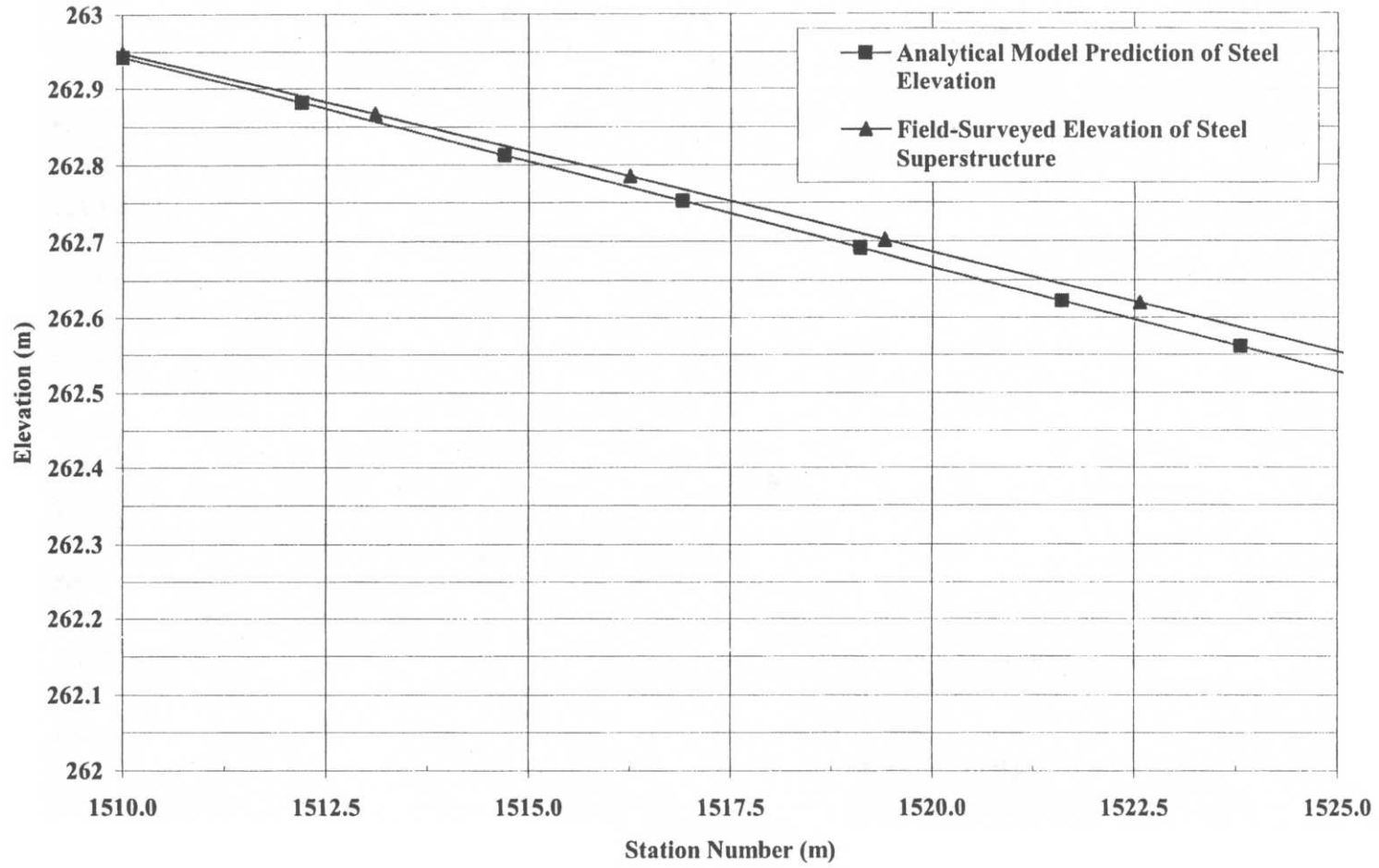


**Figure D-31** G4 – Elevation profile, STA 1+510 to 1+525; Analytical model versus field-surveyed data

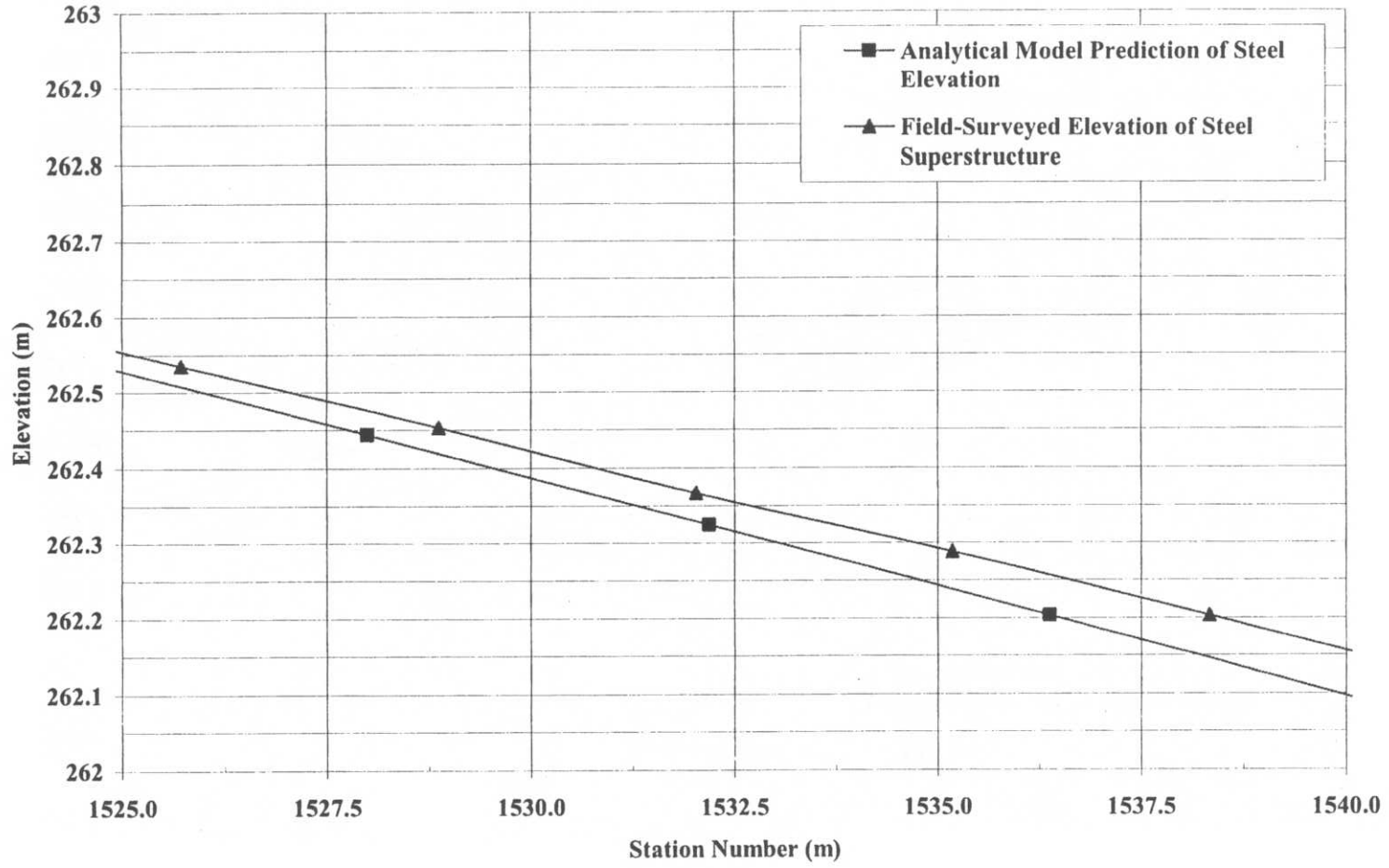


**Figure D-32** G4 – Elevation profile, STA 1+525 to 1+540; Analytical model versus field-surveyed data

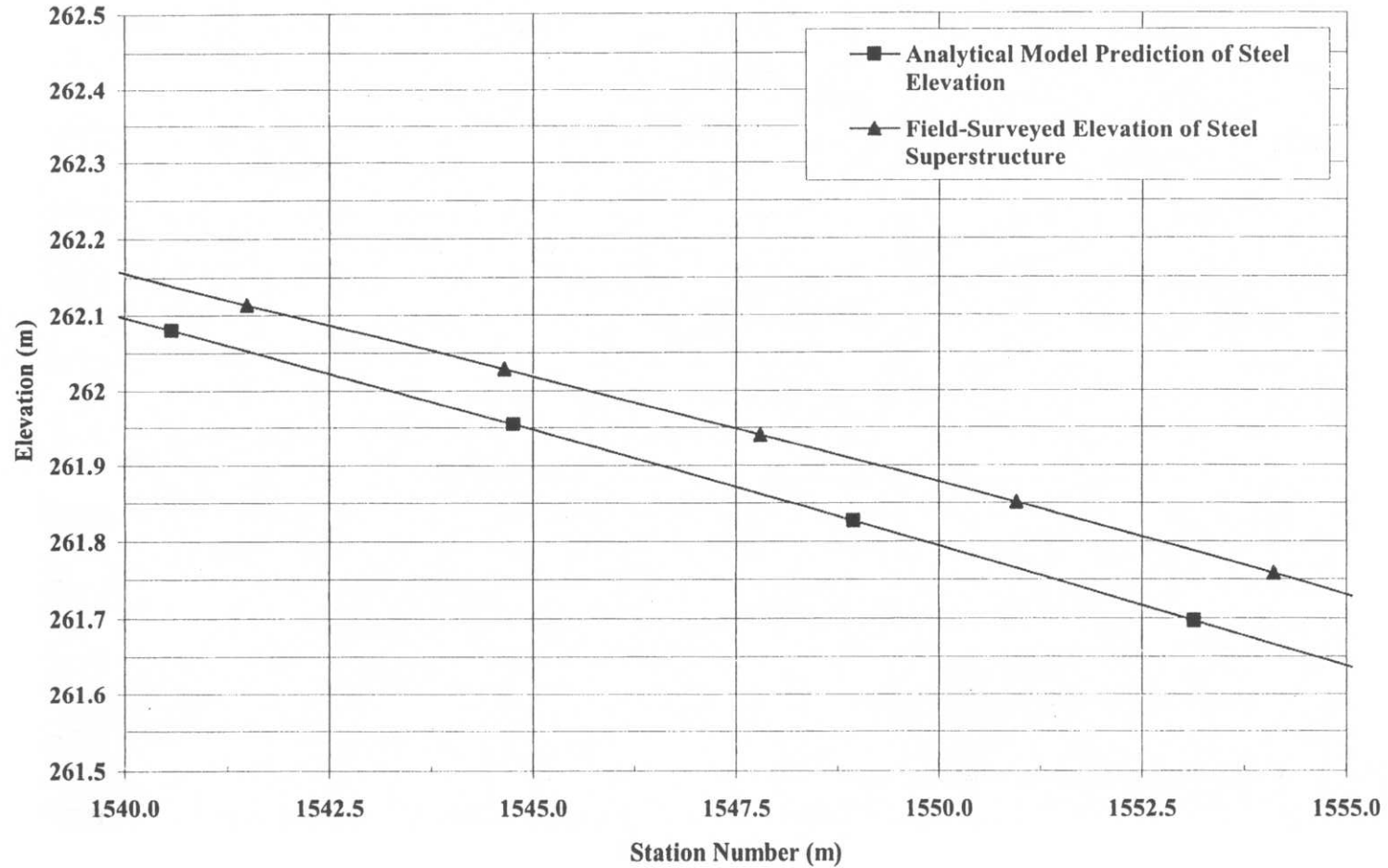


**Figure D-33 G4** – Elevation profile, STA 1+540 to 1+555; Analytical model versus field-surveyed data

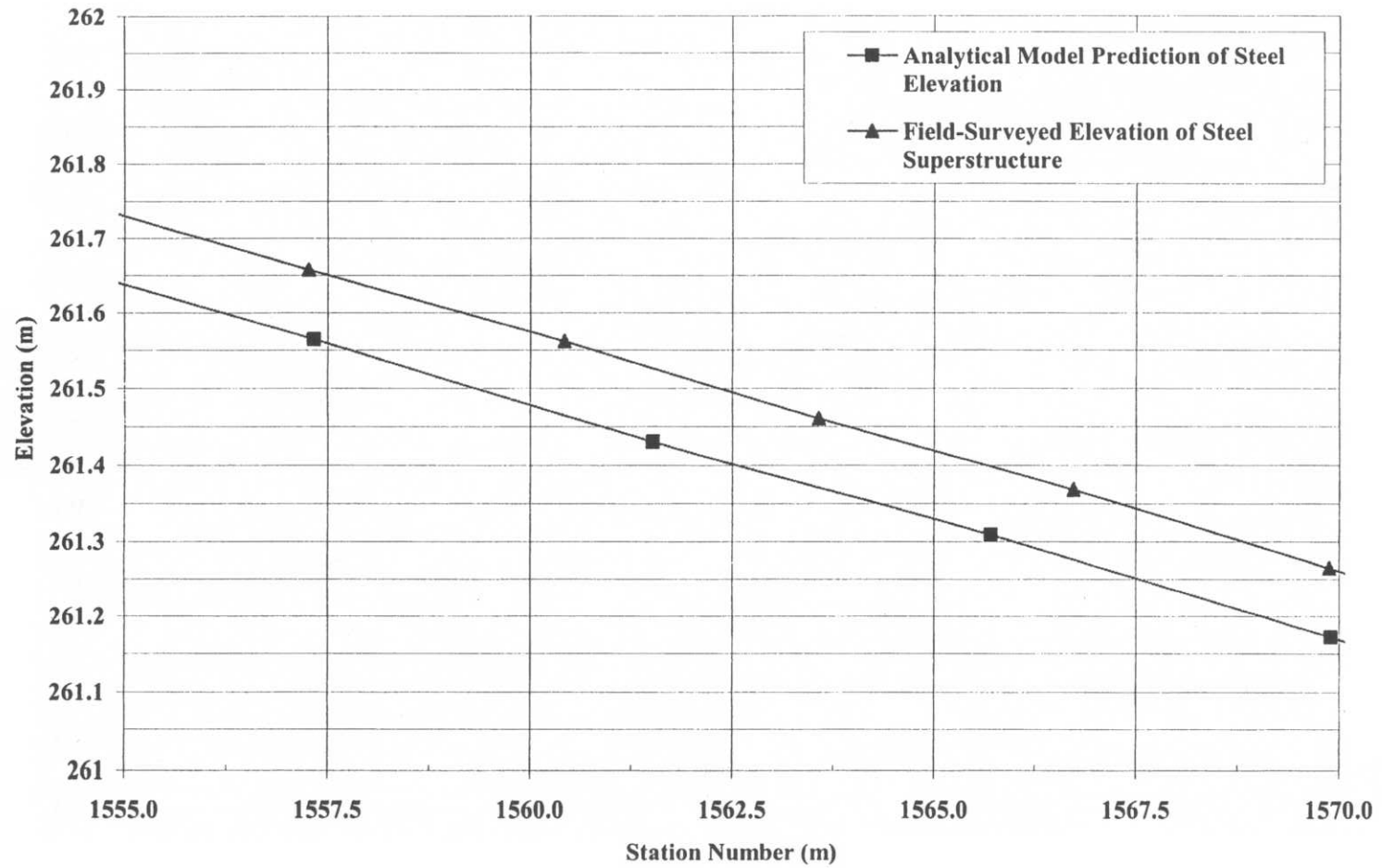


**Figure D-34 G4** – Elevation profile, STA 1+555 to 1+570; Analytical model versus field-surveyed data

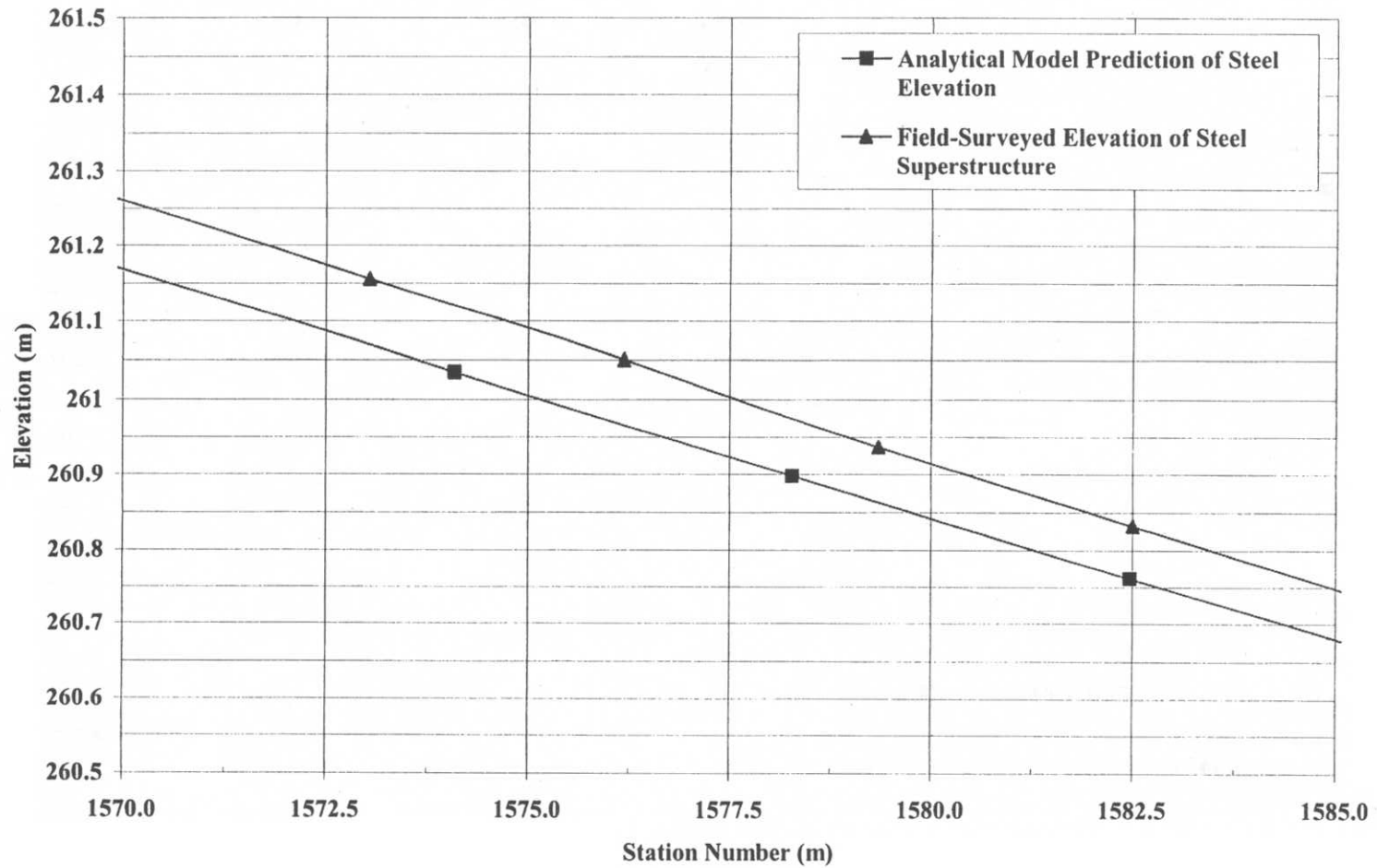


Figure D-35 G4 – Elevation profile, STA 1+570 to 1+585; Analytical model versus field-surveyed data

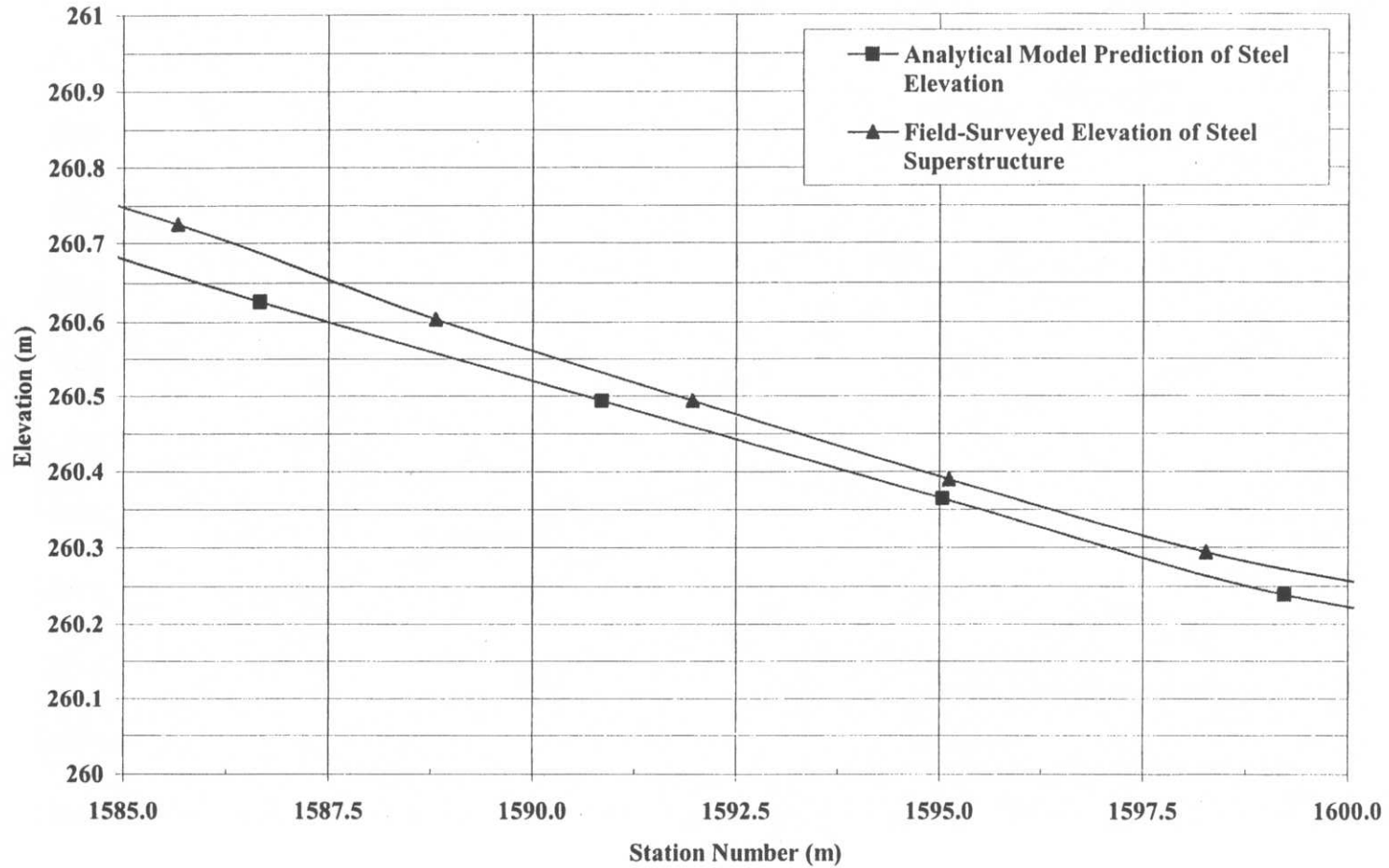
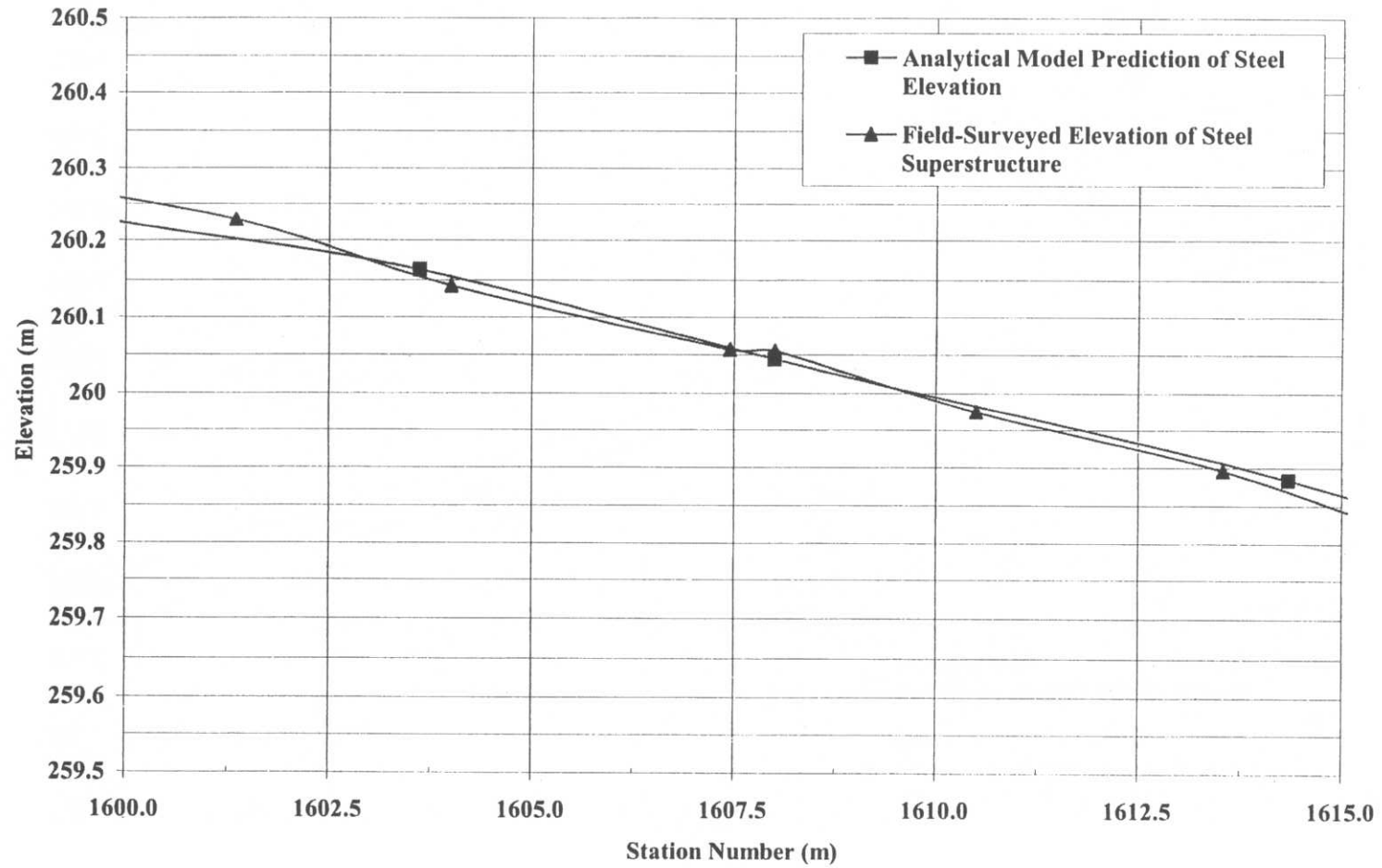


Figure D-36 G4 – Elevation profile, STA 1+585 to 1+600; Analytical model versus field-surveyed data



**Figure D-37 G4** – Elevation profile, STA 1+600 to 1+615; Analytical model versus field-surveyed data

## **APPENDIX E**

## APPENDIX E

### E.1 HAND CALCULATION OF CROSS-FRAME MEMBER LENGTH FOR THE WEB-OUT-OF-PLUMB CONDITION AT THE NO-LOAD POSITION

This calculation is accomplished using the results from the finite element analysis of the entire Ford City Bridge (curved and straight spans), subjected to steel self-weight only. The cross-frame member lengths are calculated for cross-frame 14A, which is the location of the largest difference in the diagonal cross-frame member lengths for those detailed to web-plumb at the no-load position and those detailed to web out-of-plumb at the no-load position.

Also, as part of this appendix, the girder displacements due to steel self-weight only, resulting from the finite element analysis of the entire Ford City Bridge are given following the example hand calculation.

#### **1. Data:**

Cross-frame 14A

ABAQUS  $\theta = 107.04$  deg.

Bridge STA = 1553.136

#### **2. Prior to Load Application (i.e no-load):**

Note: Elevations are at the Web – Cross-frame junction, not at the actual flanges; Bottom and Top flange references are used for simplicity. Furthermore, the elevations given are those of the fully-cambered girder, and with the change in elevation from abutment 1 to abutment 2 included.

#### **Girder G1:**

Radius ( $R_{G1}$ ) = 162065mm

Bottom Flange Elevation ( $Z_{BFG1}$ ) = 3021.65mm

Top Flange Elevation ( $Z_{TFG1}$ ) = 6861.65mm

#### **Girder G2:**

Radius ( $R_{G2}$ ) = 157965mm

Bottom Flange Elevation ( $Z_{BFG2}$ ) = 2921.23mm

Top Flange Elevation ( $Z_{TFG2}$ ) = 6761.23mm

### 3. Results From the Finite Element Analysis After Application of Steel Self-Weight Only:

See figure (Figure E-1) below for notations. (The figure is an enlargement of the entire cross-section, however only cross-frame A is shown.)

Girder G1:

$$X_B = 39.85\text{mm}$$

$$X_T = 131.2\text{mm}$$

$$Y_{G1} = 313.8\text{mm}$$

Girder G2:

$$X_B = 41.68\text{mm}$$

$$X_T = 131.3\text{mm}$$

$$Y_{G2} = 224.3\text{mm}$$

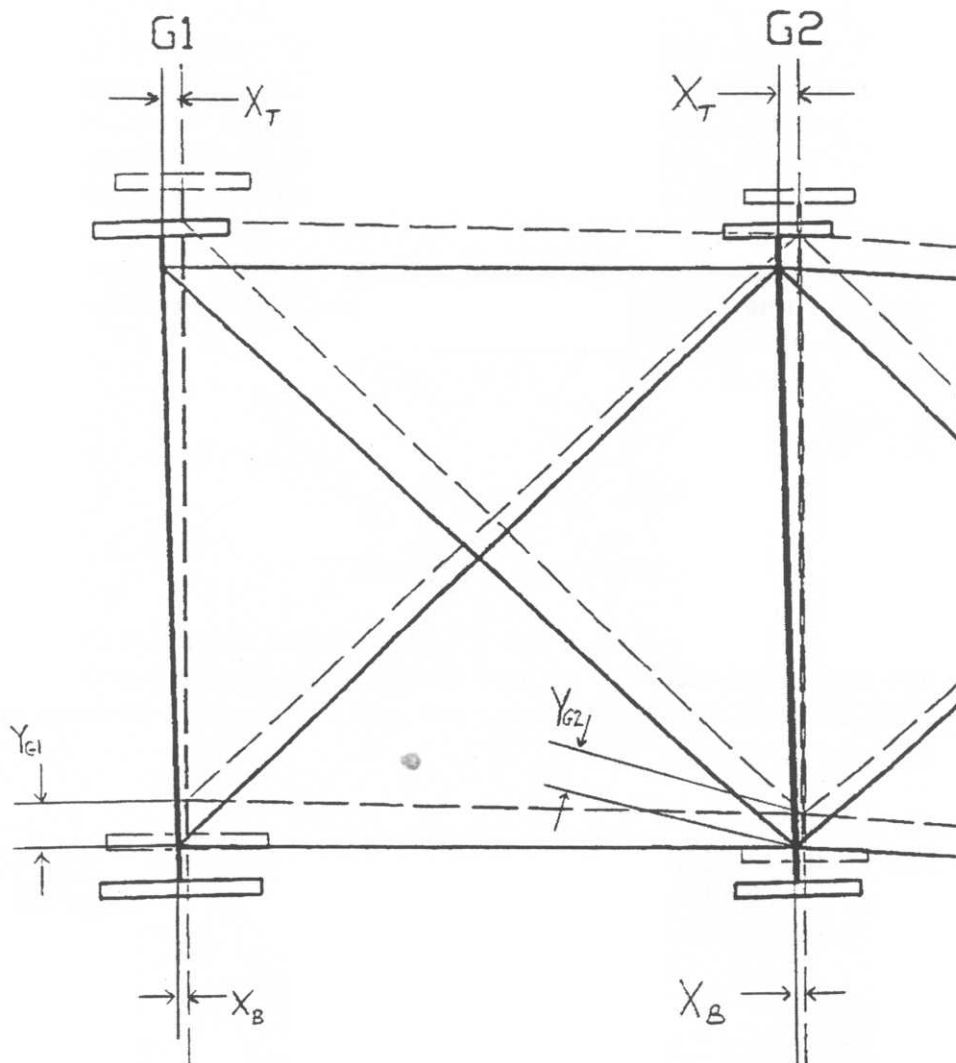


**Figure E-1** Girder Displacements for Hand Calculation

#### 4. Rotate the Girder Webs to a Plumb Position:

Rotate the displaced girders about the bottom flange-web junction to position the girders in a web-plumb state. The amount of rotation is equal to the displaced rotation of the girders due to the application of steel self-weight, and is equal for each girder. In other words: at the top web-cross-frame junction the lateral (out-of-plane, radial) displacement is ( $X_T$ ) 131.2mm, and at the bottom web-cross-frame junction the lateral displacement is ( $X_B$ ) 39.85mm.

$$X_T - X_B = 131.2\text{mm} - 39.85\text{mm} = 91.35\text{mm}$$

Therefore, the top flange is moved laterally 91.35mm (to the right, inward of curve), so that the web of the girder is now plumb.

With the girder webs plumb, new cross-frame members are drawn in using the same web-cross-frame junction locations, as shown in the next figure (Figure E-2), and now the member lengths can be determined as follows.

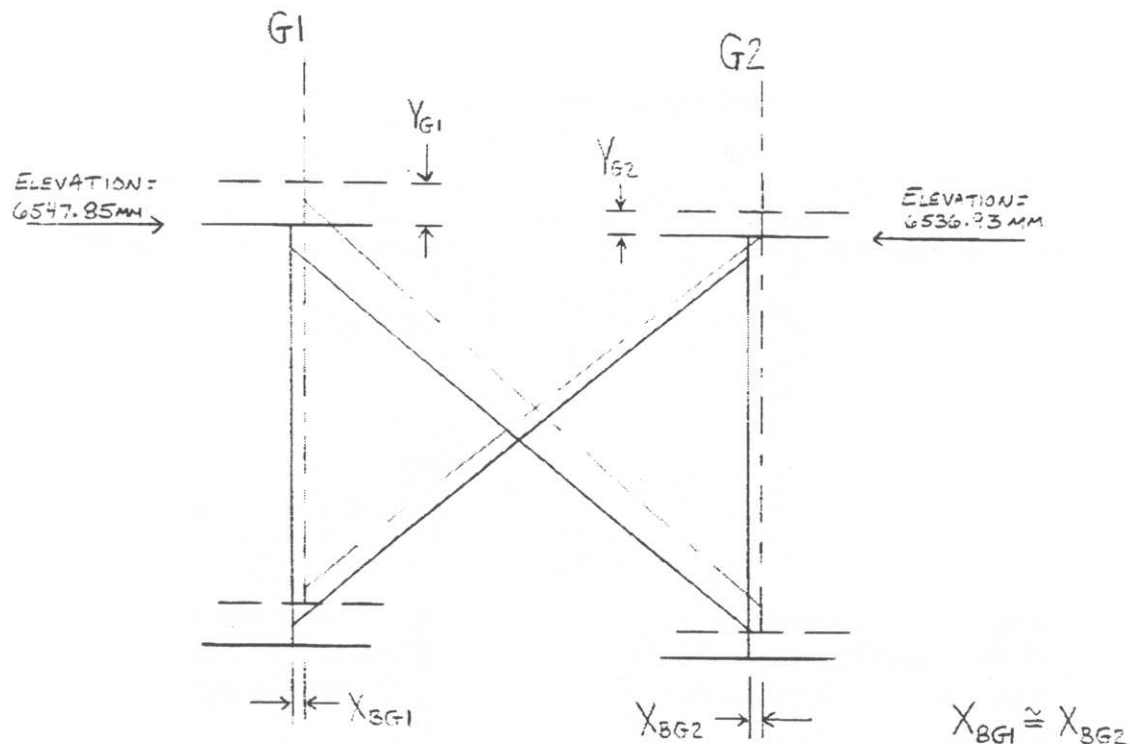


**Figure E-2** Web-Out-of-Plumb Cross-Frames Inserted for Hand Calculation

### **5. Determine New Cross-Frame Member Lengths:**

$$Z_{\text{NEW}} \text{ (displaced elevation)} = Z_{\text{TFG* or BFG*}} \text{ (no-load elevation)} - Y \text{ (vertical displacement)}$$

#### Girder G1:

$$Z_{\text{NEW BFG1}} = Z_{\text{BFG1}} - Y_{\text{G1}} = 6861.65\text{mm} - 313.8\text{mm} = 2707.85\text{mm}$$

$$Z_{\text{NEW TFG1}} = Z_{\text{TFG1}} - Y_{\text{G1}} = 3021.65\text{mm} - 313.8\text{mm} = 6547.85\text{mm}$$

#### Girder G2:

$$Z_{\text{NEW BFG2}} = Z_{\text{BFG2}} - Y_{\text{G2}} = 2921.23\text{mm} - 224.3\text{mm} = 2696.93\text{mm}$$

$$Z_{\text{NEW TFG2}} = Z_{\text{TFG2}} - Y_{\text{G2}} = 6761.23\text{mm} - 224.3\text{mm} = 6536.93\text{mm}$$

Note that the inside girder G2 is actually higher than the outside girder G1, this is due to the superelevation of the structure and is acceptable in determining cross-frame member lengths.

Using a typical bracing formula, with the previous figure (Step 4), the member lengths can be calculated:

$$b = 3840\text{mm}$$

$$w = 4100\text{mm}$$

$$n = p = 2696.93\text{mm} - 2707.85\text{mm} = -10.92\text{mm}$$

#### Equations:

$$F = [(b + p)^2 + w^2]^{1/2}$$

$$\text{Bottom Chord} = [n^2 + w^2]^{1/2}$$

$$M = [(b - n)^2 + w^2]^{1/2}$$

$$\text{Top Chord} = [p^2 + w^2]^{1/2}$$

*Therefore:*

$$F = 5609.98\text{mm}$$

$$\text{Bottom Chord} = 4100.01 \text{ mm}$$

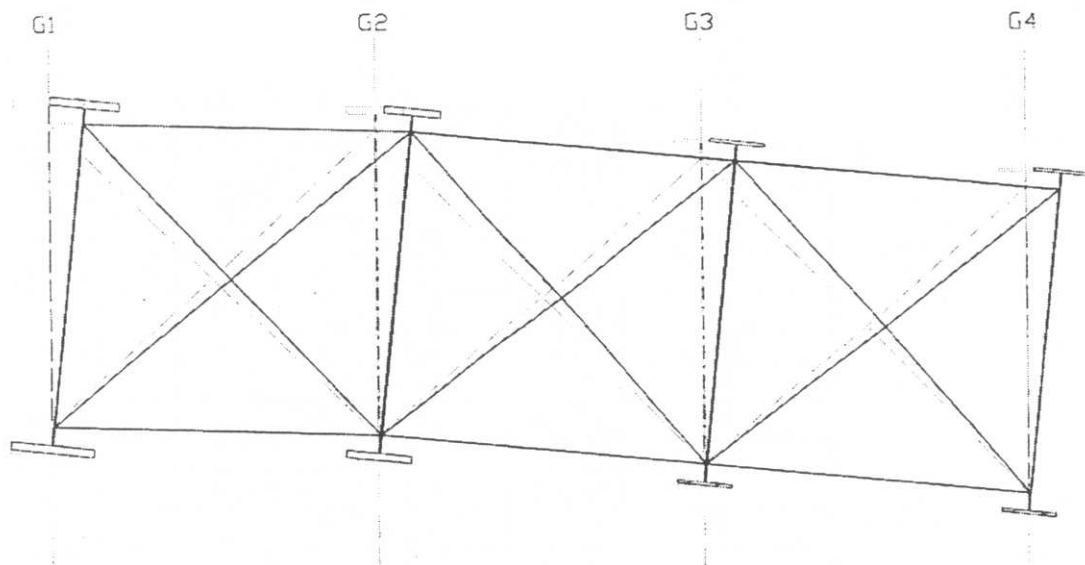
$$M = 5624.91\text{mm}$$

$$\text{Top Chord} = 4100.01 \text{ mm}$$

These cross-frame lengths are then used for girders erected with their webs out-of-plumb at the beginning of construction. After steel erection is completed, and temporary supports removed, the girder webs will rotate to a vertically plumb position.

### **6. Position of Girders at the Beginning of Construction:**

The entire bridge cross-section is then rotated back by the same angle it deflected due to the application of steel self-weight. The vertical and horizontal displacements due to the application of steel self-weight are also “reversed,” such that the midpoint of the bottom of each girder bottom flange is in the same location as it is in the no-load, web-plumb position. The figure below (displacement/rotation is magnified by a factor of 5 for illustrative purposes) illustrates the starting point of bridge erection for cross-frames detailed such that the girder webs are vertically plumb after the application of steel self-weight (removal of temporary supports).



WEB-PLUMB AT BEGINNING OF CONSTRUCTION (NO-LOAD)

—— NON-WEB-PLUMB AT BEGINNING OF CONSTRUCTION (NO-LOAD)

**Figure E-3** Girder position for girder webs out-of-plumb at the beginning of construction

**Table E-1** Analytical girder G1 displacements of the entire Ford City Bridge due to steel self-weight only

Cross-Frame Location	STA (m)	G1 Bottom Flange		G1 Top Flange
		Out-of-Plane (Radial) (mm)	Vertical (mm)	Out-of-Plane (Radial) (mm)
1	1510.00	-4.17	0.00	21.82
2	1512.20	-1.41	-26.03	30.62
3	1514.70	2.00	-54.98	40.54
4	1516.90	5.12	-80.03	49.35
5	1519.11	8.03	-104.30	58.55
6	1521.60	11.76	-130.80	68.02
7	1523.81	15.42	-153.00	75.25
8	1528.00	21.59	-191.70	89.23
9	1532.19	27.20	-226.00	102.20
10	1536.38	32.16	-255.30	113.20
11	1540.57	36.15	-279.10	122.00
12	1544.76	38.89	-297.00	128.10
13	1548.95	40.16	-308.60	131.20
14	1553.14	39.85	-313.80	131.20
15	1557.33	37.96	-312.70	128.10
16	1561.52	34.63	-305.40	122.30
17	1565.71	30.28	-292.20	113.50
18	1569.90	25.17	-273.70	102.80
19	1574.09	19.67	-250.30	90.67
20	1578.28	14.21	-223.00	77.60
21	1582.47	9.26	-192.40	64.26
22	1586.66	5.19	-159.40	51.18
23	1590.85	2.58	-125.10	38.74
24	1595.04	1.78	-90.81	27.43
25	1599.23	0.34	-57.75	17.75
26	1603.61	-0.10	-27.34	8.77
27	1608.00	0.00	0.00	0.15
28	1614.35	-0.84	29.74	-11.64
29	1620.70	-4.15	51.60	-24.13
30	1624.93	-9.95	61.63	-33.53

**Table E-2** Analytical girder G2 displacements of the entire Ford City Bridge due to steel self-weight only

Cross-Frame Location	STA (m)	G2 Bottom Flange		G2 Top Flange
		Out-of-Plane (Radial) (mm)	Vertical (mm)	Out-of-Plane (Radial) (mm)
1	1510.00	2.12	0.00	21.37
2	1512.20	4.87	-18.54	30.31
3	1514.70	8.29	-39.20	40.39
4	1516.90	11.48	-57.09	49.16
5	1519.11	14.49	-74.46	58.19
6	1521.60	18.28	-93.39	67.74
7	1523.81	21.78	-109.30	75.25
8	1528.00	26.91	-137.00	89.45
9	1532.19	31.94	-161.60	102.40
10	1536.38	36.34	-182.60	113.50
11	1540.57	39.72	-199.00	122.20
12	1544.76	41.85	-212.40	128.30
13	1548.95	42.53	-220.60	131.30
14	1553.14	41.68	-224.30	131.30
15	1557.33	39.31	-223.40	128.20
16	1561.52	35.54	-218.00	122.00
17	1565.71	30.81	-208.50	113.50
18	1569.90	25.43	-195.10	103.00
19	1574.09	19.71	-178.20	90.85
20	1578.28	14.11	-158.40	77.82
21	1582.47	9.02	-136.30	64.43
22	1586.66	4.89	-112.50	51.19
23	1590.85	2.10	-88.17	38.97
24	1595.04	0.41	-63.78	27.60
25	1599.23	-0.03	-40.55	17.85
26	1603.61	-0.07	-18.99	8.76
27	1608.00	0.00	0.00	0.09
28	1614.35	0.05	16.51	-11.92
29	1620.70	-3.83	32.93	-24.60
30	1624.93	-9.43	38.87	-33.47

**Table E-3** Analytical girder G3 displacements of the entire Ford City Bridge due to steel self-weight only

Cross-Frame Location	STA (m)	G3 Bottom Flange		G3 Top Flange
		Out-of-Plane (Radial) (mm)	Vertical (mm)	Out-of-Plane (Radial) (mm)
1	1510.00	7.27	0.00	19.47
2	1512.20	9.75	-11.14	28.01
3	1514.70	12.63	-23.60	37.75
4	1516.90	15.21	-34.39	46.20
5	1519.11	17.69	-44.90	54.60
6	1521.60	20.56	-56.40	63.85
7	1523.81	23.17	-66.10	71.55
8	1528.00	27.74	-83.17	85.38
9	1532.19	31.81	-98.22	97.86
10	1536.38	35.24	-111.00	108.60
11	1540.57	37.73	-121.30	117.00
12	1544.76	39.06	-128.90	122.90
13	1548.95	39.05	-133.80	125.90
14	1553.14	37.67	-135.90	125.90
15	1557.33	34.91	-135.20	122.90
16	1561.52	30.92	-131.80	117.00
17	1565.71	26.17	-125.70	108.70
18	1569.90	20.91	-117.30	98.54
19	1574.09	15.46	-106.80	86.86
20	1578.28	10.25	-94.41	74.30
21	1582.47	5.67	-80.66	61.44
22	1586.66	2.14	-66.04	48.86
23	1590.85	-0.09	-51.15	37.13
24	1595.04	-1.21	-36.50	26.32
25	1599.23	-1.20	-22.83	17.03
26	1603.61	-0.60	-10.38	8.36
27	1608.00	0.00	0.00	0.05
28	1614.35	-0.44	8.57	-11.88
29	1620.70	-2.97	12.52	-24.91
30	1624.93	-7.03	12.64	-33.57

**Table E-4** Analytical girder G4 displacements of the entire Ford City Bridge due to steel self-weight only

Cross-Frame Location	STA (m)	G4 Bottom Flange		G4 Top Flange
		Out-of-Plane (Radial) (mm)	Vertical (mm)	Out-of-Plane (Radial) (mm)
1	1510.00	12.42	0.00	17.48
2	1512.20	14.63	-3.26	25.77
3	1514.70	17.07	-7.90	35.27
4	1516.90	19.22	-11.89	43.56
5	1519.11	21.40	-15.77	51.62
6	1521.60	23.73	-19.98	60.63
7	1523.81	25.67	-23.51	68.31
8	1528.00	29.14	-29.76	81.90
9	1532.19	32.17	-35.23	94.09
10	1536.38	34.59	-39.82	104.50
11	1540.57	36.14	-43.45	112.80
12	1544.76	36.61	-46.06	118.50
13	1548.95	35.88	-47.63	121.40
14	1553.14	33.90	-48.13	121.40
15	1557.33	30.70	-47.58	118.40
16	1561.52	26.45	-46.01	112.60
17	1565.71	21.62	-43.52	104.60
18	1569.90	16.44	-40.13	94.64
19	1574.09	11.26	-35.88	83.29
20	1578.28	6.45	-30.96	71.11
21	1582.47	2.37	-25.59	58.66
22	1586.66	-0.55	-20.02	46.54
23	1590.85	-2.16	-14.57	35.24
24	1595.04	-2.66	-9.45	24.89
25	1599.23	-2.13	-5.01	16.06
26	1603.61	-0.97	-1.68	7.90
27	1608.00	0.00	0.00	0.02
28	1614.35	-0.14	-2.83	-11.59
29	1620.70	-1.87	-9.45	-24.66
30	1624.93	-5.10	-15.89	-33.14

## **APPENDIX F**

## APPENDIX F

### F.1 SUMMARY OF CONSEQUENCES RELATED TO INCONSISTENT DETAILING OF CROSS-FRAMES

This Appendix briefly lists some of the consequences related to the inconsistent detailing of cross-frame members in curved steel I-girder bridges. This information can also be found in section 8.0 of the current report.

#### F.1.1 Cross-Frames

- Diagonal members of 'X' type cross-frames will be either too long to too short.
- Gaps in the cross-frame connections will result from incorrect cross-frame member lengths.
- Cross-frames may have to be forced into place during steel erection of the bridge.
- Additional external forces may have to be applied during steel erection in order to bring cross-frames and girders into alignment.

#### F.1.2 Girders

- Bolt holes on the cross-frame connection plates attached to the girders will not align properly with inconsistently detailed cross-frames.
- The cross-frame connection plates may be at the wrong locations.
- Difficulties in closing field-splices will develop; field-splice bolt holes in the web and flanges may not align as anticipated by the design. Transitions in flange thickness at the field-splices may also complicate the alignment of bolt holes.
- Additional forces applied to the girders in order to bring components (cross-frames and girders) into alignment may be unacceptable (too large), or may cause girder instabilities.

### **F.1.3 General**

- Girder and bridge system instabilities may result from the unclosed gaps in cross-frame connections caused by inconsistently detailed cross-frame members.
- The final girder elevations after steel erection may not be in the designed locations, resulting in design changes to the concrete deck thickness and haunch at each girder.
- It may be necessary to acquire larger capacity cranes to bring components into alignment.
- Additional jacking frames / devices and temporary supports may be required.
- Predetermined construction costs assumed for a consistently detailed bridge will increase in proportion to problems resulting from inconsistent detailing.

## **BIBLIOGRAPHY**

## BIBLIOGRAPHY

ABAQUS, (2001), ABAQUS Standard User's Manual, Version 6.2, Volumes 1 to 3, Hibbit, Karlsson & Sorensen, Inc., Pawtucket, Rhode Island, USA.

American Association of State Highway and Transportation Officials (AASHTO), (1993), *Guide Specifications for Horizontally Curved Highway Bridges*, Washington, D.C.

Burrell, J.D., Zureick, A., and Grubb, M.A., (1997), "FHWA Curved Steel-Girder Research Project: Analysis of Curved Steel I-Girder Test Frame," *Building to Last – Proceedings of the XV Structures Congress*, Portland, Oregon, pp. 1632-1636.

Brennan, P.J., Antoni, C.M., Leininger, R., and Mandel, J.A., (1970), "Analysis for Stress and Deformation of a Horizontally Curved Girder Bridge Through a Geometric Structural Model," Research Report Submitted to New York State Department of Transportation, Engineering Research and Development Bureau, Department of Civil Engineering, Syracuse University, August.

Brennan, P.J. and Mandel, J.A., (1979), "Multiple Configuration Curved Bridge Model Studies," *Journal of the Structural Division*, ASCE, Vol. 105, No. ST5, May, pp. 875-890.

Davidson, J.S., (1996), "Nominal Bending and Shear Strength of Horizontally Curved Steel I-Girder Bridges," Ph.D. Dissertation, Auburn University, Auburn, Alabama.

Davidson, J.S., Keller, M.A., and Yoo, C.C., (1996), "Cross-Frame Spacing and Parametric Effects in Horizontally Curved I-Girder Bridges," *Journal of Structural Engineering*, ASCE, Vol. 122, No. 9, September, pp. 1089-1096.

Davidson, J.S., Balance, S.R., Yoo, C.H., (1999a), "Analytical Model of Curved I-Girder Web Panels Subjected to Bending," *Journal of Bridge Engineering*, ASCE, Vol. 4, No. 3, August, pp. 204-212.

Davidson, J.S., Balance, S.R., Yoo, C.H., (1999b), "Finite Displacement Behavior of Curved I-Girder Webs Subjected to Bending," *Journal of Bridge Engineering*, ASCE, Vol. 4, No. 3, August, pp. 213-220.

Davidson, J.S., Balance, S.R., Yoo, C.H., (2000a), "Behavior of Curved I-Girder Webs Subjected to Combined Bending and Shear," *Journal of Bridge Engineering*, ASCE, Vol. 5, No. 2, May, pp. 165-170.

Davidson, J.S., Balance, S.R., Yoo, C.H., (2000b), "Effects of Longitudinal Stiffeners on Curved I-Girder Webs," *Journal of Bridge Engineering*, ASCE, Vol. 5, No. 2, May, pp. 171-178.

Davidson, J.S. and Yoo, C.H., (2000c), "Evaluation of Strength Formulations for Horizontally Curved Flexural Members," *Journal of Bridge Engineering*, ASCE, Vol. 5, No. 3, August, pp. 200-207.

Duwadi, S.R., Grubb, M.A., Yoo, C.H., and Hartmann, J., (2000), "Federal Highway Administration's Horizontally Curved Steel Bridge Research Project: An Update," *Transportation Research Record 1696, Vol. 1*, Transportation Research Board, National Research Council, Washington, D.C, pp. 152-161.

Galambos, T.V., (1978), "Tentative Load Factor Design Criteria for Curved Steel Bridges, Research Report No. 50," Department of Civil Engineering, Washington University, St. Louis, Missouri.

Galambos, T.V., Hajjar, J.F., Leon, R.T., Huang, W.-H., Pulver, B.E., and Rudie, B.J., (1996), "Stresses in a Steel Curved Girder Bridge," Report No. MN/RC-96/28, Minnesota Department of Transportation, St. Paul, Minnesota.

Galambos, T.V., Hajjar, J.F., Huang, W.-H., Pulver, B.E., Leon, R.T., and Rudie, B.J., (2000), "Comparison of Measured and Computed Stresses in a Steel Curved Girder Bridge," *Journal of Bridge Engineering*, ASCE, Vol. 5, No. 3, August, pp. 191-199.

Grubb, M.A., Yadlosky, J.M., and Duwadi, S.R., (1996), "Construction Issues in Steel Curved-Girder Bridges," *Transportation Research Record 1544*, Transportation Research Board, National Research Council, Washington, D.C., pp. 64-70.

Hall, D.H., Grubb, M.A., and Yoo, C.H., (1999), *National Cooperative Highway Research Program Report 424: Improved Design Specifications for Horizontally Curved Steel Girder Highway Bridges*, Transportation Research Board, National Research Council, Washington, D.C.

HDR Engineering, Inc., Ford City Bridge Erection Procedure Staging Drawings, Armstrong County, S.R. 0128, Sec. 013, Pittsburgh, Pennsylvania, August, 1999.

Hilton, M.H., (1984), "Deflections and Camber Loss in Heat-Curved Girders," *Transportation Research Record 950, Vol 2*, Transportation Research Board, National Research Council, Washington, D.C, pp. 51-59.

Huang, W.-H., (1996), "Curved I-Girder Systems," Ph.D. Dissertation, Department of Civil Engineering, University of Minnesota, Minneapolis, Minnesota.

Linzell, D.G., (1999), “Studies of Full-Scale Horizontally Curved Steel I-Girder Bridge Systems Under Self Weight,” Ph.D. Dissertation, School of Civil and Environmental Engineering, Georgia Institute of Technology.

Linzell, D.G., (2000), “How Much Influence Does Construction Have on Curved Steel Bridges? Results From Analytical and Experimental Studies,” *17<sup>th</sup> International Bridge Conference*, Pittsburgh, Pennsylvania.

Mozer, J. and Culver, C., (1970), “Horizontally Curved Highway Bridges – Stability of Curved Plate Girders, Report No. P1,” Report Submitted to the Department of Transportation, Federal Highway Administration, Department of Civil Engineering, Carnegie-Mellon University, Pittsburgh, Pennsylvania.

Mozer, J., Ohlson, R., and Culver, C., (1971), “Horizontally Curved Highway Bridges – Stability of Curved Plate Girders, Report No. P2,” Report Submitted to the Department of Transportation, Federal Highway Administration, Department of Civil Engineering, Carnegie-Mellon University, Pittsburgh, Pennsylvania.

Mozer, J., Cook, J., and Culver, C., (1973), “Horizontally Curved Highway Bridges – Stability of Curved Plate Girders, Report No. P3,” Report Submitted to the Department of Transportation, Federal Highway Administration, Department of Civil Engineering, Carnegie-Mellon University, Pittsburgh, Pennsylvania.

Pennsylvania Department of Transportation (PennDOT), Ford City Bridge Design Plans, Armstrong County, S.R 0128, Sec. 013, January, 1998

Personal Communication with John M. Yadlosky, P.E. Vice President, HDR Engineering, Inc., Pittsburgh, Pennsylvania, September 2001.

Pulver, B.E., (1996), “Measured Stresses in A Steel Curved Girder Bridge System,” MCE Report, Department of Civil Engineering, University of Minnesota, Minneapolis, Minnesota.

Simpson, M.D., (2000), “Analytical Investigation of Curved Steel Girder Behavior,” Ph.D. Dissertation, Department of Civil Engineering, University of Toronto, Toronto, Ontario, Canada.

Schelling, D., Namini, A., Fu, C.C., (1989), “Construction Effects on Bracing on Curved I-Girders,” *Journal of Structural Engineering*, ASCE, Vol. 115, No. 9, September, pp. 2145-2165.

Stegmann, T.H., (1975), “Load Factor Design Criteria for Curved Steel Girders,” M.S. Thesis, Washington University, St. Louis, Missouri.

Zureick, A., Naqib, R., and Yadlosky, J.M., (1994), "Curved Steel Bridge Research Project, Interim Report I: Synthesis," FHWA-RD-93-129, Federal Highway Administration, U.S. Department of Transportation, December.

Zureick, A. and Naqib, R., (1999), "Horizontally Curved steel I-Girders State-of-the-Art Analysis Methods," *Journal of Bridge Engineering*, Vol. 4, No. 1, February, pp. 38-47.

## REFERENCES NOT CITED

Althoff, J.C., (1972), "Theoretical and Experimental Investigation of Horizontally Curved Girder Highway Bridges," M.S. Thesis, Department of Civil and Mineral Engineering, University of Alabama, Alabama.

Brockenbrough, R.L. and Ives, K.D., (1970), "Experimental Stresses and Strains from Heat Curving," *Journal of the Structural Division*, ASCE, Vol. 96, No. ST7, July, pp. 1305-1331.

Brockenbrough, R.L., (1970), "Theoretical Stresses and Strains from Heat Curving," *Journal of the Structural Division*, ASCE, Vol. 96, No. ST7, July, pp. 1421-1444.

Brockenbrough, R.L., (1970), "Criteria for Heat Curving Steel Beams and Girders," *Journal of the Structural Division*, ASCE, Vol. 96, No. ST10, October, pp. 2209-2226.

Brockenbrough, R.L., (1986), "Distribution Factors for Curved I-Girder Bridges," *Journal of Structural Engineering*, ASCE, Vol. 112, No. 10, October, pp. 2200-2215.

Chini, A. and Genauer, G., (1997), "Technical Guidance Available to designers of Temporary Structures," *Building to Last-Proceedings of the XV Structures Congress*, Portland, Oregon, pp. 979-984.

Dunsberry, D.O., (1997), "Environmental Loads on Structures During Construction," *Building to Last-Proceedings of the XV Structures Congress*, Portland, Oregon, pp. 991-995.

Funkhouser, D.W. and Heins, C.P., (1974), "Skew and Elevated Support Effects on Curved Bridges," *Journal of the Structural Division*, ASCE, Vol. 100, No. ST7, July, pp. 1379-1396.

Ghaboussi, J. and Pecknold, D.A., (1984), "Incremental Finite Element Analysis of Geometrically Altered Structures," *International Journal for Numerical Methods in Engineering*, Vol. 20, pp. 2051-2064.

Grubb, M.A., (1984), "Horizontally Curved I-Girder Bridge Analysis: V-Load Method," *Transportation Research Record 982*, Transportation Research Board, National Research Council, Washington, D.C., pp. 26-35.

Hall, D.H., (1997), "Proposed Curved Girder Provisions for AASHTO," *Building to Last-Proceedings of the XV Structures Congress*, Portland, Oregon, pp. 151-154.

Heins, C.P., Bonakdarpour, B., and Bell, L.C., (1972), "Multicell Curved Girder Model Studies," *Journal of the Structural Division*, ASCE, Vol. 98, No. ST4, April, pp. 831-843.

Heins, C.P. and Spates, K.R., (1970), "Behavior of single Horizontally Curved Girder," *Journal of the Structural Division*, ASCE, Vol. 96, No. ST7, July, pp. 1511-1524.

Nakai, H. and Heins, C.P., (1977), "Analysis Criteria for Curved Girder Bridges," *Journal of the Structural Division*, ASCE, Vol. 103, No. ST7, July, pp. 1419-1427.

Nakai, H. and Yoo, C.H., (1988), *Analysis and Design of Curved Steel Bridges*, McGraw Hill Book Company, New York, New York.

Pi, Y.-L. and Trahair, N.S., (1997), "Nonlinear Elastic Behavior of I-Beams Curved in Plan," *Journal of Structural Engineering*, Vol. 123, No. 9, September, pp. 1201-1209.

Reddy, P., Ghaboussi, J., and Hawkins, N.M., (1999), "Simulation of Construction of Cable-Stayed Bridges," *Journal of Bridge Engineering*, ASCE, Vol. 4, No. 4, November, pp. 249-257.

Roeder, C.W., (1987), "Prediction of Deformations Due to Heat Curving," *Bridges and Transmission Line Structures, Proceedings of the Sessions at Structures Congress 1987, Orlando, FL, USA*, ASCE, New York, New York, pp. 101-110.

Shanmugam, N.E., Thevendran, V., Richard Liew, J.Y., and Tan, L.O., (1995), "Experimental Study on Steel Beams Curved in Plan," *Journal of Structural Engineering*, ASCE, Vol. 121, No. 2, February, pp. 249-259.

Stallings, J.M. and Cousins, T.E., (1997), "Evaluation of Diaphragm Requirements in Existing Bridges." *Building to Last-Proceedings of the XV Structures Congress*, Portland, Oregon, pp. 1494-1498.

Thatcher, W.M., (1967), "Horizontally Curved Steel Girders – Fabrication and Design Considerations," *Engineering Journal*, AISC, July, pp. 107-112.

Thevendran, V., Shanmugam, N.E., and Richard Liew, J.Y., (1998), *Journal of Constructional Steel Research*, Elsevier Science Ltd., Vol. 46:1-3, Paper No. 345.

Weinhold, S.A., (1997), "Erection Engineering for Steel Bridge Superstructures," *Modern Steel Construction*, AISC, Vol. 37, Issue 10, October, pp. 15-18.

Yang, Y.-B. and Kuo, S.-R., (1987), "Effect of Curvature on Stability of Curved Beams," *Journal of Structural Engineering*, ASCE, Vol. 113, No. 6, June, pp.1185-1202.

Yoo, C.H. and Heins, C.P., (1972), "Plastic Collapse of Horizontally Curved Bridge Girders," *Journal of the Structural Division*, ASCE, Vol. 98, No. ST4, April, pp. 899-914.

Yoo, C.H. and Littrell, P.C., (1986), "Cross-Bracing Effects in Curved Stringer Bridges," *Journal of Structural Engineering*, ASCE, Vol. 112, No. 9, September, pp. 2127-2140.

